Preparation of Polysubstituted Pyrans Toward the Synthesis of Biologically Active Compounds

by

Taras Ivan Rybak

A thesis submitted in partial fulfillment of the requirements for the degree of
Doctor of Philosophy

Department of Chemistry
University of Alberta

Abstract

Polyfunctionalized pyrans are among the most common structures in bioactive molecules. Based on the ubiquity of the pyran framework in natural and synthetic molecules, there is a need to develop more efficient methods of synthesizing and functionalizing the pyran motif. Due to recent interest in increasing the three-dimensionality of potentially bioactive molecules, applying asymmetric reactions to access the pyran framework is highly desirable. This thesis describes new efforts to develop and utilize stereochemically enriched dihydropyrans for the synthesis of biologically-active molecules.

Chapter 1 provides a summary of the most common methods to synthesize and functionalize pyran structures. These methods were effectively used towards the syntheses of diverse classes of biologically active molecules containing polyfunctionalized pyran cores. Chapter 2 describes efforts made toward the synthesis of small dihydropyran-containing molecules analogous to laulimalide, an antimitotic and potentially useful chemotherapeutic natural product. Previous work attempting to identify the key pharmacophores of laulimalide was used to propose structurally simpler analogues. These analogues were modeled for binding affinity using computational analysis to propose a synthetic target. Early attempts were made at developing a short synthetic route to this target compound.

In Chapter 3, early efforts towards expanding the utility of the Suzuki-Miyaura reaction beyond the classical sp^2–sp^2 bond formation are summarized. The analysis of novel cross-coupling reactions led to the first stereospecific and regiodivergent allylic Suzuki-Miyaura cross-coupling reaction. This unique method, which forms carbon-carbon sp^3–sp^2 bonds on enantioenriched heterocyclic allylboronates, is discussed. The ligand-controlled cross-coupling reaction effectively produces a broad range of aryl- and alkenyl-coupled pyrans with high

stereospecificity and regioselectivity. Enantioenriched 2-ethoxy dihydropyranyl boronate substrates, synthesized from an asymmetric inverse electron demand oxa-[4+2] cycloaddition, were used in the cross-coupling reaction. The allylic cross-coupling was applied to the synthesis of polyfuntionalized pyrans. Furthermore, based on the spectroscopic and X-ray crystallographic analysis of the derivatized products, the stereospecificity of these reactions was confirmed and a more generalized mechanism was proposed. Lastly, this method was utilized towards the synthesis of the natural product goniothalesdiol A, as well as the successful total synthesis of the antiosteoporotic natural product diospongin B.

Preface

Chapter 3 of this thesis has been published as Ding, J.; Rybak, T.; Hall, D. G. "Synthesis of Chiral Heterocycles by Ligand-controlled Regiodivergent and Enantiospecific Suzuki Miyaura Cross-coupling", *Nature Communications* 5:5474. My colleague Jinyue Ding was responsible for the reaction optimization for the cross-coupling of chiral dehydropiperidinyl and dihydropyranyl boronates. He was also responsible for the study of the substrate scope, data collection and analysis for the cross-coupling of chiral dehydropiperidinyl boronates and partly for dihydropyranyl boronates, which is described in Chapter 3. I was partly responsible for the study of the substrate scope, data collection and analysis that involved the cross-coupling of chiral dihydropyranyl boronates. Prof. Hall was the supervisory author and was involved with concept formation and manuscript composition.

Chapter 4 of this thesis has been published as Rybak, T.; Hall, D. G. "Stereoselective and Regiodivergent Allylic Suzuki-Miyaura Cross-Coupling of 2-Ethoxydihydropyranyl Boronates: Synthesis and Confirmation of Absolute Stereochemistry of Diospongin B.", *Organic Letters* **2015**, *17:*4156–4159. As the sole experimentalist, I was responsible for the reaction optimization, study of substrate scope, data collection and analysis for the cross-coupling of chiral 2-ethoxydihydropyranyl boronates as well as the total synthesis of diospongin B. I also wrote the manuscript with assistance from D. G. Hall. Prof. Hall, was the supervisory author and was involved with concept formation and project initiation.

Acknowledgements

I would like to express my gratitude to Prof. Dennis Hall, who has guided and supported me during my graduate degree. His research expertise, comprehensive understanding of the work related to my thesis, and patience have given me the opportunity to excel in synthetic chemistry and to improve on my research skills. He has provided me the opportunity to attend and present at several conferences and symposia. During our group and biweekly meetings, he has helped in further improving my education in synthetic chemistry. I am very thankful and indebted to him for his support.

I am very thankful for the assistance of the administrative and research services at the University of Alberta. Specifically, I am particularly thankful for the help provided by Lynne Lechelt, Anita Weiler, Ryan Lewis and Matthew Kingston. In regards to the Scientific Services Staff, I am particularly thankful to Wayne Moffat (spectroscopy), Mark Miskolzie (NMR), Dr. Robert McDonald (X-Ray crystallography) and Ed Fu (HPLC) for their expertise in providing advice and assistance to my scientific research. Furthermore, I am thankful to other staff members of the NMR, Mass Spectrometry, X-ray Crystallographic and Analytical labs, as well as the machine shop, the storeroom, and the glass shop.

I am also thankful to my Supervisory Committee and Ph. D. Examination Committee members: Prof. Derrick Clive, Prof. John C. Vederas, Prof. Mariusz Klobukowski, Prof. John Klassen and Prof. Cathleen Crudden. I am grateful for the comments, suggestions, and guidance they have provided me over the years.

I am also grateful to all my lab mates, past and present, with whom I have had the pleasure to work with. They are all hard working and very talented individuals who have helped support and guide me over the years. I am specifically thankful to Dr. Sylvain Bernard, Dr. Sergey

Vshyvenko and Youri Kim for their friendship and support. Most of all, I am grateful to Burcin Akgun, my supportive lab mate and closest friend. She provided unwavering friendship, patience, and advice during my degree. I am thankful to those who have provided advice while writing my dissertation, which are Dr. Olivier Soueidan, Dr. Mickey Richards and Dr. Timothy Morgan. I would also like to thank Dr. Hayley Wan for being a supportive lab coordinator. Her patience, friendliness and guidance made my teaching experience very enjoyable.

Last, and not least, I am thankful to my friends and family for all the support and advice they have given me throughout my graduate degree. To Pavan Kondapi and Claude Larrivee Aboussafy, my two oldest and dearest friends in Alberta, are both trustworthy and supportive colleagues. Also graduate students studying synthetic organic chemistry, we have shared research related ideas among one another throughout our degree. Specifically to Pavan, I am honored to have accompanied his family on countless occasions. Both Dr. Ho-Yan Sun and Roger Ashmus, friends that I have accompanied on several occasions, have been very supportive during my graduate degree. To my gang of “Aliens”, my group of friends who I have also had fun and exciting experiences with, which include Nada Djokic, Dr. Yazeed Nabeeh Al Hamarneh, Dr. Maica and Dr. Leonidas Perez, Dr. Elena and Dr. Nikolaus Klamerth, Burcin and Burak Akgun, Daniel Hernandez and Dr. Vanessa Incani. They have all treated me as family and I will always be indebted to them. To my family, which include my Mom, Dad, Anastazia, Dr. Adrian Rybak, the love and support they have given me is immeasurable. Once more, both my friends and family encouraged me to persevere during the difficult times in my graduate degree. I am forever grateful for everything they have done for me. I wouldn’t succeed without their advice, love and patience.

List of Abbreviations

9-BBN	9-Borabicyclo(3.3.1)nonane
Ac	Acetyl
ACS	American Chemical Society
Ar	Aryl group
BINAP	2,2'-Bis(diphenylphosphino)-1,1'-binaphthyl
BINOL	2,2′-Dihydroxy-1,1′-dinaphthyl
Boc	*tert*-Butyloxycarbonyl
Bn	Benzyl
br	Broad
n-Bu	Normal butyl
t-Bu	*tert*-Butyl
calcd	Calculated
cataCXium A-Pd-G2	Chloro[(di(1-adamantyl)-N-butylphosphine)-2-(2-aminobiphenyl)]palladium(II)
cm^{-1}	Wavenumbers
COSY	Correlation spectroscopy
CPME	Cyclopentyl methyl ether
CM	Cross metathesis
CSA	Camphorsulfonic acid
Cy	Cyclohexyl
CyJohnPhos	2-(Dicyclohexylphosphino)biphenyl
Dan	1,8-Diaminonaphthalene

DCC	*N*,*N*'-Dicyclohexylcarbodiimide
DIC	*N*,*N*'-Diisopropylcarbodiimide
dba	Dibenzylideneacetone
DMAP	4-(Dimethylamino)pyridine
DBU	1,8-Diazabicyclo[5.4.0]undec-7-ene
DIAD	Diisopropyl azodicarboxylate
DIPEA	*N*,*N*-Diisopropylethylamine
DIPCl	*B*-Chlorodiisopinocampheylborane
dd	Doublet of doublets
ddd	Doublet of doublet of doublets
dq	Doublet of quartets
dt	Doublet of triplets
dr	Diastereomeric ratio
DFT	Density functional theory
DIBAL-H	Diisobutylaluminium hydride
dppb	1,4-Bis(diphenylphosphino)butane
dppp	1,3-Bis(diphenylphosphino)propane
dppf	1,1'-Bis(diphenylphosphino)ferrocene
dippf	1,1′-Bis(di-isopropylphosphino)ferrocene
DME	Dimethoxyethane
DMF	*N,N*-Dimethylformamide
DMSO	Dimethyl sulfoxide
dppb	1,4-Bis(diphenylphosphino)butane

dppf	1,1'-Bis(diphenylphosphino)ferrocene
D-t-BPF	1,1'-Bis(di-tert-butylphosphino)ferrocene
ee	Enantiomeric excess
er	Enantiomeric ratio
EDG	Electron donating group
EWG	Electron withdrawing group
EI	Electron impact
eq	Equation
equiv	Equivalents
ESI	Electrospray ionization
Et	Ethyl
fod	tris(6,6,7,7,8,8,8-Heptafluoro)-2,2-dimethyl-3,5-octanedionate
G-H II	Grubbs-Hoveyda second generation catalyst
h	Hour
HDA	Hetero-Diels-Alder
HDX	Hydrogen/deuterium exchange
HPLC	High performance liquid chromatography
HRMS	High resolution mass spectrometry
HSQC	Heteronuclear single-quantum correlation spectroscopy
HMBC	Heteronuclear multiple-bond correlation spectroscopy
IR	Infrared spectroscopy
*i*Pr	Isopropyl
*i*Pent	Isopentyl

KHMDS	Potassium hexamethyldisilazide
LDA	Lithium diisopropylamide
LHMDS	Lithium hexamethyldisilazide
LTMP	Lithium tetramethylpiperidide
m	Multiplet
MSA	Microtubule-stabilizing agent
MDA	Microtubule-destabilizing agent
mol	mole
*m*CPBA	*meta*-Chloroperoxybenzoic acid
mp	melting point
Me	Methyl
MeOH	Methanol
MS	Molecular sieves
MTPA	Methoxy(trifluoromethyl)phenylacetic acid
NMO	*N*-Methylmorpholine *N*-oxide
nOe	Nuclear Overhauser effect
NHC	*N*-Heterocyclic carbene
NMR	Nuclear magnetic resonance
NOESY	Nuclear Overhauser effect spectroscopy
Nu	Nucleophile
ORTEP	Oak Ridge thermal ellipsoid plot
PEPPSI	Pyridine-enhanced precatalyst preparation stabilization and initiation

Ph	Phenyl
pin	Pinacolato
PMP	*p*-Methoxyphenyl
PMB	*p*-Methoxybenzyl
PPTS	Pyridinium *p*-toluenesulfonate
Pyr	pyridine
q	Quartet
qd	Quartet of doublets
rt	Room temperature
ROESY	Rotating-frame nuclear Overhauser effect correlation spectroscopy
RCM	Ring-closing metathesis
ROM	Ring-opening metathesis
RuPhos	2-Dicyclohexylphosphino-2′,6′-diisopropoxybiphenyl
SAR	Structure-activity relationship
S_E	Electrophilic substitution
SPINOL	1,1′-Spirobiindane-7,7′-diol
SPhos	2-Dicyclohexylphosphino-2′,6′-dimethoxybiphenyl
TBAF	Tetra-*n*-butylammonium fluoride
TMS	Trimethylsilyl
TES	Triethylsilyl
TBS	*tert*-Butyldimethylsilyl
TIPS	Triisopropylsilyl
TBDPS	*tert*-Butyldiphenylsilyl

t	Triplet
td	Triplet of doublets
TFA	Trifluoroacetic acid
THF	Tetrahydrofuran
TLC	Thin-layer chromatography
TMEDA	*N*, *N*, *N′*, *N′*-Tetramethylethylenediamine
TANIAPHOS	(Dimethylamino)[2-(diphenylphosphino)phenyl]methyl]-2-(diphenylphosphino)ferrocene
XantPhos	4,5-Bis(diphenylphosphino)-9,9-dimethylxanthene
XPhos	2-Dicyclohexylphosphino-2′,4′,6′-triisopropylbiphenyl
UV	Ultraviolet

Table of Contents

Chapter 1. Introduction: Synthesis and Modification of Pyran Building Blocks 1

1.1 The pyran motif in biologically-relevant compounds 1

1.2 Common methods of synthesizing pyrans. 5

1.2.1 Classical methods 6

1.2.2 Prins cyclization 8

1.2.3 Hetero-Diels-Alder cycloadditions 12

1.2.4 Olefin Metathesis 19

1.3 Forming carbon–carbon bonds onto the pyran framework 23

1.4 Thesis objectives 29

1.5 References 30

Chapter 2. Synthetic Efforts Towards the Development of Simplified Laulimalide Analogues 35

2.1.1 Introduction 35

2.1.2 Targeting the cell cycle for chemotherapeutic treatment 37

2.1.3 Locating the binding site of laulimalide 38

2.1.4 Function-oriented synthesis and drug design 43

2.1.5 An overview of previously reported analogues 45

2.1.5.1 Synthesis of analogues by Gallagher 46

2.1.5.2 Synthesis of analogues by Koert 47

2.1.5.3 Synthesis of analogues by Mulzer 48

2.1.5.4 Synthesis of analogues by Wender 50

2.1.5.5 Synthesis of analogues by Paterson 51

2.2 Objectives 53

2.3 Synthesis of laulimalide analogues 55

2.4 Summary 73

2.5 Supporting Information 76

2.5.1 General information 76

2.5.2 Experimental procedures and spectral data 77

2.6 References 77
Chapter 3. Accessing Chiral Dihydropyrans Through a Stereospecific and Regiovergent Allylic Suzuki-Miyaura Cross-Coupling Reaction 114
3.1.1 Introduction 114
3.1.2 Methods towards carbon-carbon cross-coupling of pyran substrates 114
3.1.3 Advances in stereospecific Suzuki-Miyaura cross-coupling 117
3.1.4 Recent advances in the allylic Suzuki-Miyaura cross-coupling reaction 124
3.1.5 Optimization of the yield and regioselectivity of the Suzuki-Miyaura cross-coupling of dihydropyranyl boronate 128
3.2 Objectives 132
3.3 Substrate scope for the regioselective and stereospecific Suzuki-Miyaura cross-coupling . 133
3.4 Elucidating the stereochemistry of the allylic Suzuki-Miyaura cross-coupling reaction 141
3.5 First proposed mechanistic cycle 143
3.6 Summary 150
3.7 Experimental 150
3.7.1 General information 150
3.7.2 Experimental and spectral data 152
3.7.3 Derivatization of selected substrates for determination of enantiomeric ratio 171
3.8 References 173
Chapter 4. Expanding the Allylic Suzuki-Miyaura Cross-Coupling Reaction Towards Chiral Polyfunctionalized Dihydropyrans 177
4.1 Towards the formation of 2,4- and 2,6-functionalized dihydropyrans 177
4.2 Objectives 180
4.3 Optimization of the yield and regioselectivity of the Suzuki-Miyaura cross-coupling of the 2-dihydropyranyl boronate 181
4.4 Substrate scope for the stereospecific cross-coupling reaction 184
4.5 Clarifying the mechanism of the allylic Suzuki-Miyaura cross-coupling of dihydropyranyl boronates 188
4.6 Utilizing the regiodivergent and stereospecific Suzuki-Miyaura cross-coupling reaction towards the synthesis of bioactive natural products 195

4.6.1 Synthetic efforts towards the synthesis of goniothalesdiol A 195
4.6.2 Total synthesis and stereochemical assessment of diospongin B 201
4.7 Summary 209
4.8 Experimental 209
4.8.1 General information 209
4.8.2 Experimental procedures and spectral data 211
4.8.3 Derivatization of selected substrates for determination of diastereomeric ratio 223
4.8.4 Synthesis efforts toward the synthesis of goniothalesdiol A 229
4.8.5 Synthesis of diospongin B 233
4.8.6 Comparison of synthetic and natural products of diospongin B 239
4.9 References 240

Chapter 5. Conclusions 242

5.1 Conclusions and Future Perspectives 242
5.2 References 245

Bibliography 246

Appendices 257

Appendix 1: Selected copies of NMR spectra 257
Appendix 2: Chromatograms for enantiomeric excess measurement (selected) 316
Appendix 3: Crystal Structure Report 327

List of Tables

Table 2-1: Silyl protection of alcohol **2-35a**. 62

Table 3-1: Optimized conditions and key test reactions for α- and γ-regioisomers..... 130

Table 3-2: Scope of electrophiles in the α-selective stereospecific Suzuki-Miyaura cross-coupling with chiral dihydropyranyl boronate **3-50**. 135

Table 3-3: Scope of electrophiles in the γ-selective stereospecific Suzuki-Miyaura cross-coupling with chiral dihydropyranyl boronate **3-50**. 138

Table 3-4: Control experiment for the coupling of the cyclic non-heteroatom-conjugated allylboronate examined by Dr. Ding..... 147

Table 4-1: Optimized conditions for the synthesis of α-regioisomers 182

Table 4-2: Optimized conditions for the synthesis of γ-regioisomers..... 183

Table 4-3: Scope of electrophiles in the α- and γ-selective stereospecific Suzuki-Miyaura cross-coupling with chiral 2-ethoxy dihydropyranyl boronate 4-4. 186

List of Figures

Figure 1-1: Natural products containing a pyran core. 2

Figure 1-2: Bioactive pyran-based compounds within the genus Goniothalamus. 3

Figure 1-3: Synthetic and bioactive compounds containing a pyran-core. 4

Figure 1-4: Various bioactive C-glycosides. 5

Figure 1-5: Synthesis of pyrans following Baldwin's Rules. 6

Figure 2-1: Structure, cytotoxicity and resistance factor of paclitaxel and laulimalide. 36

Figure 2-2: The mitotic cycle. 38

Figure 2-3: Basic concept and methodology of HDX-MS. 40

Figure 2-4: The located laulimalide binding site reported by a) Schriemer and b) Steinmetz and a close-up view of c) Tuszynski's predicted and d) Steinmetz's observed laulimalide-tubulin complex. 42

Figure 2-5: Compared structure and activity of isolaulimalide, neolaulimalide and laulimalide over various cancer cell lines. 44

Figure 2-6: Representative bryostatin analog designed through function-oriented synthesis. 45

Figure 2-7: MCA's with in vitro inhibition results on the MDA-MB-435 cell line: a) modified sites of all derivatives and b) modified sites of the most active laulimalide analogues. 46

Figure 2-8: Select examples of laulimalide-based analogues having cell growth inhibition. 49

Figure 2-9: MCAs with in vitro inhibition results of several cancer cell lines. 51

Figure 2-10: Inhibitory effects of ligands on growth of human ovarian carcinoma cells lines. .. 52

Figure 2-11: Initial computational binding affinity tests for **2-18** relative to laulimalide. 54

Figure 2-12: Initial screening of compounds analogous to **2-25** through HDX mass-perturbation

analysis of microtubulin performed by the Schriemer group (Unpublished)..... 55

Figure 2-13: 2D NMR analysis of **2-41a**. 68

Figure 2-14: 2D NMR analysis of **2-51b**. 72

Figure 2-15: Problems addressed with the current synthetic route. 74

Figure 2-16: Potential analogue designed through function-oriented synthesis. 74

Figure 3-1: Generic types of cross-coupling onto the pyran framework. 115

Figure 3 2: Catalytic cycle and mechanistic features for the Suzuki-Miyaura cross-coupling of chiral sp^3-hybridized organoboron substrates. 118

Figure 3-3: Addressing the issue of regioselectivity in cross-coupling of allylic boronates. 124

Figure 3-4: Potential enantioselective borylation/Suzuki-Miyaura cross-coupling..... 129

Figure 3-5: Proposed Suzuki-Miyaura cross-coupling of dihydropyranyl boronates..... 132

Figure 3-6: Important structural features of the γ-promoting phosphine ligand..... 137

Figure 3-7: Mechanistic predictions on the 2-boryl dehydroheterocycle. 144

Figure 4-1: Facial selectivity influenced by favored conformation of oxocarbenium species.. 179

Figure 4-2: Preferred nucleophilic trajectories onto substituted oxocarbenium species. 180

Figure 4-3: ORTEP structures of **4-8**, **4-9**, and **4-10**. 190

Figure 4-4: Spectral confirmation of relative stereochemistry of derivatives. 192

Figure 4-5: Chosen synthetic targets accessible using the allylic cross-coupling method. 195

List of Schemes

Scheme 1-1: Synthesis of pyrans via an intramolecular cyclization. 7

Scheme 1-2: The first Prins reactions developed by Kriewitz and Prins as well as the first Prins cyclization by Hanschke. 9

Scheme 1-3: Mechanism of the Prins cyclization toward the synthesis of pyrans. 10

Scheme 1-4: Utilization of the Prins cyclization towards the synthesis of (+)-civet and (–)-exiguolide. 11

Scheme 1-5: Possible stereochemical conformation of dihydropyrans in the HDA reaction. 13

Scheme 1-6: Early discovery towards the synthesis of dihydropyrans via the HDA reaction. 14

Scheme 1-7: Strategies for generating absolute stereochemistry in the HDA reaction. 15

Scheme 1-8: Synthesis of (+)-ambruticin via an asymmetric HDA reaction. 16

Scheme 1-9: Branched synthesis of natural products from a single substrate. 17

Scheme 1-10: Synthesis of natural products through an asymmetric HDA/allylboration process. 18

Scheme 1-11: Mechanism of the ring-closing metathesis. 19

Scheme 1-12: First reported synthesis of dihydropyrans through the RCM process. 19

Scheme 1-13: Synthesis of the dihydropyran of (+)-cacospongionolide B through RCM. 20

Scheme 1-14: Asymmetric ROM/CM toward the synthesis of tetrahydropyrans. 22

Scheme 1-15: Surveying approaches toward carbon–carbon bond formations onto pyrans. 24

Scheme 1-16: Nucleophilic attack of Lewis acid-activated acetal-functionalized pyrans. 25

Scheme 1-17: Epoxide-coordinated syn-S_N2’ addition of organometallic nucleophile. 26

Scheme 1-18: Syn- and anti-S_N2' addition of organometallic nucleophiles. 28

Scheme 2-1: Key reaction steps in the synthesis of the laulimalide analogue **2-7** 48

Scheme 2-2: Retrosynthetic pathway towards the analogue framework of laulimalide. 56

Scheme 2-3: Synthesis and isolation of diastereomers **2-34a** and **2-34b**..... 57

Scheme 2-4: Synthesis of *R*- and *S*-Mosher esters from the generic alcohol..... 58

Scheme 2-5: Determination of the stereochemistry and identity of the diastereomer **2-34a**..... 59

Scheme 2-6: Determination of the stereochemistry and identity of the diastereomer **2-34b**..... 60

Scheme 2-7: Cross-metathesis of **2-34a** with acrolein..... 61

Scheme 2-8: Brown allylation and confirmation of the stereochemistry of **2-37a**. 63

Scheme 2-9: Synthesis of **2-40a**..... 69

Scheme 2-10: Synthesis of the laulimalide analogues **2-41a** to **2-50a**. 66

Scheme 2-11: Mechanistic rational behind the 1,2-acyl migration..... 67

Scheme 2-12: Synthesis of **2-37b**..... 68

Scheme 2-13: Brown allylation and confirmation of the stereochemistry of **2-37b**..... 69

Scheme 2-14: Synthesis of target intermediate **2-40b**. 70

Scheme 2-15: Preliminary scope of synthesized analogues..... 71

Scheme 2-16: Mechanistic rational for 1,2-acyl migration of analogues derived from **2-40b**. ... 73

Scheme 2-17: Retrosynthesis of a new class of laulimalide analogues implementing the sequential enantioselective hetero[4+2] cycloaddition/allylboration reaction followed by a Claisen-Ireland [3,3] rearrangement..... 75

Scheme 2-18: Possible solution to address the 1,2-acyl migration. 76

Scheme 3-1: Representative examples of cross-coupling onto dihydropyrans. 116

Scheme 3-2: Suzuki-Miyaura cross-coupling of sp^3-hybridized organoboronate species. 120

Scheme 3-3: A divergent pathway towards retention or inversion of stereochemistry in Suzuki-Miyaura cross-coupling products..... 122

Scheme 3-4: Recent advances in doubly inverted stereospecific cross-coupling of 1,1-diboron. 123

Scheme 3-5: Gamma-selective Suzuki-Miyaura cross-coupling of allylboron derivatives. 125

Scheme 3-6: Alpha-selective Suzuki-Miyaura cross-coupling of allylboronates. 126

Scheme 3-7: Highly enantiospecific synthesis of α- and γ-regioisomers. 127

Scheme 3-8: Highly regioselective divergent synthesis of α- and γ-regioisomers. 128

Scheme 3-9: Derivatization of dihydropyrans **3-32** and **3-53** for HPLC analysis. 140

Scheme 3-10: Formal synthesis of (+)-anabasine and (+)-paroxetine, and compared 142

Scheme 3-11: Attempts at accessing 2-boronate dehydropiperidines 145

Scheme 3-12: Synthetic efforts to the 2-boryl dihydropyran **3-66**. 146

Scheme 3-13: Proposed mechanistic paths for the ligand-controlled regioselective Suzuki-Miyaura cross-coupling of heterocyclic allylic boronates **3-66** and **3-67**. 149

Scheme 4-1: The synthesis of the 2-ethoxy dihydropyranyl boronate **4-4** through the catalytic enantioselective oxa-[4+2] cycloaddition. 177

Scheme 4-2: The synthesis of the 2-ethoxy dihydropyran boronate **4-4** through the 184

Scheme 4-3: Modification of cross-coupling products. 189

Scheme 4-4: A generalized ligand-controlled catalytic cycle for the Suzuki-Miyaura cross-coupling of dihydropyranyl boronates. 194

Scheme 4-5: Protecting-group-free total synthesis of goniothalesdiol A. 196

Scheme 4-6: Short synthesis of goniothalesdiol A from 2-deoxy-D-ribose. 198

Scheme 4-7: Retrosynthetic analysis of goniothalesdiol A. 199

Scheme 4-8: Synthesis and protection of diol **4-10.** 200

Scheme 4-9: Screening of various Lewis acids for the Mukaiyama-type aldol reaction. 201

Scheme 4-10: Total synthesis of diospongin B by Hashimoto and co-workers. 202

Scheme 4-11: Retrosynthetic analysis of diospongin B. 203

Scheme 4-12: Efforts toward the synthesis of **4-34** through hydroboration/oxidation. 203

Scheme 4-13: Scale-up allylic cross-coupling toward the synthesis of alcohol **4-34**. 205

Scheme 4-14: Protection of the alcohol **4-34**. 206

Scheme 4-15: Synthesis of diospongin B. 207

Scheme 4-16: Synthesis of diospongin A from diospongin B and optical rotation data by Hashimoto and co-workers 208

Scheme 5-1: Current methods and future prospects of functionalizing enantioenriched dihydropyranyl boronates. 244

Scheme 5-2: Potential access to unique heterocycles using the ligand-controlled 245

Chapter 1. Introduction: Synthesis and Modification of Pyran Building Blocks

1.1 The pyran motif in biologically-relevant compounds

Lipinski's "Rule of Five" is a generalized tool to measure druglikeness by focusing on specific parameters related to the physical and chemical properties of a molecule.[1] This seminal work contributed to the development of libraries that collected and categorized physical and chemical properties of marketed drugs to measure the druggability of future compounds. Among them, the investigation of the three-dimensionality of drugs concluded that the fraction of sp^3 carbons (fsp^3) present in a molecule correlated with its druggability.[2] In an attempt to distinguish between relevant fsp^3 values, drugs with sp^3-carbon-containing rings were evaluated by Taylor, Chan and co-workers.[3,4] These authors observed that the frequency and shape-diversity of these three-dimensional rings contributed to the bioactivity of these molecules.[3,4] Furthermore, both reports listed pyran rings as one of the most frequently used fragments in bioactive drugs.[3,4]

Pyrans are six-membered oxygen-containing heterocycles that are a common structural motif present in a variety of natural products, from monosaccharides to structurally complex metabolites and marine natural products. These structures have a vast array of functionalization, with various combinations of stereogenic centers present. Due to the wide scope of medicinal applications of pyran-based compounds, there have been exhaustive efforts devoted to their preparation.[5,6,7] The pyran motif - including tetrahydropyrans, dihydropyrans, δ-lactones, and lactols - are ubiquitous in nature (Figure 1-1).[8] This can be exemplified by their presence in pyranose-based carbohydrates, as well as macrolides such as the antimitotic natural products laulimalide and zampanolide.[9,10] Paecilomycin B, an antimalarial macrolide recently isolated[11] and synthesized,[12] is the only known paecilomycin derivative containing a pyran motif. A large

subset of pyran-based natural products contain 2,6-*cis*- or 2,6-*trans*-difunctionalized pyran rings, such as the anti-inflammatory, antibacterial, and antileishmanial diarylheptanoid, (–)-centrolobine.[13,14] Also, the antiosteoporotic natural products diospongin A and B are diarylheptanoids that are isomers of one another, differing only in the relative stereochemistry of the C6-position.[15] A 2,6-*cis*-difunctionalized natural product containing three contiguous stereocenters, goniothalesdiol A was isolated in 2006 by Wu and co-workers from a southern Taiwan tree, *Goniothalamus amuyon*.[16]

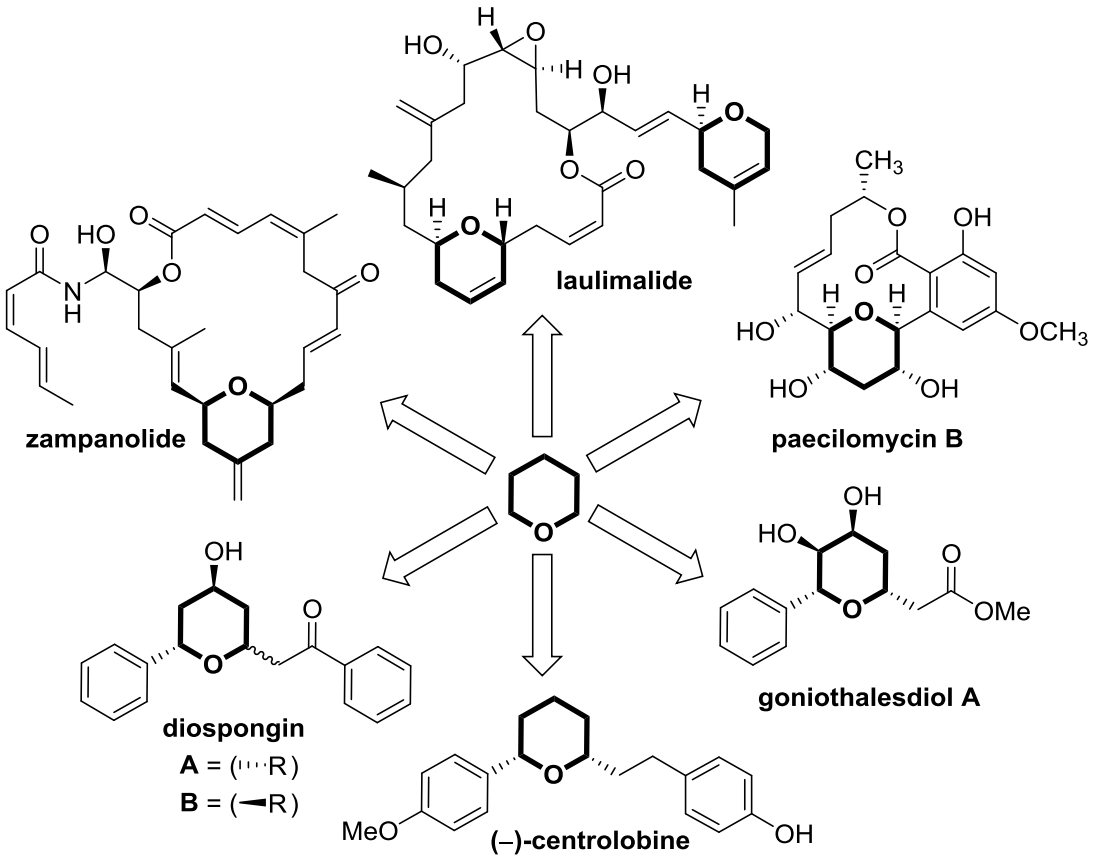

Figure 1-1: Natural products containing a pyran core.

Various species within the genus *Goniothalamus* provide a variety of pyran-based bioactive compounds, such as (*R*)-goniothalamin (Figure 1-2), which is a potent mosquito larvicide[17] with antimicrobial,[18,19] as well as antitumor activity.[20] Other compounds within the *Goniothalamus* family, such as 8-*epi*-goniodiol, exhibit strong cytotoxicity towards human lung carcinoma and one was used as a synthetic precursor towards the bioactive styryllactone 9-deoxygoniopypyrone.[21]

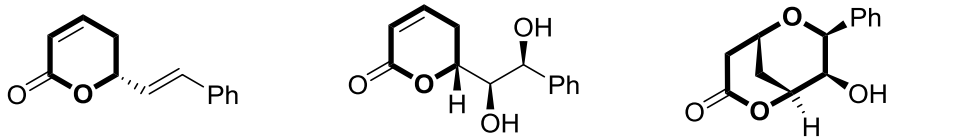

Figure 1-2: Bioactive pyran-based compounds within the genus *Goniothalamus*.

The pyran motif has demonstrated its value as a pharmacophore in medicinally-relevant drugs, as shown in the unnatural enantiomer (*S*)-goniothalamin and analogues synthesized to improve the efficacy and selectivity of the natural product (*R*)-goniothalamin (Figure 1-3). As a result, these compounds demonstrate a variety of bioactivities.[20,22,23] The potential type 2 anti-diabetic drug omarigliptin (MK-3102), created by Merck, is another example of a medicinally-relevant compound containing a pyran moiety.[24] An analogue to aprepitant is a potential alternative for the treatment of chemotherapeutic-induced nausea and vomiting.[25] Simvastatin (MK-733), a derivative of the natural product lovastatin, is used as a preventative treatment against cardiovascular disease as well as treatment for dyslipidemia, which is the over-accumulation of cholesterol or fats in the bloodstream.[26]

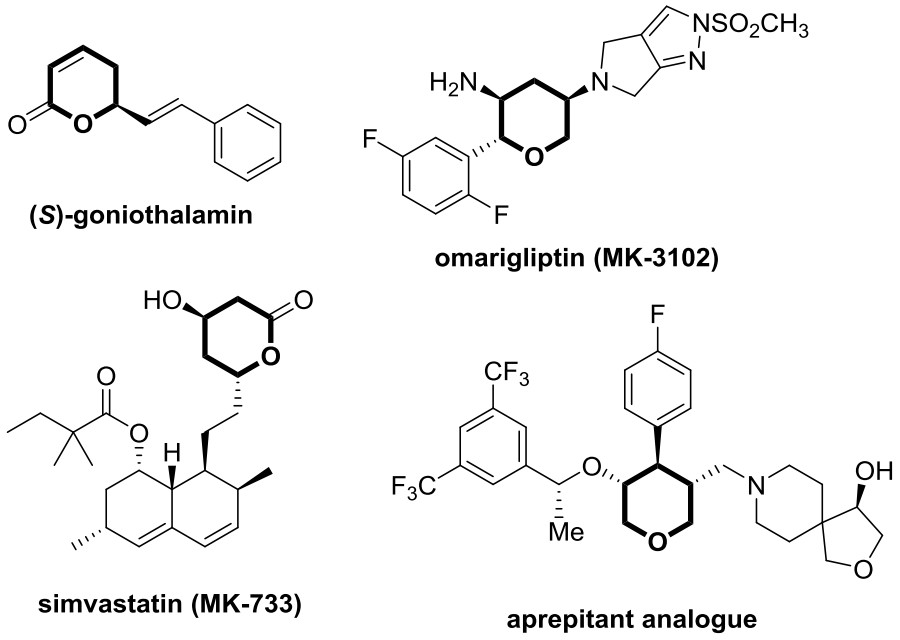

Figure 1-3: Synthetic and bioactive compounds containing a pyran-core.

An important class of pyran-containing compounds that possess relevant bioactivity is the *C*-glycosides.[27] The structures of these compounds consist of a pyranose derivative functionalized at the C1-position through a carbon–carbon bond. Several examples of naturally occurring and biologically-relevant *C*-glycosides include vitexin, a *C*-glycoside containing a flavone aglycone (Figure 1-4). Other examples of biologically-relevant *C*-glycosides are the α-*C*-mannosyltryptophan[28] and bergenin.[29] Bergenin is a secondary metabolite that was reported to have antitussive, antiplasmodial, anti-inflammatory, and antiviral activities.[30] Dapagliflozin, developed by AstraZeneca and Bristol-Myers Squibb, is an antidiabetic drug that selectively and reversibly inhibits sodium–glucose cotransporter 2.[31] The abundance of natural and synthetic biologically-relevant compounds containing a pyran motif demonstrates the importance of developing new synthetic techniques to synthesize and modify these heterocyclic structures.

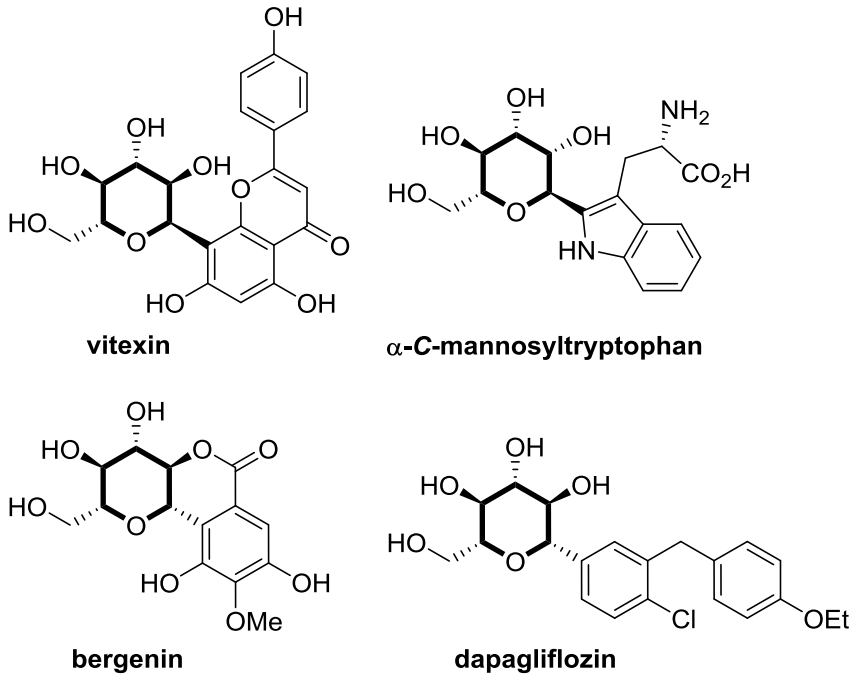

Figure 1-4: Various bioactive *C*-glycosides.

1.2 Common methods of synthesizing pyrans.

Reaction diversity of tetrahydropyrans and dihydropyrans – both synthesis and modification – have been explored thoroughly by practitioners of synthetic organic chemistry. Although lactones are another valued pyran-based building block, there are a wide variety of ways of synthesizing these structures, especially through the use of tetrahydropyran- and dihydropyran-based substrates. In this regard, the synthesis of tetrahydropyrans and dihydropyrans will only be evaluated.

1.2.1 Classical methods

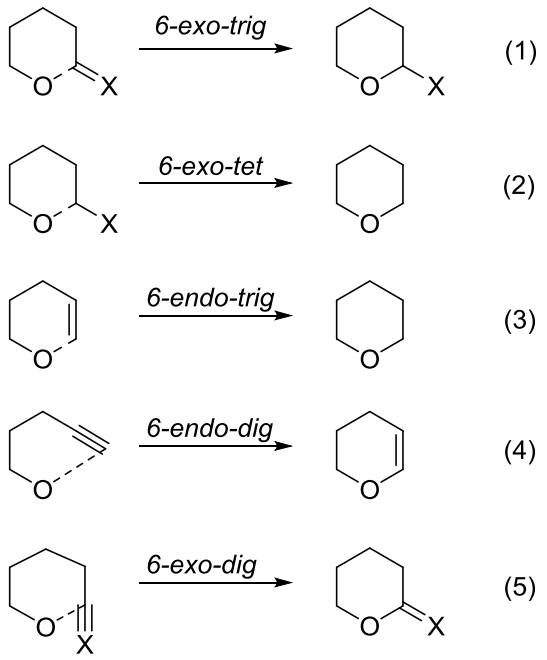

Figure 1-5: Synthesis of pyrans following Baldwin's Rules.

Pyrans may be constructed with the use of classical reaction methods, where the use of acyclic intermediates undergo inter- or intramolecular cyclizations. The ubiquity of the pyrans present in various natural compounds can be rationalized by the ease of their formation in an intramolecular reaction as defined by Baldwin's rules, where a six-membered ring can be formed either through a 6-*exo-trig*, 6-*exo-tet*, 6-*endo-trig,* 6-*endo-dig* or 6-*exo-dig* cyclization (Figure 1-5).[32] The 6-*exo-trig* cyclization to form pyrans can be accessed through a conjugate addition pathway onto α,β-unsaturated carbonyls. This is a common method used frequently toward the synthesis of various pyran-based natural products such as (+)-decarestrictine L, where the desilylated intermediate **1-1**, proceeds to form the natural product through a dipole-stabilized chair-like transition state **1-2** (Scheme 1-1, Equation 1).[33]

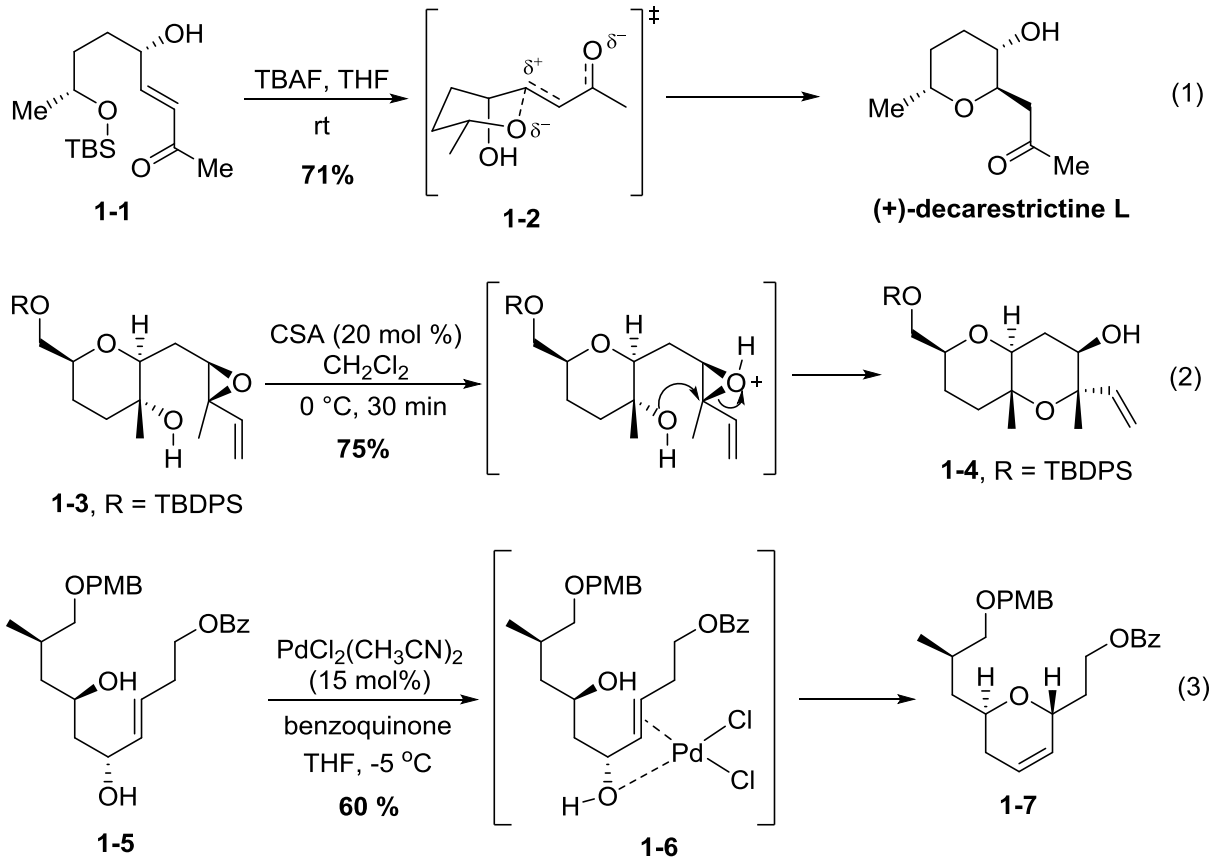

Scheme 1-1: Synthesis of pyrans via an intramolecular cyclization.

Pyrans can also be formed through the 6-*exo-tet* cyclization that can be exemplified by an S_N2 reaction onto an oxirane adjacent to an alkenyl substituent, a frequently used strategy toward the synthesis of several natural products such as brevetoxin[34] and amphidinol 3.[35] More recently, this method was used in the formal synthesis of maitotoxin (Scheme 1-1, Equation 2), one of the largest secondary metabolites isolated in nature.[36] This method proved to be beneficial after a failed attempt was made toward a cascade reaction involving a series of allylic epoxides.[36] This reaction is made possible due to the presence of an alkenyl substituent adjacent to the oxirane group. This configuration limits the substrate scope, since without the presence the alkenyl group the reaction would instead proceed through the kinetically favorable 5-*exo-tet* cyclization.[37] Towards the synthesis of laulimalide, Uenishi and coworkers demonstrated an effective synthesis

of the dihydropyran subunit contained within the macrocyclic core of the natural product, through a 6-*endo-trig* cyclization involving the activation of the chiral allylic alcohol in **1-5** using a catalytic palladium(II) species (Scheme 1-1, Equation 3).[38] The reaction proceeds with the formation of **1-6**, a palladium (II)-complex with the allylic alcohol of **1-5**. The oxo-palladium complex induces an *syn*-S_N2'-like process with the nearby alcohol to afford the 2,6-trans dihydropyran intermediate **1-7**. A recurring limitation in utilizing these reactions towards the synthesis of biologically-relevant compounds is the necessity of synthesizing complex-functionalized substrates containing stereogenic centers before the cyclization step. Other methods may also be burdened by other competing side-reactions due to poor control of regioselectivity.

1.2.2 Prins cyclization

The predominant method used toward the synthesis of the pyran motif for the production of natural products is the Prins cyclization, an acid-mediated condensation of an aldehyde with a nucleophilic alkene. The Prins reaction was initially observed by Kriewitz and coworkers in 1899 for the preparation of homoallylic alcohols from pinene **1-8** and formaldehyde under thermal conditions.[39] It was fully investigated by Prins using aqueous sulphuric acid to induce the reaction between formaldehyde and various alkenyl-based substrates (Scheme 1-2, Equations 1 and 2).[40] The first synthesis of pyran-based compounds involving a Prins reaction process was documented by Hanschke in 1955, when he performed a Brønsted acid-induced cyclization using 3-buten-1-ol with a variety of aldehydes and ketones (**1-12)** to form various tetrahydropyrans 1-**1-13** (Scheme 1-2, Equation 3).[41] Later reports described the formation of pyran byproducts when reacting various olefins with aldehydes under similar reaction conditions.[42]

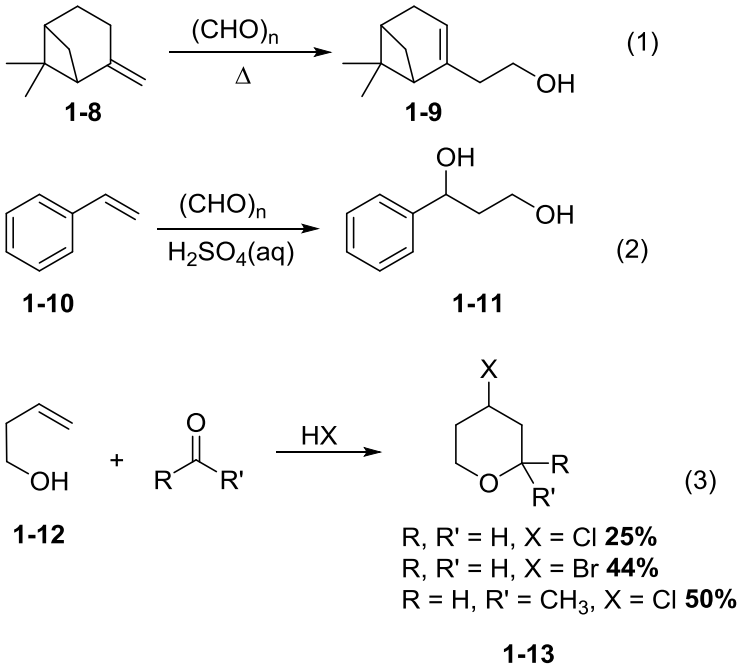

Scheme 1-2: The first Prins reactions developed by Kriewitz and Prins as well as the first Prins cyclization by Hanschke.

In regards to pyran synthesis, the mechanism proceeds through the condensation of a nucleophilic allylic alcohol **1-14** with an electrophilic aldehyde to generate a reactive oxonium species **1-15** (Scheme 1-3). This reactive species is sufficiently electrophilic to react with the alkene group, proceeding toward an intramolecular 6-*endo*-*trig* cyclization.[40a,40b] The Prins cyclization is considered a valuable method toward the synthesis of natural products due to the high stereocontrol that is dictated by the lowest energy conformation, as shown in the transition state **1-16**. [43] The resulting cationic intermediate **1-17** is captured by any spectator nucleophile present during the reaction.

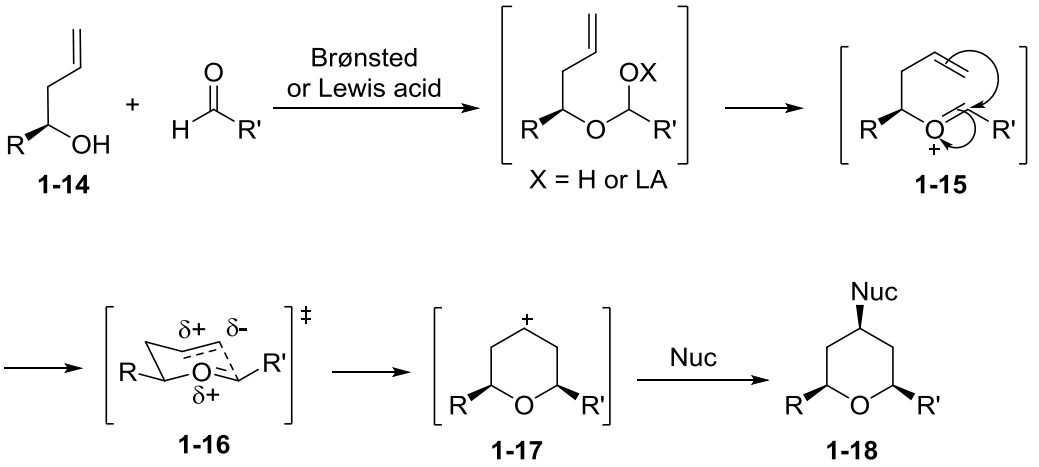

Scheme 1-3: Mechanism of the Prins cyclization toward the synthesis of pyrans.

Among the numerous natural products synthesized via a Prins cyclization is the perfume additive naturally produced from the glands of the civet cat, (+)-civet (Scheme 1-4, Equation 1).[44] The reaction mechanism for the synthesis of (+)-civet differs from the generalized reaction mechanism due to the presence of the weakly nucleophilic triflate anion, leading to an elimination step towards a dihydropyran intermediate **1-23**. This highly effective method can be used to form a variety of pyran derivatives as shown in the synthesis of (–)-exiguolide, an anticancer agent isolated from a marine sponge in 2006 (Scheme 1-4, Equation 2).[45,46] Toward the synthesis of this natural product, Song and co-workers successfully formed the first pyran **1-24** within the macrocycle through a Lewis acid-catalyzed silyl-Prins cyclization. The intermediate, **1-24**, was modified further for a second Prins cyclization/bromination step, which formed a significant portion of the macrocycle towards the final product. A major drawback of the Prins cyclization, as is evident from the mechanism (Scheme 1-3), is that the synthesis is restricted to the production of 2,6-*cis*-functionalized pyrans; 2,6-*trans*-isomers cannot be formed.

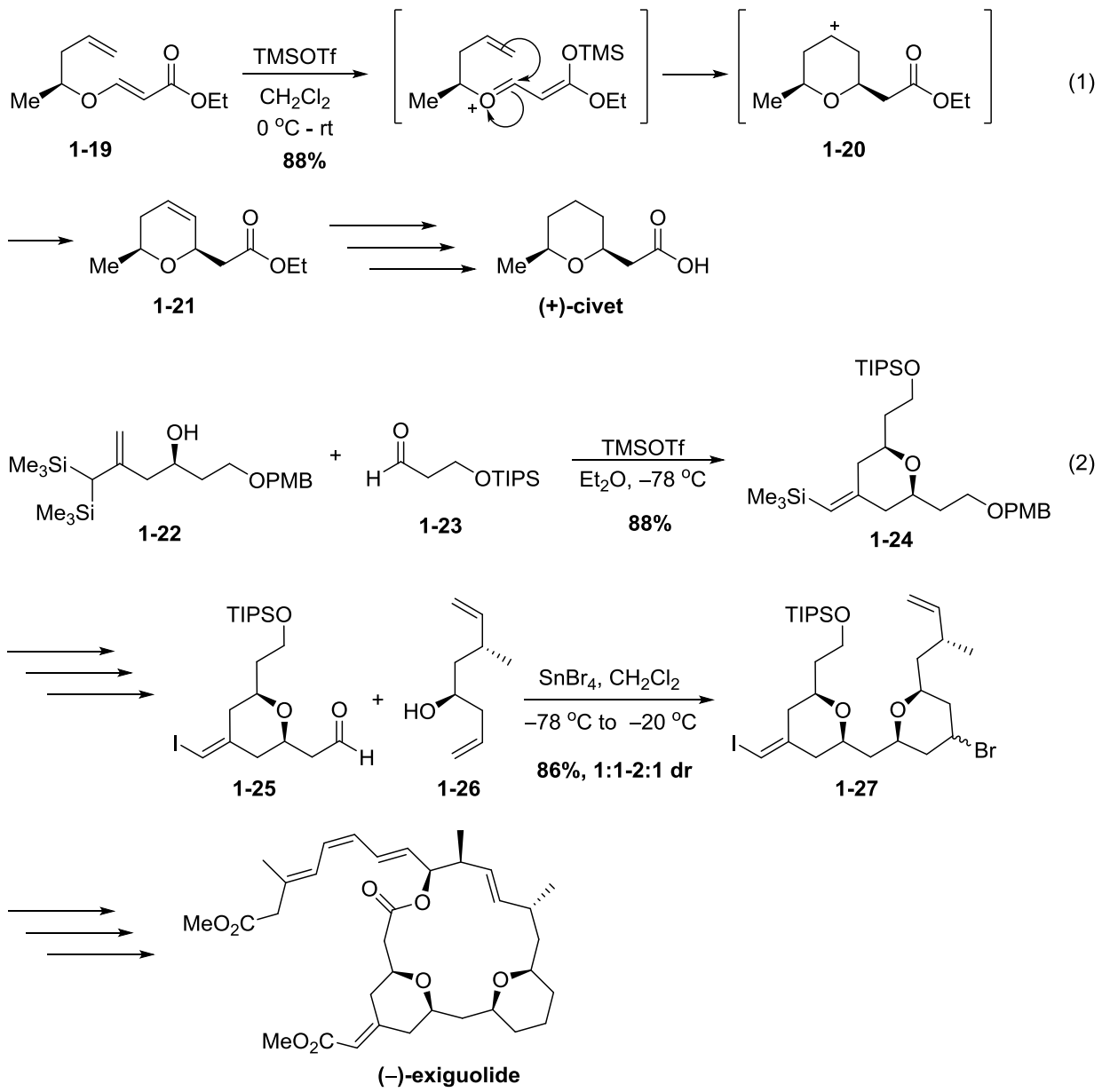

Scheme 1-4: Utilization of the Prins cyclization towards the synthesis of (+)-civet and (–)-exiguolide.

1.2.3 Hetero-Diels-Alder cycloadditions

The hetero-Diels–Alder (HDA) reaction is an efficient method to produce dihydropyrans of moderate complexity. The advantages of utilizing the HDA reaction towards the synthesis of biologically-relevant pyran-containing compounds are the one-step formation of complex compounds, mild reaction conditions, atom economy, and functional group tolerance.[47] Complex molecules can be produced with high regio- and diastereoselectivity, where one product can be made out of up to potentially eight isomers. The high selectivity is a result of the electronic configuration of the diene and dienophile, where the secondary orbital interactions between the diene and dienophile can be enhanced by the electron-donating or withdrawing functional groups on either substrate.[47] In regards to the synthesis of dihydropyrans there are two modes of synthesis, one being the normal electron-demand HDA reaction that involves a reaction between an electron-rich diene with an electrophilic carbonyl-based dienophile to form either 2,6-*trans*- or 2,6-*cis*-functionalized dihydropyrans, **1-28** and **1-29** (Scheme 1-5). On the other hand, the inverse electron-demand HDA reaction involves the use of a nucleophilic dienophile and a α,β-unsaturated carbonyl as a diene to form 2,4-*trans*- or 2,4-*cis*-functionalized dihydropyrans, **1-30** and **1-31**. Another important factor for the high selectivity is the orientation of the dienophile caused by steric effects, secondary orbital interactions, or a combination of the two factors, leading to either the *endo* or *exo* model for the transition state.[47] For the inverse and normal electron-demand HDA reactions, the *exo*-transition state leads to the respective formation of **1-28** and **1-30** due to the steric effects caused by the bulky substituents on the dienophile. Whereas, the *endo*-transition state that forms **1-29** and **1-31** is favored as a result of secondary orbital interactions between the diene and dienophile. The reaction also offers high enantioselectivity depending on whether a chiral Lewis or Brønsted acid is used.[47]

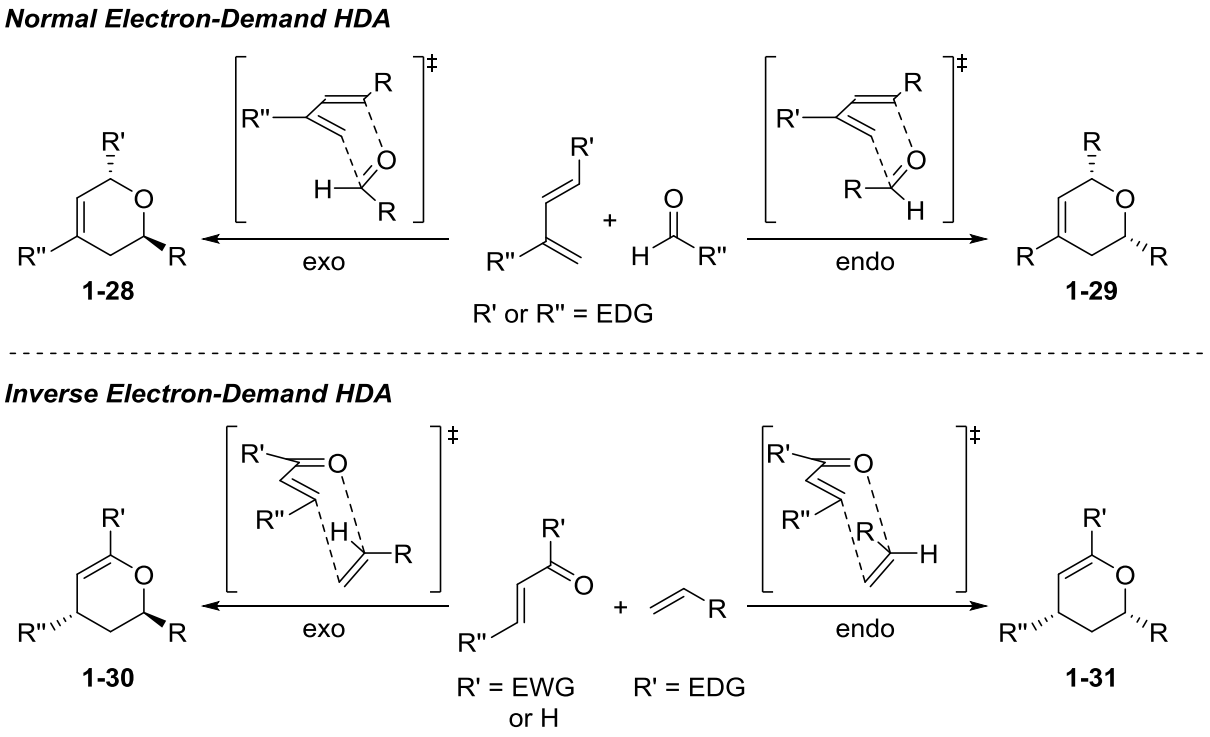

Scheme 1-5: Possible stereochemical conformation of dihydropyrans in the HDA reaction.

Since the discovery of the Diels-Alder reaction in 1928,[48] which consisted in a [4+2] cycloaddition between cyclopentadiene **1-32** and quinone **1-33** (Scheme 1-6, Equation 1), the first synthesis of 3,6-dihydro-2*H*-pyrans **1-36** was reported only a decade later by Steadman and Gresham (Scheme 1-6, Equation 2).[49] Their work involved a thermal oxa-[4+2]-cycloaddition between 2-methyl-1,3-pentadiene (**1-35**) and formaldehyde at 180 °C under solventless conditions. This method was further optimized with the incorporation of electron-donating groups on the dienophile **1-37**, which enhanced the yield and regioselectivity of the reaction to afford alkoxy-5,6-dihydro-2*H*-pyrans **1-38** (Scheme 1-6, Equation 3).[50] Early investigations into the development of pyrans relied on the use of activated carbonyl dienophiles, such as glyoxylates, or electron-rich dienes such as Danishefsky's diene.[51] Performing reactions under high-pressure or using Lewis acid catalysts broadened the scope of dienes and dienophiles that could be applied to the HDA reaction.[47,52]

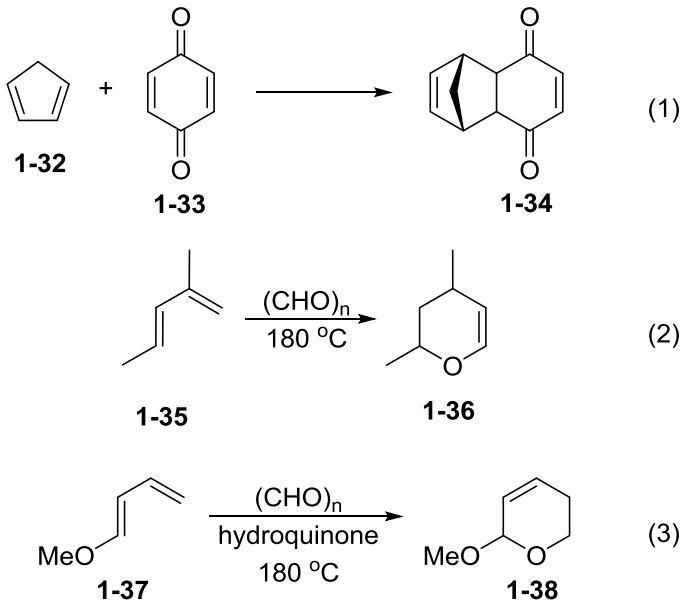

Scheme 1-6: Early discovery towards the synthesis of dihydropyrans via the HDA reaction.

There are a large variety of catalytic asymmetric HDA reactions using either a chiral auxiliary, such as the europium-catalyzed reaction using chiral bornanesulfones,[53] or reactions involving bisoxazoline-. BINOL-, other chiral ligand-coordinated Lewis acid catalysts (Scheme 1-7).[52] Only a few examples described herein demonstrate the potential to form optically pure pyrans through an asymmetric HDA reaction. The auxiliary is designed to assist in the activation of the dienophile by chelating to the Lewis acidic lanthanide (Scheme 1-7, entry 1). Due to the steric repulsion from the chiral auxiliary, the *exo*-transition state is preferred and affords 2,6-*trans*-cycloadducts.[7] Although the products contained the auxiliary group, they were obtained in high yields and high diastereoselectivity (95:5 dr). The second method involves a chiral Lewis acid to coordinate to and activate the carbonyl dienophile, as well as forcing the diene to approach only one face of the dienophile.[7] This method is more beneficial due to the reduced number of reaction steps since there is no need to incorporate and later remove an auxiliary group. Additionally, a broad set of unactivated carbonyl dienophiles can also be used. The catalytic

enantioselective HDA reaction was first demonstrated by Yamamoto using an aluminum-based chiral Lewis acid to form dihydropyranones with high enantio- and *endo*-selectivity (Scheme 1-7, Equation 2).

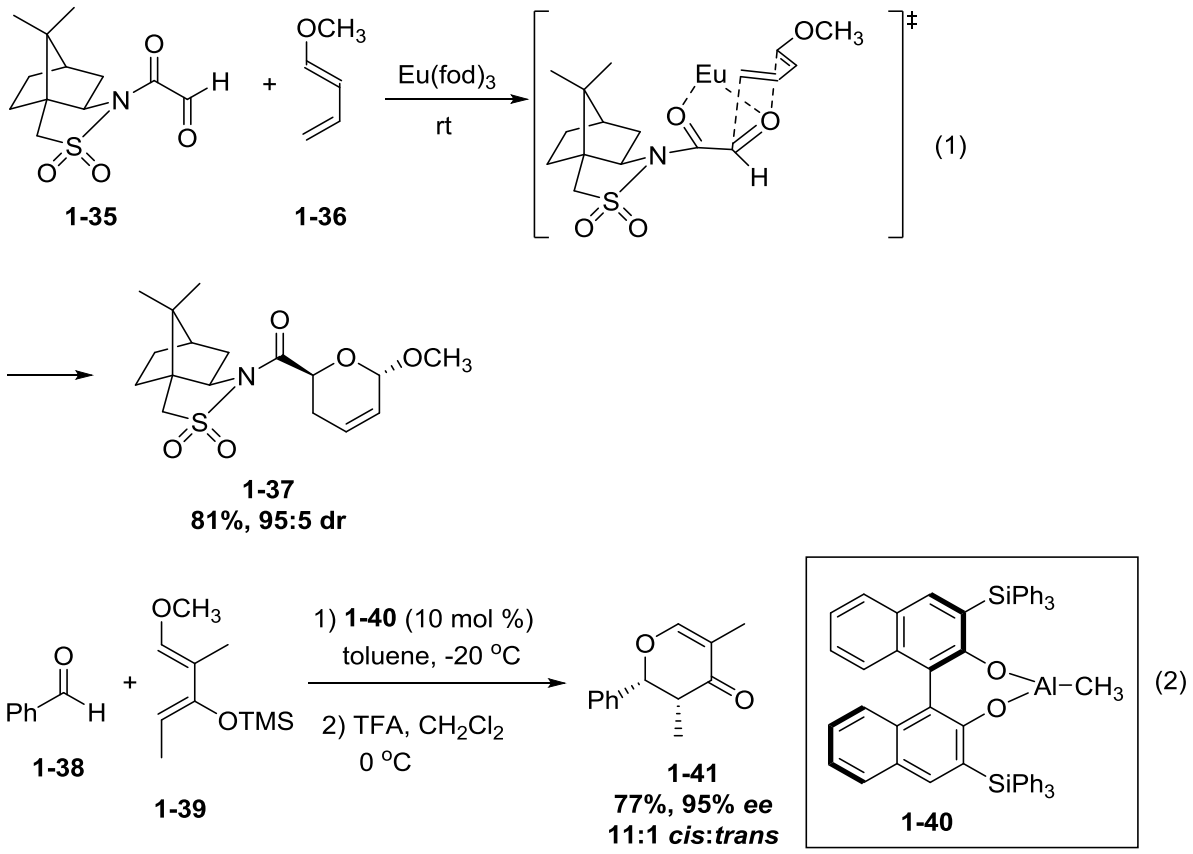

Scheme 1-7: Strategies for generating absolute stereochemistry in the HDA reaction.

Because of its high enantio- and diastereoselectivity for a broad set of inactivated substrates, one of the most common methods used in asymmetric HDA reactions involves Jacobsen's tridentate chromium complex as the chiral Lewis acid catalyst.[54,55] This established catalytic process was used by Liu and Jacobsen in the total synthesis of (+)-ambruticin (Scheme 1-8).[56] The stereoselectivity is a result of two structural features of the chromium complex, the bulky adamantyl group and the chiral indanone moiety. When the dienophiles **1-43** and **1-47** are activated by the chiral Lewis acid catalysts **1-44** and **1-48**, the indanone dictates the approach of

the dienophile on the less sterically hindered face of the catalyst, while the orientation of the alkyl chain is away from the adamantyl group. As a result, an enantioselective approach of the dienes **1-42** and **1-46** onto the corresponding dienophiles occurs as shown in the predicted transition state conformation, **1-50**, of this HDA system.[56] The two HDA products **1-45** and **1-49** are eventually combined to form (+)-ambruticin with a 12% yield within 16 steps as the longest linear sequence.

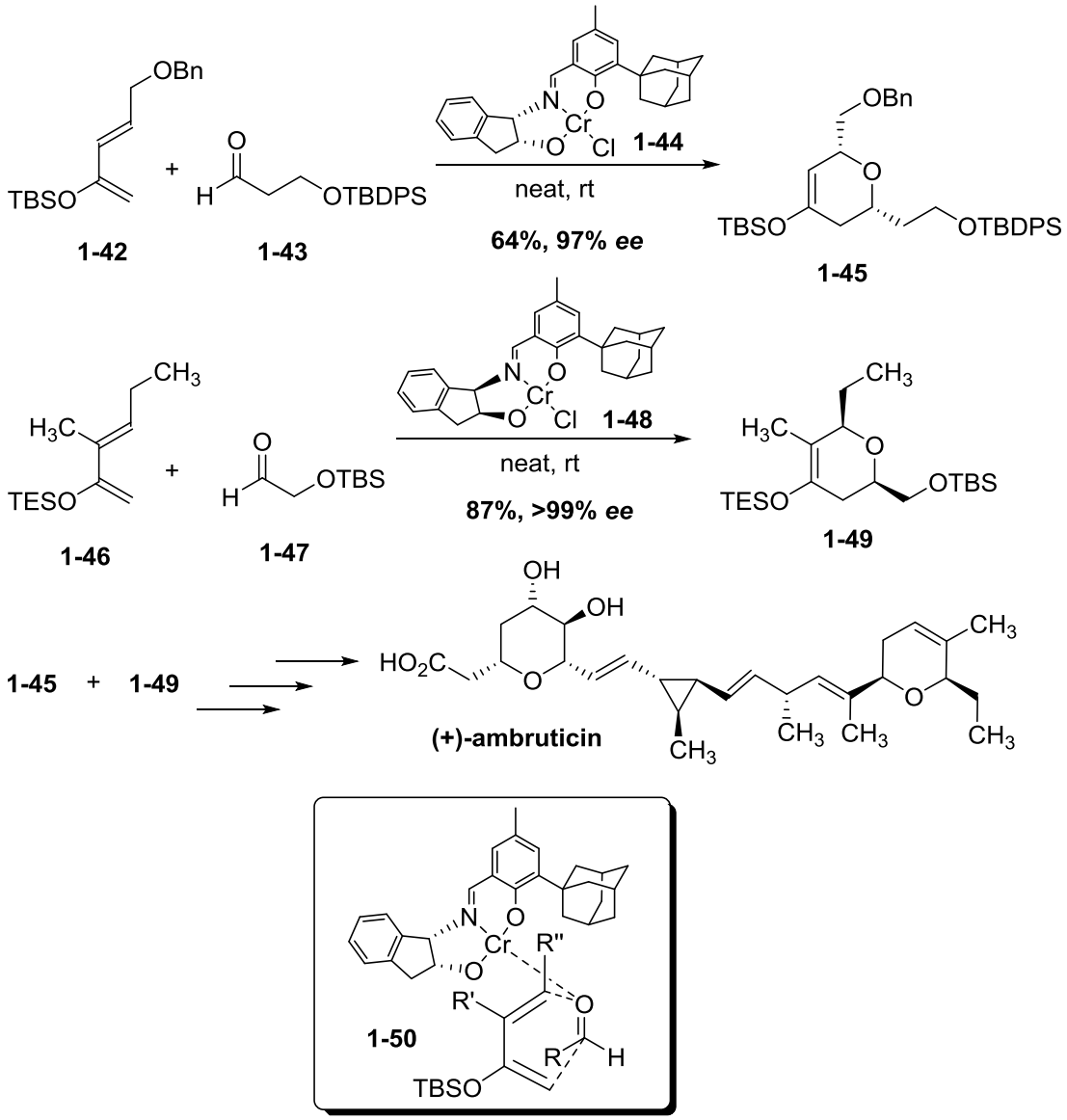

Scheme 1-8: Synthesis of (+)-ambruticin via an asymmetric HDA reaction.

Another example of an enantioselective oxa-[4+2]-cycloaddition catalyzed by Jacobsen's tridentate chromium complex involves a neat reaction between boronoacrolein pinacolate (**1-51**) and ethyl vinyl ether. This transformation, which was developed by Hall and Carboni, can be achieved at an impressively low catalyst loading ranging from 1–5 mol% in the presence of 4Å molecular sieves at ambient temperatures.[57,58,59,60] The resulting enantiomerically enriched allylboronate **1-52** has been applied in a number of stereoselective, tandem oxa-[4+2]-cycloaddition/allylboration reactions toward the synthesis of numerous bioactive molecules.[57,61]

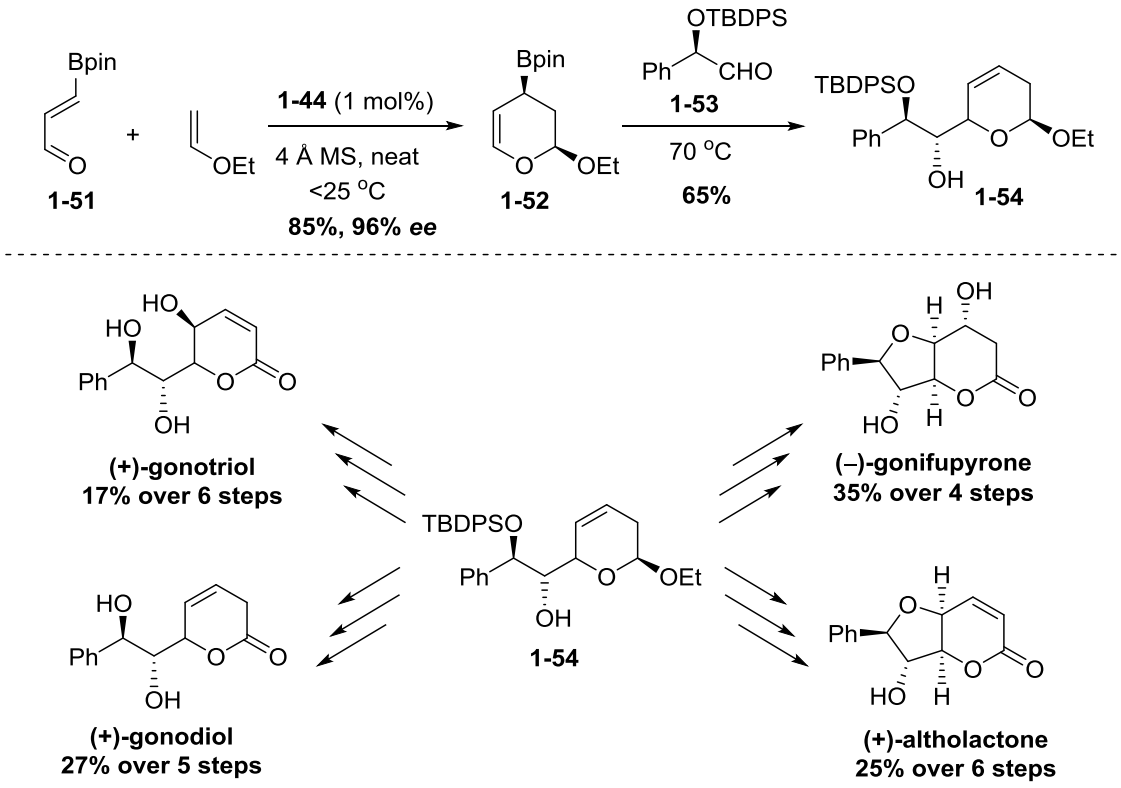

Scheme 1-9: Branched synthesis of natural products from a single substrate.

Carboni and co-workers produced a variety of natural products from the *Goniothalamus sp.* by synthesizing a core building block **1-54** through an allylboration between a chiral aldehyde **1-53** and the designated allylboronate **1-52** (Scheme 1-9).[62] The resulting intermediate provided access to multiple natural products: (+)-gonotriol, (+)-gonodiol, (+)-altholactone, and (–)-gonifupyrone. The oxo-[4+2]-cycloaddition/allylboration sequence was performed differently by Hall and coworkers, where the sequence was performed in a one pot procedure preventing any decomposition of the allylboronate intermediate.[57] This variation to the method offered access to structurally complex natural products such as a natural derivative of thiomarinol A[63] as well as the highly cytotoxic macrolide palmerolide A (Scheme 1-10).[26] The utility of the HDA reaction toward the synthesis of natural products is only diminished by the limited type of dienes and dienophiles that are capable of performing these highly regio- and stereoselective processes.

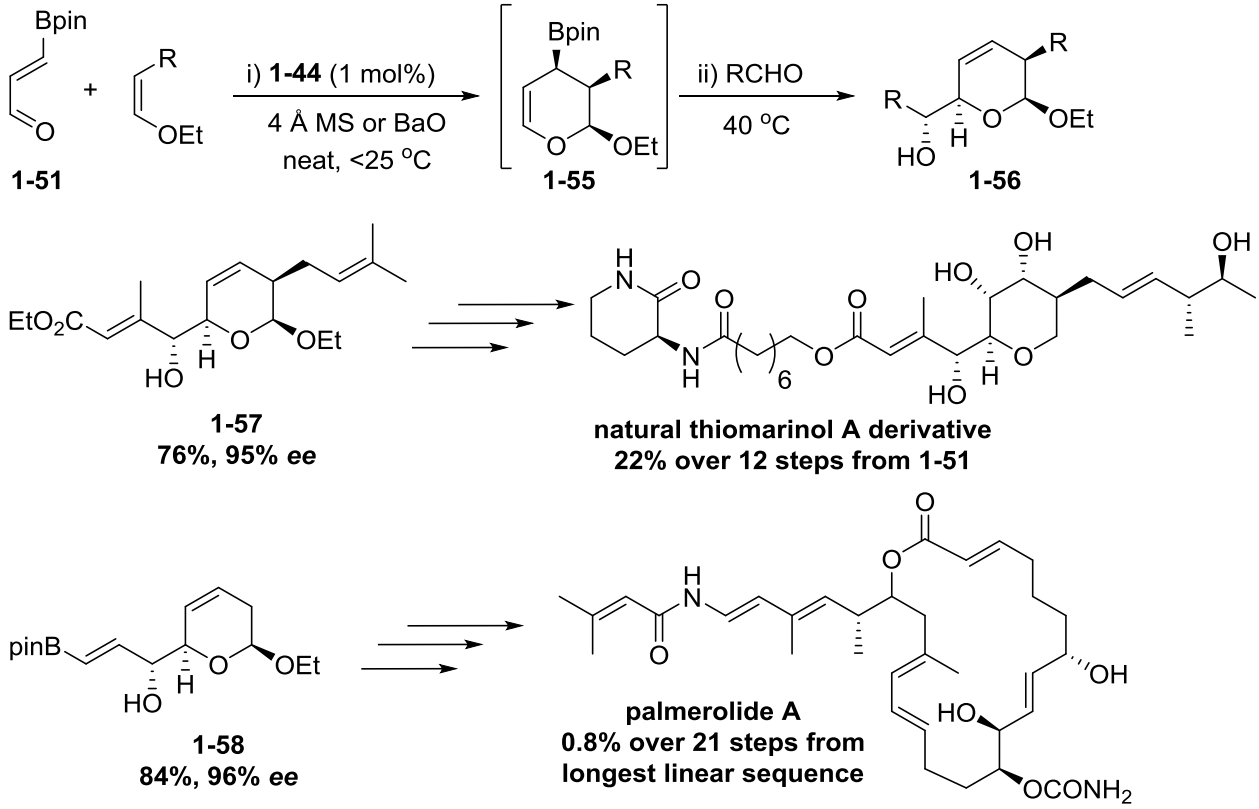

Scheme 1-10: Synthesis of natural products through an asymmetric HDA/allylboration process.

1.2.4 Olefin Metathesis

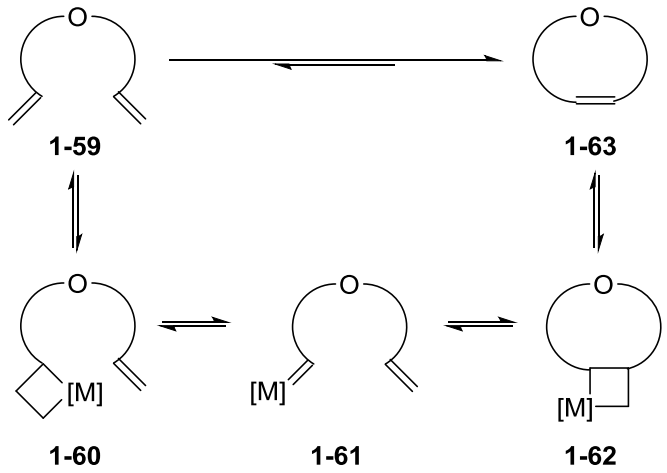

Scheme 1-11: Mechanism of the ring-closing metathesis.

Catalytic olefin metathesis is an invaluable method of forming carbon–carbon bonds due to its functional group tolerance, mild reaction conditions, and chemoselectivity.[7] In regards to formation of dihydropyrans, oxygen heterocycles can be synthesized through a ring-closing metathesis (RCM), where the metalocarbene undergoes with a [2+2]-cycloaddition with an olefin to form a metallacyclobutane species **1-60** (Scheme 1-11). This process is entropically-driven, where **1-60** reverts to release a volatile by-product and form the metallocarbene **1-61**. This process is repeated until the unsaturated heterocycle **1-63** is formed.

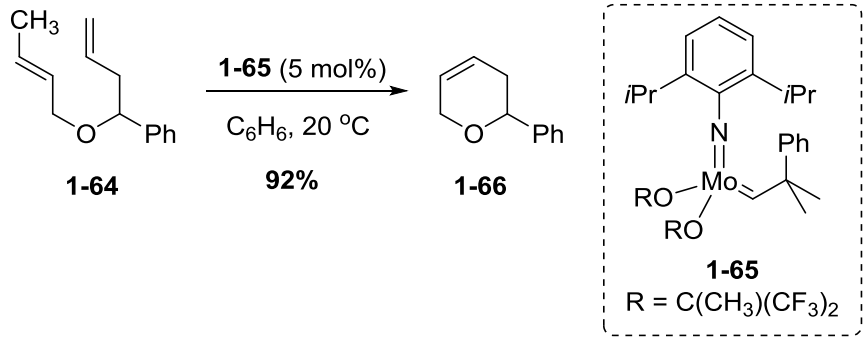

Scheme 1-12: First reported synthesis of dihydropyrans through the RCM process.

The first example of ring-closing metathesis of heterocycles was achieved by Grubbs using the molybdenum-based catalyst **1-65**, where a dihydropyran was formed in 92% yield in 15 minutes (Scheme 1-12).[64] The main pathway to access dihydropyrans involves the RCM to form the C3–C4/C4–C5 bond.[7] This strategy has been applied in the synthesis of the natural antimicrobial[65] compound (+)-cacospongionolide B, where the furan-bound dihydropyran was formed with a 91% yield using the first-generation Grubbs catalyst (Scheme 1-13).[66]

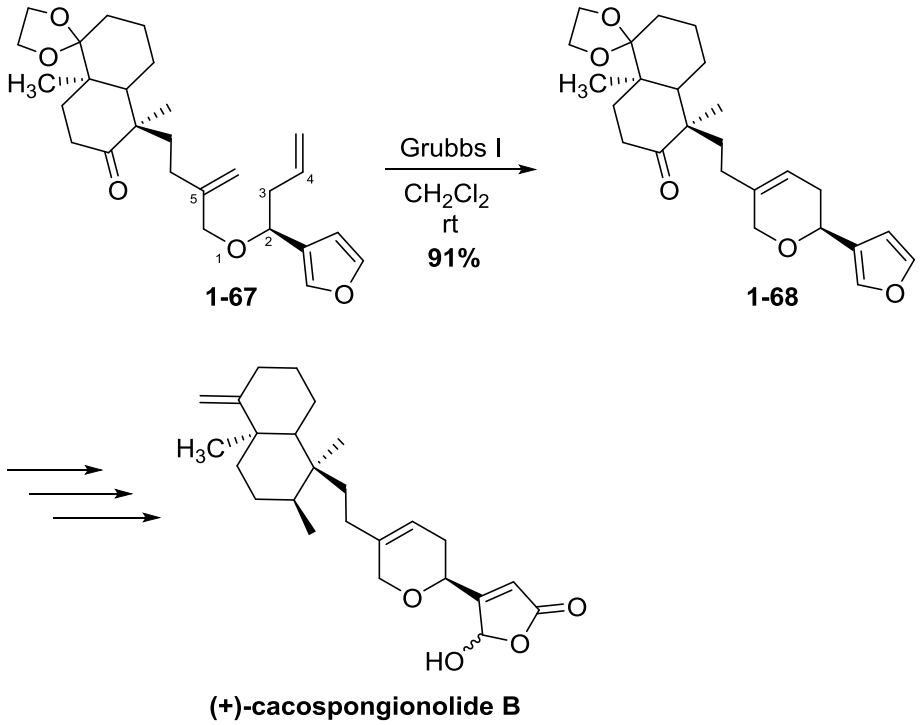

Scheme 1-13: Synthesis of the dihydropyran of (+)-cacospongionolide B through RCM.

The main drawback of classical ring-closing metathesis is the required pre-installation of stereochemistry before the formation of the pyran motif. Efforts toward asymmetric olefin metathesis have made some progress in resolving this issue for example, the development of a Ru-catalyzed asymmetric ring-opening/cross-metathesis reactions (ROM/CM) to produce 2,6-cis functionalized tetrahydropyrans in high optical purity (Scheme 1-14, Equation 1).[67] Hoveyda and Schrock expanded on this concept with the selective formation of *Z*-olefins under asymmetric

conditions (Scheme 1-14, Equation 2).[68,69] This study led to their collaborative work in which (+)-neopeltolide A was synthesized using a variety of asymmetric olefin metathesis catalysts that are proposed for either cross-metathesis, macrocyclic olefin metathesis, and the ROM/CM (Scheme 1-14, Equation 3).[70] The asymmetric ROM/CM reaction step afforded **1-77** at 88% yield with *Z*-selectivity and high enantiopurity (98% *ee*). This synthetic route efficiently gave (+)-neopeltolide with an overall yield of 21% with 11 steps as the longest linear sequence.

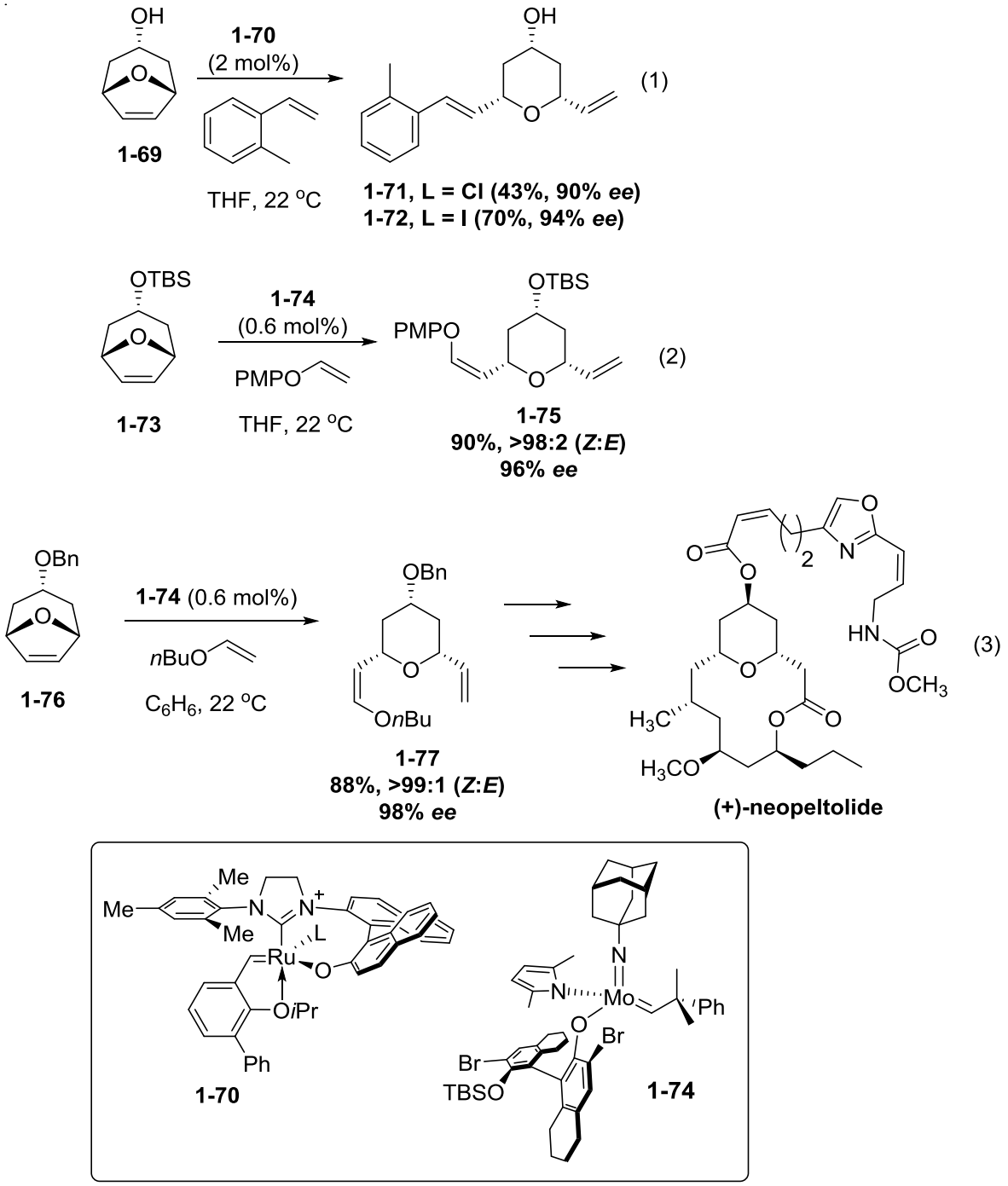

Scheme 1-14: Asymmetric ROM/CM toward the synthesis of tetrahydropyrans.

Although there are a wide variety of methods of making pyrans, including the aforementioned methods, each one can be utilized to produce a variety of pyran-based bioactive compounds. Each method also has its own limitations that include the requirement of highly functionalized

starting materials for a late-stage formation of a functionalized pyran core, which would reduce the possibility of product derivatization and lead to a finite set of compounds. For some of these methods, there are regio- and stereochemical constraints, inlcuding competing side-reactions or stereogenic centers that must be made before the cyclization. In addition to these disadvantages, some reactions have low functional group tolerance. As a result, these problems may lead to setbacks and occasionally create lengthier syntheses to overcome these obstacles. To mitigate or avoid these problems, alternate methods of creating pyran-based moieties are needed for these important building blocks.

1.3 Forming carbon–carbon bonds onto the pyran framework

In order to make these pyran derivatives applicable towards the synthesis of biologically-active molecules, the pyran ring must be capable of further modification after formation. There are a variety of ways of introducing heteroatoms onto a pyran core, but there are few methods available to form carbon–carbon bonds. Due to continuous interest in the synthesis of *C*-glycosides, the most common site in the pyran structure that is investigated toward incorporating function groups is at the C1-position.[71] Reactions that have been used to target this position are the intra- and intermolecular enolsilane addition (Scheme 1-15, Equation 1 and 2), and the Hosomi-Sakurai reaction (Scheme 1-15, Equation 3).[72] The *syn*- or *anti*-S_N2' γ-functionalization are also typically studied toward the formation of *C*-glycosides, where 2,6-*cis*- or 2,6-*trans*-products are formed (Scheme 1-15, Equation 4). The intramolecular aldol reaction has been used in the synthesis of (+)-goniodiol, whereupon exposure of the Lewis acidic TMSOTf to **1-78** lead toward the *in situ* formation of an oxocarbenium species **1-79** and the release of the silyl enol ether **1-80** (Scheme 1-16, Equation 1).[73] The nucleophilic silyl enol ether **1-80** is then able to react with the oxocarbenium of **1-79** to form the desired ketone **1-81** with a yield of 85%. The

intermolecular variant of this reaction involves the formation of the oxocarbenium species from an acetal starting material and stoichiometric amounts of the nucleophilic silyl enol ether. This method was used towards the synthesis of ircinastatin A (Scheme 1-16, Equation 2), where the TBS-protected enol ether **1-83** reacted with the 2-acetyl tetrahydropyran **1-82** to give **1-84** with a 59% yield.[74] The Hosomi-Sakurai reaction onto pyrans also relies on the *in situ* generation of an oxocarbenium species, but differs in the formation of an allyl group using an allylsilane as a mild nucleophile. This method has been applied on numerous total syntheses, such as the synthesis of brevetoxin A and more recently the synthesis of (–)-apicularen A (Scheme 1-16, Equation 3).[75]

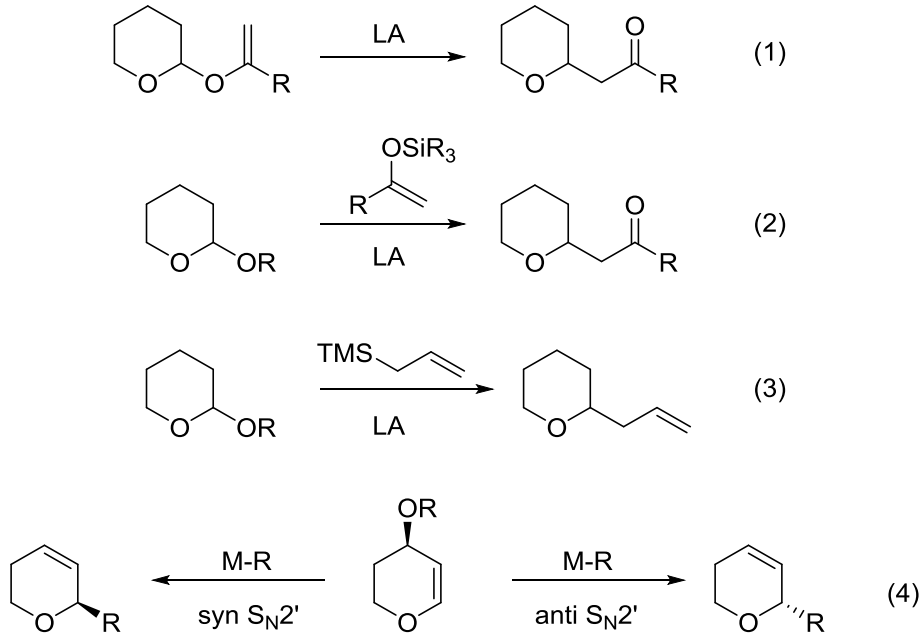

Scheme 1-15: Surveying approaches toward carbon–carbon bond formations onto pyrans.

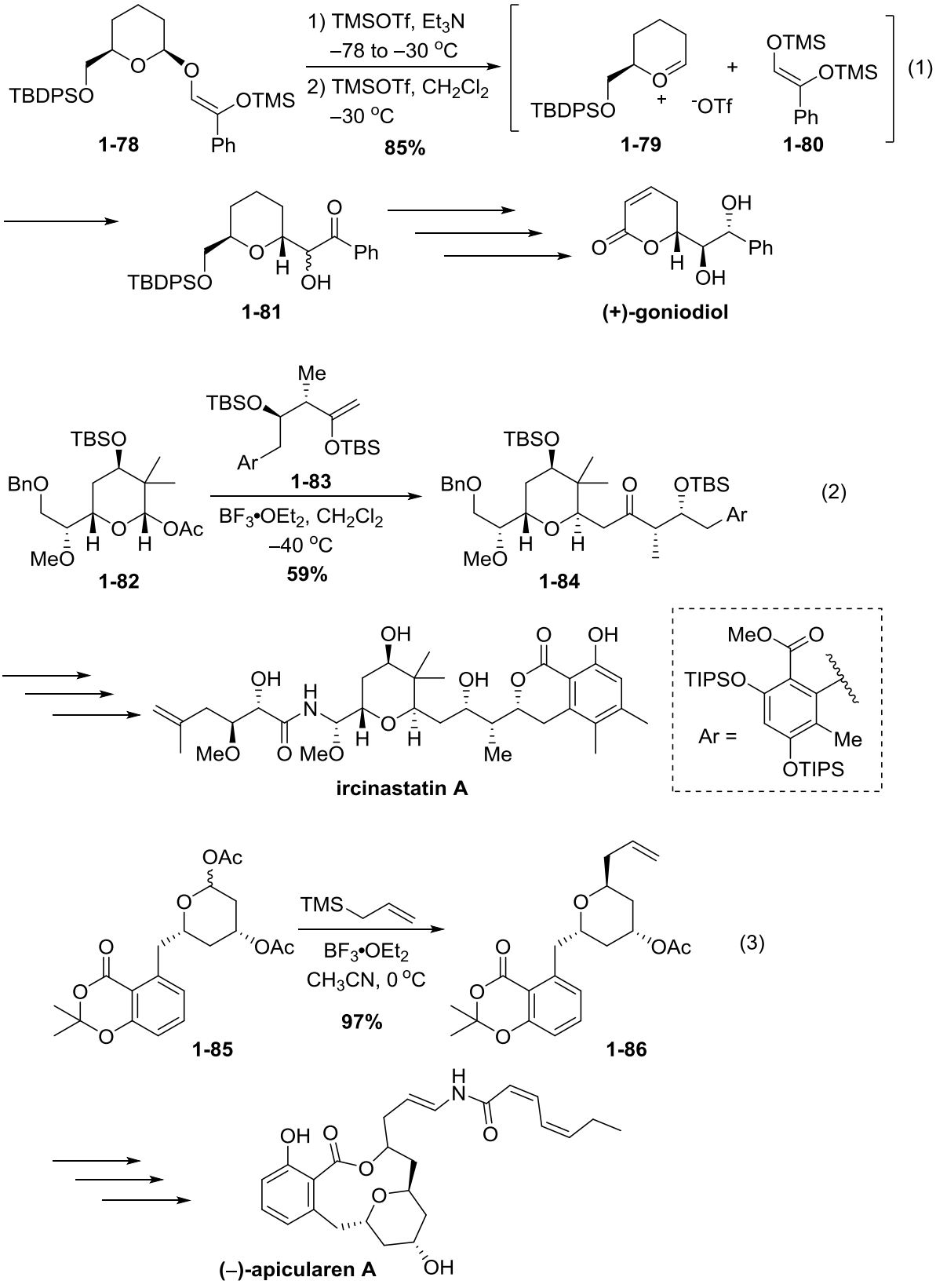

Scheme 1-16: Nucleophilic attack of Lewis acid-activated acetal-functionalized pyrans.

Research toward the development *C*-glycosides have made great strides in regio- and stereoselective functionalization of dihydropyrans. Crotti and co-workers effectively demonstrated *C*-glycosidation towards the formation of 3-epoxy dihydropyrans **1-88** by incorporating electrophilic allylic epoxides into the pyran ring (Scheme 1-17, Equation 1).[76,77] Due to an epoxide-nucleophile coordination (**1-89**), a *syn*-S_N2' reaction occurs where the oxygen atom coordinates the nucleophile synfacial to the γ-position to afford compounds such as **1-91** and **1-92** with high regio- and enantioselectivity (Scheme 1-17, Equation 2 and 3).

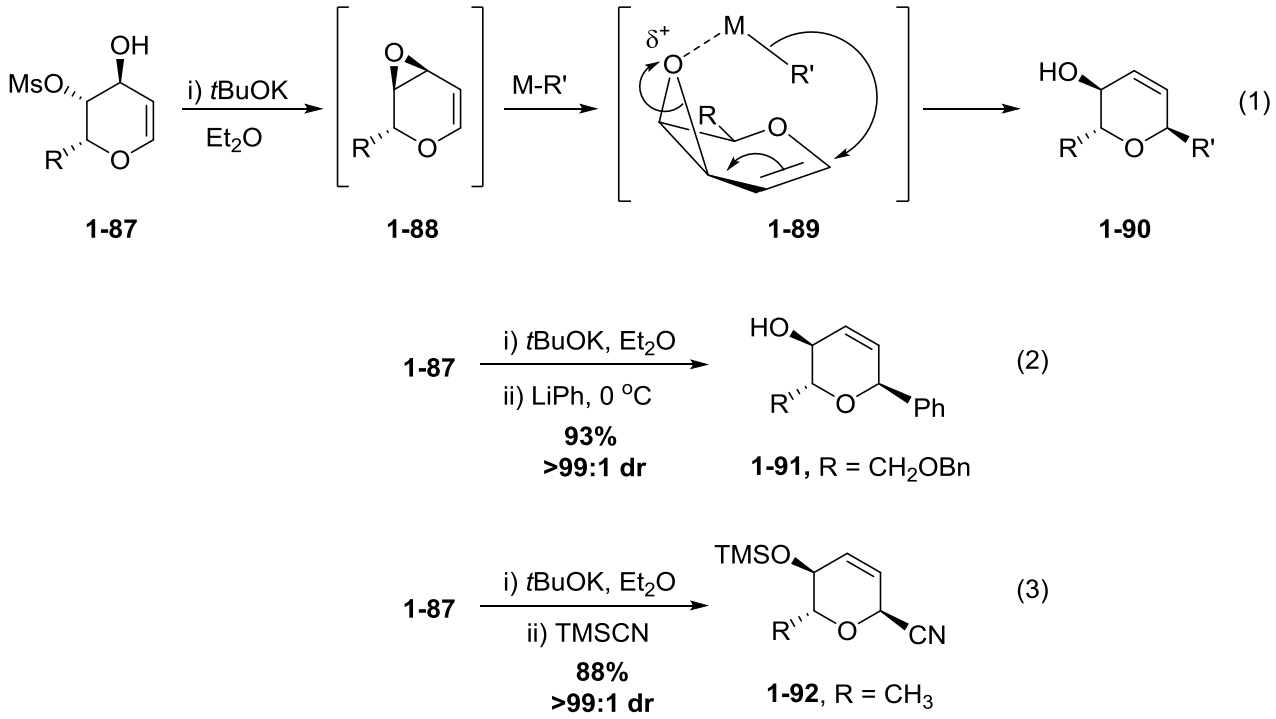

Scheme 1-17: Epoxide-coordinated syn-S_N2' addition of organometallic nucleophile.

The Ferrier rearrangement, an *anti*-S_N2' reaction, is an effective method to access 2,3-unsaturated glycosides, usually requiring strong carbon-nucleophiles and a variety of strong Lewis acids to promote this transformation.[78] Recent developments in the Ferrier rearrangement have resolved the initial need of stoichiometric amounts of a strong Lewis acid, where in some

cases it has been reduced to catalytic amounts and using milder reagents.[78] Milder nucleophiles can also be used in the Ferrier rearrangement, such as the reaction between the alkynyl trifluoroborate and the glycal **1-93**, which required the use of stoichiometric amounts of $BF_3 \cdot OEt_2$ to selectively afford the 2,6-*trans*-product **1-94** (Scheme 1-18, Equation 1).[79] Kobayashi developed a mild method of C1-allylation with high regioselectivity (>10:1 dr) using catalytic amounts of the mild Lewis acid InOTf and the mild allylboronic acid pinacol ester as the pronucleophile to afford the allyl-functionalized dihydropyran **1-95** (Scheme 1-18, Equation 2).[80] A significant limitation of the Ferrier rearrangement, as shown in these two methods, is that the reactions typically favor the formation of 2,6-*trans*-products/α-glycosides; the 2,6-*cis*-products/β-glycosides are rendered inaccessible or difficult to produce. Due to the presence of an acyl allylic system in these glycals, a convenient π-allyl palladium species can be accessed through a Tsuji-Trost-like reaction. This allylpalladium-complex offers the potential application of forming C–C bonds through a cross-coupling pathway. In light of this, Liu and co-workers developed a stereo- and regioselective intramolecular decarboxylative coupling reaction, which afforded the desired 2,6-*cis*-products/β-glycosides such as **1-97** in high stereo- and regioselectivity.[81] To demonstrate the utility of this method, an effective formal total synthesis of aspergillide A was accomplished, where the natural product could be accessed from intermediate **1-98** in one step (Scheme 1-18, Equation 3).[81,82] Although these methods are affective at controlling the stereochemistry of the reactions – through stereospecificity and the coordination-capability of the substrate – these reactions fail to regioselectively functionalize the C1 position or the C3 position. A regiodivergent pathway to incorporate a functional group stereospecifically, with retention or inversion of stereochemistry, would be highly advantageous.

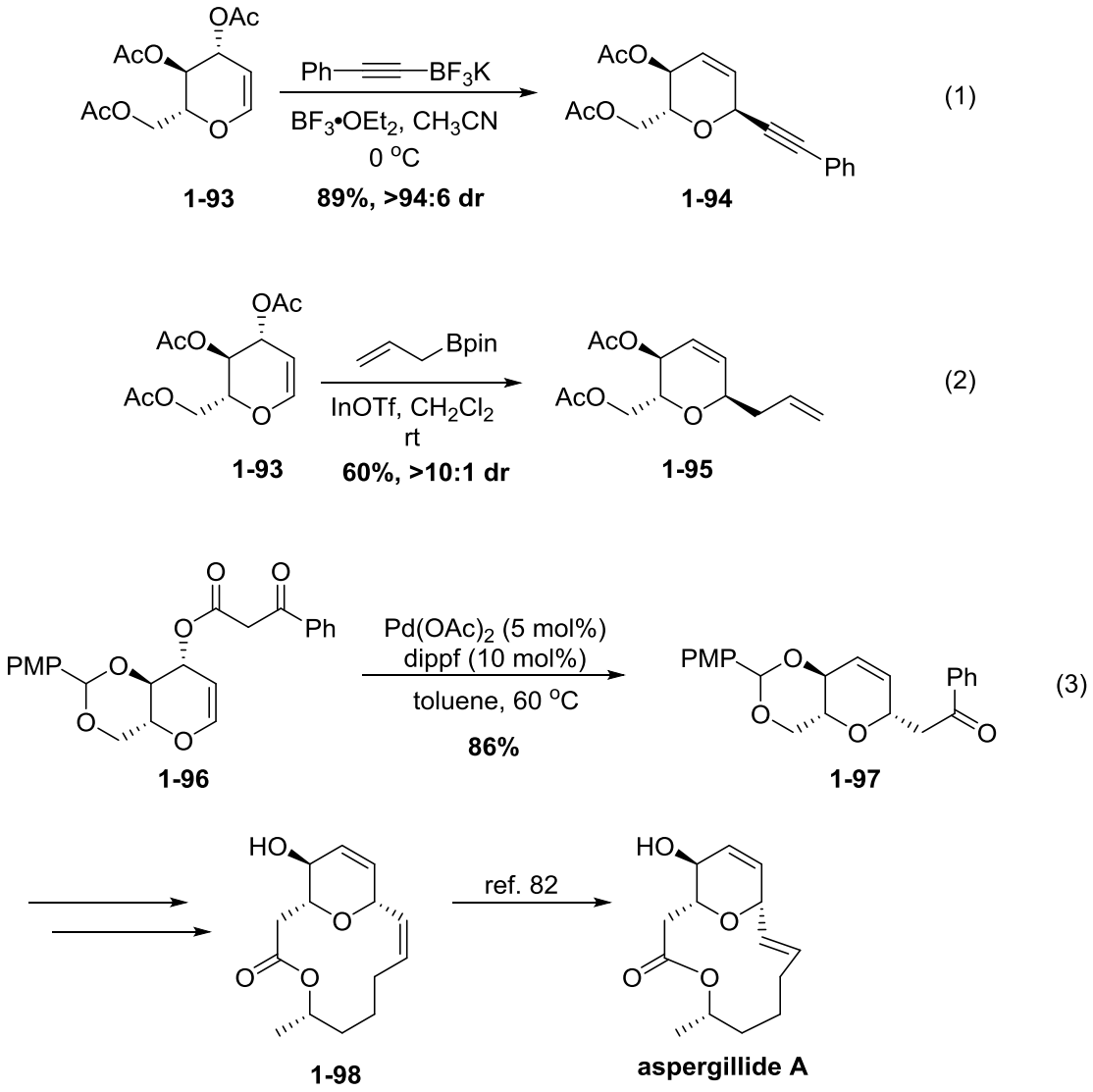

Scheme 1-18: Syn- and anti-S_N2' addition of organometallic nucleophiles.

1.4 Thesis objectives

The goal of the work described in this thesis is to contribute to the functionalization and utilization of pyran moieties toward medicinal applications, such as drug development and natural product synthesis. The second chapter will focus on the efforts made in developing a synthetic pathway toward potentially active dihydropyran-containing compounds analogous to the potent anticancer natural product, laulimalide. This synthetic pathway offers insight into necessary reaction methods needed in the creation of key intermediates and is offered as a guideline for future investigations into discovering the key pharmacophores of laulimalide. The third chapter in this thesis will introduce the assisted development of an advanced sp^3-sp^2 cross-coupling of dihydropyranyl boronates, a stereospecific and regioselective allylic Suzuki-Miyaura cross-coupling reaction that is challenging to achieve by other means. In chapter 4, the Suzuki-Miyaura cross-coupling reaction is expanded further with the use of the 2-ethoxy dihydropyranyl boronate as the cross-coupling substrate. The high regioselectivity of the Suzuki-Miyaura reaction methodology – based on the previous cross-coupling conditions developed by Dr. Jinyue Ding – has been further improved by evaluating additional ligands and optimizing the reaction conditions. Furthermore, the utility of the products was evaluated for additional modification to demonstrate the potential application of this method toward the synthesis of biologically-relevant compound. These studies led to the successful synthesis of the antiosteoporotic diospongin B.

1.5 References

[1] Lipinski, C. A.; Lombardo, F.; Dominy, B. W.; Feeney, P. J. *Adv. Drug Delivery Rev.* **1997**, *23*, 3–25.

[2] Lovering, F.; Bikker, J.; Humblet, C. *J. Med. Chem.* **2009**, *52*, 6752–6756.

[3] Taylor, R. D.; MacCoss, M.; Lawson, A. D. *J. Med. Chem.* **2014**, *57*, 5845–5859.

[4] Aldeghi, M.; Malhotra, S.; Selwood, D. L.; Chan, A. W. *Chem. Biol. Drug Des.* **2014**, *83*, 450–461.

[5] Clarke, P. A.; Santos, S. *Eur. J. Org. Chem.* **2006**, 2045–2053.

[6] Nicolas, L.; Butkevich, A. N.; Guérinot, A.; Corbu, A.; Reymond, S.; Cossy, J. *Pure Appl. Chem.* **2013**, *85*, 1203–1213.

[7] Perry, M. A.; Rychnovsky, S. D.; Sizemore, N. *Synthesis of Saturated Tetrahydropyrans*. Springer-Verlag: Berlin, 2014; Vol. 35.

[8] Elliott, M. C. *J. Chem. Soc., Perkin Trans. 1* **2002**, 2301–2323.

[9] Tanaka, J.; Higa, T. *Tetrahedron Lett.* **1996**, *37*, 5535–5538.

[10] Corley, D. G.; Herb, R.; Moore, R. E.; Scheuer, P. J.; Paul, V. J. *J. Org. Chem.* **1988**, *53*, 3644–3646.

[11] Xu, L.; He, Z.; Xue, J.; Chen, X.; Wei, X. *J. Nat. Prod.* **2010**, *73*, 885–889.

[12] Ohba, K.; Nakata, M. *Org. Lett.* **2015**, *17*, 2890–2893.

[13] De Albuquerque, I. L.; Galeffi, C.; Casinovi, C. G.; Marini-Bettolo, G. B. *Gazz. Chim. Ital.* **1964**, *94*, 287–295.

[14] Galeffi, C.; Casinovi, C. G.; Marini-Bettòlo, G. B. *Gazz. Chim. Ital.* **1965**, *95*, 95–100.

[15] Yin, J.; Kouda, K.; Tezuka, Y.; Tran, Q. L.; Miyahara, T.; Chen, Y.; Kadota, S. *Planta Med.* **2004**, *70*, 54–58.

[16] Lan, Y. H.; Chang, F. R.; Yang, Y. L.; Wu, Y. C. *Chem. Pharm. Bull.* **2006**, *54*, 1040–1043.

[17] de Fatima, A.; Kohn, L. K.; Antonio, M. A.; de Carvalho, J. E.; Pilli, R. A. *Bioorg. Med. Chem.* **2005**, *13*, 2927–2933.

[18] Mosaddik, M. A.; Haque, M. E. *Phytother. Res.* **2003**, *17*, 1155–1157.

[19] de Fatima, A.; Marquissolo, C.; de Albuquerque, S.; Carraro-Abrahao, A. A.; Pilli, R. A.

Eur. J. Med. Chem. **2006**, *41*, 1210–1213.

[20] de Fatima, A.; Kohn, L. K.; Carvalho, J. E.; Pilli, R. A. *Bioorg. Med. Chem.* **2006**, *14*, 622–631.

[21] (a) Prasad, K. R.; Gholap, S. L. *Tetrahedron Lett.* **2007**, *48*, 4679–4682; (b) Veena, B.; Sharma, G. *Synlett* **2014**, *25*, 1283–1286; (c) Chen, J.; Lin, G. Q.; Liu, H. Q. *Tetrahedron Letters* **2004**, *45*, 8111–8113; (d) Chen, J.; Lin, G.; Wang, Z.; Liu, H. *Synlett* **2002**, *8*, 1265–1268.

[22] Semprebon, S. C.; de Fatima, A.; Lepri, S. R.; Sartori, D.; Ribeiro, L. R.; Mantovani, M. S. *Hum. Exp. Toxicol.* **2014**, *33*, 3–13.

[23] de Fatima, A.; Zambuzzi, W. F.; Modolo, L. V.; Tarsitano, C. A.; Gadelha, F. R.; Hyslop, S.; de Carvalho, J. E.; Salgado, I.; Ferreira, C. V.; Pilli, R. A. *Chem. Biol. Interact.* **2008**, *176*, 143–150.

[24] (a) Biftu, T.; Qian, X.; Chen, P.; Feng, D.; Scapin, G.; Gao, Y. D.; Cox, J.; Roy, R. S.; Eiermann, G.; He, H.; Lyons, K.; Salituro, G.; Patel, S.; Petrov, A.; Xu, F.; Xu, S. S.; Zhang, B.; Caldwell, C.; Wu, J. K.; Lyons, K.; Weber, A. E. *Bioorg. Med. Chem. Lett.* **2013**, *23*, 5361–5366; (b) Xu, F.; Zacuto, M. J.; Kohmura, Y.; Rosen, J.; Gibb, A.; Alam, M.; Scott, J.; Tschaen, D. *Org. Lett.* **2014**, *16*, 5422–5425.

[25] Raubo, P.; Giuliano, C.; Hill, A. W.; Huscroft, I. T.; London, C.; Reeve, A.; Seward, E. M.; Swain, C. G.; Kulagowski, J. J. *Synlett* **2006**, 600–604.

[26] Penner, M.; Rauniyar, V.; Kaspar, L. T.; Hall, D. G. *J. Am. Chem. Soc.* **2009**, *131*, 14216–14217.

[27] (a) Jan, Š.; Hocek, M.; K., P. *Chem. Rev.* **2009**, *109*, 6729–6764; (b) Compain, P.; Martin, O. R. *Bioorg. Med. Chem.* **2001**, *9*, 3077–3092; (c) Bililign, T.; Griffith, B. R.; Thorson, J. S. *Nat. Prod. Rep.* **2005**, *22*, 742–760.

[28] Nishikawa, T.; Koide, Y.; Kajii, S.; Wada, K.; Ishikawa, M.; Isobe, M. *Org. Biomol. Chem.* **2005**, *3*, 687–700.

[29] Frick, W.; Hofmann, J.; Fischer, H.; Schmidt, R. R. *Carbohydr. Res.* **1991**, *210*, 71–77.

[30] Bajracharya, G. B. *Fitoterapia* **2015**, *101*, 133–152.

[31] (a) Washburn, W. N. *Expert Opin. Ther. Patents* **2009**, *19*, 1485–1499; (b) Hardman, T. C.; Dubrey, S. W. *Diabetes Ther.* **2011**, *2*, 133–145.

[32] Baldwin, J. *J. Chem. Soc., Chem. Commun.* **1976**, 734–736.

[33] Risi, R. M.; Maza, A. M.; Burke, S. D. *J. Org. Chem.* **2014**, *80*, 204−216.

[34] Nicolaou, K. C.; Duggan, M. E.; Hwang, C. K.; Somers, P. K. *J. Chem. Soc., Chem.*

Commun. **1985**, 1359–1362.

[35] Kanemoto, M.; Murata, M.; Oishi, T. *J. Org. Chem.* **2009**, *74*, 8810–8813.

[36] Nicolaou, K. C.; Seo, J. H.; Nakamura, T.; Aversa, R. J. *J. Am. Chem. Soc.* **2010**, *133*, 214–219.

[37] Larrosa, I.; Romeab, P.; Urpí, F. *Tetrahedron* **2008**, *64*, 2683–2723.

[38] Uenishi, J.; Ohmi, M. *Angew. Chem. Int. Ed.* **2005**, *44*, 2756–2760.

[39] Kriewitz, O. *Ber.* **1899**, *32*, 57–60.

[40] (a) Prins, H. J. *Chem. Weekbl.* **1919**, *16*, 1072–1073; (b) Prins, H. J. *Chem. Weekbl.* **1919**, *16*, 1510–1526.

[41] Hanschke, E. *Chem. Ber.* **1955**, *88*, 1053–1061.

[42] Adams, D. R.; Bhatnagar, S. P. *Synthesis* **1977**, *10*, 661–672.

[43] Olier, C.; Kaafarani, M.; Gastaldi, S.; Bertrand, M. P. *Tetrahedron* **2010**, *66*, 413–445.

[44] Sultana, S.; Indukuri, K.; Deka, M. J.; Saikia, A. K. *J. Org. Chem.* **2013**, *78*, 12182–12188.

[45] Ohta, S.; Uy, M. M.; Yanai, M.; Ohta, E.; Hirata, T.; Ikegami, S. *Tetrahedron Lett.* **2006**, *47*, 1957–1960.

[46] Li, H.; Xie, H.; Zhang, Z.; Xu, Y.; Lu, J.; Gao, L.; Song, Z. *Chem. Commun.* **2015**, *51*, 8484–8487.

[47] Waldmann, H. *Synthesis* **1994**, 535–551.

[48] Diels, O.; Alder, K. *Liebigs Ann. Chem.* **1928**, *460*, 98–122.

[49] Gresham, T. L.; Steadman, T. R. *J. Am. Chem. Soc.* **1949**, *71*, 737–738.

[50] Kubler, D. G. *J. Org. Chem.* **1962**, *27*, 1435–1436.

[51] Danishefsky, S.; Harvey, D. F.; Quallich, G.; Uang, B. J. *J. Org. Chem.* **1984**, *49*, 392–393.

[52] Jorgensen, K. A. *Angew. Chem. Int. Ed.* **2000**, *39*, 3558–3588.

[53] Bauer, T.; Chapuis, C.; Kozak, J.; Jurczak, J. *Helv. Chim. Acta* **1989**, *72*, 482–486.

[54] Dossetter, A. G.; Jamison, T. F.; Jacobsen, E. N. *Angew. Chem. Int. Ed.* **1999**, *38*, 2398–2400.

[55] Gademann, K.; Chavez, D. E.; Jacobsen, E. N. *Angew. Chem. Int. Ed.* **2002**, *114*, 3185–3187.

[56] Liu, P.; Jacobsen, E. N. *J. Am. Chem. Soc.* **2001**, *123*, 10772–10773.

[57] Gao, X.; Hall, D. G. *J. Am. Chem. Soc.* **2003**, *125*, 9308–9309.

[58] Deligny, M.; Carreaux, F.; Carboni, B.; Toupet, L.; Dujardin, G. *Chem. Commun.* **2003**, 276–277.

[59] Deligny, M.; Carreaux, F.; Toupet, L.; Carboni, B. *Adv. Synth. Catal.* **2003**, *345*, 1215–1219.

[60] Gao, X.; Hall, D. G.; Deligny, M.; Favre, A.; Carreaux, F.; Carboni, B. *Chem. Eur. J.* **2006**, *12*, 3132–3142.

[61] Carreaux, F.; Deligny, M.; Carboni, B. *Synlett* **2005**, 1462–1464.

[62] Favre, A.; Carreaux, F.; Deligny, M.; Carboni, B. *Eur. J. Org. Chem.* **2008**, *2008*, 4900–4907.

[63] Gao, X.; Hall, D. G. *J. Am. Chem. Soc.* **2005**, *127*, 1628– 1629.

[64] Fu, G. C.; Grubbs, R. H. *J. Am. Chem. Soc.* **1992**, *114*, 5426–5427.

[65] De Rosa, S.; Crispino, A.; De Giulio, A.; Iodice, C.; Pronzato, R.; Zavodnik, N. *J. Nat. Prod.* **1995**, *58*, 1776−1780.

[66] Cheung, A. K.; Murelli, R.; Snapper, M. L. *J. Org. Chem.* **2004**, *69*, 5712–5719.

[67] Gillingham, D. G.; Kataoka, O.; Garber, S. B.; Hoveyda, A. H. *J. Am. Chem. Soc.* **2004**, *126*, 12288–12290.

[68] Ibrahem, I.; Yu, M.; Schrock, R. R.; Hoveyda, A. H. *J. Am. Chem. Soc.* **2009**, *131*, 3844–3845.

[69] Yu, M.; Ibrahem, I.; Hasegawa, M.; Schrock, R. R.; Hoveyda, A. H. *J. Am. Chem. Soc.* **2012**, *134*, 2788–2799.

[70] Y., M.; Schrock, R. R.; Hoveyda, A. H. *Angew. Chem. Int. Ed.* **2014**, *54*, 215–220.

[71] Nicotra, F., Synthesis of C-glycosides of biological interest. In *Glycoscience Synthesis of Substrate Analogs and Mimetics*, Driguez, H.; Thiem, J., Eds. Springer Berlin Heidelberg: 1998; Vol. 187, pp 55-83.

[72] Frein, J. D.; Rovis, T. *Tetrahedron* **2006**, *62*, 4573–4583.

[73] Crimmins, M. T.; Stevens, J. M.; Schaaf, G. M. *Org. Lett.* **2009**, *11*, 3990–3993.

[74] Tate, E. W.; Dixon, D. J.; Ley, S. V. *Org. Biomol. Chem.* **2006**, *4*, 1698–1706.

[75] Nicolaou, K. C.; Kim, D. W.; Baati, R.; O'Brate, A.; Giannakakou, P. *Chem. Eur. J.* **2003**, *9*, 6177–6191.

[76] Di Bussolo, V.; Caselli, M.; Pineschi, M.; Crotti, P. *Org. Lett.* **2003**, *5*, 2173–2176.

[77] Di Bussolo, V.; Favero, L.; Romano, M. R.; Pineschi, M.; Crotti, P. *Tetrahedron* **2008**, *64*, 8188–8201.

[78] Gómez, A. M.; Lobo, F.; Uriel, C.; López, J. C. *Eur. J. Org. Chem.* **2013**, *2013*, 7221–7262.

[79] Vieira, A. S.; Fiorante, P. F.; Hough, T. L. S.; Ferreira, F. P.; Lüdtke, D. S.; Stefani, H. A. *Org. Lett.* **2008**, *10*, 5215–5218.

[80] Dao, H. T.; Schneider, U.; Kobayashi, S. *Chem. Asian J.* **2011**, *6*, 2522–2529.

[81] Zeng, J.; Ma, J.; Xiang, S.; Cai, S.; Liu, X.-W. *Angew. Chem. Int. Ed.* **2013**, *52*, 5134–5137.

[82] Díaz-Oltra, S.; Angulo-Pachón, C. A.; Murga, J.; Carda, M.; Marco, J. A. *J. Org. Chem.* **2010**, *75*, 1775-1778.

Chapter 2. Synthetic Efforts Towards the Development of Simplified Laulimalide Analogues

2.1 Introduction

Breast cancer is the leading cancer amongst women in the world as of 2015, where it accounts for an estimated 29% of all cases reported in the United States.[1] It is also expected to be the second leading cause of death for cancer-stricken women.[1] Ovarian cancer, another deadly disease that threatens women, is expected to account for 5% of cancer-related deaths in 2015.[1] A common method of treating breast and ovarian cancer is through chemotherapy, where anticancer drugs are used to stop the proliferation of cancers cells. These drugs function by targeting various metabolic mechanisms in the cell and may trigger the malignous cells to undergo apoptosis. Modern chemotherapeutic drugs may consist of natural cytotoxic or unnatural synthetic compounds that exhibit similar bioactivity to their natural counterparts. A distinct class of drugs used in chemotherapy are microtubule-stabilizing agents (MSAs) or microtubule-destabilizing agents (MDAs); compounds that target microtubules formed during mitosis. Mitosis is the process that enables the duplication of a cell's chromosomes, after which the cell is split into two daughter cells.[2] The microtubules formed are necessary for the proper function of the mitotic process where, once distorted by a MSA or MDA, key steps in the cellular mechanism of mitosis are disrupted.[3] This is an advantageous method of targeting tumor cells, where once their mitotic cycle is dysfunctional, these cells would be signaled to undergo apoptosis.[3] The first MSA used for cancer treatment is the taxane, Paclitaxel.[2] Once considered a "wonder drug", this compound is listed as an essential medication by the World Health Organization.[4,5] Although paclitaxel is still used in treating various diseases, it suffers from cardiac toxicity,[6,7] low solubility,[8] and poor multidrug resistance[9] (Figure 2-1). Fortunately, the

efficacy of paclitaxel has been proven to be enhanced through synergistic interactions with laulimalide, another natural product that is also an effective MSA.[10,11,12]

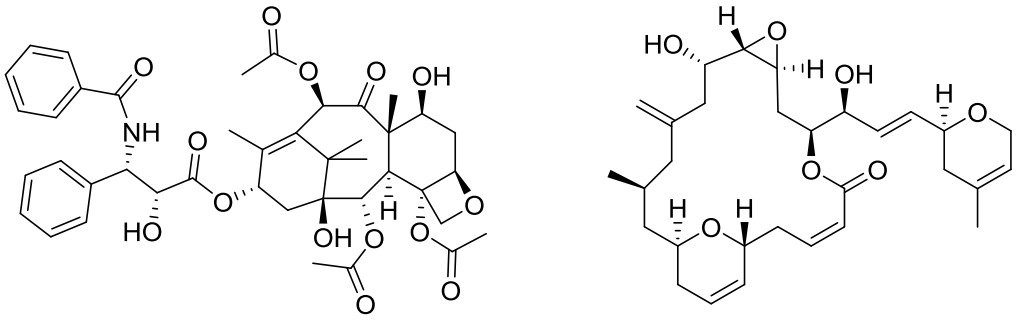

paclitaxel
MDA-MB-435: IC_{50} = 1.02 nM
SK-OV-3: IC_{50} = 1.71 nM
SKVLB: IC_{50} > 100,000 nM
Resistance factor >58,480

laulimalide
MDA-MB-435: IC_{50} = 5.74 nM
SK-OV-3: IC_{50} = 11.53 nM
SKVLB: IC_{50} = 1,210 nM
Resistance factor = 105

Figure 2-1: Structure, cytotoxicity and resistance factor of paclitaxel and laulimalide.

Laulimalide consists of an 18-membered macrocyclic lactone containing two unique dihydropyran moieties (Figure 2-1). Also known as fijianolide B, it was isolated 1988 from two sources of marine sponge, *Cacospongia mycofijiensis*[13] and *Hyattella sponge*, as well as a nudibranch predator.[14] In 1999, Bernardinelli and co-workers determined the absolute stereochemistry after isolating it from another marine sponge, *Fasciospongia rimosa*.[15] The cytoxicity of this marine-based MSA was comparable to the more commonly used paclitaxel (Figure 2-1), where the inhibition concentration of laulimalide towards cell proliferation of melanoma cells (MDA-MB-435) was five times in magnitude relative to paclitaxel.[9] The inhibition of cell proliferation of ovarian carcinoma cells (SK-OV-3 and SKVLB), when using laulimalide was approximately eleven times larger compared to paclitaxel. Furthermore, laulimalide has gained considerable interest due to its significantly lower multi-drug resistance – a cell's ability to resist the effects of a drug – relative to other chemotherapeutic drugs.[9,16] The multidrug resistance of paclitaxel has a reported resistance factor of greater than 58,000 relative

to laulimalide, which has just above 100.[9] Since these two MSAs exhibit synergistic effects with each other toward microtubule stabilization, developing a new active laulimalide-based compound would be an attractive next-generation MSA toward combination chemotherapy with taxane-based drugs.

2.1.2 Targeting the cell cycle for chemotherapeutic treatment

The mitotic cycle consists of several unique stages involved in the growth and proliferation of cells: the prophase, the prometaphase, the metaphase, the anaphase, and the telophase (Figure 2-2). Microtubules, protein-based polymers consisting of the heterodimers α- and β-tubulin, make up the majority of mitotic spindles, an essential subcellular structure involved in the mitotic cycle.[17] Although microtubules are required for all stages of mitosis, they play a significant role in the splitting of chromosomes, at specific stages in the cell cycle. During the prometaphase, microtubules probe the cell until they attach to the chromosomes at their kinetochores.[18] Once the microtubules attach to the chromosomes, in the metaphase, the microtubules align all chromosomes at the equator of the cell, or metaphase plate.[2] Afterwards, the metaphase–anaphase checkpoint occurs, a system that ensures that the cell is properly set up to form two daughter cells with an identical set of chromosomes.[2] Once this checkpoint is passed, the chromosomes are synchronously split in two during the anaphase and telophase.[2] These split chromosomes are then incorporated into each daughter cell, which are formed at the end of the cycle.[2] The proper function of the mitotic spindle depends on the length and tension caused by the microtubules, which is regulated by a polymerization and depolymerisation mechanism.[2] Any disturbances to these mechanisms would interrupt the metaphase–anaphase checkpoint, where not all chromosomes are attached to a mitotic spindle or they are not properly aligned at the equator of the cell during the metaphase.[2] If the cell fails to pass the metaphase–anaphase

checkpoint, the cell is signalled to undergo cell apoptosis.[2] Since tumour cells proliferate at a higher rate compared to normal cells, and thus undergo mitosis more frequently, MSAs are beneficial in regulating and eradicating these cancer cells.

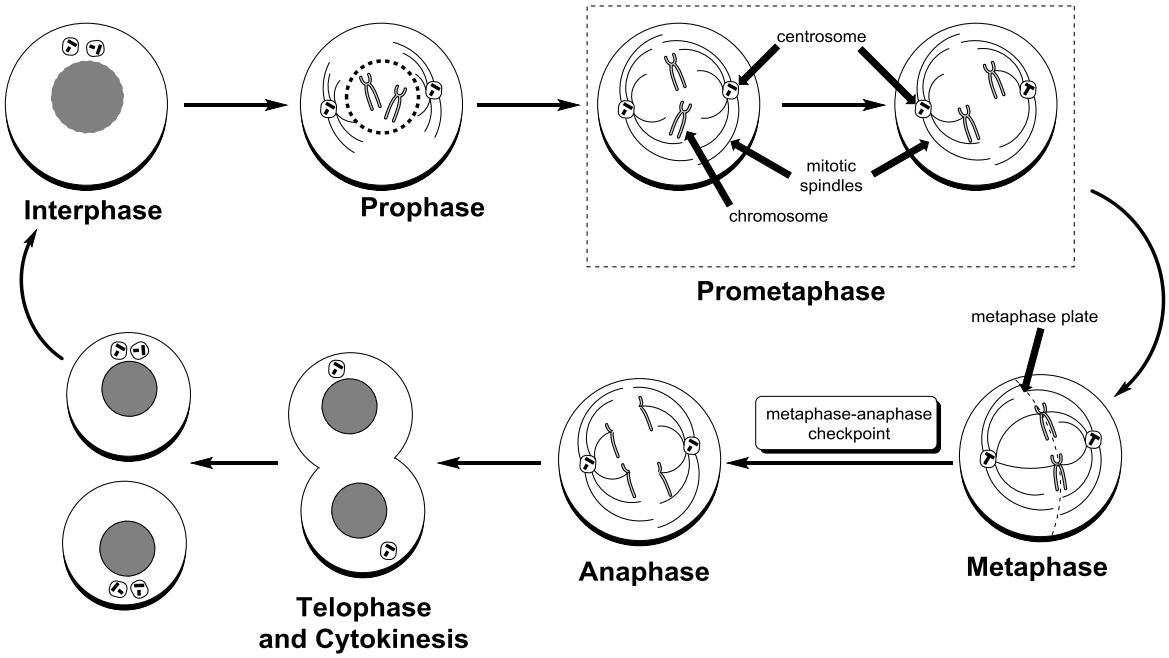

Figure 2-2: The mitotic cycle.[19]

2.1.3 Locating the binding site of laulimalide

The laulimalide binding site, as initially proposed by Hamel and co-workers, was suspected of binding to microtubules at an alternate and unknown binding pocket to the paclitaxel binding site.[16] Initial unveiling of the laulimalide binding site was determined by the Schriemer group using hydrogen-deuterium exchange (HDX) mass-spectrometric analysis,[20] a process that is used often in the study of protein folding.[21]

The HDX MS analysis of proteins conformations and ligand interactions works by exploiting the proton exchange between the solution medium and any protic amino acid residue in the protein's peptide chain.[21,22] Using deuterated water (D_2O), a hydrogen-deuterium exchange occurs on the amide backbone as well as any nitrogen, oxygen, or sulfur containing residues.[23] In

the native state, the amide-bound hydrogen atoms and the weak hydrogen-bound residues located on the surface of the folded protein would undergo hydrogen-deuterium exchange and – given that the conformation of proteins are dynamic and can on occasion partially unfold – protic sources inside the protein exchange more slowly.[22,24,25] The process for which the amount of deuterium incorporated on the protein surface is measured begins with the exposure and deuteration of the target protein **A** (Figure 2-3a).[25] Afterwards, the deuterated protein **B** is unfolded under an acidic buffered environment (pH 2.5) and kept at cold temperatures (0 ^{o}C) in order to reduce the backward rate of deuterium-hydrogen exchange.[22,25] The denatured protein is digested using protease enzymes, which fragment the peptide chains at specific sites. Fragmention of the protein improves the resolution of MS detection by increasing the population of the fragments.[22,25] The peptide fragments are separated by liquid chromatography followed by MS detection. The percent of deuterium exchange for each peptide is measured by calculating the average mass to charge ratio (m/z) of the deuterated peptide ion of protein **B** relative to the corresponding nondeuterated peptide fragment of protein **A**.[25] From these results, the conformation of the protein can be determined by mapping out which peptides had an increased percent of deuterium exchange.[25] In the presence of a ligand that would interact with the target protein, the binding site can be determined by measuring the decreased percent of deuterium exchange between the deuteration of a ligand-bound protein **C** relative to a ligand-free deuterated protein **B** (Figure 2-3b).

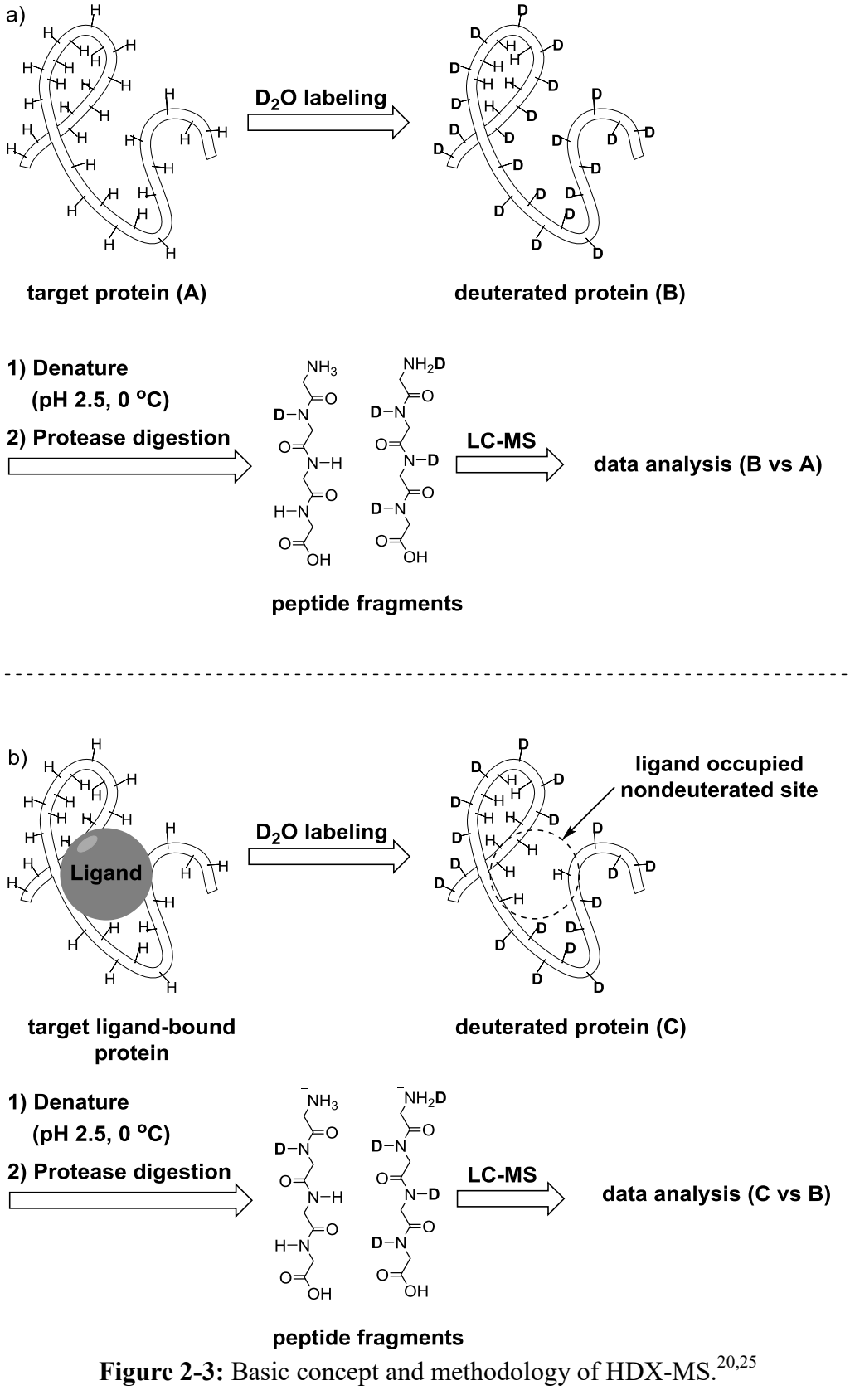

Figure 2-3: Basic concept and methodology of HDX-MS.[20,25]

Using this method, the microtubule-laulimalide binding site can be predicted indirectly, and is easier to determine compared to the recrystallization of a ligand-bound protein. Furthermore, this HDX MS analysis may represent a more realistic analysis of the natural protein-ligand interaction compared to X-ray crystallographic analysis, where the free-floating protein and ligand are interacting in a physiologically relevant buffer solution. As a result, the laulimalide-tubulin binding interactions, under HDX MS analysis, are determined under a more native state.

Using the HDX MS technique, Schriemer and co-workers determined that laulimalide-microtubule interaction was located on the exterior surface of microtubules at the β-tubulin site (Figure 2-4a).[20] Through molecular docking simulations performed by the Tuszynski group, a model of the laulimalide-tubulin binding interaction was predicted (Figure 2-4b).[20] Based on the proposed conformation, the hydroxyl group of laulimalide is believed to undergo a hydrogen-bond interaction with the nearby asparagine residue (N337).[20] The H-bonding interaction between the exomacrocyclic dihydropyran and the arginine residue (R306) may further increase the stability of the tubulin-ligand binding affinity.[20] The importance of the hydroxyl group and exomacrocyclic dihydropyran moiety has been addressed by several research groups, where laulimalide-based analogues with modifications at these sites demonstrated significantly lower activities.[26]

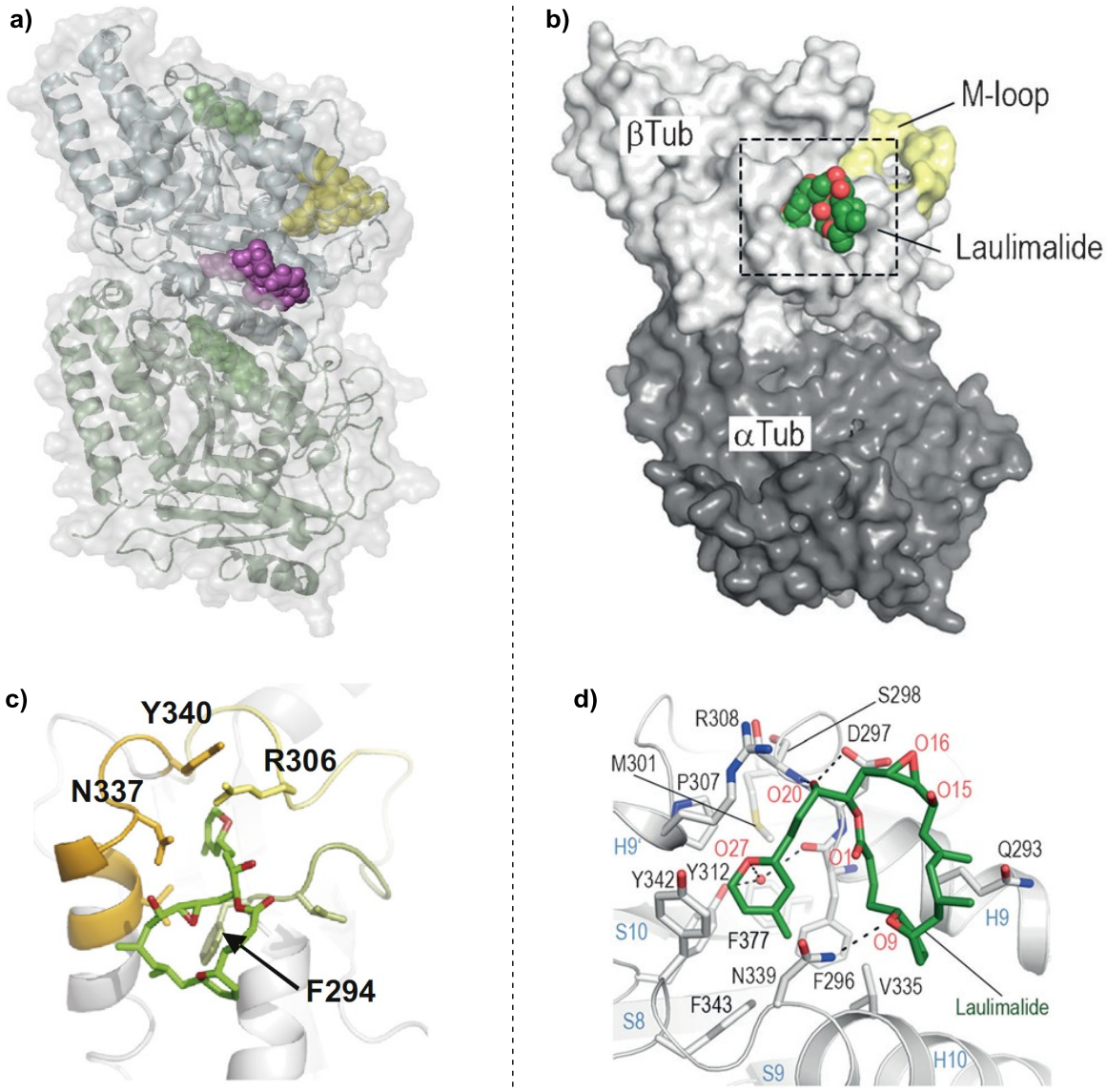

Figure 2-4: The located laulimalide binding site reported by a) Schriemer[20] and b) Steinmetz[27] and a close-up view of c) Tuszynski's predicted[20] and d) Steinmetz's observed[27] laulimalide-tubulin complex. Reprinted with permission from John Wiley and Sons[27] and Elsevier.[20]

A more direct method that confirmed the location of the laulimalide binding site was determined in 2014 by Steinmetz and co-workers through an X-ray crystallographic analysis,[27] the gold standard in determining the structural conformations of proteins (Figure 2-4c).[24] Although the binding site is not the same as the one predicted by the Schriemer group, both

binding sites were fairly close to one another and located on β-tubulin. Furthermore, the Steinmetz group determined the conformation of laulimalide and its interaction with key residues in the binding site.[27] Unlike the predicted models proposed by the Tuszynski group, where only the exomacrocyclic dihydropyran undergoes a hydrogen-bonding interaction with the surface of β-tubulin, both dihydropyran moieties in laulimalide appeared to be relevant to the natural product's interaction with the binding site (Figure 2-4d).[27] The endomacrocyclic dihydropyran, fused to the macrocycle of laulimalide, forms hydrogen-bonding interactions with an asparagine residue (N339), while the exomacrocyclic dihydropyran moiety formed a water-mediated hydrogen-bonding interaction with a tyrosine residue (Y312).[27] Interestingly, the Steinmetz group observed that laulimalide, when bound to microtubules, did not affect the global conformation of the protein-based structure.[27]

2.1.4 Function-oriented synthesis and drug design

A major drawback of this potentially useful cytotoxic compound is that the concentration of laulimalide from the natural source is approximately 0.00016%.[28] To extract a sufficient amount of this compound from the marine sponge would create deleterious effects on the marine ecosystem. In addition to this, laulimalide is known to decompose into the isomer isolaulimalide (Figure 2-5).[14] Another isomer of laulimalide, neolaulimalide, which was extracted from the marine sponge *Fasciospongia rimosa* also decomposes into isolaulimalide, albeit more slowly.[29] The efficacy of both isomers was compared to laulimalide over a variety of cell lines, which include breast adenocarcinoma (MCF-7), prostatic carcinoma (PC-3M), colon carcinoma (HCT-116), and melanoma (MDA-MB-435) cell lines.[26c] Isolaulimalide had significantly lower inhibition of cell proliferation relative to laulimalide, whereas neolaulimalide had comparable efficacy toward irradication of cancer cells.[26c] Due to the structural complexity of laulimalide,

the alternative method of obtaining this molecule through total synthesis would not be economically viable as it requires a large number steps and would afford a low overall yield. Thus, laulimalide is currently regarded as an impractical MSA for chemotherapy.

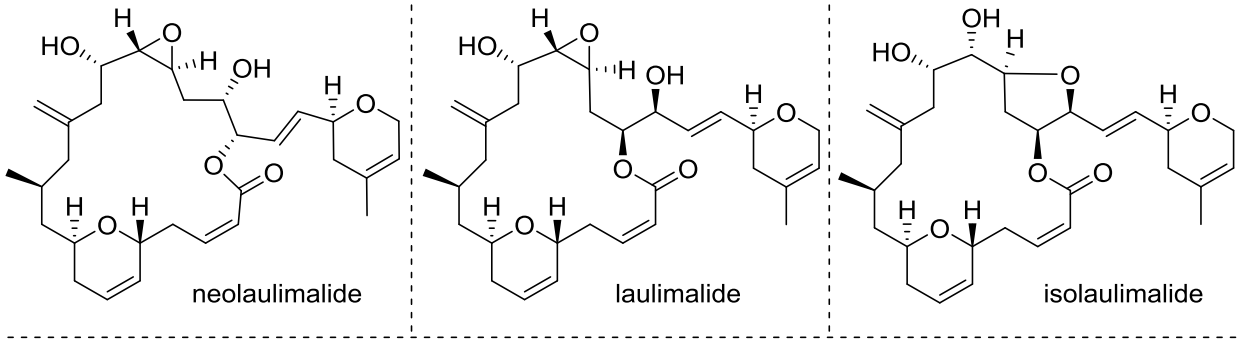

	Inhibition of cell proliferation IC_{50} (nM)			
compound	**MCF-7**	**PC-3M**	**HCT-116**	**MDA-MB-435**
laulimalide:	11.6	5.9	7.8	5.7
isolaulimalide:	4900	4400	4800	1970
neolaulimalide:	13.2	8.4	4.5	N/A

Figure 2-5: Compared structure and activity of isolaulimalide, neolaulimalide and laulimalide over various cancer cell lines.

A solution to the problems that arise in obtaining laulimalide as a potential chemotherapeutic drug is by using the strategy of function-oriented synthesis. This can be achieved by harnessing the structure-activity of the complex natural product, by simplifying the core structure and incorporating the pharmacophores of that natural product.[28] This approach would be very economical towards the synthesis of laulimalide analogues by addressing the issues involved in synthesizing this complex natural product, such a step-economy, poor supply from natural sources, and structural stability. [28] This strategy can be exemplified with the development of compounds analogous to bryostatin, a structurally complex natural product possessing a range of biological activities (Figure 2-6).[28] When the Wender group synthesized various analogues of bryostatin, a lead compound containing a simpler macrocyclic core possessed a more potent

inhibition activity relative to the natural product.[30] This process demonstrates that more potent and synthetically accessible drug targets can be obtained, which may be applicable to the synthesis of laulimalide-based analogues.

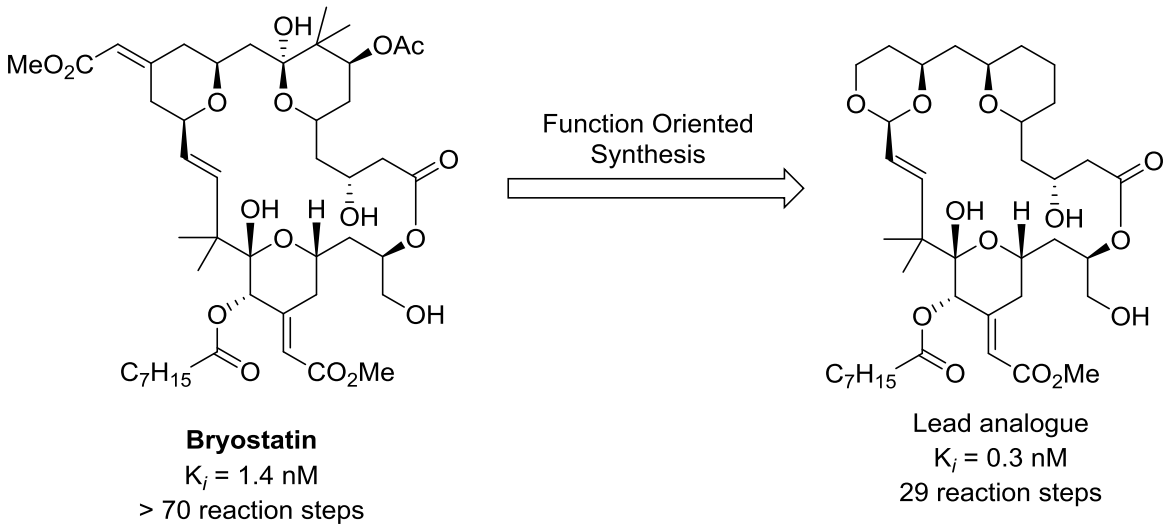

Figure 2-6: Representative bryostatin analog designed through function-oriented synthesis.[28,30]

2.1.5 An overview of previously reported analogues

The exceptional biological activity and structural complexity of laulimalide gave several research groups an incentive to develop simplified biologically active and more stable analogs of the natural product. This objective was addressed by modifying specific sections of the natural product in order to design simplified derivatives, while maintaining several core features that resembled the natural product. This campaign was led by the Gallagher, Paterson, Koert, Mulzer and Wender groups, who provided the seminal work in elucidating the key pharmacophores of the natural product. By evaluating the structure-activity relationship (SAR) data obtained by these research groups, clinically superior laulimalide analogues, with rationally designed and simpler structures, may be designed to create clinically viable chemotherapeutic agents.

2.1.5.1 Synthesis of analogues by Gallagher

In 2004, Gallagher and co-workers investigated the structure-activity relationship between microtubulin stabilization with analogues of laulimalide.[26a] The main sites in laulimalide that were modified for functional group-related activity were the type of unsaturated esters that constituted the lactone macrocycle (**X**; Figure 2-7a), the stereochemistry and presence of the epoxide (**Y**; Figure 2-7a), the functionalization of the free hydroxyl group within the macrocycle (**R**^{1}, **R**^{2}; Figure 2-7a) and nearest to the dihydropyran (**R**^{3}; Figure 2-7a).[26a] Although all analogues had activities lower than that of the natural product, the most active analogues, with an IC_{50} lower than 0.1 μM for the melanoma (MDA-MB-435) cell line, were **2-1**, **2-2** and **2-3** (Figure 2-7b).[26a] Each of these analogues differed from the natural product by one functional group, which indicated that any changes may have affected the shape of the macrocyclic core or interrupted any potential hydrogen-bonding interactions within the binding site and thereby decreasing the binding affinity of these analogues.

a)

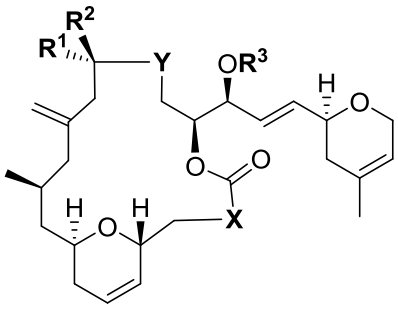

b)

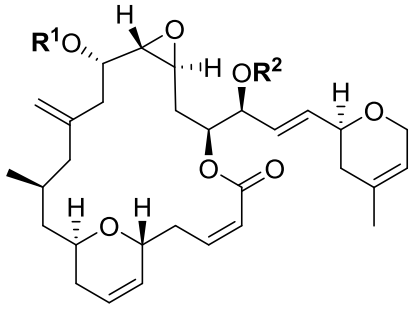

analogue	R^1	R^2	IC_{50} (nM) MDA-MB-435
laulimalide:	H	H	2.3
2-1:	H	Ac	91
2-2:	p-$NO_2(C_6H_4)C(O)$	H	37
2-3:	Ac	H	23

Figure 2-7: MCAs with *in vitro* inhibition results on the MDA-MB-435 cell line: a) modified sites of all derivatives and b) modified sites of the most active laulimalide analogues.

2.1.5.2 Synthesis of analogues by Koert

In an effort to determine the significance of the exomacrocyclic dihydropyranyl group, Koert and co-workers developed the phenyl laulimalide analogue **2-7** (Scheme 2-1).[26b] A key step toward the synthesis of laulimalide and its derivatives was the macrolactonization of **2-4**, where **2-5** was formed under Yamaguchi conditions with an unexpected *E*- to *Z*-isomerization in a 1:1.3 ratio (Scheme 2-1, Equation 1).[26b] Another obstacle toward the synthesis of **2-7** was the cleavage of the MOM-ether protecting group on **2-6**, which required the use of the harsh Lewis acid, Me_2BBr (Scheme 2-1, Equation 2).[26b] These conditions lead to an inseparable mixture of the desired product **2-7** and the isolaulimalide isomer **2-8**, and the mixture was not reported to have been subjected to *in vitro* testing for microtubulin stabilization or mitotic inhibition.[26b]

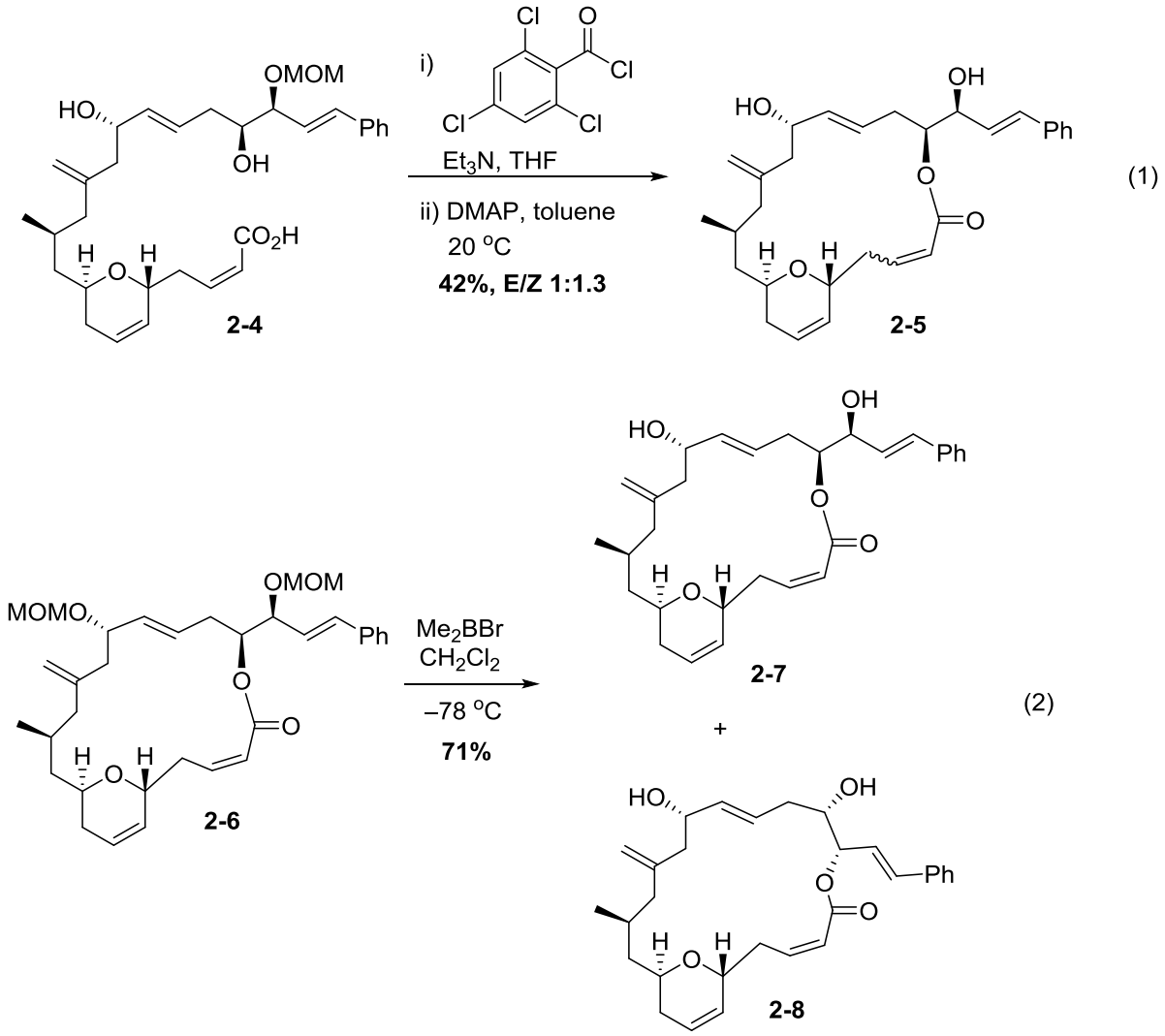

Scheme 2-1: Key reaction steps in the synthesis of the laulimalide analogue **2-7**.

2.1.5.3 Synthesis of analogues by Mulzer

Mulzer and co-workers have investigated the bioactivity of a variety of laulimalide analogues. In 2003, the Mulzer group investigated various synthetic pathways to the total synthesis of laulimalide as well as the synthesis of three analogues: 16-desepoxy laulimalide **2-9**, desepoxy *E*-enoate **2-10**, and **2-11** (Figure 2-8).[31] A simpler analogue was synthesized by the Mulzer group in 2009, which was the des-dihydropyranyl **2-12**.[32] From both reported experiments, several cancer cell lines were tested: breast cancer (MCF-7, MaTu, and

MaTu/ADR), ovarian tumor (NCI/ADR), prostate cancer (PC-3 M), and the colorectal carcinoma (HCT-116).[31,32] All laulimalide-based analogues had activities lower than that of the natural product.[31,32] The analogues **2-9** and **2-11**, however, had comparable activity relative to laulimalide. Furthermore, the desepoxy laulimalide, **2-10** did not inhibit any of the cancer cell lines when tested at 100 nM.[31] The significantly simpler analogue, **2-12**, also had no activity for any tested cell line, which supported that the endomacrocyclic dihydropyranyl group is relevant to the activity of the natural product.

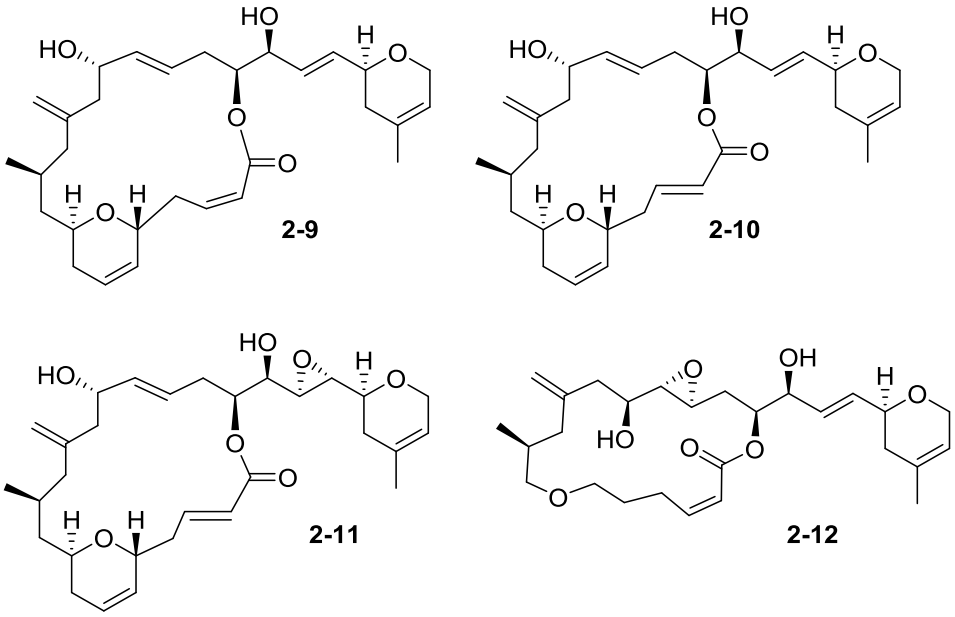

	IC_{50} (nM)					
analogue	**MCF-7**	**NCI/ADR**	**MaTu**	**MaTu/ADR**	**PC-3 M**	**HCT-116**
laulimalide:	3.8 (11.6)	36	3.8	6.0	5.9	7.8
2-9:	89	n/i	43	170	–	–
2-10:	n/i	n/i	n/i	n/i	–	–
2-11:	54	n/i	38	250	–	–
2-12:	>10,000	–	–	–	>10,000	>10,000

n/i = no inhibition measured up to 100 nM

Figure 2-8: Select examples of laulimalide-based analogues having cell growth inhibition.

2.1.5.4 Synthesis of analogues by Wender

The Wender group has made several contributions toward the function-oriented synthesis of laulimalide analogues.[26d,26e,33] Furthermore, in collaboration with Mooberry, they have tested these analogues on several cancer cell lines, which include cervix carcinoma (HeLa), melanoma (MDA-MB-435) and the ovarian tumor (NCI/ADR) cell line (Figure 2-9).[12,26d] Although the most active analogues had inhibition activity significantly lower than that of laulimalide, compounds **2-13** to **2-16** demonstrated low resistance factors relative to paclitaxel.[26d,26e,33] Similar to the findings by the Gallagher group, the lower activities measured are believed to be a result of the analogues forming inactive structural conformations that would not permit proper binding to the binding site. Since the activity of **2-16** was not significantly lower than the natural product, the removal of the methyl group in the macrocyclic ring indicates that the hydrophobic part of the macrocyclic ring possibly has little or no interaction with the binding site.[26e] When the authors replaced the exomacrocyclic dihydropyran with a cyclohexyl group **2-17**, the inhibitory power was significantly lower than that of the natural product suggesting that the external dihydropyran is essential to the activity of the natural product.

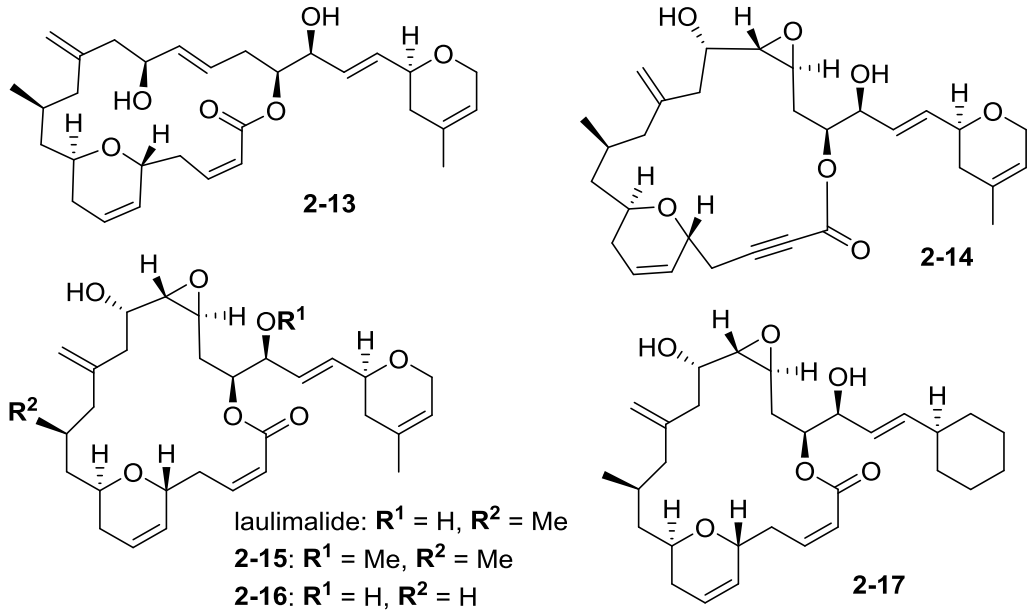

	IC$_{50}$ (nM)			Resistance factor for **NCI/ADR**
analogue	**HeLa**	**MDA-MB-435**	**NCI/ADR**	
laulimalide:	–	5.7	–	–
2-13:	100	120	370	3.1
2-14:	2200	2500	13700	5.5
2-15:	180	240	470	2.0
2-16:	38.5	49	292	6.0
2-17:	–	1170	–	–
paclitaxel:	–	1.15	2454	2134

Figure 2-9: MCAs with *in vitro* inhibition results of several cancer cell lines.

2.1.5.5 Synthesis of analogues by Paterson

In 2005, Paterson and co-workers developed a variety of analogues related to the 11-desmethyllaulimalide derivative or the desmethyl-/desepoxy-variant and tested their ability to inhibit cell growth on ovarian carcinoma (A2780 and A2780/AD10) cell lines (Figure 2-10).[26f] The authors focused on derivitizing the dihydropyran moiety that was separate from the macrocyclic core of laulimalide. The moieties replacing the dihydropyran include truncated (R^2 = H) a simpler (R^2 = cyclohexane) functional groups and the thiazole-based moiety inspired from epothilones;[34] MCA's known to have strong cytotoxic activity. Other than **2-16**, none of the analogues (**2-18** to **2-24**) demonstrated any activity close to laulimalide. Based on the results of

the *in vitro* study, currently there are no suitable functional groups to replace dihydropyran moiety.

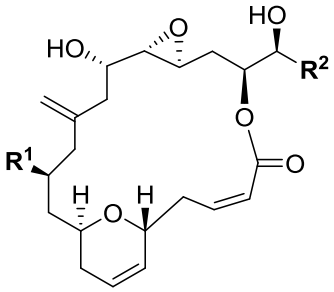

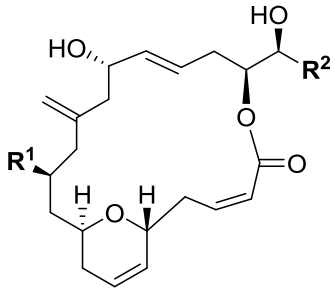

compound	R^1	R^2
laulimalide	Me	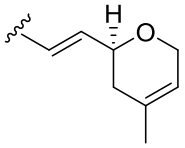
2-16	H	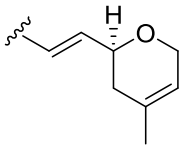
2-18	H	
2-19	H	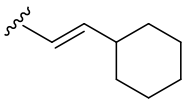
2-20	H	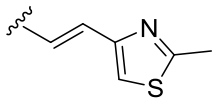

compound	R^1	R^2
2-21	Me	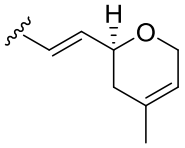
2-22	H	
2-23	H	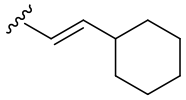
2-24	H	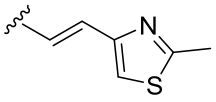

compound	IC_{50} (nM) A2780	A2780/AD10
laulimalide:	3.4	7.5
2-16:	50	74
2-18:	40,000	44,000
2-19:	9000	8300
2-20:	n/i	n/i
2-21:	430	1100
2-22:	n/i	n/i
2-23:	n/i	n/i
2-24:	n/i	n/i
taxol:	1.1	1500

n/i = no inhibition measured below 50,000 nM

Inspiration for compounds **2-20** and **2-24:**

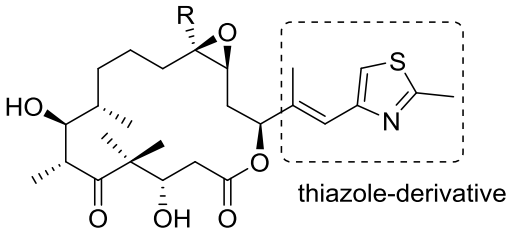

epothilone A, R = H
epothilone B, R = Me

Figure 2-10: Inhibitory effects of ligands on growth of human ovarian carcinoma cells lines.

2.2 Objectives

Using the strategy of function-oriented synthesis, potential chemotherapeutic drugs could be accessed through a shorter and more cost-effective synthesis. Although this problem has been addressed by the work of the Gallagher, Paterson, Koert, Mulzer and Wender groups, these structures relied on maintaining the closed macrocyclic ring. Instead, simpler structures analogous to laulimalide and without the rigid macrocyclic core were subjected to computerized modeling of the ligand-tubulin interactions by our collaborator Melissa Gajewski from the Tuszynski group at the University of Alberta. This study was achieved using generalized Born surface area (MM-GBSA) calculations, a computational method of calculating the free energy difference (ΔG) between the bound and unbound state of laulimalide with the tubulin binding site. The results of the β–tubulin binding affinity studies indicated that the structurally simpler and smaller dihydropyran-based compound **2-25** had significant potency relative to laulimalide (Figure 2-11). The calculated ligand-tubulin binding affinity of **2-25** was measured at –25 kcal/mol, which was similar to the measured binding affinity calculated for laulimalide (ΔG = –38 kcal/mol). Although the magnitude of these measured binding affinities are abnormally large, they are a result of neglecting the entropy due to the amount of processing power required to account for the solvent effects in the study. The epoxide group in laulimalide was not incorporated into **2-25** since it was believed that this functional group would make the analogues more prone to decomposition. This stability issue can be exemplified with laulimalide, where the natural product decomposes into the less potent isolaulimalide (Section 2.4, Figure 2-5).

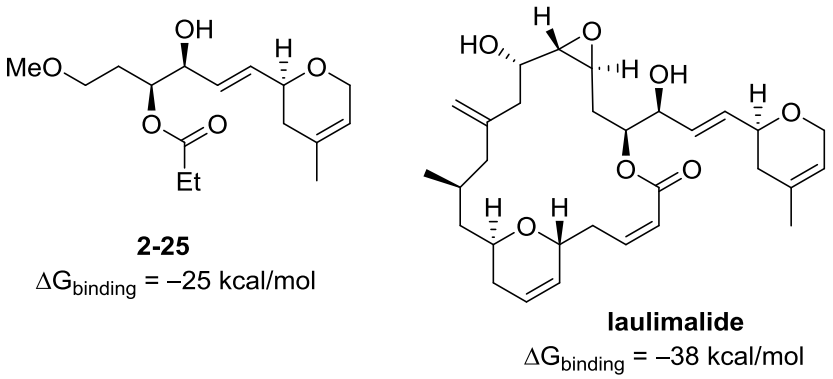

Figure 2-11: Initial computational binding affinity tests for **2-18** relative to laulimalide.

Based on the structural design of **2-25**, the initial study resulted in the design and synthesis of analogues A and B, which were unique from one another based on the relative stereochemistry of the dihydropyran stereocenter (Figure 2-12). These two compounds, with undefined stereochemistry and resembling compound **2-25**, were subjected to HDX MS analysis of the laulimalide-tubulin binding site, which was performed by the Schriemer group. Although these analogues were incapable of inducing polymerization of tubulin to form microtubules at 100 μM, the results from the HDX-MS experiment indicated that these analogues had weak binding at the laulimalide binding site. Several peptide fragments that were correlated to the peptide sequence of β-tubulin (331-340 and 332-340) showed a decrease in deuteration when either of the two analogues were tested. Since these peptide sequences were part of the laulimalide-tubulin binding site, as confirmed by the Schriemer group, a short synthetic pathway was implemented to access compounds analogous to **2-25**. Furthermore, a core structure would be chosen in order to develop a library of drug targets, where the propionic ester group would be replaced with a variety of ester groups or other potentially active fragments such as various peptides. Since the stereochemistry of the original samples were not determined, a consequence of an accelerated effort to determine if there was any precedence to the computation result made by the Tuszynski

group, efforts were made to fully characterize each intermediate to confirm what isomers would be tested. Using HDX MS analysis, the Schriemer group at the University of Calgary would test every synthesized analogue for *in vitro* binding affinity and microtubule stabilization.

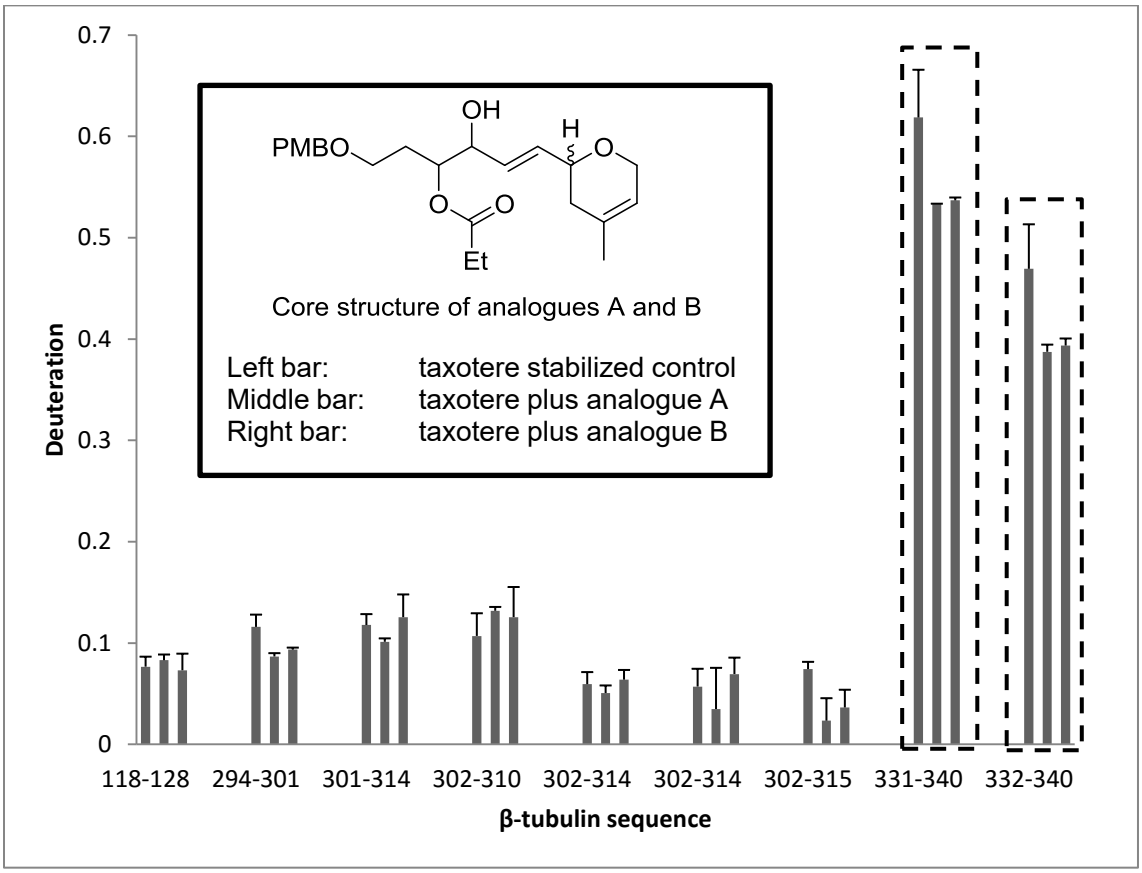

Figure 2-12: Initial screening of compounds analogous to **2-25** through HDX mass-perturbation analysis of microtubulin performed by the Schriemer group (Unpublished).

2.3 Synthesis of laulimalide analogues

Our retrosynthetic plan involved the ring-closing metathesis to form **2-27**, the main structure needed to develop a library of analogues **2-26** (Scheme 2-2). The key step towards the formation of the dihydropyran would involve a stereoselective allylboration of the unsaturated aldehyde **2-28**. The latter would originate from a cross-metathesis (CM) between **2-29** and acrolein. The

vinyl group used in the CM would be formed through a Grignard reaction using vinylmagnesium bromide and the corresponding aldehyde **2-30**. In turn, the aldehyde of **2-30** would be prepared through the Swern oxidation of **2-31**. Fortunately, **2-31** can be derived from the natural chiral building block, L-(–)-malic acid, which contains a stereogenic secondary alcohol with stereochemistry necessary for the synthesis of **2-27**.

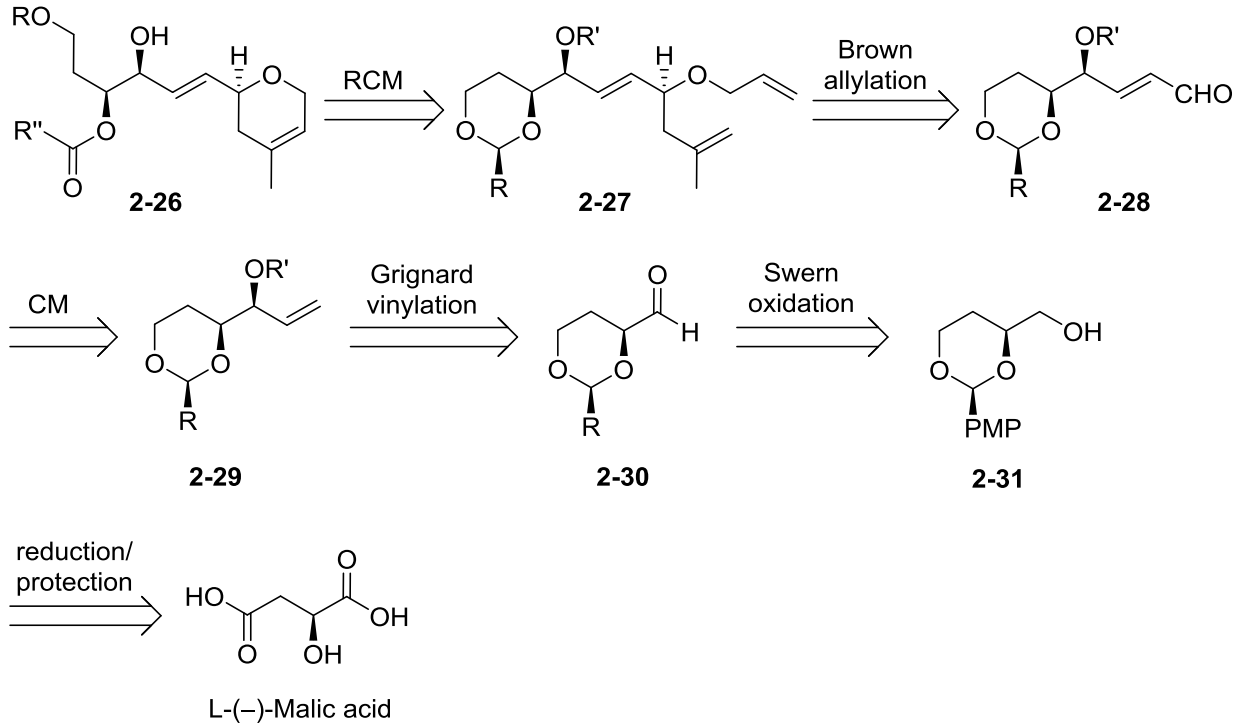

Scheme 2-2: Retrosynthetic pathway towards the analogue framework of laulimalide.

The synthetic route began with the reduction of L-(–)-malic acid using a mixture of BH_3•Me_2S and trimethylborate at room temperature (Scheme 2-3). After acetal protection of the crude triol, **2-32** was produced with a 54% yield over two steps. The *para*-methoxyphenyl acetal-protected product **2-32** underwent a Swern oxidation to afford the aldehyde **2-33**, which was subsequently subjected to alkenylation using vinylmagnesium bromide to afford a mixture of **2-34a** and **2-34b** in a 30:70 diastereomeric ratio with an overall yield of 40% over two steps. The low yield was likely a result of the benzylidene group's sensitivity to the Lewis acidic $MgBr_2$

present in the Grignard reagent. As a result, the protecting group may be prematurely removed during the reaction.

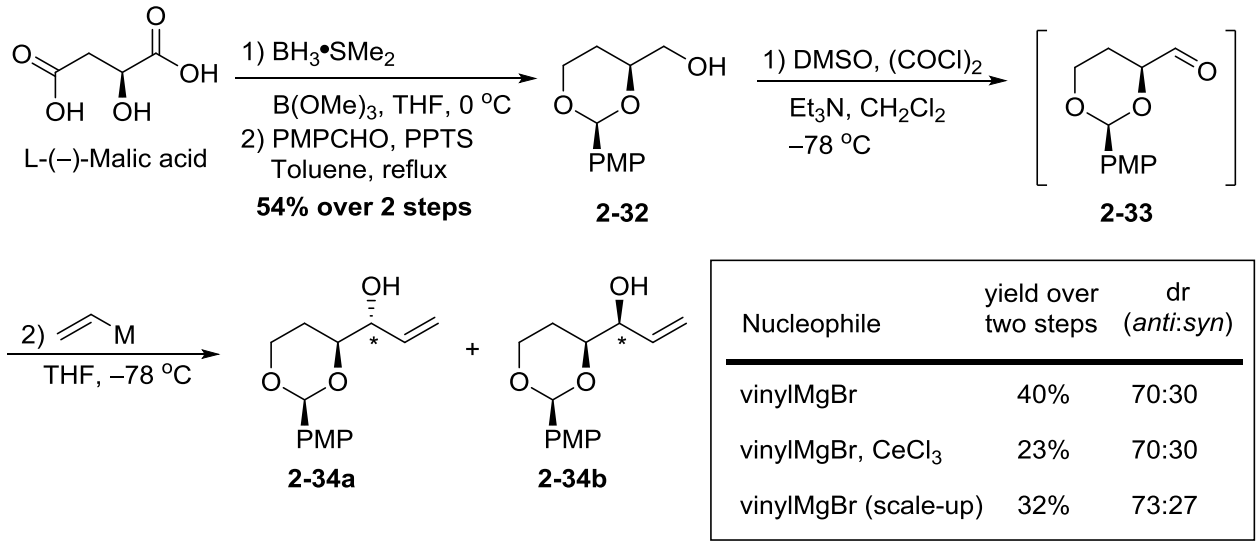

Nucleophile	yield over two steps	dr (*anti*:*syn*)
vinylMgBr	40%	70:30
vinylMgBr, $CeCl_3$	23%	70:30
vinylMgBr (scale-up)	32%	73:27

Scheme 2-3: Synthesis and isolation of diastereomers **2-34a** and **2-34b**.

The stereochemistry of each diastereomer was confirmed through ^{1}H NMR analysis of the corresponding Mosher esters. Using the conformational models assigned to the corresponding Mosher esters in Scheme 2-4, one can determine the absolute stereochemistry by analyzing the change in the chemical shifts of the protons occupied near the substituents of the target stereocenter.[35] This difference is caused by the anisotropic effects imposed by the phenyl group of the Mosher ester, where the chemical shift of protons in the proximity of the aryl group are shifted upfield due to the magnetic shielding effects.[35]

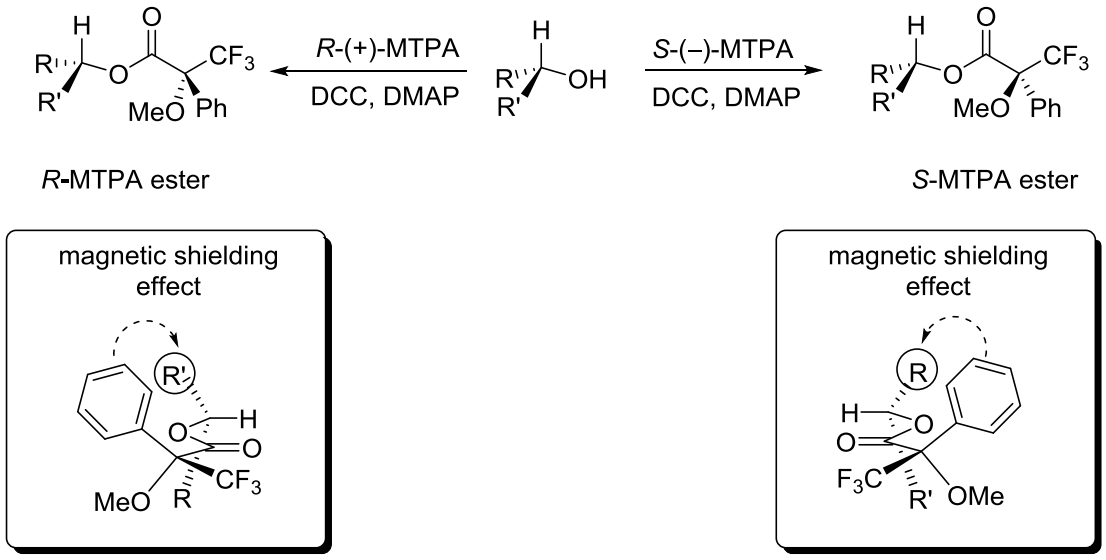

Scheme 2-4: Synthesis of *R*- and *S*-Mosher esters from the generic alcohol.

When analyzing the Mosher esters of **2-34a**, as shown in Scheme 2-5, the alkenyl proton (H^A) of the *S*-MTPA ester had a chemical shift more downfield (δ 6.29) relative to the same proton in the *R*-MTPA ester (δ 5.91). This indicated that for the *S*-MTPA ester, H^A was not proximal to the phenyl group. This conclusion was confirmed with inspection of the corresponding proton in *R*-MTPA ester, which had a more upfield chemical shift and indicated that the phenyl group was in the same plane to the proton of interest. Based on these results, the newly formed stereocenter can be assigned the *R*-configuration. Consequently, the major product assigned as **2-34a** was confirmed to be the undesired stereoisomer.

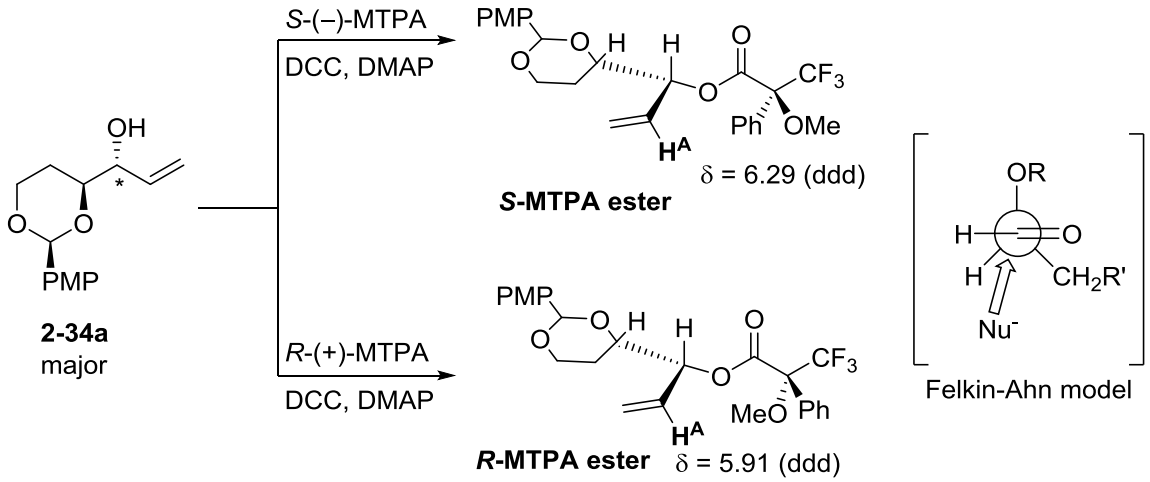

Scheme 2-5: Determination of the stereochemistry and identity of the diastereomer **2-34a**.

To confirm the absolute stereochemistry of both diastereomers, the minor product **2-34b** was also subjected to Mosher esterification. The same alkenyl proton (H^A) that was analyzed for the Mosher esters of **2-34a** were also examined for **2-34b**. The alkenyl proton of the *S*-MTPA ester had a chemical shift more upfield (δ 5.76) relative to the same proton in the *R*-MTPA ester (δ 5.88). The ^{1}H NMR results of the Mosher esters indicated that H^A was proximal to the phenyl group for the *S*-MTPA ester and in opposite plane of the phenyl group in the *R*-MTPA ester. From these results, an *S*-configuration was assigned to the newly formed stereocenter in **2-34b**. To improve the yield and increase the ratio in favor of the *syn*-diastereomer **2-34b**, the corresponding organocerium reagent was generated and reacted with the aldehyde substrate to afford the product at a 23% yield and the same diastereoselectivity was obtained (30:70 dr). Based on the ratio of diastereomers, the reaction mixture is believed to follow a polar Felkin-Ahn model, where the Grignard or organocerium reagent attacks opposite to the bulky acetal-protected diol (Scheme 2-5). This result was unexpected, since the Lewis acidity of the magnesium and cerium counter ion would typically favor a Cram-chelate model involving the basic oxygen atom on the acetal (Scheme 2-6).

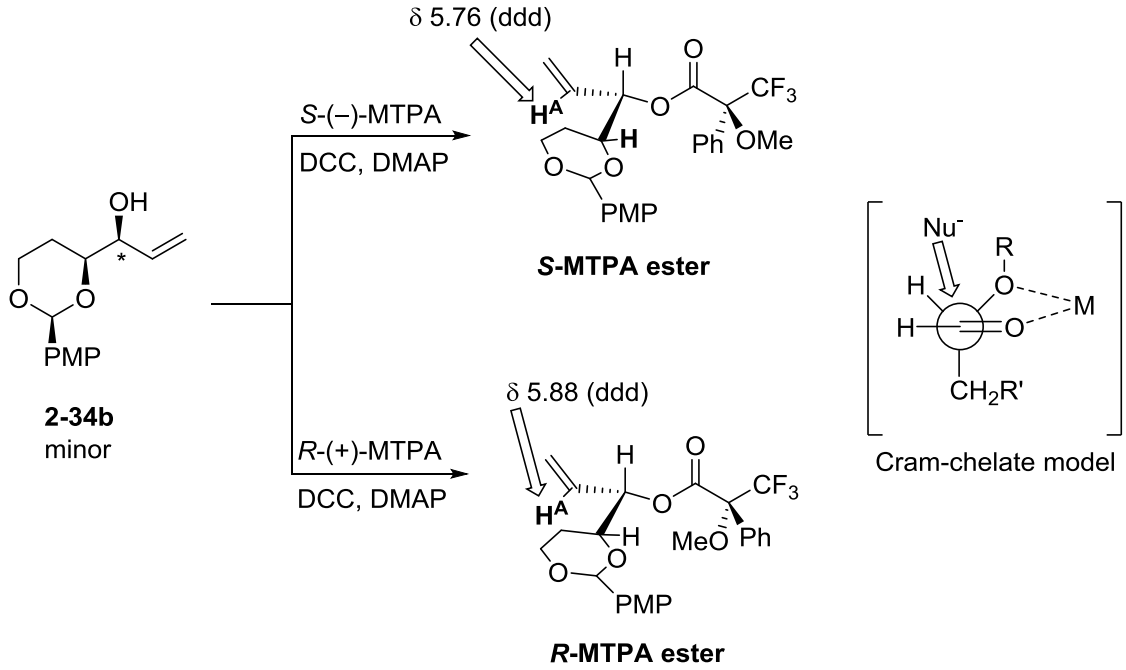

Scheme 2-6: Determination of the stereochemistry and identity of the diastereomer **2-34b**

To salvage this synthetic route, the major diastereomer was employed as a test substrate to evaluate the efficiency of the remaining steps in the pathway. Additionally, the analogues generated from the undesired diastereomer **2-34a** could be tested to confirm whether the stereochemistry of the alcohol is relevant to the biological activity of the natural product, a parameter that was not investigated in previous syntheses of laulimalide analogues. To help in correlating between the two epimeric reaction pathways, similar substrates were designated with the labels **a** or **b,** depending on which of the original two diastereomers were used (**2-34a** and **2-34b**).

Using the "undesired" epimer **2-34a**, the efficiency of the cross-metathesis was tested using an excess of acrolein and Grubbs second-generation catalyst in an efficient catalyst loading of 3 mol% (Scheme 2-7). This is made possible due to catalytic amounts of copper iodide provided (5 mol%), which, as reported by Lipshutz and co-workers, is suspected of stabilizing and

accelerating the rate of reaction.[36] Under reflux conditions in Et_2O, the α,β-unsaturated aldehyde **2-35a** was obtained in a 62% yield. An excess of acrolein was required since both olefinic substrates, the allyl alcohol **2-34a** and the acrolein reagent, are both considered as Type-II coupling partners and, as such, are only moderately reactive and are prone to form homocoupling products.[37]

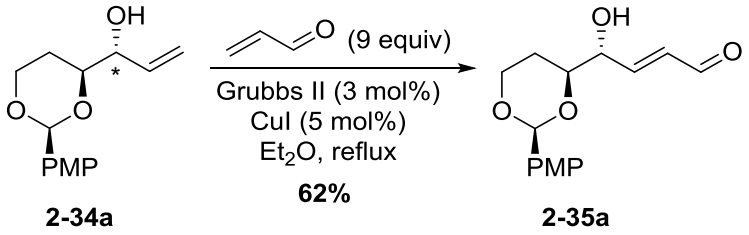

2-34a **2-35a**

Scheme 2-7: Cross-metathesis of **2-34a** with acrolein.

The initial strategy in selecting a suitable protecting group for the alcohol of **2-35a** was that it would resist the acidic conditions of subsequent reaction methods and was not benzylic due to the similarities with the *p*-anisyl acetal group. Under various conditions, the triisopropylsilyl (TIPS) group could not be installed onto the alcohol group, resulting in recovery of starting material or decomposition under the reaction conditions (Table 2-1, entries 1 to 6). Fortunately, the alcohol could be protected using a *tert*-butyldiphenylsilyl (TBDPS) group, where the conditions consisting of TBDPSCl and imidazole in CH_2Cl_2 afforded **2-36a** in a 70% yield (Table 2-1, entry 9). It should be noted that, when using pyridine as the base, the product yields were lower relative to using the milder Brønsted base, imidazole. The lower yield might be a result of poorer chemoselectivity, where pyridine is more nucleophilic and may be more prone to undergo a Michael addition with the conjugate aldehyde relative to imidazole (Table 2-1, entry 7). Furthermore, the additive $AgNO_3$ was not useful in raising the activity of the silyl chloride reagent (Table 2-1, entry 8), where the yield was comparable to the reaction without the additive (Table 2-1, entry 7).

Table 2-1: Silyl protection of alcohol **2-35a**.

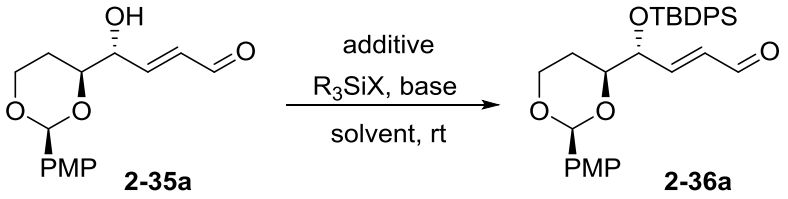

entry	R_3SiX	additive	base	solvent	yield (%)
1	TIPSOTf		imidazole	CH_2Cl_2	0
2	TIPSOTf		2,6-lutidine	CH_2Cl_2	0
3	TIPSOTf		pyridine	CH_2Cl_2	0
4	TIPSOTf		DIPEA	CH_2Cl_2	0
5	TIPSOTf		Et_3N	CH_2Cl_2	0
6	TIPSOTf	$AgNO_3$	2,6-lutidine	2:1 THF/DMF	0
7	TBDPSCl		pyridine	CH_2Cl_2	58
8	TBDPSCl	$AgNO_3$	pyridine	DMF	60
9	TBDPSCl		imidazole	CH_2Cl_2	70

Following the protection of the hydroxyl, aldehyde **2-36a** was subjected to a Brown allylation to afford the desired diastereomer **2-37a** with a 89% yield in high diastereoselectivity (96:4 dr) (Scheme 2-8). The rationale for using this synthetic method, where stoichiometric amounts of the chiral allylboronate (–)-*B*-allyldiisopinocampheylborane was used, was that this method is reliable in obtaining very high stereoselectivity for a broad range of substrates, and more importantly, its applicability to unsaturated aldehydes. Furthermore, other methods that may have demonstrated activity to unsaturated aldehydes require the use of expensive Brønsted acid catalysts or catalysts that cannot be easily synthesized, such as SPINOL-[38] or BINOL-derived[39] phosphoric acids.

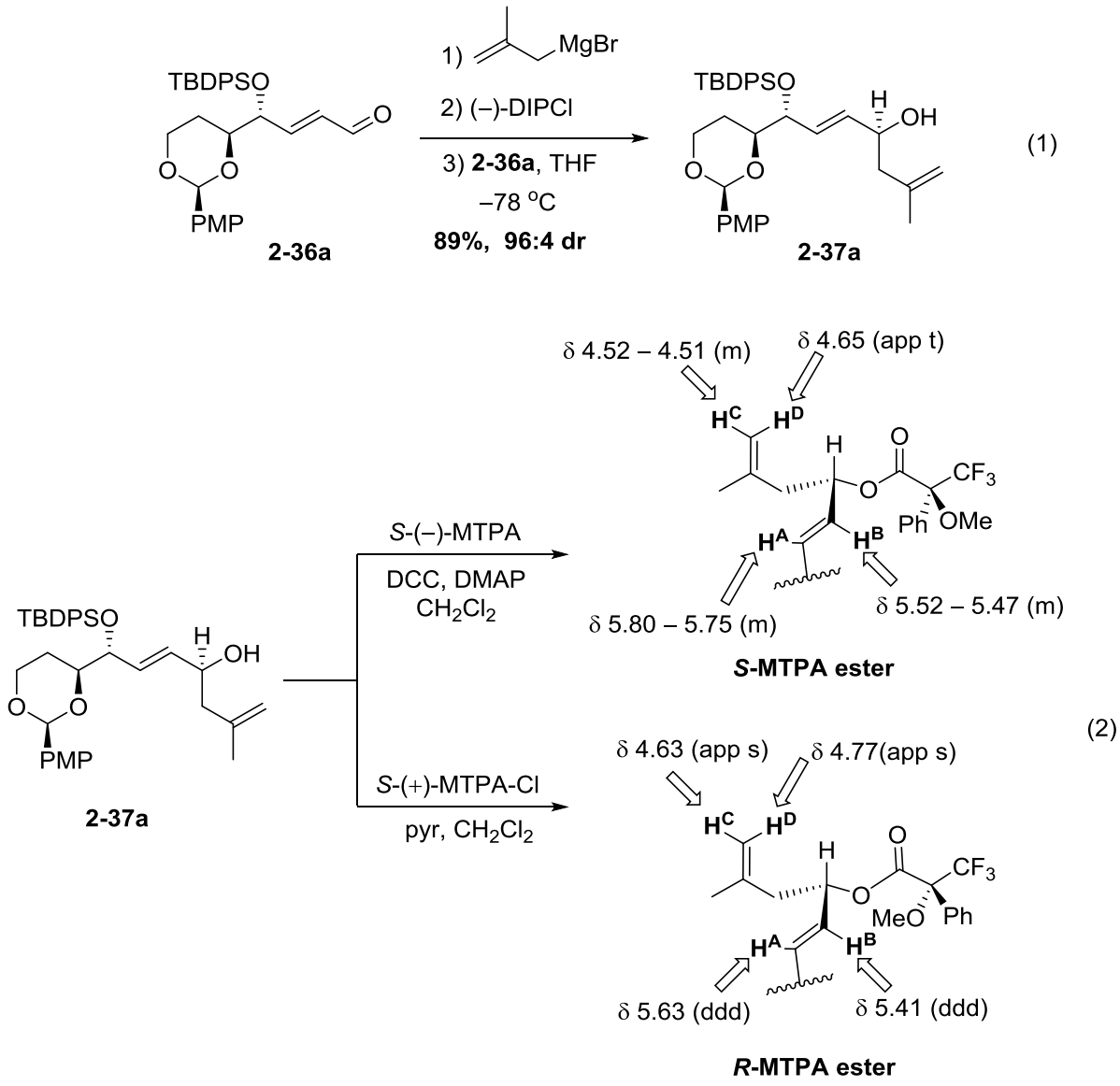

Scheme 2-8: Brown allylation and confirmation of the stereochemistry of **2-37a**.

The stereochemistry of the newly formed hydroxyl group of **2-37a** was confirmed through the ^{1}H NMR analysis of the Mosher ester derivatives (Scheme 2-8). This analysis was achieved by inspecting the internal (H^A and H^B) and terminal (H^C and H^D) alkenyl protons of the corresponding Mosher esters of **2-37a**. The internal alkenyl proton (H^A) of the *S*-MTPA ester had a chemical shift more downfield (δ 5.80 – 5.75) relative to the same proton in the *R*-MTPA ester (δ 5.63). This effect was similarly observed for internal proton H^B in both Mosher esters. Based

on these ^{1}H NMR results, the lack of magnetic shielding of H^{A} and H^{B} in the *S*-MTPA ester, compared to the *R*-MTPA ester, indicated that these protons were on the opposite plane to the phenyl group. The terminal alkenyl proton (H^{C}) of the *S*-MTPA ester had a chemical shift more upfield (δ 4.52 – 4.51) relative to the same proton in the *R*-MTPA ester (δ 4.63). To confirm this result, H^{D} was also confirmed to follow this same trend of magnetic shielding. The protons H^{C} and H^{D}, on the other hand, were proximal to the phenyl group and, thus, shielded. These results strongly supported that product **2-37a** possessed a *S*-configuration.

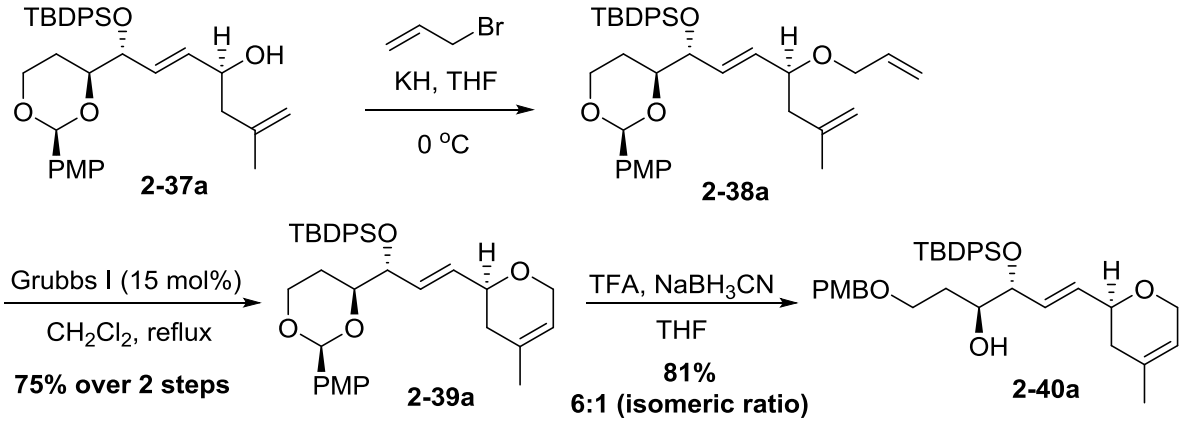

Scheme 2-9: Synthesis of **2-40a**.

With the alcohol product **2-37a** in hand, the pyran motif was synthesized through a ring-closing metathesis (RCM) – after *O*-allylation of **2-37a** – to afford **2-39a** with a 75% yield over two steps (Scheme 2-9). Lastly, the target structure **2-40a** was isolated with a 81% yield after a regioselective reductive ring opening (6:1 ratio of isomers) using TFA and $NaBH_3CN$. Several ester products were formed using either ester anhydrides under basic conditions (Method A) or carboxylic acids with DMAP and DCC (Method B) as shown in Scheme 2-10. A broad range of functionalized carboxylic esters and acid anhydrides were chosen to see if the ester functional group had an influence on the binding affinity of the final analogues. To closely resemble the endomacrocyclic dihydropyran contained in laulimalide, which was believed to interact with the

laulimalide binding site as proposed by Steinmetz and co-workers,[27] structures with similar electronic characteristics were chosen. These ester fragments include the furanyl (**2-43a** and **2-45a**) pyridinyl (**2-44a**) pyrone (**2-48a**) and thiophenyl (**2-49a**) groups. The importance of the endomacrocyclic dihydropyran in the natural product would also be confirmed by inserting nonpolar ester fragments (**2-41a**, **2-42a**, **2-46a** and **2-47a**), where the activity of these analogues would confirm if a coordinating group on the ester is necessary. To closely resemble the *Z*-α,β-unsaturated lactone in laulimalide, several *E*-α,β-unsaturated esters (**2-42a**, **2-44a**, **2-45a**, **2-47a** and **2-50a**) were synthesized from their corresponding carboxylic acids, which can be easily obtained from commercial sources or synthesized through a Knoevenagel condensation. Through careful removal of the TBDPS group using excess amounts of buffered HF•pyr, the ester products were obtained with moderate to high yields over two steps, which include esterification and desilylation. The propionic ester **2-41a**, which resembles the target analogue **2-25** that was originally proposed, according to computer modelling, to have similar binding affinity relative to laulimalide (Figure 2-11), was obtained with a 41% yield. Analogues **2-45a** and **2-50a**, which contain electron-rich α,β-unsaturated esters were obtained with moderate yields (49% and 55% consecutively). The crotonic ester **2-47a** was obtained with a 53% yield, whereas the cinnamic ester **2-42a** was obtained with a 70% yield. Surprisingly, the more basic ester **2-44a** was obtained a 96% yield. The benzyl ester **2-46a** was obtained with a 52% yield. The heterocyclic esters **2-43a**, **2-48a** and **2-49a** were obtained with moderate to high yields (89%, 51% and 66% respectively).

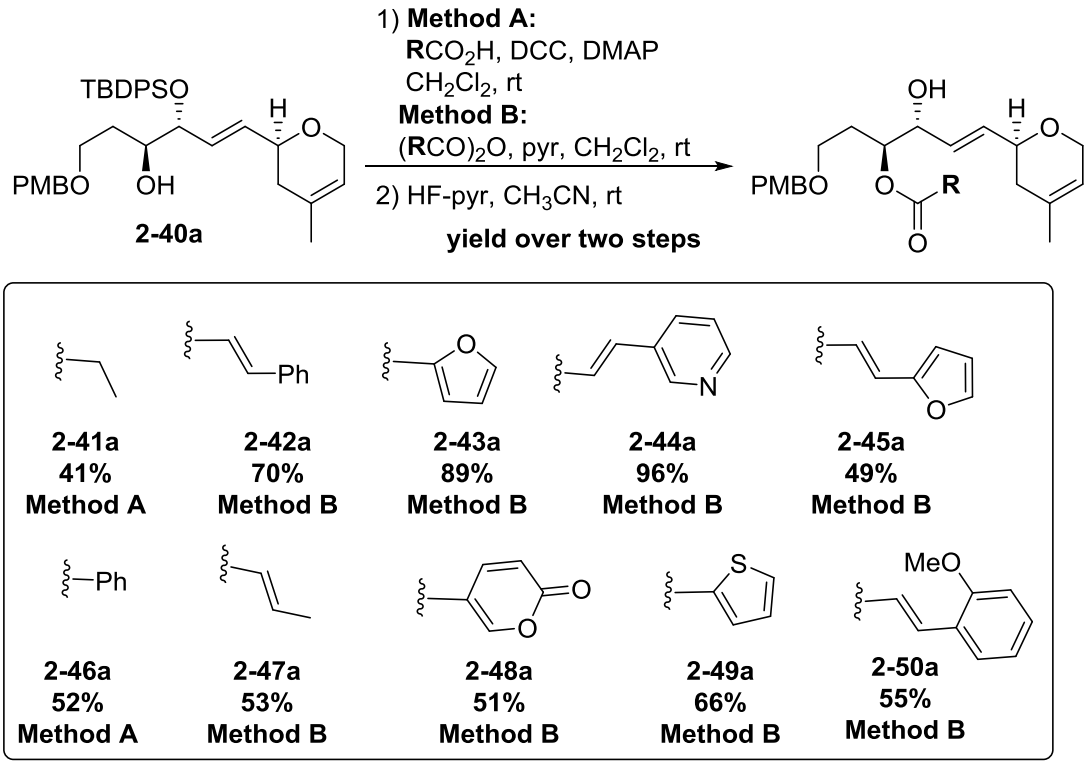

Scheme 2-10: Synthesis of the laulimalide analogues **2-41a** to **2-50a**.

During the deprotection of the TBDPS group, all esters were prone to migration to the adjacent allylic alcohol, resulting in a mixture of regioisomers (Scheme 2-11). This process would be hindered by the steric repulsions of the eclipsed substituents. The separation of the regioisomers could not be achieved using typical flash chromatography techniques. Instead, to isolate the desired regioisomer, preparative TLC was heavily relied upon. Furthermore, the challenges of separating these isomers was further exacerbated by the observed decomposition while purification. Since the 1,2-acyl migration occurred under the Brønsted acidic conditions of the desilylation step, one could predict that the chemical stability of ester linkage and its stability under mildly acidic silica during purification would result in the moderate yields obtained for most of the analogues (Scheme 2-11). Esters with more electron-rich π-systems, on the other hand, may be more stable from 1,2-acyl migrations as demonstrated by the higher yields.

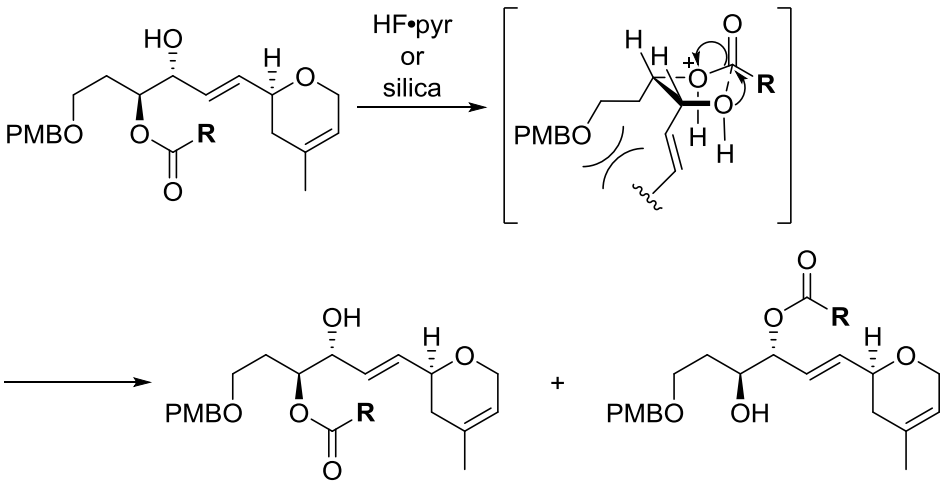

Scheme 2-11: Mechanistic rational behind the 1,2-acyl migration of analogues derived from **2-40a**.

In order to confirm that the correct regioisomer was obtained, sample **2-41** and **2-42** were examined using 2D NMR techniques, such as COSY, HSQC and HMBC (Figure 2-13). The proton geminal to the propionic ester (H^D) was confirmed based on the downfield chemical shift (δ 5.05) as well as the COSY correlation data, where it correlated to the vicinal proton H^E. Likewise, H^E was confirmed to be geminal to the hydroxyl group based on its downfield chemical shift (δ 4.24). The relevant correlations between H^E and the vinylic protons (H^A and H^B) supported that H^E, not H^D, was closest to the alkenyl group. The combined results of HSQC and HMBC were also useful in confirming the structure of **2-41a**. After correlating the protons of interest to their corresponding carbons, the carbonyl carbon (C1) exhibited a ^3J heteronuclear correlation to H^D, indicating that H^D is geminal to the ester group. The other proton, H^E, did not have the same correlation effect to the C1. Thus, **2-41a** was confirmed to be the correct regioisomer. Based on the compared retention factors (R_f's) between **2-41a** and its corresponding regioisomer, where **2-41a** would elute more slowly than the undesired regioisomer, other analogues were isolated following the R_f's of the desired products relative to their regioisomers. Lastly, analogues **2-41a** to **2-50a**, which were examined by the Schriemer group, showed no

binding affinity to the laulimalide binding site. These analogues were also unable to induce tubulin polymerization.

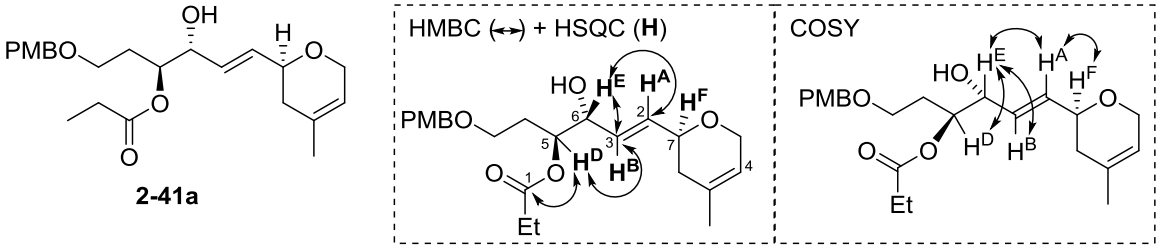

Figure 2-13: 2D NMR analysis of **2-41a**.

Based on the successful formation of analogues derived from diastereomer **2-34a**, the epimeric allylic alcohol **2-34b** was subjected to the same synthetic route in order to discover an active analogue. Using **2-34b**, a CM reaction was achieved followed by protection of the crude **2-35b** with TBDPSCl to afford the aldehyde **2-36b** with a 29% yield over two steps (Scheme 2-12). When attempting the CM using the previous conditions that afforded **2-35a**, the reaction afforded the **2-35b** with a 18% yield. As a result, the more reactive Grubbs-Hoveyda second generation catalyst (G-H II) was used at 7 mol% in order to improve the yield of the reaction. Afterward silyl-protection of **2-35b**, the Brown allylation of **2-36b** resulted in exclusive formation of the desired diastereomer **2-37b** with a 92% yield.

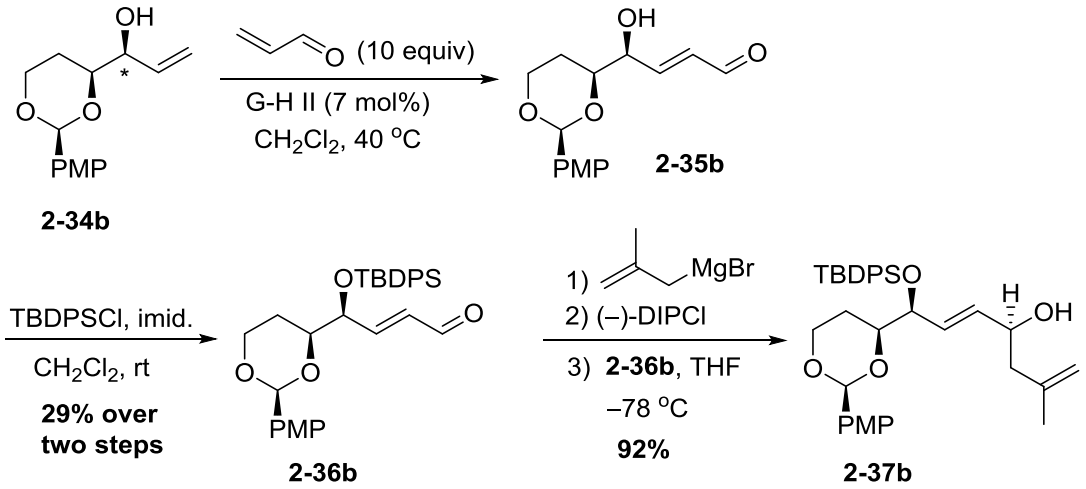

Scheme 2-12: Synthesis of **2-37b**.

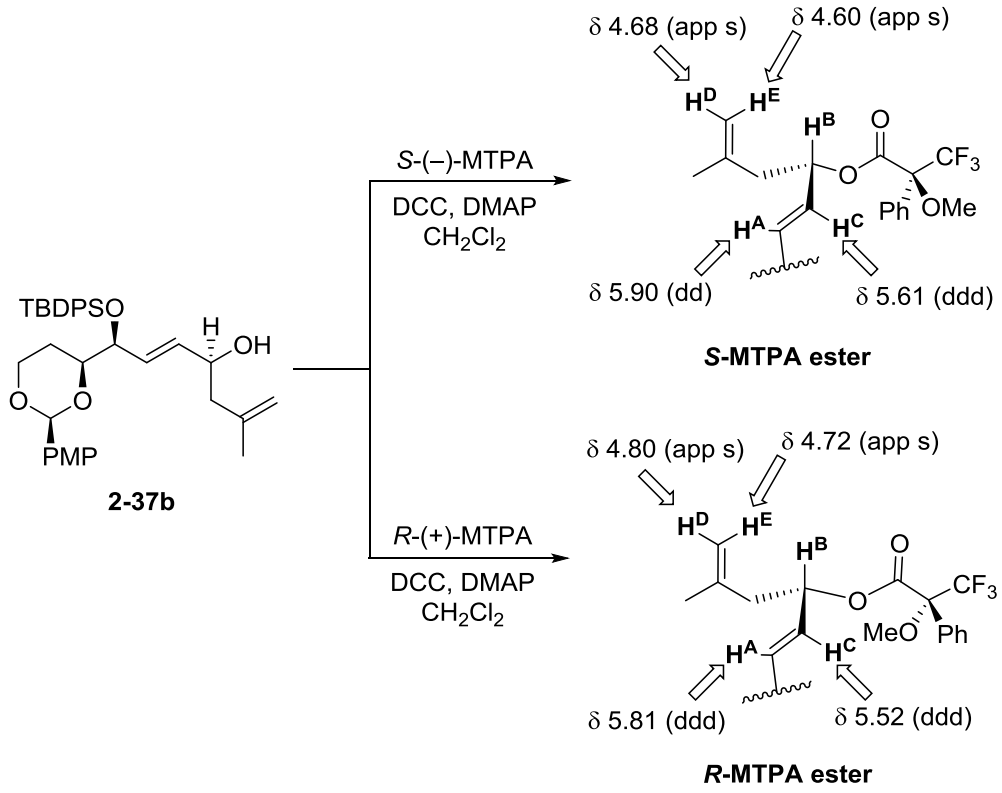

Scheme 2-13: Brown allylation and confirmation of the stereochemistry of **2-37b**.

Following the same method of analyzing the stereochemistry of **2-37a** (Scheme 2-8), the stereochemistry of the newly formed hydroxyl group of **2-37b** was investigated (Scheme 2-13). The stereochemistry of the new stereocenter of **2-37b** was confirmed through Mosher esterification analysis, where the internal (H^A and H^B) and terminal (H^C and H^D) alkenyl protons of the corresponding Mosher esters of **2-37b** were examined. The internal alkenyl proton (H^A) of the *S*-MTPA ester had a chemical shift more downfield (δ 5.90) relative to the same proton in the *R*-MTPA ester (δ 5.81). This effect was similarly observed for internal proton H^B in both Mosher esters. Based on these ^{1}H NMR results, the lack of magnetic shielding of H^A and H^B in the *S*-MTPA ester, compared to the *R*-MTPA ester, indicated that these protons were on the opposite plane to the phenyl group. Additionally, The terminal alkenyl proton (H^C) of the *S*-MTPA ester had a chemical shift more upfield (δ 4.68) relative to the same proton in the *R*-MTPA ester (δ

4.80). The other terminal alkenyl proton, H^D, also followed the same trend of magnetic shielding. protons H^C and H^D were proximal to the phenyl group and, thus, shielded. Consequently, it can be stated with high confidence that the new stereocenter of **2-37b** has a *S*-configuration.

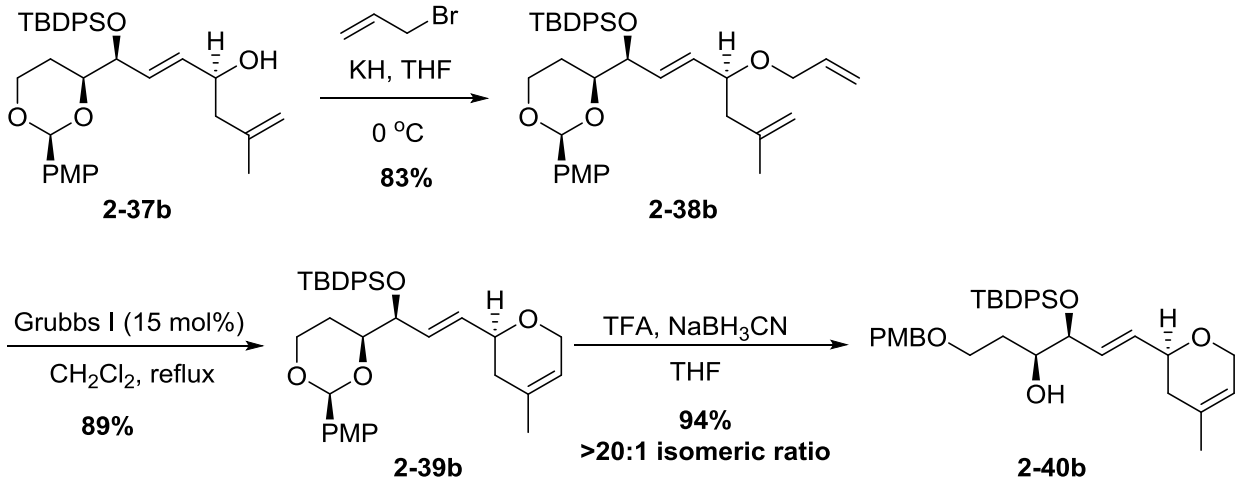

Scheme 2-14: Synthesis of target intermediate **2-40b**.

After confirming the stereochemistry of **2-37b**, the homoallylic alcohol was subjected to *O*-allylation to form **2-38b** with a 83% yield over two steps using distilled allylbromide and potassium hydride (Scheme 2-14). A RCM reaction of **2-38b** using the first-generation Grubbs catalyst at 15 mol% generated **2-39b** with a 89% yield. With **2-39b** in hand, a reductive ring-opening of the benzylidene group gave, based on ^{1}H NMR analysis of the crude reaction, nearly exclusive formation of the desired regioisomer **2-40b** with a 94% yield.

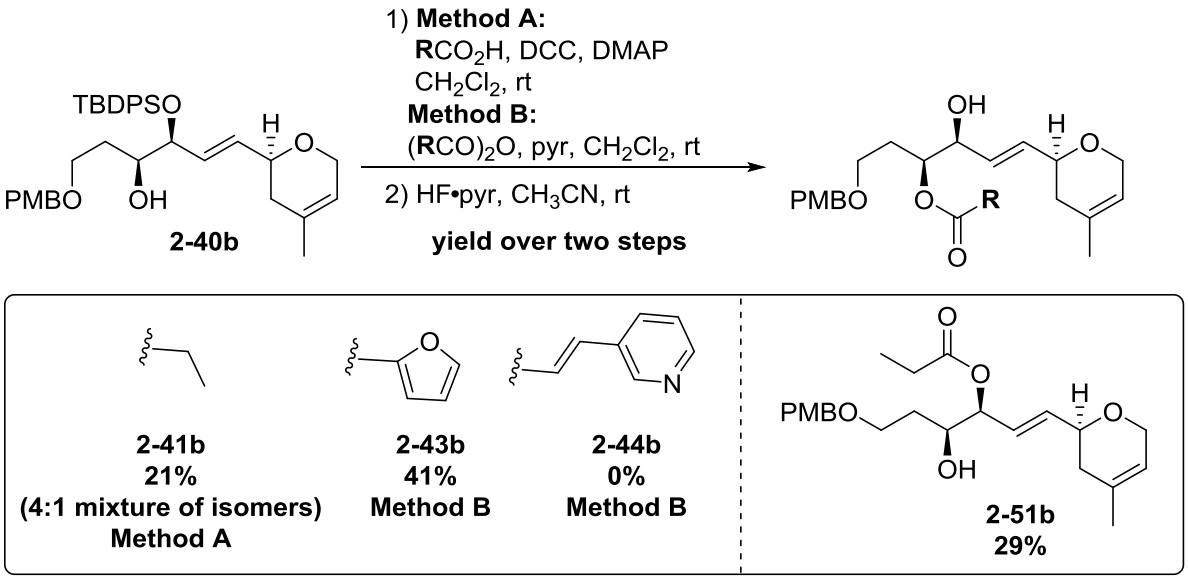

Scheme 2-15: Preliminary scope of synthesized analogues

Esterification of **2-40b** was achieved by either reacting with an acid anhydride [Method A: $(RCO)_2O$, pyridine in CH_2Cl_2 at rt)] or by using a carboxylic acid [(Method B: RCO_2H, DCC, and DMAP in CH_2Cl_2 at rt)] (Scheme 2-15). The crude product obtained from this reaction was desilylated using an excess of the HF•pyr complex. The products derived from **2-40b** were more prone to isomerization during purification relative to **2-40a**. This behavior was demonstrated during the attempted synthesis of **2-41a**, which resulted in a complicated mixture of regioisomers **2-41b** and **2-51b**. The structure of **2-51b**, the undesired regioisomer isolated with a 29% yield from the mixture of regioisomers, was confirmed by 2D NMR analysis (Figure 2-14). When analyzing the COSY spectra, the proton geminal to the propionic ester (H^D) was determined from its downfield chemical shift (δ 5.27) and the correlation to the vicinal protons, H^B and H^F. Since H^D had a strong correlation to the alkenyl proton H^B, there was little doubt that the structure of **2-51b** was the undesired regioisomer. To further support the proposed structure, the HMQC and HMBC spectra of **2-51b** were analyzed. First, when the HMQC spectra was analyzed, the protons of interest were designated to the corresponding carbons atoms that they are bound to.

Through HMBC analysis, it was observed that H^D is geminal to the ester group, since this proton had a ^3J correlation to the carbonyl-based carbon (C1). Furthermore, H^D had strong ^2J- and ^3J-correlations to the neighboring alkenyl groups (C2 and C3 respectively), whereas H^F does not. Therefore, the stereochemistry of **2-51** was confirmed to be of the undesired regioisomer.

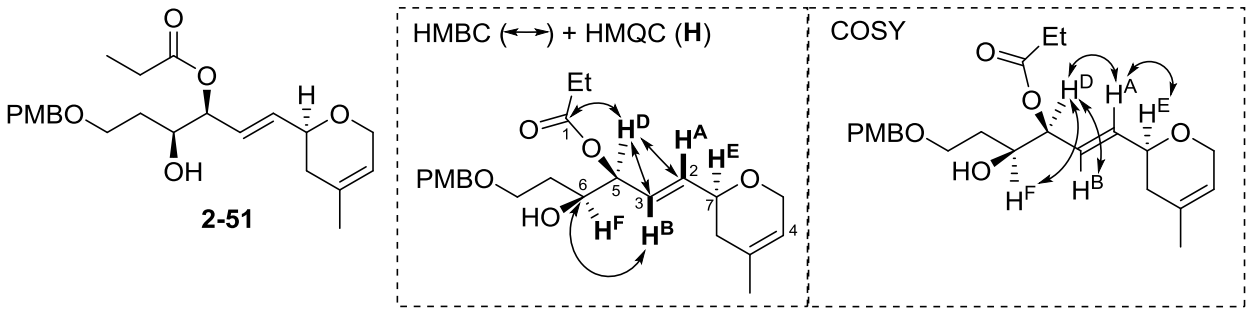

Figure 2-14: 2D NMR analysis of **2-51b.**

When the 2-furanyl carboxylate ester **2-43b** was synthesized, the regioisomers were separable allowing for the isolation of the desired analogue in a 41% yield. When attempting the same conditions to form the *anti*-3-(3-pyridyl) acrylic ester **2-44b**, the product could not be obtained due to decomposition during purification. These products were more prone to 1,2-acyl migrations, where repeated efforts were required to obtain a partial purification of **2-41b** and an isolated yield of **2-43b**. The ease of the 1,2-acyl migration can be rationalized where, unlike the analogues derived from **2-40a** (Scheme 2-11), the vicinal hydroxyl group is more able to approach the ester due to a decrease in steric repulsion of the pseudo-eclipsed substituents (Scheme 2-16).

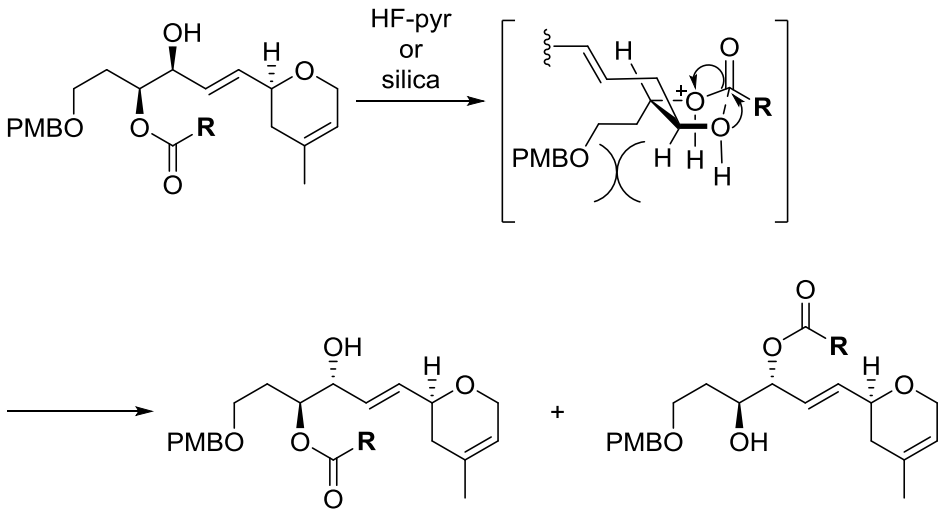

Scheme 2-16: Mechanistic rational for 1,2-acyl migration of analogues derived from **2-40b**.

2.4 Summary

Following our synthetic route to form the target analogue that was initially proposed by Melissa Gajewski from the Tuszynski group, several preliminary issues were addressed (Figure 2-15). The organometallic vinyl addition onto the corresponding aldehyde **2-26** was not diastereoselective, unfortunately it did not follow a Cram-chelate model to selectively form **2-27b** with the correct *syn*-diol stereochemistry. Instead, the Felkin-Ahn model led to the synthesis of the undesired product **2-27a**. Secondly, the CM reaction, though a powerful method of coupling two olefinic species, was inconsistent in forming products with acceptable yields. On the other hand, the asymmetric Brown allylboration proved to be a reliable method for a highly diastereoselective allylation of the unsaturated aldehyde, allowing a nearly exclusive formation of the desired diastereomer. The Brønsted acid-driven reductive ring-opening of the *para*-methoxybenzylidene group favoured the formation of the desired isomer with excellent regioselectivity. Lastly, the desilylation of the secondary alcohol was complicated by a 1,2-acyl migration. This inconvenience was further exacerbated upon purification of the products either

by preparative TLC or flash chromatography. This outcome may indicate a closer connection between laulimalide and neolaulimalide, where, over time, laulimalide might decompose or metabolize into neolaulimalide. HDX MS analysis of the analogues derived from **2-40a**, tested by the Schriemer group showed no binding affinity or ability to promote tubulin polymerization. The evaluation of analogues **2-40b**, **2-41b**, **2-43b** and **2-51b**, by the the Schriemer group are ongoing.

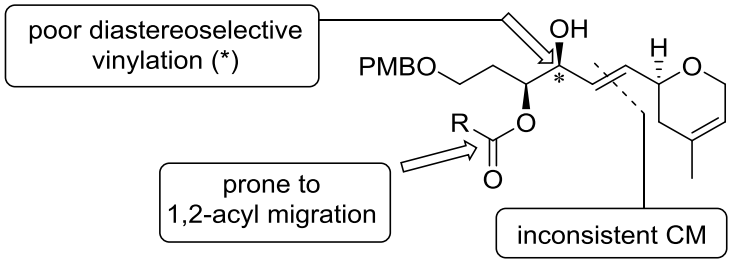

Figure 2-15: Problems addressed with the current synthetic route.

There are several ways to address the issues mentioned above. Using the remaining amounts of **2-40b,** one final analogue, **2-52b**, can be made that contains the endomacrocyclic dihydropyran similar to laulimalide (Figure 2-16). This motivation behind designing this synthetic target can be justified by the X-ray crystallographic result obtained by the Steinmetz group (Section 2.3, Figure 2-4), where the second dihydropyran was believed to interact with the binding site.

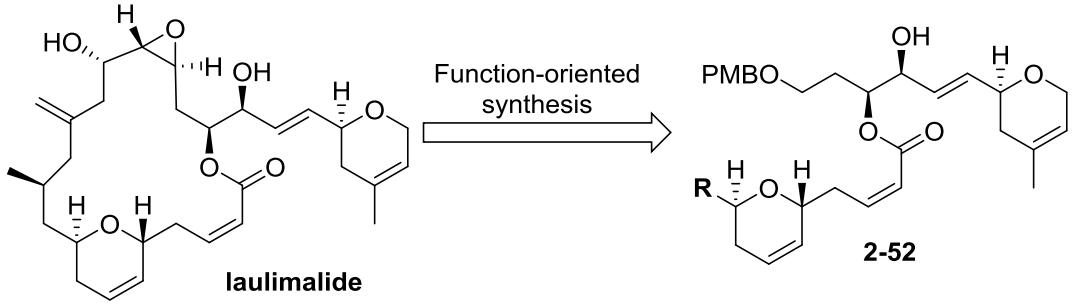

Figure 2-16: Potential analogue designed through function-oriented synthesis.

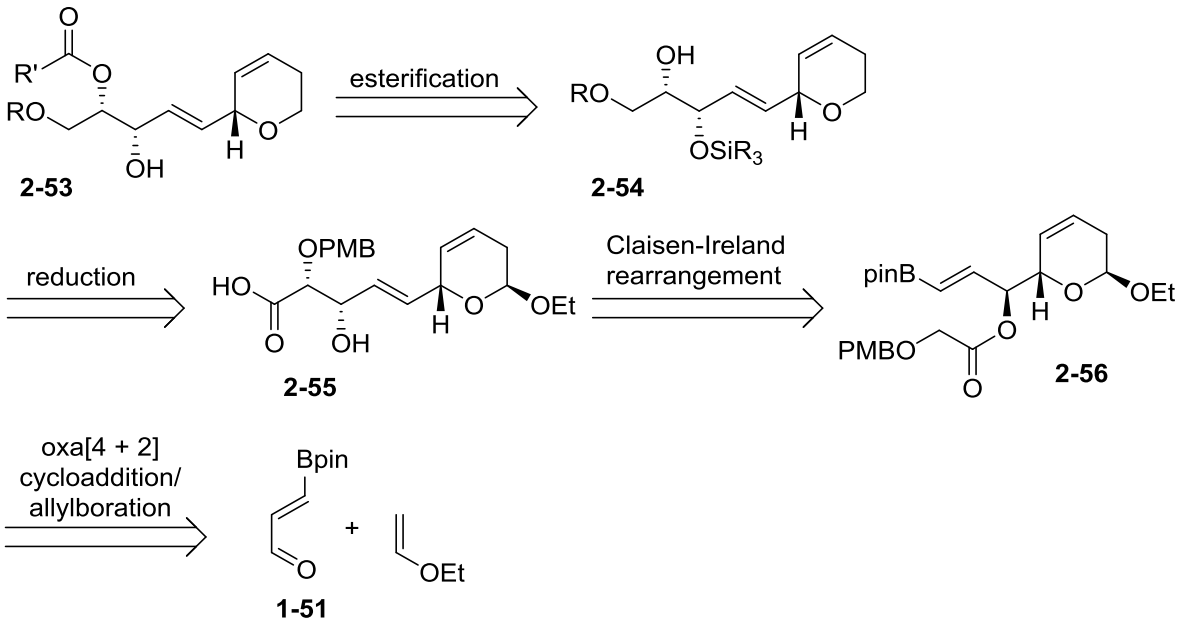

Scheme 2-17: Retrosynthesis of a new class of laulimalide analogues implementing the sequential enantioselective hetero[4+2] cycloaddition/allylboration reaction followed by a Claisen-Ireland [3,3] rearrangement.

Furthermore, another class of potentially active analogues (**2-53**) could be investigated (Scheme 2-17). The synthesis of these derivatives would begin with using the in-house asymmetric oxa[4+2] cycloaddition/allylboration between boronoacrolein pinacolate (**1-51**) and ethyl vinyl ether, which was developed by the Hall group.[40,41] The derivatives of **2-53**, could be made through a more optimal method of esterification of **2-54**, where the 1,2-acyl migration would be minimized. Compound **2-54** may be accessed through a reduction of the carboxylic acid of **2-55** followed by reductive displacement of the ethoxy group. Lastly, **2-55** would be accessed through a Claisen-Ireland rearrangement from **2-56**, a process that has been previously implemented toward the synthesis of palmerolide A.[41] To address the issue of the 1,2-acyl migration, which plagued the synthesis of analogues described in this chapter, would be to modify the target analogue such that the ester group was replaced with an amide (Scheme 2-18). This could be achieved through a possible chemo-, regio- and stereoselective formation of amino alcohols.

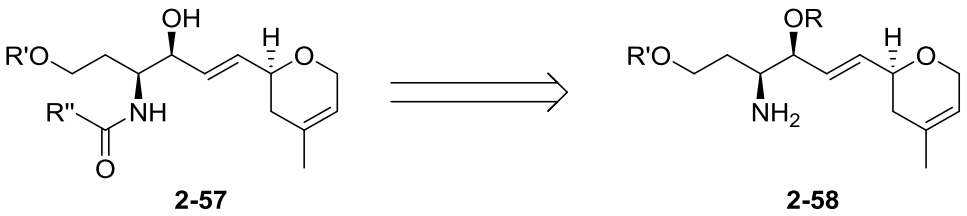

Scheme 2-18: Possible solution to address the 1,2-acyl migration.

2.5 Supporting Information

2.5.1 General information

Unless otherwise stated, all reactions were performed under a nitrogen atmosphere using flame-dried glassware. Hydroboration of L-(–)-malic acid was done following the literature procedure.[42] The *para*-methoxybenzylidene protection to form **2-25** was achieved following the reported procedure in literature, but with the benzene solvent replaced with toluene.[43] When following the literature procedure, **2-26** was formed through a Swern oxidation and was used immediately in the subsequent reaction after purification.[44] The reactant, *trans*-furan-2-acrylic acid, was synthesized following the reported procedure in literature.[45] Before using in a reaction, KH was prewashed with hexanes, filtered and dried *in vacuo*. Powdered 4Å molecular sieves (<5 micron, Aldrich) were dried in an oven (300 ^{o}C) followed by flame-drying in a dry round bottom flask *in vacuo*. Acrolein was distilled before use. THF and dichloromethane were obtained from a MBraun MB SPS* solvent system prior to use. The anhydrous acetonitrile was purchased from Sigma-Aldrich (99.8% purity). Unless otherwise stated, all reagents were purchased from Sigma-Aldrich and used as received. Thin layer chromatography (TLC) was performed on Merck Silica Gel 60 F254 plates and was visualized with UV light, *p*-anisaldehyde and $KMnO_4$ stain. NMR spectra were recorded on INOVA-400, INOVA-500 or INOVA-700 MHz instruments. The residual solvent protons (^{1}H) of $CDCl_3$ (7.26 ppm) or C_6D_6 (7.15 ppm) and the solvent carbons

(^{13}C) of $CDCl_3$ (77.06 ppm) were used as internal standards. ^{1}H NMR data is presented as follows: chemical shift in ppm (δ) downfield from tetramethylsilane (multiplicity, coupling constant, integration). The following abbreviations are used in reporting NMR data: s, singlet; br s, broad singlet; d, doublet; t, triplet; q, quartet; dd, doublet of doublets; ddd, doublet of doublet of doublets; dddd, doublet of doublet of doublet of doublets; app s, apparent singlet; app ddt, apparent doublet of doublet of triplets; m, multiplet. High-resolution mass spectra (HRMS) were recorded by the University of Alberta Mass Spectrometry Services Laboratory using either electron impact (EI) or electrospray ionization (ESI) techniques. Infrared spectra were obtained on a Nicolet Magna-IR with frequencies expressed in cm^{-1}. Optical rotations were measured using a 1 mL cell with a 1 dm length on a Perkin Elmer 241 polarimeter. Melting points were determined in a capillary tube using a Gallenkamp melting point apparatus and are uncorrected.

2.5.2 Experimental procedures and spectral data

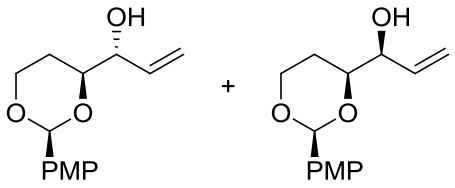

2-34a **2-34b**

(1*R*)-1-[(2*S*,4*S*)-2-(4-Methoxyphenyl)-1,3-dioxan-4-yl]prop-2-en-1-ol (2-34a) and (1*S*)-1-[(2*S*,4*S*)-2-(4-Methoxyphenyl)-1,3-dioxan-4-yl]prop-2-en-1-ol (2-34b)

A solution of aldehyde **2-26** (4.79 g, 21.6 mmol) in THF (44 mL) was treated with vinylmagnesium chloride solution (1.5 M in THF, 27 mL, 27 mmol) dropwise at –78 °C. The mixture was stirred overnight at –78 °C. Once the reaction was complete, the reaction mixture was treated with saturated NH_4Cl (100 mL) then allowed to warm to 0 °C. After 30 minutes, the

solution was transfered into a separatory funnel and washed with CH_2Cl_2 (3 × 30 mL). The organic fraction was washed with water (50 mL), brine (50 mL) then dried ($MgSO_4$). The solution was filtered then concentrated to obtain a crude mixture of diastereomers. Once the reaction was repeated two more times at similar scales, the crude products were pooled together and were subjected to flash chromatography on silica gel (5% acetone and 30% hexanes in CH_2Cl_2) to obtain the diastereomers **2-34b** (1.50 g, 9%) and **2-34a** (4.00 g, 24%).

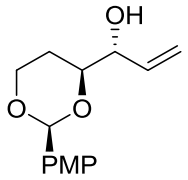

(1*R*)-1-[(2*S*,4*S*)-2-(4-Methoxyphenyl)-1,3-dioxan-4-yl]prop-2-en-1-ol (2-34a)

Clear oil; R_f = 0.42 (5% acetone and 40% petroleum ether in CH_2Cl_2);

$[\alpha]^{20}_{D}$ +5.73 (*c* 1.34, CH_2Cl_2).

^{1}H NMR (400 MHz, $CDCl_3$) δ 7.47–7.36 (m, 2 H), 6.97–6.83 (m, 2 H), 5.91 (ddd, *J* = 17.3, 10.6, 5.9 Hz, 1 H), 5.51 (s, 1 H), 5.38 (ddd, *J* = 17.3, 1.6, 1.6 Hz, 1 H), 5.26 (ddd, *J* = 10.7, 1.4, 1.2 Hz, 1 H), 4.29 (ddd, *J* = 11.4, 5.1, 1.3 Hz, 1 H), 3.93–3.89 (m, 2 H), 3.84–3.76 (m, 3 H), 2.29 (d, *J* = 3.8 Hz, 1 H), 2.03 (dddd, *J* = 13.3, 12.5, 11.7, 5.1 Hz, 1 H), 1.62 (s, 1 H), 1.46 (dddd, *J* = 13.6, 2.8, 2.6, 1.4 Hz, 1 H).

^{13}C NMR (101 MHz, $CDCl_3$) δ 160.1, 135.7, 131.0, 127.4, 117.1, 113.7, 101.2, 79.4, 74.3, 66.8, 55.3, 24.8.

IR (cast film, cm^{-1}) 3427, 2961, 2928, 2853, 1680, 1614, 1599, 1248.

HRMS (EI) for $C_{14}H_{18}O_4$ (m/z): calcd. 250.12051; found 250.12048.

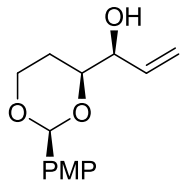

2-27b

(1*S*)-1-[(2*S*,4*S*)-2-(4-Methoxyphenyl)-1,3-dioxan-4-yl]prop-2-en-1-ol (2-34b)

Clear oil; R_f = 0.50 (5% acetone and 40% petroleum ether in CH_2Cl_2);

$[\alpha]^{20}_{D}$ +4.92 (*c* 1.34, CH_2Cl_2).

^{1}H NMR (700 MHz, $CDCl_3$) δ 7.43–7.39 (m, 2 H), 6.92–6.88 (m, 2 H), 5.85 (ddd, *J* = 17.1, 10.5, 6.6 Hz, 1 H), 5.49 (s, 1 H), 5.42 (app dt, *J* = 17.2, 1.4 Hz, 1 H), 5.30–5.26 (m, 1 H), 4.28 (ddd, *J* = 11.5, 5.1, 1.3 Hz, 1 H), 4.10–4.06 (m, 1H), 3.93 (ddd, *J* = 12.4, 11.6, 2.6 Hz, 1 H), 3.81 (s, 3 H), 3.75 (ddd, *J* = 11.5, 7.2, 2.4 Hz, 1 H), 2.68 (d, *J* = 3.1 Hz, 1 H), 1.87 (dddd, *J* = 13.2, 12.5, 11.6, 5.2 Hz, 1 H), 1.51 (dddd, *J* = 13.3, 2.6, 2.5, 1.5 Hz, 1 H).

^{13}C NMR (176 MHz, $CDCl_3$) δ 160.1, 135.5, 130.9, 127.5, 118.3, 113.7, 101.3, 79.8, 75.7, 66.6, 55.4, 27.1.

IR (cast film, cm^{-1}) 3476, 2931, 2855, 1615, 1588, 1518, 1249.

HRMS (ESI) for $C_{14}H_{18}NaO_4$ $[M + Na]^+$ (m/z): calcd. 273.1097; found 273.1097, for $C_{14}H_{19}O_4$ $[M + H]^+$ (m/z): calcd. 251.1278; found 251.1277.

Synthesis of diastereomer 2-40a

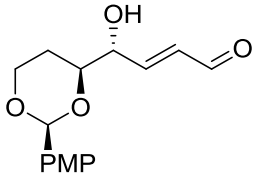

(2*E*,4*R*)-4-Hydroxy-4-[(2*S*,4*S*)-2-(4-methoxyphenyl)-1,3-dioxan-4-yl]but-2-enal (2-35a)

To a degassed solution of diether ether containing allylic alcohol **2-34a** (2.38 g, 9.51 mmol) was added CuI (90.2 mg, 0.474 mmol, 5 mol%), followed by acrolein (6.00 mL, 87.2 mmol, 9.2

equiv). The solution was degassed for an additional 30 minutes followed by slow addition of a solution of Grubbs second-generation catalyst in diethyl ether (14 mL, 258 mg, 0.304 mmol, 3 mol%). The reaction was stirred overnight under reflux with nitrogen bubbling. Then, the mixture was allowed to cool to room temperature. The reaction mixture was concentrated and the crude product was immediately subjected to flash chromatography on silica gel to afford the title compound (1.63 g, 62%).

White amorphous solid; R_f = 0.22 (50% EtOAc/hexanes).

$[\alpha]^{20}_D$ +30.3 (*c* 1.39, CH_2Cl_2).

^{1}H NMR (400 MHz, $CDCl_3$) δ 9.61 (d, *J* = 7.8 Hz, 1 H), 7.45–7.36 (m, 2 H), 6.93–6.88 (m, 2 H), 6.85 (dd, *J* = 15.8, 4.4 Hz, 1 H), 6.43 (ddd, *J* = 15.8, 7.8, 1.8 Hz, 1 H), 5.52 (s, 1 H), 4.57 (dd, *J* = 4.3, 1.6 Hz, 1 H), 4.31 (ddd, *J* = 11.4, 5.1, 1.2 Hz, 1 H), 4.02 (ddd, *J* = 11.6, 4.3, 2.6 Hz, 1 H), 3.95 (ddd, *J* = 12.3, 11.7, 2.5 Hz, 1 H), 3.81 (s, 3 H), 2.54 (d, *J* = 4.3 Hz, 1 H), 2.03 (ddd, *J* = 25.4, 12.6, 5.1 Hz, 1 H), 1.47 (ddd, *J* = 13.3, 3.9, 2.5 Hz, 1 H).

^{13}C NMR (100 MHz, $CDCl_3$) δ 193.2, 160.2, 153.2, 132.7, 130.6, 127.4, 113.8, 101.4, 78.6, 72.8, 66.6, 55.4, 25.4.

IR (cast film, cm^{-1}) 3436, 2964, 2930, 2851, 2733, 1688, 1614, 1518, 1250, 1105.

HRMS (ESI) for $[M + Na]^+$ $C_{15}H_{18}NaO_5$ (m/z): calcd. 301.1046; found 301.1044.

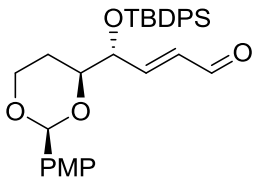

(2*E*,4*R*)-4-{[*tert*-Butyl(diphenyl)silyl]oxy}-4-[(2*S*,4*S*)-2-(4-methoxyphenyl)-1,3-dioxan-4-yl]but-2-enal (2-36a)

To a solution of conjugated aldehyde **2-35a** (1.60 g, 5.74 mmol) in CH_2Cl_2 (29 mL) was added

imidazole (794 mg, 11.5 mmol, 2.01 equiv) followed by TBDPSCl (3.26 g, 6.31 mmol, 1.1 equiv) at 0°C. After consumption of starting material, saturated NH_4Cl (30 mL) was added. The resulting biphasic solution was added to a separatory funnel followed by extracting using CH_2Cl_2 (2 × 20 mL). The organic phase was separated and subsequently washed with brine (30 mL) then dried ($MgSO_4$), filtered, and concentrated. The crude product was subjected to flash chromatography on silica gel (5 to 30% EtOAc/hexanes) to afford the title compound (2.29 g, 77%).

white waxy oil; R_f = 0.40 (30% EtOAc/hexanes).

$[\alpha]^{20}_D$ +20.2 (*c* 1.22, CH_2Cl_2).

^{1}H NMR (500 MHz, $CDCl_3$) δ 9.39 (d, *J* = 7.9 Hz, 1 H), 7.77–7.61 (m, 3 H), 7.48–7.41 (m, 2 H), 7.39–7.32 (m, 3 H), 6.95–6.86 (m, 2 H), 6.72 (dd, *J* = 15.8, 6.0 Hz, 1 H), 6.09 (ddd, *J* = 15.8, 7.9, 1.3 Hz, 1 H), 5.43 (s, 1 H), 4.54 (ddd, *J* = 5.9, 4.7, 1.2 Hz, 1 H), 4.32–4.23 (m, 1 H), 3.95–3.86 (m, 2 H), 3.85 (s, 3 H), 1.94 (dddd, *J* = 12.5, 12.2, 12.1, 5.2 Hz, 1 H), 1.51 (dd, J = 13.2, 1.4 Hz, 1 H), 1.14 (s, 9 H).

^{13}C NMR (126 MHz, $CDCl_3$) δ 193.2, 160.0, 155.1, 136.1, 136.0, 133.2, 133.0, 132.8, 130.9, 130.1, 130.0, 127.8, 127.7, 127.4, 113.6, 101.2, 79.7, 76.8, 75.2, 66.7, 55.3, 27.0, 26.6, 19.5.

IR (cast film, cm^{-1}) 3071, 2999, 2960, 2931, 2857, 1693, 1615, 1588, 1517, 1112.

HRMS (ESI) for $[M + K]^+$ $C_{31}H_{36}KO_5Si$ (m/z): calcd. 555.1964; found 555.1960, $[M + Na]^+$ $C_{31}H_{36}NaO_5Si$ (m/z): calcd. 539.2224; found 539.2218, $[M + H]^+$ $C_{31}H_{37}O_5Si$ (m/z): calcd. 517.2405; found 517.2400.

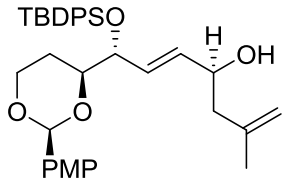

(4*S*,5*E*,7*R*)-7-{[*tert*-Butyl(diphenyl)silyl]oxy}-7-[(2*S*,4*S*)-2-(4-methoxyphenyl)-1,3-dioxan-4-yl]-2-methylhepta-1,5-dien-4-ol (2-37a)

To a solution of (−)-DIPCl (0.98 M in THF, 17.5 mL, 4.00 equiv) at 0 °C was added a solution of β-methallylmagnesium chloride in THF (0.45 M in THF, 23 mL, 2.40 equiv). The reaction mixture was stirred for 2 h at 0°C. After cooling the reaction mixture to −78 °C, a solution of enal **2-36a** (2.19 g, 4.25 mmol) in THF (21 mL) was slowly added over a period of 30 min then stirred overnight at −78 °C. The reaction was treated with 1N NaOH (35 mL) then warmed to 0 °C at which point H_2O_2 (1.8 mL) was added then the reaction mixture was allowed to warm to rt. The resulting mixture was extracted with CH_2Cl_2 (3 × 30 mL). The organic fractions were pooled together and washed with brine (30 mL), and dried over $MgSO_4$. The solution was filtered and concentrated to obtain a crude mixture of diastereomers in >10:1 dr based on ^{1}H NMR analysis. The crude product was subjected to flash chromatography (45% petroleum ether/CH_2Cl_2 then 5% acetone and 40% petroleum ether in CH_2Cl_2) to afford the title compound (2.24 g, 92%).

Clear oil; R_f = 0.36 (30% EtOAc/hexanes).

$[\alpha]^{20}_D$ +5.92 (*c* 1.22, CH_2Cl_2).

^{1}H NMR (500 MHz, C_6D_6) δ 7.93–7.87 (m, 2 H), 7.84–7.77 (m, 2 H), 7.65–7.58 (m, 2 H), 7.24–7.17 (m, 6 H), 6.87–6.80 (m, 2 H), 5.69 (ddd, *J* = 15.5, 7.5, 1.2 Hz, 1 H), 5.41 (s, 1 H), 5.33 (ddd, *J* = 15.5, 5.8, 0.7 Hz, 1 H), 4.74 (d, *J* = 1.4 Hz, 1 H), 4.67 (d, *J* = 0.9 Hz, 1 H), 4.43 (dd, *J* = 7.5, 3.7 Hz, 1 H), 4.06 (dd, *J* = 11.3, 4.4 Hz, 1 H), 3.93 (d, *J* = 5.1 Hz, 1 H), 3.64 (ddd, *J* = 11.3, 3.5, 2.4 Hz, 1 H), 3.54 (app td, *J* = 12.6, 2.4 Hz, 1 H), 3.27 (s, 3 H), 2.12 (ddd, *J* = 24.3,

12.7, 5.1 Hz, 1 H), 1.98 (dd, *J* = 13.8, 8.2 Hz, 1 H), 1.92 (dd, *J* = 13.8, 5.2 Hz, 1 H), 1.52 (s, 3 H), 1.26–1.22 (m, 10 H), 1.01 (d, *J* = 3.4 Hz, 1 H).

^{13}C NMR (126 MHz, $CDCl_3$) δ 159.8, 142.0, 136.3, 136.2, 135.1, 135.1, 134.6, 133.6, 131.4, 129.9, 129.6, 129.6, 127.5, 127.4, 127.4, 113.4, 101.1, 80.4, 76.23, 69.4, 69.3, 67.0, 55.3, 45.4, 45.3, 29.7, 27.0, 26.0, 22.4, 19.4.

IR (cast film, cm^{-1}) 3471, 3071, 2997, 2961, 2930, 2894, 2856, 1615, 1518, 1463, 1111.

HRMS (ESI) for $[M + K]^+$ $C_{35}H_{44}KO_5Si$ (m/z): calcd. 611.259; found 611.2593, $[M + Na]^+$ $C_{35}H_{44}NaO_5Si$ (m/z): calcd. 595.285; found 595.2849, $[M + NH_4]^+$ $C_{35}H_{48}NaO_5Si$ (m/z): calcd. 590.3296; found 590.3304, $[M + H]^+$ $C_{35}H_{45}O_5Si$ (m/z): calcd. 573.3031; found 573.3027.

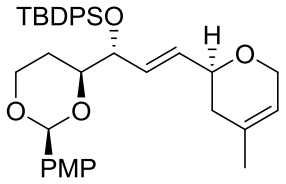

***tert*-Butyl({(1*R*,2*E*)-1-[(2*S*,4*S*)-2-(4-methoxyphenyl)-1,3-dioxan-4-yl]-3-[(2*S*)-4-methyl-3,6-dihydro-2*H*-pyran-2-yl]prop-2-en-1-yl}oxy)diphenylsilane (2-39a)**

To a solution of homoallylic alcohol **2-37a** (2.12 g, 3.70 mmol) and allyl bromide (0.910 mL, 10.4 mmol, 2.81 equiv) in THF (74 mL) was added KH (443 mg, 11.0 mmol, 3.0 equiv) at 0°C and the solution was stirred vigorously, while gradually allowed to rt, for 3 h. The solution was cooled to 0 °C then treated with saturated NH_4Cl solution (50 mL) and the resulting biphasic solution was extracted with Et_2O (100 mL). The organic fraction was separated, washed with brine (50 mL), dried ($MgSO_4$), filtered, and concentrated. The crude oil was subjected to flash chromatography (10 to 15% Et_2O/hexanes) to afford the allylic intermediate **2-38a** (1.83 g, 81%). The allylic intermediate **2-38a** (1.59 g, 2.60 mmol) was diluted in CH_2Cl_2 (260 mL) and Grubbs first generation catalyst (106 mg, 0.129 mmol, 5 mol%) was added and stirred overnight

at room temperature. The reaction mixture was concentrated and the crude product was subjected to flash chromatography on silica gel (10 to 15% EtOAc/hexanes) to afford the title compound (1.20 g, 79%).

Clear oil; R_f = 0.18 (10% EtOAc/hexanes).

$[\alpha]^{20}_{D}$ –22.0 (*c* 1.46, CH_2Cl_2).

^{1}H NMR (500 MHz, C_6D_6) δ 7.93–7.89 (m, 2 H), 7.86–7.80 (m, 2 H), 7.63–7.58 (m, 2 H), 7.21–7.19 (m, 6 H), 6.86–6.81 (m, 2 H), 5.84 (ddd, *J* = 15.7, 7.0, 1.5 Hz, 1 H), 5.60 (ddd, *J* = 15.7, 5.1, 1.0 Hz, 1 H), 5.39 (br s, 1 H), 5.12 (s, 1 H), 4.49 (dd, *J* = 7.0, 3.4 Hz, 1 H), 4.11–3.99 (m, 2 H), 3.98–3.92 (m, 1 H), 3.80–3.72 (m, 1 H), 3.66–3.59 (m, 1 H), 3.50 (ddd, *J* = 12.5, 12.0, 1.7 Hz, 1 H), 3.27 (s, 3 H), 2.13 (dddd, *J* = 13.0, 13.5, 12.1, 5.0 Hz, 1 H), 1.84–1.74 (m, 1 H), 1.48 (d, *J* = 15.8 Hz, 4 H), 1.27–1.19 (m, 11 H).

^{13}C NMR (126 MHz, C_6D_6) δ 160.3, 136.8, 136.7, 134.8, 134.3, 133.9, 132.3, 131.2, 129.8, 129.8, 129.1, 128.1, 127.8, 120.4, 113.6, 101.6, 80.6, 76.7, 73.1, 66.8, 65.6, 54.7, 35.8, 30.4, 27.4, 25.6, 22.9, 19.8.

IR (cast film, cm^{-1}) 3071, 2961, 2930, 2855, 1615, 1517, 1249, 1112.

HRMS (ESI) for $[M + Na]^+$ $C_{36}H_{44}NaO_5Si$ (m/z): calcd. 607.2850; found 607.2855, $[M + H]^+$ $C_{36}H_{45}O_5Si$ (m/z): calcd. 585.3031; found 585.3017.

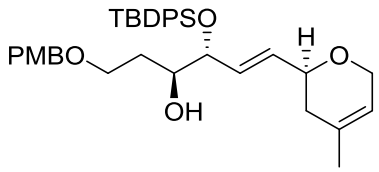

(3*S*,4*R*,5*E*)-4-{[*tert*-Butyl(diphenyl)silyl]oxy}-1-[(4-methoxybenzyl)oxy]-6-[(2*S*)-4-methyl-3,6-dihydro-2*H*-pyran-2-yl]hex-5-en-3-ol (2-40a)

To a solution of **2-39a** (570 mg, 0.975 mmol) in DMF (19.5 mL) was added 4Å MS (165 mg)

followed by $NaBH_3CN$ (397 mg, 6.3 mmol, 6.5 equiv) at 0 °C. The reaction mixture was treated with TFA (0.278 mL, 3.63 mmol, 3.7 equiv) then the reaction mixture was gradually allowed to warm to rt overnight. When the starting material was fully consumed, the reaction was treated with Et_3N (0.5 mL) then the solution was diluted with saturate NH_4Cl (100 mL) then extracted with CH_2Cl_2 (5 × 25 mL). The organic fractions were pooled together and washed with brine (25 mL) then dried ($MgSO_4$), filtered, and concentrated to afford a crude mixture of the desired regioisomer in a 6:1 mixture of isomers as confirmed by ^1H NMR. The crude product was purified by flash chromatography (10 to 50% Et_2O/hexanes) to afford the title compound (462 mg, 81%).

Clear oil; R_f = 0.24 (50% Et_2O/hexanes).

$[\alpha]^{20}_D$ –47.8 (*c* 1.39, CH_2Cl_2).

^{1}H NMR (500 MHz, C_6D_6) δ 7.87–7.76 (m, 4 H), 7.21–7.19 (m, 6 H), 7.16–7.11 (m, 2 H), 6.80–6.73 (m, 2 H), 5.95 (ddd, *J* = 15.8, 7.5, 1.5 Hz, 1 H), 5.57 (ddd, *J* = 15.8, 5.0, 0.8 Hz, 1 H), 5.11 (br s, 1 H), 4.35 (dd, *J* = 7.5, 3.5 Hz, 1 H), 4.28–4.18 (m, 2 H), 4.11–4.02 (m, 1 H), 4.01–3.90 (m, 2 H), 3.81–3.73 (m, 1 H), 3.56–3.41 (m, 2 H), 3.30 (s, 3 H), 2.69 (d, *J* = 3.0 Hz, 1 H), 1.91–1.73 (m, 3 H), 1.53–1.45 (m, 4 H), 1.18 (s, 9 H).

^{13}C NMR (126 MHz, C_6D_6) δ 159.6, 136.6, 136.4, 134.5, 134.4, 134.4, 131.22, 131.1, 130.0, 129.8, 129.3, 128.6, 128.3, 128.1, 127.9, 120.4, 114.0, 78.3, 73.7, 73.1, 72.8, 68.04, 65.6, 54.7, 35.8, 32.6, 27.3, 22.9, 19.7.

IR (cast film, cm^{-1}) 3478, 3071, 2957, 2930, 2856, 1612, 1513, 1248, 1111.

HRMS (ESI) for $[M + Na]^+$ $C_{36}H_{46}NaO_5Si$ (m/z): calcd. 609.3007; found 609.2998, $[M + NH_4]^+$ $C_{36}H_{50}NO_5Si$ (m/z): calcd. 604.3453; found 604.3454.

General procedure for esterification of products derived from 2-34a

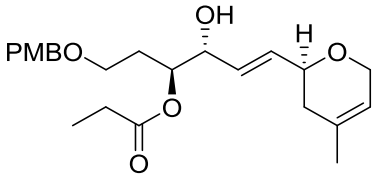

(1*S*,2*R*,3*E*)-2-Hydroxy-1-{2-[(4-methoxybenzyl)oxy]ethyl}-4-[(2*S*)-4-methyl-3,6-dihydro-2*H*-pyran-2-yl]but-3-en-1-yl propionate (2-41a)

To a solution of alcohol **2-40a** (15.9 mg, 0.0271 mmol) in THF (0.500 mL) was added DMAP (1.8 mg, 0.015 mmol, 54 mol%), pyridine (7.00 μL, 0.0922 mmol, 3.4 equiv) then propionic anhydride (7.00 μL, 0.0570 mmol, 2.1 equiv). After stirring the solution overnight at rt, the solution was concentrated and the residue was directly subjected to flash chromatography (5% to 20% Et_2O/hexanes) to afford the ester product. The silyl-protected product was then transferred to a plastic vessel containing a stir bar using CH_3CN (0.300 mL). After pyridine (0.044 mL, 0.542 mmol, 20 equiv) was added, the solution was cooled to 0 ^oC followed by dropwise addition of HF•pyr complex (0.140 mL, 1.08 mmol, 40 equiv) then gradually allowed to warm to rt. After stirring the reaction mixture for several days the solution was cooled to 0 ^oC and treated with saturated NH_4Cl (10 mL). The solution was extracted with CH_2Cl_2 (3 × 10 mL) and the organic fractions were pooled together. The organic phase was washed with brine (10 mL), dried (Na_2SO_4), filtered, and concentrated. The crude product was purified by preparative TLC (10% EtOAc/CH_2Cl_2) to afford the title compound (4.50 mg, 41%).

Clear oil; R_f = 0.14 (50% Et_2O/hexanes).

$[\alpha]^{20}_D$ –52 (*c* 0.55, $CHCl_3$).

^{1}H NMR (500 MHz, $CDCl_3$) δ 7.26–7.22 (m, 2 H), 6.89–6.85 (m, 2 H), 5.84 (ddd, *J* = 15.7, 5.4, 1.2 Hz, 1 H), 5.72 (ddd, *J* = 15.7, 6.2, 1.3 Hz, 1 H), 5.41 (br s, 1 H), 5.05 (ddd, *J* = 6.0, 6.0, 4.5 Hz, 1 H), 4.44 (d, *J* = 11.4 Hz, 1 H), 4.40 (d, *J* = 11.4 Hz, 1 H), 4.24 (dd, *J* = 10.6, 4.8 Hz, 1 H),

4.21–4.12 (m, 2 H), 4.05–3.99 (m, 1 H), 3.80 (s, 3 H), 3.53 (ddd, *J* = 9.5, 5.7, 5.5 Hz, 1 H), 3.46 (ddd, *J* = 9.5, 6.2, 6.0 Hz, 1 H), 2.78 (d, *J* = 4.8 Hz, 1 H), 2.36–2.24 (m, 2 H), 2.08–1.98 (m, 1 H), 1.93 (q, *J* = 5.9 Hz, 1 H), 1.88 (d, *J* = 16.8 Hz, 1 H), 1.70 (s, 3 H), 1.12 (t, 3 H).

^{13}C NMR (126 MHz, $CDCl_3$) δ 174.3, 159.3, 133.6, 131.4, 130.0, 129.4, 128.7, 119.7, 113.9, 74.2, 73.6, 73.2, 72.9, 65.9, 65.7, 55.3, 35.7, 30.0, 27.8, 23.0, 9.2.

IR (cast film, cm^{-1}) 3441, 2930, 2855, 1735, 1612, 1586, 1513, 1248, 1182.

HRMS (ESI) for $[M+Na]^+$ $C_{23}H_{32}NaO_6$ (m/z): calcd. 427.2091; found 427.2095.

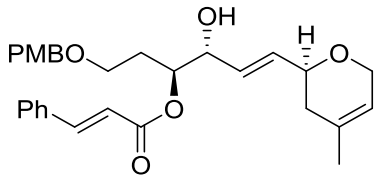

(1*S*,2*R*,3*E*)-2-Hydroxy-1-{2-[(4-methoxybenzyl)oxy]ethyl}-4-[(2*S*)-4-methyl-3,6-dihydro-2*H*-pyran-2-yl]but-3-en-1-yl (2*E*)-but-2-enoate (2-42a)

To a solution of alcohol **2-40a** (10.3 mg, 0.0176 mmol) in CH_2Cl_2 (0.350 mL) was added DMAP (4.00 μL, 0.0327 mmol, 1.9 equiv), DIC (4.00 μL, 0.0256 mmol, 1.5 equiv) then *trans*-cinnamic acid (6.40 mg, 0.0432 mmol, 2.4 equiv). After stirring the solution overnight at rt, the solution was concentrated and then transferred to a plastic vessel containing a stir bar using CH_3CN (0.350 mL). After pyridine (0.016 mL, 0.198 mmol, 11 equiv) was added, the solution was cooled to 0 °C followed by dropwise addition of HF•pyr complex (0.0300 mL, 0.233 mmol, 13 equiv) then gradually allowed to warm to rt. After stirring the reaction mixture for several days the solution was cooled to 0 °C and treated with saturated NH_4Cl (10 mL). The solution was extracted with CH_2Cl_2 (3 × 10 mL) and the organic fractions were pooled together. The organic phase was washed with brine (10 mL), dried (Na_2SO_4), filtered, and concentrated. The crude product was purified by preparative TLC (10% EtOAc/CH_2Cl_2) to afford the title compound

(12.6 mg, 70%).

Clear oil; R_f = 0.17 (30% EtOAc/hexanes).

$[\alpha]^{20}_D$ –33 (*c* 0.47, $CHCl_3$).

^{1}H NMR (500 MHz, $CDCl_3$) δ 7.67 (d, *J* = 16.0 Hz, 1 H), 7.55–7.49 (m, 2 H), 7.42–7.37 (m, 3 H), 7.26–7.22 (m, 2 H), 6.87–6.82 (m, 2 H), 6.43 (dd, *J* = 16.0, 2.5 Hz, 1 H), 5.87 (ddd, *J* = 15.7, 5.5, 1.1 Hz, 1 H), 5.77 (ddd, *J* = 15.7, 6.1, 1.2 Hz, 1 H), 5.39 (br s, 1 H), 5.18 (ddd, *J* = 6.7, 5.0, 4.7 Hz, 1 H), 4.45 (d, *J* = 11.5 Hz, 1 H), 4.42 (d, *J* = 12.0 Hz, 1 H), 4.33 (s, 1 H), 4.45 (d, *J* = 11.4 Hz, 1 H), 4.42 (d, *J* = 11.4 Hz, 1 H), 4.04–4.01 (m, 1 H), 3.74 (s, 3 H), 3.62–3.55 (m, 1 H), 3.51 (ddd, *J* = 9.5, 6.8, 5.6 Hz, 1 H), 2.90 (d, *J* = 3.7 Hz, 1 H), 2.07–1.96 (m, 3 H), 1.86 (d, *J* = 16.8 Hz, 1 H), 1.65 (s, 3 H).

^{13}C NMR (126 MHz, $CDCl_3$) δ 166.8, 159.3, 145.3, 134.4, 133.6, 131.4, 130.4, 130.0, 129.5, 128.9, 128.8, 128.2, 119.7, 118.0, 113.9, 74.6, 73.6, 73.3, 72.9, 65.9, 65.6, 55.2, 35.8, 30.0, 22.9.

IR (cast film, cm^{-1}) 3424, 2959, 2928, 2854, 1709, 1636, 1612, 1512, 1247, 1171.

HRMS (ESI) for $[M + Na]^+$ $C_{29}H_{34}NaO_6$ (m/z): calcd. 501.2248; found 501.2244, $[M + NH_4]^+$ $C_{29}H_{38}NO_6$ (m/z): calcd. 496.2694; found 496.2694.

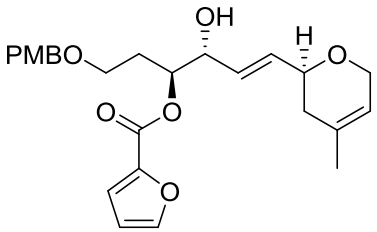

(1*S*,2*R*,3*E*)-2-Hydroxy-1-{2-[(4-methoxybenzyl)oxy]ethyl}-4-[(2*S*)-4-methyl-3,6-dihydro-2*H*-pyran-2-yl]but-3-en-1-yl 2-furoate (2-43a)

To a solution of alcohol **2-40a** (20.6 mg, 0.0351 mmol) in CH_2Cl_2 (0.700 mL) was added DMAP (27.3 mg, 0.223 mmol, 6.6 equiv), DCC (45.0 mg, 0.218 mmol, 6.2 equiv) then 2-furanoic acid (17.4 mg, 0.152 mmol, 4.3 equiv). After stirring the solution overnight at rt, the solution was

concentrated and directly subjected to flash chromatography (15 to 20% Et_2O/hexanes) to afford the ester product. The silyl-protected product was then transferred to a plastic vessel containing a stir bar using CH_3CN (0.350 mL). After pyridine (0.057 mL, 0.705 mmol, 20 equiv) was added, the solution was cooled to 0 °C followed by dropwise addition of HF•pyr complex (0.090 mL, 0.699 mmol, 20 equiv) then gradually allowed to warm to rt. After stirring the reaction mixture for several days the solution was cooled to 0 °C and treated with saturated NH_4Cl (10 mL). The solution was extracted with CH_2Cl_2 (3 × 10 mL) and the organic fractions were pooled together. The organic phase was washed with brine (10 mL), dried (Na_2SO_4), filtered, and concentrated. The crude product was purified by preparative TLC (10% EtOAc/CH_2Cl_2) to afford the title compound (13.8 mg, 89%).

Clear oil; R_f = 0.28 (40% EtOAc/hexanes).

$[\alpha]^{20}_D$ –54.4 (*c* 1.52, $CHCl_3$).

^{1}H NMR (500 MHz, $CDCl_3$) δ 7.58 (dd, *J* = 1.7, 0.8 Hz, 1 H), 7.24–7.20 (m, 2 H), 7.15 (dd, *J* = 3.5, 0.8 Hz, 1 H), 6.86–6.80 (m, 2 H), 6.50 (dd, *J* = 3.5, 1.7 Hz, 1 H), 5.85 (ddd, *J* = 15.7, 5.6, 1.0 Hz, 1 H), 5.76 (ddd, *J* = 15.7, 6.2, 1.1 Hz, 1 H), 5.38 (br s, 1 H), 5.25 (ddd, *J* = 6.5, 5.5, 5.2 Hz, 1 H), 4.44 (d, *J* = 11.5 Hz, 1 H), 4.40 (d, *J* = 11.5 Hz, 1 H), 4.34 (dd, *J* = 10.1, 4.9 Hz, 1 H), 4.19–4.09 (m, 2 H), 4.04–3.97 (m, 1 H), 3.78 (s, 3 H), 3.60 (ddd, *J* = 9.6, 5.5, 5.5 Hz, 1 H), 3.52 (ddd, *J* = 9.5, 6.8, 5.7 Hz, 1 H), 2.81 (d, *J* = 4.6 Hz, 1 H), 2.08–2.01 (m, 2 H), 1.97–1.89 (m, 1 H), 1.79 (d, *J* = 16.6 Hz, 1 H), 1.65 (s, 3 H).

^{13}C NMR (126 MHz, $CDCl_3$) δ 159.3, 158.5, 146.5, 144.6, 133.9, 131.3, 130.0, 129.4, 128.7, 119.7, 118.2, 113.8, 111.9, 74.9, 73.6, 73.3, 72.9, 65.8, 65.6, 55.3, 35.6, 30.0, 22.9.

IR (cast film, cm^{-1}) 3440, 2960, 2930, 2857, 1723, 1612, 1580, 1513, 1296, 1180.

HRMS (ESI) for $[M + Na]^+$ $C_{25}H_{30}NaO_7$ (m/z): calcd. 465.1884; found 465.1878, $[M + NH_4]^+$ $C_{25}H_{34}NO_7$ (m/z): calcd. 460.2330; found 460.2329.

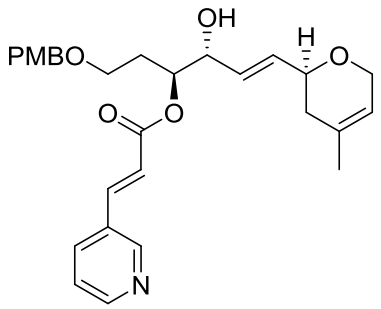

(1*S*,2*R*,3*E*)-2-Hydroxy-1-{2-[(4-methoxybenzyl)oxy]ethyl}-4-[(2*S*)-4-methyl-3,6-dihydro-2*H*-pyran-2-yl]but-3-en-1-yl (2*E*)-3-pyridin-3-ylacrylate (2-44a)

To a solution of alcohol **2-40a** (20.5 mg, 0.0356 mmol) in CH_2Cl_2 (0.700 mL) was added DMAP (30.0 mg, 0.243 mmol, 6.8 equiv), DCC (52.0 mg, 0.250 mmol, 7 equiv) then *trans*-3-(3-pyridyl) acrylic acid (28.0 mg, 0.188 mmol, 5.3 equiv). After stirring the solution overnight at rt, the solution was concentrated and the residue was directly subjected to flash chromatography (15 to 25% EtOAc/CH_2Cl_2) to afford the ester product. The silyl-protected product was then transferred to a plastic vessel containing a stir bar using CH_3CN (0.360 mL). After pyridine (0.024 mL, 0.297 mmol, 8.3 equiv) was added, the solution was cooled to 0 ^oC followed by dropwise addition of HF•pyr complex (0.040 mL, 0.310 mmol, 8 equiv) then gradually allowed to warm to rt. After stirring the reaction mixture for several days the solution was cooled to 0 ^oC and treated with saturated NH_4Cl (10 mL). The solution was extracted with CH_2Cl_2 (3 × 10 mL) and the organic fractions were pooled together. The organic phase was washed with brine (10 mL), dried (Na_2SO_4), filtered, and concentrated. The crude product was purified by preparative TLC (25% EtOAc/CH_2Cl_2) to afford the title compound (16.4 mg, 96%).

Clear oil; R_f = 0.23 (40% EtOAc/CH_2Cl_2).

$[\alpha]^{20}_D$ –41.3 (*c* 1.50, $CHCl_3$).

^{1}H NMR (500 MHz, $CDCl_3$) δ 8.73 (d, *J* = 1.2 Hz, 1 H), 8.61 (d, *J* = 3.7 Hz, 1 H), 7.81 (ddd, *J* = 7.1, 2.0, 1.7 Hz, 1 H), 7.64 (d, *J* = 16.1 Hz, 1 H), 7.33 (dd, *J* = 7.9, 4.8 Hz, 1 H), 7.26–7.22 (m, 2 H), 6.87–6.80 (m, 2 H), 6.48 (d, *J* = 16.1 Hz, 1 H), 5.87 (ddd, *J* = 15.7, 5.4, 1.0 Hz, 1 H), 5.77 (ddd, *J* = 15.7, 6.0, 1.2 Hz, 1 H), 5.40 (br s, 1 H), 5.19 (ddd, *J* = 5.5, 5.0, 4.7 Hz, 1 H), 4.44 (d, *J* = 11.4 Hz, 1 H), 4.41 (d, *J* = 11.4 Hz, 1 H), 4.33 (dd, *J* = 8.8, 4.1 Hz, 1 H), 4.22–4.11 (m, 2 H), 4.07–3.99 (m, 1 H), 3.74 (s, 3 H), 3.58 (ddd, *J* = 9.5, 5.7, 5.5 Hz, 1 H), 3.51 (ddd, *J* = 9.5, 6.9, 5.5 Hz, 1 H), 2.93 (d, *J* = 4.6 Hz, 1 H), 2.07–1.96 (m, 3 H), 1.86 (d, *J* = 16.7 Hz, 1 H), 1.66 (s, 3 H).

^{13}C NMR (126 MHz, $CDCl_3$) δ 166.0, 159.3, 151.1, 149.8, 141.5, 134.3, 133.8, 131.3, 130.2, 130.0, 129.5, 128.6, 123.8, 120.2, 119.7, 113.9, 74.9, 73.5, 73.2, 72.9, 65.9, 65.6, 55.2, 35.8, 29.9, 22.9.

IR (cast film, cm^{-1}) 3411, 3032, 2928, 2854, 1713, 1641, 1612, 1513, 1248, 1173.

HRMS (ESI) for $[M + Na]^+$ $C_{28}H_{33}NNaO_6$ (m/z): calcd. 502.2200; found 502.2201, $[M + H]^+$ $C_{28}H_{34}NO_6$ (m/z): calcd. 480.2381; found 480.2383.

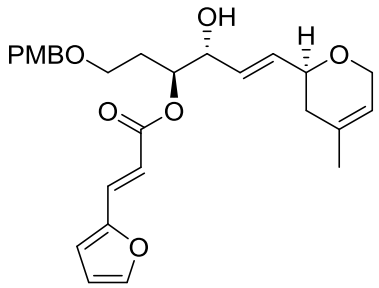

(1*S*,2*R*,3*E*)-2-Hydroxy-1-{2-[(4-methoxybenzyl)oxy]ethyl}-4-[(2*S*)-4-methyl-3,6-dihydro-2*H*-pyran-2-yl]but-3-en-1-yl (2*E*)-3-(2-furyl)acrylate (2-45a)

To a solution of alcohol **2-40a** (21.2 mg, 0.0361 mmol) in CH_2Cl_2 (0.350 mL) was added DMAP (30.0 mg, 0.246 mmol, 6.8 equiv), DCC (26.0 mg, 0.126 mmol, 3.5 equiv) then *trans*-furan-2-acrylic acid (6.40 mg, 0.0432 mmol, 2.4 equiv). After stirring the solution overnight at rt, the

solution was concentrated and the residue was directly subjected to flash chromatography (15 to 25% EtOAc/CH_2Cl_2) to afford the ester product. The silyl-protected product was then transferred to a plastic vessel containing a stir bar using CH_3CN (0.400 mL). After pyridine (0.072 mL, 0.890 mmol, 25 equiv) was added, the solution was cooled to 0 ^oC followed by dropwise addition of HF•pyr complex (0.120 mL, 0.932 mmol, 26 equiv) then gradually allowed to warm to rt. After stirring the reaction mixture for several days the solution was cooled to 0 ^oC and treated with saturated NH_4Cl (10 mL). The solution was extracted with CH_2Cl_2 (3 × 10 mL) and the organic fractions were pooled together. The organic phase was washed with brine (10 mL), dried (Na_2SO_4), filtered, and concentrated. The crude product was purified by preparative TLC (10% EtOAc/CH_2Cl_2) to afford the title compound (7.70 mg, 49%).

Clear oil; R_f = 0.33 (40% EtOAc/hexanes).

$[\alpha]^{20}_D$ –59.5 (*c* 0.780, $CHCl_3$).

^{1}H NMR (500 MHz, $CDCl_3$) δ 7.49 (d, *J* = 1.5 Hz, 1 H), 7.41 (d, *J* = 15.7 Hz, 1 H), 7.25–7.21 (m, 2 H), 6.87–6.82 (m, 2 H), 6.62 (d, *J* = 3.4 Hz, 1 H), 6.48 (dd, *J* = 3.4, 1.8 Hz, 1 H), 6.30 (d, *J* = 15.7 Hz, 1 H), 5.86 (ddd, *J* = 15.7, 5.5, 1.1 Hz, 1 H), 5.75 (ddd, *J* = 15.7, 6.1, 1.2 Hz, 1 H), 5.39 (br s, 1 H), 5.15 (ddd, *J* = 6.5, 5.0, 4.7 Hz, 1 H), 4.44 (d, *J* = 11.4 Hz, 1 H), 4.41 (d, *J* = 11.4 Hz, 1 H), 4.30 (dd, *J* = 10.5, 4.9 Hz, 1 H), 4.22–4.11 (m, 2 H), 4.05–3.99 (m, 1H), 3.77 (s, 3 H), 3.57 (ddd, *J* = 9.5, 6.0, 5.7 Hz, 1 H), 3.49 (ddd, *J* = 9.4, 6.7, 6.0 Hz, 1 H), 2.88 (d, *J* = 4.9 Hz, 1 H), 2.06–1.95 (m, 3 H), 1.86 (d, *J* = 16.7 Hz, 1 H), 1.66 (s, 3 H).

^{13}C NMR (126 MHz, $CDCl_3$) δ 166.8, 159.3, 150.9, 144.9, 133.6, 131.6, 131.4, 130.0, 129.5, 128.7, 119.7, 115.6, 115.0, 113.9, 112.4, 74.5, 73.6, 73.3, 72.9, 65.9, 65.6, 55.3, 35.8, 30.0, 22.9.

IR (cast film, cm^{-1}) 3439, 2960, 2929, 2855, 1707, 1637, 1613, 1513, 1249, 1167.

HRMS (ESI) for $[M+Na]^+$ $C_{27}H_{32}NaO_7$ (m/z): calcd. 491.2040; found 491.2031.

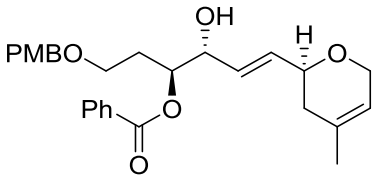

(1*S*,2*R*,3*E*)-2-Hydroxy-1-{2-[(4-methoxybenzyl)oxy]ethyl}-4-[(2*S*)-4-methyl-3,6-dihydro-2*H*-pyran-2-yl]but-3-en-1-yl benzoate (2-46a)

To a solution of alcohol **2-40a** (13.8 mg, 0.0235 mmol) in THF (0.500 mL) was added DMAP (1.3 mg, 0.0106 mmol, 45 mol%), pyridine (6.00 μL, 0.0742 mmol, 3.4 equiv) then benzoic anhydride (12.5 mg, 0.0553 mmol, 2.4 equiv). After stirring the solution overnight at rt, the solution was concentrated and the residue was directly subjected to flash chromatography (5 to 20% Et_2O/hexanes) to afford the ester product. The silyl-protected product was then transferred to a plastic vessel containing a stir bar using CH_3CN (0.300 mL). After pyridine (0.038 mL, 0.470 mmol, 20 equiv) was added, the solution was cooled to 0 ^oC followed by dropwise addition of HF•pyr complex (0.120 mL, 0.940 mmol, 40 equiv) then gradually allowed to warm to rt. After stirring the reaction mixture for several days the solution was cooled to 0 ^oC and treated with saturated NH_4Cl (10 mL). The solution was extracted with CH_2Cl_2 (3 × 10 mL) and the organic fractions were pooled together. The organic phase was washed with brine (10 mL), dried (Na_2SO_4), filtered, and concentrated. The crude product was purified by preparative TLC (10% EtOAc/CH_2Cl_2) to afford the title compound (10.8 mg, 52%).

Clear oil; R_f = 0.26 (10% EtOAc/CH_2Cl_2).

$[\alpha]^{20}_D$ –51.9 (*c* 0.620, $CHCl_3$).

^{1}H NMR (500 MHz, $CDCl_3$) δ 8.03–7.98 (m, 2 H), 7.60–7.53 (m, 1 H), 7.46–7.40 (m, 2 H), 7.24–7.19 (m, 2 H), 6.86–6.79 (m, 2 H), 5.86 (ddd, *J* = 15.7, 5.5, 0.9 Hz, 1 H), 5.78 (ddd, *J* = 15.7, 6.1, 1.0 Hz, 1 H), 5.37 (br s, 1 H), 5.28 (ddd, *J* = 7.0, 5.0, 4.7 Hz, 1 H), 4.44 (d, *J* = 11.5

Hz, 1 H), 4.41 (d, *J* = 11.5 Hz, 1 H), 4.38 (dd, *J* = 5.5. 5.5 Hz, 1 H), 4.20–4.09 (m, 2 H), 4.04–3.97 (m, 1 H), 3.77 (s, 3 H), 3.62 (app dt, *J* = 9.5, 5.7 Hz, 1 H), 3.54 (ddd, *J* = 9.5, 7.2, 5.2 Hz, 1 H), 2.90 (s, 1 H), 2.14–2.01 (m, 2 H), 1.96–1.85 (m, 1 H), 1.77 (d, *J* = 16.9 Hz, 1 H), 1.63 (s, 3 H).

^{13}C NMR (126 MHz, $CDCl_3$) δ 166.3, 159.3, 133.8, 133.1, 131.4, 130.2, 130.0, 129.8, 129.5, 128.9, 128.4, 119.6, 113.8, 75.0, 73.7, 73.3, 72.9, 65.8, 65.6, 55.3, 35.6, 30.2, 22.9.

IR (cast film, cm^{-1}) 3421, 2960, 2927, 2854, 1717, 1612, 1585, 1513, 1274, 1113.

HRMS (ESI) for $[M + K]^+$ $C_{23}H_{32}KO_6$ (m/z): calcd. 491.183; found 491.1838; $[M + Na]^+$ $C_{23}H_{32}NaO_6$ (m/z): calcd. 475.2091; found 475.2088; $[M + NH_4]^+$ $C_{23}H_{36}NO_6$ (m/z): calcd. 470.2537; found 470.2539.

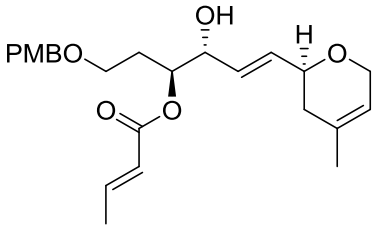

(1*S*,2*R*,3*E*)-2-Hydroxy-1-{2-[(4-methoxybenzyl)oxy]ethyl}-4-[(2*S*)-4-methyl-3,6-dihydro-2*H*-pyran-2-yl]but-3-en-1-yl (2*E*)-but-2-enoate (2-47a)

To a solution of alcohol **2-40a** (19.5 mg, 0.0332 mmol) in CH_2Cl_2 (0.700 mL) was added DMAP (13.0 mg, 0.106 mmol, 3.2 equiv), DCC (21.0 mg, 0.101 mmol, 3.1 equiv) then crotonic acid (7.00 mg, 0.0813 mmol, 2.4 equiv). After stirring the solution overnight at rt, the solution was concentrated and the residue was directly subjected to flash chromatography (5 to 15% Et_2O/hexanes) to afford the ester product. The silyl-protected product was then transferred to a plastic vessel containing a stir bar using CH_3CN (0.300 mL). After pyridine (0.0270 mL, 0.332 mmol, 10 equiv) was added, the solution was cooled to 0 ^oC followed by dropwise addition of HF•pyr complex (0.085 mL, 0.664 mmol, 20 equiv) then gradually allowed to warm to rt. After

stirring the reaction mixture for several days the solution was cooled to 0 °C and treated with saturated NH_4Cl (10 mL). The solution was extracted with CH_2Cl_2 (3 × 10 mL) and the organic fractions were pooled together. The organic phase was washed with brine (10 mL), dried (Na_2SO_4), filtered, and concentrated. The crude product was purified by preparative TLC (10% EtOAc/CH_2Cl_2) to afford the title compound (7.30 mg, 56%).

Clear oil; R_f = 0.21 (10% EtOAc/CH_2Cl_2).

$[\alpha]^{20}_D$ –41.2 (*c* 0.490, $CHCl_3$).

^{1}H NMR (500 MHz, $CDCl_3$) δ 7.25–7.22 (m, 2 H), 6.97 (app dq, *J* = 15.5, 6.9 Hz, 1 H), 6.89–6.84 (m, 2 H), 5.87–5.81 (m, 2 H), 5.72 (ddd, *J* = 15.7, 6.1, 1.2 Hz, 1 H), 5.40 (br s, 1 H), 5.09 (app dt, *J* = 6.6, 5.0 Hz, 1 H), 4.45–4.38 (m, 2 H), 4.27– 4.26 (m, 1 H), 4.21–4.11 (m, 2 H), 4.04–4.00 (m, 1 H), 3.80 (s, 3 H), 3.55 (app dt, *J* = 9.5, 5.7 Hz, 1 H), 3.50–3.43 (m, 1 H), 2.85 (d, *J* = 4.4 Hz, 1 H), 2.08–1.91 (m, 3 H), 1.91–1.82 (m, 4 H), 1.69 (s, 3 H).

^{13}C NMR (126 MHz, $CDCl_3$) δ 166.3, 159.3, 145.3, 133.6, 131.4, 130.1, 129.4, 128.7, 122.6, 119.7, 113.9, 74.2, 73.6, 73.3, 72.9, 65.9, 65.6, 55.3, 35.8, 30.0, 23.0, 18.0.

IR (cast film, cm^{-1}) 3441, 2929, 2960, 2854, 1717, 1656, 1513, 1248, 1182.

HRMS (ESI) for $C_{24}H_{32}NaO_6$ $[M + Na]^+$ (m/z): calcd. 439.2091; found 439. 2084.

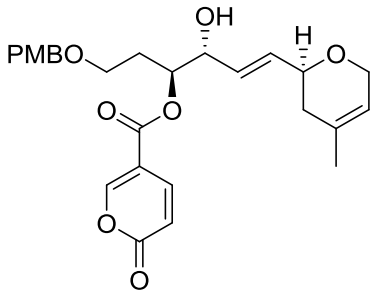

(1*S*,2*R*,3*E*)-2-Hydroxy-1-{2-[(4-methoxybenzyl)oxy]ethyl}-4-[(2*S*)-4-methyl-3,6-dihydro-2*H*-pyran-2-yl]but-3-en-1-yl 2-oxo-2*H*-pyran-5-carboxylate (2-48a)

To a solution of alcohol **2-40a** (36.2 mg, 0.0616 mmol) in CH_2Cl_2 (1.2 mL) was added DMAP (23.0 mg, 0.188 mmol, 3.1 equiv), DCC (40.0 mg, 0.194 mmol, 3.1 equiv) then coumalic acid (19.1 mg, 0.136 mmol, 2.2 equiv). After stirring the solution overnight at rt, the solution was concentrated and the residue was directly subjected to flash chromatography (5 to 50% Et_2O/hexanes) to afford the ester product. The silyl-protected product was then transferred to a plastic vessel containing a stir bar using CH_3CN (0.400 mL). After pyridine (0.032 mL, 0.396 mmol, 6.4 equiv) was added, the solution was cooled to 0 ^oC followed by dropwise addition of HF•pyr complex (0.050 mL, 0.388 mmol, 6.3 equiv) then gradually allowed to warm to rt. After stirring the reaction mixture for several days the solution was cooled to 0 ^oC and treated with saturated NH_4Cl (10 mL). The solution was extracted with CH_2Cl_2 (3 × 10 mL) and the organic fractions were pooled together. The organic phase was washed with brine (10 mL), dried (Na_2SO_4), filtered, and concentrated. The crude product was purified by preparative TLC (10% EtOAc/CH_2Cl_2) to afford the title compound (7.80 mg, 51%).

Clear oil; R_f = 0.33 (25% EtOAc/CH_2Cl_2).

$[\alpha]^{20}_D$ –29.9 (*c* 0.630, $CHCl_3$).

^{1}H NMR (500 MHz, $CDCl_3$) δ 8.17 (dd, *J* = 2.6, 1.1 Hz, 1 H), 7.69 (dd, *J* = 9.8, 2.6 Hz, 1 H), 7.22–7.17 (m, 2 H), 6.85–6.80 (m, 2 H), 6.29 (dd, *J* = 9.8, 1.1 Hz, 1 H), 5.86 (ddd, *J* = 15.7, 5.3,

1.1 Hz, 1 H), 5.74 (ddd, *J* = 15.7, 6.2, 1.3 Hz, 1 H), 5.41 (br s, 1 H), 5.23 (ddd, *J* = 7.0, 4.5, 4.5 Hz, 1 H), 4.41 (d, *J* = 11.5 Hz, 1 H), 4.38 (d, *J* = 11.5 Hz, 1 H), 4.34–4.30 (m, 1 H), 4.19–4.15 (m, 2 H), 4.04–4.00 (m, 1 H), 3.79 (s, 3 H), 3.58–3.52 (m, 1 H), 3.49 (ddd, *J* = 9.6, 7.0, 5.0 Hz, 1 H), 2.68 (s, 1 H), 2.05–1.95 (m, 2 H), 1.85 (d, *J* = 16.7 Hz, 1 H), 1.69 (s, 3 H), 1.59 (br s, 1 H).

^{13}C NMR (126 MHz, $CDCl_3$) δ 162.8, 159.8, 159.4, 158.2, 141.6, 134.2, 131.2, 129.7, 129.6, 128.3, 119.8, 115.2, 113.8, 112.1, 75.8, 73.4, 73.1, 73.0, 65.7, 65.6, 55.3, 35.7, 29.8, 23.0.

IR (cast film, cm^{-1}) 3451, 2929, 2855, 1755, 1721, 1637, 1612, 1290, 1246, 1088.

HRMS (ESI) for $[M + Na]^+$ $C_{26}H_{30}NaO_8$ (m/z): calcd. 493.1833; found 493.1824.

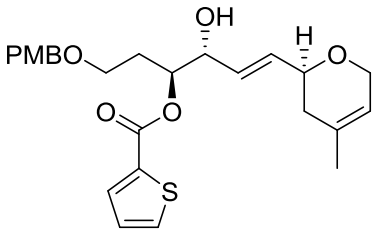

(1*S*,2*R*,3*E*)-2-Hydroxy-1-{2-[(4-methoxybenzyl)oxy]ethyl}-4-[(2*S*)-4-methyl-3,6-dihydro-2*H*-pyran-2-yl]but-3-en-1-yl thiophene-2-carboxylate (2-49a)

To a solution of alcohol **2-40a** (20.5 mg, 0.0349 mmol) in CH_2Cl_2 (0.700 mL) was added DMAP (14.0 mg, 0.115 mmol, 3.3 equiv), DCC (20.0 mg, 0.0969 mmol, 2.8 equiv) then 2-thiophenecarboxylic acid (9.2 mg, 0.0711 mmol, 2.0 equiv). After stirring the solution overnight at rt, the solution was concentrated and transferred to a plastic vessel containing a stir bar using CH_3CN (0.300 mL). After pyridine (0.024 mL, 0297 mmol, 8.5 equiv) was added, the solution was cooled to 0 ^oC followed by dropwise addition of HF•pyr complex (0.040 mL, 0.311 mmol, 8.9 equiv) then gradually allowed to warm to rt. After stirring the reaction mixture for several days the solution was cooled to 0 ^oC and treated with saturated NH_4Cl (10 mL). The solution was extracted with CH_2Cl_2 (3 × 10 mL) and the organic fractions were pooled together. The organic phase was washed with brine (10 mL), dried (Na_2SO_4), filtered, and concentrated. The crude

product was purified by preparative TLC (10% EtOAc/CH_2Cl_2) to afford the title compound (10.7 mg, 66%).

Clear oil; R_f = 0.15 (10% EtOAc/CH_2Cl_2).

$[\alpha]^{20}_D$ –28.9 (*c* 0.160, $CHCl_3$).

^{1}H NMR (500 MHz, $CDCl_3$) δ 7.78 (dd, *J* = 3.7, 1.2 Hz, 1 H), 7.56 (dd, *J* = 5.0, 1.2 Hz, 1 H), 7.24–7.20 (m, 2 H), 7.10 (dd, *J* = 4.9, 3.8 Hz, 1 H), 6.85–6.80 (m, 2 H), 5.89–5.82 (m, 1 H), 5.76 (ddd, *J* = 15.7, 6.2, 1.0 Hz, 1 H), 5.38 (br s, 1 H), 5.22 (ddd, *J* = 7.0, 5.0, 5.0 Hz, 1 H), 4.44 (d, *J* = 11.5 Hz, 1 H), 4.41(d, *J* = 11.5 Hz, 1 H), 4.35 (dd, *J* = 10.4, 5.0 Hz, 1 H), 4.20–4.09 (m, 2 H), 4.04–3.97 (m, 1 H), 3.78 (s, 3 H), 3.61 (ddd, *J* = 9.5, 5.5, 5.5 Hz, 1 H), 3.53 (ddd, *J* = 9.5, 6.9, 5.6 Hz, 1 H), 2.84 (d, *J* = 4.7 Hz, 1 H), 2.05 (ddd, *J* = 7.2, 6.2, 1.8 Hz, 2 H), 1.91 (dd, *J* = 16.6, 10.2 Hz, 1 H), 1.78 (d, *J* = 16.7 Hz, 1 H), 1.64 (s, 3 H).

^{13}C NMR (126 MHz, $CDCl_3$) δ 161.9, 159.3, 133.9, 133.8, 133.7, 132.6, 131.4, 130.0, 129.4, 128.8, 127.8, 119.6, 113.8, 75.2, 73.6, 73.3, 72.9, 65.8, 65.6, 55.3, 35.6, 30.1, 22.9.

IR (cast film, cm^{-1}) 3415, 2929, 2854, 1706, 1612, 1585, 1513, 1259, 1095.

HRMS (ESI) for $[M + Na]^+$ $C_{25}H_{30}NaO_6S$ (m/z): calcd. 481.1655; found 481.1656, $[M + NH_4]^+$ $C_{25}H_{34}NO_6S$ (m/z): calcd. 476.2101; found 476.2105.

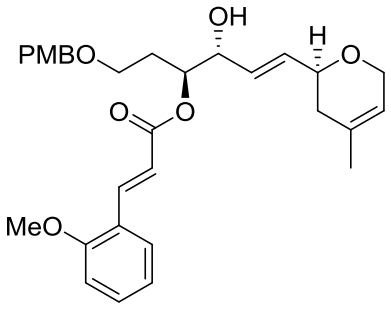

(1*S*,2*R*,3*E*)-2-Hydroxy-1-{2-[(4-methoxybenzyl)oxy]ethyl}-4-[(2*S*)-4-methyl-3,6-dihydro-2*H*-pyran-2-yl]but-3-en-1-yl (2*E*)-3-(2-methoxyphenyl)acrylate (2-50a)

To a solution of alcohol **2-40a** (20.9 mg, 0.0349 mmol) in CH_2Cl_2 (0.700 mL) was added DMAP (13.6 mg, 0.111 mmol, 3.1 equiv), DCC (23.0 mg, 0.111 mmol, 3.1 equiv) then 2-methoxycinnamic acid (14.0 mg, 0.0786 mmol, 2.1 equiv). After stirring the solution overnight at rt, the solution was concentrated and the residue was directly subjected to flash chromatography (15 to 20% Et_2O/hexanes) to afford the ester product. The silyl-protected product was then transferred to a plastic vessel containing a stir bar using CH_3CN (0.400 mL). After pyridine (0.0560 mL, 0.698 mmol, 20 equiv) was added, the solution was cooled to 0 ^oC followed by dropwise addition of HF•pyr complex (0.180 mL, 1.40 mmol, 40 equiv) then gradually allowed to warm to rt. After stirring the reaction mixture for several days the solution was cooled to 0 ^oC and treated with saturated NH_4Cl (10 mL). The solution was extracted with CH_2Cl_2 (3 × 10 mL) and the organic fractions were pooled together. The organic phase was washed with brine (10 mL), dried (Na_2SO_4), filtered, and concentrated. The crude product was purified by preparative TLC (5% *i*PrOH/hexanes) to afford the title compound (9.90 mg, 55%).

Clear oil; R_f = 0.44 (20% EtOAc/CH_2Cl_2).

$[\alpha]^{20}_D$ –40.6 (*c* 0.690, $CHCl_3$).

^{1}H NMR (500 MHz, $CDCl_3$) δ 7.99 (d, *J* = 16.2 Hz, 1 H), 7.50 (dd, *J* = 7.7, 1.6 Hz, 1 H), 7.39–7.33 (m, 1 H), 7.25–7.24 (m, 2 H), 6.96 (dd, *J* = 11.0, 4.0 Hz, 1 H), 6.92 (d, *J* = 8.3 Hz, 1 H),

6.87–6.82 (m, 2 H), 6.52 (d, *J* = 16.1 Hz, 1 H), 5.87 (ddd, *J* = 15.7, 5.5, 1.0 Hz, 1 H), 5.77 (ddd, *J* = 15.7, 6.0, 1.1 Hz, 1 H), 5.39 (br s, 1 H), 5.17 (ddd, *J* = 6.6, 5.0, 4.7 Hz, 1 H), 4.45 (d, *J* = 11.0 Hz, 1 H), 4.42 (d, *J* = 11.5 Hz, 1 H), 4.33 (dd, *J* = 10.4, 4.9 Hz, 1 H), 4.17–4.15 (m, 2 H), 4.06–4.00 (m, 1 H), 3.89 (s, 3 H), 3.75 (s, 3 H), 3.59 (ddd, *J* = 10.6, 5.5, 3.5 Hz, 1 H), 3.55–3.48 (m, 1 H), 2.91 (d, *J* = 4.9 Hz, 1 H), 2.06–1.97 (m, 3 H), 1.87 (d, *J* = 14.8 Hz, 1 H), 1.65 (s, 3 H).

^{13}C NMR (126 MHz, $CDCl_3$) δ 167.4, 159.3, 158.5, 140.9, 133.6, 131.6, 131.4, 130.1, 129.4, 129.1, 128.8, 123.4, 120.8, 119.7, 118.4, 113.9, 111.2, 74.4, 73.7, 73.4, 72.9, 66.0, 65.6, 55.5, 55.3, 35., 30.4, 30.0, 22.9.

IR (cast film, cm^{-1}) 3430, 3002, 2928, 2853, 1708, 1629, 1513, 1488, 1248, 1172.

HRMS (ESI) for $[M + Na]^+$ $C_{30}H_{36}NaO_7$ (m/z): calcd. 531.2353; found 531.2348, $[M + NH_4]^+$ $C_{30}H_{40}NO_7$ (m/z): calcd. 526.2799; found 526.2800.

Synthesis of diastereomer 2-40b

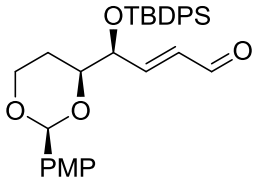

(2*E*,4*S*)-4-{[*tert*-Butyl(diphenyl)silyl]oxy}-4-[(2*S*,4*S*)-2-(4-methoxyphenyl)-1,3-dioxan-4-yl]but-2-enal (2-36b)

Through nitrogen bubbling, a solution of CH_2Cl_2 (9.5 mL) containing alkene **2-34b** (902 mg, 3.60 mmol) was degassed for 15 minutes before addition of acrolein (2.70 mL, 36.4 mmol, 10 equiv). The solution was degassed for an additional 30 minutes followed by slow addition of a solution of Grubbs-Hoveyda second generation catalyst in CH_2Cl_2 (2.0 mL). The reaction mixture was stirred overnight at 40 ^oC. After the reaction mixture was allowed to cool to room temperature, the crude conjugated aldehyde was concentrated and was immediately subjected to

flash chromatography on silica gel to afford the semi-pure intermediate which was immediately used in the subsequent reaction.

Crude conjugated aldehyde **2-35b**; R_f = 0.23 (50% EtOAc/hexanes).

To a solution of the crude conjugated aldehyde **2-35b** (592 mg, 2.13 mmol) in CH_2Cl_2 (11 mL) was added imidazole (299 mg, 4.39 mmol, 2.1 equiv) followed by TBDPSCl (620 mg, 2.26 mmol, 1.1 equiv) at 0°C. After consumption of starting material, saturated NH_4Cl (20 mL) was added. The resulting biphasic solution was extracted with CH_2Cl_2. The organic phase was separated and subsequently washed with brine, then dried ($MgSO_4$), filtered and concentrated. The crude product was subjected to flash chromatography on silica gel (25% EtOAc/hexanes) to afford the title compound with (538 mg, 29%).

Clear oil; R_f = 0.62 (25% EtOAc/hexanes).

$[\alpha]^{20}_D$ –51.0 (*c* 3.17, $CHCl_3$).

^{1}H NMR (500 MHz, $CDCl_3$) δ 9.54 (d, *J* = 8.0 Hz, 1 H), 7.69–7.67 (m, 2 H), 7.61–7.59 (m, 2 H), 7.50–7.32 (m, 6 H), 7.31–7.27 (m, 2 H), 6.90 (dd, *J* = 15.7, 4.1 Hz, 1 H), 6.87–6.83 (m, 2 H), 6.41 (ddd, *J* = 15.7, 8.0, 1.7 Hz, 1 H), 5.20 (s, 1 H), 4.72 (ddd, *J* = 5.6, 4.2, 1.7 Hz, 1 H), 4.22 (dd, *J* = 11.5, 3.9 Hz, 1 H), 3.83–3.71 (m, 5 H), 1.74 (ddd, *J* = 25.1, 12.3, 5.0 Hz, 1 H), 1.57 (dd, *J* = 13.3, 1.4 Hz, 1 H), 1.12 (s, 9 H).

^{13}C NMR (126 MHz, $CDCl_3$) δ 193.3, 160.0, 155.5, 135.8, 135.8, 133.4, 132.8, 132.6, 130.7, 130.2, 130.2, 127.9, 127.8, 127.4, 113.6, 101.3, 78.5, 73.6, 66.8, 55.3, 27.1, 25.4, 19.4.

IR (cast film, cm^{-1}) 2960, 2931, 2857, 1692, 1615, 1518, 1114.

HRMS (ESI) for $C_{31}H_{36}NaO_5Si$ $[M + Na]^+$ (m/z): calcd. 539.2224; found 539.2224, for $C_{31}H_{37}O_5Si$ $[M + H]^+$ (m/z): calcd. 517.2405; found 517.2406.

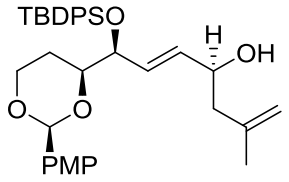

(4*S*,5*E*,7*S*)-7-{[*tert*-Butyl(diphenyl)silyl]oxy}-7-[(2*S*,4*S*)-2-(4-methoxyphenyl)-1,3-dioxan-4-yl]-2-methylhepta-1,5-dien-4-ol (2-37b)

To a solution of (−)-DIPCl (1.0 M in THF, 4.0 mL, 4.0 equiv) was added a solution of β-methallylmagnesium chloride in THF (0.44 M in THF, 5.5 mL, 2.4 equiv) at 0 °C. The reaction mixture was stirred for 2 h followed by cooling the solution to −78 °C. A solution of enal **2-36b** (0.519 g, 1.00 mmol) in THF (5 mL) was cooled to −78 °C then slowly added, over a period of 30 min, to the reaction mixture and then stirred overnight at −78 °C. The reaction mixture was treated with 1N NaOH (8.5 mL) then allowed to warm to 0 ^{o}C, at which point H_2O_2 (0.450 mL) was added and the solution was allowed to warm to rt. The resulting biphasic solution was extracted with CH_2Cl_2 (3 × 30 mL). The organic fractions were pooled together and washed with brine (30 mL), dried ($MgSO_4$), filtered, and concentrated to obtain exclusively a single diastereomer based on ^{1}H NMR analysis. The crude product was subjected to flash chromatography (5 to 30% EtOAc/hexanes) to afford the title compound (531 mg, 92%).

Clear oil; R_f = 0.23 (20% EtOAc/hexanes).

$[\alpha]^{20}_D$ +16.7 (*c* 0.840, CH_2Cl_2).

^{1}H NMR (700 MHz, C_6D_6) δ 7.85–7.83 (m, 2 H), 7.81–7.77 (m, 2 H), 7.54–7.52 (m, 2 H), 7.23–7.17 (m, 6 H), 6.83–6.79 (m, 2 H), 5.77 (ddd, *J* = 15.5, 6.8, 1.3 Hz, 1 H), 5.54 (ddd, J = 15.5, 5.5, 0.8 Hz, 1 H), 5.33 (s, 1 H), 4.75 (s, 1 H), 4.71 (s, 1 H), 4.46 (t, *J* = 6.4 Hz, 1 H), 3.99 (dd, *J* = 10.7, 4.6 Hz, 2 H), 3.76 (ddd, *J* = 11.5, 6.2, 2.3 Hz, 1 H), 3.52 (ddd, *J* = 11.9, 11.9, 2.8 Hz, 1 H), 3.26 (s, 3 H), 2.01 (dd, *J* = 13.8, 8.5 Hz, 1 H), 1.96 (dd, *J* = 13.8, 4.8 Hz, 1 H), 1.69 (ddd, *J* =

24.7, 12.5, 5.1 Hz, 1 H), 1.55 (s, 3 H), 1.25–1.15 (m, 11 H).

^{13}C NMR (126 MHz, $CDCl_3$) δ 159.8, 142.1, 136.1, 136.0, 134.9, 134.1, 134.0, 131.3, 129.6, 129.6, 128.7, 127.5, 127.4, 113.6, 113.5, 101.2, 79.9, 75.3, 69.3, 66.9, 55.3, 45.8, 27.1, 26.1, 22.4, 19.4.

IR (cast film, cm^{-1}) 3446, 2960, 2931, 2856, 1615, 1518, 1112.

HRMS (ESI) for $[M + Na]^+$ $C_{35}H_{44}NaO_5Si$ (m/z): calcd. 595.2850; found 595.2834, $[M + NH_4]^+$ $C_{35}H_{48}NO_5Si$ (m/z): calcd. 590.3296; found 590.3297, $[M + H]^+$ $C_{35}H_{45}O_5Si$ (m/z): calcd. 573.3031; found 573.3021.

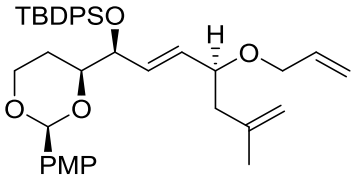

({(1*S*,2*E*,4*S*)-4-(Allyloxy)-1-[(2*S*,4*S*)-2-(4-methoxyphenyl)-1,3-dioxan-4-yl]-6-methylhepta-2,6-dien-1-yl}oxy)(*tert*-butyl)diphenylsilane (2-38b)

A solution of **2-37b** (500 mg, 0.873 mmol) in THF (18 mL) was cooled to –10 °C, treated with KH (110 mg, 2.74 mmol, 3.1 equiv) then the reaction mixture was allowed to warm to 0 °C. After stirring the orangy-yellow reaction mixture at 0 °C for 1 h, allylbromide (0.250 mL, 3.3 equiv) was slowly added, whereupon the solution colour appeared white. After stirring the reaction mixture for 1 h, the reaction mixture was treated with saturated NH_4Cl (30 mL) and the resulting biphasic solution was extracted with Et_2O (3 × 20 mL). The organic phase was washed with water (20 mL), brine (20 mL), dried (Na_2SO_4), filtered, and concentrated to give the crude product as a yellow oil. The crude product was subjected to flash chromatography (5-10% Et_2O/hexanes) to afford the title compound (0.443 g, 83%).

Clear oil; R_f = 0.67 (20% EtOAc/hexanes).

$[\alpha]^{20}_{D}$ –28.0 (c = 1.94, $CHCl_3$).

^{1}H NMR (500 MHz, $CDCl_3$) δ 7.68–7.66 (m, 2 H), 7.65–7.63 (m, 2 H), 7.44–7.37 (m, 2 H), 7.35–7.30 (m, 4 H), 7.30–7.26 (m, 2 H), 6.85–6.81 (m, 2 H), 5.84 (dddd, *J* = 17.2, 10.5, 6.1, 5.1 Hz, 1 H), 5.71 (ddd, *J* = 15.6, 6.0, 0.6 Hz, 1 H), 5.47 (ddd, *J* = 15.6, 7.6, 1.2 Hz, 1 H), 5.27 (s, 1 H), 5.20 (ddd, *J* = 17.2, 3.4, 1.7 Hz, 1 H), 5.12 (ddd, *J* = 10.4, 3.1, 1.3 Hz, 1 H), 4.77–4.69 (m, 2 H), 4.41 (app td, *J* = 5.8, 1.1 Hz, 1 H), 4.22 (dd, *J* = 11.4, 3.9 Hz, 1 H), 3.93 (app ddt, *J* = 12.9, 5.0, 1.5 Hz, 1 H), 3.88–3.80 (m, 2 H), 3.79 (s, 3 H), 3.77–3.68 (m, 2 H), 2.27 (dd, *J* = 14.1, 7.5 Hz, 1 H), 2.05 (dd, *J* = 14.1, 5.7 Hz, 1 H), 1.79 (ddd, *J* = 17.1, 12.5, 5.0 Hz, 1 H), 1.72 (s, 3 H), 1.50 (dd, *J* = 13.3, 1.4 Hz, 1 H), 1.06 (d, *J* = 2.4 Hz, 9 H).

^{13}C NMR (126 MHz, $CDCl_3$) δ 159.9, 142.2, 136.0, 135.9, 135.1, 134.1, 133.8, 132.8, 131.2, 131.0, 129.7, 129.6, 127.6, 127.5, 127.5, 116.6, 113.5, 112.6, 101.2, 79.6, 77.9, 74.8, 69.1, 67.0, 55.3, 44.2, 27.1, 25.7, 22.9, 19.5.

IR (cast film, cm^{-1}) 3072, 2961, 2856, 1615, 1518, 1112.

HRMS (ESI) for $[M + Na]^+$ $C_{38}H_{48}NaO_5Si$ (m/z): calcd. 635.3163; found 635.3154, $[M + NH_4]^+$ $C_{38}H_{52}NO_5Si$ (m/z): calcd. 630.3609; found 630.3606, $[M + H]^+$ $C_{38}H_{49}O_5Si$ (m/z): calcd. 613.3344; found 613.3329.

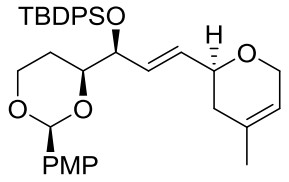

***tert*-Butyl({(1*S*,2*E*)-1-[(2*S*,4*S*)-2-(4-methoxyphenyl)-1,3-dioxan-4-yl]-3-[(2*S*)-4-methyl-3,6-dihydro-2*H*-pyran-2-yl]prop-2-en-1-yl}oxy)diphenylsilane (2-39b)**

To a solution of **2-38b** (440 mg, 0.720 mmol) in CH_2Cl_2 (77 mL) was added Grubbs first generation catalyst (120 mg, 0.146 mmol, 20 mol%) and the reaction mixture was heated at 40 ^oC overnight. The reaction mixture was filtered over a silica pad (1% Et_3N in Et_2O) then concentrated. The crude product was purified by flash chromatography on silica gel (0.5% Et_3N in a solution of 5 to 25% Et_2O/hexanes) to afford the title compound (374 mg, 89%).

Clear oil; R_f = 0.38 (30% Et_2O/hexanes).

$[\alpha]^{20}_D$ –22.0 (*c* 1.46, CH_2Cl_2).

^{1}H NMR (400 MHz, $CDCl_3$) δ 7.69–7.62 (m, 4 H), 7.41–7.36 (m, 2 H), 7.30–7.28 (m, 6 H), 6.85–6.82 (m, 2 H), 5.74 (ddd, *J* = 15.7, 6.4, 1.1 Hz, 1 H), 5.58 (ddd, *J* = 15.8, 5.6, 0.9 Hz, 1 H), 5.38 (br s, 1 H), 5.30 (s, 1 H), 4.34 (dd, *J* = 6.2, 6.0 Hz, 1 H), 4.22–4.18 (m, 1 H), 4.15–4.12 (m, 2 H), 3.95–3.87 (m, 1 H), 3.87–3.71 (m, 5 H), 1.89–1.70 (m, 3 H), 1.67 (s, 3 H), 1.45 (d, *J* = 13.7 Hz, 1 H), 1.05 (d, *J* = 3.7 Hz, 9 H).

^{13}C NMR (126 MHz, C_6D_6) δ 160.3, 136.8, 136.7, 134.8, 134.3, 133.9, 132.3, 131.2, 129.8, 129.8, 129.1, 128.1, 127.8, 120.4, 113.6, 101.6, 80.6, 76.7, 73.1, 66.8, 65.6, 54.7, 35.8, 30.4, 27.4, 25.6, 22.9, 19.8.

IR (cast film, cm^{-1}) 3071, 2961, 2930, 2855, 1615, 1517, 1249, 1112.

HRMS (ESI) for $[M + Na]^+$ $C_{36}H_{44}NaO_5Si$ (m/z): calcd. 607.2850; found 607.2855, $[M + H]^+$ $C_{36}H_{45}O_5Si$ (m/z): calcd. 585.3031; found 585.3017.

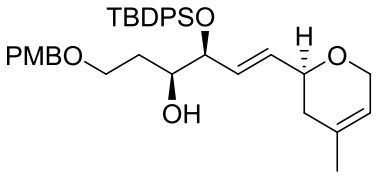

(3*S*,4*S*,5*E*)-4-{[*tert*-Butyl(diphenyl)silyl]oxy}-1-[(4-methoxybenzyl)oxy]-6-[(2*S*)-4-methyl-3,6-dihydro-2*H*-pyran-2-yl]hex-5-en-3-ol (2-40b)

To a solution of **2-39b** (356 mg, 0.609 mmol) in DMF (12.4 mL) was added 4Å MS (184 mg) followed by $NaBH_3CN$ (294 mg, 4.67 mmol, 7.7 equiv) at 0 °C. After adding TFA (0.260 mL, 3.43 mmol, 5.6 equiv) the reaction mixture was allowed to gradually warm to rt overnight. When the starting material was fully consumed, the reaction mixture was treated with Et_3N (1.0 mL) then the solution was diluted with saturated NH_4Cl (100 mL). The resulting biphasic solution was extracted with Et_2O (5 × 50 mL) and the organic fractions were pooled together. The organic fraction was washed with brine (25 mL), dried ($MgSO_4$), filtered, and concentrated to afford a crude mixture of the desired regioisomer in a >20:1 mixture of isomers as confirmed by ^1H NMR. The crude product was subjected to flash chromatography (5 to 40% Et_2O/hexanes) to afford the title compound (338 mg, 94%).

Clear oil; R_f = 0.29 (50% Et_2O/hexanes).

$[\alpha]^{20}_D$ –47.8 (*c* 1.39, CH_2Cl_2).

^1H NMR (500 MHz, C_6D_6) δ 7.86–7.76 (m, 4 H), 7.21–7.19 (m, 6 H), 7.17–7.12 (m, 2 H), 6.80–6.74 (m, 2 H), 5.95 (ddd, *J* = 15.8, 7.5, 1.5 Hz, 1 H), 5.57 (ddd, *J* = 15.8, 5.0, 0.8 Hz, 1 H), 5.11 (br s, 1 H), 4.35 (app dd, *J* = 7.5, 3.5 Hz, 1 H), 4.26–4.18 (m, 2 H), 4.11–4.02 (m, 1 H), 4.01–3.90 (m, 2 H), 3.80–3.73 (m, 1 H), 3.56–3.41 (m, 2 H), 3.30 (s, 3 H), 2.69 (d, *J* = 3.0 Hz, 1 H), 1.91–1.73 (m, 3 H), 1.52–1.46 (m, 4 H), 1.18 (s, 9 H).

^{13}C NMR (126 MHz, $CDCl_3$) δ 159.2, 136.1, 136.0, 134.1, 133.9, 133.5, 131.4, 130.5, 129.8,

129.6, 129.6, 129.3, 127.7, 127.7, 127.4, 119.6, 113.8, 77.7, 73.5, 73.1, 72.8, 67.8, 65.4, 55.3, 35.3, 32.3, 27.1, 22.9, 19.5.

IR (cast film, cm^{-1}) 3478, 3071, 2957, 2930, 2856, 1612, 1513, 1248, 1111.

HRMS (ESI) for $[M + Na]^+$ $C_{36}H_{46}NaO_5Si$ (m/z): calcd. 609.3007; found 609.2998, $[M + NH_4]^+$ $C_{36}H_{50}NO_5Si$ (m/z): calcd. 604.3453; found 604.3454.

General procedure for ester analogues derived from 2-34b

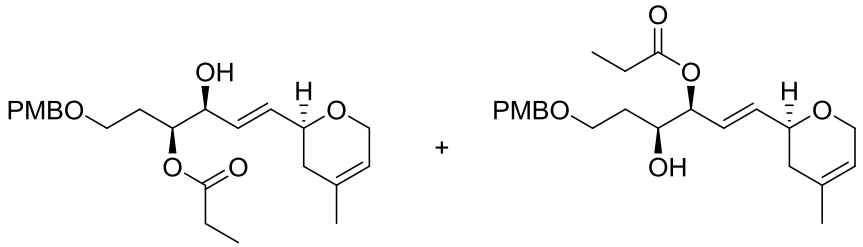

(1*S*,2*S*,3*E*)-2-Hydroxy-1-{2-[(4-methoxybenzyl)oxy]ethyl}-4-[(2*S*)-4-methyl-3,6-dihydro-2*H*-pyran-2-yl]but-3-en-1-yl propionate (2-41b) and (1*S*,2*E*)-1-{(1*S*)-1-Hydroxy-3-[(4-methoxybenzyl)oxy]propyl}-3-[(2*S*)-4-methyl-3,6-dihydro-2*H*-pyran-2-yl]prop-2-en-1-yl propionate (2-51) To a solution of alcohol **2-40b** (35.4 mg, 0.0604 mmol) in CH_2Cl_2 (1.0 mL) was added DMAP (1.00 mg, 0.00818 mmol, 14 mol%), then propionic anhydride (9.00 µL, 0.0691 mmol, 1.1 equiv). After stirring the reaction mixture overnight at rt, the solution was concentrated and the residue was directly subjected to flash chromatography (5 to 20% Et_2O/hexanes) to afford the ester product. The silyl-protected product was then transferred to a plastic vessel containing a stir bar using CH_3CN (0.600 mL). After pyridine (0.098 mL, 1.21 mmol, 20 equiv) was added, the solution was cooled to 0 ^oC followed by dropwise addition of HF•pyr complex (0.110 mL, 1.74 mmol, 29 equiv) then gradually allowed to warm to rt. After stirring the reaction for several days, the solution was cooled to 0 ^oC and treated with saturated NH_4Cl (10 mL). The solution was extracted with CH_2Cl_2 (3 × 10 mL) and the organic fractions were pooled together. The organic phase was washed with brine (10 mL), dried (Na_2SO_4),

filtered, and concentrated. The crude product was subjected to flash chromatography (10% EtOAc/CH_2Cl_2) to afford a 4:1 mixture of **2-41b**:**2-51** (5.00 mg, 21%) and **2-51** as a single isomer (7.00 mg, 29%).

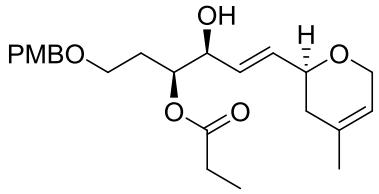

2-41b : 2-51 = 4:1

(1*S*,2*S*,3*E*)-2-Hydroxy-1-{2-[(4-methoxybenzyl)oxy]ethyl}-4-[(2*S*)-4-methyl-3,6-dihydro-2*H*-pyran-2-yl]but-3-en-1-yl propionate (2-41b)

Clear oil; R_f = 0.13 (10% EtOAc/CH_2Cl_2).

$[\alpha]^{20}_D$ –62.3 (*c* 0.580, $CHCl_3$).

^{1}H NMR (500 MHz, $CDCl_6$) δ 7.24 (app d, *J* = 7.7 Hz, 2 H), 6.87 (app d, *J* = 7.4 Hz, 2 H), 5.85 (dd, *J* = 15.7, 5.4 Hz, 1 H), 5.74 (dd, *J* = 15.7, 5.3 Hz, 1 H), 5.41 (br s, 1 H), 5.10–5.00 (m, 1 H), 4.41 (dd, *J* = 15.7, 10.5 Hz, 2 H), 4.27–4.11 (m, 3 H), 4.06–3.97 (m, 1 H), 3.80 (d, *J* = 1.1 Hz, 3 H), 3.57–3.41 (m, 2 H), 2.54 (d, *J* = 4.6 Hz, 1 H), 2.39–2.24 (m, 2 H), 2.02 (ddd, *J* = 19.0, 12.3, 5.7 Hz, 2 H), 1.94–1.81 (m, 2 H), 1.69 (s, 3 H), 1.13 (app dtd, *J* = 8.7, 7.5, 1.2 Hz, 3 H).

^{13}C NMR (126 MHz, $CDCl_3$) δ 174.2, 173.7, 159.3, 135.2, 132.9, 131.4, 130.0, 129.6, 129.5, 129.4, 129.34, 129.30, 125.6, 119.75, 119.70, 113.90, 113.88, 74.0, 73.9, 73.4, 73.2, 73.07, 73.06, 73.00, 72.98, 72.9, 72.8, 72.0, 68.0, 66.1, 65.71, 65.66, 55.3, 35.73, 35.66, 32.5, 32.0, 30.8, 29.8, 29.7, 29.6, 29.41, 29.38, 27.8, 27.7, 23.0, 22.9, 22.7, 14.2, 9.24, 9.18.

IR (cast film, cm^{-1}) 3424, 2927, 2854, 1735, 1612, 1513, 1248, 1182.

HRMS (ESI) for $[M + Na]^+$ $C_{23}H_{32}NaO_6$ (m/z): calcd. 427.2091; found 427.2094, $[M + NH_4]^+$ $C_{36}H_{50}NO_5Si$ (m/z): calcd. 422.2537; found 422.2550.

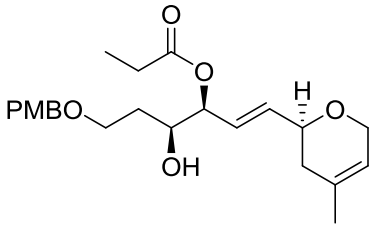

(1*S*,2*E*)-1-{(1*S*)-1-Hydroxy-3-[(4-methoxybenzyl)oxy]propyl}-3-[(2*S*)-4-methyl-3,6-dihydro-2*H*-pyran-2-yl]prop-2-en-1-yl propionate (2-51b)

Clear oil; R_f = 0.12 (10% EtOAc/CH_2Cl_2).

[α]$^{20}_{D}$ –44.8 (*c* 0.690, $CHCl_3$).

^{1}H NMR (500 MHz, $CDCl_3$) δ 7.25–7.22 (m, 2 H), 6.89–6.85 (m, 2 H), 5.86 (dd, *J* = 15.8, 4.7 Hz, 1 H), 5.75 (ddd, *J* = 15.7, 6.7, 1.2 Hz, 1 H), 5.41 (br s, 1 H), 5.27 (app t, *J* = 6.1 Hz, 1 H), 4.44 (app s, 2 H), 4.23–4.11 (m, 2 H), 4.05–3.99 (m, 1 H), 3.89 (ddd, *J* = 8.5, 5.2, 3.0 Hz, 1 H), 3.80 (s, 3 H), 3.71–3.65 (m, 1 H), 3.61 (ddd, *J* = 9.3, 7.5, 4.9 Hz, 1 H), 2.84 (s, 1 H), 2.37 (qd, *J* = 7.6, 1.9 Hz, 2 H), 2.09–1.99 (m, 1 H), 1.89 (app d, *J* = 16.7 Hz, 1 H), 1.80–1.69 (m, 5H), 1.14 (t, *J* = 7.6 Hz, 3 H).

^{13}C NMR (126 MHz, $CDCl_3$) δ 173.7, 159.3, 135.2, 131.4, 130.0, 129.4, 125.6, 119.7, 113.9, 76.4, 73.1, 73.0, 72.0, 68.0, 65.7, 55.3, 35.7, 32.5, 27.8, 22.9, 9.2.

IR (cast film, cm^{-1}) 3461, 2927, 2854, 1736, 1612, 1513, 1248, 1181.

HRMS (ESI) for $[M + Na]^+$ $C_{23}H_{32}NaO_6$ (m/z): calcd. 427.2091; found 427.2082, $[M + NH_4]^+$ $C_{36}H_{50}NO_5Si$ (m/z): calcd. 422.2538; found 422.2537.

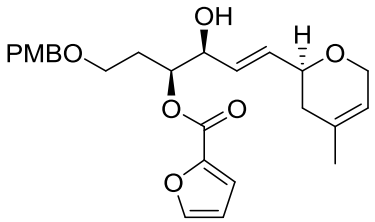

(1*S*,2*S*,3*E*)-2-Hydroxy-1-{2-[(4-methoxybenzyl)oxy]ethyl}-4-[(2*S*)-4-methyl-3,6-dihydro-2*H*-pyran-2-yl]but-3-en-1-yl 2-furoate (2-43b)

To a solution of alcohol **2-40b** (15.5 mg, 0.0264 mmol) in CH_2Cl_2 (0.510 mL) was added DMAP (21.4 mg, 0.175 mmol, 6.6 equiv), DCC (37.0 mg, 0.179 mmol, 6.8 equiv) then 2-furanoic acid (12.7 mg, 0.111 mmol, 4.2 equiv). After stirring the solution overnight at rt, the reaction mixture was concentrated and the residue was directly subjected to flash chromatography (5% Et_2O/hexanes) to afford the ester product. The silyl-protected product was then transferred to a plastic vessel containing a stir bar using CH_3CN (0.500 mL). After pyridine (0.043 mL, 0.532 mmol, 20 equiv) was added, the solution was cooled to 0 ^oC followed by dropwise addition of HF•pyr complex (0.065 mL, 1.03 mmol, 39 equiv) then gradually warmed to rt. After stirring the reaction mixture for several days the solution was cooled to 0 ^oC and treated with saturated NH_4Cl (10 mL). The solution was extracted with CH_2Cl_2 (3 × 10 mL) and the organic fractions were pooled together. The organic phase was washed with brine (10 mL), dried (Na_2SO_4), filtered, and concentrated. The crude product was subjected to preparative TLC (5% EtOAc/CH_2Cl_2) to afford the title compound (7.40 mg, 41%).

Clear oil; R_f = 0.17 (10% EtOAc/CH_2Cl_2).

$[\alpha]^{20}_D$ –56.4 (*c* 0.480, $CHCl_3$).

^{1}H NMR (500 MHz, $CDCl_3$) δ 7.58 (app s, 1 H), 7.22 (app d, *J* = 8.6 Hz, 2 H), 7.17 (d, *J* = 3.5 Hz, 1 H), 6.84 (app d, *J* = 8.6 Hz, 2 H), 6.50 (dd, *J* = 3.4, 1.7 Hz, 1 H), 5.87 (dd, *J* = 15.8, 5.6 Hz, 1H), 5.79 (dd, *J* = 15.7, 5.2 Hz, 1H), 5.38 (br s, 1 H), 5.27 (app dt, *J* = 8.0, 4.9 Hz, 1 H),

4.46–4.36 (m, 2 H), 4.32 (dd, *J* = 10.4, 5.2 Hz, 1 H), 4.15 (d, *J* = 1.9 Hz, 2 H), 4.04–3.97 (m, 1 H), 3.79 (s, 3 H), 3.58 (app dt, *J* = 10.7, 5.5 Hz, 1 H), 3.54–3.48 (m, 1 H), 2.56 (d, *J* = 6.2 Hz, 1 H), 2.18–2.07 (m, 1 H), 2.05–1.89 (m, 2 H), 1.79 (d, *J* = 16.9 Hz, 1 H), 1.66 (s, 3 H).

^{13}C NMR (126 MHz, $CDCl_3$) δ 159.3, 158.4, 146.5, 144.5, 133.3, 131.4, 130.0, 129.5, 129.4, 119.7, 118.2, 113.8, 111.9, 74.7, 73.4, 73.0, 73.0, 66.0, 65.6, 55.3, 35.6, 30.9, 22.9.

IR (cast film, cm^{-1}) 3433, 2930, 1724, 1612, 1579, 1513, 1473, 1295.

HRMS (ESI) for $[M + Na]^+$ $C_{25}H_{30}NaO_7$ (m/z): calcd. 465.1884; found 465.1876, $[M + NH_4]^+$ $C_{25}H_{34}NO_7$ (m/z): calcd. 460.2330; found 460.2325.

2.6 References

[1] Siegel, R. L.; Miller, K. D.; Jemal, A. *Ca-Cancer J. Clin.* **2015**, *65*, 5-29.

[2] Jordan, M. A.; Wilson, L. *Nat. Rev. Cancer* **2004**, *4*, 253–265.

[3] Fanale, D.; Bronte, G.; Passiglia, F.; Calo, V.; Castiglia, M.; Di Piazza, F.; Barraco, N.; Cangemi, A.; Catarella, M.; Insalaco, L.; Listi, A.; Maragliano, R.; Massihnia, D.; Perez, A.; Toia, F.; Cicero, G.; Bazan, V. *Anal. Cell. Pathol.* **2015**, *2015*, 1–19.

[4] Henderson, M., The Story of Taxol: Nature and Politics in the Pursuit of an Anti-Cancer Drug. 2001.

[5] *WHO Model List of Essential Medicines* World Health Organization: April 2015.

[6] Frishman, W. H.; Sung, H. M.; Yee, H. C. M.; Liu, L. L.; Einzig, A. I.; Dutcher, J.; Keefe, D. *Curr. Probl. Cardiol.* **1996**, *21*, 227–286.

[7] Alagaratnam, T. *J.-Lancet* **1993**, *342*, 1232–1233.

[8] Sharma, U. S.; Balasubramanian, S. V.; Straubinger, R. M. *J. Pharm. Sci.* **1995**, *84*, 1223-1230.

[9] Mooberry, S. L.; Tien, G.; Hernandez, A. H.; Plubrukarn, A.; Davidson, B. S. *Cancer Res.* **1999**, *59*, 653–660.

[10] Gapud, E. J.; Bai, R.; Ghosh, A. K.; Hamel, E. *Mol. Pharmacol.* **2004**, *66*, 113–121.

[11] Hamel, E.; Day, B. W.; Miller, J. H.; Jung, M. K.; Northcote, P. T.; Ghosh, A. K.; Curran, D. P.; Cushman, M.; Nicolaou, K. C.; Paterson, I.; Sorensen, E. J. *Mol. Pharmacol.* **2006**,

70, 1555–1564.

[12] Clark, E. A.; Hills, P. M.; Davidson, B. S.; Wender, P. A.; Mooberry, S. L. *Mol. Pharm.* **2006**, *3*, 457–467.

[13] Quinoa, E.; Kakou, Y.; Crews, P. *J. Org. Chem.* **1988**, *53*, 3642–3644.

[14] Corley, D. G.; Herb, R.; Moore, R. E.; Scheuer, P. J.; Paul, V. J. *J. Org. Chem.* **1988**, *53*, 3644–3646.

[15] Jefford, C. W.; Bernardinelli, G.; Tanaka, J.; Higa, T. *Tetrahedron Lett.* **1996**, *37*, 159–162.

[16] Pryor, D. E.; O'Brate; Bilcer, G.; Díaz, J. F.; Wang, Y.; Wang, Y.; Kabaki, M.; Jung, M. K.; Andreu, J. M.; Ghosh, A. K.; Giannakakou, P.; Hamel, E. *Biochemistry* **2002**, *41*, 9109–9115.

[17] Mitchison, T. J. *Annu. Rev. Cell Biol.* **1988**, *4*, 527–545.

[18] Hayden, J. H.; Bowser, S. S.; Rieder, C. L. *J. Cell Biol.* **1990**, *111*, 1039–1045.

[19] Alberts, B.; Bray, D.; Hopkin, K.; Johnson, A. D.; Lewis, J.; Raff, M.; Roberts, K.; Walter, P. *Essential Cell Biology*. 4th edition ed.; Garland Science: New York, 2013.

[20] Bennett, M. J.; Barakat, K.; Huzil, J. T.; Tuszynski, J.; Schriemer, D. C. *Chemistry & Biology* **2010**, *17*, 725–734.

[21] Engen, J. R. *Anal. Chem.* **2009**, *81*, 7870–7875.

[22] Percy, A. J.; Rey, M.; Burns, K. M.; Schriemer, D. C. *Anal. Chim. Acta* **2012**, *721*, 7–21.

[23] Englander, S. W.; Mayne, L.; Bai, Y.; Sosnick, T. R. *Protein Sci.* **1997**, *6*, 1101–1109.

[24] Konermann, L.; Pan, J.; Liu, Y. *Chem. Soc. Rev.* **2011**, *40*, 1224–1234.

[25] Lee, J.; Park, Y.; Lee, K. *Arch. Pharmacal Res.* **2015**, *38*, 1737–1745.

[26] (a) Gallagher, B. M.; Fang, F. G.; Johannes, C. W.; Pesant, M.; Tremblay, M. R.; Zhao, H.; Akasaka, K.; Li, X.; Liu, J. G.; Littlefield, B. A. *Bioorg. Med. Chem. Lett.* **2004**, *14*, 575–579; (b) Faveau, C.; Mondon, M.; Gesson, J.; Mahnke, T.; Gebhardt, S.; Koert, U. *Tetrahedron Lett.* **2006**, *47*, 8305–8308; (c) Gollner, A.; Altmann, K. H.; Gertsch, J.; Mulzer, J. *Chemistry* **2009**, *15*, 5979–5997; (d) Wender, P. A.; Hegde, S. G.; Hubbard, R. D.; Zhang, L.; Mooberry, S. L. *Org. Lett.* **2003**, *5*, 3507–3509; (e) Wender, P. A.; Hilinski, M. K.; Soldermann, N.; Mooberry, S. L. *Org. Lett.* **2006**, *8*, 1507–1510; (f) Paterson, I.; Menche, D.; Håkansson, A. E.; Longstaff, A.; Wong, D.; Barasoain, I.; Buey, R. M.; Díaz, J. F. *Bioorg. Med. Chem. Lett.* **2005**, *15*, 2243–2247.

[27] Prota, A. E.; Bargsten, K.; Northcote, P. T.; Marsh, M.; Altmann, K.-H.; Miller, J. H.;

Díaz, J. F.; Steinmetz, M. O. *Angew. Chem. Int. Ed.* **2014**, *53*, 1621–1625.

[28] Wender, P. A.; Verma, V. A.; Paxton, T. J.; Pillow, T. H. *Acc. Chem. Res.* **2008**, *41*, 40–49.

[29] Tanaka, J.; Higa, T.; Bernardinelli, G.; Jefford, C. W. *Chem. Lett.* **1996**, *25*, 255–256.

[30] Wender, P. A.; Baryza, J. L.; Bennett, C. E.; Bi, F. C.; Brenner, S. E.; Clarke, M. O.; Horan, J. C.; Kan, C.; Lacôte, E.; Lippa, B.; Nell, P. G.; Turner, T. M. *J. Am. Chem. Soc.* **2002**, *124*, 13648–13649.

[31] Ahmed, A.; Hoegenauer, E. K.; Enev, V. S.; Hanbauer, M.; Kaehlig, H.; Mulzer, J. *J. Org. Chem.* **2003**, *68*, 3026–3042.

[32] Gollner, A.; Altmann, K. H.; Gertsch, J.; Mulzer, J. *Tetrahedron Lett.* **2009**, *50*, 5790–5792.

[33] Wender, P. A.; Hilinski, M. K.; Skaanderup, P. R.; Soldermann, G. S.; Mooberry, S. L. *Org. Lett.* **2006**, *8*, 4105–4108.

[34] Bollag, D. M.; McQueney, P. A.; Zhu, J.; Hensens, O.; Koupal, L.; Liesch, J.; Goetz, M.; Lazarides, E.; Woods, C. M. *Cancer Res.* **1995**, *55*, 2325–2333.

[35] Hoye, T. R.; Jeffrey, C. S.; Shao, F. *Nat. Protocols* **2007**, *2*, 2451–2458.

[36] Voigtritter, K.; Ghorai, S.; Lipshutz, B. H. *J. Org. Chem.* **2011**, *76*, 4697–4702.

[37] Chatterjee, A. K.; Choi, T.; Sanders, D. P.; Grubbs, R. H. *J. Am. Chem. Soc.* **2003**, *125*, 11360–11370.

[38] Xing, C.; Liao, Y.; Zhang, Y.; Sabarova, D.; Bassous, M.; Hu, Q. *Eur. J. Org. Chem.* **2012**, *2012*, 1115–1118.

[39] Jain, P.; Antilla, J. C. *J. Am. Chem. Soc.* **2010**, *132*, 11884–11886.

[40] Gao, X.; Hall, D. G. *J. Am. Chem. Soc.* **2003**, *125*, 9308–9309.

[41] Penner, M.; Rauniyar, V.; Kaspar, L. T.; Hall, D. G. *J. Am. Chem. Soc.* **2009**, *131*, 14216–14217.

[42] Shiina, I.; Kikuchi, T.; Sasaki, A. *Org. Lett.* **2006**, *8*, 4955–4958.

[43] Judd, W. R.; Ban, S.; Aubé, J. *J. Am. Chem. Soc.* **2006**, *128*, 13736–13741.

[44] (a) Kato, Y.; Hashimoto, Y.; Nagasawa, K. *Molecules* **2003**, *8*, 488–499; (b) Kato, Y.; Nakano, Y.; Sano, H.; Tanatani, A.; Kobayashi, H.; Shimazawa, R.; Koshino, H.; Hashimoto, Y.; Nagasawa, K. *Bioorg. Med. Chem. Lett.* **2004**, *14*, 2579–2583.

[45] Yang, S.; Kang, T.; Rui, C.; Yang, X.; Sun, Y.; Cui, Z.; Ling, Y. *Chin. J. Chem.* **2011**, *29*, 2394–2400.

Chapter 3. Accessing Chiral Dihydropyrans Through a Stereospecific and Regiodivergent Allylic Suzuki-Miyaura Cross-Coupling Reaction

3.1.1 Introduction

As discussed in Chapter 1, a large set of bioactive molecules that contain a polyfunctionalized pyran core other than polysaccharides exhibit 2-, 4-, or 6-positioned carbon-based fragments. Although there are numerous ways of synthesizing pyrans, deciding which method that can access a broad set of pyran-derived compounds relies on the modification of these molecules. Dihydropyrans are a suitable building block owing to the presence of unsaturation to access a variety of pyran derivatives, such as δ-lactones or tetrahydropyrans. Furthermore, there are various ways to introduce heteroatoms onto a dihydropyran framework.[1] One aspect of pyran functionalization that requires further investigation is to selectively install carbon-based fragments, especially through catalytic C–C coupling. The profusion of natural products and druggable compounds containing aryl- or alkenyl-functionalized pyrans further justifies the development of novel methods to functionalize these building blocks.

3.1.2 Methods towards carbon-carbon cross-coupling of pyran substrates

In general, the invaluable class of palladium-catalyzed cross-coupling reactions allows a chemoselective carbon–carbon bond formation to occur that would otherwise be viewed as extremely difficult to achieve. Due to the extensive research into the synthesis of *C*-glycosides, there are numerous examples of Negishi, Heck, Stille and Suzuki-Miyaura cross-coupling at the C1-position of the dihydropyran moiety (Figure 3-1).[2]

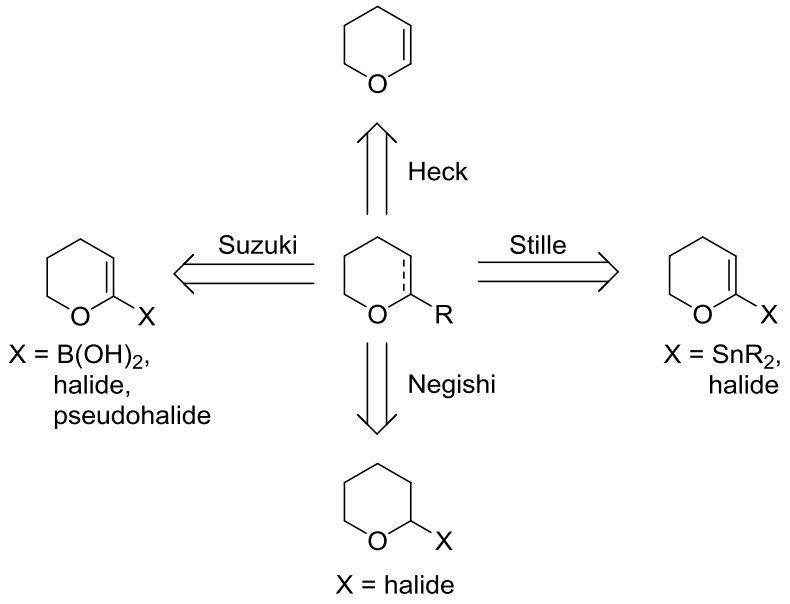

Figure 3-1: Generic types of cross-coupling onto the pyran framework.

In regards to dihydropyrans, an example of cross-coupling onto the pyran framework can be shown in the Heck coupling onto 2,3-dihydropyrans **3-1** (Scheme 3-1, Equation 1). Depending on the reaction conditions, the Heck reaction can favor the formation of 2,6-*trans* products with a (sp^2)-C(sp^3) bond at the C1-position. Based on the mechanism of a Heck reaction, these products consist of 3,4-dihydropyrans, where the unsaturation is a result of either *anti* elimination to form **3-2**[3] or β-hydride elimination[4] to afford **3-3**. There have also been numerous attempts at forming C(sp^2)-C(sp^2) bonds on dihydropyrans through Suzuki-Miyaura cross-coupling reactions. This cross-coupling reaction can be achieved with an electrophilic halide/pseudo-halide-glycal[5] or the boronic acid-[6] or ester-[7] bound glycal (Scheme 3-1, Equation 2). The Stille reaction with glycals has also been investigated, where it was shown to offer variable yields due to the formation of the glycal homodimer (Scheme 3-1, Equation 3).[8] This method was similarly used under Negishi conditions to develop a limited set of *C*-glycosides (Scheme 3-1, Equation 4).[9] Although these transition metal-catalyzed cross-coupling reactions are capable of forming C(sp^2)-C(sp^2) bonds –

other than the aforementioned Heck reaction – there are only rare examples of stereoselective transformations to form $C(sp^2)$-$C(sp^3)$ and $C(sp^3)$-$C(sp^3)$ bonds.[10] Furthermore, unlike the advantageous application of the Tsuji-Trost π-allyl cross-coupling method, these transformations are limited to functionalizing a single site on the pyran core. Thus, there is demand for the development of a regio- and stereoselective cross-coupling at various positions onto a pyran framework.

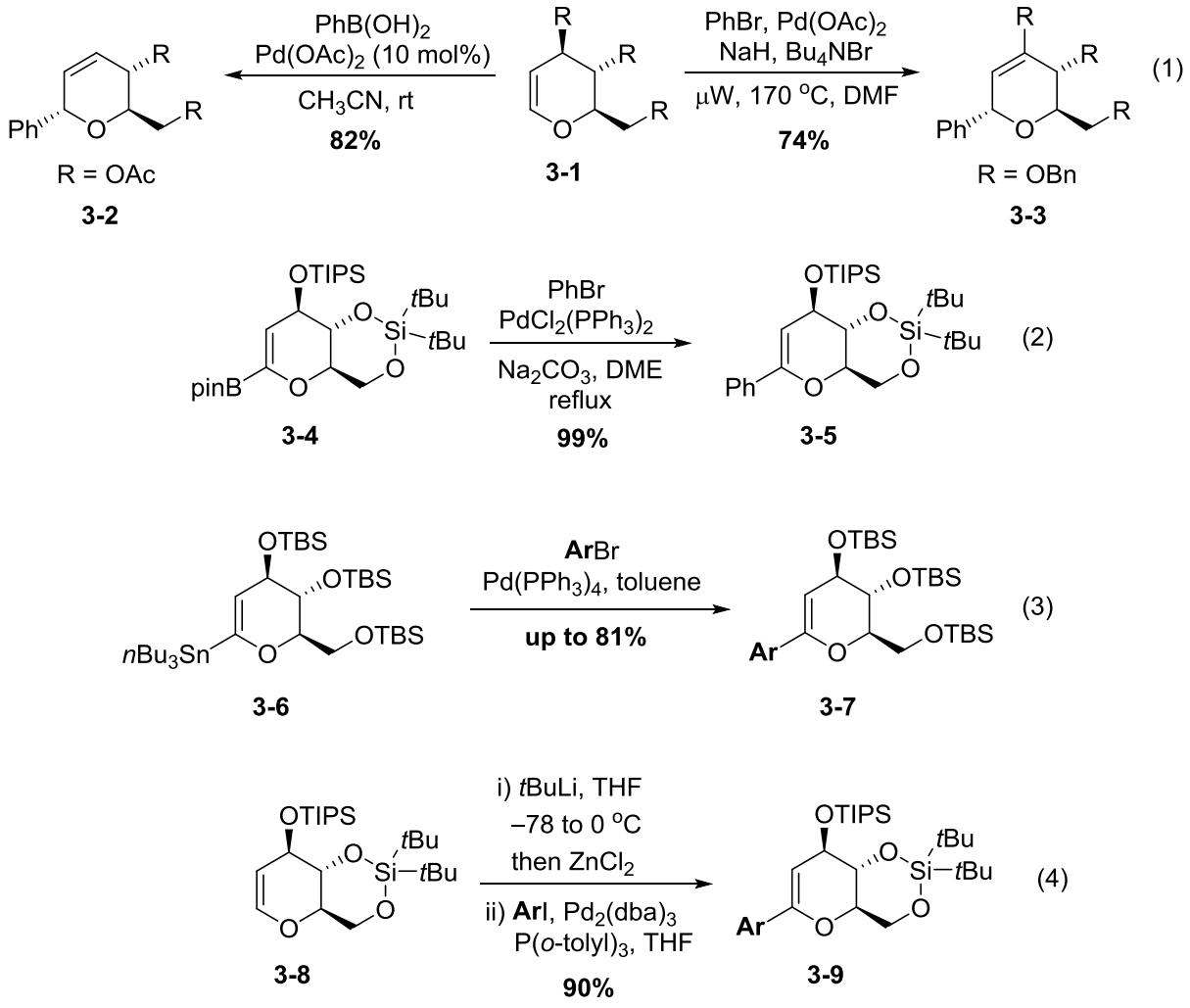

Scheme 3-1: Representative examples of cross-coupling onto dihydropyrans.

3.1.3 Advances in stereospecific Suzuki-Miyaura cross-coupling

The classical reactions of the Suzuki–Miyaura cross-coupling of organoboron substrates involved the formation of $C(sp^2)$-$C(sp^2)$ bonds, affording an invaluable reaction process that earned their creators a Nobel prize in 2010. Cross-coupling of sp^3-hybridized organoboron compounds to form $C(sp^2)$-$C(sp^3)$ and $C(sp^3)$-$C(sp^3)$ bonds offer a greater challenge and with advantages as it would be more applicable toward the formation of a variety of synthetically-relevant compounds that contain aryl, alkenyl as well as saturated hydrocarbon-functionalized species. Furthermore, sp^3-hybridized organoboron compounds offer an additional access to a new stereocenter at the $C(sp^2)$-$C(sp^3)$ bond, leading to potentially optically pure stereoisomers under stereochemically invertive or retentive conditions. In the past decade, there has been sufficient advances towards asymmetric synthesis of secondary and tertiary boronates[11,12] and, in conjuction, the stereospecific cross-coupling of these organoboronate substrates.[13,14] Controlling the stereoselectivity of sp^3-sp^2 and sp^3-sp^3 bonds is considered the final frontier in the Suzuki-Miyaura cross-couping reaction.

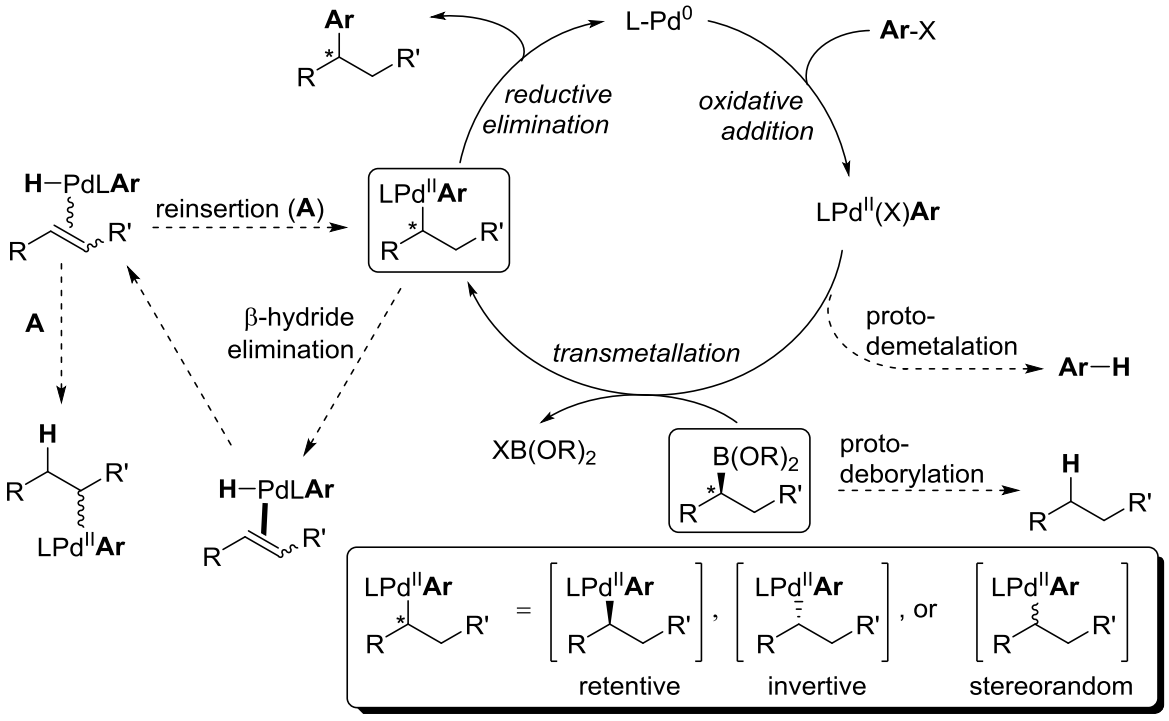

Figure 3-2: Catalytic cycle and mechanistic features for the Suzuki-Miyaura cross-coupling of chiral sp^3-hybridized organoboron substrates.

There are several potential drawbacks to the cross-coupling of alkyl boronates as shown in the reaction mechanism of a typical Suzuki-Miyaura reaction (Figure 3-2). After the oxidative addition of the Pd(0) catalyst, a relatively slow transmetallation step proceeds as a result of the less reactive sp^3-hybridized boronate.[13] Concurrently, the increased lifetime of the early-stage reaction species encourages protodeborylation of the alkyl boronate and protodemetallation of the organopalladium(II) species.[13] During the transmetallation step, poor stereocontrol would lead to erosion of stereochemistry leading to reduced enantiopurity; which is a result of a combined occurrence of inversion and retention of stereochemistry or a radical pathway.[14] The sp^3-hybridized organopalladium species is also susceptible to the formation of other side products that typically plague cross-coupling reactions, such as the β-hydride elimination,

leading to an alkene product, followed by reinsertion that may potentially lead to further racemization of the stereocenter or formation of alternate isomers.[14]

Recent progress in the coupling of chiral secondary alkylboron intermediates, albeit limited in scope and tolerance of the type of C-B functional group, have shown high enantiocontrol with either retention or inversion of the carbon stereocenter (Schemes 3-2 to 3-4).[14] In regards to stereoselective cross-coupling of sp^3-hybridized organoboron reagents to alkenyl and aryl halides, the initial investigations by Woerpel[15] and Soderquist[16] demonstrated that the cross-coupling of deuterated organoboranes proceeds with stereoretention. This assertion was confirmed through the measured coupling constants of the resulting products; later, similar studies by Jarvo[17] and Morken[18] would further support these observations. These seminal results motivated others to investigate stereocontrolled cross-coupling of various optically enriched organoboron substrates.

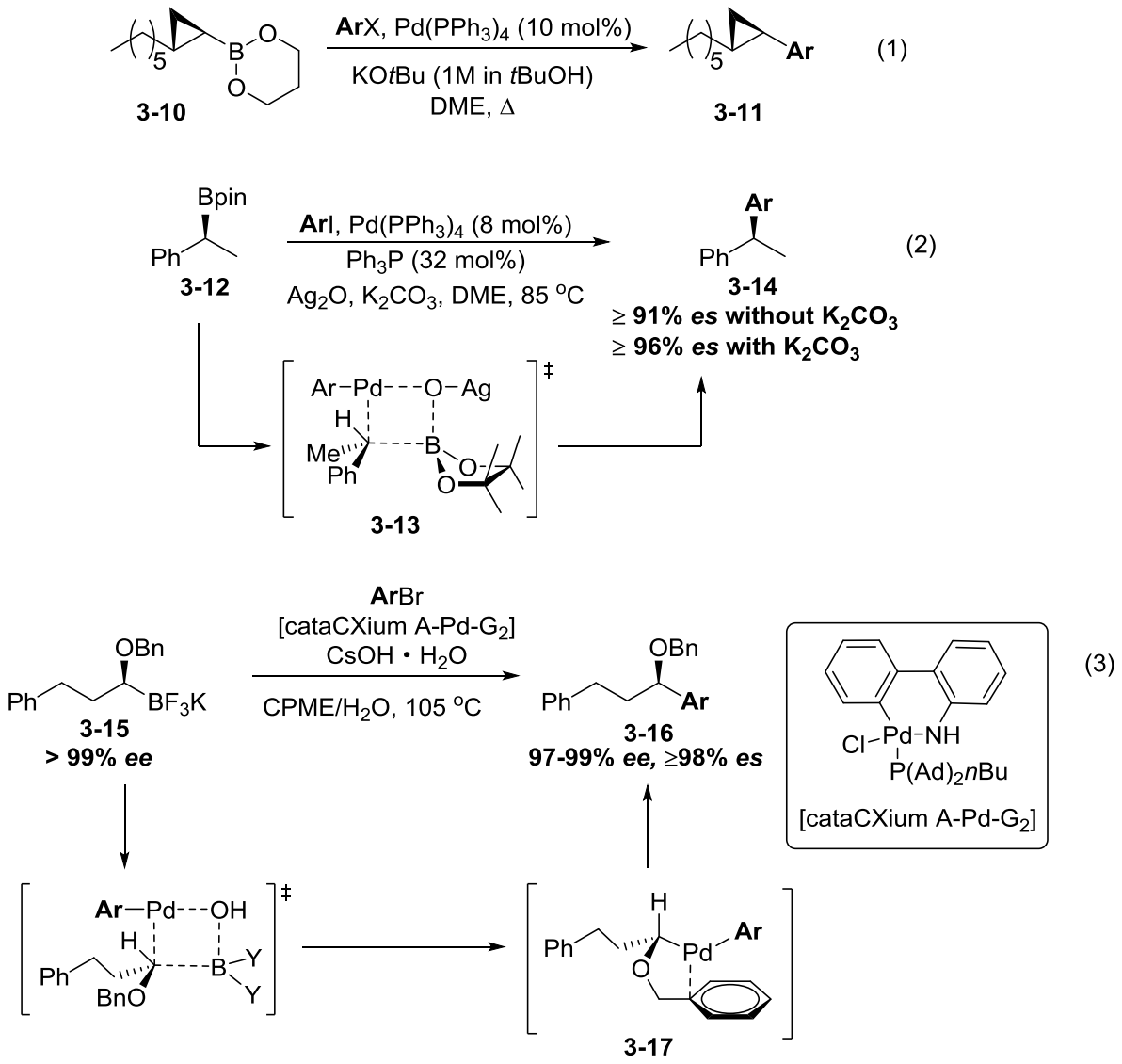

Scheme 3-2: Suzuki-Miyaura cross-coupling of sp3-hybridized organoboronate species.

Cyclopropylboronates were the first class of optically pure organoboron species used in the enantiospecific Suzuki-Miyaura cross-coupling (Scheme 3-2, Equation 1).[19] The reactivity of substrate **3-10** is believed to be a result of the increased "p"-character of the neighboring cyclopropane moiety, offering increased stabilization of the palladium-complexed intermediate formed after transmetallation. These reactions were later reported to have retention of stereochemistry, which was confirmed through 2D NOESY experiments.[20]

In 2009, Crudden and co-workers demonstrated the highly stereospecific cross-coupling of the enantioenriched 1-arylethylboronic esters **3-12**.[21] The conditions of this cross-coupling reaction involved the use of Ag_2O as base in the reaction; an essential additive in order to obtain high yields and stereospecificity.[21] The rationale behind the use of Ag_2O pertained to the knowledge of this additive's ability to accelerate the transmetallation step, thereby preventing the formation of side products and erosion of stereochemistry.[22] A follow-up to this work showed that the stereospecificity could be improved with the introduction of potassium carbonate, where the percent enantiospecificity of **3-14** increased from 91% *es* to 96% *es* (Scheme 3-2 Equation 2).[23] This base is believed to prevent the formation of the palladium hydride complex that leads to erosion of enantiopurity.[23] The stereoretention – as observed by the Crudden group – was believed to be a result of the four-membered transition state in the transmetallation step. In this transition state **3-13**, the oxo-palladium species transferred the aryl substituent synfacial to the activated sp^3-hybridized organoboronate species; a mechanism proposed previously by Soderquist and co-workers.[16] Based on the successful asymmetric cross-coupling reaction by the Crudden group, Molander and co-workers achieved the asymmetric cross-coupling of optically pure secondary sp^3-hybridized trifluoroborates containing a geminal-ether group **3-15**.[24] This reaction involves the cross-coupling of **3-15** with sp^2-hybridized organochlorides to afford aryl-substituted secondary benzylic alcohols **3-16** in high enantiomeric purity with high retention of stereochemistry.[25] The high enantiocontrol and yield are believed to be a result of the electron-withdrawing effect of the geminal-benzylether that prevents the palladium(II) species from undergoing a β-hydride elimination and thereby eroding the enantiomeric purity.[25] Furthermore, the organopalladium species **3-17** would be stabilized by the benzylic group, which is able to coordinate to the palladium(II) species through π-interactions.[25]

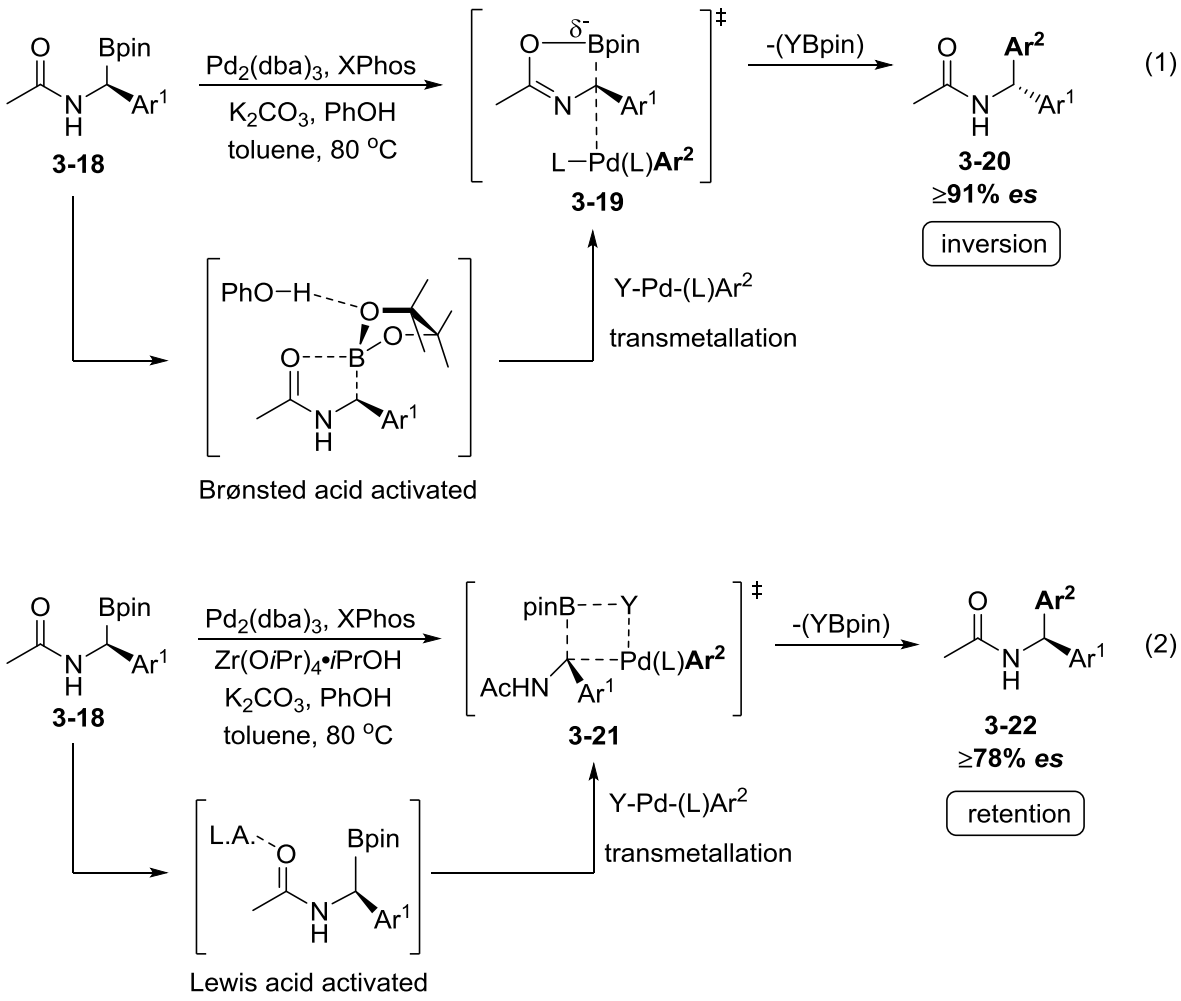

Scheme 3-3: A divergent pathway towards retention or inversion of stereochemistry in Suzuki-Miyaura cross-coupling products.

Ohmura and Suginome demonstrated that the inversion of stereochemistry of the amide carbonyl using chiral α-(acylamino)benzylboronates **3-18**, where an intramolecular coordination to the boronate could promote a backside attack from the palladium(II) species (Scheme 3-3).[26] This inversion pathway was also observed in Molander's cross-coupling of organotrifluoroborates using a similar amide-coordinating group.[27] Following this initial report, the Suginome group developed a divergent pathway where products **3-20** and **3-22** formed selectively with retention or inversion of stereochemistry.[28] This control was made possible by

activating the substrate with a suitable Brønsted or Lewis acid. The phenol additive promoted the inversion pathway by increasing the reactivity of the Lewis acidic boronate through hydrogen bonding. This effect would increase the electrophilicity of the boronate, thereby promoting effective coordination with the neighboring amide group to form the inversion transition state **3-19**. To promote the stereoretentive pathway, the Lewis acidic catalyst, $Zr(OiPr)_4$, is used to coordinated to the amide group. This interaction hinders the amide-boronate activation, leading to the more familiar four-coordinate transition state **3-21**. Cognizant of the successful work achieved by the Suginome, Molander, and Crudden, the Hall group successfully coupled aryl groups enantiospecifically and sequentially onto optically pure 1,1-diboron substrates (Scheme 3-4).[29] These innovative methods of stereospecific cross-coupling lay the groundwork for the potential application towards pyran functionalization.

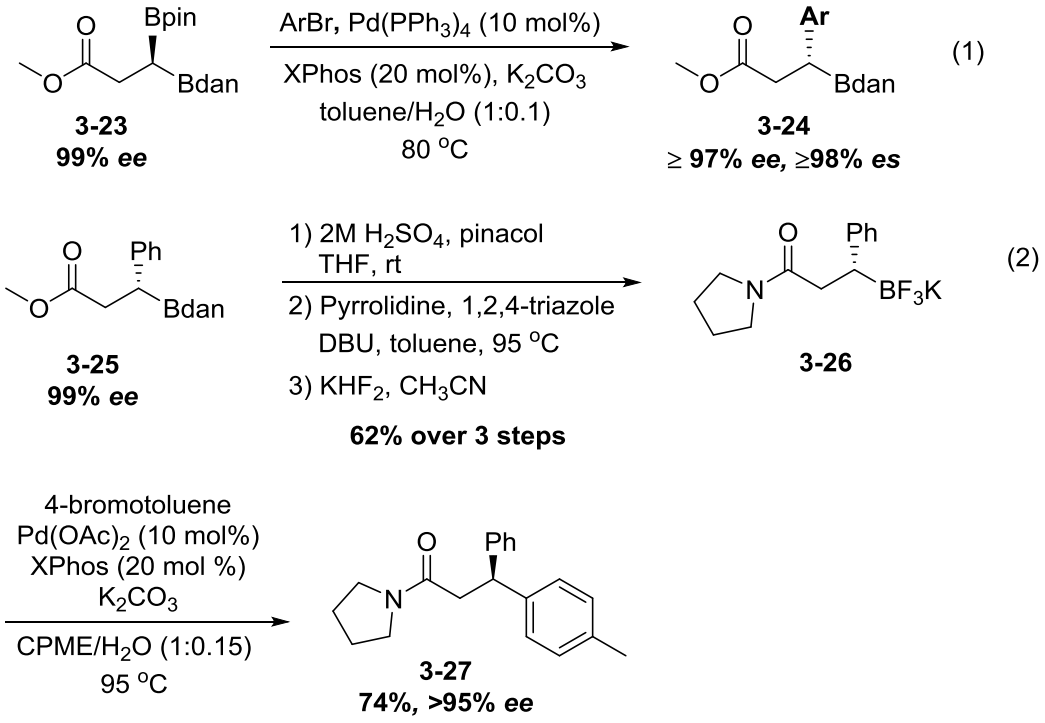

Scheme 3-4: Recent advances in doubly inverted stereospecific cross-coupling of 1,1-diboron.

3.1.4 Recent advances in the allylic Suzuki-Miyaura cross-coupling reaction

Other aspects of the Suzuki-Miyaura reaction that have recently been addressed include "site-selectivity" with respect to allylic boronates. These substrates offer the additional challenge of regioselectivity in a cross-coupling reaction, where the C-C bond can form at the alpha (α) or gamma (γ) site of the allylic-functional group (Figure 3-3). This issue was first investigated by Yamamoto and co-workers, where potassium allyltrifluoroborates **3-28** were coupled to an aryl bromide substrate using a Pd(0)/bisphosphine catalyst to afford only the γ-regioisomer **3-29** (Scheme 3-2, Equation 1).[30] Similarly, Szabó and co-workers demonstrated the same γ-selectivity by coupling highly reactive allylboronic acids **3-30** with aryl iodides using tetrakis palladium triphenylphosphine as catalyst (Scheme 3-5, Equation 2).[31] Based on the exclusive formation of the γ-regioisomer **3-31**, as well as mechanistic investigations, the authors concluded that the reaction did not proceed through the formation of a η^3 π-allyl palladium complex **3-34** and instead occurred *via* a S_E2' transmetallation from the complex **3-32**.[31,32] Through DFT studies, the Miyaura group proposed that this S_E2' pathway occurred *via* a potential coordination of the palladium(II) species toward the γ-position before transmetallation. Unfortunately, the authors did not have sufficient evidence in their theoretical studies to support this chelation effect.

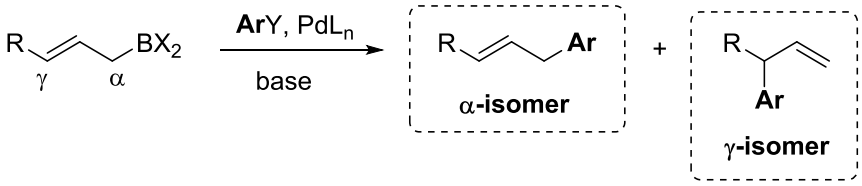

Figure 3-3: Addressing the issue of regioselectivity in cross-coupling of allylic boronates.

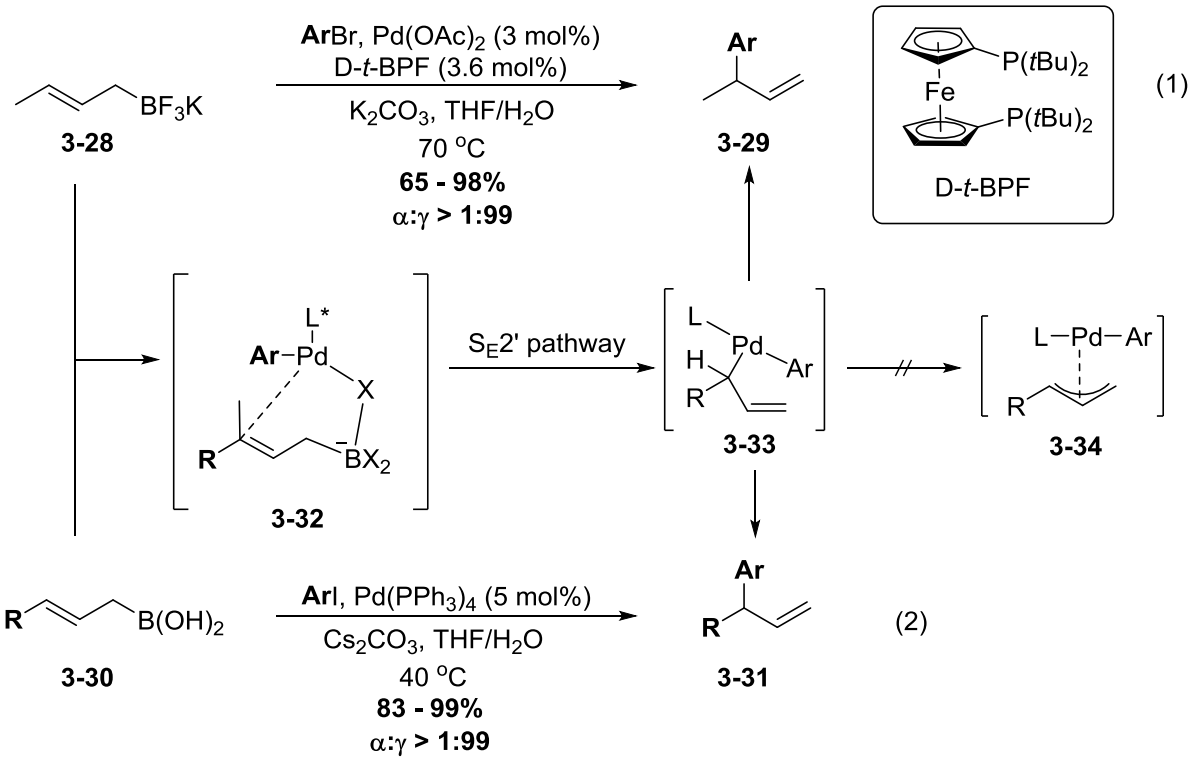

Scheme 3-5: Gamma-selective Suzuki-Miyaura cross-coupling of allylboron derivatives.

A complementary approach towards the exclusive formation of the α-regioisomers was achieved by the Organ group using their in-house developed electron rich *N*-heterocyclic carbene-ligated catalyst, Pd-PEPPSI-IPENT (Scheme 3-6).[33] In contrast to the results reported by Yamamoto and Szabó, this catalyst produced the α-regioisomer **3-36** exclusively from **3-35**. The bulkiness of the NHC ligand was credited for the absolute α-regioselectivity, where the S_E2' pathway could not be accessed and instead a S_E2-pathway was achieved.[33] Additionally, due to the nature of the bulky ligand, a fast reductive elimination would also proceed.[33] This characteristic would impede any possible σ-π isomerization and subsequent formation of the η^3 π-allyl palladium(II) complex.

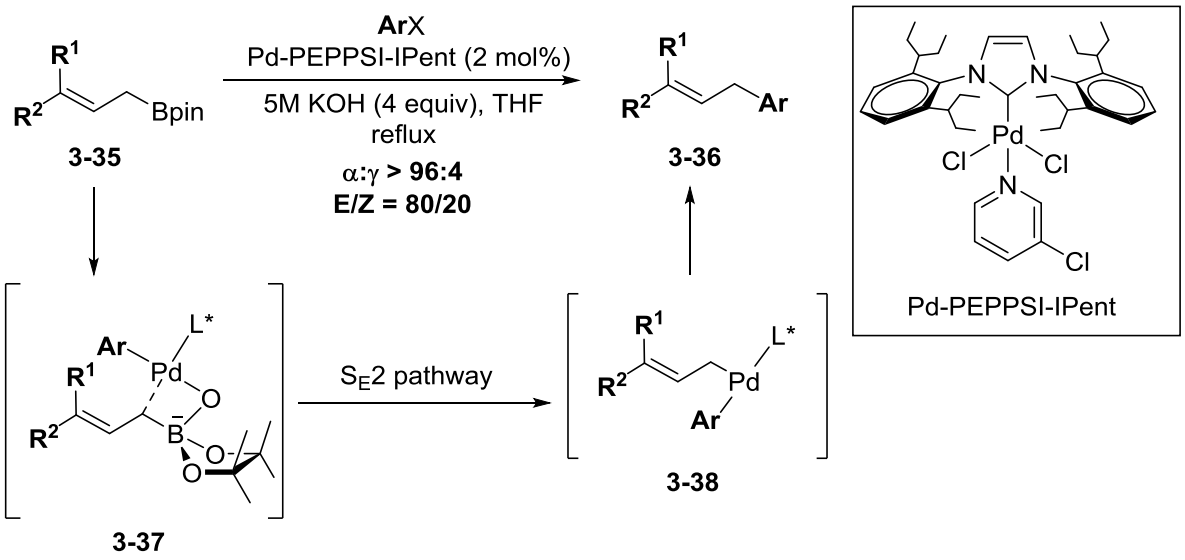

Scheme 3-6: Alpha-selective Suzuki-Miyaura cross-coupling of allylboronates.

Following their initial investigations into the cross-coupling of allylboronates,[34] Crudden and co-workers demonstrated that a combination of high γ-regioselectivity and stereospecificity was achieved using optically pure allylboronate substrates **3-39** (Scheme 3-7).[24] Based on the retention of stereochemistry – reporting an stereospecificity greater than 92% *es* – the authors proposed that the reaction proceeded through a *syn*-S_E2' pathway, where the oxyborate-coordinated palladium(II) intermediate **3-42** is coordinated to the γ-site. Although both regioisomers are produced in the allylic cross-coupling reaction, the α-product was not believed to be accessed through the π-allyl palladium(II) species **3-44**, formed *via* a σ-π-σ isomerization of the palladium species **3-43**. Instead, α-regioisomers are produced from a S_E transmetallation similar to **3-37**. The *E*-isomerization of these acyclic allylboronates is another obstacle that had not been addressed by previous investigations into the allylic Suzuki-Miyaura cross-coupling reaction. These secondary boronates would form a low energy chair conformation **3-42** in the transition state of the S_E2' transmetallation, where the substituent (R^1) would be positioned

equatorial. This effect was claimed to be a result of avoiding the 1,3-allylic strain between the substituents R^1 and R^2 and, as a result, *E*-isomers were the major products.[24,35]

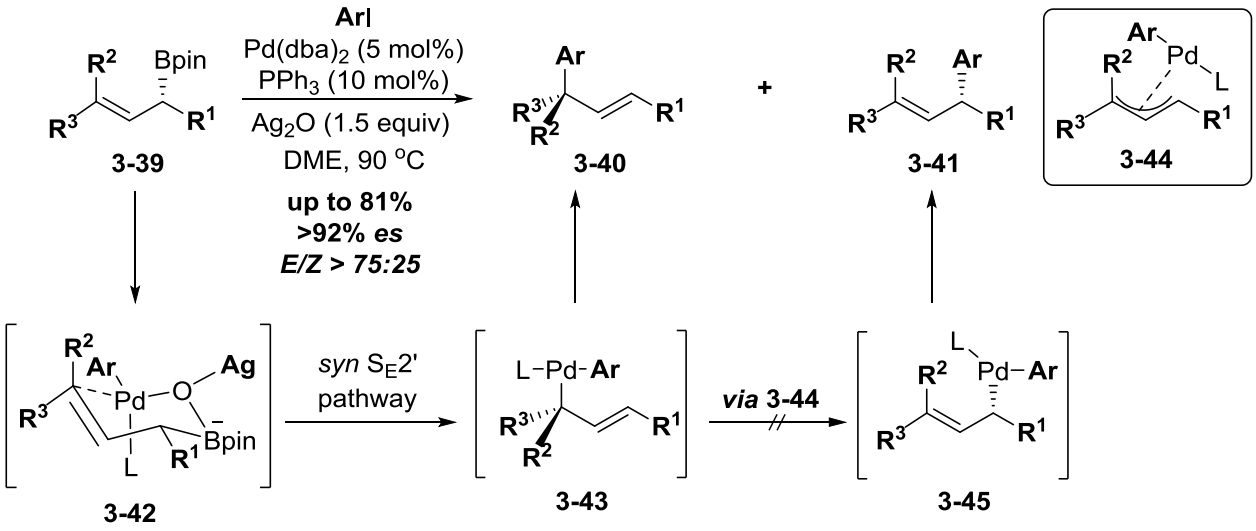

Scheme 3-7: Highly enantiospecific synthesis of α- and γ-regioisomers.

A ligand-controlled regiodivergent process was developed by Buchwald and coworkers, where the α-regioisomer **3-47** was formed when using ligand **3-49**, and likewise, the γ-regioisomer **3-48** was formed using ligand **3-50** (Scheme 3-8).[36] Based on the regioselectivity of the substrate scope as well as mechanistic investigations, the difference in regioselectivity in forming both isomers in high yield was a result of the relative steric-congestion on the corresponding ligands. The sterically-congested ligand **3-49** promoted the S_E2 pathway. The sufficiently less bulky ligand **3-50** was able to drive reaction through the S_E2' pathway to afford the γ-regioisomers. Based on the high regioselectivity, each pathway would result in a fast reductive elimination, thereby hindering the σ-π-σ interconversion involving the η^3 π-allyl palladium complex.

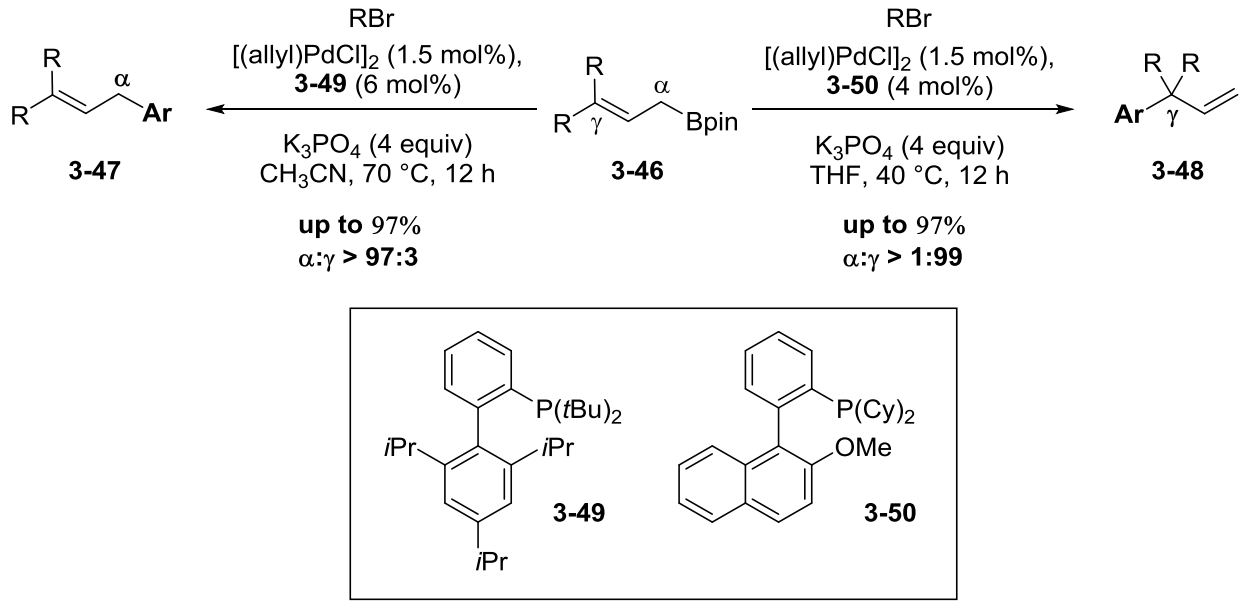

Scheme 3-8: Highly regioselective divergent synthesis of α- and γ-regioisomers.

Based on the current trends in the cross-coupling of allylboronates, both steric and electronic effects of the ligand as well as the allylboronate species govern the regioselectivity of Suzuki-Miyaura reaction. A combined asymmetric and regiodivergent pathway to access either isomer from a single substrate, simply by changing the catalyst, would be beneficial in accessing a broad spectrum of chiral-containing building blocks.

3.1.5 Optimization of the yield and regioselectivity of the Suzuki-Miyaura cross-coupling of dihydropyranyl boronate

As discussed in Chapter 1, new methods for the synthesis and functionalization of pyrans are needed in order to access these "privileged" building blocks. Using the methods of synthesizing chiral heterocyclic allylic boronates developed in the Hall group,[37] a combined regiodivergent and stereospecific Suzuki-Miyaura cross-coupling reaction to access 2- or 4-aryl- and alkenyl-substituted pyrans was envisioned. This would be a challenging feat, given that the allylic cross-

coupling reaction has only been used on simple allylboronates. Furthermore, elucidating the mechanism of the regio- and stereospecific formation of $C(sp^3)$-$C(sp^2)$ bonds will further expand the utility of the Suzuki-Miyaura reaction.

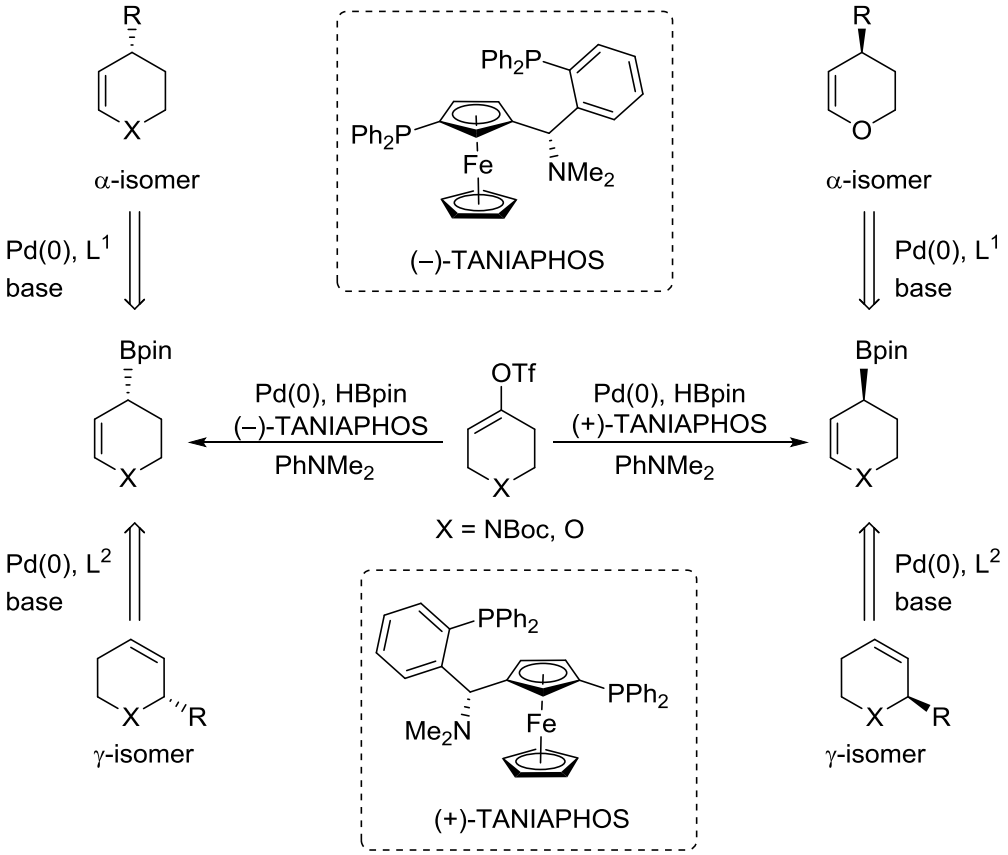

Figure 3-4: Potential enantioselective borylation/Suzuki-Miyaura cross-coupling leading to 2- and 4-substituted heterocycles.

The substrates required to study this method were obtained from our in-house methodology on the catalytic enantioselective borylative isomerization of heterocyclic alkenyl triflates to afford pyranyl and piperidinyl allylic boronates (Figure 3-4).[37] Using the enantiomers of the chiral ligand, TANIAPHOS, both enantiomers can be accessed through a catalytic enantioselective borylation in high selectivity using the achiral enol triflate. The chiral allylic boronates produced from this method could then undergo Suzuki-Miyaura cross-coupling with

organohalides to form both α- or γ-regioisomers. By controlling the regioselectivity of this reaction, this method would provide a concise access to optically-enriched 2- and 4-substituted pyran building blocks.

Table 3-1: Optimized conditions and key test reactions for α- and γ-regioisomers.[a]

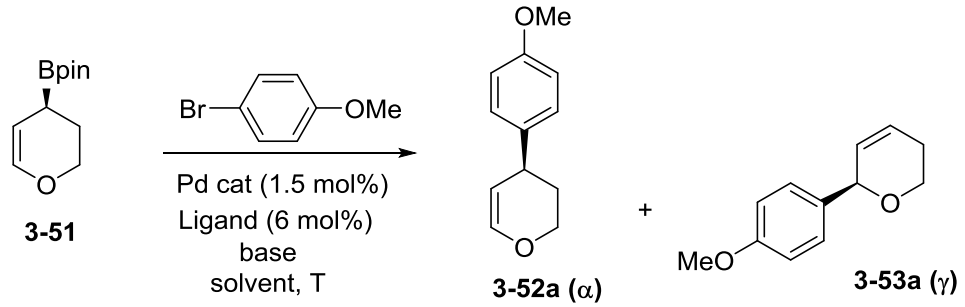

α-selectivity[c]

Pd cat	Ligand (6 mol%)	base	solvent, T	yield (%)[b] γ + α
$(AllylPdCl)_2$	$(p\text{-}CF_3C_6H_5)_3P$	K_3PO_4	CH_3CN, 70 °C	4 + 75
Pd-PEPPSI-IPr	–	K_3PO_4	CH_3CN, 70 °C	10 + 58
Pd-PEPPSI-IPent	–	K_3PO_4	THF, 70 °C	3 + 63

γ-selectivity[c]

Pd cat	Ligand (6 mol%)	base	solvent, T	yield (%)[b] γ + α
$Pd_2(dba)_3$	PPh_3	Ag_2O	THF, 40 °C	0
$(AllylPdCl)_2$	*t*BuXPhos	K_3PO_4	THF, 40 °C	85 + 0
$(AllylPdCl)_2$	XPhos	K_3PO_4	THF, 40 °C	92 + 0

[a] Reaction scale: **3-51** (0.30 mmol, 1.2 equiv), 4-bromoanisole (0.25 mmol, 1.0 equiv), Pd catalyst (3.8 μmol, 1.5 mol%), ligand (15 μmol, 6 mol%), base (1.3 mmol, 5 equiv).[b] Isolated yields of each regioisomer.[c] Optimization developed by Dr. Jinyue Ding.

Based on previous observations on the regioselective allylic Suzuki-Miyaura cross-coupling reaction – as discussed in Section 3.1.4 – the regioselectivity was dependent on the nature of the transmetallation step, where the 2- or 4-substituted heterocycles form. The initial optimization of the regioselectivity was conducted by Dr. Jinyue Ding, a former lab mate, using the racemic dihydropyranyl boronate **3-51** with 4-bromoanisole as the corresponding cross-coupling partner (Table 3-1). Initially, the conditions and catalysts that were chosen were based on previous methods that were known to favor the allylic Suzuki-Miyaura cross-coupling reaction. After screening through a variety of reaction conditions, Dr. Ding observed that the optimal synthesis of the α-isomer **3-52a** was provided using a weakly σ-donating triarylphosphine ligand (p-$CF_3C_6H_5)_3P$ with $[(allyl)PdCl]_2$ as the palladium catalyst, potassium phosphate as the base, and acetonitrile as solvent at 70 ^oC. The aqueous base K_3PO_4, gave efficient reactivity that may be a result of promoted oxo-palladium complex (i.e. conversion of $Ar{-}PdL_2{-}X$ to $Ar{-}PdL_2{-}OH$) or an anionic borate species formation, two active species that accelerate the transmetallation step.[38,39] Organ's Pd-PEPPSI-IPr catalyst,[33] which was previously used to promote α-regioselectivity, gave comparable selectivity to the optimal conditions.[40] Ding also identified conditions that promote the formation of the γ-regioisomer **3-53a** through the use of a strongly sigma-donating alkylphosphine ligand XPhos combined with the same palladium catalyst. The most effective base was K_3PO_4 using THF as the solvent at 40 ^oC. Other bases, such as Ag_2O, which was crucial towards the cross-coupling of aryl iodides to synthesize γ-regioisomers, as reported by Crudden and co-workers,[24] gave little or no products using an aryl bromide substrate.

3.2 Objectives

Dr. Jinyue Ding was able to address the initial challenge toward the optimization of this novel cross-coupling reaction, which consisted in identifying the type of palladium catalyst and ligand needed to produce both regioisomers selectively. With these conditions in hand, the next step was to examine the scope of this reaction, where a diverse range of electrophilic cross-coupling partners including aryl, heteroaryl or alkenyl halides were used (Figure 3-5). It was understood that the reaction conditions may require some fine-tuning depending on specific substrates. With each example of α- and γ-regioisomers, the level of regioselectivity was measured by ^{1}H NMR analysis of the crude reaction mixtures. The enantiomeric purity of the products were measured by HPLC analysis, which also allowed us to determine the enantiospecificity of this method. Lastly, attempts at elucidating the reaction mechanism were explored. These challenges are addressed in detail in the following sections.

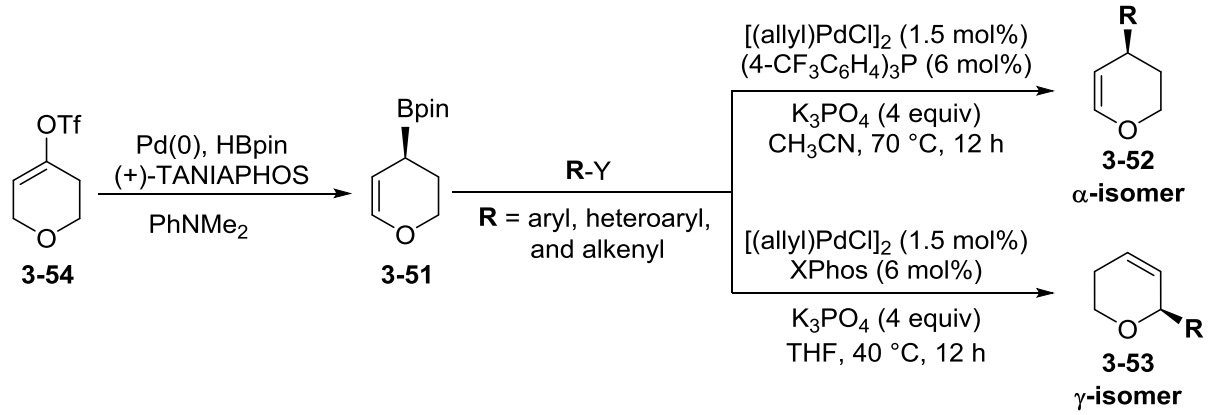

Figure 3-5: Proposed Suzuki-Miyaura cross-coupling of dihydropyranyl boronates.

3.3 Substrate scope for the regioselective and stereospecific Suzuki-Miyaura cross-coupling

A variety of substrates were investigated to examine the scope of suitable coupling partners for the optically enriched dihydropyranyl boronate **3-51** (Table 3-2 and Table 3-3). In order to produce sufficient amounts of the chiral allylic boronate **3-51** for testing, the substrate was synthesized in gram scale with high enantiomeric purity (93% *ee*) via the Pd-catalyzed asymmetric borylation/isomerization reaction using (+)-TANIAPHOS as the chiral ligand (Figure 3-5).[37] Initially, a portion of the substrate scope was conducted by my colleague Dr. Jinyue Ding as indicated specifically in the legend Table 3-2 and Table 3-3. In addition, Dr. Ding assisted in the determination of the enantiomeric purity of several substrates as specified in the legend of Table 3-2 and Table 3-3.[40] This information was included for the comprehensiveness of this chapter.

Using the optimal conditions that promoted the synthesis of the α-regioisomers **3-52** (Table 3-2), which involve the use of the weakly σ-donating tris-4-trifluoromethylphenyl phosphine ligand, a variety of diversified sp^2-hybridized electrophiles were investigated. The electrophiles used included aryl bromides with electron-donating and withdrawing substituents, heteroaryl bromides, as well as alkenyl bromides. All electrophiles tested were successfully coupled, producing the 4-substituted regioisomers **3-52a** to **3-52k** with regioselectivity ratios ranging from 3:1 to 15:1. The electron-rich substrates 4-methoxyphenyl bromide and 1-bromo-3,4,5-trimethoxybenzene afforded products **3-52a** and **3-52d** in good to high yields with excellent regioselectivity. The products of the sterically congested substrate, 2-bromoanisole, and substrate with an electron deficient CF_3-substituent were obtained at lower regioselectivity, **3-52b** (α/γ = 5:1) and **3-52c** (α/γ = 6:1), for the cross-coupling relative to the case of the 4-methoxyphenyl

bromide (**3-52a**, α/γ = 15:1). All regioisomers can be easily separated by flash column chromatography. The napthyl-product **3-52e** was obtained in good yield and regioselectivity (70%, α/γ = 7:1). The heteroaryl product **3-52f** was obtained in a high yield (93%) through the highly regioselective reaction (α/γ = 10:1) between **3-51** and 8-bromoquinoline. The reaction between **3-51** and *N*-Boc-5-bromoindole could not afford the α-product **3-52k** at such a high yield or regioselectivity (α/γ = 3:1) compared to the previous heteroaryl example, which was suspected of being a result of a poorer rate of transmetallation and likely required increased temperatures. To our surprise, for all products that afforded a measurable optical purity by chiral HPLC, the coupling process occurred with near to absolute stereospecificity. This outcome was verified by the exceptional enantiomeric ratios measured for the set of cross-coupling products. With the exception of products **3-51c** to **3-51e**, the enantiomeric ratios of the remaining optically pure products could not be measured directly by chiral HPLC, since they could not be resolved using different HPLC conditions. Thus, these products, **3-52b** and **3-52f to 3-52h,** underwent further chemical derivatization with the help of Dr. Ding (see Scheme 3-9).[40] The remaining examples, compound **3-52i** to **3-52k**, only had a yield and regioselectivity reported since we were unable to determine the optical purity of the products or their derivatized counterparts by HPLC analysis (see footnote of Table 3-2 and Table 3-3). Nonetheless, these products were included to further exemplify the regioselectivity of this process. It can be reasonably assumed that products **3-52i** to **3-52k** were formed in high enantiomeric purity.

Table 3-2: Scope of electrophiles in the α-selective stereospecific Suzuki-Miyaura cross-coupling with chiral dihydropyranyl boronate **3-51**.[a]

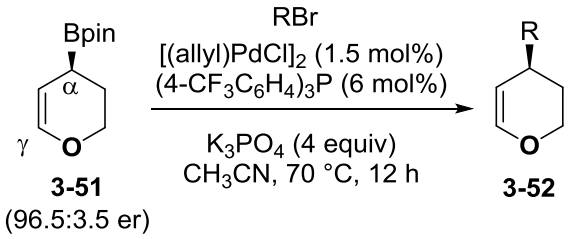

3-51 (96.5:3.5 er) → **3-52**

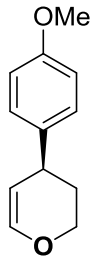

3-52a
78%[b,h]
α/γ = 15:1[c]
95:5 er[d]

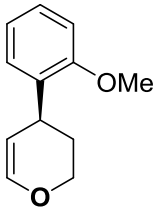

3-52b
71%[b]
α/γ = 5:1[c]
95:5 er[f]

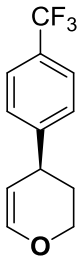

3-52c
72%[b]
α/γ = 6:1[c]
95:5 er[d]

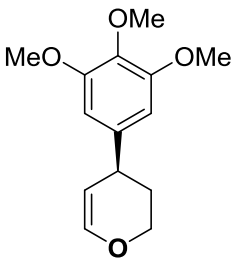

3-52d
76%[b,h]
α/γ = 9:1[c]
95:5 er[d]

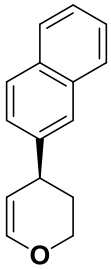

3-52e
70%[b,h]
α/γ = 7:1[c]
96:4 er[d]

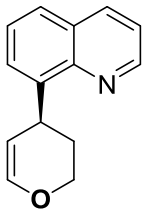

3-52f
93%[b]
α/γ = 10:1[c]
96.5:3.5 er[f]

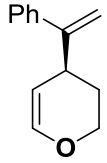

3-52g
86%[b]
α/γ = 7:1[c]
95:5 er[f]

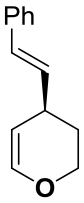

3-52h
78%[b]
α/γ = 9:1[c]
96:4 er[e]

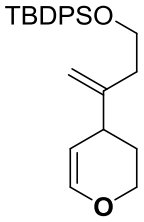

3-52i
85%[b,g]
α/γ = 6:1[c]
– er[g]

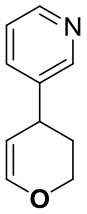

3-52j
60%[b,g]
α/γ = 8:1[c]
– er[g]

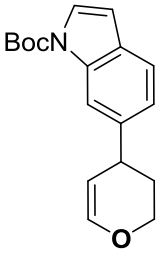

3-52k
78%[b,g]
α/γ = 3:1[c]
– er[g]

[a] [(allyl)PdCl]$_2$ (1.4 mg, 3.8 μmol), (4-$CF_3C_6H_4$)$_3$P (7.0 mg, 15.0 μmol) **3-50** (63.0 mg, 0.30 mmol), R-Br (0.25 mmol) and K_3PO_4 (2.5M in H_2O, 2.5 mL, 1.0 mmol) in dry CH_3CN (2.5 mL) at 70 °C. [b] Isolated yields of the major, separated regioisomers. [c] Regioisomer ratio (α/γ) was measured from the ^{1}H NMR spectra of crude products. [d] The enantiomeric ratio (er) was obtained directly from the pure coupling product by chiral HPLC analysis. [e] er was measured after chemical derivatization (see Scheme 3-9). [f] er was measured after chemical derivatization with the assistance of Dr. Jinyue Ding, which was included for the comprehensiveness of this chapter (see Scheme 3-9). [g] er of products could not be obtained, yield and regioselectivity are determined from racemic **3-51**. [h] Product was synthesized by my colleague Dr. Jinyue Ding, which was included for the comprehensiveness of this chapter.

Additionally, the highly regioselective formation of 1- and 2-substituted alkenyl products, as exemplified by compounds **3-52g** (α/γ = 7:1, 86%) and **3-52h** (α/γ = 9:1, 78%) (Table 3-2), demonstrates the broad utility of this method to couple various sp^2-hybridized organobromides. Although these enantioenriched 4-alkenyl dihydropyran products were obtained with excellent yields and very good regioselectivities, a *tert*-butyldiphenylsilyl-protected alkenyl halide afforded **3-52i** with a slightly lower regioselectivity and a yield comparable to the other alkenyl products (α/γ = 6:1, 85%). The reduced regioselectivity may in part be caused by the bulkiness of the silyl-protecting group on the alkenyl halide. It is noteworthy that the β-bromostyrene substrate is a mixture consisting of *E/Z*-stereoisomers (*E/Z* = 80/20) that – when subjected to the α-coupling conditions – afforded the (*E*)-β-bromostyrene-coupled product which was separable from the (*Z*)-isomer.

The same substrates used in the α-selective Suzuki-Miyaura cross-coupling reaction were also used in the synthesis of the γ-regioisomers **3-53** (Table 3-3). Using the previously optimized conditions that favored the formation of γ-regioisomers, with the strongly σ-donating and sterically bulky XPhos ligand, slightly improved yields and regioselectivity were observed relative to the α-isomers. The XPhos ligand, like other similar ligands developed by the Buchwald group,[41] are known to exhibit high reactivity in cross-coupling reactions due to their unique structural features (Figure 3-6).[42] The large cyclohexyl substituents create an electron-rich phosphine that enhances the rate of oxidative addition of the cross-coupling process. In addition to this, the bulkiness of the biaryl-backbone and the phosphine substituents accelerate the reductive elimination step. The electronic and structural features, in part, contribute to the enhanced regioselectivity and yields due to a reduced stagnation at key steps in the mechanism that would otherwise lead to side products.

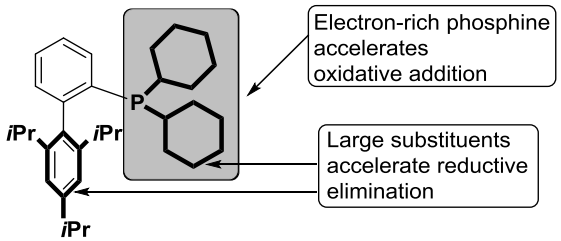

Figure 3-6: Important structural features of the γ-promoting phosphine ligand.

All products with measureable enantioselectivity were obtained with good to excellent yields, with excellent enantiomeric ratios (≥ 95:5 er) and nearly all substrates led to exclusive formation of the γ-regioisomer. Once more, the cross-coupling of the electron-rich methoxy-substituted aryl substrates afforded **3-53a** (74%) and **3-53d** (71%) in good yields. Additionally, exclusive formation of the γ-substituted naphthyl- and quinoline-based products were obtained in high yield, **3-53e** (98%) and **3-53f** (86%). The regioselectivity for the *N*-Boc indole-substituted product **3-53k** improved relative to the synthesis of the α-isomer **3-52k** (1:10 α:γ versus 3:1 α:γ), whereas the regioselectivity dramatically decreased for the 3-pyridyl-substituted products (**3-52j**, 1:3 α:γ versus **3-53**, 8:1 α:γ). Again, the model 1- and 2-substituted alkenyl halides were suitable electrophiles for this method, leading to the enantioenriched 2-substituted alkenyl dihydropyran products with good yields. Unfortunately, the regioselectivity under the γ-selective cross-coupling conditions (α:γ = 3:1 for both **3-53g** and **3-53h**), was lower than the regioselectivity of the α-promoted conditions (7:1 α:γ and 9:1 α:γ for **3-52g** and **3-52h**). Surprisingly, the *tert*-butylsilyl-protected alkenyl product **3-53i** was obtained at a higher yield and regioselectivity relative to the other two alkenyl products (α:γ = 1:50 for **3-53i**). Once more, in regards to the impure β-bromostyrene substrate of (*E*/*Z* = 80/20), the reaction afforded the (*E*)-β-bromostyrene-substituted product that was separable from the minor isomer, the (*Z*)-β-bromostyrene-substituted product. The poor regioselectivity observed for several substrates may be a result of a

slower rate of reductive elimination, thereby allowing for a diminished regioselectivity through a σ-π isomerization to form the π-allyl palladium species.

Table 3-3: Scope of electrophiles in the γ-selective stereospecific Suzuki-Miyaura cross-coupling with chiral dihydropyranyl boronate **3-51**.[a]

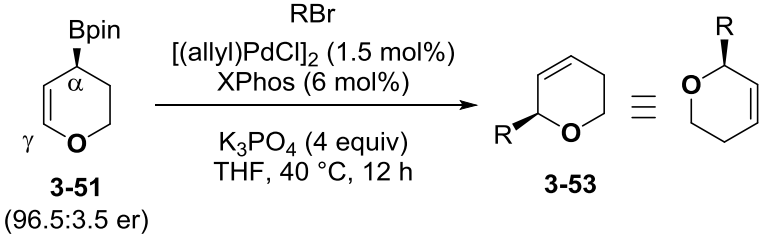

3-51
(96.5:3.5 er)

3-53

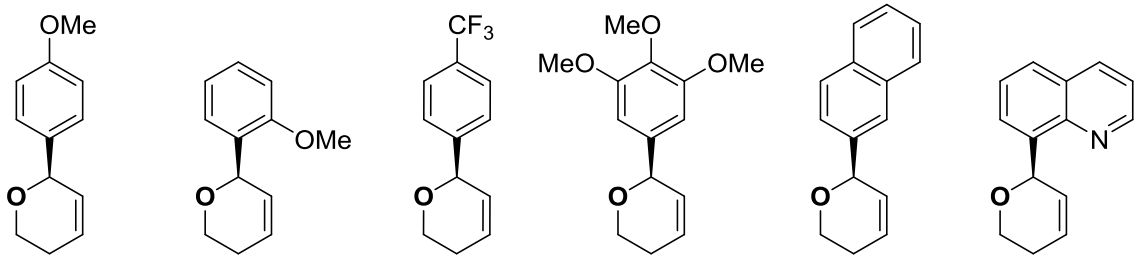

3-53a	**3-53b**	**3-53c**	**3-53d**	**3-53e**	**3-53f**
74%[b,h]	74%[b]	97%[b]	71%[b]	98%[b]	86%[b]
γ/α = >98:2[c]	γ/α = >98:2[c]	γ/α = >98:2[c]	γ/α = >98:2[c]	γ/α = >98:2[c]	γ/α = >98:2[c]
96:4 er[d]	96:4 er[d]	95:5 er[d]	95.5:4.5 er[f]	96.5:3.5 er[d]	96:4 er[d]

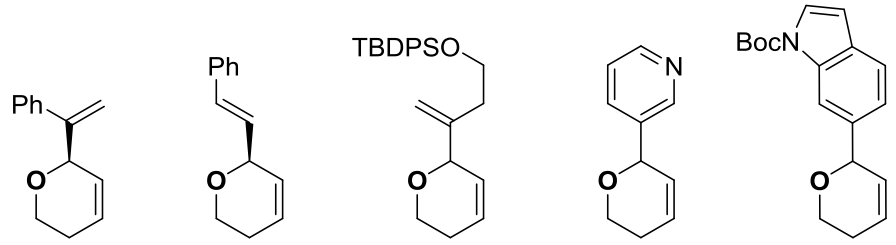

3-53g	**3-53h**	**3-53i**	**3-53j**	**3-53k**
72%[b]	70%[b]	98%[b,f]	66%[b,f]	96%[b,f]
γ/α = 3:1[c]	γ/α = 3:1[c]	γ/α >98:2[c]	γ/α = 3:*1*[c]	γ/α = 10:1[c]
95.5:4.5 er[d]	96:4 er[d]	– er[g]	– er[g]	– er[g]

[a] [(allyl)PdCl]$_2$ (1.4 mg, 3.8 μmol), XPhos (7.2 mg, 15 μmol), chiral **3-50** (63.0 mg, 0.30 mmol), R-Br (0.25 mmol) and K_3PO_4 (2.5M in H_2O, 2.5 mL, 1.0 mmol) in dry THF (2.5 mL) at 40 °C. [b] Isolated yields of the major, separated regioisomers. [c] Regioisomer ratio (α/γ) was measured from the ^{1}H NMR spectra of crude products. [d] The enantiomeric ratio (*er*) was obtained directly from the pure coupling product by chiral HPLC analysis. [e] er was measured after chemical derivatization (see Scheme 3-9). [f] er was measured after chemical derivatization with the assistance of Dr. Jinyue Ding, which was included for the comprehensiveness of this chapter (see Scheme 3-9). [g] er of products could not be obtained, yield and regioselectivity are determined from racemic **3-52**. [h] Product was synthesized by my colleague Dr. Jinyue Ding, which was included for the comprehensiveness of this chapter.

Since the enantiomeric ratio of several substrates could not be determined directly by chiral HPLC analysis, these compounds were further derivatized with the help of Dr. Ding (Scheme 3-9). For the α-coupled products, the electron-rich olefin was used as a reactive site for functionalization. Compounds **3-52b** and **3-52f** were subjected to a borylation/oxidation reaction to afford products **3-54** (46%) and **3-55** (86%). These products contained an alcohol group at the C2-position. The substrates **3-52g** and **3-52h** underwent an Upjohn dihydroxylation reaction, which gave an inseparable mixture of 2,3-hydroxy-substituted diastereomers (1:1 dr), **3-56a/b** and **3-57a/b** for both alkenyl-based substrates. The yield of the alkenyl product **3-56a/b** (75%) was significantly higher than **3-57a/b** (8%), which was likely a result of the chemoselectivity of dihydroxylation between the electron-rich olefin and the substituted alkenyl groups. The relative stereochemistry of the hydroxyl[43] or dihydroxyl groups[44] was proposed based on the precedence for an *anti* insertion relative to the aryl and alkenyl substituents on a dihydropyran framework. Lastly, the alkenyl group of compound **3-53d** was reduced using the *in situ*-generated diimide to afford **3-58** in a very high yield (95%).

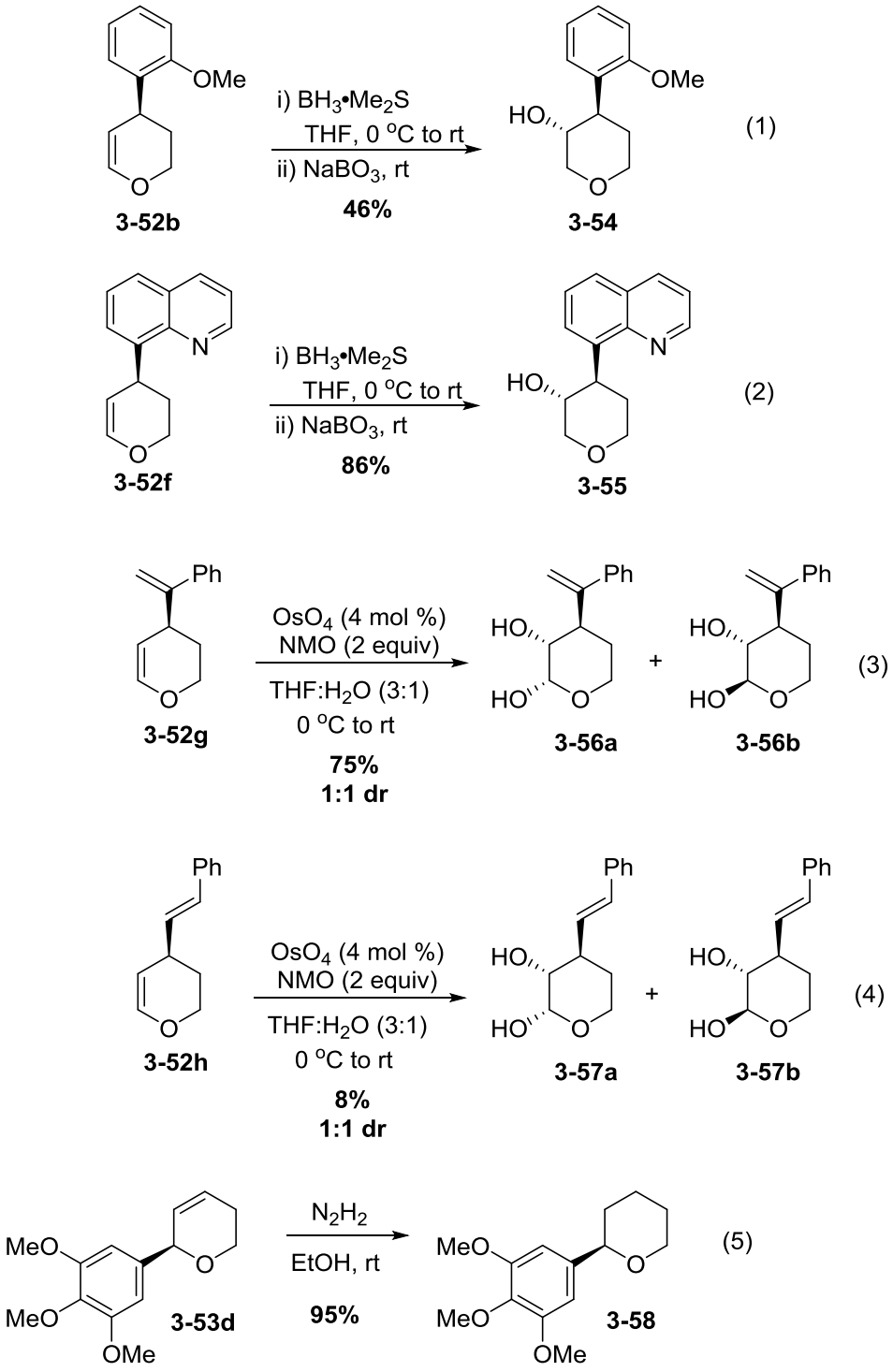

Scheme 3-9: Derivatization of dihydropyrans **3-32** and **3-53** for HPLC analysis.

3.4 Elucidating the stereochemistry of the allylic Suzuki-Miyaura cross-coupling reaction

In regards to clarifying whether the reaction proceeds with stereochemical retention or inversion of the allylboronate stereocenter, we were unable to address this issue unequivocally for the coupling of dihydropyran products. Fortunately, we were able to elucidate the absolute stereochemistry of the resulting cross-coupling products corresponding to the piperidyl boronate based on a concise formal synthesis of the alkaloid (+)-anabasine as well as the formal synthesis of the antidepressant drug (+)-paroxetine (Scheme 3-10); both developed by Dr. Ding. In the formal synthesis of (+)-anabasine, the enantiomer of the intermediate **3-61** was also a key substrate used in the literature to synthesize the natural product.[45] The observed optical rotation for **3-61**, $[\alpha]^{20}_{D}$ = –95.3 (*c* 0.13, $CHCl_3$), had an opposite sign to the literature value of **3-62**, $[\alpha]^{20}_{D}$ = +88.6 (*c* 1.00, $CHCl_3$).[45] Although the literature example was of lower enantiomeric purity (88:12 er), the opposite sign indicated that the stereogenic center at the C1-position for **3-60** had a (*S*)-configuration. Similarly, in the formal synthesis of (+)-paroxetine the optical rotation of intermediate **3-65**, $[\alpha]^{20}_{D}$ = +4.98 (*c* 0.87, MeOH), had the same sign to the literature example, $[\alpha]^{20}_{D}$ = +5.13 (*c* 1.13, MeOH), as well as confirming a (*S*)-configuration at the C3-position.[46] By comparing the optical rotation of the optically enriched piperidine derivatives to the literature examples, we were able to confirm that this cross-coupling process proceeded with stereoretention. In chapter 4, we obtained indisputable evidence that the allylic cross-coupling reaction of dihydropyranyl boronates proceeds with retention of stereochemistry from the analysis of derivatives of cross-coupling products (1D NOESY and X-ray crystallography) and the synthesis and structural analysis of the natural product diospongin B.

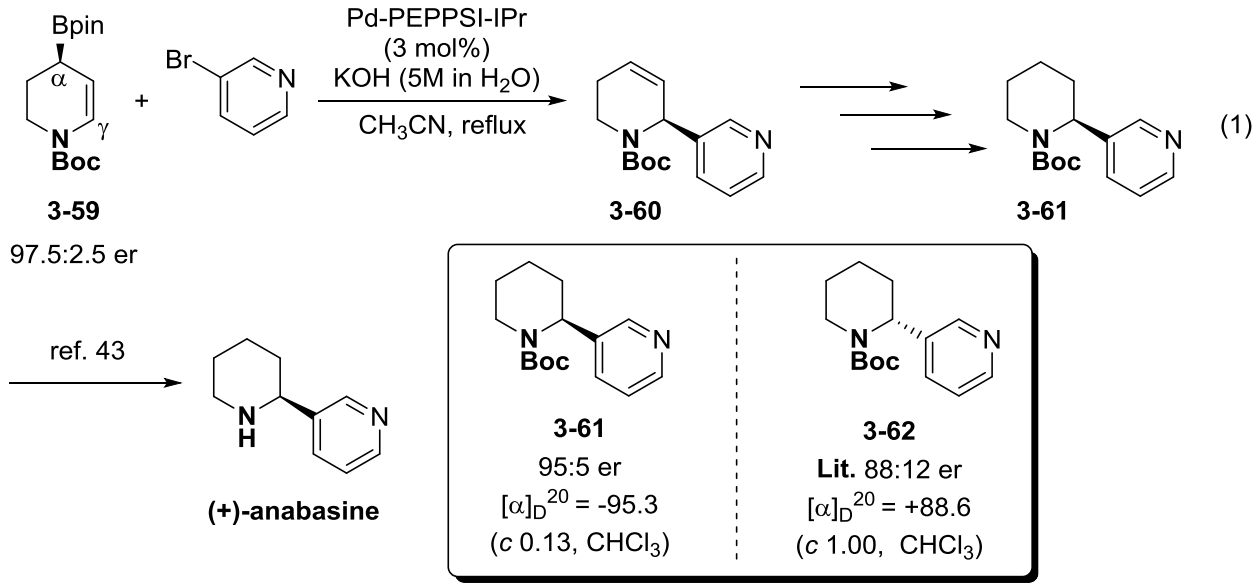

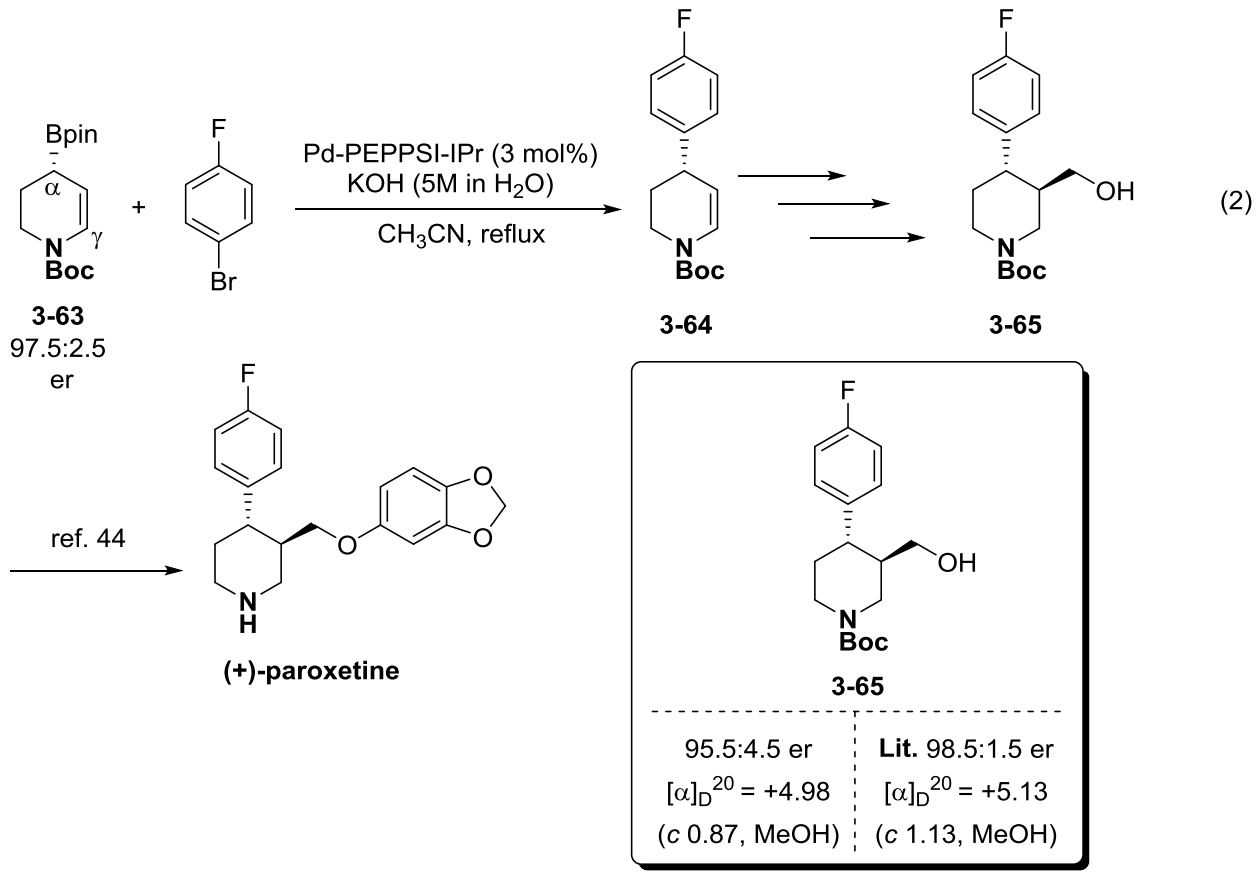

Scheme 3-10: Formal synthesis of (+)-anabasine and (+)-paroxetine, and compared optical rotation to literature example developed by Dr. Ding.

3.5 First proposed mechanistic cycle

To further elucidate the mechanism of the allylic Suzuki-Miyaura cross-coupling of dehydropiperidine and dihydropyran-derived allylboronates, we attempted to access the C2-positioned allylboronates on either a dehydropiperidine or dihydropyran framework. Depending on which ligand was used, these regioisomers could provide further insight on whether the ligands promote a S_E2 or an S_E2' pathway as well as confirming if a π-allyl palladium species forms through a σ-π transformation (Figure 3-7). In regards to the NHC-ligated palladium catalyst, we sought a way to confirm that the Pd-PEPPSI-IPr catalyst follows an S_E2 pathway as proposed by Organ (see Section 3-3).[33] Additionally, we wanted to determine if the reactivity of the catalyst was driven by the inherent electron-rich donation of the NHC ligand that would promote a fast reductive elimination or, alternatively, the inherent steric-bulkiness of the ligand. Either of these conclusions would further explain the catalyst's ability to promote α-regioselectivity as well as offer an opportunity in designing more reactive and selective catalysts. In light of the reaction mechanism of the allylic Suzuki-Miyaura cross-coupling reaction using the phosphine ligands, as proposed by Crudden and Aggarwal (see Section 3-3),[34,24] it was not conclusive that the electron-poor, α-promoting, phosphine ligand proceeded through an S_E2' pathway followed by transitioning to the α-positioned palladium species – through the elusive π-allyl palladium intermediate – instead proceeding through an S_E2 pathway. This issue could be further addressed with the results that would be obtained from using the γ-promoting conditions on α-boryl substrate **3-66** or **3-67** using the XPhos ligand.

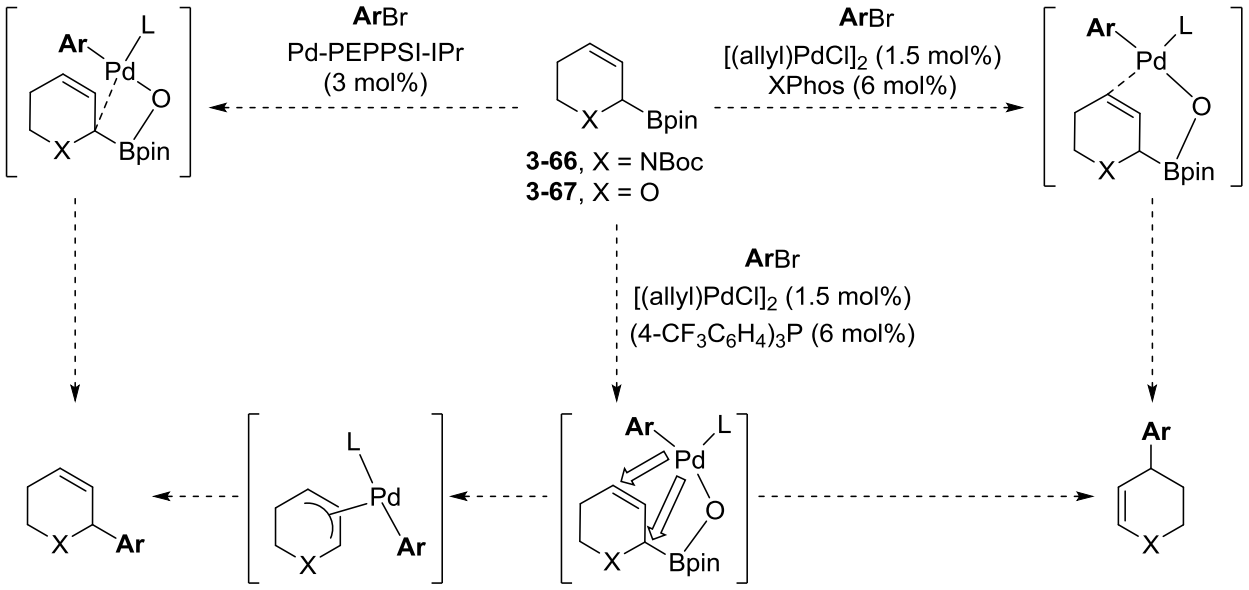

Figure 3-7: Mechanistic predictions on the 2-boryl dehydroheterocycle.

Before we could address the uncertainty of the cross-coupling mechanism, we first had to synthesize the 2-boryl dehydroheterocycle, either containing dehydropiperidine **3-66** or dihydropyran **3-67**. Using the commercially available *N*-Boc-protected 1,2,3,6-tetrahydropyridine, we attempted to directly insert the boronyl group. Using either *sec*BuLi or LTMP, the piperidine **3-68** was lithiated at the 2-position at –78 ^{o}C (Scheme 3-11). Afterwards, several borate reagents were tested on the lithiated substrate in order to form the boronate product **3-66**. Instead, we observed decomposition, recovery or isomerization of the dehydropiperidine starting material.

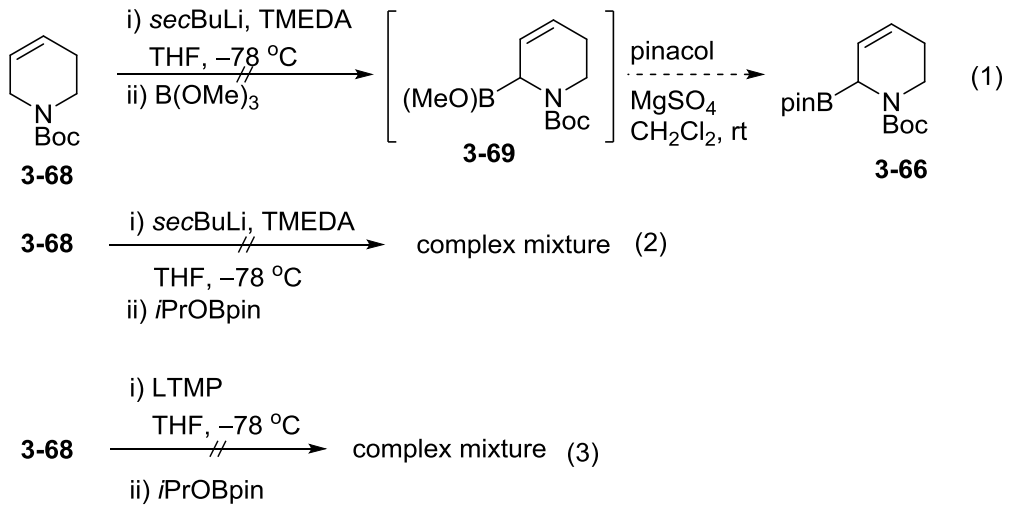

Scheme 3-11: Attempts at accessing 2-boronate dehydropiperidines under organolithium conditions.

An alternative route to **3-66** involved the formation of the allylic alcohol **3-72** from the *N*-Boc-protected piperidine **3-70**. Although dehydroheterocycles have not been tested, the desired C1-borylated product **3-66** may be formed using **3-72** through a transition metal-catalyzed allylic borylation. The allylic alcohol substrate, **3-72** was synthesized through a palladium-catalyzed dehydrogenation of the heterocyclic ketone, *N*-Boc-protected 4-dioxopiperidine **3-70**.[47] The reaction resulted in an inseparable mixture containing the α,β-unsaturated ketone **3-71** and the starting material **3-70**. The crude mixture was subjected to a Luche reduction to form **3-72** at a 47% yield over two steps. The first method tested involved a conjugate borylation substitution developed by Ito and Sawamura.[48] This method required the formation of the carbonate intermediate that would act as a suitable leaving group during the *anti*-S_N2' reaction (Scheme 3-12, Equation 1). After the formation of the carbonate species using methyl chloroformate and DMAP in pyridine, the carbonate product could not be isolated since it would decompose during purification by flash chromatography. We expected that the carbonate **3-73** decomposed during workup conditions due to the acidic nature of the silica. Using the crude carbonate product, we

were unsuccessful in forming **3-66** through conjugate boryl substitution. Alternatively, we attempted a direct borylation of the allylic alcohol by accessing the allylpalladium(II) complex **3-74**, an efficient method developed by the Szabó group (Scheme 3-12, Equation 2).[49] Again we observed that the starting material was fully consumed, but did not form **3-66**. After exhausting our efforts toward the synthesis of **3-66**, we wanted to confirm the importance of the heteroatom that is conjugated to the allylboronate in these heterocyclic boronate substrates.

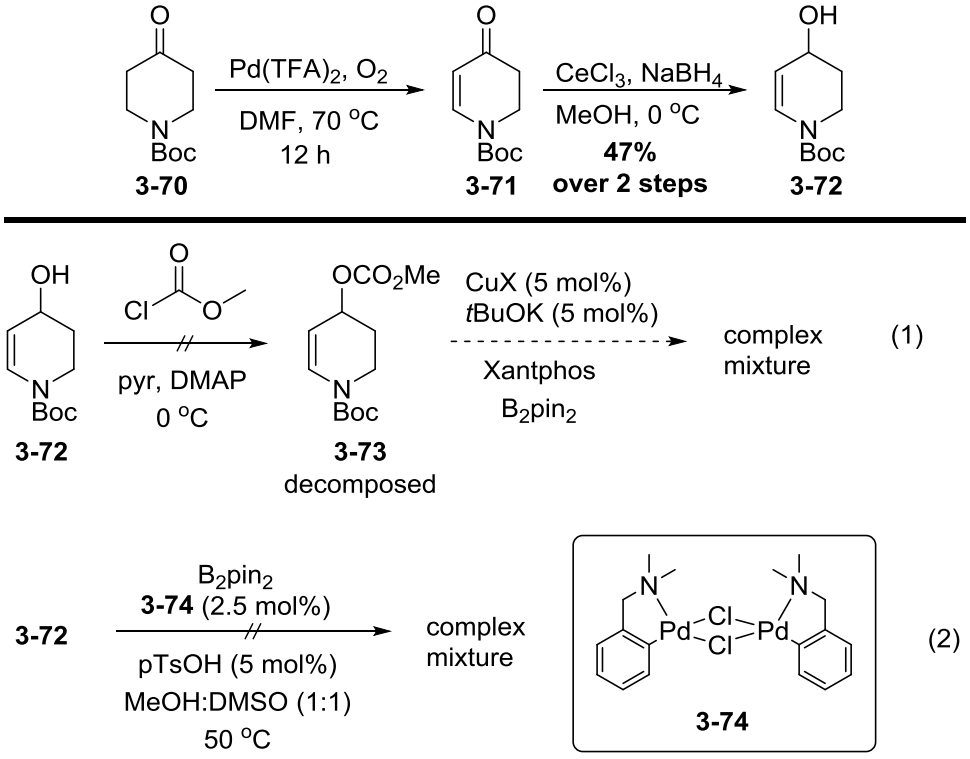

Scheme 3-12: Synthetic efforts to the 2-boryl dihydropyran **3-66**.

Using the carbocyclic allylboronate **3-75**, Dr. Ding confirmed that the level of reactivity of the allylic Suzuki-Miyaura cross-coupling method depended on the presence of an electron-rich heteroatom-conjugated allylboronate system. This was achieved by testing all of the optimized regiodivergent cross-coupling conditions on boronate **3-75** (Table 3-4). The Pd-PEPPSI-IPr catalytic system successfully coupled the carbocyclic allylboronate to 4-bromoanisole to afford

3-76 with a 46% yield. This was made possible since the Pd-PEPPSI-IPr catalyst promoted the S_E2 pathway. On the other hand, the phosphine ligands do not form any product and, as a result, may require a strong π-donating alkene to access the S_E2' pathway. This outcome further confirmed that the NHC-ligated palladium system proceeded through an alternate pathway to the phosphine-ligated palladium system.

Table 3-4: Control experiment for the coupling of the cyclic non-heteroatom-conjugated allylboronate examined by Dr. Ding**.**

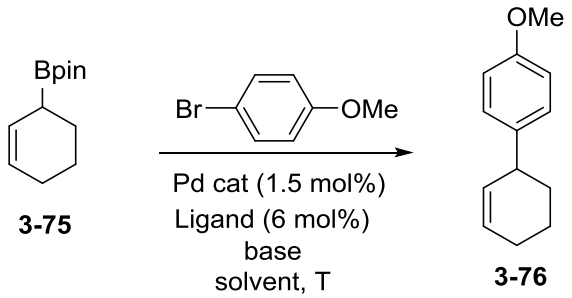

entry	Pd cat	Ligand	yield (%)
1[a]	$(AllylPdCl)_2$	$(p\text{-}CF_3Ph)_3P$	0
2[b]	**Pd-PEPPSI-IPr**	**–**	**46**
3[c]	$(AllylPdCl)_2$	XPhos	0

[a] $[(allyl)PdCl]_2$ (1.4 mg, 3.8 μmol), $(4\text{-}CF_3C_6H_4)_3P$ (7.0 mg, 15.0 μmol) **3-69** (56.5 mg, 0.30 mmol), 4-bromoanisole (0.25 mmol) and K_3PO_4 (2.5M in H_2O, 2.5 mL, 1.0 mmol) in dry CH_3CN (2.5 mL) at 70 °C. [b] Pd-PEPPSI-iPr (5.1 mg, 7.5 μmol), **3-69** (56.5 mg, 0.30 mmol), 4-bromoanisole (0.25 mmol) and KOH (5M in H_2O, 250 μL, 1.25 mmol) in dry CH_3CN (2.5 mL) at 83 °C.[c] $[(allyl)PdCl]_2$ (1.4 mg, 3.8 μmol), XPhos (7.2 mg, 15 μmol), chiral **3-69** (56.5 mg, 0.30 mmol), 4-bromoanisole (0.25 mmol) and K_3PO_4 (2.5M in H_2O, 2.5 mL, 1.0 mmol) in dry THF (2.5 mL) at 40 °C.

.

The allylic cross-coupling of heterocyclic allylboronates provides exceptional regioselectivity with nearly absolute retention of stereochemistry. Based on the products and mechanistic investigations performed, three different ligand systems have been identified to give

the regioselectivity observed in the optimization and reaction scope. In order to rationalize the results obtained from this method, a mechanism was proposed for all three ligands: the N-heterocyclic carbene, (Pd-PEPPSI-IPr), XPhos, and $(4\text{-}CF_3\text{-}C_6H_4)_3P$ (Scheme 3-13). In the presence of an aqueous base, either a hydroxyl-Pd(II) complex or a boronate anion species forms in the pre-transmetallation step.[38,39] Afterwards, the transmetallation step proceeds through either a *syn*-S_E or *syn*-S_E' mechanism from an oxyborate-coordinated palladium species **A**. The mechanism is presumed to proceed through a *syn*-transmetallation due the retention of stereochemistry, which was confirmed when analyzing the intermediates toward the formal synthesis of (+)-anabasine and (+)-paroxetine (Section 3.4, Scheme 3-10). Based on previous investigations into the allylic cross-coupling mechanism as well as the results from the scope of dihydropyranyl products, the phosphine-ligated Pd(II) species proceeds through a *syn*-S_E' transmetallation.[24,31,32,36] Consequently, both XPhos and $(4\text{-}CF_3\text{-}C_6H_4)_3P$ promote the formation of the η^1 σ-bonded palladium(II) complex **B**. As observed from the reaction scope (Table 3-3), the bulky and strong σ-donating phosphine ligand XPhos promotes a fast reductive elimination to afford exclusive formation of the γ-isomer. With the smaller and weaker σ-donating phosphine ligand $(4\text{-}CF_3\text{-}C_6H_4)_3P$, the reductive elimination is less favored and subsequently proceeds through a σ-π interconversion to form the π-allylpalladium species **C**. Afterwards, complex **C** equilibrates between the two η^1 σ-bonded palladium regioisomeric complexes **B** and **D**, and eventually forming the thermodynamically favorable isomer **D**. An alternative *syn*-S_E mechanism would proceed when using the NHC-ligated catalyst Pd-PEPPSI-IPr, which was previously claimed by the Organ group.[33] Furthermore, the results from the allylic cross-coupling of the carbocyclic allylboronate **3-75** further supports that the NHC-ligated catalyst behaves differently in comparison to the phosphine-ligated catalysts. Due to the fast reductive elimination

of the S_E transmetallation using electron-rich and bulky catalyst, an α-regioisomer is formed in high regioselectivity. Although an erosion of stereochemistry is possible for chiral π-allylpalladium complexes,[50] the effect is only minimal for this allylic cross-coupling reaction.

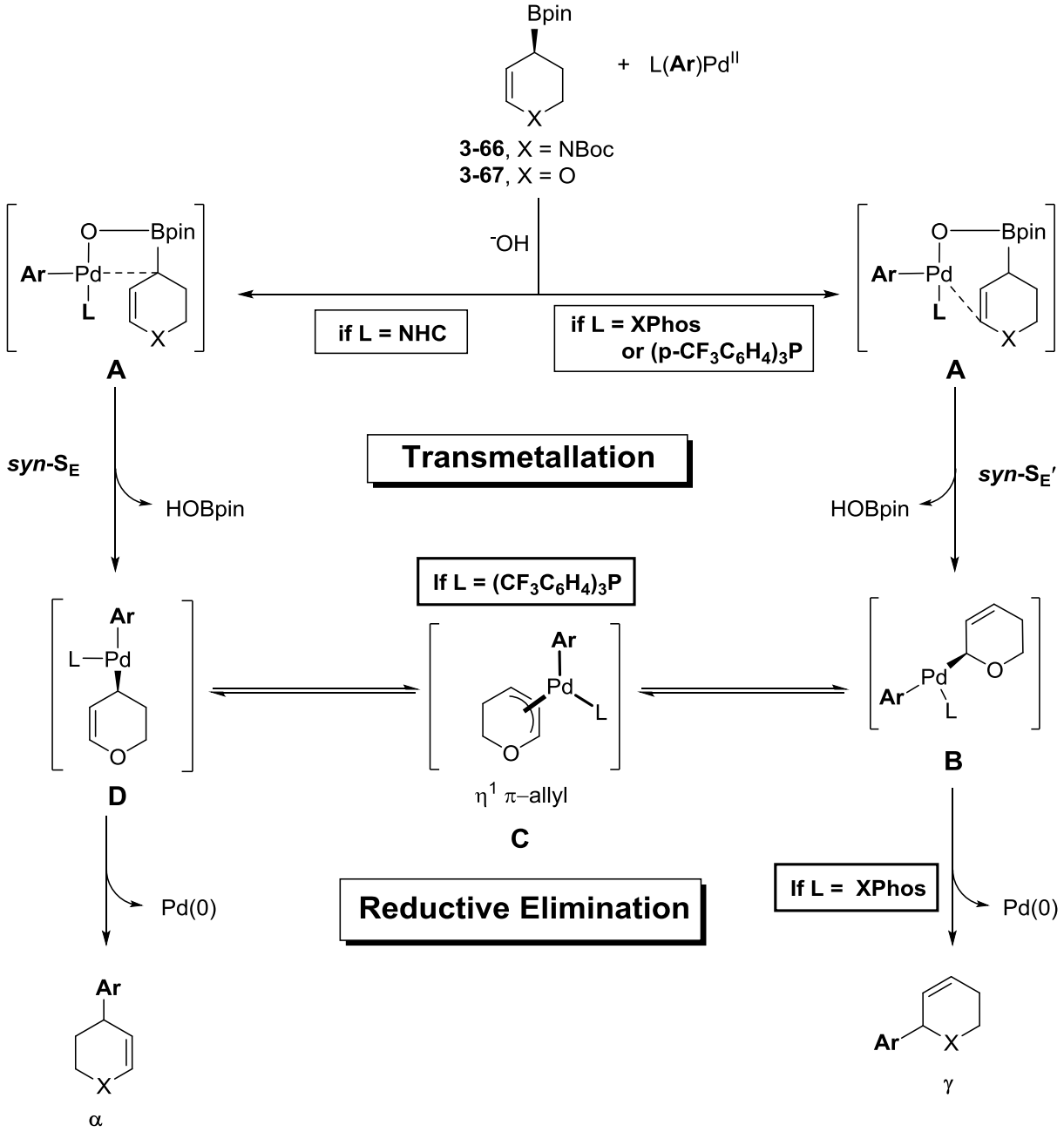

Scheme 3-13: Proposed mechanistic paths for the ligand-controlled regioselective Suzuki-Miyaura cross-coupling of heterocyclic allylic boronates **3-66** and **3-67**.

3.6 Summary

In regards to the palladium-catalyzed allylic Suzuki-Miyaura cross-coupling reaction of heterocyclic allylboronates, the regioselectivity and stereospecificity of this process is dictated by the careful choice of ligands used. The divergent control of regioselectivity, using the dihydropyran-based allylboronate, offers an access to a variety 2- or 4-substituted dihydropyrans; through direct sp^2-sp^3 cross-coupling. This method could potentially be utilized towards diversity oriented synthesis, where this complexity-generating method leads to a branching pathway to afford a broad scope of potentially biologically-relevant compounds containing the "privileged" pyran structure.[51] Additionally, this method further expands on the Suzuki-Miyaura cross-coupling reaction from the traditional coupling of sp^2-hybridized substrates to the asymmetric cross-coupling of optically pure sp^3-carbon centers.[14]

3.7 Experimental

3.7.1 General information

Unless otherwise stated, all reactions were performed under a nitrogen atmosphere using flame-dried glassware. Acetonitrile was distilled from CaH_2. THF, toluene, dichloromethane, and methanol were obtained from a MBraun MB SPS* solvent system prior to use. The anhydrous 1,4-dioxane was purchased from Sigma-Aldrich, 99.8%, and it was deoxygenated with dry nitrogen for 3 hours before use. $Pd(OAc)_2$ was purchased from Sigma-Aldrich, ≥99.9%; chiral ligands (+)-TANIAPHOS and (−)-TANIAPHOS were synthesized on gram-scale respectively according to the literature procedure.[52] Other ligands and palladium catalysts were obtained from commercial sources. Thin layer chromatography (TLC) was performed on Merck Silica Gel 60 F254 plates and was visualized with UV light and $KMnO_4$ stain. NMR spectra were recorded on

Varian INOVA-300, INOVA-400 or INOVA-500 MHz instruments. The residual solvent protons (^{1}H) or the solvent carbons (^{13}C) were used as internal standards. ^{1}H NMR data is presented as follows: chemical shift in ppm (δ) downfield from tetramethylsilane (multiplicity, coupling constant, integration). The following abbreviations are used in reporting NMR data: s, singlet; br s, broad singlet; d, doublet; t, triplet; q, quartet; dd, doublet of doublets; qt, quartet of triplets; dtd, doublet of triplet of doublets; dse, double of septets; m, multiplet. High-resolution mass spectra were recorded by the University of Alberta Mass Spectrometry Services Laboratory using either electron impact (EI) ion source with double focussing sector analyzer (Kratos Analytical MS-50G) or electrospray (ESI) ion source with orthogonal acceleration TOF analyzer (Agilent Technologies 6220 oaTOF). Infrared spectra were obtained on a Nicolet Magna-IR with frequencies expressed in cm^{-1}. The enantiomeric excesses for chiral compounds were determined using a HPLC Agilent instrument with Chiralcel-OD (4.6 × 250 mm, inner diameter × length; particle size 5 μm), Chiralpak-AS (4.6 × 250 mm, inner diameter × length; particle size 5 μm), Chiralpak-IC (4.6 × 150 mm, inner diameter × length; particle size 5 μm) or Chiralpak-IB (4.6 × 150 mm, inner diameter × length; particle size 5 μm) columns.

Enol triflate **3-54**, as well as allylic boronate **3-50** were all prepared on gram-scale (0.5 mmol) following our previously published procedures.[37] Careful purification of the allylic boronate **3-50** was required prior to the cross-coupling reactions. When purified *via* silica gel flash chromatography, the air-sensitive allylic boronate tends to develop considerable affinity to the silica gel over time, resulting in a difficult purification, especially on a smaller scale (below 0.5 mmol). To obtain good purity without diminishing the isolated yield on a small scale, some important technical tips need to be considered: 1) after evaporating the solvent from the crude reaction, immediately run a quick silica gel flash chromatography; 2) use silica columns that are

short and wide to avoid long elution times; 3) quantitate the silica gel (around 100/1, w/w, silica gel to crude compound ratio).

3.7.2 Experimental and spectral data

General procedure A towards 4-substituted pyran:

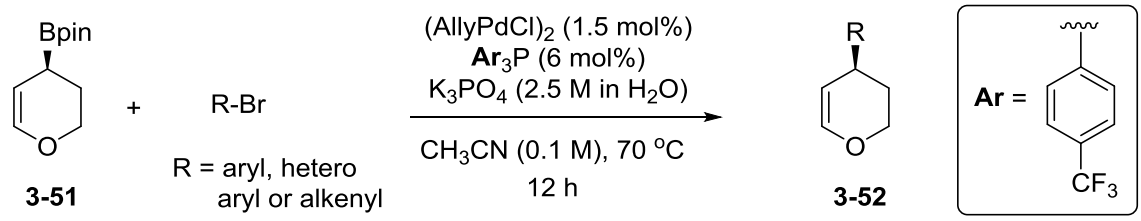

Complex $[(allyl)PdCl]_2$ (1.4 mg, 3.8 μmol) and $(4\text{-}CF_3C_6H_4)_3P$ (7.0 mg, 15 μmol) was added in a flamed-dried reaction tube, which was then flushed with nitrogen. The dry acetonitrile (1.0 mL) was added and the mixture was stirred for 10 minutes. Allylic heterocyclic boronic ester **3-51** (0.30 mmol, 1.2 equiv) was added *via* syringe, which was washed three times with dry acetonitrile (0.5 mL portion). Organobromide (0.25 mmol) and aqueous K_3PO_4 solution (2.5 M in H_2O, 0.5 mL, 5 equiv) were added and the resulting reaction mixture was allowed to stir under nitrogen at 70 °C for 12 h. The mixture was allowed to cool down to room temperature, passed through a short pipette loaded with silica gel, and rinsed with 15 mL ethyl acetate. The solvents were then evaporated to yield a crude oil, which was subjected to flash chromatography to afford the pure 4-substituted pyran product.

<u>General procedure B</u> towards 2-substituted pyran:

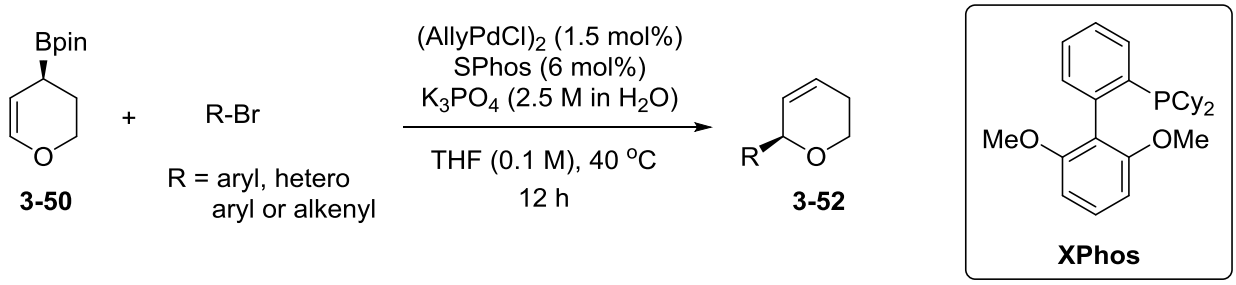

Complex $[(allyl)PdCl]_2$ (1.4 mg, 3.8 μmol) and XPhos (6.4 mg, 15 μmol) was added in a flamed-dried reaction tube, which was then flushed with nitrogen. The dry THF (1.0 mL) was added and the mixture was stirred for 10 minutes. Allylic heterocyclic boronic ester **3-51** (0.3 mmol, 1.2 equiv) was added *via* syringe, which was washed three times with dry THF (0.5 mL portion). Organobromide (0.25 mmol) and aqueous K_3PO_4 solution (2.5 M in H_2O, 0.5 mL, 5 equiv) were then added, and the resulting reaction mixture was allowed to stir under nitrogen at 40 °C for 12 h. The mixture was cooled down to room temperature, passed through a short pipette loaded with silica gel, and rinsed with 15 mL ethyl acetate. The solvents were then evaporated to yield a crude oil, which was subjected to flash chromatography to afford the pure 2-substituted pyran product.

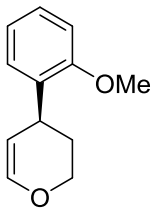

(4*S*)-4-(2-Methoxyphenyl)-3,4-dihydro-2*H*-pyran (3-52b)

By following the general procedure A, the title compound **3-52b** was synthesized from **3-51** and the corresponding aryl bromide. The crude sample, containing **3-52b** in a 5 : 1 mixture of regioisomers, was subjected to flash chromatography (20% Et_2O/Hexane) to afford the title compound (34 mg, 71%).

Clear oil; TLC (Et_2O:Hexane, 15:85 v/v): R_f = 0.51.

$[\alpha]_D^{20}$: −32 (*c* 0.32, $CHCl_3$).

^{1}H NMR (500 MHz, $CDCl_3$) δ 7.32 (dd, *J* = 7.5, 1.7 Hz, 1H), 7.18 (ddd, *J* = 7.7, 7.5, 1.5 Hz, 1H), 6.95 (ddd, *J* = 7.5, 7.5, 1.0 Hz, 1H), 6.87 (dd, *J* = 8.2, 0.8 Hz, 1H), 6.62 (dd, *J* = 6.3, 1.9 Hz, 1H), 4.72 (dd, *J* = 6.3, 3.8 Hz, 1H), 4.00 (ddd, *J* = 10.4, 7.2, 3.0 Hz, 1H), 3.93 (ddd, *J* = 10.9, 8.2, 2.9 Hz, 1H), 3.88 (dd, *J* = 3.8, 2.0 Hz, 1H), 3.85 (s, 3H), 2.20 (dddd, *J* = 14.6, 9.6, 3.2, 3.0 Hz, 1H), 1.82–1.73 (m, 1H).

^{13}C NMR (126 MHz, $CDCl_3$) δ 156.9, 145.1, 133.6, 128.8, 127.3, 120.3, 110.1, 103.4, 63.8, 55.3, 29.9, 29.2.

IR (microscope, cm^{-1}) 3057, 2957, 2932, 2875, 2835, 1645, 1598, 1585.

HRMS (EI) for $C_{12}H_{14}O_2$: calcd. 190.0994; found 190.0994.

Enantiomeric ratio of compound **3-52b** could not be determined directly, due to the difficult HPLC separation. The er determination was determined by Dr. Ding after hydroboration/oxidation of **3-52b**.[40]

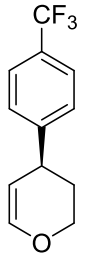

(4*S*)-4-[4-(Trifluoromethyl)phenyl]-3,4-dihydro-2*H*-pyran (3-52c)

By following the general procedure A, the title compound **3-52c** was synthesized from **3-51** and the corresponding aryl bromide. The crude sample, containing **3-52c** in a 6 : 1 mixture of regioisomers, was subjected to flash chromatography (5% Et_2O/Hexane) to afford the title compound (41 mg, 72%).

Clear oil; TLC (Et_2O:Hexane, 20:80 v/v): R_f = 0.55.

$[\alpha]_D^{20}$: −53 (*c* 0.50, $CHCl_3$).

^{1}H NMR (500 MHz, $CDCl_3$) δ 7.57 (d, *J* = 8.0 Hz, 2 H), 7.39 (dd, *J* = 8.0, 0.5 Hz, 2 H), 6.60 (dd, *J* = 6.3, 1.9 Hz, 1 H), 4.75 (dddd, *J* = 6.2, 3.4, 3.4, 0.5 Hz, 1 H), 4.07–3.93 (m, 2 H), 3.58–3.54 (m, 1 H), 2.21 (dddd, *J* = 13.3, 6.6, 6.5, 3.0 Hz, 1 H), 1.84 (dddd, *J* = 14.0, 7.2, 3.6, 3.5 Hz, 1 H).

^{13}C NMR (126 MHz, $CDCl_3$) δ 149.7, 145.4, 128.0, 125.4, 125.4, 125.3, 125.3, 102.62, 63.7, 36.2, 32.0.

IR (microscope, cm^{-1}) 3062, 2932, 2877, 1645, 1618.

HRMS (EI) for $C_{12}H_{11}F_3O$ (m/z): calcd. 228.0762; found 228.0767.

HPLC (Chiralcel IB): 5:95 *i*-PrOH/Hexane, 0 °C, 0.5 mL/minute, λ = 230 nm, t_{major} = 27.6 min, t_{minor} = 25.1 min, 95:5 er.

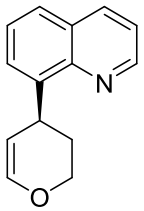

8-[(4*S*)-3,4-Dihydro-2*H*-pyran-4-yl]quinolone (3-52f)

By following the general procedure A, the title compound **3-52f** was synthesized from **3-51** and the corresponding aryl bromide. The crude sample, containing **3-52f** in a 10 : 1 mixture of regioisomers, was subjected to flash chromatography (20% Et_2O/Hexane) to afford the title compound (49 mg, 93%) .

Clear oil; TLC (EtOAc:Hexane, 20:80 v/v): R_f = 0.43.

$[\alpha]_D^{20}$: +60 (*c* 0.33, $CHCl_3$).

^{1}H NMR (500 MHz, $CDCl_3$) δ 8.94 (dd, *J* = 4.2, 1.8 Hz, 1 H), 8.16 (dd, *J* = 8.2, 1.8 Hz, 1 H),

7.71 (ddd, *J* = 9.5, 7.6, 1.3 Hz, 2 H), 7.52 (dd, *J* = 8.0, 7.5 Hz, 1 H), 7.41 (dd, *J* = 8.2, 4.2 Hz, 1 H), 6.74–6.67 (m, 1 H), 4.92–4.82 (m, 2 H), 4.10 (ddd, *J* = 10.3, 7.2, 3.0 Hz, 1 H), 3.99 (ddd, *J* = 10.8, 7.9, 2.9 Hz, 1 H), 2.53–2.40 (m, 1 H), 1.92–1.87 (m, 1 H).

^{13}C NMR (100 MHz, $CDCl_3$) δ 149.4, 146.1, 145.4, 143.9, 136.5, 128.9, 128.2, 126.4, 126.3, 121.0, 103.9, 64.1, 30.9, 30.3.

IR (microscope, cm^{-1}) 3054, 3001, 2964, 2873, 1644, 1612, 1596, 1574, 1497.

HRMS (EI) for $C_{14}H_{13}NO$ (m/z): calcd. 211.0997; found 211.099.

Enantiomeric ratio of compound **3-52f** could not be determined directly, due to the difficult HPLC separation. The er determination was determined by Dr. Ding after hydroboration/oxidation of **3-52f**.[40]

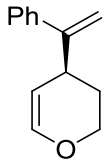

(4*S*)-4-(1-Phenylvinyl)-3,4-dihydro-2*H*-pyran (3-52g)

By following the general procedure A, the title compound **3-52g** was synthesized from **3-51** and the corresponding aryl bromide. The crude sample, containing **3-52g** in a 7 : 1 mixture of regioisomers, was subjected to flash chromatography (4% Et_2O/Hexane) to afford the title compound (40 mg, 86%).

Clear oil; TLC (Et_2O:Hexane, 10:90 v/v): R_f = 0.60.

$[\alpha]_D^{20}$: −110 (*c* 0.20, $CHCl_3$).

^{1}H NMR (500 MHz, $CDCl_3$) δ 7.41–7.28 (m, 4 H), 6.54 (dd, *J* = 6.3, 1.8 Hz, 1 H), 5.40 (d, *J* = 1.3 Hz, 1 H), 5.18 (dd, *J* = 1.2, 1.0 Hz, 1 H), 4.77 (ddd, *J* = 5.9, 3.9, 0.8 Hz, 1 H), 3.98–3.90 (m, 2 H), 3.42 (dd, *J* = 10.1, 4.7 Hz, 1 H), 2.04–1.95 (m, 1 H), 1.67–1.59 (m, 1 H).

^{13}C NMR (126 MHz, $CDCl_3$) δ 151.9, 144.8, 141.1, 128.4, 127.5, 126.6, 114.5, 102.9, 63.1, 34.5, 27.9.

IR (microscope, cm^{-1}) 3079, 3058, 2951, 2928, 2874, 1646, 1624, 1598, 1493.

HRMS (EI) for $C_{13}H_{14}O$ (m/z): calcd. 186.1045; found 186.1047.

Enantiomeric ratio of compound **3-52g** could not be determined, due to the difficult HPLC separation. The er determination was determined by Dr. Ding after dihydroxylation of **3-52g**.[40]

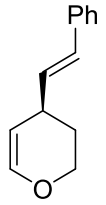

(4*R*)-4-[(*E*)-2-Phenylvinyl]-3,4-dihydro-2*H*-pyran (3-52h)

By following the general procedure A, the title compound **3-52h** was synthesized from **3-51** and the corresponding aryl bromide. The crude sample, containing **3-52h** in a 9 : 1 mixture of regioisomers, was subjected to flash chromatography (2% Et_2O:Hexane) to afford the title compound (36 mg, 78%).

Clear oil; TLC (Et_2O:Hexane, 2:98 v/v): R_f = 0.29.

$[\alpha]_D^{20}$: −307 (*c* 0.41, $CHCl_3$).

^{1}H NMR (500 MHz, $CDCl_3$) δ 7.38–7.35 (m, 2 H), 7.32–7.29 (m, 2 H), 7.23–7.20 (m, 1 H), 6.48 (dd, *J* = 6.5, 2.0 Hz , 1 H), 6.43 (d, *J* = 15.0 Hz , 1 H), 6.17 (dd, *J* = 15.7, 7.0 Hz , 1 H), 4.70 (dd, *J* = 6.0, 3.5 Hz , 1 H), 4.01 (dd, *J* = 5.98 Hz , 2 H), 3.05–3.00 (m, 1 H), 2.09–2.05 (m, 1 H), 1.79–1.75 (m, 1 H).

^{13}C NMR (125 MHz, $CDCl_3$) δ 144.4, 137.5, 133.8, 130.2, 128.6, 127.2, 126.2, 103.0, 63.6, 33.3, 29.1.

IR (microscope, cm^{-1}) 3058, 3026, 2955, 2924, 2853, 1644, 1600, 1493, 1451.

HRMS (EI) for $C_{13}H_{14}O$: calcd. 186.1045; found 186.1041.

Enantiomeric ratio of compound **3-52h** could not be determined directly, due to the difficult HPLC separation. The er determination was determined after dihydroxylation of **3-52h**.[40]

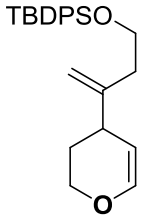

***tert*-Butyl{[3-(3,4-dihydro-2*H*-pyran-4-yl)but-3-en-1-yl]oxy}diphenylsilane (3-52i)**

By following the general procedure A, the title compound **3-52i** was synthesized from **3-51** and the corresponding aryl bromide. The crude sample, containing **3-52i** in a 6 : 1 mixture of regioisomers, was subjected to flash chromatography (5 to 10% Et_2O:Hexane) to afford the title compound (83 mg, 85%).

Clear oil; TLC (Et_2O:Hexane, 5:95 v/v): $R_f = 0.47$.

^{1}H NMR (500 MHz, $CDCl_3$) δ 7.72–.64 (m, 4 H), 7.46–7.35 (m, 6 H), 6.43 (dd, *J* = 6.3, 1.8 Hz, 1 H), 4.91–4.84 (m, 2 H), 4.55 (dd, *J* = 6.2, 3.6 Hz, 1 H), 3.93–3.86 (m, 2 H), 3.78 (app t, *J* = 7.0 Hz, 2 H), 2.77–2.69 (m, 1 H), 2.36–2.24 (m, 2 H), 1.88 (ddd, *J* = 10.7, 9.0, 5.2 Hz, 1 H), 1.68–1.58 (m, 1 H), 1.06 (s, 9 H).

^{13}C NMR (126 MHz, $CDCl_3$) δ 149.2, 144.4, 135.6, 133.9, 133.9, 129.6, 127.7, 112.6, 103.2, 63.5, 63.4, 37.2, 36.2, 27.7, 26.9, 19.2.

IR (microscope, cm^{-1}) 2955, 2930, 2857, 1646, 1472, 1428, 1111.

HRMS (EI) for $C_{26}H_{32}O_2Si$: calcd. 392.2172; found 392.2173.

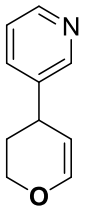

3-(3,4-Dihydro-2*H*-pyran-4-yl)pyridine (3-52j)

By following the general procedure A, the title compound **3-52j** was synthesized from **3-51** and the corresponding aryl bromide. The crude sample, containing **3-52j** in a 8 : 1 mixture of regioisomers, was subjected to flash chromatography (25 to 50% EA:DCM) to afford the title compound with a (24 mg, 60%).

Clear oil; TLC (MeOH:DCM, 5:95 v/v): $R_f = 0.34$.

^{1}H NMR (500 MHz, $CDCl_3$) δ 8.53 (d, *J* = 2.1 Hz, 1 H), 8.47 (dd, *J* = 4.8, 1.5 Hz, 1 H), 7.59 (app dt, *J* = 7.8, 1.8 Hz, 1 H), 6.60 (dd, *J* = 6.3, 1.9 Hz, 1 H), 4.73 (dd, *J* = 6.2, 3.3 Hz, 1 H), 4.08–3.92 (m, 2 H), 3.53 (ddd, *J* = 9.1, 6.4, 2.8 Hz, 1 H), 2.22 (app tdd, *J* = 9.2, 6.2, 2.8 Hz, 1 H), 1.91–1.77 (m, 1 H).

^{13}C NMR (125 MHz, $CDCl_3$) δ 149.6, 147.9, 145.6, 140.8, 135.1, 123.4, 102.3, 63.6, 34.0, 31.9.

IR (microscope, cm^{-1}) 3056, 3028, 2970, 2950, 2929, 2874, 1644, 1574, 1422, 1243.

HRMS (EI) for $C_{10}H_{11}NO$: calcd. 161.0841; found 161.0842.

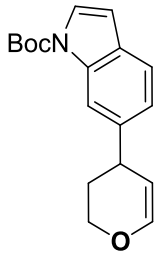

***tert*-Butyl 6-(3,4-dihydro-2*H*-pyran-4-yl)-1*H*-indole-1-carboxylate (3-52k)**

By following the general procedure A, the title compound **3-52k** was synthesized from **3-51** and the corresponding aryl bromide. The crude sample, containing **3-52k** in a 3 : 1 mixture of regioisomers, was subjected to flash chromatography (0 to 2% Et_2O:Hexane) to afford the title compound (58 mg, 78%).

Clear oil; TLC (Et_2O:Hexane, 10:90 v/v): $R_f = 0.31$.

^{1}H NMR (400 MHz, $CDCl_3$) δ 8.11 (s, 1 H), 7.57 (d, *J* = 3.6 Hz, 1 H), 7.50 (d, *J* = 8.1 Hz, 1 H), 7.16 (dd, *J* = 8.0, 1.5 Hz, 1 H), 6.60 (dd, *J* = 6.2, 1.9 Hz, 1 H), 6.54 (d, *J* = 3.7 Hz, 1 H), 4.85 (dd, *J* = 6.3, 3.4 Hz, 1 H), 4.07–3.99 (m, 2 H), 3.68–3.59 (m, 1 H), 2.30–2.19 (m, 1 H), 1.92 (app dt, *J* = 11.4, 6.0 Hz, 1 H), 1.68 (s, 9 H).

^{13}C NMR (126 MHz, $CDCl_3$) 149.9, 144.8, 142.3, 135.4, 129.1, 125.8, 122.7, 120.7, 114.4, 107.1, 104.1, 83.6, 63.8, 36.6, 32.6, 28.3.

IR (microscope, cm^{-1}) 3151, 3115, 3057, 2975, 2874, 1731, 1643, 1529, 1335.

HRMS (EI) for $C_{18}H_{21}NO_3$: calcd. 299.1521; found 299.1520.

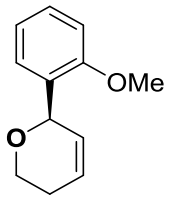

(6*R*)-6-(2-Methoxyphenyl)-3,6-dihydro-2*H*-pyran (3-53b)

By following the general procedure B, the title compound **3-53b** was synthesized as a single regioisomer from **3-51** and the corresponding aryl bromide. The crude sample was subjected to flash chromatography (2.5% Et_2O/Hexane) to afford the title compound (35 mg, 74%).

Clear oil; TLC (Et_2O:Hexane, 20:80 v/v): $R_f = 0.38$.

$[\alpha]_D^{20}$: +88 (*c* 0.28, $CHCl_3$).

^{1}H NMR (500 MHz, $CDCl_3$) δ 7.43 (dd, *J* = 7.5, 1.7 Hz, 1 H), 7.29–7.23 (m, 1 H), 6.96 (ddd, *J* = 7.5, 7.2, 0.5 Hz, 1 H), 6.89 (dd, *J* = 8.2, 0.6 Hz, 1 H), 5.97 (dddd, *J* = 7.6, 7.5, 2.5, 2.5 Hz, 1 H), 5.79 (dddd, *J* = 10.1, 4.0, 2.0, 2.0, 2.0 Hz, 1 H), 5.63 (ddd, *J* = 5.1, 2.5, 2.5 Hz, 1 H), 4.02 (ddd, *J* = 11.2, 4.7, 4.5 Hz, 1 H), 3.88–3.78 (m, 4 H), 2.40–2.28 (m, 1 H), 2.14–2.03 (m, 1 H).

^{13}C NMR (126 MHz, $CDCl_3$) δ 156.8, 129.5, 129.3, 128.8, 128.1, 124.9, 120.5, 110.6, 69.9, 63.1, 55.5, 25.3.

IR (microscope, cm^{-1}) 3035, 2999, 2958, 2922, 2853, 2836, 1720, 1601, 1589, 1491, 1463.

HRMS (EI) for $C_{12}H_{14}O_2$ (m/z): calcd. 190.0994; found 190.0997.

HPLC (Chiralcel IC): 1:99 *i*-PrOH/Hexane, 20 °C, 0.5 mL/minute, λ = 230 nm, t_{major} = 11.2 min, t_{minor} = 23.9 min, 96:4 er.

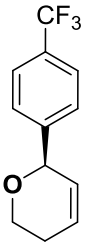

(6*R*)-6-[4-(Trifluoromethyl)phenyl]-3,6-dihydro-2*H*-pyran (3-53c)

By following the general procedure B, the title compound **3-53c** was synthesized as a single regioisomer **3-51** and the corresponding aryl bromide. The crude sample was subjected to flash chromatography (15% ethyl acetate/Hexane) to afford the title compound (55 mg, 97%).

Yellow oil; TLC (EtOAc:Hexane, 15:85 v/v): $R_f = 0.57$.

$[\alpha]_D^{20}$: –8.7 (*c* 0.12, $CHCl_3$).

^{1}H NMR (500 MHz, $CDCl_3$) δ 7.61 (d, *J* = 8.1 Hz, 2 H), 7.50 (d *J* = 8.1, 2 H), 6.02 (dddd, *J* = 10.2, 5.0, 2.5, 2.0 Hz, 1 H), 5.79 (dddd, *J* = 10.3, 2.0, 2.0, 2.0 Hz, 1 H), 5.19 (ddd, *J* = 5.2, 3.0, 2.7 Hz, 1 H), 4.01 (ddd, *J* = 11.4, 5.5, 3.5 Hz, 1 H), 3.83 (ddd, *J* = 11.3, 8.9, 4.1 Hz, 1 H), 2.42–2.32 (m, 1 H), 2.14–2.05 (m, 1 H).

^{13}C NMR (126 MHz, $CDCl_3$) δ 145.5, 128.8, 127.6, 125.8, 125.5, 125.4, 125.4, 125.4, 77.3, 63.3, 25.1.

IR (microscope, cm^{-1}) 3039, 2966, 2926, 2858, 1645, 1619.

HRMS (EI) for $C_{12}H_{11}F_3O$ (m/z): calcd. 228.0762; found 228.0765.

HPLC (Chiralcel IB): 2:98 *i*-PrOH/Hexane, 20 °C, 0.5 mL/minute, λ = 210 nm, t_{major} = 48.7 min, t_{minor} = 44.0 min, 95:5 er.

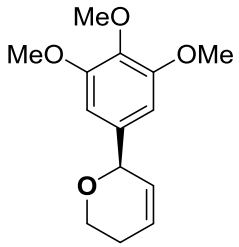

(6*R*)-6-(3,4,5-Trimethoxyphenyl)-3,6-dihydro-2*H*-pyran (3-53d)

By following the general procedure B, the title compound **3-53d** was synthesized as a single regioisomer from **3-51** and the corresponding aryl bromide. The crude sample was subjected to flash chromatography (50% Et_2O/Hexane) to afford the title compound (44 mg, 71%).

Clear oil; TLC (EtOAc:Hexane, 50:50 v/v): $R_f = 0.31$.

$[\alpha]_D^{20}$: +32 (*c* 0.36, $CHCl_3$).

^{1}H NMR (500 MHz, $CDCl_3$) δ 6.61 (s, 2 H), 6.0 (dddd, *J* = 7.0, 6.4, 5.0, 2.5 Hz, 1 H), 5.81 (dddd, *J* = 10.6, 2.0, 2.0, 2.0 Hz, 1 H), 5.06 (ddd, *J* = 4.7, 3.0, 2.5 Hz, 1 H), 4.02 (ddd, *J* = 11.1, 5.5, 3.0 Hz, 1 H), 3.93–3.74 (m, 8 H), 2.38 (dddd, *J* = 14.3, 11.3, 5.5, 2.6 Hz, 1 H), 2.12–2.02 (m, 1 H).

^{13}C NMR (100 MHz, $CDCl_3$) δ 153.3, 137.7, 137.0, 129.4, 125.6, 104.6, 63.4, 60.8, 56.1, 25.1.

IR (microscope, cm^{-1}) 3032, 2994, 2958, 2937, 2837, 1591, 1506.

HRMS (EI) for $C_{14}H_{18}O_4$ (m/z): calcd. 250.1205; found 250.1201.

Enantiomeric ratio of compound **3-53d** could not be determined directly, due to the difficult HPLC separation. The er determination was determined by Dr. Ding after diimide reduction of **3-53d**.[40]

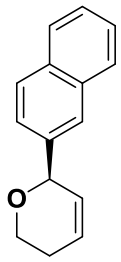

(6*R*)-6-(2-Naphthyl)-3,6-dihydro-2*H*-pyran (3-53e)

By following the general procedure B, the title compound **3-53e** was synthesized as a single regioisomer from **3-51** and the corresponding aryl bromide. The crude sample was subjected to flash chromatography (10% Et_2O/Hexane) to afford the title compound (52 mg, 98%).

White solid; (m.p.: 63.0–65.1 °C); TLC (Et_2O:Hexane, 20:80 v/v): R_f = 0.60.

$[\alpha]_D^{20}$: +147 (*c* 1.02, $CHCl_3$).

^{1}H NMR (500 MHz, $CDCl_3$) δ 7.87–7.81 (m, 3 H), 7.53 (dd, *J* = 8.5, 1.7 Hz, 1 H), 7.50–7.45 (m, 2 H), 6.06 (dddd, *J* = 10.1, 5.0, 2.7, 2.5 Hz, 1 H), 5.92 (dddd, *J* = 10.2, 2.0, 2.0, 2.0 Hz, 1 H), 5.32 (ddd, *J* = 2.6, 2.5, 2.5 Hz, 1 H), 4.06 (ddd, *J* = 11.2, 5.4, 3.8 Hz, 1 H), 3.87 (dddd, *J* = 11.3, 8.6, 4.2 Hz, 1 H), 2.48–2.35 (m, 1 H), 2.20–2.08 (m, 1 H).

^{13}C NMR (126 MHz, $CDCl_3$) δ 138.8, 133.3, 133.1, 129.5, 128.3, 128.1, 127.7, 126.3, 126.0, 125.9, 125.6, 125.5, 77.7, 76.2, 63.1, 25.3.

IR (microscope, cm^{-1}) 3055, 3034, 2960, 2921, 2856, 1688, 1646, 1600, 1508.

HRMS (EI) for $C_{15}H_{14}O$ (m/z): calcd. 210.1045; found 210.1044.

HPLC (Chiralcel IC): 2:98 *i*-PrOH/Hexane, 20 °C, 0.5 mL/minute, λ = 230 nm, t_{major} = 18.7 min, t_{minor} = 5.0 min, 96.5:3.5 er.

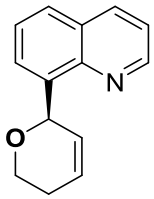

8-[(2*R*)-5,6-Dihydro-2*H*-pyran-2-yl]quinoline (3-53f)

By following the general procedure B, the title compound **3-53f** was synthesized as a single regioisomer from **3-51** and the corresponding aryl bromide. The crude sample was subjected to flash chromatography (20% Et_2O/Hexane) to afford the title compound (45 mg, 86%).

Yellow oil: TLC (Et_2O:Hexane, 20:80 v/v): $R_f = 0.28$.

$[\alpha]_D^{20}$: +129 (*c* 0.81, $CHCl_3$).

^{1}H NMR (500 MHz, $CDCl_3$) δ 8.96 (dd, *J* = 4.2, 1.8 Hz, 1 H), 8.15 (dd, *J* = 8.3, 1.8 Hz, 1 H), 7.90 (dd, *J* = 7.0, 1.5 Hz, 1 H), 7.76 (dd, *J* = 8.2, 1.4 Hz, 1 H), 7.55 (dd, *J* = 8.0, 7.3 Hz, 1 H), 7.41 (dd, *J* = 8.3, 4.2 Hz, 1 H), 6.53–6.52 (m, 1 H), 6.05–5.94 (m, 2 H), 4.15 (ddd, *J* = 11.2, 5.4, 3.0 Hz, 1 H), 3.99 (ddd, *J* = 11.2, 9.2, 4.0 Hz, 1 H), 2.51–2.38 (m, 1 H), 2.19–2.05 (m, 1 H).

^{13}C NMR (126 MHz, $CDCl_3$) δ 149.7, 145.7, 139.3, 136.4, 130.2, 128.3, 127.5, 127.4, 126.4, 124.6, 121.0, 77.3, 71.1, 63.7, 25.4.

IR (microscope, cm^{-1}) 3037, 2957, 2919, 2852, 1615, 1596, 1577, 1498.

HRMS (EI) for $C_{14}H_{13}NO$ (m/z): calcd. 211.0997; found 211.0993.

HPLC (Chiralcel IB): 25:75 *i*-PrOH/Hexane, 20 °C, 0.5 mL/minute, λ = 280 nm, t_{major} = 9.1 min, t_{minor} = 35.7 min, 96:4 er.

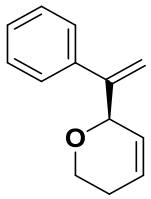

(6*R*)-6-(1-Phenylvinyl)-3,6-dihydro-2*H*-pyran (3-53g)

By following the general procedure B, the title compound **3-53g** was synthesized from **3-51** and the corresponding aryl bromide. The crude sample, containing **3-53g** as the major isomer in a 3 : 1 mixture of regioisomers, was subjected to flash chromatography (2.5% Et_2O/Hexane) to afford the title compound (30 mg, 65%).

Clear oil; TLC (Et_2O:Hexane, 10:90 v/v): $R_f = 0.45$.

$[\alpha]_D^{20}$: +3.0 (*c* 0.40, $CHCl_3$).

^{1}H NMR (400 MHz, $CDCl_3$) δ 7.51–7.47 (m, 2 H), 7.36–7.27 (m, 3 H), 5.94 (ddd, *J* = 10.2, 6.2, 3.8 Hz, 1 H), 5.73 (ddd, *J* = 10.3, 4.2, 2.1 Hz, 1 H), 5.50 (d, *J* = 1.4 Hz, 1 H), 5.37 (app s, 1 H), 5.13–5.08 (m, 1 H), 4.00 (ddd, *J* = 11.1, 5.5, 5.0 Hz, 1 H), 3.79 (ddd, *J* = 11.5, 7.0, 4.5 Hz, 1 H), 2.29–2.21 (m, 1 H), 2.16–2.05 (m, 1 H).

^{13}C NMR (126 MHz, $CDCl_3$) δ 147.6, 139.9, 128.5, 128.3, 127.6, 126.8, 125.5, 115.6, 77.3, 75.3, 62.2, 25.3.

IR (microscope, cm^{-1}) 3081, 3055, 3033, 2961, 2922, 2855, 1628, 1600, 1574, 1494.

HRMS (EI) for $C_{13}H_{14}O$ (m/z): calcd. 186.1045; found 186.1040.

HPLC (Chiralcel IB): 1:99 *i*-PrOH/Hexane, 0 °C, 0.3 mL/minute, λ = 254 nm, t_{major} = 12.1 min, t_{minor} = 11.0 min, 95.5:4.5 er.

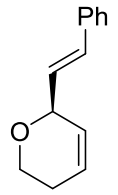

(6*R*)-6-[(*E*)-2-Phenylvinyl]-3,6-dihydro-2*H*-pyran (3-53h)

By following the general procedure B, the title compound **3-53h** was synthesized from **3-51** and the corresponding aryl bromide. The crude sample, containing **3-53h** as the major isomer in a 3 : 1 mixture of regioisomers, was subjected to flash chromatography (2% Et_2O/Hexane) to afford the title compound (33 mg, 70%).

Clear oil; TLC (Et_2O:Hexane, 2:98 v/v): $R_f = 0.27$.

$[\alpha]_D^{20}$: 130 (*c* 1.33, $CHCl_3$).

^{1}H NMR (500 MHz, $CDCl_3$) δ 7.40–7.38 (m, 2 H), 7.32–7.29 (m, 2 H), 7.25–7.22 (m, 1 H), 6.62 (dd, *J* = 16.0, 0.5 Hz, 1 H), 6.22 (dd, *J* = 15.7, 6.5 Hz, 1 H), 5.97–5.93 (m, 1 H), 5.74 (app. dq, *J* = 10.0, 2.5 Hz, 1 H), 4.78–4.74 (m, 1 H), 4.00 (ddd, *J* = 11.5, 5.0, 5.0 Hz, 1 H), 3.77 (ddd, *J* = 11.9, 7.2, 4.0 Hz, 1 H).

^{13}C NMR (126 MHz, $CDCl_3$) δ 136.8, 131.8, 128.9, 128.6, 128.6, 127.7, 126.6, 125.4, 62.4, 25.2.

IR (cast film, cm^{-1}) 3082, 3029, 2960, 2922, 2855, 1599, 1577, 1494, 1460.

HRMS (EI) for $C_{13}H_{14}O$ (m/z): calcd. 186.10446; found 186.10417.

HPLC (Chiralcel IC): 2:98 *i*-PrOH/Hexane, 20 °C, 0.5 mL/minute, λ = 280 nm, t_{major} = 9.8 min, t_{minor} = 11.6 min, 96:4 er.

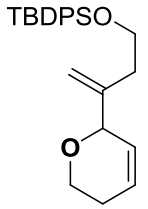

***tert*-Butyl{[3-(5,6-dihydro-2*H*-pyran-2-yl)but-3-en-1-yl]oxy}diphenylsilane (3-53i)**

By following the general procedure B, the title compound **3-53i** was synthesized from **3-51** and the corresponding aryl bromide. The crude sample, containing **3-53i** in a >98 : 2 mixture of regioisomers, was subjected to flash chromatography (5 to 10% Et_2O:Hexane) to afford the title compound (96 mg, 98%).

Clear oil; TLC (Et_2O:Hexane, 5:95 v/v): $R_f = 0.26$.

^{1}H NMR (500 MHz, $CDCl_3$) δ 7.70–7.65 (m, 4 H), 7.45–7.35 (m, 6 H), 5.90–5.86 (m, 1 H), 5.61 (ddd, *J* = 10.3, 4.1, 2.2 Hz, 1 H), 5.09–4.92 (m, 2 H), 4.54–4.45 (m, 1 H), 3.86 (ddd, *J* = 12.3, 8.6, 3.8 Hz, 1 H), 3.83–3.75 (m, 2 H), 3.64 (ddd, *J* = 11.2, 8.0, 4.3 Hz, 1 H), 2.46–2.31 (m, 2 H), 2.15 (app ddtd, *J* = 18.7, 11.0, 5.3, 2.7 Hz, 1 H), 2.04–1.93 (m, 1 H), 1.08–1.00 (m, 9 H).

^{13}C NMR (126 MHz, $CDCl_3$) δ 145.8, 135.6, 134.1, 134.0, 129.6, 128.6, 127.6, 125.6, 114.4, 63.4, 62.3, 35.5, 26.9, 25.2, 19.2.

IR (microscope, cm^{-1}) 2958, 2929, 2857, 1472, 1462, 1427, 1111.

HRMS (EI) for $C_{21}H_{23}O_2Si$ $[M - tBu]^+$: calcd. 335.1467; found 335.1474.

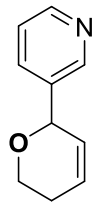

3-(5,6-Dihydro-2*H*-pyran-2-yl)pyridine (3-53j)

By following the general procedure B, the title compound **3-53j** was synthesized from **3-51** and the corresponding aryl bromide. The crude sample, containing **3-53j** in a 3 : 1 mixture of regioisomers, was subjected to flash chromatography (2.5 to 5% *i*PrOH:Hexane) to afford the title compound (27 mg, 66%).

Clear oil; TLC (MeOH:DCM, 5:95 v/v): $R_f = 0.28$.

^{1}H NMR (500 MHz, $CDCl_3$) = 7.2, 4.8, 2.3 Hz, 1 H), 5.78 (ddd, *J* = 10.2, 4.0, 2.1 Hz, 1 H), 5.23–5.12 (m, 1 H), 3.99 (ddd, *J* = 11.3, 5.3, 3.7 Hz, 1 H), 3.81 (ddd, *J* = 11.3, 8.7, 4.2 Hz, 1 H), 2.42–2.30 (m, 1 H), 2.10 (ddt, *J* = 10.6, 6.8, 2.4 Hz, 1 H).

^{13}C NMR (125 MHz, $CDCl_3$) δ 149.3, 149.2, 136.8, 135.0, 128.4, 126.1, 123.4, 73.9, 63.2, 25.1.

IR (microscope, cm^{-1}) 3034, 2962, 2922, 2855, 1578, 1477, 1462, 1425, 1084.

HRMS (EI) for $C_{10}H_{11}NO$: calcd. 161.0841; found 161.0842.

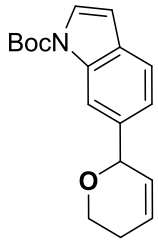

***tert*-Butyl 6-(5,6-dihydro-2*H*-pyran-2-yl)-1*H*-indole-1-carboxylate (3-53k)**

By following the general procedure B, the title compound **3-53k** was synthesized from **3-51** and the corresponding aryl bromide. The crude sample, containing **3-53k** in a 10 : 1 mixture of regioisomers, was subjected to flash chromatography (0 to 2% Et_2O:Hexane) to afford the title compound (72 mg, 96%).

Clear oil; TLC (Et_2O:Hexane, 10:90 v/v): $R_f = 0.14$.

^{1}H NMR (500 MHz, $CDCl_3$) δ 8.19 (s, 1H), 7.59 (d, *J* = 3.5 Hz, 1 H), 7.53 (d, *J* = 8.0 Hz, 1 H), 7.28 (dd, *J* = 8.2, 1.3 Hz, 1 H), 6.55 (dd, *J* = 3.7, 0.6 Hz, 1 H), 6.03 (app ddt, *J* = 9.6, 4.7, 2.3 Hz, 1 H), 5.89 (ddd, *J* = 10.2, 3.9, 2.1 Hz, 1 H), 5.32–5.21 (m, 1 H), 4.06–4.00 (m, 1 H), 3.83 (ddd, *J* = 11.2, 8.6, 4.2 Hz, 1 H), 2.38 (dddd, *J* = 17.0, 8.4, 5.4, 2.7 Hz, 1 H), 2.15–2.05 (m, 1 H), 1.68 (s, 9 H).

^{13}C NMR (100 MHz, $CDCl_3$) δ 149.8, 137.6, 135.2, 130.4, 129.9, 126.3, 125.2, 122.6, 120.9, 114.6, 107.2, 83.7, 63.0, 28.2, 25.3.

IR (microscope, cm^{-1}) 2977, 2922, 2854, 1734, 1613, 1528, 1438, 1344, 1148.

HRMS (EI) for $C_{18}H_{21}NO_3$: calcd. 299.1521; found 299.1522.

3.7.3 Derivatization of selected substrates for determination of enantiomeric ratio

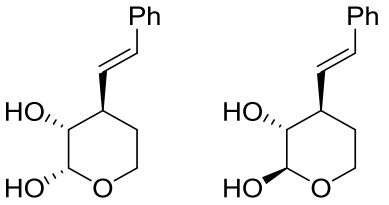

R_f (**3-57a** and **3-57b**) = 0.33 (Et_2O)

(2*S*,3*R*,4*R*)-4-[(*E*)-2-Phenylethenyl]oxane-2,3-diol (3-57a)

and (2*R*,3*R*,4*R*)-4-[(*E*)-2-Phenylethenyl]oxane-2,3-diol (3-57b)

Dihydro heterocyclic **3-52h** (0.1 mmol) was dissolved in 1 mL of acetone and 250 μL of distilled water. The solution was cooled to 0 °C in an ice bath. *N*-methylmorpholine *N*-oxide (50% w/w aq. soln., 41 μL, 0.20 mmol) and osmium(VIII) oxide (4% w/w aq. soln., 23 μL, 4.0 μmol) were added sequentially. The reaction mixture was slowly warmed up to room temperature overnight. After conventional workup, the crude product was purified by flash chromatography to give the desired 1,2-diol with high regioselectivity. The title α,β-diol compounds **3-57a** and **3-57b** were obtained as a 1/1 ratio of an unseparable mixture (8%).

White solid: (m.p.: 127.8–138.3 °C); TLC (Et_2O): R_f = 0.33 (**3-57a** and **3-57b**).

$[\alpha]_D^{20}$: +119(*c* 0.59, $CHCl_3$).

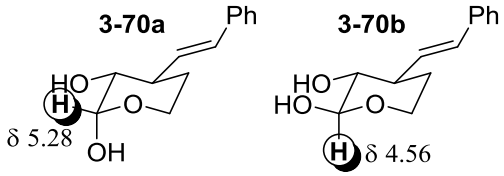

^{1}H NMR (498 MHz, $CDCl_3$): δ 7.39–7.29 (m, 4 H), 7.24–7.21 (m, 1 H), 6.54 (d, *J* = 15.9 Hz, 1 H), 6.17 (ddd, *J* = 15.9, 8.0, 8.0 Hz, 1 H), 5.27 (d, *J* = 2.5 Hz, 0.5 H, 15a, equatorial proton more deshielded due to magnetic anisotropy effects), 4.56 (d, *J* = 7.5 Hz, 1 H, 15b, axial proton more

shielded due to magnetic anisotropy effects), 4.05–4.00 (m, 1 H), 3.66–3.59 (m, 1 H), 3.50–3.49 (m, 0.5 H), 3.23 (dd, J = 10.0, 7.5 Hz, 0.5 H), 3.09 (br s, 0.5 H), 2.79 (br s, 0.5 H), 2.72–2.73 (m, 0.5 H), 2.46–2.39 (m, 0.5 H), 2.28 (br s, 0.5 H), 2.04–2.01 (m, 0.5 H), 1.80–1.56 (m, 2 H).

^{13}C NMR (126 MHz, $CDCl_3$) δ 137.02, 137.00, 131.9, 131.8, 130.4, 129.7, 128.63, 128.60, 127.6, 127.5, 126.32, 126.28, 126.25, 98.8, 98.7, 77.0, 76.94, 76.92, 76.8, 76.67, 76.66, 74.8, 71.9, 65.1, 60.4, 59.0, 45.1, 40.9, 31.2, 30.5, 30.4, 21.1, 14.2. (33 carbon signals result from mixture of **3-57a** and **3-57b**).

IR (cast film, cm^{-1}) 3376, 2957, 2885, 2853, 1598, 1493, 1447.

HRMS (ESI) for $[M+NH_4]^+$ $C_{13}H_{20}NO_3$: calcd. 238.1438; found 238.1436, $[M+Na]^+$ $C_{13}H_{16}NaO_3$: calcd. 243.0992; found 243.0989.

HPLC of 3-57a (Chiralcel IC): 5:95 *i*-PrOH/Hexane, 20 °C, 0.5 mL/minute, λ = 254 nm, t_{major} = 33.9 min, t_{minor} = 37.6 min, 96:5 er.

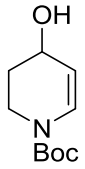

***tert*-Butyl 4-hydroxy-3,4-dihydropyridine-1(2*H*)-carboxylate (3-72)**

To a 25 ml round-bottom flask equipped with a stir bar was added $Pd(TFA)_2$ (7.8 mg, 0.020 mmol, 4 mol%) and *N*-Boc-4-piperidone **3-70** (110 mg, 0.6 mmol) in DMSO (2.5 mL). The reaction mixture was stirred at 80 °C under O_2 for 12 h. The crude product was subjected to flash chromatography purification (40% Et_2O/Hexane) to afford an inseparable mixture of the starting material and product. The mixture was then dissolved in methanol (1.4 mL) followed by addition of cerium trichloride heptahydrate (209 mg, 0.55 mmol) and cooled to 0 ºC. After stirring for several minutes, sodium borohydride (21.0 mg, 0.55 mmol) was added slowly over 20 minutes. After the starting material was consumed, the reaction mixture was diluted with water (40 mL),

concentrated then extracted with ether (4 × 40 mL). The combined organic extracts were dried ($MgSO_4$), filtered, and concentrated. The crude product was subject to flash chromatography (10-70% Et_2O:Hexane) to afford the title compound (210 mg, 49%).

Amorphous solid; TLC (70% Et_2O): $R_f = 0.32$.

^{1}H NMR (500 MHz, $CDCl_3$, 25 ^{o}C) δ 7.01–6.87 (m, 1 H), 5.05–4.95 (m, 1 H), 4.27–4.13 (m, 1 H), 3.89–3.83 (m, 1 H), 3.33 (t, *J* = 11.5 Hz, 1 H), 1.97–1.73 (m, 2 H), 1.57–1.44 (m, 10 H). (Rotamers present at room temperature)

^{13}C NMR (125 MHz, $CDCl_3$, 25 ^{o}C) δ 152.6, 152.0, 128.2, 106.6, 106.2, 81.3, 61.0, 38.0, 37.0, 30.5, 28.3. (Rotamers present at room temperature).

IR (microscope, cm^{-1}) 3420, 2976, 2931, 2879, 1704, 1640, 1366, 1054.

HRMS (ESI) for $C_{10}H_{17}NNaO_3$ $(M + Na)^+$: calcd. 222.1101; found 222.1098, for $C_{20}H_{29}N_2O_4$ $(M + NH_4)^+$: calcd. 361.2122; found 361.2119, for $C_{20}H_{26}NO_4$ $(M + H)^+$: calcd. 344.1856; found 344.1855.

3.8 References

[1] de la Pradilla, R. F.; Lwoff, N.; Viso, A. *Eur. J. Org. Chem.* **2009**, *2009*, 2312–2322.

[2] Lalitha, K.; Muthusamy, K.; Prasad, Y. S.; Vemula, P. K.; Nagarajan, S. *Carbohydr. Res.* **2015**, *402*, 158–171.

[3] (a) Ramnauth, J.; Poulin, O.; Rakhit, S.; Maddaford, S. P. *Org. Lett.* **2001**, *3*, 2013–2015; (b) Bai, Y.; Kim, L. M. H.; Liao, H.; Liu, X. W. *J. Org. Chem.* **2013**, *78*, 8821–8825; (c) Bai, Y.; Leow, M. L.; Zeng, J.; Liu, X.-W. *Org. Lett.* **2011**, *13*, 5648–5651.

[4] (a) Farr, R. N.; Outten, R. A.; Cheng, J. C. Y.; Daves, G. D. *Organometallics* **1990**, *9*, 3151–3156; (b) Kwok, D. L.; Farr, R. N.; Daves, G. D. *J. Org. Chem.* **1991**, *56*, 3711–3713; (c) Lei, M.; Gao, L.; Yang, J. S. *Tetrahedron Lett.* **2009**, *50*, 5135–5138; (d) Xiang, S.; Cai, S.; Zeng, J.; Liu, X. W. *Org. Lett.* **2011**, *13*, 4608–4611.

[5] Leidy, M. R.; Hoffman, J. M.; Pongdee, R. *Tetrahedron Lett.* **2013**, *54*, 6889–6891.

[6] Bower, J. F.; Guillaneux, D.; Nguyen, T.; Wong, P. L.; Snieckus, V. *J. Org. Chem.* **1998**,

63, 1514–1518.

[7] Sakamaki, S.; Kawanishi, E.; Nomura, S.; Ishikawa, T. *Tetrahedron* **2012**, *68*, 5744–5753.

[8] Friesen, R. W.; Loo, R. W.; Sturino, C. F. *Can. J. Chem.* **1994**, *72*, 1262–1272.

[9] Ousmer, M.; Boucard, V.; Lubin-Germain, N.; Uziel, J.; Augé, J. *Eur. J. Org. Chem.* **2006**, *2006*, 1216–1221.

[10] (a) Gong, H.; Gagné, M. R. *J. Am. Chem. Soc.* **2008**, *130*, 12177–12183; (b) Gong, H.; Sinisi, R.; Gagné, M. R. *J. Am. Chem. Soc.* **2007**, *129*, 1908–1909.

[11] Ito, H.; Kunii, S.; Sawamura, M. *Nat. Chem.* **2010**, *2*, 972–976.

[12] Leonori, D.; Aggarwal, V. K. *Acc. Chem. Res.* **2014**, *47*, 3174–3183.

[13] Jana, R.; Pathak, T. P.; Sigman, M. S. *Chem. Rev.* **2011**, *111*, 1417–1492.

[14] Leonori, D.; Aggarwal, V. K. *Angew. Chem. Int. Ed.* **2015**, *54*, 1082–1096.

[15] Ridgway, B. H.; Woerpel, K. A. *J. Org. Chem.* **1998**, *63*, 458–460.

[16] Matos, K.; Soderquist, J. A. *J. Org. Chem.* **1998**, *63*, 461–470.

[17] Taylor, B. L. H.; Jarvo, E. R. *J. Org. Chem.* **2011**, *76*, 7573–7576.

[18] Mlynarski, S. N.; Schuster, C. H.; Morken, J. P. *Nature* **2014**, *505*, 386–390.

[19] Hildebrand, J. P.; Marsden, S. P. *Synlett* **1996**, *1996*, 893–894.

[20] (a) Fang, G.; Yan, Z.; Deng, M. *Org. Lett.* **2004**, *6*, 357–360; (b) Charette, A. B.; Mathieu, S.; Fournier, J. *Synlett* **2005**, *2005*, 1779–1782.

[21] Imao, D.; Glasspoole, B. W.; Laberge, V. S.; Crudden, C. M. *J. Am. Chem. Soc.* **2009**, *131*, 5024–5025.

[22] (a) Uenishi, J.; Beau, J. M.; Armstrong, R. W.; Kishi, Y. *J. Am. Chem. Soc.* **1987**, *109*, 4756–4758; (b) Hirabayashi, K.; Kawashima, J.; Nishihara, Y.; Mori, A.; Hiyama, T. *Org. Lett.* **1999**, *1*, 299–302.

[23] Crudden, C. M.; Glasspoole, B. W.; Oderinde, M.; Moore, B.; Antoft-Finch, A. *Synthesis* **2013**, *45*, 1759–1763.

[24] Chausset-Boissarie, L.; Ghozati, K.; LaBine, E.; Chen, J. L.; Aggarwal, V. K.; Crudden, C. M. *Chem. Eur. J.* **2013**, *19*, 17698–17701.

[25] Molander, G. A.; Wisniewski, S. R. *J. Am. Chem. Soc.* **2012**, *134*, 16856–16868.

[26] Ohmura, T.; Awano, T.; Suginome, M. *J. Am. Chem. Soc.* **2010**, *132*, 13191–13193.

[27] Sandrock, D. L.; Jean-Gérard, L.; Chen, C.; Dreher, S. D.; Molander, G. A. *J. Am. Chem. Soc.* **2010**, *132*, 17108–17110.

[28] Awano, T.; Ohmura, T.; Suginome, M. *J. Am. Chem. Soc.* **2011**, *133*, 20738–20741.

[29] (a) Lee, J. C. H.; McDonald, R.; Hall, D. G. *Nat. Chem.* **2011**, *3*, 894–899; (b) Lee, J. C.; Sun, H. Y.; Hall, D. G. *J. Org. Chem.* **2015**, *80*, 7134–7143.

[30] Yamamoto, Y.; Takada, S.; Miyaura, N. *Chem. Lett.* **2006**, *35*, 704–705.

[31] Sebelius, S.; Olsson, V. J.; Wallner, O. A.; Szabó, K. J. *J. Am. Chem. Soc.* **2006**, *128*, 8150−8151.

[32] Yamamoto, Y.; Takada, S.; Miyaura, N.; Iyama, T.; Tachikawa, H. *Organometallics* **2009**, *28*, 152–160.

[33] Farmer, J. L.; Hunter, H. N.; Organ, M. G. *J. Am. Chem. Soc.* **2012**, *134*, 17470–17473.

[34] Glasspoole, B. W.; Ghozati, K.; Moir, J. W.; Crudden, C. M. *Chem. Commun.* **2012**, *48*, 1230–1232.

[35] Denmark, S. E.; Werner, N. S. *J. Am. Chem. Soc.* **2010**, *132*, 3612–3620.

[36] Yang, Y.; Buchwald, S. L. *J. Am. Chem. Soc.* **2013**, *135*, 10642–10645.

[37] Lessard, S.; Peng, F.; Hall, D. G. *J. Am. Chem. Soc.* **2009**, *131*, 9612–9613.

[38] (a) Suzuki, A. *J. Organomet. Chem.* **1999**, *576*, 147–168; (b) Carrow, B. P.; Hartwig, J. F. *J. Am. Chem. Soc.* **2011**, *133*, 2116–2119.

[39] (a) Lennox, A. J.; Lloyd-Jones, G. C. *Angew. Chem. Int. Ed.* **2013**, *52*, 7362–7370; (b) Lennox, A. J. J.; Lloyd-Jones, G. C. *Chem. Soc. Rev.* **2014**, *43*, 412–443.

[40] Ding, J.; Rybak, T.; Hall, D. G. *Nat. Commun.* **2014**, *5*.

[41] Huang, X.; Anderson, K. W.; Zim, D.; Jiang, L.; Klapars, A.; Buchwald, S. L. *J. Am. Chem. Soc.* **2003**, *125*, 6653–6655.

[42] Surry, D. S.; Buchwald, S. L. *Chem. Sci.* **2011**, *2*, 27–50.

[43] (a) Brown, E.; Dujardin, G.; Maudet, M. *Tetrahedron* **1997**, *53*, 9679–9694; (b) Postema, M. H. D.; Piper, J. L.; Liu, L.; Shen, J.; Faust, M.; Andreana, P. *J. Org. Chem.* **2003**, *68*, 4748–4754; (c) Huang, C.; Liu, R.; Wu, T.; Cheng, W. *Tetrahedron Lett.* **2008**, *49*, 2895–2898.

[44] (a) Fakha, G.; Sinou, D. *Molecules* **2005**, *10*, 859–870; (b) She, X.; Xie, X.; Li, J.; Zheng, H.; Su, Y. *Synlett* **2010**, *2010*, 2283–2284.

[45] Beng, T. K.; Gawley, R. E. *Org. Lett.* **2011**, *13*, 394–397.

[46] (a) Amat, M.; Bosch, J.; Hidalgo, J.; Cantó, M.; Pérez, M.; Llor, N.; Molins, E.; Miravitlles, C.; Orozco, M.; Luque, J. *J. Org. Chem.* **2000**, *65*, 3074–3084; (b) de Gonzalo, G.; Brieva, R.; Sánchez, V. M.; Bayod, M.; Gotor, V. *J. Org. Chem.* **2001**, *66*, 8947–8953.

[47] Diao, T.; Stahl, S. S. *J. Am. Chem. Soc.* **2011**, *133*, 14566–14569.

[48] Ito, H.; Kawakami, C.; Sawamura, M. *J. Am. Chem. Soc.* **2005**, *127*, 16034–16035.

[49] Dutheuil, G.; Selander, N.; Szabó, K. J.; Aggarwal, V. K. *Synthesis* **2008**, 2293–2297.

[50] (a) Pregosin, P. S.; Salzmann, R. *Coord. Chem. Rev.* **1996**, *155*, 35–68; (b) Trost, B. M.; Van Vranken, D. L. *Chem. Rev.* **1996**, *96*, 395–422.

[51] Spring, D. R. *Org. Biomol. Chem.* **2003**, *1*, 3867–3870.

[52] Ireland, T.; Tappe, K.; Grossheimann, G.; Knochel, P. *Chem. Eur. J.* **2002**, *8*, 843–852.

Chapter 4. Expanding the Allylic Suzuki-Miyaura Cross-Coupling Reaction Towards Chiral Polyfunctionalized Dihydropyrans

4.1 Towards the formation of 2,4- and 2,6-functionalized dihydropyrans

In Chapter 3, a highly controlled regiodivergent synthesis of 2- or 4-substituted dihydropyrans with high stereochemical retention using enantiomerically enriched heterocyclic allylic boronates was demonstrated. The regioselective and stereospecific Suzuki-Miyaura cross-coupling reaction forms $C(sp^3)$-$C(sp^2)$ bonds onto a dihydropyranyl framework using aryl and alkenyl halides. Thus far, this method has not accounted for the consequential stereochemical effects induced by additional chirality that may be present in a pyran framework; potentially affecting the selectivity of the cross-coupling reaction. As mentioned in Chapter 1, there are numerous bioactive molecules containing a 2,4- or 2,6-functionalized pyran motif (Chapter 1, Figure 1-1). Utilizing the allylic cross-coupling reaction to access this class of compounds requires a suitable allylboronate substrate.

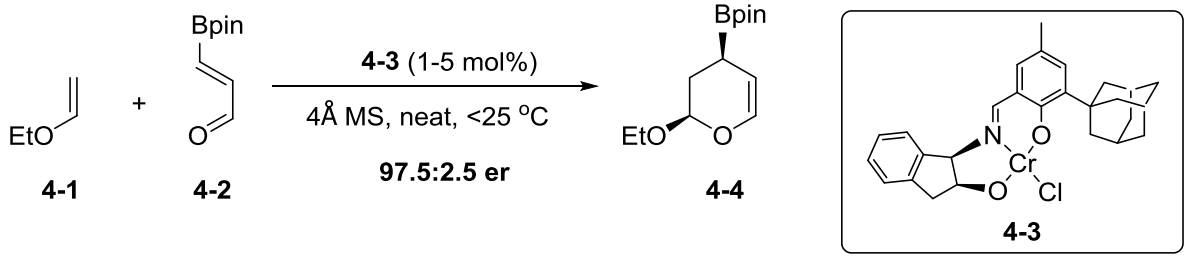

Scheme 4-1: The synthesis of the 2-ethoxy dihydropyranyl boronate **4-4** through the catalytic enantioselective oxa-[4+2] cycloaddition.

The 2-ethoxy dihydropyranyl boronate **4-4**, as described in Chapter 1, originates from the enantioselective oxa-[4+2] cycloaddition between ethyl vinyl ether **4-1** and boronoacrolein **4-2** catalyzed by Jacobsen's tridentate chromium complex **4-3** (Scheme 4-1).[1] Due to the broad applicability of this substrate **4-4** toward the synthesis of numerous bioactive molecules, this heterocyclic allylboronate would be a suitable choice to expand on the allylic Suzuki-Miyaura cross-coupling reaction.[2]

Additionally, the 2-ethoxy group is another handle for functionalization, involving the formation of, and reactions to, the oxocarbenium ion. As described earlier, several methods exploit functionalization at the C1-position through the formation of the oxocarbenium ion, specifically reactions with enol silanes and allyl silanes (see Chapter 1, Section 1.3). Various diastereoselective reactions onto the oxocarbenium electrophile have been examined previously by Woerpel and co-workers, where they observed that substituent-controlled conformational preferences of the pyran ring influenced the trajectory of the approaching nucleophile (Figure 4-1, Equation 1).[3] Typically, nucleophiles would preferentially attack the oxocarbenium species to from the lower energy half-chair transition state rather than the higher energy twist-boat conformation (Figure 4-1, Equation 2).

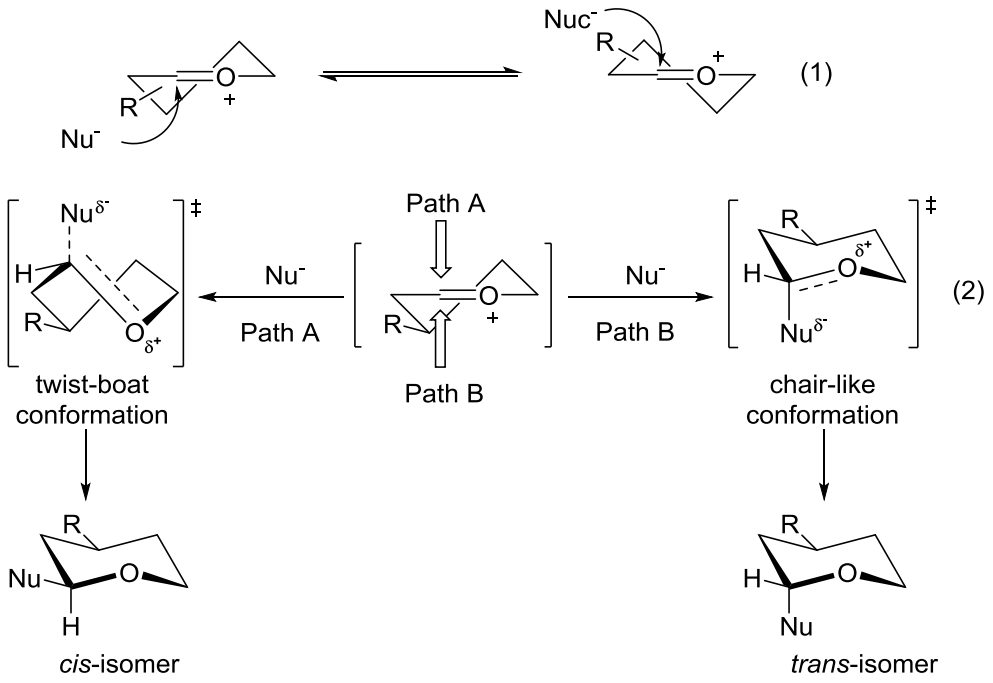

Figure 4-1: Facial selectivity influenced by favored conformation of oxocarbenium species.

In regards to substituent-dependent conformations, aliphatic substituents would typically favor a pseudoequatorial conformation to minimize steric repulsions. Specifically to the C2-position, alkoxy substituents would favor a pseudoequatorial conformation to form *cis*-2,3-functionalized tetrahydropyrans, a result of improved hyperconjugation stabilization of the oxocarbenium species (Figure 4-2, Equation 1). On the other hand, bulky aliphatic substituents would favor the higher energy twist-boat transition state to form *trans*-2,3-functionalized tetrahydropyrans as a result of decreased steric repulsion between the nucleophile and the substituent. Specific to substituents located at the C3- or C4-position, polar functional groups would typically favor a pseudoaxial conformation due to improved electrostatic interactions between the electron-rich substituent and the electron-deficient oxocarbenium group (Figure 4-2, Equations 2 and 3).[4] Equipped with this knowledge, a late stage facial selective functionalization of the anomeric site of **4-4** can be utilized towards the synthesis of bioactive 2,4- or 2,6-functionalized bioactive products.

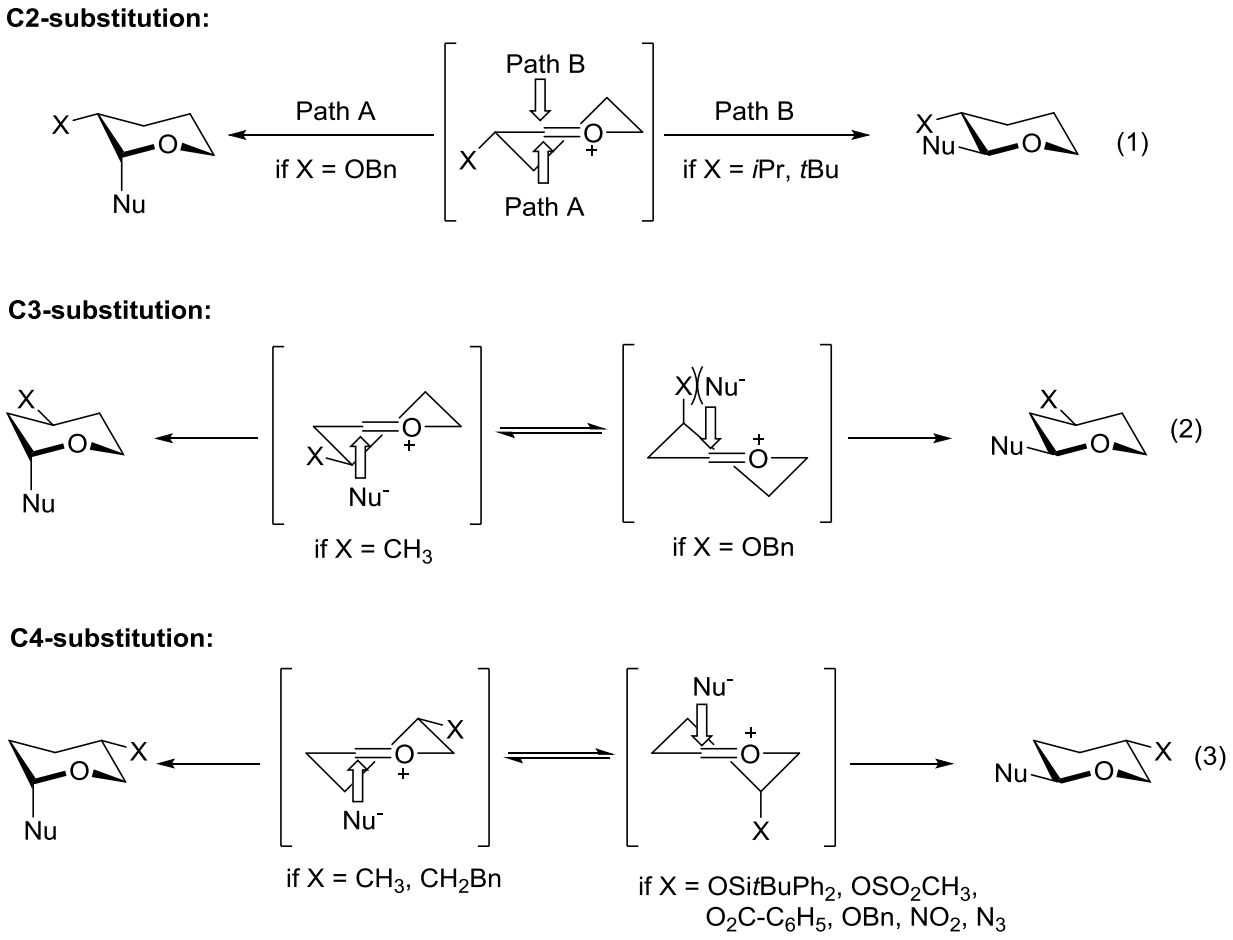

Figure 4-2: Preferred nucleophilic trajectories onto substituted oxocarbenium species.

4.2 Objectives

Due to a large number of bioactive molecules containing a 2,4- or 2,6-functionalized pyran motif, the allylic Suzuki-Miyaura cross-coupling method may be utilized in forming complex aryl- and alkenyl-functionalized pyran derivatives using the 2-ethoxy-substituted dihydropyranyl boronate substrate **4-4**. Additionally, given that the cross-coupling reaction was not directly confirmed to proceed with retention of stereochemistry to form 2- or 4-functionalized dihydropyrans, the stereospecificity of this method was examined. Using the data described in Chapter 3, both the scope and investigation of the mechanism, a generalized reaction mechanism

was proposed for the cross-coupling reaction. Lastly, the cross-coupling of **4-4** – aware of potential diastereoselective methods of functionalizing the C1-position – was applied towards the attempted synthesis of goniothalesdiol A and the successful synthesis of the antiosteoporotic natural product diospongin B.

4.3 Optimization of the yield and regioselectivity of the Suzuki-Miyaura cross-coupling of the 2-dihydropyranyl boronate

At first, it was uncertain whether the previously optimized cross-coupling conditions for the dihydropyranyl boronate **3-51** would be suitable for **4-4**. Initially, the previous reaction conditions (Chapter 3, Section 3.5, Table 3-1) were used to optimize the regioselectivity of α- and γ- products, **4-5** and **4-6** (Table 4-1 and 4-2). The standard conditions used for the synthesis of the des-ethoxy α-regioisomer **3-52** – $[(allyl)PdCl]_2$ with potassium phosphate as a base in acetonitrile – formed **4-5** in good regioselectivity and moderate yield (Table 4-1, entry 1). By altering the base to KOH, the optimal base previously used toward the synthesis of piperidine-based α-regioisomers, the regioselectivity (α:γ = 83:17) and yield (26%) could not be improved (Table 4-1, entry 2). Previous work on **3-51** showed that α-selectivity was favored with the use of weaker sigma-donating ligands. However, when using the tris(4-fluorophenyl)phosphine ligand, the yield and selectivity (54%, α:γ = 85:15) could not be improved (Table 4-1, entry 3). Similarly, the more electron-rich triphenylphosphine ligand could not improve the regioselectivity and afforded a lower yield (43%, α:γ = 84:16) compared to other phosphine ligands (Table 4-1, entry 4). Several achiral bisphosphine ligands that were tested were also not suitable replacements over the monophosphine ligands (Table 4-1, entries 5 to 8). Organ's NHC-ligated palladium catalysts – previously known to offer comparable α-selectivity relative to the tris(p-trifluoromethylphenyl)phosphine ligand – showed no improvement towards α-selectivity

(Table 4-1, entries 9 and 10).[2d] Upon increasing the reaction temperature to 85 °C and using the conditions of entry 1, an acceptable yield and regioselectivity (73%, α:γ = 83:17) was obtained (Table 4-1, entry 11).

Table 4-1: Optimized conditions for the synthesis of α-regioisomers.[a]

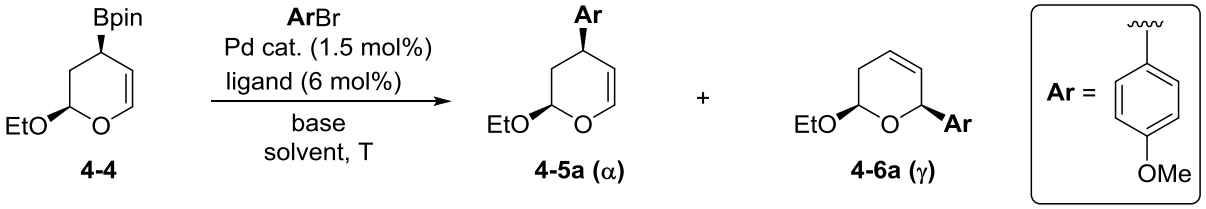

entry	Pd cat	ligand (6 mol%)	base	solvent, T (°C)	yield (%)[c]	isomeric ratio (α:γ)[d]
1	$(AllylPdCl)_2$	$(p\text{-}CF_3C_6H_4)_3P$	K_3PO_4	CH_3CN, 70	64	84:16
2	$(AllylPdCl)_2$	$(p\text{-}CF_3C_6H_4)_3P$	KOH	CH_3CN, 70	26	83:17
3	$(AllylPdCl)_2$	$(p\text{-}FC_6H_4)_3P$	K_3PO_4	CH_3CN, 70	54	85:15
4	$(AllylPdCl)_2$	PPh_3	K_3PO_4	CH_3CN, 70	43	83:17
5	$(AllylPdCl)_2$	XantPhos[b]	K_3PO_4	CH_3CN, 70	16	55:45
6	$(AllylPdCl)_2$	dppf[b]	K_3PO_4	CH_3CN, 70	50	55:45
7	$(AllylPdCl)_2$	dppp[b]	K_3PO_4	CH_3CN, 70	32	57:43
8	$(AllylPdCl)_2$	dppb[b]	K_3PO_4	CH_3CN, 70	21	76:24
9	Pd-PEPPSI-IPr	–	K_3PO_4	CH_3CN, 70	49	50:50
10	Pd-PEPPSI-IPent	–	K_3PO_4	CH_3CN, 70	16	74:26
11	**$(AllylPdCl)_2$**	**$(p\text{-}CF_3C_6H_4)_3P$**	**K_3PO_4**	**CH_3CN, 85**	**73**	**83:17**

[a] Reaction scale: **4-4** (0.30 mmol, 1.2 equiv), 4-bromoanisole (0.25 mmol, 1.0 equiv), Pd catalyst (3.75 μmol, 1.5 mol %), ligand (15 μmol, 6 mol %), base (1.25 mmol, 4 equiv) unless indicated otherwise. [b] 3.1 mol % of ligand used. [c] Isolated yield of the major regioisomer **4-5a**. [d] Regioisomer ratio (α:γ) was measured from the ^1H NMR spectra of crude products.

As discussed in Chapter 3, the reaction conditions used toward the efficient synthesis of the γ-isomer **3-53** were tested first towards the optimization of **4-6** (Table 4-2). Using the strong sigma-donating alkylphosphine ligand, XPhos, the reaction was highly regioselective (α:γ = 7:93) towards the formation of the γ-product **4-6** (Figure 4-2, entry 1). Other dialkylarylphosphines of this class of ligands gave similar regioselectivities (Table 4-2, entry 3 and 4). The optimal ligand that promoted the γ-isomer (α:γ = 5:95) with a high yield (86%) was SPhos (Table 4-2, entry 4). With the optimized conditions in hand, the regiodivergent synthesis of both α- and γ-regioisomers was explored with the use of various aryl bromides.

Table 4-2: Optimized conditions for the synthesis of γ-regioisomers.[a]

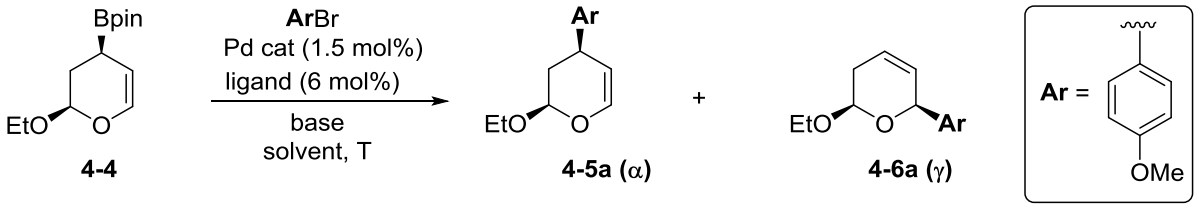

entry	Pd cat	ligand	base	solvent, T (°C)	yield (%)[b]	isomeric ratio (α:γ)[c]
1	$(AllylPdCl)_2$	XPhos	K_3PO_4	THF, 40	82	7:93
2	$(AllylPdCl)_2$	CyJohnPhos	K_3PO_4	THF, 40	61	6:94
3	$(AllylPdCl)_2$	RuPhos	K_3PO_4	THF, 40	75	5:95
4	**$(AllylPdCl)_2$**	**SPhos**	**K_3PO_4**	**THF, 40**	**86**	**5:95**

[a] Reaction scale: **4-4** (0.30 mmol, 1.2 equiv), 4-bromoanisole (0.25 mmol, 1.0 equiv), Pd catalyst (3.75 μmol, 1.5 mol %), ligand (15 μmol, 6 mol %), base (1.25 mmol, 4 equiv) unless indicated otherwise. [b] Isolated yield of the major regioisomer **4-6a**. [c] Regioisomer ratio (α:γ) was measured from the ^1H NMR spectra of crude products.

4.4 Substrate scope for the stereospecific cross-coupling reaction

In order to evaluate the scope of substrates for the regiodivergent and stereospecific allylic Suzuki-Miyaura cross-coupling reaction, the optically pure allylboronate **4-4** was prepared with a good yield with high enantioselectivity (77%, 97.5:2.5 er) using the enantioselective oxa-[4+2] cycloaddition between ethyl vinyl ether **4-1** and boronacrolein **4-2** (Scheme 4-2).[5] This inverse electron-demand hetero-Diels-Alder (HDA) reaction was catalyzed by Jacobsen's tridentate chromium complex **4-3** at an impressively low catalyst loading (3 mol%).[5] As reported previously by Hall and co-workers, the high enantioselectivity was dependent on the purity of **4-2** as well as maintaining an ambient temperature below 20 ^{o}C.[5] In order to achieve a good yield and enantioselectivity, **4-2** had to be distilled thoroughly beforehand. Afterwards, the catalyzed reaction ran under neat conditions between **4-1** and **4-2** with 4Å molecular sieves as the drying agent.

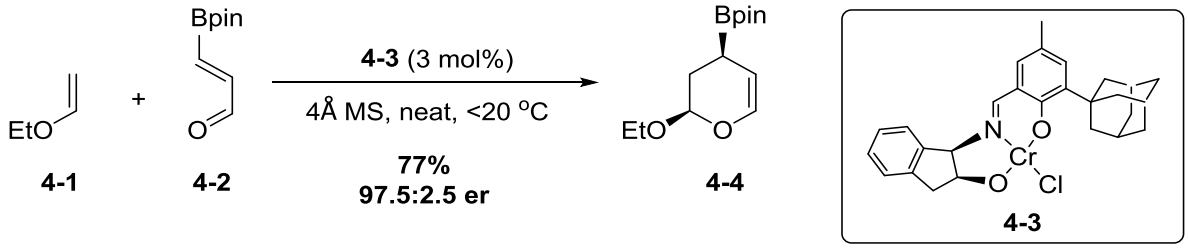

Scheme 4-2: The synthesis of the 2-ethoxy dihydropyran boronate **4-4** through the inverse electron-demand oxa-[4+2] cycloaddition.

With the enantiopure allylboronate **4-4** in hand, various classes of sp^2-hybridized organobromide substrates were tested to demonstrate the general efficiency of this method (Table 4-3). These classes of organohalides include neutral, electron-rich and electron-poor aryl bromides, a heteroaryl bromide and an alkenyl bromide. Beginning with the synthesis of α-regioisomers, all electrophiles tested were coupled in moderate to good yields to produce 2,4-

substituted products **4-5a** and **4-5e** with regioselectivity ratios ranging from 83:17 to 93:7. Surprisingly, all products had near to full preservation of stereospecificity as measured by chiral HPLC (97:3 to 97.5:2.5 dr). This was confirmed by the diasteriomeric ratios (dr) measured for the set of cross-coupling products. With the exception of products **4-5a**, **4-5d** and **4-5e**, the diastereomeric ratios of the remaining optically pure products could not be measured directly by chiral HPLC, since they could not be resolved using different HPLC conditions. Thus, these products, **4-5b** and **4-5c**, underwent further chemical derivatization (see Scheme 4-4, Equations 1 and 2). The electron-rich para-methoxyphenyl bromide afforded a lower regioselectivity of the coupling product **4-5a** (α:γ = 83:17) relative to the electron-poor para-trifluoromethylphenyl bromide, which gave a high α-selectivity (α:γ = 93:7) for **4-5b**. Initially, when phenyl bromide was subjected to the reaction conditions, the product **4-5c** was obtained with a 49% yield and good regioselectivity (α:γ = 83:17). To confirm whether the aryl bromide may be too volatile under the reaction conditions that would result in a low yield, the reaction vessel was adjusted to minimize evaporation and performed once more to afford **4-5c** at a higher yield and nearly identical regioselectivity (59%, α:γ = 84:16). The *N*-Boc-5-bromoindole substrate, which could not be examined for optical purity in the previous work (see Chapter 3, Section 3.3, Table 3-2), afforded **4-5d** in high regioselectivity (α:γ = 90:10). Alkenyl bromides also appeared to be suitable substrates for this method, as shown with the reaction of *β*-bromostyrene afforded **4-5e** in high yield and high regioselectivity (81%, α:γ = 91:9). Furthermore, since the alkenylbromide substrate consists of a *E/Z*-mixture of stereoisomers (*E/Z* = 80/20) the crude product contains both isomers that were easily separable to afford the (*E*)-β-bromostyrene-coupled product.

Table 4-3: Scope of electrophiles in the α- and γ-selective stereospecific Suzuki-Miyaura cross-coupling with chiral 2-ethoxy dihydropyranyl boronate **4-4**.[a]

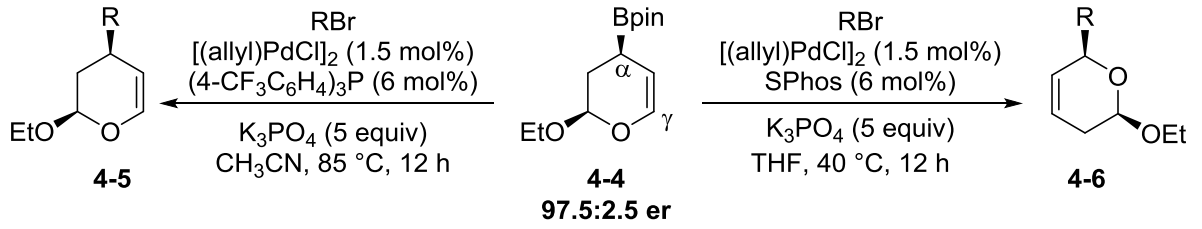

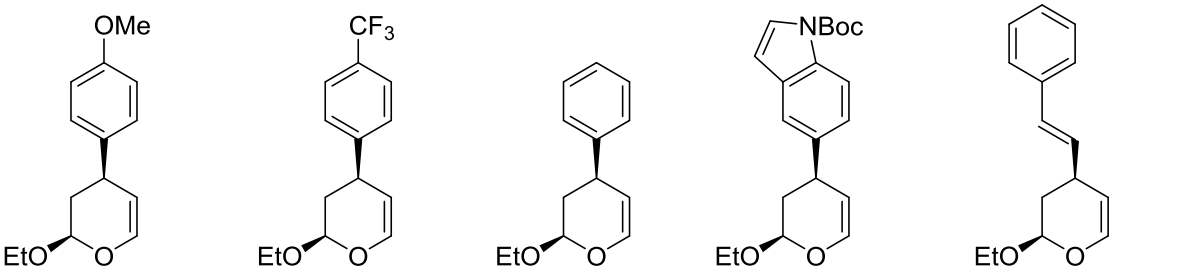

4-5a 73% α/γ = 83:17[b] 97.5:2.5 dr

4-5b 76% α/γ = 93:7[b] 97:3 dr[c]

4-5c 59% α/γ = 84:16[b] 97.5:2.5 dr[c]

4-5d 79% α/γ = 90:10[b] 97.5:2.5 dr

4-5e 81% α/γ = 91:9[b] 97.5:2.5 dr

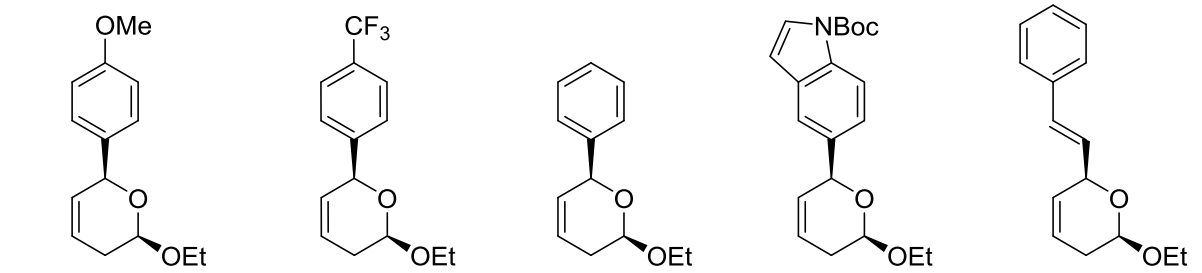

4-6a 86% α/γ = 5:95[b] 97.5:2.5 dr

4-6b 80% α/γ = 8:92[b] 97.5:2.5 dr

4-6c 74% α/γ = 3:97[b] 97.5:2.5 dr[c]

4-6d 97% α/γ = 3:97[b] 97.5:2.5 dr[c]

4-6e 80% α/γ = 2:98[b] 97.5:2.5 dr

[a] Reaction scale: **4-4** (0.30 mmol, 1.2 equiv), RBr (0.25 mmol, 1.0 equiv), Pd catalyst (3.75 μmol, 1.5 mol %), ligand (15 μmol, 6 mol%), base (1.25 mmol, 4 equiv). [b] Regioisomer ratio (α:γ) was measured from the ^{1}H NMR spectra of crude products. [c] Diastereomeric ratio was determined by chiral HPLC analysis of modified products (see Scheme 4-3).

The organobromide substrates used in the synthesis of the α-regioisomers **4-5** were also employed in the cross-coupling to form the γ-regioisomers **4-6** under previously optimized conditions using SPhos (Table 4-2, entry 4). Overall, there was an improvement in regioselectivity and yield for the γ-products relative to the α-isomers. Additionally, the stereospecificity was completely preserved based on the diastereomeric ratios (97.5:2.5 dr) measured by chiral HPLC analysis. The diastereomeric ratios of **4-5a** and **4-5e** could be measured directly, while the remaining optically pure products could not be measured directly by chiral HPLC, since they could not be resolved using different HPLC conditions. Consequently, these products, **4-5b** to **4-5d**, underwent further chemical derivatization (see Scheme 4-4, Equations 3 to 5). Once more, the para-methoxyphenyl bromide afforded product **4-6a** in a slightly higher yield (86%) and regioselectivity (α/γ = 5:95) compared to trifluoromethylphenyl bromide, which resulted in the formation of **4-6b** (80%, α/γ = 8:92). The *N*-Boc-indole-substituted γ-regioisomer **4-6d** was obtained in a much higher yield and regioselectivity (97%, α/γ = 3:97) compared to the α-regioisomer (79%, α/γ = 90:10). This trend is consistent with the previous work with *N*-Boc-indole-substituted pyrans (see Chapter 3, Section 3.3, Table 3-3). Surprisingly, the reaction between **4-4** and *β*-bromostyrene afforded **4-6e** with a yield and regioselectivity (80%, α/γ = 2:98) higher than that obtained in the previous example between **3-50** and *β*-bromostyrene (70%, α/γ = 1:3) described in Chapter 3. It is important to mention that 2,4-*tran*s- or 2,6-*trans*-diastereomers were not observed when using this cross-coupling method. Based on a limited set of aryl halides explored, these results indicate that the 2-ethoxy dihydropyranyl boronate **4-4** displays a scope comparable to that of **3-51**.

4.5 Clarifying the mechanism of the allylic Suzuki-Miyaura cross-coupling of dihydropyranyl boronates

In the previous investigation of the regiodivergent asymmetric Suzuki-Miyaura cross-coupling of the dihydropyran allylboronate **3-51**, the mechanism of the reaction was confirmed to proceede with retention of stereochemistry (see Chapter 3, Section 3-4). At the time, the tentative assignment relied on a correlation with the piperidine-based substrates that were synthesized and used toward the formal synthesis of (+)-anabasine and (+)-paroxetine (see Chapter 3, Section 3-4, Scheme 3-10). Since **4-4** could theoretically form two diastereomers where the newly formed $C(sp^2)$-$C(sp^3)$ bond could be *cis* or *trans* to the 2-ethoxy group, stronger evidence was needed to support that the cross-coupling mechanism was stereoretentive. Due to the half-chair conformations of the dihydropyran-based cross-coupling products, **4-5** and **4-6**, as well as their non-crystalline properties, these compounds were not believed to be suitable for determining whether the cross-coupling reaction is stereoretentive. Therefore, the derivitized products of **4-5** and **4-6**, which were initially synthesized to measure the diastereomeric ratios of the cross-coupling products by chiral HPLC analysis, were examined by advanced spectral analysis and X-ray crystallographic diffraction to confirm the relative stereochemistry (Scheme 4-3). Based on the successful derivatization of the des-ethoxy dihydropyranyl products (Chapter 3, Section 3-3, Scheme 3-9), select products derived from **4-5** and **4-6** were subject to the same conditions. The α-regioisomers, **4-5b** and **4-5c** underwent hydroboration and oxidation to exclusively form **4-7** and **4-8**, with a 3-hydroxy group *trans* to the aryl and ethoxy substituents, consecutively at moderate and good yields (Scheme 4-3, Equation 1 and 2). The γ-regioisomers, **4-6b** to **4-5d** were subject to a diastereoselective Upjohn dihydroxylation exclusively formed the *cis*-diol products **4-9** to **4-11** in low to good yields (Scheme 4-3, Equation 3 to 5). Based on ^{1}H

NMR analysis, the *cis*-diol groups were *trans* to the remaining substituents. One should note that when the quinuclidine reagent was added to accelerate the reaction, trace amounts of the other diastereomer, where the diols are *cis* to the other substituents, were observed. Thus, no additives were included to accelerate the Upjohn dihydroxylation. The yield for **4-9** (35%) was significantly lower than **4-10** and **4-11** due to the difficulties of observing this product by TLC.

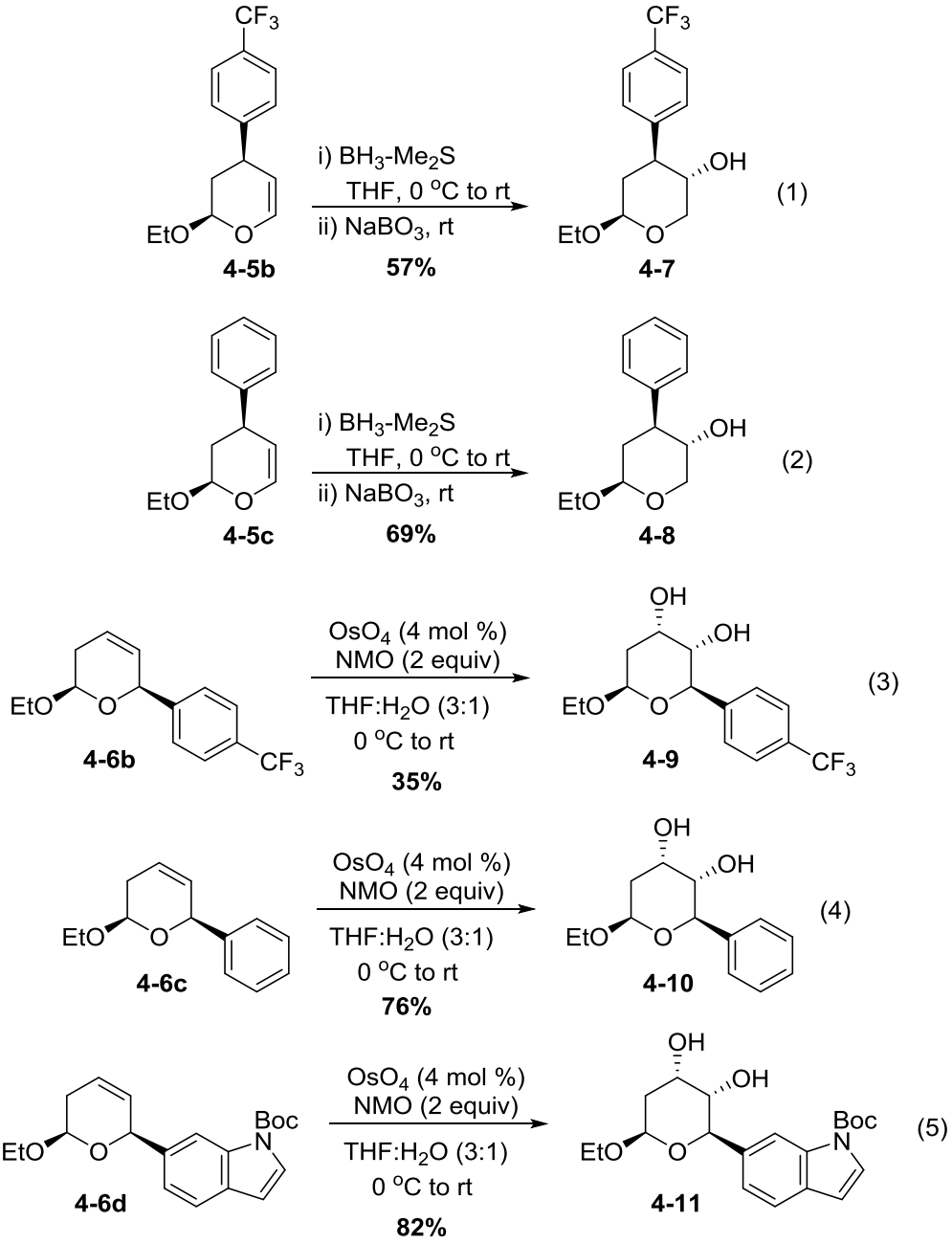

Scheme 4-3: Modification of cross-coupling products.

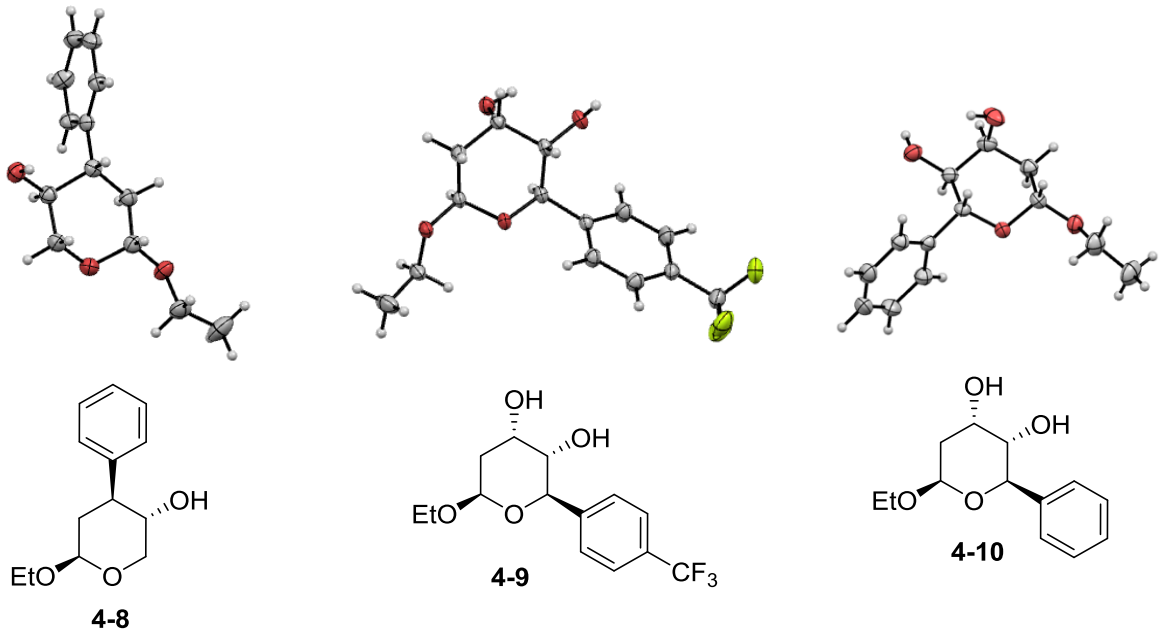

Figure 4-3: ORTEP structures of **4-8**, **4-9**, and **4-10**.

In the interest of obtaining X-ray crystallographic diffraction data, products **4-7** to **4-11** were subjected to recrystallization techniques. Among the derivatives formed, only compounds **4-8**, **4-9** and **4-10** afforded crystals of suitable quality for X-ray crystallographic analysis (Figure 4-3). The ORTEP models developed from the X-ray crystal diffraction data indicate that 2,4-*cis* disubstituted products are formed with the α-regioisomers, as shown with compound **4-8**. In regards to compounds **4-9** and **4-10**, derived from the γ-regioisomers, the cross-coupling reaction forms 2,6-*cis* products. Furthermore, relevant spatial correlations by nOe enhancement NMR analysis of compounds **4-8** to **4-10** supported the X-ray crystallographic data, where the only observed spatial correlations for each product were listed in Figure 4-4. Upon inspecting the ^{1}H NMR spectra of **4-8**, the conformation of the dihydropyran derivative was further confirmed when analyzing the coupling constants. The coupling constant between protons H^{A} and H^{B} of **4-8** is 9.7 Hz, which indicates that the protons are *trans* to one another (Figure 4-4a). Protons H^{C} and H^{D} are listed as a reference point in Figure 4-4a to trace the neighboring hydrogen atoms, H^{A}

and H^B, in the pyran framework. Using the Karplus curve to approximate the dihedral angles between H^A and H^B for **4-9**, with a coupling constant of 9.6 Hz, the phenyl group is believed to be oriented *trans* to the hydroxyl group. Lastly, the diol substituents of **4-10** were confirmed to be *trans* to the C5 substituted phenyl group since the coupling constants between H^A and H^B was measured at 9.5 Hz. These results supported the fact that no *trans*-disubstituted diastereomer had formed from the cross-coupling reaction as shown in Figure 4-4, where the structures of the possible derivitized diastereomers did not correlate with any of the data provided. As a result, the hydroxyl substituents formed in these products were confirmed to be *trans* to the aryl and ethoxy substituents based on the cross-coupling data measured in the corresponding ^{1}H NMR, as well as the 1D NOESY and X-ray crystallographic analysis.

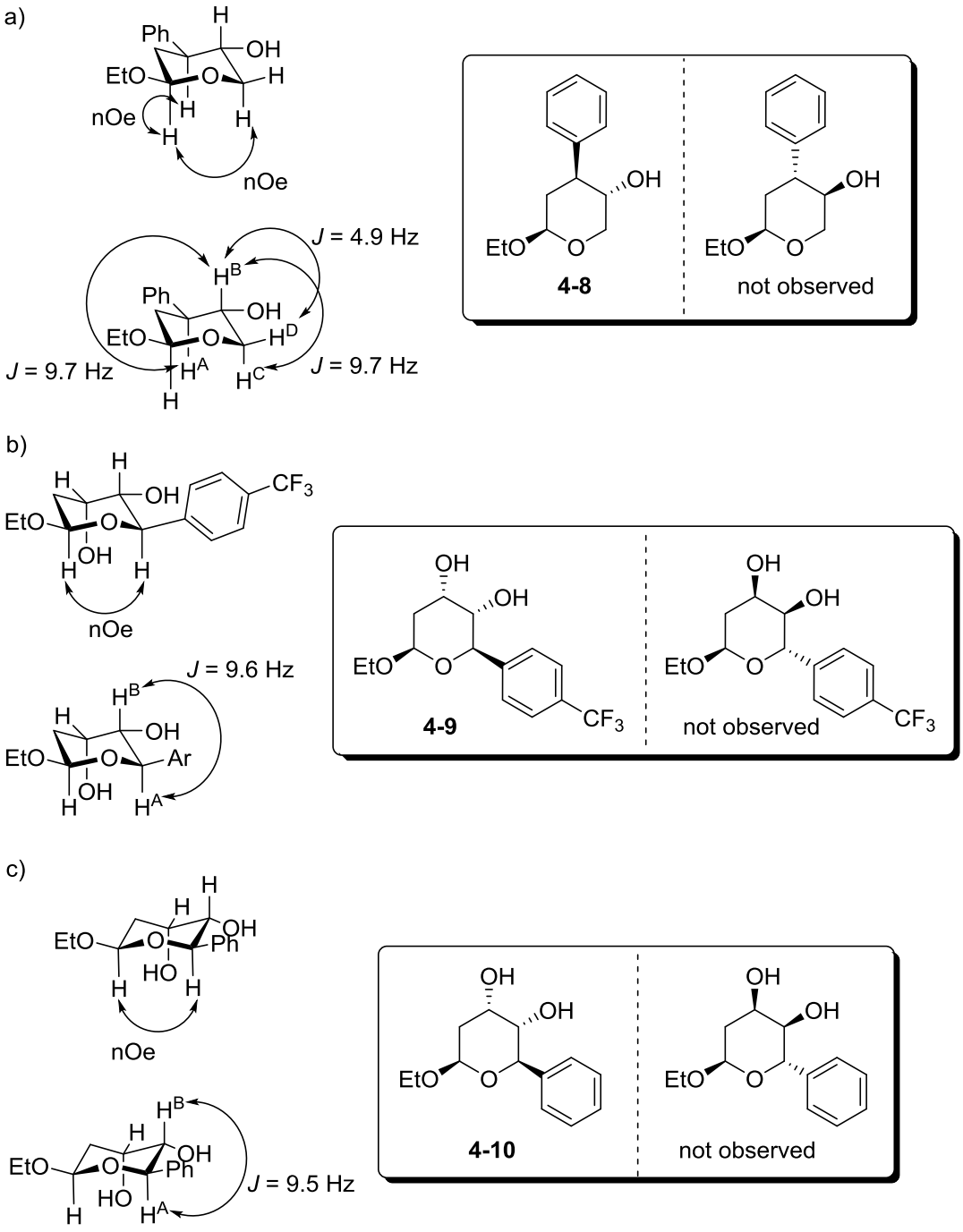

Figure 4-4: Spectral confirmation of relative stereochemistry of derivatives.

Based on the previous mechanism proposed for these allylic sp^3-sp^2 cross-coupling reactions (Chapter 3, Section 3.5, Scheme 3-13), as well as the X-ray crystallographic and spectral data that supported a retention of stereochemistry of the B-C center, a general mechanism for the

cross-coupling of dihydropyranyl boronates was proposed (Scheme 4-4). It was previously suggested that, depending on the catalyst used, the reaction proceeds through either a *syn*-S_E or *syn*-S_E' transmetallation, from the same oxyborate-coordinated palladium species **A** (see Chapter 3, Section 3.5).[2e,2f] With acyclic allylboronates, catalysts ligated by phosphines demonstrated γ-selectivity;[2c,2e,2f] thus both SPhos and $(4\text{-}CF_3\text{-}C_6H_4)_3P$ were suspected of promoting a S_E' transmetallation to form the η^1 γ-allylpalladium species **B**. Since both regioisomers were formed using either cross-coupling conditions, complex **B** is believed to isomerize to the higher-valency π-allyl intermediate **C** and eventually to the η^1 α-palladium complex **D**. Due to the weaker σ-donating capability of $(4\text{-}CF_3\text{-}C_6H_4)_3P$, the formation of the thermodynamic, heteroatom-conjugated σ-bonded Pd(II) complex **D** can be promoted via a σ–π equilibration leading to the α-coupling isomers **3-52** and **4-5**. On the other hand, strong σ-donating and bulky ligands such as XPhos and SPhos may suppress the formation of the allylpalladium intermediate **C** due to their well-known ability to promote a faster rate of reductive elimination (see Chapter 3).[6] By virtue of this effect, the allyl-isomerization is avoided and leads to the formation of the kinetically favored γ-isomers **3-53** and **4-6**. The rate of reductive elimination may be further enhanced specifically for **4-4** due to the σ-inductive electron-withdrawing ethoxy group present on the dihydropyranyl framework.[7] Thus, compared to substrate **3-51** (Chapter 3, Section 3.3), **4-4** may be more effective in suppressing an erosion of regioselectivity as observed by the increased regioselectivity of a number of substrates such as the α-substituted trifluoromethylphenyl compound [13:1 (α:γ) from **4-5b** as opposed to 6:1 (α:γ) from **3-52c**] the α-substituted *N*-Boc indole compound [9:1 (α:γ) from **4-5d** as opposed to 3:1 (α:γ) from **3-52k**], and the γ-substituted β-styrene [1:50 (α:γ) from **4-6e** as opposed to 1:3 (α:γ) from **3-53h**].

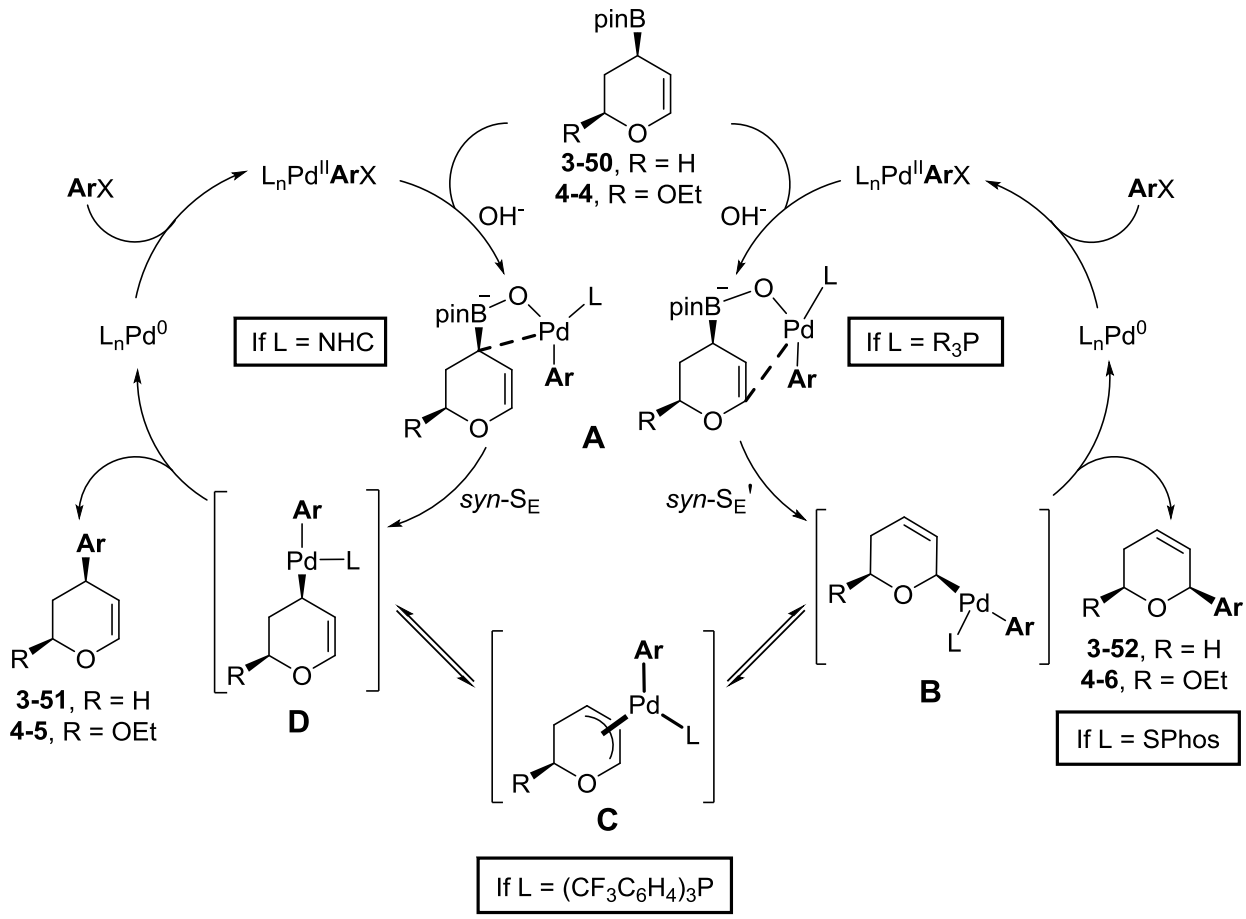

Scheme 4-4: A generalized ligand-controlled catalytic cycle for the Suzuki-Miyaura cross-coupling of dihydropyranyl boronates.

When using a NHC-ligated catalyst, such as Pd-PEPPSI-IPr, the mechanism is believed to proceed through a S_E mechanism, possibly through a fast reductive elimination caused by the electron-rich and bulky catalyst as proposed by the Organ group (Chapter 3, Section 3.9, Scheme 3-15).[2d] Although the des(2-ethoxy) dihydropyranyl boronate **3-51** has demonstrated good selectivity to form α-regioisomers using NHC-ligated catalysts, these catalysts were not efficient in producing α-coupled products when using **4-4**. The α-selectivity may be a result of the NHC-ligated catalyst's poor ability to form the π-allyl intermediate, due to the bulkiness of the ligand, as demonstrated when using the Pd-PEPPSI-IPent catalyst (Section 4.3, Table 4-1, entry 10),

where the α-coupled isomer formed at a regioselectivity comparable to the phosphine-ligated catalyst (Section 4.3, Table 4-1, entries 1 and 11). The poor yield, on the other hand, may be a result of the catalyst's bulkiness, disfavoring the transmetallation as a result of the catalyst's difficulty to coordinate to the boron-species.

4.6 Utilizing the regiodivergent and stereospecific Suzuki-Miyaura cross-coupling reaction towards the synthesis of bioactive natural products

In order to demonstrate the utility of the allylic Suzuki-Miyaura cross-coupling reaction, various biologically-relevant compounds were investigated to determine whether they were suitable examples for synthesis utilizing the allylic Suzuki-Miyaura cross-coupling reaction. Potential target compounds required a 2,4- or 2,6-functionalized pyran motif that contains either an aryl or alkenyl group. Since goniothalesdiol A and diospongin B both exhibit these structural characteristics, efforts were made toward the synthesis of these natural products (Figure 4-5).

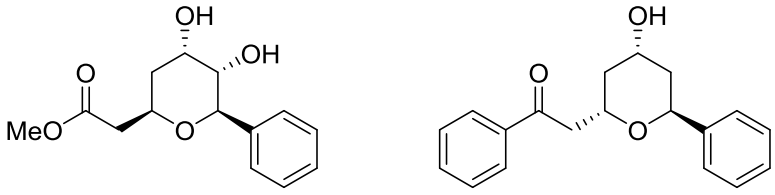

goniothalesdiol A **diospongin B**

Figure 4-5: Chosen synthetic targets accessible using the allylic cross-coupling method.

4.6.1 Synthetic efforts towards the synthesis of goniothalesdiol A

In 2006, goniothalesdiol A was isolated from a southern Taiwanese tree, *Goniothalamus amuyon*.[8] Although this compound does not appear to exhibit any biological activity, it has been a target of synthetic interest on numerous occasions.[9] One of the shortest synthetic routes in forming goniothalesdiol A was achieved by She and co-workers, which featured a protecting-

group-free reaction pathway and a silyl-Prins cyclization as the key reaction step (Scheme 4-6). The synthetic route began with the optically pure *R*-epichlorohydrin **4-12**,[9b] which was regioselectively opened using with the trimethysilyl acetylide to afford **4-13** with a 96% yield. Trans-hydrogenation of alkene **4-13** using DIBAL-H formed the *Z*-alkenyltrimethylsilyl in the presence of intermediate **4-14** followed by alkylation using orthothioformate to form **4-15** with a 60% yield over two steps. After a subsequent conversion of the orthothioester of **4-15** to form the methyl ester **4-16**, an indium(III)-catalyzed Prins reaction afforded the dihydropyran **4-17** with a 58% yield over two steps. The target natural product was obtained after a diastereoselective Upjohn dihydroxylation with a 92% yield. Although this protecting-group-free reaction pathway was efficient in forming goniothalesdiol A in only six steps with an overall yield of 30%, the pratical value of this synthesis, however, is diminished by the use of toxic and expensive *R*-epichlorohydrin as a starting material.

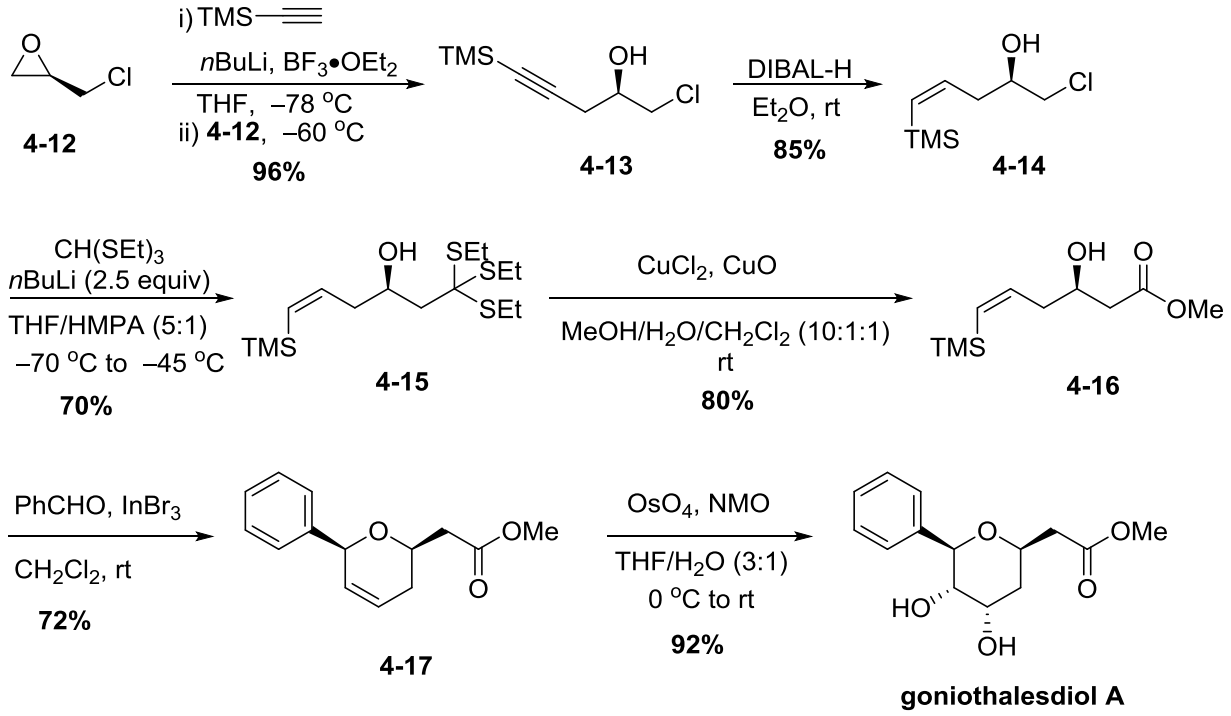

Scheme 4-5: Protecting-group-free total synthesis of goniothalesdiol A.[9b]

Another short synthesis of goniothalesdiol A was achieved by Bandichhor and co-workers, where 2-deoxy-D-ribose was used as the starting material (Scheme 4-7).[9e] Using the 2-deoxy-D-ribose the authors performed a Brønsted acid-catalyzed acetonide protection to form **4-18** with a 90% yield.[9e] Afterwards, the pyran ring was opened through a Wittig olefination to form **4-19** with a 66% yield.[9e] The primary alcohol of **4-19** was oxidized under Swern conditions followed by a diastereoselective (4.5:1 dr) Grignard reaction to form **4-21** with a 63% yield over two steps.[9e] Based on the stereochemical outcome of the Grignard reaction, the mechanism may have followed a polar Felkin-Ahn model, where the phenylmagnesium bromide nucleophile approaches the aldehyde **4-20** antarafacial to the alpha ketal-protected alcohol. Afterwards, a cross-metathesis (CM) between methyl acrylate and the alkenyl group of **4-21** using the Grubbs second generation catalyst to afford the α,β-unsaturated methyl ester **4-22** with a 97% yield.[9e] Lastly, **4-22** was subjected to a highly diastereoselective Michael addition catalyzed by *p*TsOH followed by deprotection of goniothalesdiol with a 86% yield over two steps.[9e] Currently this reaction pathway is the most concise synthesis of goniothalesdiol A, which consists of six steps with an overall yield of 31%. Although this synthetic pathway – unlike the route proposed by the She group (Scheme 4-6) – began with a non-toxic and less expensive starting material, there are several inefficient reaction steps. The Grignard reaction displayed a low diastereoselectivity, forming **4-21** at a moderate yield. Lastly, the CM reaction required excess methyl acrylate.

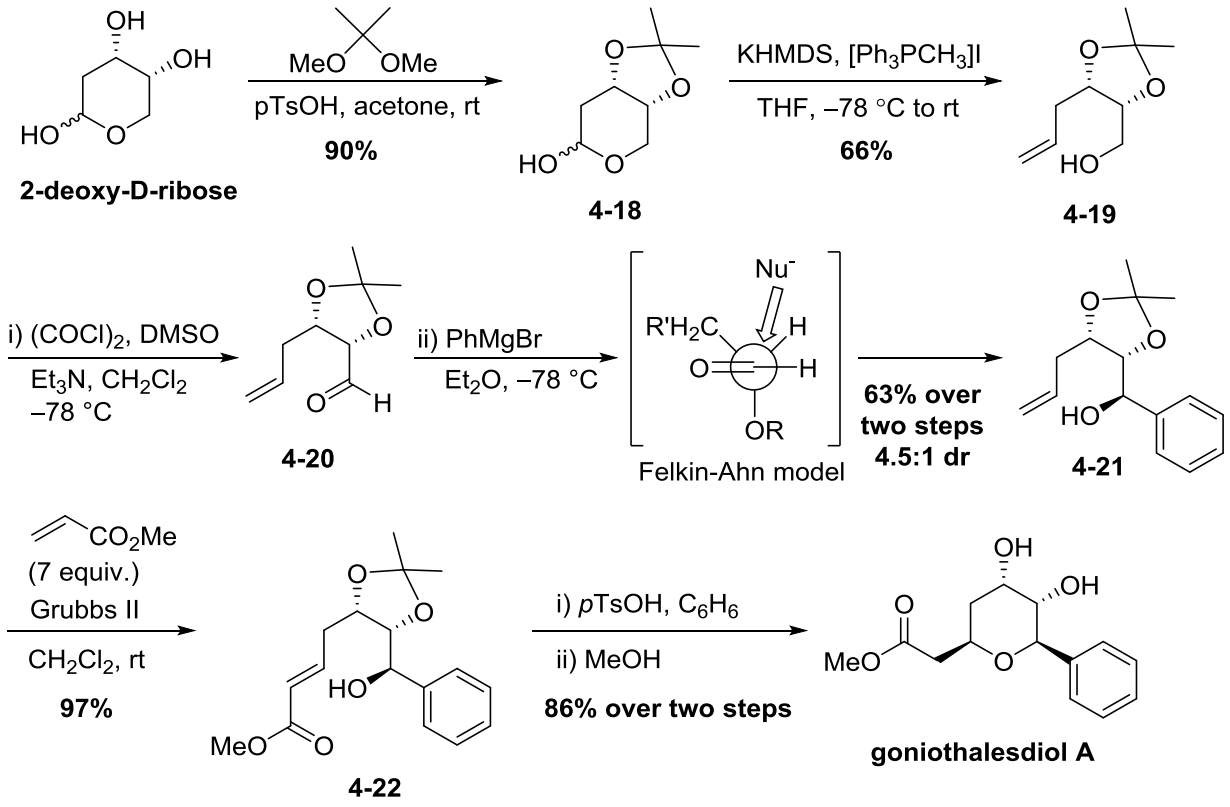

Scheme 4-6: Short synthesis of goniothalesdiol A from 2-deoxy-D-ribose.

Based on the toxicity of the reagents used in the aforementioned total synthesis of goniothalesdiol A, as well the convenient in-house synthesis of optically enriched aryl-substituted dihydropyrans within the Hall group, the allylic cross-coupling reaction was believed to be an efficient and concise access to this natural product. The retrosynthetic pathway proposed involved the synthesis of **4-23** through a late-stage insertion of the methyl ester group involving a Mukaiyama aldol-type reaction of **4-24** followed by isomerization to form the natural product (Scheme 4-8). The *trans* diol would be installed onto the phenyl-derivative **4-6c** through an Upjohn dihydroxylation to produce goniothalesdiol A. Fortunately, the starting material required for the proposed synthetic pathway, **4-6c**, can be accessed through the allylic Suzuki-Miyaura cross-coupling reaction with a good yield and high regioselectivity and diastereoselectivity.

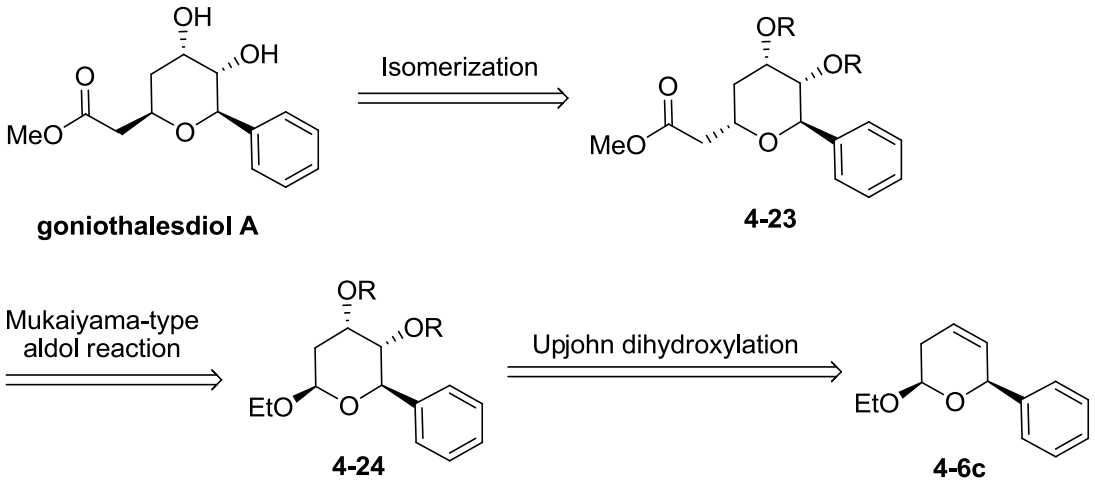

Scheme 4-7: Retrosynthetic analysis of goniothalesdiol A.

The synthesis of goniothalesdiol A began with the scale-up preparation of the starting material **4-6c** (Scheme 4-9), which afforded this product with a 78% yield and high regio- and diastereoselectivity (7:93 α:γ; 97.5:2.5 dr). The diastereoselectivity was measured after the Upjohn dihydroxylation of the *cis*-2,6-substituted dihydropyran, giving the *trans*-diol **4-10** with a 75% yield. Because there was no certainty to which protecting group would be stable under the Lewis acidic conditions of the Mukaiyama-type aldol reaction, several diol-protected derivatives were synthesized. Using 2,2-dimethoxy propane and *p*-toluenesulfonic acid at 40 ^{o}C, the acetonide-protected diol **4-25** was formed with a 87% yield. Afterwards, using acetic anhydride and DMAP, **4-26** was produced with a 86% yield. The silylation of **4-10** using TBSCl and imidazole in CH_2Cl_2 afforded the protected diol **4-27** with a quantitative yield. Lastly, the dibenzyl-protected product **4-28** was obtained with a 88% yield using sodium hydride and benzylbromide in THF.

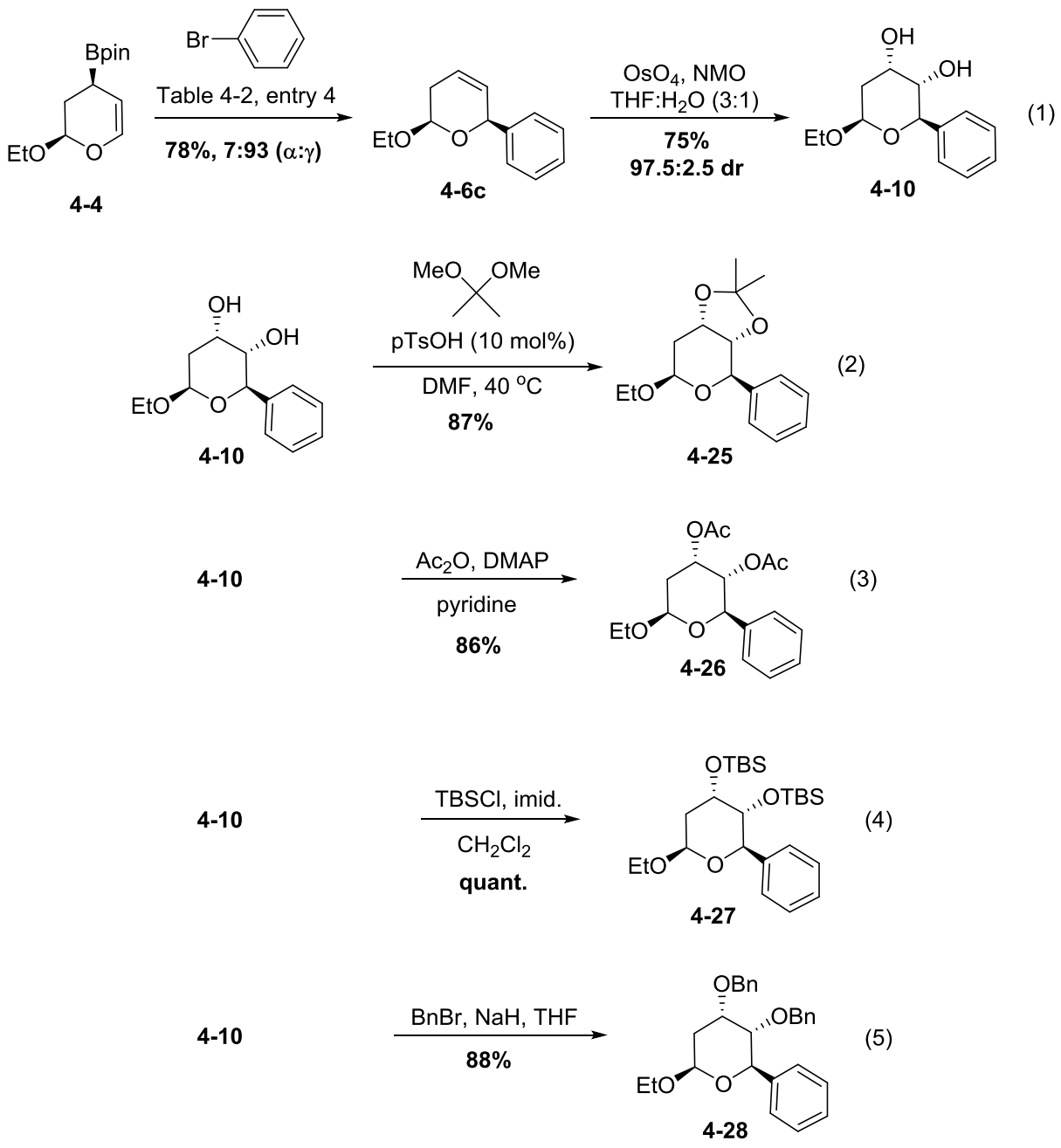

Scheme 4-8: Synthesis and protection of diol **4-10.**

After synthesizing the silyl enol ether **4-29** from methyl acetate, several Lewis acids typically used to promote the Mukaiyama-type aldol reaction were tested (Scheme 4-10). Below –10 °C, the typical Lewis acids used, BF_3•OEt_2 or TMSOTf, did not promote any reactivity. Furthermore, when replacing these reagents with $SnCl_4$, or just using excess amounts of Lewis acids, the

starting materials **4-25** to **4-28** would not react. Interchanging between the two aprotic solvents, typically used in a Mukaiyama-type aldol reaction, with either of the Lewis acids tested also had no improvement in the reactivity. Upon increasing the temperature to 0 ^{o}C or rt, either full recovery of starting material or decomposition would occur. The Lewis acid used might have had poor chemoselectivity, where the silyl enol ether **4-29** was targeted and decomposed into methyl acetate. Consequently, compounds **4-25** to **4-28** could not react with **4-29** to form analogues of **4-23**. The pyran substrates might also exist in an unfavorable conformation, thereby preventing the oxocarbenium intermediate to be generated. After efforts toward the synthesis of goniothalesdiol A were exhausted, the synthesis of diospongin B was investigated.

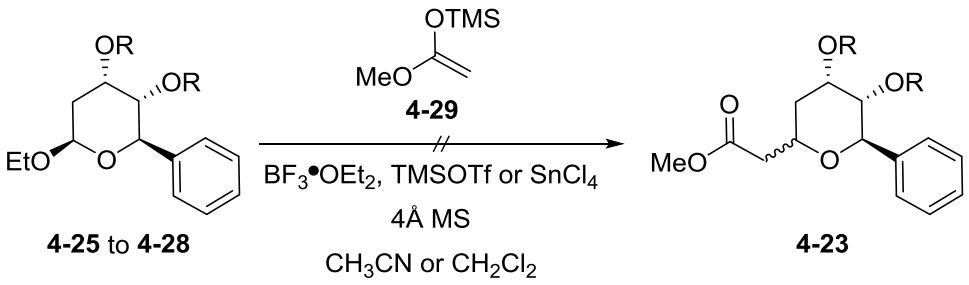

Scheme 4-9: Screening of various Lewis acids for the Mukaiyama-type aldol reaction.

4.6.2 Total synthesis and stereochemical assessment of diospongin B

Based on the structural similarities to goniothalesdiol A, diospongin B was chosen as an alternate synthetic target to demonstrate the applicability of the allylic Suzuki-Miyaura cross-coupling reaction. Diospongin B, a diarylheptanoid natural product that was extracted from rhizomes of *Dioscorea spongiosa* in 2004 by Kadota and co-workers.[10] Initial testing of the water extract of the plant revealed that osteoblast cell proliferation as well as inhibition of osteoclast cells occurred, which confirmed by the Kadota group that diospongin B displayed potent antiosteoporotic activity.[10]

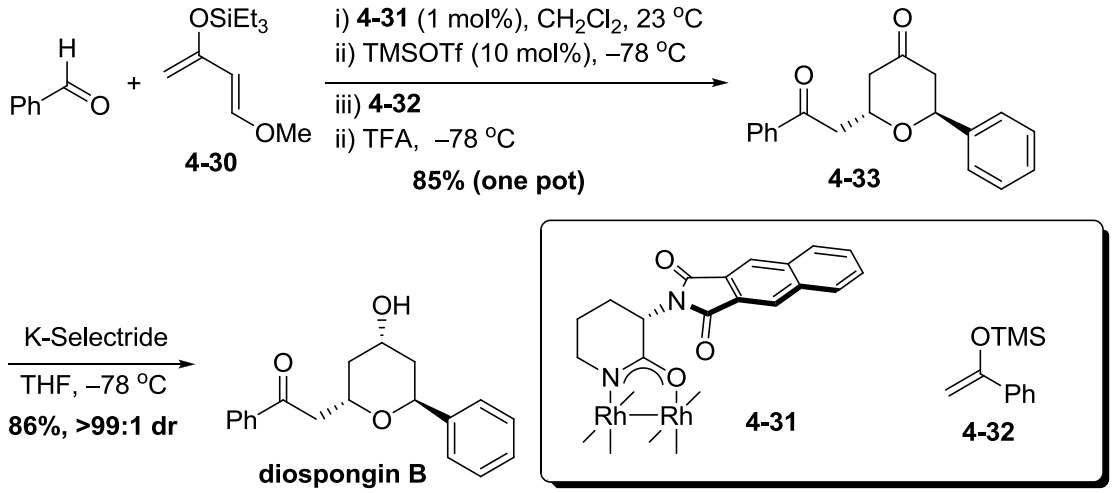

Scheme 4-10: Total synthesis of diospongin B by Hashimoto and co-workers.[11]

The shortest route towards diospongin B was achieved by Hashimoto and co-workers.[11] It began with the one-pot sequential asymmetric HDA reaction followed by a Mukaiyama–Michael reaction (Scheme 4-11). This step efficiently afforded **4-33** with a 85% yield and 95% *ee*. The first step in this process featured the asymmetric Diels-Alder reaction between benzaldehyde and the Danishefsky-type diene **4-30** using chiral Lewis acidic dirhodium(II) complex **4-31** at a low catalyst loading (1 mol%). Diketone **4-33** was then obtained upon addition of the silyl enol ether **4-32** in the presence of TMSOTf and TFA. Lastly, **4-33** was subjected to a chemoselective and diastereoselective reduction using K-Selectride to afford synthetic diospongin B with a 86% yield.

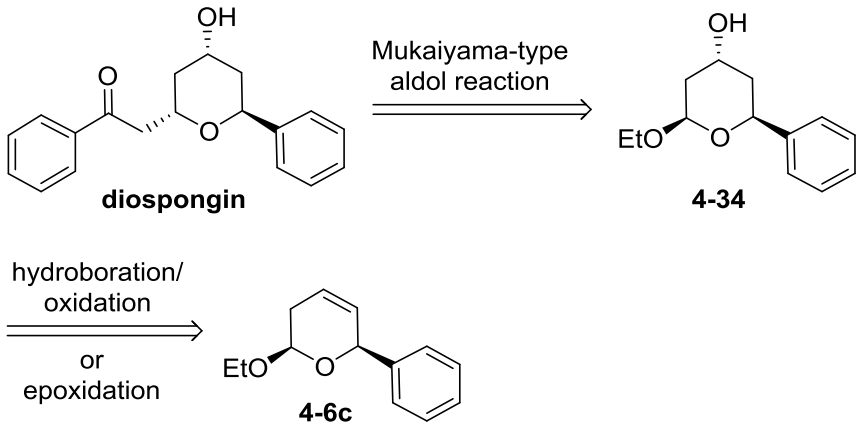

Scheme 4-11: Retrosynthetic analysis of diospongin B.

The retrosynthetic strategy proposed involves a short and concise route to diospongin B utilizing a Mukaiyama-type aldol addition onto the *in*-situ-generated oxocarbenium species of **4-34** (Scheme 4-12). This *trans*-alcohol **4-34** could be accessed from **4-6c** through a diastereoselective hydroboration-oxidation reaction. As an alternate method of forming **4-34** would be a substrate-controlled diastereoselective epoxidation followed by regioselective ring opening. Once more, the efficient scale-up preparation of **4-6c** would provide a suitable starting material towards the natural product.

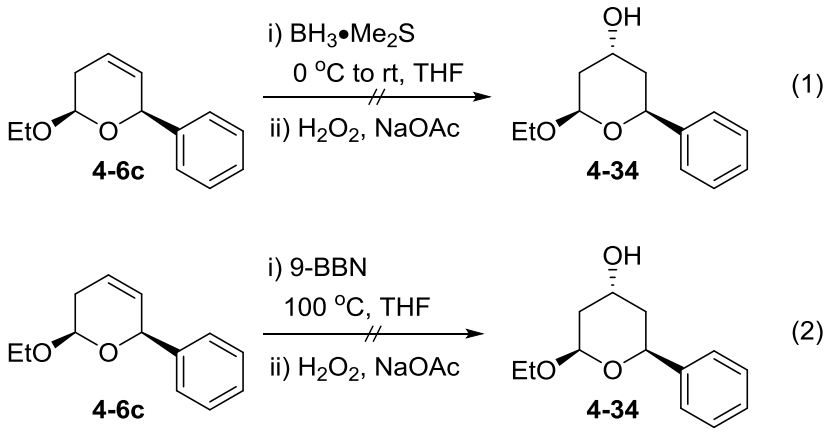

Scheme 4-12: Efforts toward the synthesis of **4-34** through hydroboration/oxidation.

With the substrate **4-6c** previously in hand, the diastereoselective formation of the alcohol at the C3-position was investigated, which would be positioned *trans* to the phenyl and ethoxy groups. Initial efforts to install the desired alcohol involved hydroboration followed by oxidation (Scheme 4-13). Since the hydroboration/oxidation step using BH_3•Me_2S followed by hydrogen peroxide treatment under basic conditions only returned complex mixtures. Controlling the selectivity using the larger reagent, 9-BBN, did not lead to any product even after raising the temperature above ambient conditions. Consequently, a diastereoselective epoxidation followed by a selective ring opening using a suitable reducing reagent was investigated. The initial epoxidation of **4-6c** using *m*CPBA in CH_2Cl_2 afforded the epoxide **4-35** with a 50% yield and low selectivity (4:1 dr). By switching the solvent from CH_2Cl_2 to $CHCl_3$, both the yield (74%) and diastereoselectivity (10:1 dr) improved significantly. The strategy of switching to a more chlorinated solvent has been exploited on numerous occasions to improve the diastereoselective epoxidation of polyfunctionalized dihydropyrans.[12,13] With the optimized conditions in hand, a scale-up preparation of **4-6c** afforded the desired product with a 93% yield (1.2 g, 6.0 mmol) with high regio- and diastereoselectivity (7:93 α:γ; 97.5:2.5 dr) (Scheme 4-14). Afterwards, using $CHCl_3$ as the solvent, the selective epoxidation using *m*CPBA afforded the epoxide **4-35** selectivly (13:1 dr) with a 70% yield. The relative stereochemistry of the insertion of the epoxide group onto **4-6c** was confirmed by the X-ray crystallographic data of **4-35** depicted in Scheme 4-10. The diastereoselectivity of the reaction is likely a result of the epoxide forming on the less sterically congested face of the dihydropyran. From **4-35**, a selective epoxide ring opening using DIBAL-H afforded the desired alcohol **4-34** with a 83% yield. The regioselective reductive ring opening of the epoxide in **4-35** may be a promoted by the preference for the lower energy chair-like transition state.

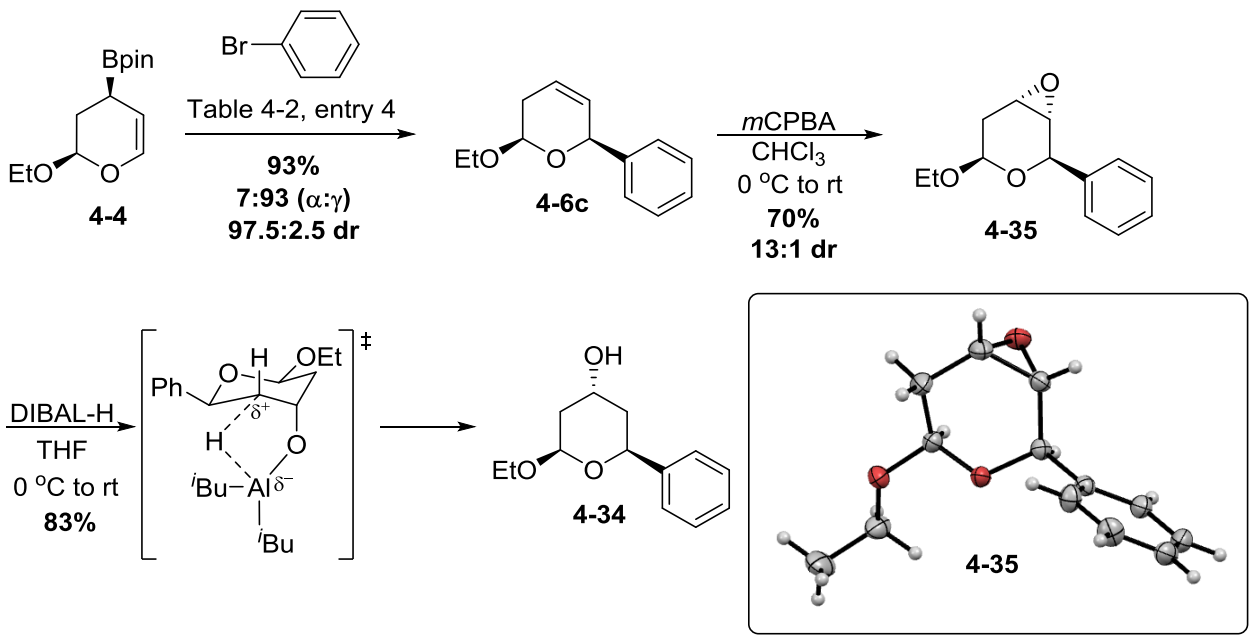

Scheme 4-13: Scale-up allylic cross-coupling toward the synthesis of alcohol **4-34**.

To avoid potential side reactions that may occur when exposing the free alcohol **4-34** under the Lewis acidic conditions of the Mukaiyama-type aldol reaction, the hydroxyl group was protected. The benzylation of **4-34** was chosen since these substrates are known to favor the formation of 2,4-*trans* products in the nucleophilic addition onto oxocarbenium species as examined by the Woerpel group.[3] Thus, **4-34** was subject to benzylation using sodium hydride and BnBr to form the benzyl ether **4-36** at a 75% yield (Scheme 4-15, Equation 1). The alcohol **4-34** was also subjected to triethylsilyl protection, because a similar silyl ether substrate was employed in a Mukaiyama-type aldol reaction toward the synthesis of diospongin B.[14] The silyl protection using chlorotriethylsilane (TESCl) afforded **4-37** with a 87% yield (Scheme 4-15).

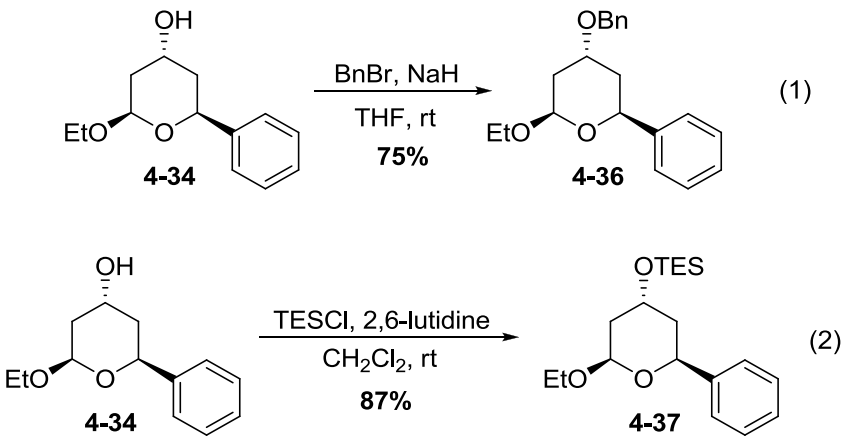

Scheme 4-14: Protection of the alcohol **4-34**.

The 2-ethoxypyran **4-37** and **4-38** were exposed to various Lewis acidic conditions to promote the Mukaiyama-type aldol addition onto the *in situ*-generated oxocarbenium species. Although the Lewis acids BF_3•OEt_2 and TMSOTf could not induce any reactivity, the reaction readily proceeded using $SnCl_4$ to give benzyl-protected 2,6-trans product **4-38** with a 79% yield (Scheme 4-16, Equation 1). Unfortunately, the benzyl protecting group could not be selectively removed under hydrogenolysis or under Lewis acidic conditions, instead resulting in the decomposition of the starting material. Using the TES-protected substrate **4-37**, however the desired 2,6-*trans* product was obtained using $SnCl_4$ and, after a final deprotection of the crude TES ether using the HF•pyridine complex, synthetic diospongin B was obtained with a 66% yield over two steps (Scheme 4-16, Equation 2). The stereoselectivity can be rationalized by the nucleophilic addition onto the favored chair-like transition state proposed by Woerpel,[3] and is supported by previous efforts by Jennings and co-workers toward the synthesis of diospongin B.[14]

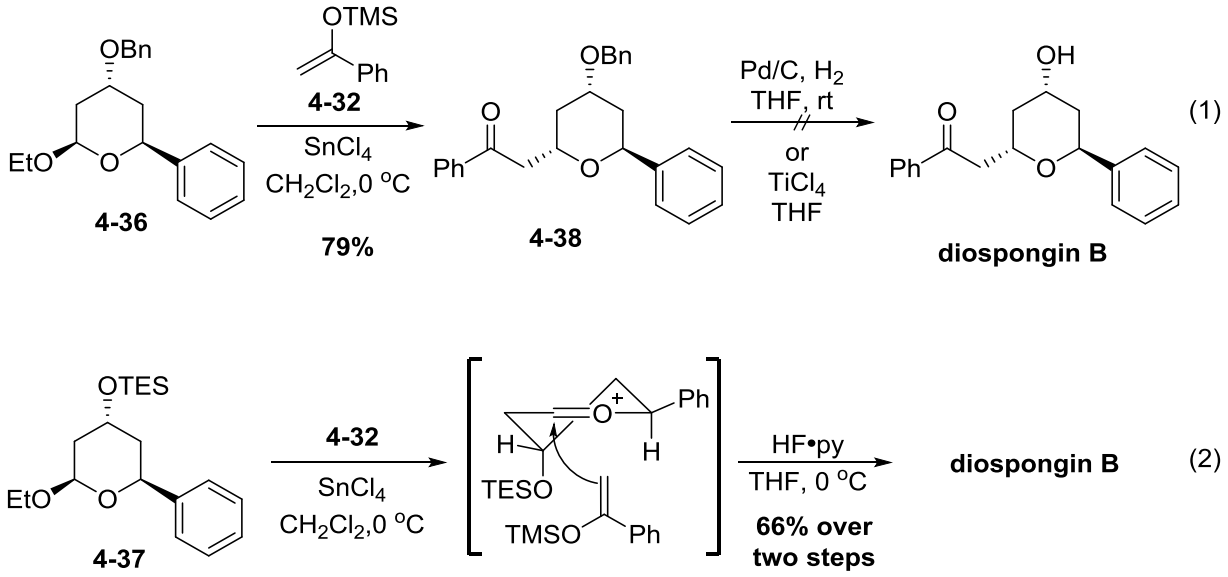

Scheme 4-15: Synthesis of diospongin B.

The spectroscopic data, such as ^{1}H and ^{13}C NMR (Section 4.8.4), IR, and HRMS, of the synthetic diospongin B were consistent with those reported for natural diospongin B.[10,11] Surprisingly, when comparing the characterization data of a sample of synthetic diospongin B with the isolated natural product originally reported by Kadota and co-workers, the sign of optical rotation of synthetic diospongin B $[\alpha]^{20}_{D}$ = +22.8 (*c* 0.70, $CHCl_3$) was opposite to that of the natural product $[\alpha]^{25}_{D}$ = –23.4 (*c* 0.60, $CHCl_3$) (Scheme 4-17).[10] Furthermore, almost all previously reported syntheses of diospongin B supported Kadota's assignment for the sign of optical rotation.[14,15] Since the configurational assignment of the allylboronate **4-4** is well documented from many previous syntheses of natural products within the Hall group, there was no doubt that there was a discrepancy in the previous reports with respect for the sign of optical rotation.[16] Furthermore, the spectral and X-ray crystallographic analysis of the derivitized cross-coupling products **4-8** to **4-10** as well as the epoxide intermediate **4-35** supported the stereochemical assignment for the hydroxyl group of diospongin B. In the end, the detailed investigation made by Hashimoto and co-workers in 2010, during their asymmetric synthesis of

diospongin B, confirmed that their recorded optical rotation was $[\alpha]^{22}_{D}$ = +22.3 (*c* 0.62, $CHCl_3$) and that the sign of optical rotation originally reported by Kadota and co-workers was erroneous.[11] Furthermore, since it was known that diospongin B can be converted into diospongin A under acidic conditions, the Hashimoto group synthesized diospongin A with a 89% yield using a mixture of 30% aqueous HCl and THF (Scheme 4-17). When comparing the spectral properties of the synthetic versus the natural diospongin A, the optical rotation obtained from the Hashimoto group, $[\alpha]^{23}_{D}$ = –21.1 (*c* 0.84, $CHCl_3$), had the correct sign and nearly the same value to the recorded data made by the Kadota group, $[\alpha]^{25}_{D}$ = –21.2 (*c* 0.80, $CHCl_3$). Furthermore, a corrigendum was made by the Kadota group supporting that the diospongin B, which was originally reported, had a positive sign in optical rotation.[10,11] These results removed any remaining doubt about the absolute stereochemistry of the synthetic natural product.

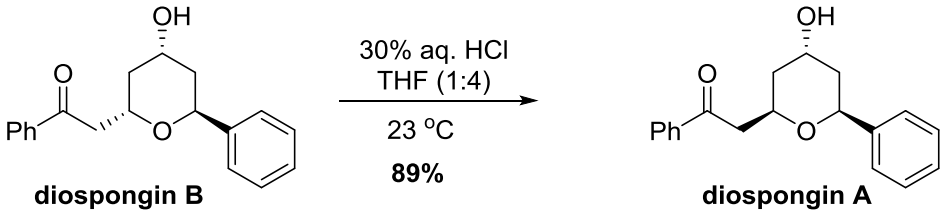

diospongin B **diospongin A**

Hall: $[\alpha]^{20}_{D}$ = +22.8 (c 0.70, $CHCl_3$)

Kadota[10]: $[\alpha]^{25}_{D}$ = –23.4 (corr. +23.4) (c 0.60, $CHCl_3$)

Hashimoto[11]: $[\alpha]^{22}_{D}$ = +22.3 (c 0.62, CHCl3)

Hashimoto: $[\alpha]^{23}_{D}$ = –21.1 (*c* 0.84, $CHCl_3$)

Kadota[10]: $[\alpha]^{25}_{D}$ = –21.2 (*c* 0.80, CHCl3)

Scheme 4-16: Synthesis of diospongin A from diospongin B and optical rotation data by Hashimoto and co-workers.[11]

4.7 Summary

In conclusion, the ligand-controlled stereospecific and regiodivergent Suzuki-Miyaura cross-coupling of heterocyclic allylboronates was applicable to the 2-ethoxy dihydropyranyl boronate substrate **4-4**, derived from a catalytic enantioselective inverse-electron demand oxa-[4+2] cycloaddition. This method was systematically optimized for substrate **4-4**, and a scope similar to the des(2-ethoxy) analog **3-51** was demonstrated with a representative set of aryl and alkenyl bromides. Both α- and γ-isomers can be obtained independently with high regio- and stereospecificity. Through advanced NMR techniques and X-ray crystallographic analyses, the coupling mechanism was determined to proceed with an overall retention of stereochemistry. This method was then applied to a concise synthesis of diospongin B. Furthermore, given the numerous discrepancies in the stereochemistry of the natural product reported in the literature, the stereochemical assignment of diospongin B was confirmed by comparing data in this study with the Hashimoto group as well as analyzing the precursors synthesized toward the natural product.

4.8 Experimental

4.8.1 General information

Catalyst **4-3** was prepared according to the procedure by Jacobsen and co-workers.[1] The chemical purity of the key substrate **4-2** is crucial in order to synthesize **4-4** in high optical purity. Boronate **4-2** was prepared according to the previous procedure from the Hall group[5] and, equipped with two Kugelrohr flasks, purified 3-4 consecutive times by Kugelrohr distillation (< 0.5 mmHg). Powdered 4A molecular sieves (<5 micron, Aldrich) were dried in an oven (300 ^{o}C) followed by flame-drying in a dry round bottom flask *in vacuo*. Compound **4-4** was synthesized

following the reported procedure of Hall and co-workers[5] with slight changes to the workup, where the celite-filtered crude product was concentrated and subjected to a silica plug (10 – 20% Et_2O/hexanes) to give **4-4** as an amber or dark brown-colored oil. Synthesis of the optically pure **4-4** was made using 3 mol % of catalyst **4-3** with 4A molecular sieves as the drying agent (77%, 95% *ee*).[5] The enantiomeric excess of **4-4** was measured on the corresponding secondary homoallylic alcohol produced from a highly diastereoselective allylboration of *p*-anisaldehyde. Synthesis of the racemic **4-4** was made using 1.5 mol % of $Yb(fod)_3$ as the catalyst and without the need for any drying agent (93%).[3] Following the reported procedures in literature, the silyl enol ethers **4-29**[17] and **4-32**[18] were synthesized.

Unless otherwise stated, all reactions were performed under a nitrogen atmosphere using flame-dried glassware. THF and dichloromethane were obtained from a MBraun MB SPS* solvent system prior to use. The anhydrous acetonitrile was purchased from Sigma-Aldrich (99.8% - purity). Unless otherwise stated, all reagents were purchased from Sigma-Aldrich and used as received. Propargylaldehyde diethyl acetal was purchased from GFS Chemicals. Commercial *β*-bromostyrene contains a mixture of *E*- and *Z*-isomer with a 8:2 ratio based on ^{1}H NMR analysis. Thin layer chromatography (TLC) was performed on Merck Silica Gel 60 F254 plates and was visualized with UV light, *p*-anisaldehyde and $KMnO_4$ stain. NMR spectra were recorded on INOVA-400, INOVA-500 or INOVA-700 MHz instruments. The residual solvent protons (^{1}H) of $CDCl_3$ (7.26 ppm) or C_6D_6 (7.15 ppm) and the solvent carbons (^{13}C) of $CDCl_3$ (77.06 ppm) were used as internal standards. ^{1}H NMR data is presented as follows: chemical shift in ppm (δ) downfield from tetramethylsilane (multiplicity, coupling constant, integration). The following abbreviations are used in reporting NMR data: s, singlet; br s, broad singlet; d, doublet; t, triplet; q, quartet; dd, doublet of doublets; ddd, doublet of doublet of doublets; dddd, doublet of doublet

of doublet of doublets; app s, apparent singlet; app ddt, apparent doublet of doublet of triplets; m, multiplet. High-resolution mass spectra (HRMS) were recorded by the University of Alberta Mass Spectrometry Services Laboratory using either electron impact (EI) or electrospray ionization (ESI) techniques. Infrared spectra were obtained on a Nicolet Magna-IR with frequencies expressed in cm^{-1}. Optical rotations were measured using a 1 mL cell with a 1 dm length on a P.E. 241 polarimeter. Melting points were determined in a capillary tube using a Gallenkamp melting point apparatus and are uncorrected. The enantiomeric excess and diastereomeric ratio for chiral compounds were determined using a HPLC Agilent instrument with Chiralcel-OD, IC, IB, or Chiralpak-AS columns as specified in the following individual procedures.

4.8.2 Experimental procedures and spectral data

<u>General procedure A</u> towards 4-substituted pyran (4-5):

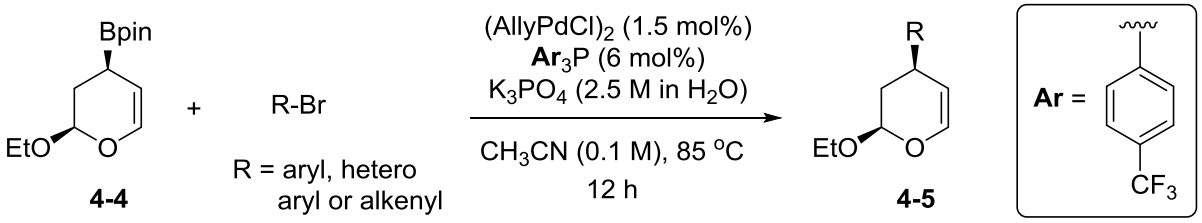

Catalyst $[(allyl)PdCl]_2$ (1.4 mg, 3.8 μmol, 1.5 mol %) and $(4\text{-}CF_3C_6H_4)_3P$ (7.3 mg, 15 μmol, 6 mol %) were added in a flamed-dried reaction tube, which was then flushed with nitrogen. The dry acetonitrile (0.2 mL) was added and the mixture was stirred for 15 minutes. Allylboronic acid pinacol ester **4-4** (76 mg, 0.30 mmol, 1.2 equiv) was added via syringe, which was washed four times with dry acetonitrile (4 × 0.2 mL). The organobromide substrate (0.25 mmol, 1 equiv) was added followed by aqueous K_3PO_4 solution (2.5 M in H_2O, 0.5 mL, 4 equiv). The resulting reaction mixture was allowed to stir under nitrogen at 85 °C for 12 h. The mixture was allowed

to cool down to room temperature, filtered through a short pad of silica and rinsed with Et_2O (20 mL). The solvents were then evaporated to yield a crude oil, which was subjected to flash chromatography to afford the 4-substituted pyran product **4-5** as the major regioisomer.

General procedure B towards 6-substituted pyran (4-6):

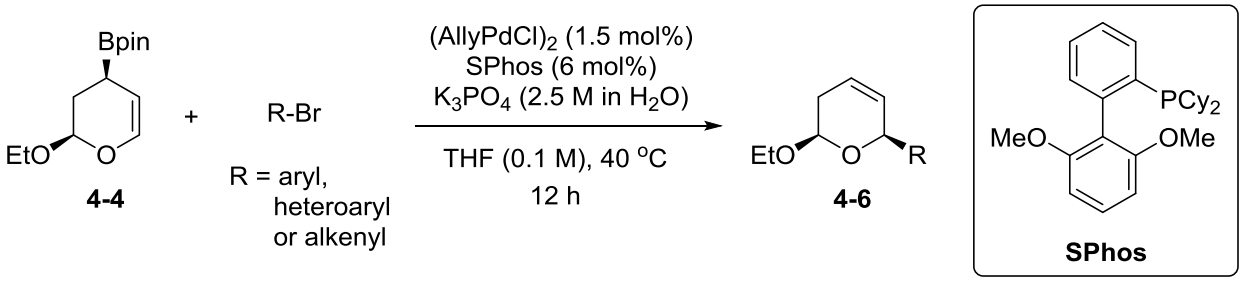

Catalyst $[(allyl)PdCl]_2$ (1.4 mg, 3.8 μmol, 1.5 mol %) and SPhos (6.3 mg, 15 μmol, 6 mol %) were added in a flamed-dried reaction tube, which was then flushed with nitrogen. Dry THF (0.2 mL) was added and the mixture was stirred for 15 minutes. Allylboronic acid pinacol ester **4-4** (76 mg, 0.30 mmol, 1.2 equiv) was added via syringe, which was washed four times with dry THF (4 × 0.2 mL). The organobromide substrate (0.25 mmol, 1 equiv) was added followed by aqueous K_3PO_4 solution (2.5 M in H_2O, 0.5 mL, 4 equiv). The resulting reaction mixture was allowed to stir under nitrogen at 40 °C for 12 h. The mixture was allowed to cool down to room temperature, filtered through a short pad of silica and rinsed with Et_2O (20 mL). The solvents were then evaporated to yield a crude oil, which was subjected to flash chromatography to afford the 6-substituted pyran product as the major regioisomer.

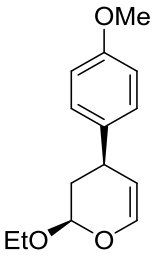

(2*R*,4*R*)-2-Ethoxy-4-(4-methoxyphenyl)-3,4-dihydro-2*H*-pyran (4-5a)

By following the general procedure A, the title compound **4-5a** was synthesized from **4-4** and 4-bromoanisole. The crude sample, containing **4-5a** in a 83 : 17 mixture of regioisomers, was subjected to flash chromatography on silica gel (5% Et_2O/hexanes) to afford the title compound (43 mg, 73%).

Clear oil; R_f = 0.44 (20% Et_2O/hexanes).

$[\alpha]^{20}_D$ +42.6 (*c* 0.310, $CHCl_3$).

^{1}H NMR (500 MHz, $CDCl_3$) δ 7.17–7.13 (m, 2 H), 6.86–6.82 (m, 2 H), 6.42 (dd, *J* = 6.1, 2.3 Hz, 1 H), 5.03 (dd, *J* = 9.2, 2.0 Hz, 1 H), 4.72 (ddd, *J* = 6.0, 2.0, 2.0 Hz, 1 H), 3.95 (dq, *J* = 9.5, 7.1 Hz, 1 H), 3.79 (s, 3 H), 3.65–3.55 (m, 2 H), 2.22 (dddd, *J* = 13.2, 6.5, 1.7, 1.5 Hz, 1 H), 1.85 (ddd, *J* = 13.2, 10.8, 9.2 Hz, 1 H), 1.25 (t, *J* = 7.1 Hz, 3 H).

^{13}C NMR (126 MHz, $CDCl_3$) δ 158.3, 142.1, 136.6, 128.2, 113.9, 105.5, 99.6, 64.4, 55.3, 38.1, 37.1, 15.2.

IR (Microscope, cm^{-1}) 3060, 2975, 2930, 1644, 1611, 1512, 1250.

HRMS (ESI-TOF) for $C_{14}H_{18}NaO_3$ $(M + Na)^+$: calcd. 257.1148; found 257.1145.

HPLC (Chiralcel IC): 1:99 *i*-PrOH/hexane, 0°C, 0.3 mL/minute, λ = 230 nm, t_{major} = 21.1 min, t_{minor} = 15.5 min, dr = 97.5:2.5.

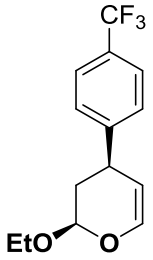

(2*R*,4*R*)-2-Ethoxy-4-[4-(trifluoromethyl)phenyl]-3,4-dihydro-2*H*-pyran (4-5b)

By following the general procedure A, the title compound **4-5b** was synthesized from **4-4** and 4-bromobenzotrifluoride. The crude sample, containing **4-5b** in a 93 : 7 mixture of regioisomers, was subjected to flash chromatography on silica gel (2.5% Et_2O/hexanes) to afford the title compound (52 mg, 76%).

Clear oil; R_f = 0.56 (10% Et_2O/hexanes).

$[\alpha]^{20}_D$ +19.1 (*c* 0.890, $CHCl_3$).

^{1}H NMR (500 MHz, $CDCl_3$) δ 7.55 (d, *J* = 8.2 Hz, 2 H), 7.36 (d, *J* = 8.1 Hz, 2 H), 6.48 (dd, *J* = 6.2, 2.2 Hz, 1 H), 5.06 (dd, *J* = 8.5, 2.1 Hz, 1 H), 4.75 (ddd, *J* = 6.2, 2.3, 1.5 Hz, 1 H), 3.94 (dq, *J* = 9.5, 7.1 Hz, 1 H), 3.68 (dddd, *J* = 10.4, 7.0, 2.2, 2.0 Hz, 1 H), 3.59 (dq, *J* = 9.5, 7.1 Hz, 1 H), 2.27 (dddd, *J* = 13.1, 6.6, 2.0, 1.7 Hz, 1 H), 1.89 (ddd, *J* = 13.3, 10.0, 8.6 Hz, 1 H), 1.22 (t, *J* = 7.1 Hz, 3 H).

^{13}C NMR (126 MHz, $CDCl_3$) δ 148.7, 142.8, 127.7, 125.5, 125.5, 125.4, 125.4, 103.9, 99.0, 64.4, 37.4, 15.2.

IR (microscope, cm^{-1}) 2978, 2932, 2875, 1645, 1619, 1326, 1125.

HRMS (EI) for $C_{14}H_{15}F_3O_2$ $(M)^+$: calcd. 272.1024; found 272.1020.

HPLC (Chiralpak AS): 1:99 *i*-PrOH/hexanes, 0°C, 0.3 mL/minute, λ = 230 nm, t_{major} = 13.0 min, t_{minor} = 14.1 min, dr = 97:3.

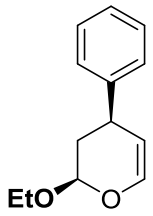

(2*R*,4*R*)-2-Ethoxy-4-phenyl-3,4-dihydro-2*H*-pyran (4-5c)

By following the general procedure A, the title compound **4-5c** was synthesized from **4-4** and bromobenzene. The crude sample, containing **4-5c** in a 84 : 16 mixture of regioisomers, was subjected to flash chromatography on silica gel (5% Et_2O/hexanes) to afford the title compound (30 mg, 59%).

Clear oil; R_f = 0.51 (20% Et_2O/hexanes).

$[\alpha]^{20}_{D}$ +33.5 (*c* 0.300, $CHCl_3$).

^{1}H NMR (500 MHz, $CDCl_3$) δ 7.32–7.29 (m, 2 H), 7.26–7.20 (m, 3 H), 6.45 (dd, *J* = 6.2, 2.3 Hz, 1 H), 5.06 (dd, *J* = 9.2, 2.0 Hz, 1 H), 4.76 (ddd, *J* = 6.1, 2.0, 2.0 Hz, 1 H), 3.96 (dq, *J* = 9.5, 7.1 Hz, 1 H), 3.67–3.57 (m, 2 H), 2.26 (dddd, *J* = 13.1, 6.2, 2.0, 1.7 Hz, 1 H), 1.90 (ddd, *J* = 13.2, 10.9, 9.2 Hz, 1 H), 1.25 (t, *J* = 7.1 Hz, 3 H).

^{13}C NMR (126 MHz, $CDCl_3$) δ 144.5, 142.3, 128.5, 127.2, 126.5, 105.0, 99.6, 64.4, 37.91, 15.2.

IR (microscope, cm^{-1}) 3061, 2976, 2930, 2871, 1643, 1234, 1099, 1031.

HRMS (EI) for $C_{13}H_{16}O_2$ $(M)^+$: calcd. 204.1150; found 204.1150; Diastereomeric ratio of compound **4-5c** could not be determined directly due to a difficult HPLC separation. See **Section 4.8.3** for dr determination of **4-8**, synthesized *via* hydroboration/oxidation of **4-5c.**

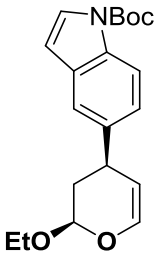

***tert*-Butyl 5-[(2*R*,4*R*)-2-ethoxy-3,4-dihydro-2*H*-pyran-4-yl]-1*H*-indole-1-carboxylate (4-5d)**

By following the general procedure A, the title compound **4-5d** was synthesized from **4-4** and *N*-boc-5-bromoindole. The crude sample, containing **4-5d** in a 90 : 10 mixture of regioisomers, was subjected to flash chromatography on silica gel (2.5 – 5% Et_2O/hexanes) to afford the title compound (68 mg, 79%).

Clear oil; R_f = 0.43 (10% Et_2O/hexanes).

$[\alpha]^{20}_D$ +26.6 (*c* 2.44, $CHCl_3$).

^{1}H NMR (500 MHz, $CDCl_3$) δ 8.07 (br s, 1 H), 7.55 (d, *J* = 3.5 Hz, 1 H), 7.48 (d, *J* = 8.1 Hz, 1 H), 7.12 (dd, *J* = 8.1, 1.5 Hz, 1 H), 6.52 (dd, *J* = 3.7, 0.5 Hz, 1 H), 6.47 (dd, *J* = 6.1, 2.3 Hz, 1 H), 5.07 (dd, *J* = 9.2, 1.9 Hz, 1 H), 4.83 (ddd, *J* = 6.3, 2.0, 2,0 Hz, 1 H), 3.97 (dq, *J* = 9.5, 7.1 Hz, 1 H), 3.77 (dddd, *J* = 10.9, 6.3, 2.2, 2.0 Hz, 1 H), 3.62 (dq, *J* = 9.5, 7.1 Hz, 1 H), 2.31 (dddd, *J* = 13.2, 6.5, 1.6, 1.6 Hz, 1 H), 1.95 (ddd, *J* = 13.2, 10.9, 9.3 Hz, 1 H), 1.67 (s, 9 H), 1.25 (t, *J* = 7.1 Hz, 3 H).

^{13}C NMR (100 MHz, $CDCl_3$) δ 149.8, 142.2, 141.0, 135.5, 129.2, 125.8, 122.2, 120.8, 113.9, 107.1, 105.5, 99.7, 83.6, 64.4, 38.5, 38.4, 28.2, 15.2.

IR (microscope, cm^{-1}) 2961, 2928, 2858, 1735, 1643, 1440, 1343, 1147.

HRMS (ESI-TOF) for $C_{20}H_{25}NaO_4$ $(M + Na)^+$: calcd. 366.1676; found 361.1672, for $C_{20}H_{29}N_2O_4$ $(M + NH_4)^+$: calcd. 361.2122; found 361.2117.

HPLC (Chiralcel OD): 0.5:99.5 to 1:99 *i*-PrOH/hexane, 5°C, 0.5 mL/minute, λ = 230 nm, t_{major} = 11.9 min, t_{minor} = 21.6 min, dr = 97.5:2.5.

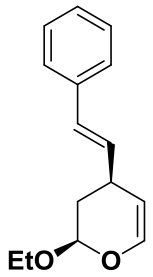

(2*R*,4*S*)-2-Ethoxy-4-[(*E*)-2-phenylvinyl]-3,4-dihydro-2*H*-pyran (4-5e)

By following the general procedure A, the title compound **4-5e** was synthesized from **4-4** and *β*-bromostyrene. The crude sample, containing **4-5e** in a 91 : 9 mixture of regioisomers, was subjected to flash chromatography on silica gel (2.5% Et_2O/hexanes) to afford the title compound (46 mg, 81%)

Clear oil; R_f = 0.64 (10% Et_2O/hexanes).

$[\alpha]^{20}_D$ +89.1 (*c* 0.920, $CHCl_3$).

^{1}H NMR (500 MHz, $CDCl_3$) δ 7.38–7.33 (m, 2 H), 7.33–7.27 (m, 2 H), 7.23–7.19 (m, 1 H), 6.42 (d, *J* = 15.8 Hz, 1 H), 6.35 (dd, *J* = 6.2, 2.1 Hz, 1 H), 6.20 (dd, *J* = 15.8, 8.1 Hz, 1 H), 5.01 (dd, *J* = 7.7, 2.2 Hz, 1 H), 4.70 (ddd, *J* = 6.2, 2.8, 1.1 Hz, 1 H), 3.94 (dq, *J* = 9.5, 7.1 Hz, 1 H), 3.60 (dq, *J* = 9.5, 7.1 Hz, 1 H), 3.18–3.10 (m, 1 H), 2.16 (dddd, *J* = 13.2, 6.5, 2.0, 1.1 Hz, 1 H), 1.81 (ddd, *J* = 13.3, 8.6, 7.9 Hz, 1 H), 1.27 (t, *J* = 7.1 Hz, 3 H).

^{13}C NMR (126 MHz, $CDCl_3$) δ 141.3, 137.4, 133.2, 129.2, 128.5, 127.2, 126.2, 104.1, 98.7, 64.3, 34.8, 34.8, 15.3.

IR (microscope, cm^{-1}) 3059, 3025, 2976, 2929, 2874, 1640, 1494, 1447, 1233, 1170, 1033.

HRMS (EI) for $C_{15}H_{18}O_2$ $(M)^+$: calcd. 230.1307; found 230.1300.

HPLC (Chiralpak AS): 1:99 *i*-PrOH/hexane, 0°C, 0.5 mL/minute, λ = 254 nm, t_{major} = 8.2 min, t_{minor} = 10.0 min, dr = 97.5:2.5.

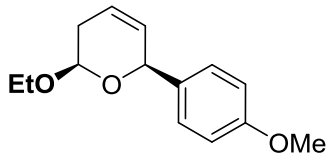

(2*R*,6*S*)-2-Ethoxy-6-(4-methoxyphenyl)-3,6-dihydro-2*H*-pyran (4-6a)

By following the general procedure B, the title compound **4-6a** was synthesized from **4-4** and 4-bromoanisole. The crude sample, containing **4-6a** in a 95 : 5 mixture of regioisomers, was subjected to flash chromatography on silica gel (5% Et_2O/hexanes) to afford the title compound (50 mg, 86%).

Clear oil: R_f = 0.16 (10% Et_2O/hexanes).

$[\alpha]^{20}_D$ −215 (*c* 1.29, $CHCl_3$).

^{1}H NMR (500 MHz, $CDCl_3$) δ 7.34–7.29 (m, 2 H), 6.90–6.85 (m, 2 H), 5.83 (dddd, *J* = 10.1, 5.0, 2.5, 2.5 Hz, 1 H), 5.72 (dddd, *J* = 10.2, 2.9, 1.7, 1.5 Hz, 1 H), 5.24–5.15 (m, 1 H), 4.84 (dd, *J* = 7.7, 3.5 Hz, 1 H), 3.88 (dq, *J* = 9.5, 7.1 Hz, 1 H), 3.80 (s, 3 H), 3.51 (dq, *J* = 9.5, 7.1 Hz, 1 H), 2.37–2.30 (m, 1 H), 2.26 (ddddd, *J* = 17.0, 6.0, 3.2, 2.5, 1.5 Hz, 1 H), 1.19 (t, *J* = 7.1 Hz, 3 H).

^{13}C NMR (126 MHz, $CDCl_3$) δ 159.3, 133.1, 129.7, 128.8, 123.3, 113.8, 98.9, 64.1, 55.4, 31.1, 15.1.

IR (microscope, cm^{-1}) 2973, 2924, 2850, 1612, 1586, 1513, 1277, 1024.

HRMS (ESI-TOF) for $C_{14}H_{18}NaO_3$ $(M + Na)^+$: calcd. 257.1148; found 257.1148, for $C_{14}H_{22}NO_3$ $(M + NH_4)^+$: calcd. 252.1594; found 252.1596, for $C_{14}H_{19}O_3$ $(M + H)^+$: calcd. 235.1329; found 235.1325.

HPLC (Chiralcel IC): 1:99 *i*-PrOH/hexane, 20°C, 0.5 mL/minute, λ = 230 nm, t_{major} = 9.9 min, t_{minor} = 11.2 min, dr = 97.5:2.5.

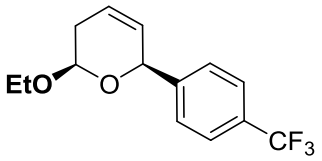

(2*R*,6*S*)-2-Ehoxy-6-[4-(trifluoromethyl)phenyl]-3,6-dihydro-2*H*-pyran (4-6b)

By following the general procedure B, the title compound **4-6b** was synthesized from **4-4** and 4-bromobenzotrifluoride. The crude sample, containing **4-6b** in a 92 : 8 mixture of regioisomers, was subjected to flash chromatography on silica gel (5% Et_2O/hexanes) to afford the title compound (54 mg, 80%).

Clear oil; R_f = 0.26 (10% Et_2O/hexanes).

$[\alpha]^{20}_D$ –144 (*c* 1.04, $CHCl_3$.

^{1}H NMR (500 MHz, $CDCl_3$) δ 7.61 (d, *J* = 8.1 Hz, 2 H), 7.52 (d, *J* = 8.5 Hz, 2 H), 5.87 (dddd, *J* = 10.2, 5.0, 2.5, 2.5 Hz, 1 H), 5.72 (dddd, *J* = 10.0, 3.4, 2.0, 1.7 Hz, 1 H), 5.31 (s, 1 H), 4.87 (dd, *J* = 7.5, 3.7 Hz, 1 H), 3.87 (dq, *J* = 9.5, 7.1 Hz, 1 H), 3.53 (dq, *J* = 9.5, 7.1 Hz, 1 H), 2.40–2.26 (m, 2 H), 1.19 (t, *J* = 7.1 Hz, 3 H).

^{13}C NMR (126 MHz, $CDCl_3$) δ 144.9, 144.8, 128.7, 127.6, 125.5, 125.4, 125.4, 125.4, 124.1, 99.0, 76.3, 64.3, 31.0, 15.1.

IR (microscope, cm^{-1}) 3041, 2979, 2933, 1432, 1415, 1164, 1127, 1066.

HRMS (ESI-TOF) for $C_{14}H_{15}F_3NaO_2$ $(M + Na)^+$: calcd. 290.1362; found 290.1364, for $C_{14}H_{19}F_3NO_2$ $(M + NH_4)^+$: calcd. 290.1362; found 290.1364; Diastereomeric ratio of compound **4-6b** could not be determined directly due to a difficult HPLC separation. See **Section 4.8.3** for dr determination of **4-9**, synthesized via Upjohn dihydroxylation of **4-6b**.

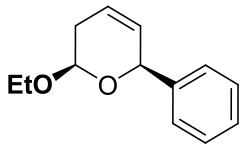

(2*R*,6*S*)-2-Ethoxy-6-phenyl-3,6-dihydro-2*H*-pyran (4-6c)

By following the general procedure B, the title compound **4-6c** was synthesized from **4-4** and *β*-bromostyrene. The crude sample, containing **4-6c** in a 97 : 3 mixture of regioisomers, was subjected to flash chromatography on silica gel (2.5% Et_2O/hexanes) to afford the title compound (38, 74%).

White solid; mp = 57.5 – 59.8 ^oC; R_f = 0.43 (10% Et_2O/hexanes).

$[\alpha]^{20}_D$ −202 (*c* 0.230, $CHCl_3$).

^{1}H NMR (500 MHz, $CDCl_3$) δ 7.41–7.39 (m, 2 H), 7.37–7.33 (m, 2 H), 7.31–7.26 (m, 1 H), 5.84 (dddd, *J* = 10.0, 5.0, 2.5, 2.5 Hz, 1 H), 5.75 (dddd, *J* = 10.0, 2.5, 1.5, 1.5 Hz, 1 H), 5.27–5.24 (m, 1 H), 4.86 (dd, *J* = 7.8, 3.5 Hz, 1 H), 3.90 (dq, *J* = 9.5, 7.1 Hz, 1 H), 3.52 (dq, *J* = 9.5, 7.1 Hz, 1 H), 2.36 (dddd, *J* = 16.8, 7.8, 3.7, 2.6 Hz, 1 H), 2.28 (dddd, *J* = 17.1, 7.7, 3.5, 2.5 Hz, 1 H), 1.19 (t, *J* = 7.1 Hz, 3 H).

^{13}C NMR (126 MHz, $CDCl_3$) δ 140.9, 129.6, 128.5, 127.9, 127.4, 123.4, 99.0, 64.1, 31.1, 15.1.

IR (microscope, cm^{-1}) 3035, 2976, 2929, 2829, 1453, 1432, 1376, 1146, 1058, 1023.

HRMS (EI) for $C_{13}H_{16}O_2$ $(M)^+$: calcd. 204.1150; found 204.1151; Diastereomeric ratio of compound **4-6c** could not be determined directly due to a difficult HPLC separation. See **Section 4.8.3** for dr determination of **4-10** after Upjohn dihydroxylation of **4-6c**.

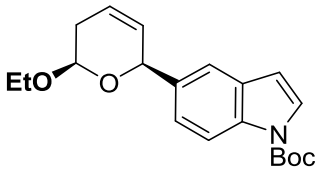

***tert*-Butyl 5-[(2*S*,6*R*)-6-ethoxy-5,6-dihydro-2*H*-pyran-2-yl]-1*H*-indole-1-carboxylate (4-6d)**

By following the general procedure B, the title compound **4-6d** was synthesized from **4-4** and *β*-bromostyrene. The crude sample, containing **4-6d** in a 97 : 3 mixture of regioisomers, was subjected to flash chromatography on silica gel (5% Et_2O/hexanes) to afford the title compound (83 mg, 97%).

Clear oil; R_f = 0.51 (20% Et_2O/hexanes).

$[\alpha]^{20}_D$ −280 (*c* 1.35, $CHCl_3$).

^{1}H NMR (500 MHz, $CDCl_3$) δ 8.21 (s, 1 H), 7.59 (d, *J* = 3.4 Hz, 1 H), 7.53 (d, *J* = 8.0 Hz, 1 H), 7.29 (dd, *J* = 8.0, 1.3 Hz, 1 H), 6.55 (d, *J* = 3.7 Hz, 1 H), 5.88–5.83 (m, 1 H), 5.82–5.80 (m, 1 H), 5.41–5.33 (m, 1 H), 4.88 (dd, *J* = 8.1, 3.3 Hz, 1 H), 3.93 (dq, *J* = 9.5, 7.1 Hz, 1 H), 3.54 (dq, *J* = 9.5, 7.1 Hz, 1 H), 2.44–2.34 (m, 1 H), 2.33–2.25 (m, 1 H), 1.68 (s, 9 H), 1.20 (t, *J* = 7.1 Hz, 3 H).

^{13}C NMR (126 MHz, $CDCl_3$) δ 149.8, 137.0, 135.2, 130.4, 130.0, 126.2, 123.2, 122.4, 120.9, 114.5, 107.1, 99.0, 83.6, 64.0, 31.2, 28.2, 15.1.

IR (microscope, cm^{-1}) 3037, 2976, 2931, 1734, 1529, 1439, 1344, 1148.

HRMS (ESI-TOF) for $C_{20}H_{25}NNaO_4$ $(M + Na)^+$: calcd. 366.1676; found 366.1674, for $C_{20}H_{29}N_2O_4$ $(M + NH_4)^+$: calcd. 361.2122; found 361.2119, for $C_{20}H_{26}NO_4$ $(M + H)^+$: calcd. 344.1856; found 344.1855; Diastereomeric ratio of compound **4-6d** could not be determined directly due to a difficult HPLC separation. See **Section 4.8.3** for dr determination of **4-34** after Upjohn dihydroxylation of **4-6d**.

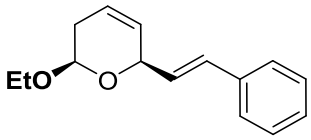

(2*R*,6*S*)-2-Ethoxy-6-[(*E*)-2-phenylvinyl]-3,6-dihydro-2*H*-pyran (4-6e)

By following the general procedure B, the title compound **4-6e** was synthesized from **4-4** and *β*-bromostyrene. The crude sample, containing **4-6e** in a 98 : 2 mixture of regioisomers, was subjected to flash chromatography on silica gel (2.5 – 10% Et_2O/hexanes) to obtain a the title compound containing the *Z*-isomer. The mixture was subsequently subjected to prep-TLC (2% Et_2O/hexanes) to afford the title compound (46 mg, 80%).

Clear oil; R_f = 0.49 (10% Et_2O/hexanes).

$[\alpha]^{20}_D$ −157 (*c* 0.820, $CHCl_3$).

^{1}H NMR (500 MHz, $CDCl_3$) δ 7.41–7.37 (m, 2 H), 7.31 (m, 2 H), 7.25–7.21 (m, 1 H), 6.63 (d, *J* = 15.9 Hz, 1 H), 6.24 (dd, *J* = 15.9, 7.3 Hz, 1 H), 5.80 (dddd, *J* = 10.1, 5.0, 4.0, 2.0 Hz, 1 H), 5.68 (dddd, *J* = 9.7, 2.0, 2.0, 2.0 Hz, 1 H), 4.89–4.84 (m, 1 H), 4.81 (dd, *J* = 5.5, 5.2 Hz, 1 H), 4.01 (dq, *J* = 9.6, 7.1 Hz, 1 H), 3.56 (dq, *J* = 9.6, 7.1 Hz, 1 H), 2.31–2.23 (m, 2 H), 1.25 (t, *J* = 7.1 Hz, 3 H).

^{13}C NMR (126 MHz, $CDCl_3$) δ 136.7, 131.5, 128.9, 128.5, 128.4, 127.7, 126.6, 123.3, 98.2, 75.3, 64.0, 30.9, 15.2.

IR (microscope, cm^{-1}) 3035, 2975, 1599, 1577, 1448, 1431, 1150, 1054, 1022.

HRMS (EI) for $C_{15}H_{18}O_2$ $(M)^+$: calcd. 230.1307; found 230.1301.

HPLC (Chiralcel OD): 1:99 *i*-PrOH/hexane, 0°C, 0.7 mL/minute, λ = 254 nm, t_{major} = 9.0 min, t_{minor} = 12.5 min, dr = 97.5:2.5 (The purified product contains trace amounts of the *Z*-isomer which is visible by ^{13}C NMR and on the HPLC chromatogram).

4.8.3 Derivatization of selected substrates for determination of diastereomeric ratio

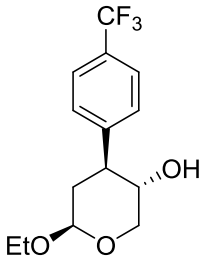

(3*S*,4*S*,6*R*)-6-Ethoxy-4-[4-(trifluoromethyl)phenyl]oxan-3-ol (4-7)

The dihydropyran substrate **4-5c** (50.3 mg, 0.184 mmol) was added in a flame-dried reaction tube under nitrogen. Dry THF (1.8 mL) was added, and the resulting solution was cooled to 0°C. BH_3•Me_2S (35.0 μL, 0.369 mmol, 2 equiv) was added dropwise to the solution and the reaction mixture was gradually allowed to warm to room temperature overnight. When the starting material was completely consumed, $NaBO_3$•$4H_2O$ (146.9 mg, 0.955 mmol, 5.2 equiv) was added and the solution was stirred vigorously at room temperature for 1 hour. The reaction mixture was cooled to 0 ^oC and followed by addition of H_2O. At 0 ^oC, the solution was diluted with water (10 mL) and extracted with EtOAc (3 × 10 mL). The organic phase was washed with brine (25 mL), dried ($MgSO_4$), filtered and concentrated. The crude product was purified by flash chromatography on silica gel (10–30% EtOAc/CH_2Cl_2) to afford the title compound (30.3 mg, 57%).

White amorphous solid; R_f = 0.44 (10% EtOAc/CH_2Cl_2).

$[\alpha]^{20}_D$ −21.7 (*c* 0.590, $CHCl_3$).

^{1}H NMR (500 MHz, $CDCl_3$) δ 7.61 (d, *J* = 8.0 Hz, 2 H), 7.38 (d, *J* = 8.2 Hz, 2 H), 4.60 (dd, *J* = 9.2, 2.2 Hz, 1 H), 4.13 (dd, *J* = 11.4, 4.9 Hz, 1 H), 3.94 (dq, *J* = 9.5, 7.1 Hz, 1 H), 3.81 (td, *J* = 9.8, 4.9 Hz, 1 H), 3.57 (dq, *J* = 9.5, 7.1 Hz, 1 H), 3.38 (dd, *J* = 11.4, 9.7 Hz, 1 H), 2.84–2.72 (m, 1 H), 2.07–2.00 (m, 1 H), 1.86 (app td, *J* = 13.3, 9.2 Hz, 1 H), 1.59 (s, 1 H), 1.24 (t, *J* = 7.1 Hz, 3 H).

^{13}C NMR (126 MHz, $CDCl_3$) δ 145.1, 130.1, 129.8, 129.5, 129.3, 128.2, 125.9, 125.9, 125.8, 1258, 101.2, 70.3, 69.0, 64.7, 48.6, 37.1, 15.3.

IR (microscope, cm^{-1}) 3434, 2977, 928 1619, 1327, 1125.

HRMS (EI) for $C_{14}H_{17}F_3O_3$ (m/z): calcd. 290.11298; found 290.11263.

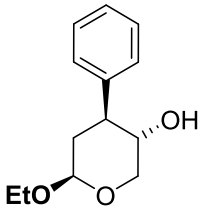

(3*S*,4*S*,6*R*)-6-Ethoxy-4-phenyloxan-3-ol (4-8)

The dihydropyran substrate **4-5c** (48.0 mg, 0.235 μmol, 1 equiv) was added in a flame-dried reaction tube under nitrogen. Dry THF (1 mL, 0.1 M) was added, and the resulting solution was cooled to 0°C. BH_3•Me_2S complex (45.0 μL, 0.474 mmol, 2 equiv) was added dropwise to the solution and the reaction mixture was gradually allowed to warm to room temperature overnight. When the starting material was completely consumed, $NaBO_3$•$4H_2O$ (190 mg, 1.23 mmol, 5.3 equiv) was added and the reaction mixture was stirred vigorously at room temperature for 1 hour. The reaction mixture was cooled to 0 ^oC and followed by addition of H_2O. At 0 ^oC, the solution was diluted with water (10 mL) and extracted with EtOAc (3 × 10 mL). The organic phase was washed with brine (25 mL), dried (Na_2SO_4), filtered and concentrated. The crude product was purified by flash chromatography on silica gel (30 – 50% EtOAc/CH_2Cl_2) to afford the title compound (36.0 mg, 69%).

White solid; mp = 57.0 – 58.7 ^oC; R_f = 0.43 (50% EtOAc/CH_2Cl_2).

$[\alpha]^{20}_D$ −27.7 (*c* 1.03, $CHCl_3$).

^{1}H NMR (500 MHz, C_6D_6) δ 7.12–7.08 (m, 2 H), 7.06–7.00 (m, 3 H), 4.30 (app dd, *J* = 8.3, 2.6

Hz, 1 H), 4.05 (dd, *J* = 11.2, 4.9 Hz, 1 H), 3.93 (dq, *J* = 9.5, 7.1 Hz, 1 H), 3.50 (ddd, *J* = 9.7, 9.7, 5.0 Hz, 1 H), 3.37 (dq, *J* = 9.5, 7.1 Hz, 1 H), 3.22 (dd, *J* = 11.2, 9.7 Hz, 1 H), 2.44 (ddd, *J* = 12.2, 9.9, 5.1 Hz, 1 H), 1.96–1.81 (m, 2 H), 1.16 (br s, 1 H), 1.13 (t, *J* = 7.1 Hz, 3 H).

^{13}C NMR (126 MHz, $CDCl_3$) δ 140.8, 128.9, 127.9, 127.4, 101.5, 70.5, 69.0, 64.6, 48.9, 37.4, 15.3.

IR (microscope, cm^{-1}) 3443, 3029, 2974, 2925, 2880, 1497, 1453, 1439, 1068.

HRMS (ESI-TOF) for $C_{13}H_{18}NaO_3$ $(M + Na)^+$: calcd. 245.1148; found 245.1144.

HPLC (Chiralcel IC): 5:95 *i*-PrOH/hexane, 5°C, 0.5 mL/minute, λ = 210 nm, t_{major} = 20.0 min, t_{minor} = 18.1 min, dr = 97.5:2.5.

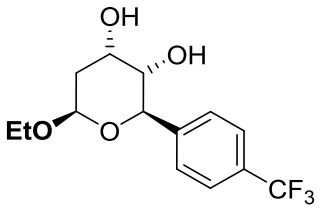

(2*R*,3*S*,4*S*,6*R*)-6-Ethoxy-2-[4-(trifluoromethyl)phenyl]oxane-3,4-diol (4-9)

To a solution containing the dihydropyran derivative **4-6b** (57.2 mg, 0.167 mmol, 1 equiv) in a mixture of THF (2.5 mL) and distilled water (0.80 mL), was added *N*-methylmorpholine *N*-oxide (50% w/w aq. soln., 60.0 μL, 0.333 mmol, 2 equiv) followed by osmium(VIII) oxide (4% w/w aq. soln., 40.0 μL, 6.29 μmol, 4 mol %) at to 0°C. The reaction mixture was gradually warmed to room temperature overnight. The reaction mixture was treated with saturated $Na_2S_2O_3$ (15 mL) and extracted with EtOAc (3 × 10 mL). The organic phase was washed with brine (25 mL), dried (Na_2SO_4), filtered and concentrated. The crude product was purified by flash chromatography on silica gel (20-30% EtOAc/CH_2Cl_2 then EtOAc) to afford the title compound (22.0 mg, 43%).

White solid; mp = 125.8 – 127.1 °C; R_f = 0.68 (EtOAc).

$[\alpha]^{20}_D$ −67.1 (*c* 0.310, $CHCl_3$).

H NMR (400 MHz, $CDCl_3$) δ 7.64 (d, J = 8.2 Hz, 2 H), 7.58 (d, J = 8.6 Hz, 2 H), 5.02 (dd, J = 9.8, 2.0 Hz, 1 H), 4.67 (d, J = 9.6 Hz, 1 H), 4.24 (ddd, J = 3.1, 3.0, 2.8 Hz, 1 H), 3.91 (dq, J = 9.6, 7.1 Hz, 1 H), 3.59–3.50 (m, 2 H), 2.53 (br s, 1 H), 2.22 (ddd, J = 14.0, 3.4, 2.2 Hz, 1 H), 1.99 (br s, 1 H), 1.87 (app ddd, J = 14.0, 9.8, 2.9 Hz, 1 H), 1.22 (t, J = 7.1 Hz, 3 H).

^{13}C NMR (100 MHz, $CDCl_3$) δ 143.2, 130.6, 130.3, 127.7, 125.5, 125.4, 125.4, 125.3, 122.8, 98.2, 75.0, 72.6, 68.3, 65.0, 37.6, 15.2.

IR (microscope, cm^{-1}) 3432, 2979, 2932, 2898, 1418, 1380, 1325, 1125, 1066.

HRMS (ESI-TOF) for $C_{14}H_{17}F_3NaO_4$ $(M + Na)^+$: calcd. 329.0971; found 329.0967.

HPLC (Chiralcel IC): 2:98 *i*-PrOH/hexane, 5°C, 0.5 mL/minute, λ = 230 nm, t_{major} = 13.3 min, t_{minor} = 16.7 min, dr = 97.5:2.5.

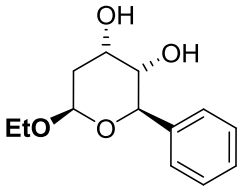

(2*R*,3*S*,4*S*,6*R*)-6-Ethoxy-2-phenyloxane-3,4-diol (4-10)

The dihydropyran derivative **4-6c** (19.8 mg, 96.9 μmol, 1 equiv) was dissolved in a mixture of THF (3.6 mL) and distilled water (1.2 mL). The solution was cooled to 0°C in an ice bath. *N*-methylmorpholine *N*-oxide (50% w/w aq. soln., 40.0 μL, 0.222 mmol, 2.3 equiv) and osmium(VIII) oxide (4% w/w aq. soln., 30.0 μL, 0.05 μmol, 5 mol %) were added sequentially. The reaction mixture was slowly warmed up to room temperature overnight. The reaction mixture was treated with saturated $Na_2S_2O_3$ (15 mL) and extracted with EtOAc (3 × 10 mL). The organic phase was washed with brine (25 mL), dried (Na_2SO_4), filtered and concentrated. The crude product was purified by flash chromatography (30 - 40% EtOAc/CH_2Cl_2 the pure EtOAc) to afford the title compound (12.9 mg, 56%).

White solid; mp = 98.2 – 100.0 °C; R_f = 0.36 (20% EtOAc/CH_2Cl_2).

$[\alpha]^{20}_D$ −101 (*c* 1.01, $CHCl_3$).

^{1}H NMR (500 MHz, $CDCl_3$) δ 7.46–7.44 (m, 2 H), 7.42–7.37 (m, 2 H), 7.36–7.32 (m, 1 H), 5.01 (dd, *J* = 9.8, 2.1 Hz, 1 H), 4.60 (d, *J* = 9.5 Hz, 1 H), 4.25 (ddd, *J* = 3.2, 3.2, 3.0 Hz, 1 H), 3.91 (dq, *J* = 9.6, 7.1 Hz, 1 H), 3.56–3.51 (m, 2 H), 2.54 (br s, 1 H), 2.22 (ddd, *J* = 14.0, 3.3, 2.2 Hz, 1 H), 1.86 (app ddd, *J* = 13.9, 9.8, 3.0 Hz, 1 H), 1.82 (app br s, 1 H), 1.21 (t, *J* = 7.1 Hz, 3 H).

^{13}C NMR (126 MHz, $CDCl_3$) δ 138.8, 128.7, 128.5, 127.5, 98.3, 75.6, 72.8, 68.1, 64.9, 37.5, 15.2.

IR (microscope, cm^{-1}) 3359, 2958, 2923, 2852, 1659, 1633, 1469, 1456, 11.41, 1050.

HRMS (EI) for $C_{13}H_{18}O_4$ $(M)^+$: calcd. 261.1097; found 261.1094.

HPLC (Chiralcel IC): 5:95 *i*-PrOH/hexane, 20°C, 0.5 mL/minute, λ = 210 nm, t_{major} = 12.6 min, t_{minor} = 17.1 min, dr = 97.5:2.5.

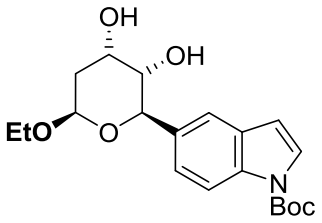

5-[(2*R*,3*S*,4*S*,6*R*)-6-Ethoxy-3,4-dihydroxyoxan-2-yl]-1*H*-indole-1-carboxylate (4-11)

The dihydropyran derivative **4-6d** (15.7 mg, 45.7 μmol, 1 equiv) was dissolved in a mixture of THF (1.7 mL) and distilled water (600 μL). The solution was cooled to 0°C in an ice bath. *N*-methylmorpholine *N*-oxide (50% w/w aq. soln., 16.0 μL, 8.88 μmol, 1.9 equiv) and osmium(VIII) oxide (4% w/w aq. soln., 14.0 μL, 2.20 μmol, 5 mol %) were added sequentially. The reaction mixture was slowly warmed up to room temperature overnight. The reaction

mixture was treated with saturated $Na_2S_2O_3$ (15 mL) and extracted with EtOAc (3 × 10 mL). The organic phase was washed with brine (25 mL), dried (Na_2SO_4), filtered and concentrated. The crude product was purified by flash chromatography on silica gel (20-30% EtOAc/CH_2Cl_2) to afford the title compound (14.1 mg, 82%).

Clear oil; R_f = 0.60 (50% EtOAc/CH_2Cl_2).

$[\alpha]^{20}_D$ −71.8 (*c* 1.14, $CHCl_3$).

^{1}H NMR (500 MHz, $CDCl_3$) δ 8.28 (s, 1 H), 7.59 (m, 2 H), 7.36 (dd, *J* = 8.1, 1.4 Hz, 1 H), 6.56 (d, *J* = 3.7 Hz, 1 H), 5.04 (dd, *J* = 9.7, 2.0 Hz, 1 H), 4.71 (d, *J* = 9.5 Hz, 1 H), 4.28 (ddd, *J* = 3.0, 3.0, 3.0 Hz, 1 H), 3.91 (dq, *J* = 9.6, 7.1 Hz, 1 H), 3.70 (dd, *J* = 9.5, 2.8 Hz, 1 H), 3.54 (dq, *J* = 9.6, 7.1 Hz, 1 H), 2.55 (br s, 1 H), 2.24 (ddd, *J* = 14.0, 3.2, 2.2 Hz, 1 H), 1.93–1.85 (m, 1 H), 1.77 (br s, 1 H), 1.67 (s, 9 H), 1.20 (t, *J* = 7.1 Hz, 3 H).

^{13}C NMR (126 MHz, $CDCl_3$) δ 149.6, 135.3, 134.6, 130.8, 126.5, 122.0, 121.4, 114.7, 107.1, 98.3, 83.9, 76.3, 72.9, 68.1, 64.8, 37.4, 28.2, 15.2.

IR (microscope, cm^{-1}) 3438, 2977, 2929, 1734, 1478, 1440, 1376, 1344, 1150.

HRMS (ESI-TOF) for $C_{20}H_{27}NNaO_6$ $(M + Na)^+$: calcd. 400.1731; found 400.1732, for $C_{20}H_{31}N_2O_6$ $(M + NH_4)^+$: calcd. 395.2177; found 395.2172.

HPLC (Chiralcel IC): 5:95 *i*-PrOH/hexane, 20°C, 0.5 mL/minute, λ = 254 nm, t_{major} = 25.7 min, t_{minor} = 38.6 min, dr = 97.5:2.5.

4.8.4 Synthesis efforts toward the synthesis of goniothalesdiol A

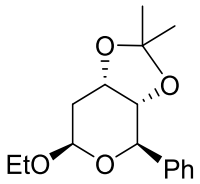

(3a*S*,4*R*,6*R*,7a*S*)-6-Ethoxy-2,2-dimethyl-4-phenyl-hexahydro-[1,3]dioxolo[4,5-c]pyran (4-25)

A mixture of **4-10** (476 mg, 2.00 mmol) and 2,2-dimethoxypropane (1.42 mL, 11.5 mmol, 5.8 equiv) in DMF (2 mL) was treated with pTsOH (4 mg, 0.021 mmol, 1 mol%) at rt. The solution was warmed to 40 ^{o}C and stirred overnight. The reaction was allowed to cool to rt and treated with saturated NH_4Cl (50 mL). The mixture was extracted with Et_2O (5 × 10 mL), then the combined organic phase was washed with brine (25 mL), dried (Na_2SO_4), filtered and concentrated. The crude product was then subjected to flash chromatography on silica gel (10% Et_2O/hexanes) to afford the title compound (584 mg, 87%).

Clear oil; R_f = 0.21 (25% Et_2O/hexanes).

$[\alpha]^{20}_D$ –0.11 (*c* 0.70, $CHCl_3$).

^{1}H NMR (500 MHz, $CDCl_3$) δ 7.47–7.46 (m, 2 H), 7.38–7.33 (m, 2 H), 7.32–7.27 (m, 1 H), 4.94 (dd, *J* = 8.7, 2.5 Hz, 1 H), 4.51 (app td, *J* = 5.0, 2.8 Hz, 1 H), 4.43 (d, *J* = 9.3 Hz, 1 H), 4.04–3.95 (m, 2 H), 3.59 (dq, *J* = 9.6, 7.1 Hz, 1 H), 2.34 (dt, *J* = 14.7, 2.6 Hz, 1 H), 2.09 (ddd, *J* = 14.6, 8.7, 4.9 Hz, 1 H), 1.61 (s, 3 H), 1.37 (s, 3 H), 1.25 (t, *J* = 7.1 Hz, 3 H).

^{13}C NMR (126 MHz, $CDCl_3$) δ 139.9, 128.4, 127.8, 126.6, 109.2, 98.6, 76.7, 76.7, 73.2, 64.6, 33.1, 28.4, 26.0, 15.3.

IR (Microscope, cm^{-1}) 2983, 2934, 2879, 1379, 1074.

HRMS (EI) for $C_{16}H_{22}O_4$ (m/z): calcd. 278.1518; found 278.1514.

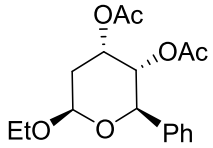

(2*R*,3*S*,4*S*,6*R*)-3-(Acetyloxy)-6-ethoxy-2-phenyloxan-4-yl acetate (4-26)

A mixture of **4-10** (299 mg, 1.26 mmol) DMAP (249 mg, 2.04 mmol, 1.6 equiv) in pyridine (31 mL) was treated with Ac_2O (1.90 mL, 20.1 mmol, 16 equiv) at 0 ^oC. The reaction mixture was gradually allowed to warm to room temperature and stirred overnight. The reaction was treated with saturated $NaHCO_3$ (25 mL). The mixture was extracted with EtOAc (2 × 20 mL). The organic phase was washed with brine (25 mL), dried (Na_2SO_4), filtered and concentrated. The crude product was then subjected to flash chromatography on silica gel (1% Et_3N in 5-20% Et_2O/hexanes) to afford the title compound (348 mg, 86%)

White amorphous solid; R_f = 0.24 (20% Et_2O/hexanes).

$[\alpha]^{20}_D$ –39.0 (*c* 3.73, $CHCl_3$).

^{1}H NMR (700 MHz, $CDCl_3$) δ 7.39 (app d, *J* = 7.3 Hz, 2 H), 7.34–7.28 (m, 3 H), 5.55 (d, *J* = 3.1 Hz, 1 H), 4.98 (dd, *J* = 9.6, 1.7 Hz, 1 H), 4.90 (dd, *J* = 10.0, 3.0 Hz, 1 H), 4.77 (d, *J* = 10.0 Hz, 1 H), 3.93 (dq, *J* = 14.2, 7.1 Hz, 1 H), 3.57–3.50 (m, 1 H), 2.18 (s, 3 H), 2.16–2.11 (m, 1 H), 2.06–1.99 (m, 1 H), 1.80 (s, 3 H), 1.21 (t, *J* = 7.1 Hz, 3 H).

^{13}C NMR (176 MHz, $CDCl_3$) δ 169.9, 169.4, 137.8, 128.3, 128.2, 127.3, 98.3, 74.1, 71.7, 68.0, 64.9, 36.0, 21.1, 20.5, 15.1.

IR (Microscope, cm^{-1}) 2974, 2886, 1732, 1373, 1253, 1044.

HRMS (ESI-TOF) for $C_{17}H_{22}NaO_6$ $[M + Na]^+$: calcd. 345.1309; found 345.1312.

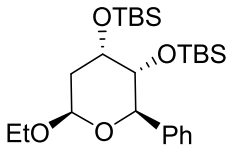

***tert*-Butyl({[(2*R*,3*R*,4*S*,6*R*)-3-[(tert-butyldimethylsilyl)oxy]-6-ethoxy-2-phenyloxan-4-yl]oxy})dimethylsilane (4-27)**

A mixture of **4-10** (372 mg, 1.56 mmol) and 2,6-lutidine (460 µL, 3.95 mmol, 2.5 equiv) in CH_2Cl_2 (5.2 mL) was treated with TBSOTf (770 µL, 3.29 mmol, 2.1 equiv) at 0 °C. The reaction mixture was gradually allowed to warm to room temperature and stirred overnight. The reaction mixture was diluted with CH_2Cl_2 (20 mL) and treated with saturated $NaHCO_3$ (25 mL). The organic phase was washed with brine (25 mL), dried ($MgSO_4$), filtered and concentrated. The crude product was then subjected to flash chromatography on silica gel (1-2.5% Et_2O/hexanes) to afford the title compound (719 mg, 99%).

White amorphous solid; R_f = 0.26 (2 × 20% Et_2O/hexanes).

$[\alpha]^{20}_D$ –8.0 (*c* 0.46, $CHCl_3$).

^{1}H NMR (700 MHz, $CDCl_3$) δ 7.39–7.38 (ddd, *J* = 6.1, 1.3, 0.6 Hz, 2 H), 7.31–7.27 (m, 2 H), 7.26–7.23 (m, 1 H), 5.02 (dd, *J* = 9.6, 2.0 Hz, 1 H), 4.76 (d, *J* = 9.0 Hz, 1 H), 4.11 (dt, *J* = 4.2, 2.2 Hz, 1 H), 3.91 (dq, *J* = 9.8, 7.1 Hz, 1 H), 3.52 (dq, *J* = 9.8, 7.1 Hz, 1 H), 3.47 (dd, *J* = 9.0, 2.3 Hz, 1 H), 2.04 (ddd, *J* = 13.4, 4.0, 2.1 Hz, 1 H), 1.82 (ddd, *J* = 13.4, 9.6, 2.1 Hz, 1 H), 1.21 (t, *J* = 7.1 Hz, 3 H), 0.97 (s, 9 H), 0.71 (s, 9 H), 0.14 (s, 3 H), 0.12 (s, 3 H), -0.22 (s, 3 H), -0.69 (s, 3 H).

^{13}C NMR (176 MHz, $CDCl_3$) δ 140.0, 128.1, 127.8, 127.6, 98.1, 75.7, 75.3, 70.6, 64.6, 40.1, 26.2, 26.0, 18.3, 18.0, 15.3.

IR (Microscope, cm^{-1}) 2955, 2930, 2887, 2857, 1472, 1462, 1380, 1361, 1252, 1089.

HRMS (EI) for $C_{25}H_{46}O_4Si_2$ $[M - tBu]^+$: calcd. 409.2230; found 409.2224.

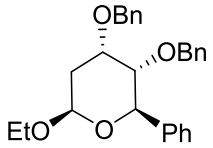

(2*R*,3*S*,4*S*,6*R*)-3,4-Bis(benzyloxy)-6-ethoxy-2-phenyloxane (4-28)

A mixture of **4-10** (545 mg, 1.17 mmol) in THF (6.5 mL) was treated with TBAF (1 M in THF, 2.90 mL, 2.90 mmol, 2.5 equiv) at 0 °C. The reaction mixture was warmed to room temperature and stirred for 6 h. The reaction mixture was allowed to cool to 0 °C and treated with saturated NH_4Cl (25 mL). The organic phase was washed with brine (25 mL), dried (Na_2SO_4), filtered and concentrated. The crude product was used immediately without further purification and transferred to a round bottom flask and diluted with THF (5 mL). At 0 °C, the reaction mixture was treated with NaH (60% w/w, 184 mg, 7.7 mmol, 6.6 equiv) followed by BnBr (309 μL, 2.60 mmol, 2.2 equiv). The reaction mixture was treated with saturated NH_4Cl (25 mL) and extracted with Et_2O (2 × 20 mL). The organic phase was washed with brine (25 mL), dried (Na_2SO_4), filtered and concentrated. The crude product was then subjected to flash chromatography on silica gel (5-10% Et_2O/hexanes) to afford the title compound (434 mg, 88%).

Clear oil; R_f = 0.32 (20% Et_2O/hexanes).

$[\alpha]^{20}_D$ +1.1 (*c* 1.2, $CHCl_3$).

^{1}H NMR (700 MHz, $CDCl_3$) δ 7.51–7.47 (m, 2 H), 7.42–7.41 (m, 2 H), 7.38–7.29 (m, 6 H), 7.21–7.17 (m, 3 H), 6.94–6.91 (m, 2 H), 5.02 (dd, *J* = 9.8, 1.9 Hz, 1 H), 4.89 (d, *J* = 9.6 Hz, 1 H), 4.81 (d, *J* = 12.4 Hz, 1 H), 4.75 (d, *J* = 12.3 Hz, 1 H), 4.12 (d, *J* = 11.9 Hz, 1 H), 4.05–4.00 (m, 2 H), 3.91 (dq, *J* = 9.7, 7.1 Hz, 1 H), 3.52 (dq, *J* = 9.7, 7.1 Hz, 1 H), 3.38 (dd, *J* = 9.6, 2.8 Hz, 1 H), 2.24 (ddd, *J* = 13.8, 3.7, 2.0 Hz, 1 H), 1.69 (ddd, *J* = 13.7, 9.8, 2.6 Hz, 1 H), 1.20 (t, *J* = 7.1 Hz, 3 H).

^{13}C NMR (176 MHz, $CDCl_3$) δ 139.9, 138.8, 138.0, 128.4, 128.2, 128.0, 127.8, 127.8, 127.8, 127.7, 127.6, 127.5, 98.3, 80.9, 75.2, 72.5, 72.1, 71.8, 64.7, 36.1, 15.3.

IR (Microscope, cm^{-1}) 3063, 3031, 74 2929, 2878, 1454, 1117, 1048.

HRMS (ESI-TOF) for $C_{27}H_{30}NaO_4$ $(M + Na)^+$: calcd. 441.2036; found 441.2035.

4.8.5 Synthesis of diospongin B

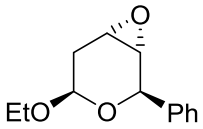

(1*S*,2*R*,4*R*,6*S*)-4-Ethoxy-2-phenyl-3,7-dioxabicyclo[4.1.0]heptane (4-35)

To a solution of **4-6c** (315 mg, 1.54 mmol, 1 equiv) in $CHCl_3$ (31 mL) was added *m*CPBA (689 mg, 3.08 mmol, 2 equiv) at 0 °C. The reaction mixture was gradually warmed to room temperature overnight. The reaction mixture was treated with saturated $Na_2S_2O_3$ (25 mL) and the organic phase was washed with saturated NH_4Cl (25 mL) followed by brine (25 mL). The organic phase was dried (Na_2SO_4), filtered and concentrated to give a crude product as a white solid containing **4-35** in a 13:1 isomeric ratio. The crude product was then subjected to flash chromatography on silica gel (5% Et_2O/hexanes) to afford the title compound (236 mg, 70%).

White solid; mp = 122.0 – 123.8 °C; R_f = 0.43 (20% Et_2O/hexanes).

$[\alpha]^{20}_D$ –180 (*c* 1.07, $CHCl_3$).

^{1}H NMR (700 MHz, $CDCl_3$) δ 7.49–7.46 (m, 2 H), 7.42–7.38 (m, 2 H), 7.35–7.31 (m, 1 H), 4.99 (s, 1 H), 4.70 (dd, *J* = 9.1, 2.7 Hz, 1 H), 3.88 (dq, *J* = 9.7, 7.1 Hz, 1 H), 3.54–3.45 (m, 2 H), 3.20 (d, *J* = 4.1 Hz, 1 H), 2.38 (ddd, *J* = 14.7, 2.1, 2.1 Hz, 1 H), 1.99 (ddd, *J* = 14.5, 9.1, 1.9 Hz, 1 H), 1.20 (t, *J* = 7.1 Hz, 3 H).

^{13}C NMR (126 MHz, $CDCl_3$) δ 139.2, 128.7, 128.2, 126.8, 96.9, 64.9, 55.9, 53.7, 31.5, 15.2.

IR (Microscope, cm^{-1}) 3006, 2982, 2950, 2923, 2898, 2875, 2425, 1379, 1356, 1142, 1088, 1012.

HRMS (EI) for $C_{13}H_{16}O_3$ $(M)^+$: calcd. 220.1099; found 220.1090.

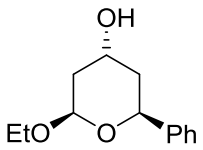

(2*R*,4*R*,6*S*)-2-Ethoxy-6-phenyltetrahydro-2*H*-pyran-4-ol (4-34)

To a solution of **4-35** (470 mg, 2.14 mmol, 1 equiv) in THF (43 mL) was added DIBAL-H (1M in toluene, 6.40 mL, 6.40 mmol, 3 equiv) at 0 °C. The solution was then gradually warmed to room temperature overnight. After complete consumption of starting material, the reaction mixture was cooled to 0 °C and treated with saturated Rochelle salt solution (50 mL) and was stirred for 30 min at room temperature. The solution was extracted with EtOAc (3 × 50 mL) and the organic fractions were washed with brine (50 mL), dried (Na_2SO_4), filtered and concentrated. The crude product was subjected to flash chromatography on silica gel (50% Et_2O/hexanes) to afford the title compound (394 mg, 83%).

Clear oil; R_f = 0.20 (50% Et_2O/hexanes).

$[\alpha]^{20}_D$ –141 (*c* 1.75, $CHCl_3$).

^{1}H NMR (700 MHz, $CDCl_3$) δ 7.41 (app d, *J* = 7.4 Hz, 2 H), 7.35 (app dd, *J* = 7.7, 7.7 Hz, 2 H), 7.28–7.26 (m, 1 H), 5.02 (dd, *J* = 10.0, 2.1 Hz, 1 H), 4.95 (dd, *J* = 11.7, 1.9 Hz, 1 H), 4.42 (app s, 1 H), 4.01 (dq, *J* = 9.7, 7.1 Hz, 1 H), 3.59 (dq, *J* = 9.7, 7.1 Hz, 1 H), 1.98 (ddd, *J* = 13.7, 5.0, 2.1 Hz, 1 H), 1.89 (ddd, *J* = 14.1, 4.9, 2.3 Hz, 1 H), 1.81–1.72 (m, 2 H), 1.64 (s, 1 H), 1.25 (t, *J* = 7.1 Hz, 3 H).

^{13}C NMR (176 MHz, $CDCl_3$) δ 142.1, 128.3, 127.4, 125.9, 98.4, 72.0, 65.9, 64.5, 40.3, 38.5, 15.3.

IR (Microscope, cm^{-1}) 3442, 3063, 3031, 2975 2929, 2878, 1380, 1343, 1136, 1039.

HRMS (EI) for $C_{13}H_{18}O_3$ $(M)^+$: calcd. 222.1256; found 222.1261.

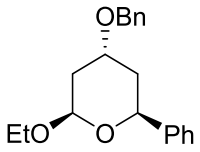

(2*R*,4*R*,6*S*)-4-(Benzyloxy)-2-ethoxy-6-phenyltetrahydro-2*H*-pyran (4-36)

To a solution of **4-34** (258 mg, 1.16 mmol) in THF (5.6 mL) was added NaH (60% w/w, 55.6 mg, 1.39 mmol, 1.2 equiv) at 0 ºC. After stirring for 30 minutes, BnBr (170 µL, 1.40 mmol, 1.2 equiv) was added dropwise to the cooled solution followed by gradually warming to rt overnight. The reaction mixture was treated with saturated NH_4Cl (25 mL) then extracted with CH_2Cl_2 (2 × 20 mL). The organic phase was washed with brine (25 mL), dried (Na_2SO_4), filtered and concentrated. The crude product was then subjected to flash chromatography on silica gel (5% Et_2O/hexanes) to afford the title compound (272 mg, 75%).

Clear oil; R_f = 0.59 (20% Et_2O/hexanes).

$[\alpha]^{20}_D$ –76.5 (*c* 1.47, $CHCl_3$).

^{1}H NMR (700 MHz, $CDCl_3$) δ 7.42–7.36 (m, 6 H), 7.36–7.30 (m, 3 H), 7.29–7.25 (m, 2 H), 5.01 (dd, *J* = 9.9, 2.1 Hz, 1 H), 4.92 (dd, *J* = 11.8, 1.9 Hz, 1 H), 4.62 (app q, *J* = 12.0 Hz, 2 H), 4.06–3.97 (m, 2 H), 3.58 (dq, *J* = 9.7, 7.1 Hz, 1 H), 2.18 (ddd, *J* = 13.6, 5.0, 2.1 Hz, 1 H), 2.09 (ddd, *J* = 14.0, 4.9, 2.2 Hz, 1 H), 1.71–1.63 (m, 2 H), 1.25 (t, *J* = 7.1 Hz, 3 H).

^{13}C NMR (176 MHz, $CDCl_3$) δ 142.2, 138.7, 128.5, 128.3, 127.7, 127.5, 127.3, 126.0, 98.8, 72.7, 72.5, 70.5, 64.5, 37.3, 35.7, 15.4.

IR (Microscope, cm^{-1}) 3030, 2973, 2928, 2869, 1496, 1453, 1039.

HRMS (ESI-TOF) for $C_{20}H_{24}NaO_3$ $(M + Na)^+$: calcd. 335.1618; found 335.1619.

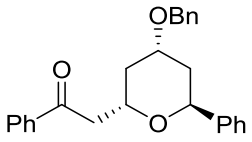

2-[(2*S*,4*S*,6*S*)-4-(Benzyloxy)-6-phenyltetrahydro-2*H*-pyran-2-yl]-1-phenylethanone (4-38)

To a solution of **4-36** (11.1 mg, 35.5 μmol) and 4Å MS (5 mg) in CH_2Cl_2 (0.15 mL) was added trimethyl((1-phenylvinyl)oxy)silane (9.0 mg, 46.8 μmol, 1.3 equiv) and stirred for 5 minutes. The solution was cooled to 0 °C then $SnCl_4$ (1M in CH_2Cl_2, 20 μL, 56 mol%) was added dropwise by syringe and stirred at 0 °C for 30 minutes. After complete consumption of starting material, Et_3N (500 μL) was added followed by saturated $NaHCO_3$ (5 mL) and the solution was allowed to warm up to room temperature. The solution was washed with EtOAc (10 mL). The resulting organic phase was washed with brine (10 mL), dried (Na_2SO_4), filtered and concentrated. The crude product was then subjected to flash chromatography on silica gel (10% Et_2O/Hexanes) to afford the title compound (10.8 mg, 79%).

Clear oil; R_f = 0.30 (20% Et_2O/Hexanes).

$[\alpha]^{20}_D$ +40.1 (*c* 0.740, $CHCl_3$).

^{1}H NMR (500 MHz, $CDCl_3$) δ 7.99–7.94 (m, 2 H), 7.60–7.53 (m, 1 H), 7.49–7.42 (m, 2 H), 7.36–7.27 (m, 8 H), 7.25–7.20 (m, 1 H), 5.16 (t, *J* = 4.7 Hz, 1 H), 4.57 (q, *J* = 11.7 Hz, 2 H), 4.33–4.26 (m, 1 H), 3.82–3.74 (m, 1 H), 3.45 (dd, *J* = 16.1, 6.7 Hz, 1 H), 3.29 (dd, *J* = 16.1, 6.3 Hz, 1 H), 2.02 (ddd, *J* = 13.7, 9.0, 4.8 Hz, 1 H), 1.66 (dt, *J* = 12.8, 8.6 Hz, 1 H).

^{13}C NMR (126 MHz, $CDCl_3$) δ 198.4, 140.7, 138.6, 137.3, 133.1, 128.6, 128.5, 128.5, 128.4, 128.3, 128.3, 127.7, 127.7, 127.1, 126.4, 71.9, 71.1, 70.2, 67.4, 44.5, 36.5, 34.5.

IR (Microscope, cm^{-1}) 3061, 3029, 2927, 1683, 1644, 1597, 1580, 1066.

HRMS (ESI-TOF) for $C_{26}H_{26}NaO_3$ $(M + Na)^+$: calcd. 409.1774; found 409.1776.

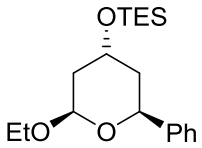

{[(2*R*,4*R*,6*S*)-2-Ethoxy-6-phenyltetrahydro-2*H*-pyran-4-yl]oxy}(triethyl)silane (4-37)

A mixture of **4-34** (394 mg, 1.77 mmol, 1 equiv) and 2,6-lutidine (0.410 mL, 3.52 mmol, 2 equiv) in CH_2Cl_2 (5.9 mL) was treated with TESCl (0.450 mL, 2.68 mmol, 1.5 equiv) at 0 °C. The reaction mixture was gradually allowed to warm to room temperature and stirred overnight. The reaction mixture was diluted with CH_2Cl_2 (20 mL) and treated with saturated $NaHCO_3$ (25 mL). The organic phase was washed with brine (25 mL), dried (Na_2SO_4), filtered and concentrated. The crude product was then subjected to flash chromatography on silica gel (2.5% Et_2O/hexanes) to afford the title compound (519 mg, 87%).

Clear oil; R_f = 0.30 (2.5% Et_2O/hexanes).

$[\alpha]^{20}_D$ –80.0 (*c* 0.870, $CHCl_3$).

^{1}H NMR (400 MHz, $CDCl_3$) δ 7.41–7.37 (m, 2 H), 7.36–7.31 (m, 2 H), 7.29–7.23 (m, 1 H), 5.00 (dd, *J* = 9.7, 2.2 Hz, 1 H), 4.95 (dd, *J* = 11.3, 2.3 Hz, 1 H), 4.34 (dddd, *J* = 2.9, 2.9, 2.8, 2.8 Hz, 1 H), 4.01 (dq, *J* = 9.6, 7.1 Hz, 1 H), 3.58 (dq, *J* = 9.6, 7.1 Hz, 1 H), 1.90 (dddd, *J* = 13.1, 3.2, 2.0, 2.0 Hz, 1 H), 1.83–1.77 (m, 1 H), 1.74–1.61 (m, 2 H), 1.25 (t, *J* = 7.2 Hz, 3 H), 1.00 (*t*, *J* = 8.0 Hz, 9 H), 0.63 (q, *J* = 7.8 Hz, 6 H).

^{13}C NMR (101 MHz, $CDCl_3$) δ 142.5, 128.3, 127.2, 125.9, 98.8, 72.2, 66.1, 64.4, 41.2, 39.3, 15.4, 6.95, 4.9.

IR (Microscope, cm^{-1}) 3060, 2975, 2930, 1644, 1611, 1512, 1250.

HRMS (ESI-TOF) for $C_{19}H_{32}NaO_3Si$ $(M + Na)^+$: calcd. 359.2013; found 359.2010.

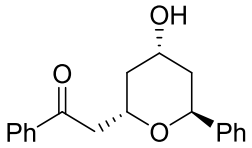

Diospongin B

To a solution of **4-37** (58.8 mg, 0.175 mmol, 1 equiv) and 4A MS (30 mg) in CH_2Cl_2 (0.4 mL) was added trimethyl((1-phenylvinyl)oxy)silane (65.8 mg, 0.342 mmol, 2 equiv) and stirred for 5 minutes. The solution was cooled to 0 ^oC then $SnCl_4$ (1M in CH_2Cl_2, 70 μL, 70.0 μmol, 40 mol %) was added dropwise by syringe and stirred at 0 ^oC for 1.5 h. After complete consumption of starting material, Et_3N (500 μL) was added followed by saturated NH_4Cl (5 mL) and the solution was allowed to warm up to room temperature. The solution was washed with EtOAc (10 mL). The resulting organic phase was washed with brine (10 mL), dried (Na_2SO_4), filtered and concentrated. The crude product was used immediately without further purification and transferred to a plastic reaction vessel using dry THF (1.8 mL). After cooling the solution to 0 ^oC, HF•pyridine complex (40.0 μL, 0.193 mmol, 1.1 equiv) was added dropwise and the reaction was stirred at 0 ^oC for 2.5 h. The reaction mixture was treated with saturated NH_4Cl (5 mL) followed by extractions with EtOAc (2 × 10 mL). The organic phase was then washed with brine (25 mL), dried (Na_2SO_4), filtered and concentrated. The crude product was then subjected to flash chromatography on silica gel (5 - 10% EtOAc/CH_2Cl_2) to afford **diospongin B** (34.0 mg, 66%).

Clear oil; R_f = 0.24 (20% EtOAc/CH_2Cl_2).

$[\alpha]^{20}_D$ +22.8 (*c* 0.710, $CHCl_3$).

^{1}H NMR (400 MHz, $CDCl_3$) δ 8.01–7.96 (m, 2 H), 7.60–7.54 (m, 1 H), 7.50–7.44 (m, 2 H), 7.39–7.29 (m, 4 H), 7.25–7.20 (m, 1 H), 5.19 (dd, *J* = 4.4, 4.2 Hz, 1 H), 4.23 (dddd, *J* = 9.5, 6.4, 6.4, 3.1 Hz, 1 H), 4.02 (app tt, *J* = 9.4, 4.4 Hz, 1 H), 3.45 (dd, *J* = 15.8, 7.2 Hz, 1 H), 3.17 (dd, *J*

= 15.8, 6.0 Hz, 1 H), 2.51 (dddd, *J* = 13.3, 3.8, 3.8, 2.0 Hz, 1 H), 2.08–2.03 (m, 1 H), 1.92 (ddd, *J* = 14.1, 9.2, 5.2 Hz, 1 H), 1.81 (br s, 1 H), 1.51 (ddd, *J* = 12.5, 9.6, 9.4 Hz, 1 H).

^{13}C NMR (101 MHz, $CDCl_3$) δ 198.4, 140.3, 137.2, 133.2, 128.7, 128.6, 128.3, 127.1, 126.4, 72.4, 67.0, 64.2, 44.7, 40.2, 36.8.

IR (Microscope, cm^{-1}) 3405, 3061, 2924, 1683, 1597, 1580, 1052.

HRMS (ESI-TOF) for $C_{19}H_{20}NaO_3$ $(M + Na)^+$: calcd. 319.1305; found 319.1305.

4.8.6 Comparison of synthetic and natural products of diospongin B

Hall ^{1}H NMR (400 MHz, $CDCl_3$)	**Hashimoto (Synthetic)[11]** ^{1}H NMR (400 MHz, $CDCl_3$)	**Kadota (Natural)[10]** ^{1}H NMR (400 MHz, $CDCl_3$)[a]
8.01 – 7.96 (m, 2 H)	7.99 (d, *J* = 7.4 Hz, 2 H)	7.98 (dd, *J* = 7.8 Hz)
7.60 – 7.54 (m, 1 H)	7.58 (t, *J* = 7.4 Hz, 1 H)	7.57 (t, *J* = 7.8 Hz)
7.50 – 7.44 (m, 2 H)	7.47 (t, *J* = 7.4 Hz, 2 H)	7.47 (t, *J* = 7.8 Hz)
7.39 – 7.29 (m, 4 H)	7.35 (m, 2 H)	7.35 (m)
	7.32 (m, 2 H)	7.32 (m)
7.25 – 7.20 (m, 1 H)	7.23 (t, *J* = 6.9 Hz, 1 H)	7.23 (t, *J* = 6.8 Hz)
5.19 (dd, *J* = 4.4, 4.2 Hz, 1 H)	5.19 (dd, *J* = 4.0, 4.0 Hz, 1 H)	5.19 (t, *J* = 4.1 Hz)
4.23 (dddd, *J* = 9.5, 6.4, 6.4, 3.1 Hz, 1 H)	4.23 (dddd, *J* = 9.7, 6.9, 6.3, 2.9 Hz, 1 H)	4.23 (dddd, *J* = 9.5, 6.8, 5.8, 3.0 Hz)
4.02 (app tt, *J* = 9.4, 4.4 Hz, 1 H)	4.02 (dddd, *J* = 9.7, 9.7, 5.1, 4.0 Hz, 1 H)	4.02 (dddd, *J* = 9.8, 9.5, 5.2, 3.9 Hz)
3.45 (dd, *J* = 15.8, 7.2 Hz, 1 H)	3.45 (dd, *J* = 16.0, 6.9 Hz, 1 H)	3.45 (dd, *J* = 15.8, 6.8 Hz)
3.17 (dd, *J* = 15.8, 6.0 Hz, 1 H)	3.17 (dd, *J* = 16.0, 6.3 Hz, 1 H)	3.17 (dd, *J* = 15.8, 5.8 Hz)
2.51 (dddd, *J* = 13.3, 3.8, 3.8, 2.0 Hz, 1 H)	2.51 (ddd, *J* = 13.2, 4.0, 4.0 Hz, 1 H)	2.51 (ddd, *J* = 13.3, 4.1, 3.9 Hz)
2.08 – 2.03 (m, 1 H)	2.05 (ddd, *J* = 12.6, 5.1, 2.9 Hz, 1 H)	2.05 (ddd, *J* = 12.4, 5.2, 3.0 Hz)
1.92 (ddd, *J* = 14.1, 9.2, 5.2 Hz, 1 H)	1.92 (ddd, *J* =13.2, 9.7, 4.0 Hz, 1 H)	1.92 (ddd, *J* = 13.3, 9.8, 4.1 Hz)
1.81 (br s, 1 H)		
1.51 (ddd, *J* = 12.5, 9.6, 9.4 Hz, 1 H)	1.50 (ddd, *J* = 12.6, 9.7, 9.7 Hz, 1 H)	1.50 (dt, *J* = 12.4, 9.5 Hz)

[a] Integrations were not listed by Kadota and co-workers.[10]

Hall ^{13}C NMR (100 MHz, $CDCl_3$)	**Hashimoto (Synthetic)[11]** ^{13}C NMR (100 MHz, $CDCl_3$)	**Kadota (Natural)[10]** ^{13}C NMR (100 MHz, $CDCl_3$)
198.4	198.4	198.4
140.3	140.1	140.3
137.2	137.1	137.2
133.2	133.2	133.2
128.7	128.6	128.6
128.6	128.5	128.5
128.3	128.2	128.3
127.1	127.0	127.1
126.4	126.3	126.4
72.4	72.3	72.4
67.0	66.9	67.0
64.2	64.1	64.2
44.7	44.6	44.6
40.2	40.1	40.1
36.8	36.6	36.8

4.9 References

[1] Gademann, K.; Chavez, D. E.; Jacobsen, E. N. *Angew. Chem. Int. Ed.* **2002**, *114*, 3185–3187.

[2] (a) Yamamoto, Y.; Takada, S.; Miyaura, N. *Chem. Lett.* **2006**, *35*, 704–705; (b) Sebelius, S.; Olsson, V. J.; Wallner, O. A.; Szabó, K. J. *J. Am. Chem. Soc.* **2006**, *128*, 8150−8151; (c) Yamamoto, Y.; Takada, S.; Miyaura, N.; Iyama, T.; Tachikawa, H. *Organometallics* **2009**, *28*, 152–160; (d) Farmer, J. L.; Hunter, H. N.; Organ, M. G. *J. Am. Chem. Soc.* **2012**, *134*, 17470–17473; (e) Glasspoole, B. W.; Ghozati, K.; Moir, J. W.; Crudden, C. M. *Chem. Commun.* **2012**, *48*, 1230–1232; (f) Chausset-Boissarie, L.; Ghozati, K.; LaBine, E.; Chen, J. L.; Aggarwal, V. K.; Crudden, C. M. *Chem. Eur. J.* **2013**, *19*, 17698–17701; (g) Yang, Y.; Buchwald, S. L. *J. Am. Chem. Soc.* **2013**, *135*, 10642–10645.

[3] (a) Romero, J. A. C.; Tabacco, S. A.; Woerpel, K. A. *J. Am. Chem. Soc.* **2000**, *122*, 168–169; (b) Ayala, L.; Lucero, C. G.; Romero, J. A. C.; Tabacco, S. A.; Woerpel, K. A. *J. Am. Chem. Soc.* **2003**, *125*, 15521–15528.

[4] (a) Woods, R. J.; Andrews, C. W.; Bowen, J. P. *J. Am. Chem. Soc.* **1992**, *114*, 859–864; (b) Miljković, M.; Yeagley, D.; Deslongchamps, P.; Dory, Y. L. *J. Org. Chem.* **1997**, *62*, 7597–7604.

[5] Gao, X.; Hall, D. G. *J. Am. Chem. Soc.* **2003**, *125*, 9308–9309.

[6] Martin, R.; Buchwald, S. L. *Acc. Chem. Res.* **2008**, *41*, 1461–1473.

[7] Hartwig, J. F. *Inorg. Chem.* **2007**, *46*, 1936–1947.

[8] Lan, Y. H.; Chang, F. R.; Yang, Y. L.; Wu, Y. C. *Chem. Pharm. Bull.* **2006**, *54*, 1040–1043.

[9] (a) Venkataiah, M.; Somaiah, P.; Reddipalli, G.; Fadnavis, N. W. *Tetrahedron: Asymmetry* **2009**, *20*, 2230–2233; (b) She, X.; Xie, X.; Li, J.; Zheng, H.; Su, Y. *Synlett* **2010**, *2010*, 2283–2284; (c) Yadav, J. S.; Rao, R. N.; Somaiah, R.; Harikrishna, V.; Reddy, B. V. S. *Helv. Chim. Acta* **2010**, *93*, 1362–1368; (d) Sabitha, G.; Rammohan R., T.; Yadav, J. S. *Tetrahedron Lett.* **2011**, *52*, 6550–6553; (e) Thakur, P.; Boyapelly, K.; Gurram, R. R.; Bandichhor, R.; Mukkanti, K. *Tetrahedron: Asymmetry* **2012**, *23*, 659–661.

[10] Yin, J.; Kouda, K.; Tezuka, Y.; Tran, Q. L.; Miyahara, T.; Chen, Y.; Kadota, S. *Planta Med.* **2004**, *70*, 54–58.

[11] Anada, M.; Washio, T.; Watanabe, Y.; Takeda, K.; Hashimoto, S. *Eur. J. Org. Chem.* **2010**, *2010*, 6850–6854.

[12] Fakha, G.; Sinou, D. *Molecules* **2005**, *10*, 859–870.

[13] (a) Huang, H.; Panek, J. S. *Org. Lett.* **2001**, *3*, 1693–1696; (b) Su, Q.; Panek, J. S. *J. Am.*

Chem. Soc. **2004**, *126*, 2425–2430.

[14] Sawant, K. B.; Jennings, M. P. *J. Org. Chem.* **2006**, *71*, 7911−7914.

[15] (a) Kawai, N.; Hande, S. M.; Uenishi, J. *Tetrahedron* **2007**, *63*, 9049–9056; (b) Sabitha, G.; Padmaja, P.; Yadav, J. S. *Helv. Chim. Acta* **2008**, *91*, 2235–2239; (c) Wang, H. M.; Shuhler, B. J.; Xian, M. *Synlett* **2008**, *2008*, 2651–2654; (d) Kumaraswamy, G.; Ramakrishna, G.; Naresh, P.; Jagadeesh, B.; Sridhar, B. *J. Org. Chem.* **2009**, *74*, 8468–8471; (e) Stefan, E.; Nalin, A. P.; Taylor, R. E. *Tetrahedron* **2013**, *69*, 7706–7712.

[16] (a) Gao, X.; Hall, D. G. *J. Am. Chem. Soc.* **2005**, *127*, 1628– 1629; (b) Penner, M.; Rauniyar, V.; Kaspar, L. T.; Hall, D. G. *J. Am. Chem. Soc.* **2009**, *131*, 14216–14217.

[17] Ainsworth, C.; Chen, F.; Kuo, Y. *J. Organomet. Chem.* **1972**, *46*, 59–71.

[18] Cazeau, P.; Duboudin, F.; Moulines, F.; Babot, O.; Dunogues, J. *Tetrahedron* **1987**, *43*, 2075–2088.

Chapter 5. Conclusions

5.1 Conclusions and Future Perspectives

In the last decade, there have been ongoing discoveries of natural and synthetic bioactive pyran-containing molecules (Chapter 1, Section 1.1). This outcome has reaffirmed that novel methods of synthesizing and utilizing the pyran motif are needed. Furthermore, the use of asymmetric reactions on a pyran framework may afford highly enantioenriched compounds that would provide a chiral pool towards the synthesis of three-dimensional, sp^3-hybridized, and clinically viable drugs. To this end, this thesis describes new avenues in developing and applying stereochemically enriched dihydropyrans towards the synthesis of bioactive compounds.

Chapter 1 briefly outlined current methods of synthesizing and functionalizing pyran structures as well as addressing certain strengths and issues in utilizing them to obtain natural products or synthetic drugs. In Chapter 2, a short route towards laulimalide analogues provided early insight into the challenges of synthesizing these compounds (Chapter 2, Section 2.8, Figure 2-15, Equation 2). The successful synthesis of the simplified laulimalide analogues did not come without pitfalls, such as poor diastereoselective transformations that favored the formation of undesired intermediates. The cross-metathesis proved to be inefficient, where excess equivalents of the highly toxic reagent acrolein was needed to form an α,β-unsaturated aldehyde. Furthermore, harsh conditions were required in the desilylation step. Lastly, the natural product, 1,2-acyl migrations was a reoccurring issue when forming and purifying these analogues. One possible way of resolving these issues requires a concise asymmetric and regioselective synthesis of a *cis*-1,2-amino alcohol intermediate that would serve as the core building block of the these potentially antimitotic compounds. Thus, replacing the ester group with an amide group would

improve the stability of these synthetic analogues and protect the compounds from esterases *in vivo*. Efforts to design a biologically more stable and active class of laulimalide analogues are ongoing.

Chapter 3 described the development of the first stereospecific and regiodivergent allylic Suzuki-Miyaura cross-coupling reaction to form chiral sp^3–sp^2 bonds from enantioenriched heterocyclic allylboronates; formed from the in-house catalytic enantioselective borylative isomerization (Scheme 5-1, Equation 1).[1] This method effectively produced two sets of dihydropyranyl regioisomers under ligand control with high stereospecificity and regioselectivity. Furthermore, these dipydropyrans can be functionalized with moderate to high diastereoselectivity, demonstrating the utility in developing these potentially useful products. In Chapter 4, the utility of this method was expanded to produce polyfunctionalized tetrahydropyrans with very high stereospecificity. This was achieved by using the enantioenriched 2-ethoxy dihydropyranyl boronate substrate made from the asymmetric inverse electron-demand oxa-[4+2] cycloaddition developed by the Hall group (Scheme 5-1, Equation 2).[2] This method was then applied towards the total synthesis of the antiosteoporotic natural product diospongin B. Looking into the future, a current limitation to the utility of these chiral dihydropyrans is the functionalization of these regioisomers at the C3-position, where diastereoselective transformations would form fully polyfunctionalized pyrans. This would be beneficial towards an alternate access to several *C*-glycosides previously mentioned in Chapter 1, such as the natural product bergenin (Scheme 5-1, Equation 3).

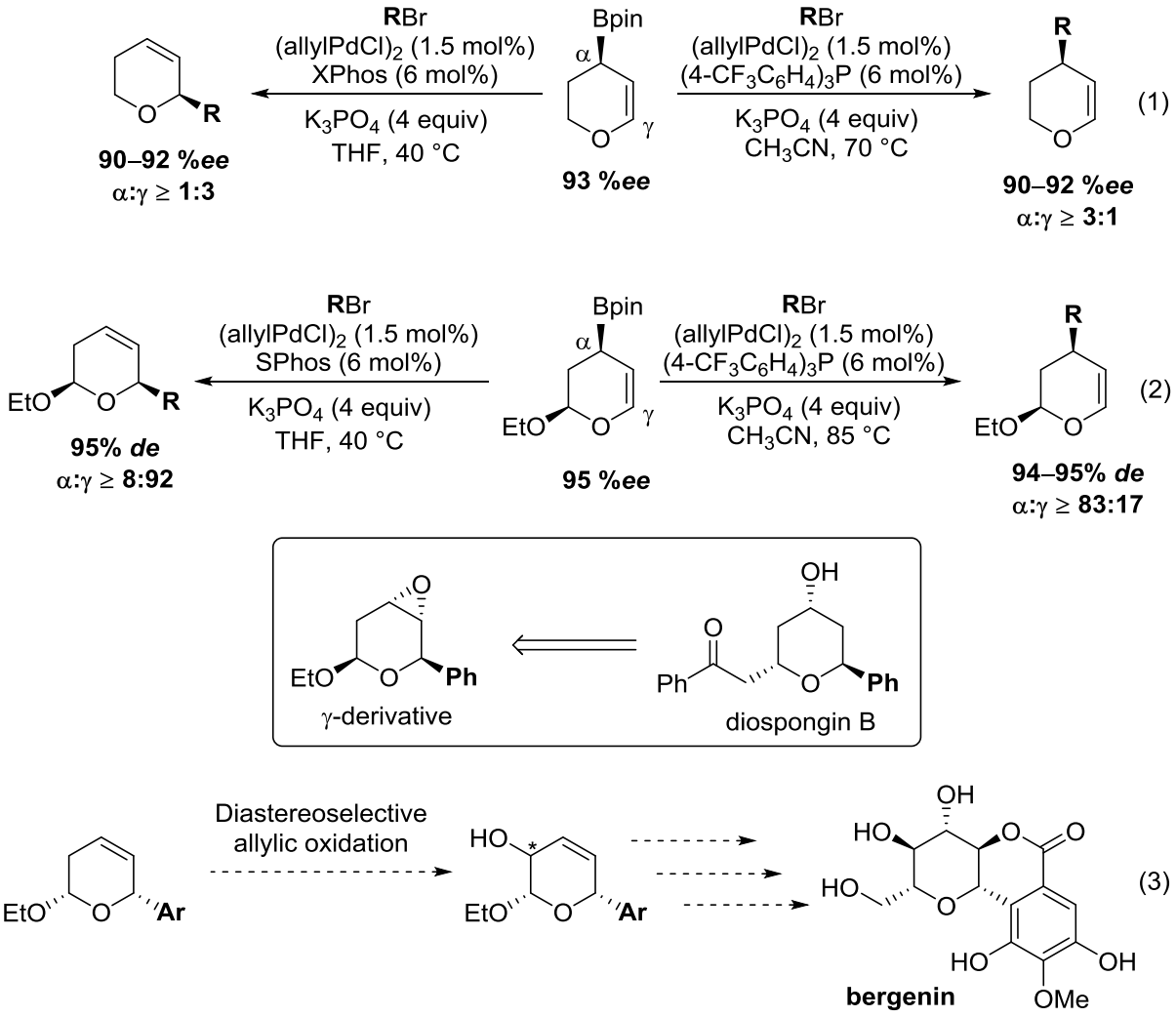

Scheme 5-1: Current methods and future prospects of functionalizing enantioenriched dihydropyranyl boronates.

To broaden the utility of this method even further, other optically pure heterocyclic allylboronates with various ring sizes could be explored (Scheme 5-2). This objective would require a concise formation of asymmetric heterocyclic allylboronates to support the applicability of these compounds. The suggested extensions to the studies described in this thesis, as mentioned above, only represent a small portion of what could be contributed to the aforementioned research. Exploring further in the utility of these projects would offer new

directions in research and contribute to the discovery of new strategies in forming synthetically viable compounds and novel methods.

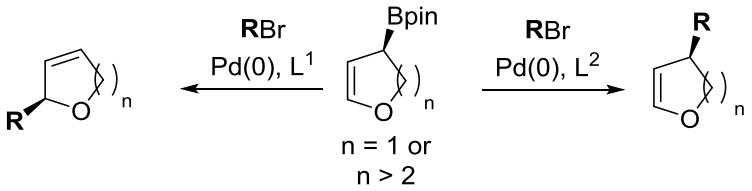

Scheme 5-2: Potential access to unique heterocycles using the ligand-controlled regiodivergent allylic cross-coupling reaction.

5.2 References

[1] Lessard, S.; Peng, F.; Hall, D. G. *J. Am. Chem. Soc.* **2009**, *131*, 9612–9613.

[2] Gao, X.; Hall, D. G. *J. Am. Chem. Soc.* **2003**, *125*, 9308–9309.

Bibliography

1. Lipinski, C. A.; Lombardo, F.; Dominy, B. W.; Feeney, P. J., *Adv. Drug Delivery Rev.* **1997,** *23* 3–25.

2. Lovering, F.; Bikker, J.; Humblet, C., *J. Med. Chem.* **2009,** *52* 6752–6756.

3. Taylor, R. D.; MacCoss, M.; Lawson, A. D., *J. Med. Chem.* **2014,** *57* 5845–5859.

4. Aldeghi, M.; Malhotra, S.; Selwood, D. L.; Chan, A. W., *Chem. Biol. Drug Des.* **2014,** *83* 450–461.

5. Clarke, P. A.; Santos, S., *Eur. J. Org. Chem.* **2006,** 2045–2053.

6. Nicolas, L.; Butkevich, A. N.; Guérinot, A.; Corbu, A.; Reymond, S.; Cossy, J., *Pure Appl. Chem.* **2013,** *85* 1203–1213.

7. Perry, M. A.; Rychnovsky, S. D.; Sizemore, N., *Synthesis of Saturated Tetrahydropyrans*. Springer-Verlag: Berlin, 2014; Vol. 35.

8. Elliott, M. C., *J. Chem. Soc., Perkin Trans. 1* **2002,** 2301–2323.

9. Tanaka, J.; Higa, T., *Tetrahedron Lett.* **1996,** *37* 5535–5538.

10. Corley, D. G.; Herb, R.; Moore, R. E.; Scheuer, P. J.; Paul, V. J., *J. Org. Chem.* **1988,** *53* 3644–3646.

11. Xu, L.; He, Z.; Xue, J.; Chen, X.; Wei, X., *J. Nat. Prod.* **2010,** *73* 885–889.

12. Ohba, K.; Nakata, M., *Org. Lett.* **2015,** *17* 2890–2893.

13. De Albuquerque, I. L.; Galeffi, C.; Casinovi, C. G.; Marini-Bettolo, G. B., *Gazz. Chim. Ital.* **1964,** *94* 287–295.

14. Galeffi, C.; Casinovi, C. G.; Marini-Bettòlo, G. B., *Gazz. Chim. Ital.* **1965,** *95* 95–100.

15. Yin, J.; Kouda, K.; Tezuka, Y.; Tran, Q. L.; Miyahara, T.; Chen, Y.; Kadota, S., *Planta Med.* **2004,** *70* 54–58.

16. Lan, Y. H.; Chang, F. R.; Yang, Y. L.; Wu, Y. C., *Chem. Pharm. Bull.* **2006,** *54* 1040–1043.

17. de Fatima, A.; Kohn, L. K.; Antonio, M. A.; de Carvalho, J. E.; Pilli, R. A., *Bioorg. Med. Chem.* **2005,** *13* 2927–2933.

18. Mosaddik, M. A.; Haque, M. E., *Phytother. Res.* **2003,** *17* 1155–1157.

19. de Fatima, A.; Marquissolo, C.; de Albuquerque, S.; Carraro-Abrahao, A. A.; Pilli, R. A.,

Eur. J. Med. Chem. **2006,** *41* 1210–1213.

20. de Fatima, A.; Kohn, L. K.; Carvalho, J. E.; Pilli, R. A., *Bioorg. Med. Chem.* **2006,** *14* 622–631.

21. (a) Prasad, K. R.; Gholap, S. L., *Tetrahedron Lett.* **2007,** *48* 4679–4682; (b) Veena, B.; Sharma, G., *Synlett* **2014,** *25* 1283–1286; (c) Chen, J.; Lin, G. Q.; Liu, H. Q., *Tetrahedron Letters* **2004,** *45* 8111–8113; (d) Chen, J.; Lin, G.; Wang, Z.; Liu, H., *Synlett* **2002,** *8* 1265–1268.

22. Semprebon, S. C.; de Fatima, A.; Lepri, S. R.; Sartori, D.; Ribeiro, L. R.; Mantovani, M. S., *Hum. Exp. Toxicol.* **2014,** *33* 3–13.

23. de Fatima, A.; Zambuzzi, W. F.; Modolo, L. V.; Tarsitano, C. A.; Gadelha, F. R.; Hyslop, S.; de Carvalho, J. E.; Salgado, I.; Ferreira, C. V.; Pilli, R. A., *Chem. Biol. Interact.* **2008,** *176* 143–150.

24. (a) Biftu, T.; Qian, X.; Chen, P.; Feng, D.; Scapin, G.; Gao, Y. D.; Cox, J.; Roy, R. S.; Eiermann, G.; He, H.; Lyons, K.; Salituro, G.; Patel, S.; Petrov, A.; Xu, F.; Xu, S. S.; Zhang, B.; Caldwell, C.; Wu, J. K.; Lyons, K.; Weber, A. E., *Bioorg. Med. Chem. Lett.* **2013,** *23* 5361–5366; (b) Xu, F.; Zacuto, M. J.; Kohmura, Y.; Rosen, J.; Gibb, A.; Alam, M.; Scott, J.; Tschaen, D., *Org. Lett.* **2014,** *16* 5422–5425.

25. Raubo, P.; Giuliano, C.; Hill, A. W.; Huscroft, I. T.; London, C.; Reeve, A.; Seward, E. M.; Swain, C. G.; Kulagowski, J. J., *Synlett* **2006,** 600–604.

26. Penner, M.; Rauniyar, V.; Kaspar, L. T.; Hall, D. G., *J. Am. Chem. Soc.* **2009,** *131* 14216–14217.

27. (a) Jan, Š.; Hocek, M.; K., P., *Chem. Rev.* **2009,** *109* 6729–6764; (b) Compain, P.; Martin, O. R., *Bioorg. Med. Chem.* **2001,** *9* 3077–3092; (c) Bililign, T.; Griffith, B. R.; Thorson, J. S., *Nat. Prod. Rep.* **2005,** *22* 742–760.

28. Nishikawa, T.; Koide, Y.; Kajii, S.; Wada, K.; Ishikawa, M.; Isobe, M., *Org. Biomol. Chem.* **2005,** *3* 687–700.

29. Frick, W.; Hofmann, J.; Fischer, H.; Schmidt, R. R., *Carbohydr. Res.* **1991,** *210* 71–77.

30. Bajracharya, G. B., *Fitoterapia* **2015,** *101* 133–152.

31. (a) Washburn, W. N., *Expert Opin. Ther. Patents* **2009,** *19* 1485–1499; (b) Hardman, T. C.; Dubrey, S. W., *Diabetes Ther.* **2011,** *2* 133–145.

32. Baldwin, J., *J. Chem. Soc., Chem. Commun.* **1976,** 734–736.

33. Risi, R. M.; Maza, A. M.; Burke, S. D., *J. Org. Chem.* **2014,** *80* 204−216.

34. Nicolaou, K. C.; Duggan, M. E.; Hwang, C. K.; Somers, P. K., *J. Chem. Soc., Chem.*

Commun. **1985,** 1359–1362.

35. Kanemoto, M.; Murata, M.; Oishi, T., *J. Org. Chem.* **2009,** *74* 8810–8813.

36. Nicolaou, K. C.; Seo, J. H.; Nakamura, T.; Aversa, R. J., *J. Am. Chem. Soc.* **2010,** *133* 214–219.

37. Larrosa, I.; Romeab, P.; Urpí, F., *Tetrahedron* **2008,** *64* 2683–2723.

38. Uenishi, J.; Ohmi, M., *Angew. Chem. Int. Ed.* **2005,** *44* 2756–2760.

39. Kriewitz, O., *Ber.* **1899,** *32* 57–60.

40. (a) Prins, H. J., *Chem. Weekbl.* **1919,** *16* 1072–1073; (b) Prins, H. J., *Chem. Weekbl.* **1919,** *16* 1510–1526.

41. Hanschke, E., *Chem. Ber.* **1955,** *88* 1053–1061.

42. Adams, D. R.; Bhatnagar, S. P., *Synthesis* **1977,** *10* 661–672.

43. Olier, C.; Kaafarani, M.; Gastaldi, S.; Bertrand, M. P., *Tetrahedron* **2010,** *66* 413–445.

44. Sultana, S.; Indukuri, K.; Deka, M. J.; Saikia, A. K., *J. Org. Chem.* **2013,** *78* 12182–12188.

45. Ohta, S.; Uy, M. M.; Yanai, M.; Ohta, E.; Hirata, T.; Ikegami, S., *Tetrahedron Lett.* **2006,** *47* 1957–1960.

46. Li, H.; Xie, H.; Zhang, Z.; Xu, Y.; Lu, J.; Gao, L.; Song, Z., *Chem. Commun.* **2015,** *51* 8484–8487.

47. Waldmann, H., *Synthesis* **1994,** 535–551.

48. Diels, O.; Alder, K., *Liebigs Ann. Chem.* **1928,** *460* 98–122.

49. Gresham, T. L.; Steadman, T. R., *J. Am. Chem. Soc.* **1949,** *71* 737–738.

50. Kubler, D. G., *J. Org. Chem.* **1962,** *27* 1435–1436.

51. Danishefsky, S.; Harvey, D. F.; Quallich, G.; Uang, B. J., *J. Org. Chem.* **1984,** *49* 392–393.

52. Jorgensen, K. A., *Angew. Chem. Int. Ed.* **2000,** *39* 3558–3588.

53. Bauer, T.; Chapuis, C.; Kozak, J.; Jurczak, J., *Helv. Chim. Acta* **1989,** *72* 482–486.

54. Dossetter, A. G.; Jamison, T. F.; Jacobsen, E. N., *Angew. Chem. Int. Ed.* **1999,** *38* 2398–2400.

55. Gademann, K.; Chavez, D. E.; Jacobsen, E. N., *Angew. Chem. Int. Ed.* **2002,** *114* 3185–3187.

56. Liu, P.; Jacobsen, E. N., *J. Am. Chem. Soc.* **2001,** *123* 10772–10773.

57. Gao, X.; Hall, D. G., *J. Am. Chem. Soc.* **2003,** *125* 9308–9309.

58. Deligny, M.; Carreaux, F.; Carboni, B.; Toupet, L.; Dujardin, G., *Chem. Commun.* **2003,** 276–277.

59. Deligny, M.; Carreaux, F.; Toupet, L.; Carboni, B., *Adv. Synth. Catal.* **2003,** *345* 1215–1219.

60. Gao, X.; Hall, D. G.; Deligny, M.; Favre, A.; Carreaux, F.; Carboni, B., *Chem. Eur. J.* **2006,** *12* 3132–3142.

61. Carreaux, F.; Deligny, M.; Carboni, B., *Synlett* **2005,** 1462–1464.

62. Favre, A.; Carreaux, F.; Deligny, M.; Carboni, B., *Eur. J. Org. Chem.* **2008,** *2008* 4900–4907.

63. Gao, X.; Hall, D. G., *J. Am. Chem. Soc.* **2005,** *127* 1628– 1629.

64. Fu, G. C.; Grubbs, R. H., *J. Am. Chem. Soc.* **1992,** *114* 5426–5427.

65. De Rosa, S.; Crispino, A.; De Giulio, A.; Iodice, C.; Pronzato, R.; Zavodnik, N., *J. Nat. Prod.* **1995,** *58* 1776−1780.

66. Cheung, A. K.; Murelli, R.; Snapper, M. L., *J. Org. Chem.* **2004,** *69* 5712–5719.

67. Gillingham, D. G.; Kataoka, O.; Garber, S. B.; Hoveyda, A. H., *J. Am. Chem. Soc.* **2004,** *126* 12288–12290.

68. Ibrahem, I.; Yu, M.; Schrock, R. R.; Hoveyda, A. H., *J. Am. Chem. Soc.* **2009,** *131* 3844–3845.

69. Yu, M.; Ibrahem, I.; Hasegawa, M.; Schrock, R. R.; Hoveyda, A. H., *J. Am. Chem. Soc.* **2012,** *134* 2788–2799.

70. Y., M.; Schrock, R. R.; Hoveyda, A. H., *Angew. Chem. Int. Ed.* **2014,** *54* 215–220.

71. Nicotra, F., Synthesis of C-glycosides of biological interest. In *Glycoscience Synthesis of Substrate Analogs and Mimetics*, Driguez, H.; Thiem, J., Eds. Springer Berlin Heidelberg: 1998; Vol. 187, pp 55-83.

72. Frein, J. D.; Rovis, T., *Tetrahedron* **2006,** *62* 4573–4583.

73. Crimmins, M. T.; Stevens, J. M.; Schaaf, G. M., *Org. Lett.* **2009,** *11* 3990–3993.

74. Tate, E. W.; Dixon, D. J.; Ley, S. V., *Org. Biomol. Chem.* **2006,** *4* 1698–1706.

75. Nicolaou, K. C.; Kim, D. W.; Baati, R.; O'Brate, A.; Giannakakou, P., *Chem. Eur. J.* **2003,** *9* 6177–6191.

76. Di Bussolo, V.; Caselli, M.; Pineschi, M.; Crotti, P., *Org. Lett.* **2003,** *5* 2173–2176.

77. Di Bussolo, V.; Favero, L.; Romano, M. R.; Pineschi, M.; Crotti, P., *Tetrahedron* **2008,** *64* 8188–8201.

78. Gómez, A. M.; Lobo, F.; Uriel, C.; López, J. C., *Eur. J. Org. Chem.* **2013,** *2013* 7221–7262.

79. Vieira, A. S.; Fiorante, P. F.; Hough, T. L. S.; Ferreira, F. P.; Lüdtke, D. S.; Stefani, H. A., *Org. Lett.* **2008,** *10* 5215–5218.

80. Dao, H. T.; Schneider, U.; Kobayashi, S., *Chem. Asian J.* **2011,** *6* 2522–2529.

81. Zeng, J.; Ma, J.; Xiang, S.; Cai, S.; Liu, X.-W., *Angew. Chem. Int. Ed.* **2013,** *52* 5134–5137.

82. Díaz-Oltra, S.; Angulo-Pachón, C. A.; Murga, J.; Carda, M.; Marco, J. A., *J. Org. Chem.* **2010,** *75* 1775-1778.

83. Siegel, R. L.; Miller, K. D.; Jemal, A., *Ca-Cancer J. Clin.* **2015,** *65* 5-29.

84. Jordan, M. A.; Wilson, L., *Nat. Rev. Cancer* **2004,** *4* 253–265.

85. Fanale, D.; Bronte, G.; Passiglia, F.; Calo, V.; Castiglia, M.; Di Piazza, F.; Barraco, N.; Cangemi, A.; Catarella, M.; Insalaco, L.; Listi, A.; Maragliano, R.; Massihnia, D.; Perez, A.; Toia, F.; Cicero, G.; Bazan, V., *Anal. Cell. Pathol.* **2015,** *2015* 1–19.

86. Henderson, M., The Story of Taxol: Nature and Politics in the Pursuit of an Anti-Cancer Drug. 2001.

87. *WHO Model List of Essential Medicines* World Health Organization: April 2015.

88. Frishman, W. H.; Sung, H. M.; Yee, H. C. M.; Liu, L. L.; Einzig, A. I.; Dutcher, J.; Keefe, D., *Curr. Probl. Cardiol.* **1996,** *21* 227–286.

89. Alagaratnam, T., *J.-Lancet* **1993,** *342* 1232–1233.

90. Sharma, U. S.; Balasubramanian, S. V.; Straubinger, R. M., *J. Pharm. Sci.* **1995,** *84* 1223-1230.

91. Mooberry, S. L.; Tien, G.; Hernandez, A. H.; Plubrukarn, A.; Davidson, B. S., *Cancer Res.* **1999,** *59* 653–660.

92. Gapud, E. J.; Bai, R.; Ghosh, A. K.; Hamel, E., *Mol. Pharmacol.* **2004,** *66* 113–121.

93. Hamel, E.; Day, B. W.; Miller, J. H.; Jung, M. K.; Northcote, P. T.; Ghosh, A. K.; Curran, D. P.; Cushman, M.; Nicolaou, K. C.; Paterson, I.; Sorensen, E. J., *Mol. Pharmacol.* **2006,** *70* 1555–1564.

94. Clark, E. A.; Hills, P. M.; Davidson, B. S.; Wender, P. A.; Mooberry, S. L., *Mol. Pharm.* **2006,** *3* 457–467.

95. Quinoa, E.; Kakou, Y.; Crews, P., *J. Org. Chem.* **1988,** *53* 3642–3644.

96. Jefford, C. W.; Bernardinelli, G.; Tanaka, J.; Higa, T., *Tetrahedron Lett.* **1996,** *37* 159–162.

97. Pryor, D. E.; O'Brate; Bilcer, G.; Díaz, J. F.; Wang, Y.; Wang, Y.; Kabaki, M.; Jung, M. K.; Andreu, J. M.; Ghosh, A. K.; Giannakakou, P.; Hamel, E., *Biochemistry* **2002,** *41* 9109–9115.

98. Mitchison, T. J., *Annu. Rev. Cell Biol.* **1988,** *4* 527–545.

99. Hayden, J. H.; Bowser, S. S.; Rieder, C. L., *J. Cell Biol.* **1990,** *111* 1039–1045.

100. Alberts, B.; Bray, D.; Hopkin, K.; Johnson, A. D.; Lewis, J.; Raff, M.; Roberts, K.; Walter, P., *Essential Cell Biology*. 4th edition ed.; Garland Science: New York, 2013.

101. Bennett, M. J.; Barakat, K.; Huzil, J. T.; Tuszynski, J.; Schriemer, D. C., *Chemistry & Biology* **2010,** *17* 725–734.

102. Engen, J. R., *Anal. Chem.* **2009,** *81* 7870–7875.

103. Percy, A. J.; Rey, M.; Burns, K. M.; Schriemer, D. C., *Anal. Chim. Acta* **2012,** *721* 7–21.

104. Englander, S. W.; Mayne, L.; Bai, Y.; Sosnick, T. R., *Protein Sci.* **1997,** *6* 1101–1109.

105. Konermann, L.; Pan, J.; Liu, Y., *Chem. Soc. Rev.* **2011,** *40* 1224–1234.

106. Lee, J.; Park, Y.; Lee, K., *Arch. Pharmacal Res.* **2015,** *38* 1737–1745.

107. (a) Gallagher, B. M.; Fang, F. G.; Johannes, C. W.; Pesant, M.; Tremblay, M. R.; Zhao, H.; Akasaka, K.; Li, X.; Liu, J. G.; Littlefield, B. A., *Bioorg. Med. Chem. Lett.* **2004,** *14* 575–579; (b) Faveau, C.; Mondon, M.; Gesson, J.; Mahnke, T.; Gebhardt, S.; Koert, U., *Tetrahedron Lett.* **2006,** *47* 8305–8308; (c) Gollner, A.; Altmann, K. H.; Gertsch, J.; Mulzer, J., *Chemistry* **2009,** *15* 5979–5997; (d) Wender, P. A.; Hegde, S. G.; Hubbard, R. D.; Zhang, L.; Mooberry, S. L., *Org. Lett.* **2003,** *5* 3507–3509; (e) Wender, P. A.; Hilinski, M. K.; Soldermann, N.; Mooberry, S. L., *Org. Lett.* **2006,** *8* 1507–1510; (f) Paterson, I.; Menche, D.; Håkansson, A. E.; Longstaff, A.; Wong, D.; Barasoain, I.; Buey, R. M.; Díaz, J. F., *Bioorg. Med. Chem. Lett.* **2005,** *15* 2243–2247.

108. Prota, A. E.; Bargsten, K.; Northcote, P. T.; Marsh, M.; Altmann, K.-H.; Miller, J. H.; Díaz, J. F.; Steinmetz, M. O., *Angew. Chem. Int. Ed.* **2014,** *53* 1621–1625.

109. Wender, P. A.; Verma, V. A.; Paxton, T. J.; Pillow, T. H., *Acc. Chem. Res.* **2008,** *41* 40–49.

110. Tanaka, J.; Higa, T.; Bernardinelli, G.; Jefford, C. W., *Chem. Lett.* **1996,** *25* 255–256.

111. Wender, P. A.; Baryza, J. L.; Bennett, C. E.; Bi, F. C.; Brenner, S. E.; Clarke, M. O.; Horan, J. C.; Kan, C.; Lacôte, E.; Lippa, B.; Nell, P. G.; Turner, T. M., *J. Am. Chem. Soc.* **2002,** *124* 13648–13649.

112. Ahmed, A.; Hoegenauer, E. K.; Enev, V. S.; Hanbauer, M.; Kaehlig, H.; Mulzer, J., *J. Org. Chem.* **2003,** *68* 3026–3042.

113. Gollner, A.; Altmann, K. H.; Gertsch, J.; Mulzer, J., *Tetrahedron Lett.* **2009,** *50* 5790–5792.

114. Wender, P. A.; Hilinski, M. K.; Skaanderup, P. R.; Soldermann, G. S.; Mooberry, S. L., *Org. Lett.* **2006,** *8* 4105–4108.

115. Bollag, D. M.; McQueney, P. A.; Zhu, J.; Hensens, O.; Koupal, L.; Liesch, J.; Goetz, M.; Lazarides, E.; Woods, C. M., *Cancer Res.* **1995,** *55* 2325–2333.

116. Hoye, T. R.; Jeffrey, C. S.; Shao, F., *Nat. Protocols* **2007,** *2* 2451–2458.

117. Voigtritter, K.; Ghorai, S.; Lipshutz, B. H., *J. Org. Chem.* **2011,** *76* 4697–4702.

118. Chatterjee, A. K.; Choi, T.; Sanders, D. P.; Grubbs, R. H., *J. Am. Chem. Soc.* **2003,** *125* 11360–11370.

119. Xing, C.; Liao, Y.; Zhang, Y.; Sabarova, D.; Bassous, M.; Hu, Q., *Eur. J. Org. Chem.* **2012,** *2012* 1115–1118.

120. Jain, P.; Antilla, J. C., *J. Am. Chem. Soc.* **2010,** *132* 11884–11886.

121. Shiina, I.; Kikuchi, T.; Sasaki, A., *Org. Lett.* **2006,** *8* 4955–4958.

122. Judd, W. R.; Ban, S.; Aubé, J., *J. Am. Chem. Soc.* **2006,** *128* 13736–13741.

123. (a) Kato, Y.; Hashimoto, Y.; Nagasawa, K., *Molecules* **2003,** *8* 488–499; (b) Kato, Y.; Nakano, Y.; Sano, H.; Tanatani, A.; Kobayashi, H.; Shimazawa, R.; Koshino, H.; Hashimoto, Y.; Nagasawa, K., *Bioorg. Med. Chem. Lett.* **2004,** *14* 2579–2583.

124. Yang, S.; Kang, T.; Rui, C.; Yang, X.; Sun, Y.; Cui, Z.; Ling, Y., *Chin. J. Chem.* **2011,** *29* 2394–2400.

125. de la Pradilla, R. F.; Lwoff, N.; Viso, A., *Eur. J. Org. Chem.* **2009,** *2009* 2312–2322.

126. Lalitha, K.; Muthusamy, K.; Prasad, Y. S.; Vemula, P. K.; Nagarajan, S., *Carbohydr. Res.* **2015,** *402* 158–171.

127. (a) Ramnauth, J.; Poulin, O.; Rakhit, S.; Maddaford, S. P., *Org. Lett.* **2001,** *3* 2013–2015;

(b) Bai, Y.; Kim, L. M. H.; Liao, H.; Liu, X. W., *J. Org. Chem.* **2013,** *78* 8821–8825; (c) Bai, Y.; Leow, M. L.; Zeng, J.; Liu, X.-W., *Org. Lett.* **2011,** *13* 5648–5651.

128. (a) Farr, R. N.; Outten, R. A.; Cheng, J. C. Y.; Daves, G. D., *Organometallics* **1990,** *9* 3151–3156; (b) Kwok, D. L.; Farr, R. N.; Daves, G. D., *J. Org. Chem.* **1991,** *56* 3711–3713; (c) Lei, M.; Gao, L.; Yang, J. S., *Tetrahedron Lett.* **2009,** *50* 5135–5138; (d) Xiang, S.; Cai, S.; Zeng, J.; Liu, X. W., *Org. Lett.* **2011,** *13* 4608–4611.

129. Leidy, M. R.; Hoffman, J. M.; Pongdee, R., *Tetrahedron Lett.* **2013,** *54* 6889–6891.

130. Bower, J. F.; Guillaneux, D.; Nguyen, T.; Wong, P. L.; Snieckus, V., *J. Org. Chem.* **1998,** *63* 1514–1518.

131. Sakamaki, S.; Kawanishi, E.; Nomura, S.; Ishikawa, T., *Tetrahedron* **2012,** *68* 5744–5753.

132. Friesen, R. W.; Loo, R. W.; Sturino, C. F., *Can. J. Chem.* **1994,** *72* 1262–1272.

133. Ousmer, M.; Boucard, V.; Lubin-Germain, N.; Uziel, J.; Augé, J., *Eur. J. Org. Chem.* **2006,** *2006* 1216–1221.

134. (a) Gong, H.; Gagné, M. R., *J. Am. Chem. Soc.* **2008,** *130* 12177–12183; (b) Gong, H.; Sinisi, R.; Gagné, M. R., *J. Am. Chem. Soc.* **2007,** *129* 1908–1909.

135. Ito, H.; Kunii, S.; Sawamura, M., *Nat. Chem.* **2010,** *2* 972–976.

136. Leonori, D.; Aggarwal, V. K., *Acc. Chem. Res.* **2014,** *47* 3174–3183.

137. Jana, R.; Pathak, T. P.; Sigman, M. S., *Chem. Rev.* **2011,** *111* 1417–1492.

138. Leonori, D.; Aggarwal, V. K., *Angew. Chem. Int. Ed.* **2015,** *54* 1082–1096.

139. Ridgway, B. H.; Woerpel, K. A., *J. Org. Chem.* **1998,** *63* 458–460.

140. Matos, K.; Soderquist, J. A., *J. Org. Chem.* **1998,** *63* 461–470.

141. Taylor, B. L. H.; Jarvo, E. R., *J. Org. Chem.* **2011,** *76* 7573–7576.

142. Mlynarski, S. N.; Schuster, C. H.; Morken, J. P., *Nature* **2014,** *505* 386–390.

143. Hildebrand, J. P.; Marsden, S. P., *Synlett* **1996,** *1996* 893–894.

144. (a) Fang, G.; Yan, Z.; Deng, M., *Org. Lett.* **2004,** *6* 357–360; (b) Charette, A. B.; Mathieu, S.; Fournier, J., *Synlett* **2005,** *2005* 1779–1782.

145. Imao, D.; Glasspoole, B. W.; Laberge, V. S.; Crudden, C. M., *J. Am. Chem. Soc.* **2009,** *131* 5024–5025.

146. (a) Uenishi, J.; Beau, J. M.; Armstrong, R. W.; Kishi, Y., *J. Am. Chem. Soc.* **1987,** *109*

4756–4758; (b) Hirabayashi, K.; Kawashima, J.; Nishihara, Y.; Mori, A.; Hiyama, T., *Org. Lett.* **1999,** *1* 299–302.

147. Crudden, C. M.; Glasspoole, B. W.; Oderinde, M.; Moore, B.; Antoft-Finch, A., *Synthesis* **2013,** *45* 1759–1763.

148. Chausset-Boissarie, L.; Ghozati, K.; LaBine, E.; Chen, J. L.; Aggarwal, V. K.; Crudden, C. M., *Chem. Eur. J.* **2013,** *19* 17698–17701.

149. Molander, G. A.; Wisniewski, S. R., *J. Am. Chem. Soc.* **2012,** *134* 16856–16868.

150. Ohmura, T.; Awano, T.; Suginome, M., *J. Am. Chem. Soc.* **2010,** *132* 13191–13193.

151. Sandrock, D. L.; Jean-Gérard, L.; Chen, C.; Dreher, S. D.; Molander, G. A., *J. Am. Chem. Soc.* **2010,** *132* 17108–17110.

152. Awano, T.; Ohmura, T.; Suginome, M., *J. Am. Chem. Soc.* **2011,** *133* 20738–20741.

153. (a) Lee, J. C. H.; McDonald, R.; Hall, D. G., *Nat. Chem.* **2011,** *3* 894–899; (b) Lee, J. C.; Sun, H. Y.; Hall, D. G., *J. Org. Chem.* **2015,** *80* 7134–7143.

154. Yamamoto, Y.; Takada, S.; Miyaura, N., *Chem. Lett.* **2006,** *35* 704–705.

155. Sebelius, S.; Olsson, V. J.; Wallner, O. A.; Szabó, K. J., *J. Am. Chem. Soc.* **2006,** *128* 8150−8151.

156. Yamamoto, Y.; Takada, S.; Miyaura, N.; Iyama, T.; Tachikawa, H., *Organometallics* **2009,** *28* 152–160.

157. Farmer, J. L.; Hunter, H. N.; Organ, M. G., *J. Am. Chem. Soc.* **2012,** *134* 17470–17473.

158. Glasspoole, B. W.; Ghozati, K.; Moir, J. W.; Crudden, C. M., *Chem. Commun.* **2012,** *48* 1230–1232.

159. Denmark, S. E.; Werner, N. S., *J. Am. Chem. Soc.* **2010,** *132* 3612–3620.

160. Yang, Y.; Buchwald, S. L., *J. Am. Chem. Soc.* **2013,** *135* 10642–10645.

161. Lessard, S.; Peng, F.; Hall, D. G., *J. Am. Chem. Soc.* **2009,** *131* 9612–9613.

162. (a) Suzuki, A., *J. Organomet. Chem.* **1999,** *576* 147–168; (b) Carrow, B. P.; Hartwig, J. F., *J. Am. Chem. Soc.* **2011,** *133* 2116–2119.

163. (a) Lennox, A. J.; Lloyd-Jones, G. C., *Angew. Chem. Int. Ed.* **2013,** *52* 7362–7370; (b) Lennox, A. J. J.; Lloyd-Jones, G. C., *Chem. Soc. Rev.* **2014,** *43* 412–443.

164. Ding, J.; Rybak, T.; Hall, D. G., *Nat. Commun.* **2014,** *5*.

165. Huang, X.; Anderson, K. W.; Zim, D.; Jiang, L.; Klapars, A.; Buchwald, S. L., *J. Am.*

Chem. Soc. **2003,** *125* 6653–6655.

166. Surry, D. S.; Buchwald, S. L., *Chem. Sci.* **2011,** *2* 27–50.

167. (a) Brown, E.; Dujardin, G.; Maudet, M., *Tetrahedron* **1997,** *53* 9679–9694; (b) Postema, M. H. D.; Piper, J. L.; Liu, L.; Shen, J.; Faust, M.; Andreana, P., *J. Org. Chem.* **2003,** *68* 4748–4754; (c) Huang, C.; Liu, R.; Wu, T.; Cheng, W., *Tetrahedron Lett.* **2008,** *49* 2895–2898.

168. (a) Fakha, G.; Sinou, D., *Molecules* **2005,** *10* 859–870; (b) She, X.; Xie, X.; Li, J.; Zheng, H.; Su, Y., *Synlett* **2010,** *2010* 2283–2284.

169. Beng, T. K.; Gawley, R. E., *Org. Lett.* **2011,** *13* 394–397.

170. (a) Amat, M.; Bosch, J.; Hidalgo, J.; Cantó, M.; Pérez, M.; Llor, N.; Molins, E.; Miravitlles, C.; Orozco, M.; Luque, J., *J. Org. Chem.* **2000,** *65* 3074–3084; (b) de Gonzalo, G.; Brieva, R.; Sánchez, V. M.; Bayod, M.; Gotor, V., *J. Org. Chem.* **2001,** *66* 8947–8953.

171. Diao, T.; Stahl, S. S., *J. Am. Chem. Soc.* **2011,** *133* 14566–14569.

172. Ito, H.; Kawakami, C.; Sawamura, M., *J. Am. Chem. Soc.* **2005,** *127* 16034–16035.

173. Dutheuil, G.; Selander, N.; Szabó, K. J.; Aggarwal, V. K., *Synthesis* **2008,** 2293–2297.

174. (a) Pregosin, P. S.; Salzmann, R., *Coord. Chem. Rev.* **1996,** *155* 35–68; (b) Trost, B. M.; Van Vranken, D. L., *Chem. Rev.* **1996,** *96* 395–422.

175. Spring, D. R., *Org. Biomol. Chem.* **2003,** *1* 3867–3870.

176. Ireland, T.; Tappe, K.; Grossheimann, G.; Knochel, P., *Chem. Eur. J.* **2002,** *8* 843–852.

177. (a) Romero, J. A. C.; Tabacco, S. A.; Woerpel, K. A., *J. Am. Chem. Soc.* **2000,** *122* 168–169; (b) Ayala, L.; Lucero, C. G.; Romero, J. A. C.; Tabacco, S. A.; Woerpel, K. A., *J. Am. Chem. Soc.* **2003,** *125* 15521–15528.

178. (a) Woods, R. J.; Andrews, C. W.; Bowen, J. P., *J. Am. Chem. Soc.* **1992,** *114* 859–864; (b) Miljković, M.; Yeagley, D.; Deslongchamps, P.; Dory, Y. L., *J. Org. Chem.* **1997,** *62* 7597–7604.

179. Martin, R.; Buchwald, S. L., *Acc. Chem. Res.* **2008,** *41* 1461–1473.

180. Hartwig, J. F., *Inorg. Chem.* **2007,** *46* 1936–1947.

181. (a) Venkataiah, M.; Somaiah, P.; Reddipalli, G.; Fadnavis, N. W., *Tetrahedron: Asymmetry* **2009,** *20* 2230–2233; (b) Yadav, J. S.; Rao, R. N.; Somaiah, R.; Harikrishna, V.; Reddy, B. V. S., *Helv. Chim. Acta* **2010,** *93* 1362–1368; (c) Sabitha, G.; Rammohan R., T.; Yadav, J. S., *Tetrahedron Lett.* **2011,** *52* 6550–6553; (d) Thakur, P.; Boyapelly, K.;

Gurram, R. R.; Bandichhor, R.; Mukkanti, K., *Tetrahedron: Asymmetry* **2012,** *23* 659–661.

182. Anada, M.; Washio, T.; Watanabe, Y.; Takeda, K.; Hashimoto, S., *Eur. J. Org. Chem.* **2010,** *2010* 6850–6854.

183. (a) Huang, H.; Panek, J. S., *Org. Lett.* **2001,** *3* 1693–1696; (b) Su, Q.; Panek, J. S., *J. Am. Chem. Soc.* **2004,** *126* 2425–2430.

184. Sawant, K. B.; Jennings, M. P., *J. Org. Chem.* **2006,** *71* 7911−7914.

185. (a) Kawai, N.; Hande, S. M.; Uenishi, J., *Tetrahedron* **2007,** *63* 9049–9056; (b) Sabitha, G.; Padmaja, P.; Yadav, J. S., *Helv. Chim. Acta* **2008,** *91* 2235–2239; (c) Wang, H. M.; Shuhler, B. J.; Xian, M., *Synlett* **2008,** *2008* 2651–2654; (d) Kumaraswamy, G.; Ramakrishna, G.; Naresh, P.; Jagadeesh, B.; Sridhar, B., *J. Org. Chem.* **2009,** *74* 8468–8471; (e) Stefan, E.; Nalin, A. P.; Taylor, R. E., *Tetrahedron* **2013,** *69* 7706–7712.

186. Ainsworth, C.; Chen, F.; Kuo, Y., *J. Organomet. Chem.* **1972,** *46* 59–71.

187. Cazeau, P.; Duboudin, F.; Moulines, F.; Babot, O.; Dunogues, J., *Tetrahedron* **1987,** *43* 2075–2088.

Appendices

Appendix 1: Selected copies of NMR spectra

^{1}H and ^{13}C spectrum for 2-34a in $CDCl_3$ at 25 ^{o}C

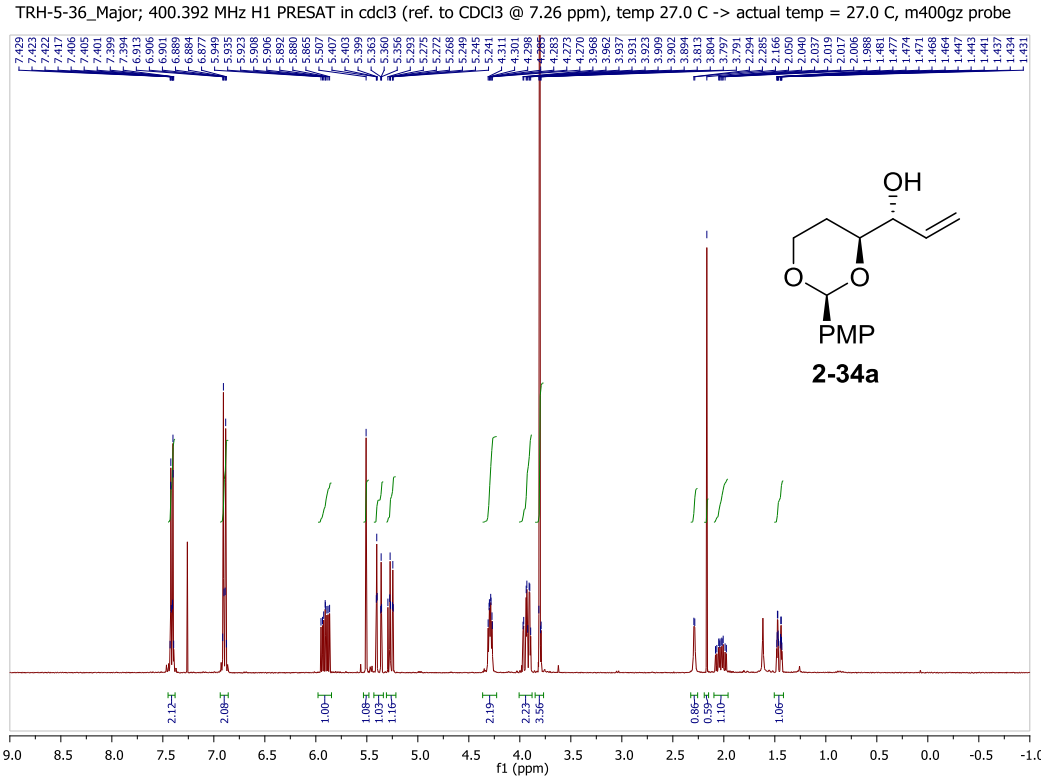

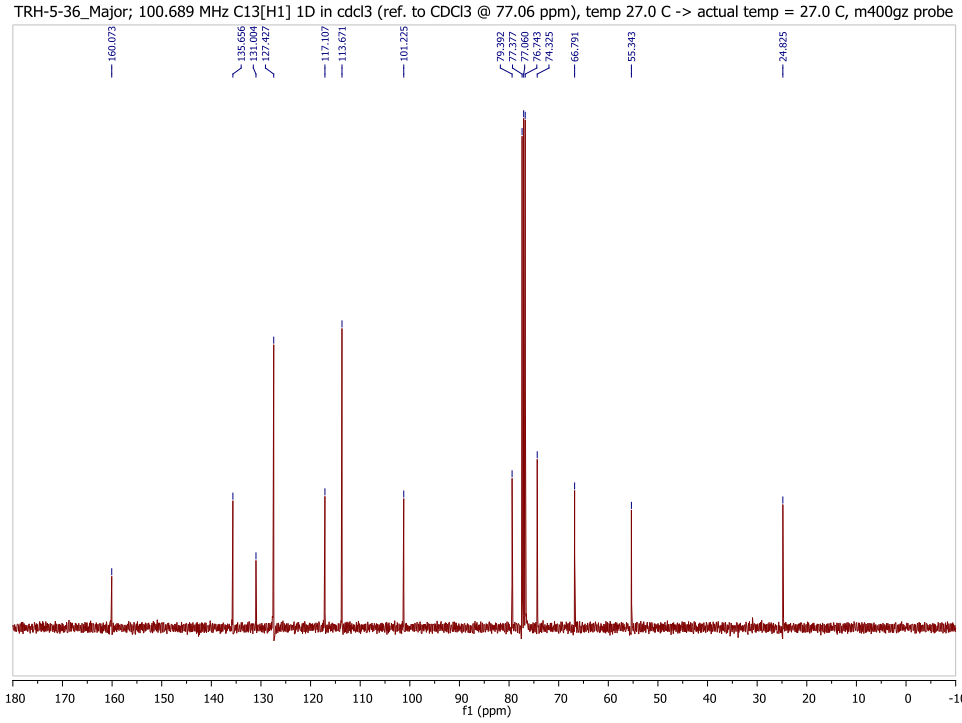

^{1}H and ^{13}C spectrum for 2-34b in $CDCl_3$ at 25 ^{o}C

TRH-5-36-Minor Diastereomer 699.769 MHz H1 PRESAT in cdcl3 (ref. to CDCl3 @ 7.26 ppm), temp 27.5 C -> actual temp = 27.0 C, coldid probe

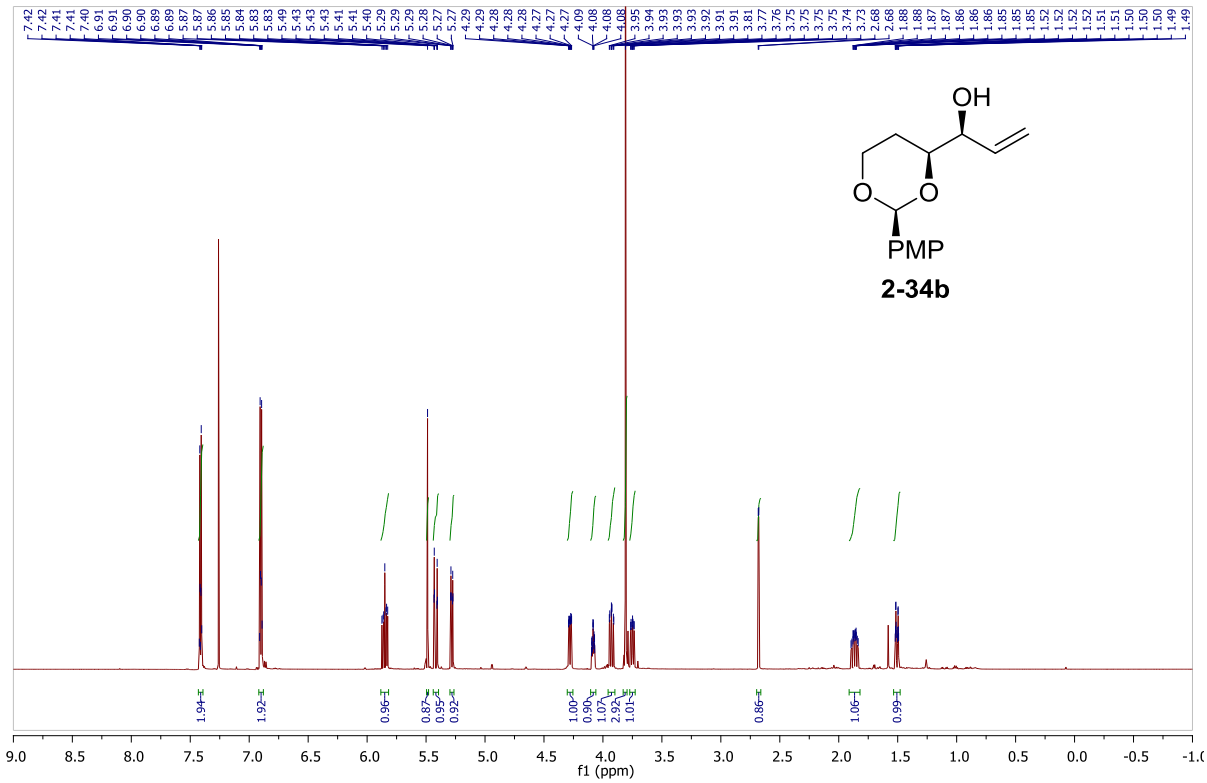

TRH-5-36_Minor_Diastereomer 175.976 MHz C13[H1] 1D in cdcl3 (ref. to CDCl3 @ 77.06 ppm), temp 27.5 C -> actual temp = 27.0 C, coldid probe

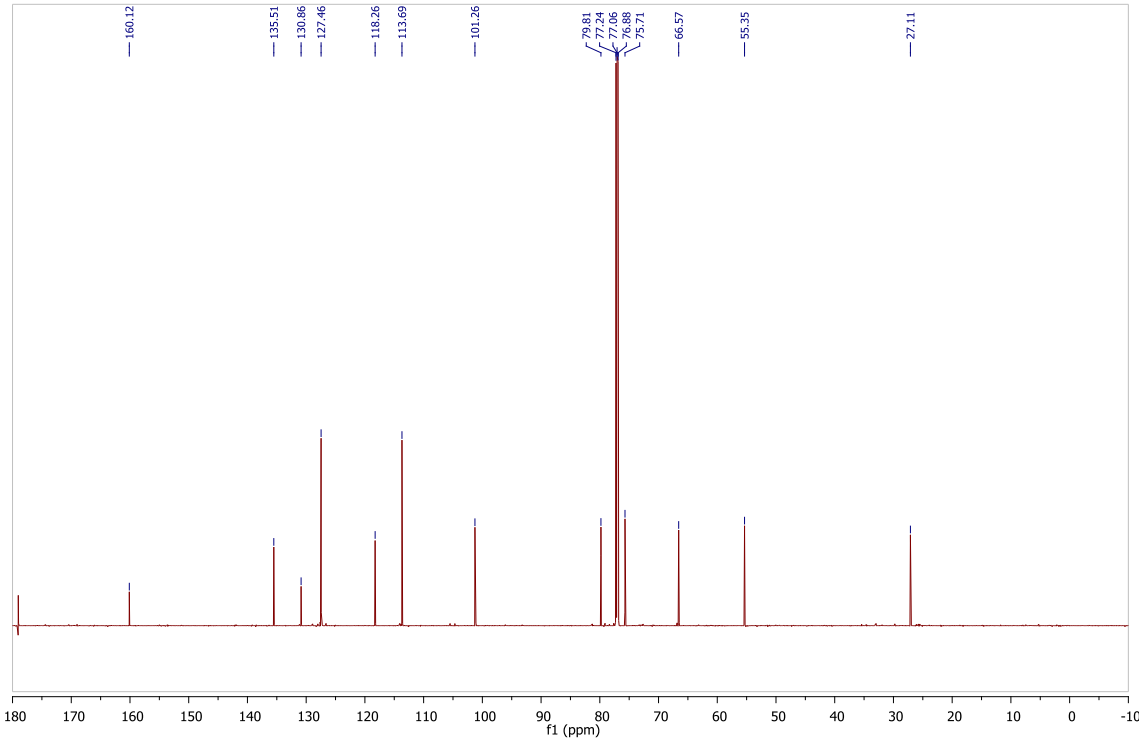

^{1}H and ^{13}C spectrum for 2-36a in $CDCl_3$ at 25 ^{o}C

TRH-6-101; 499.806 MHz H1 PRESAT in cdcl3 (ref. to CDCl3 @ 7.26 ppm), temp 27.7 C -> actual temp = 27.0 C, colddual probe

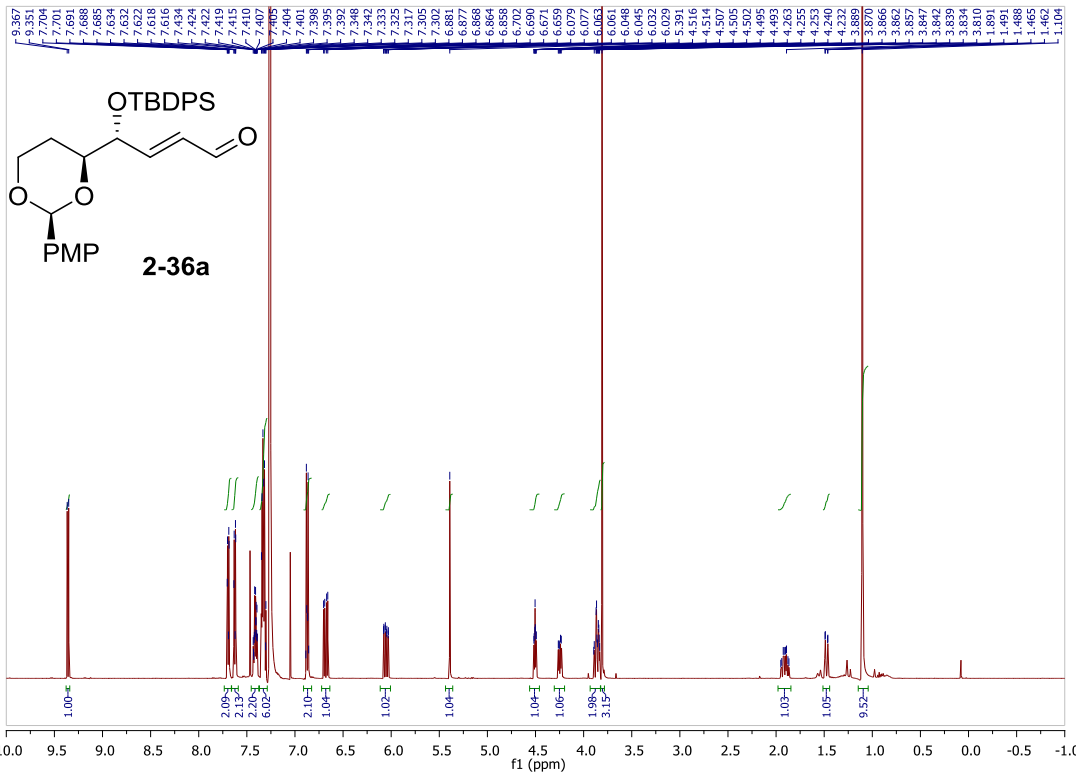

TRH-6-101; 125.691 MHz C13[H1] 1D in cdcl3 (ref. to CDCl3 @ 77.06 ppm), temp 27.7 C -> actual temp = 27.0 C, colddual probe

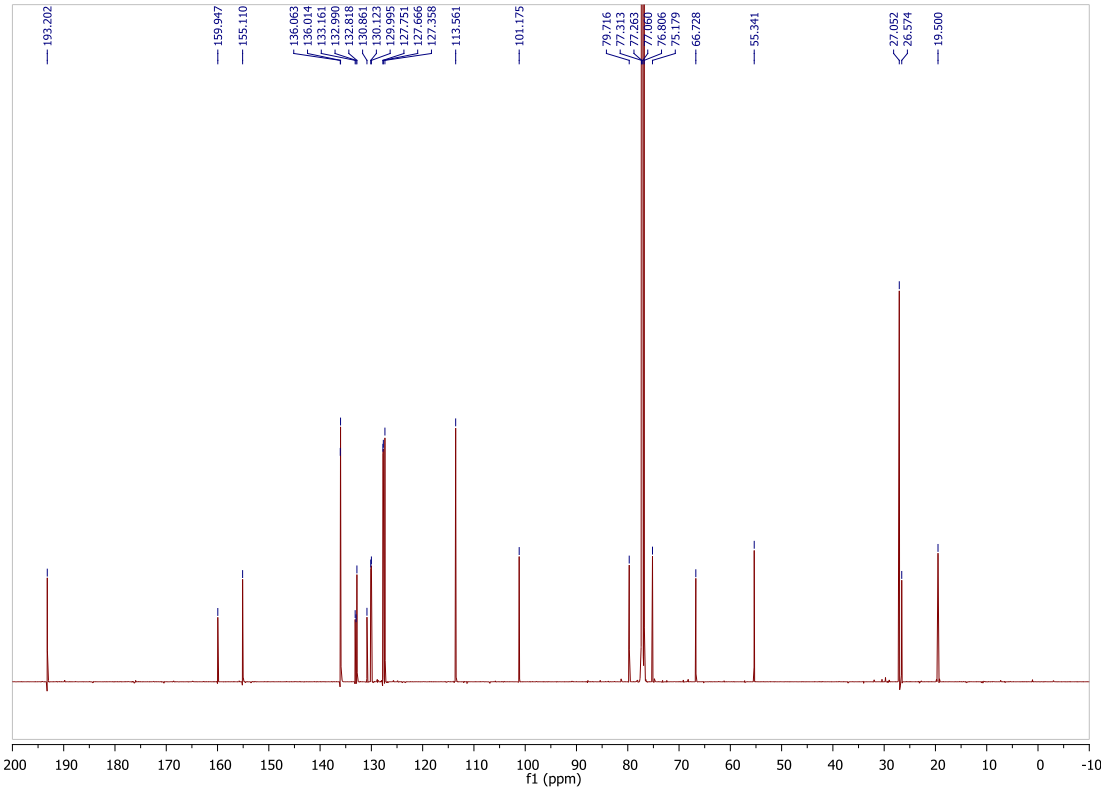

^{1}H and ^{13}C spectrum for 2-36b in $CDCl_3$ at 25 ^{o}C

TRH-11-141; 499.806 MHz H1 PRESAT in cdcl3 (ref. to CDCl3 @ 7.26 ppm), temp 27.7 C -> actual temp = 27.0 C, colddual probe

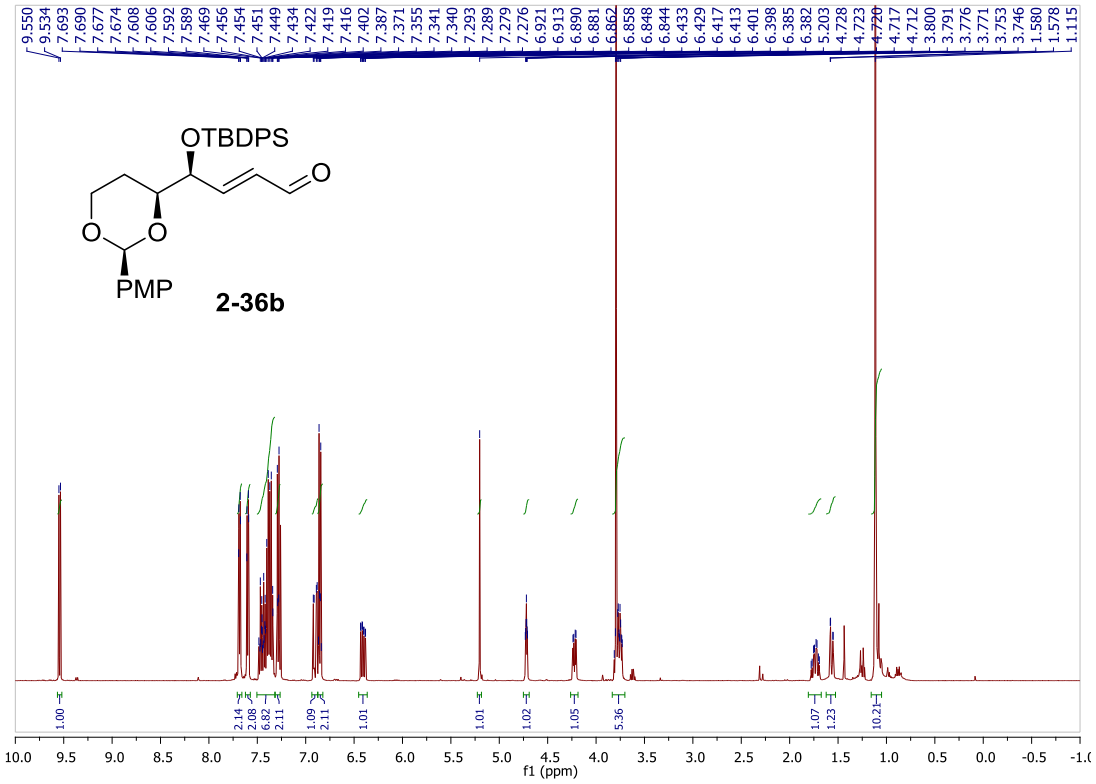

TRH-11-141; 125.691 MHz C13[H1] 1D in cdcl3 (ref. to CDCl3 @ 77.06 ppm), temp 27.7 C -> actual temp = 27.0 C, colddual probe

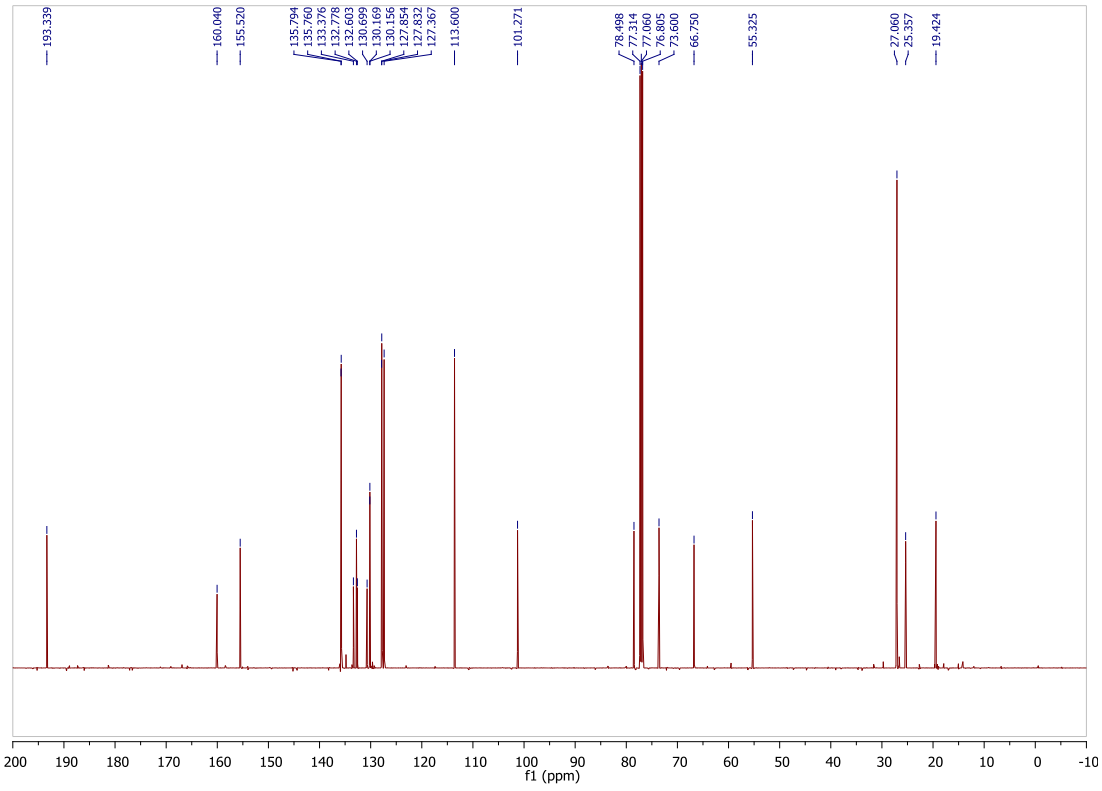

^{1}H (C_6D_6) and ^{13}C spectrum ($CDCl_3$) for 2-37a at 25 ^{o}C

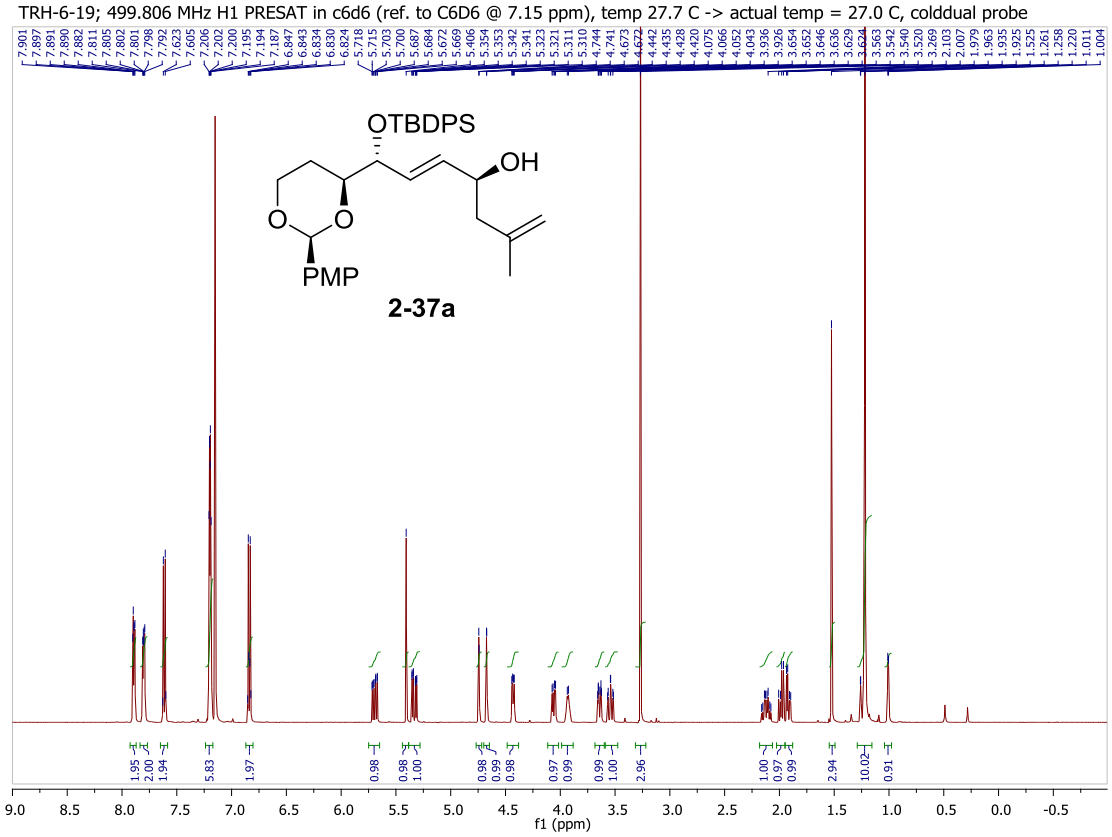

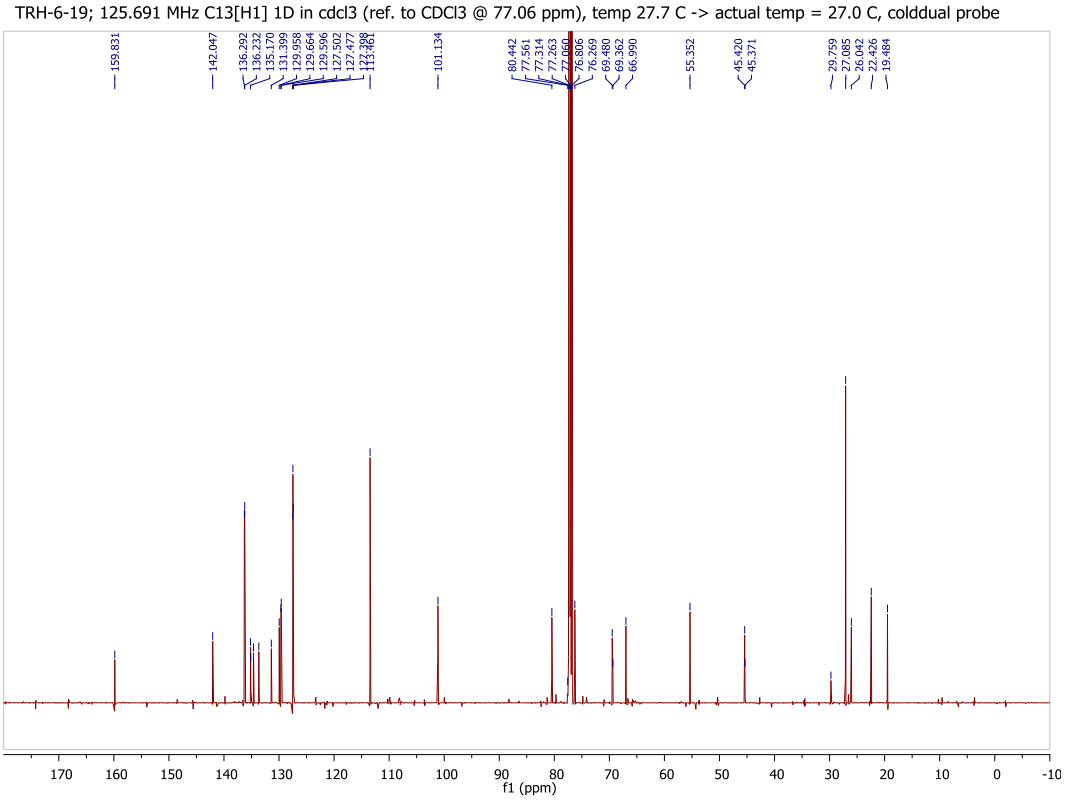

^{1}H (C_6D_6) and ^{13}C spectrum ($CDCl_3$) for 2-37b at 25 ^{o}C

TRH-11-155; 699.769 MHz H1 PRESAT in c6d6 (ref. to C6D6 @ 7.15 ppm), temp 27.5 C -> actual temp = 27.0 C, coldid probe

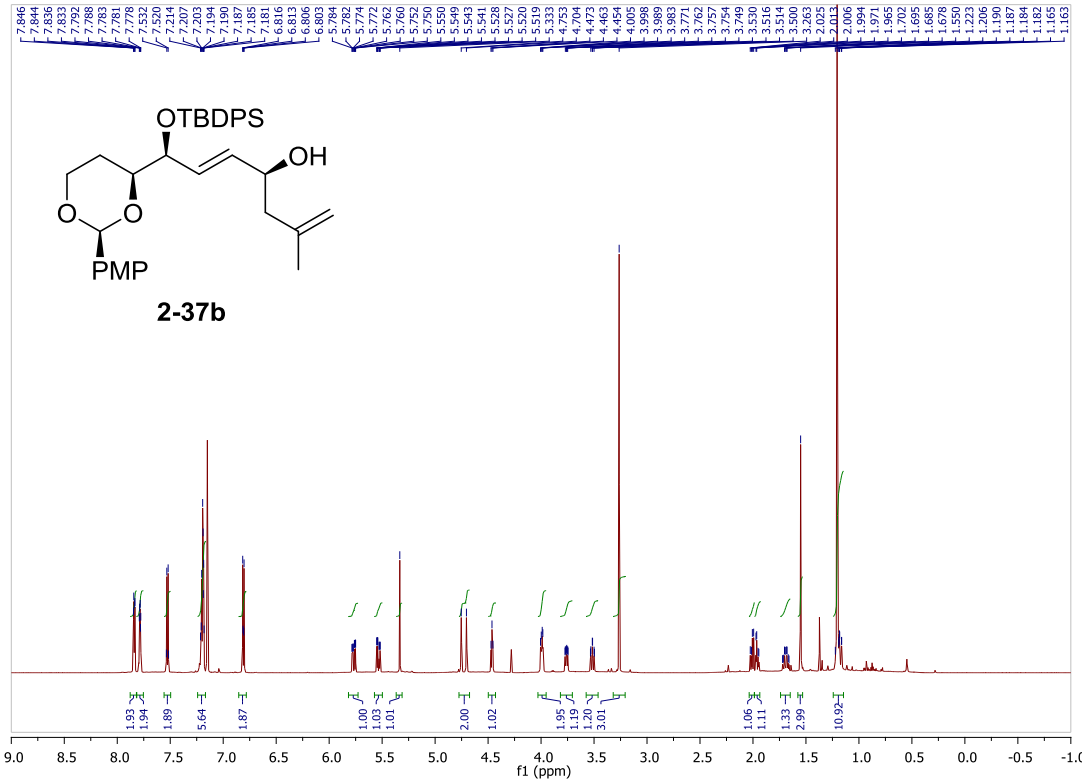

TRH-11-155; 125.691 MHz C13[H1] 1D in cdcl3 (ref. to CDCl3 @ 77.06 ppm), temp 27.7 C -> actual temp = 27.0 C, colddual probe

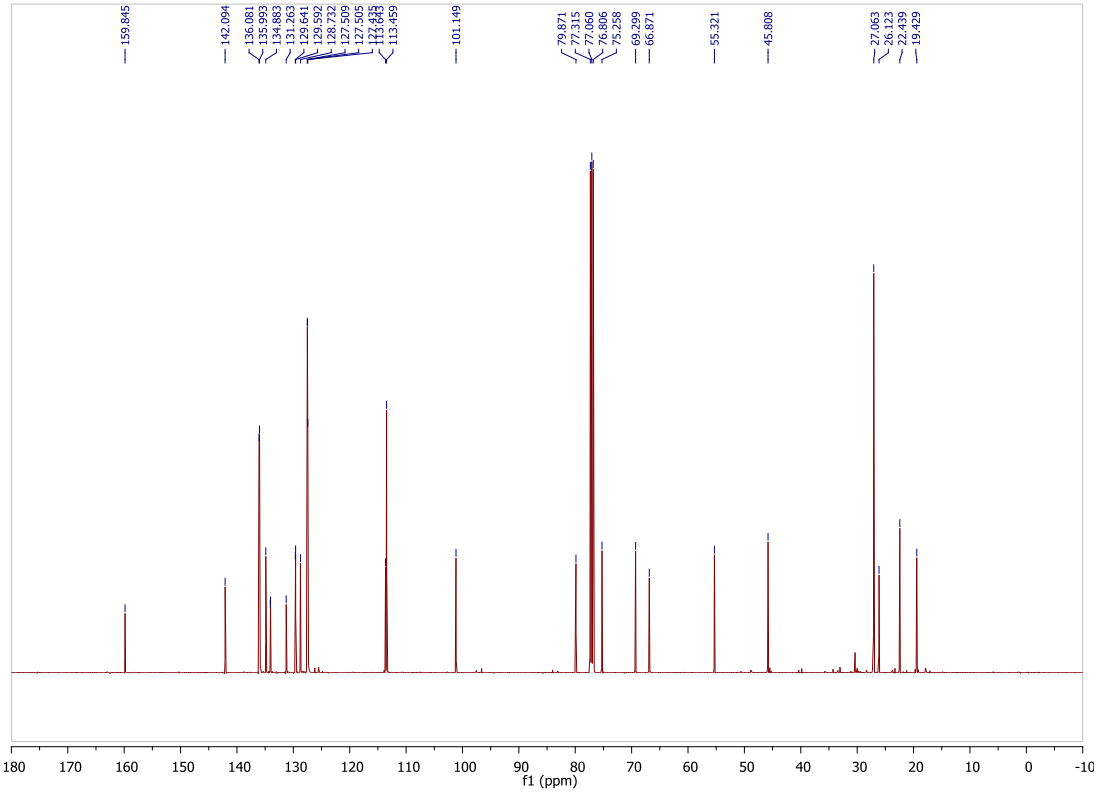

^{1}H and ^{13}C spectrum for 2-38b in $CDCl_3$ at 25 ^{o}C

TRH-11-169; 499.806 MHz H1 PRESAT in cdcl3 (ref. to CDCl3 @ 7.26 ppm), temp 27.7 C -> actual temp = 27.0 C, colddual probe

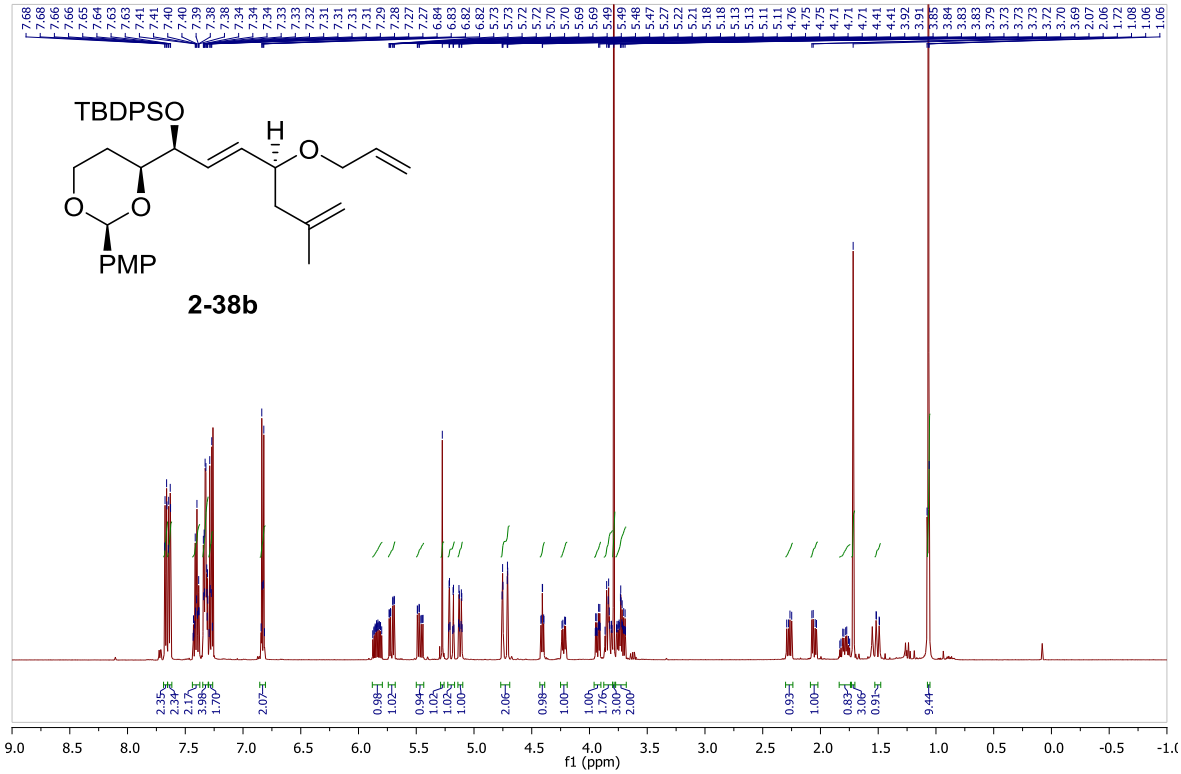

TRH-11-169; 125.691 MHz C13[H1] 1D in cdcl3 (ref. to CDCl3 @ 77.06 ppm), temp 27.7 C -> actual temp = 27.0 C, colddual probe

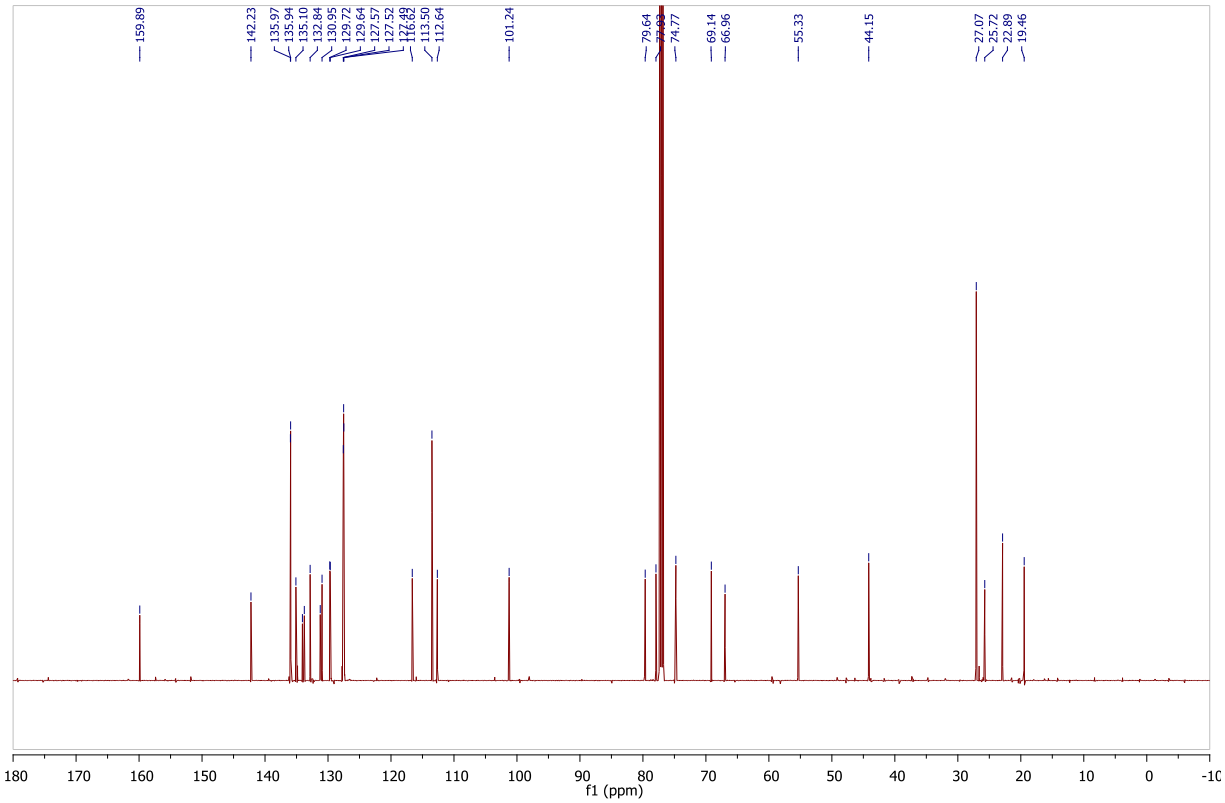

^{1}H and ^{13}C spectrum for 2-39a in $CDCl_3$ at 25 ^{o}C

TRH-7-57; 499.806 MHz H1 PRESAT in c6d6 (ref. to C6D6 @ 7.15 ppm), temp 27.7 C -> actual temp = 27.0 C, colddual probe

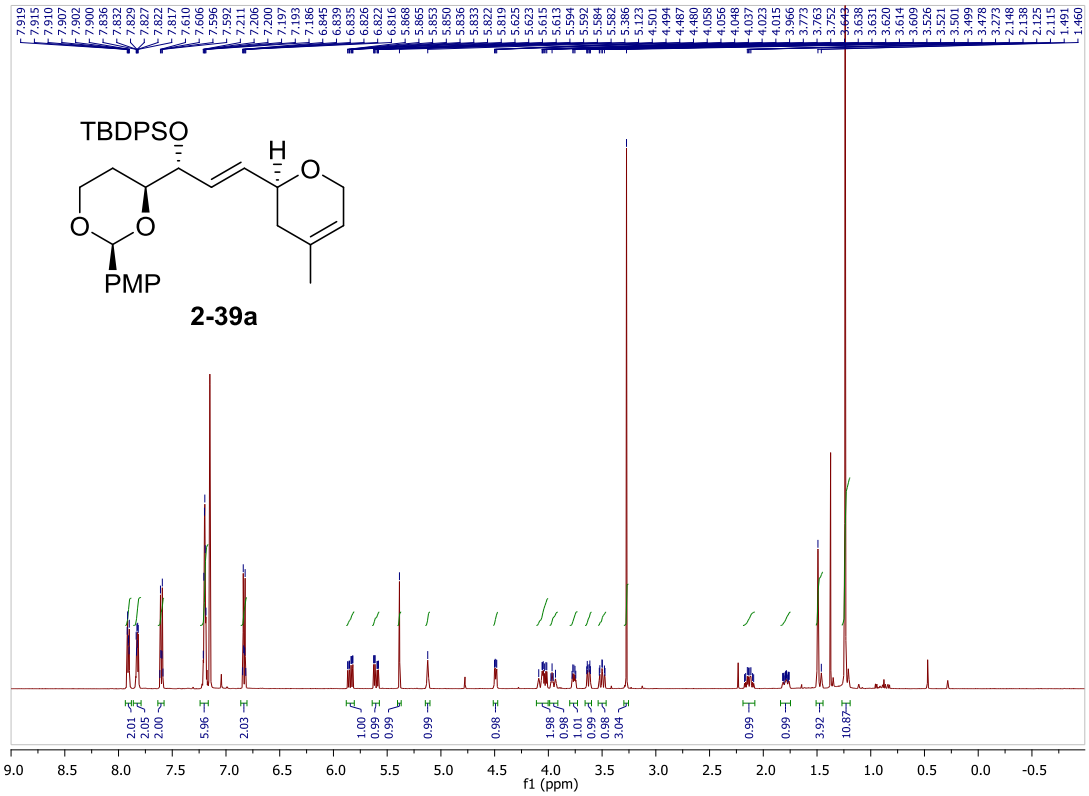

TRH-7-57; 125.691 MHz C13[H1] 1D in c6d6 (ref. to C6D6 @ 128.0 ppm), temp 27.7 C -> actual temp = 27.0 C, colddual probe

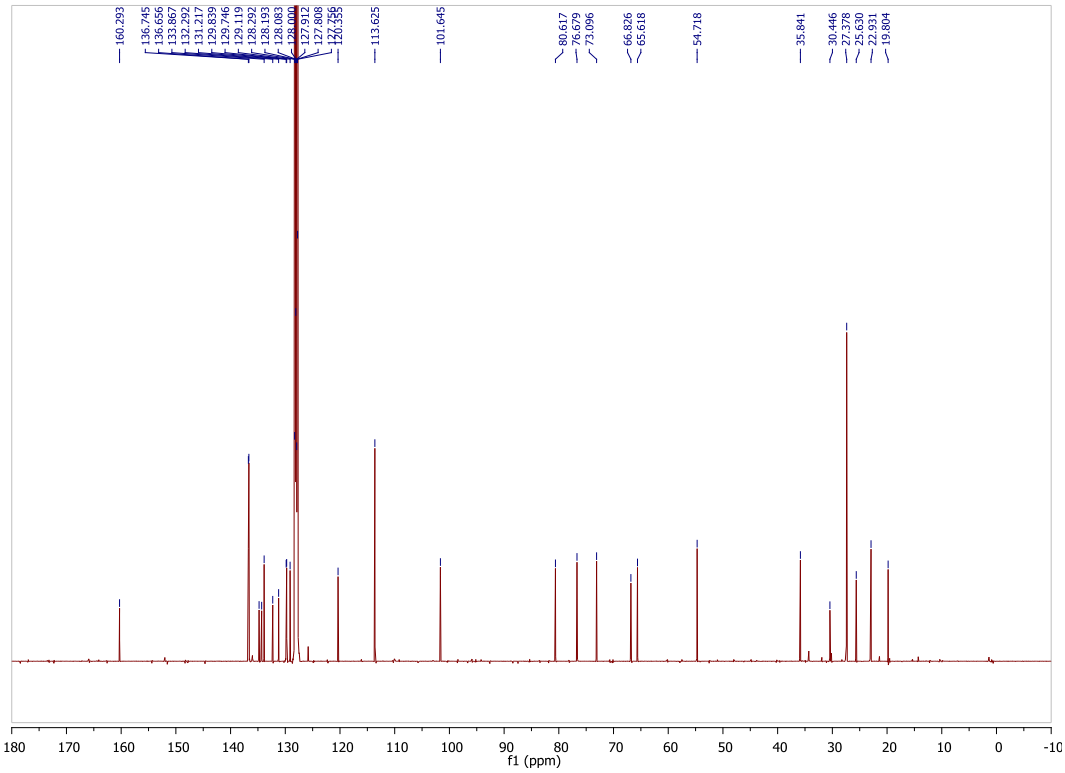

^{1}H and ^{13}C spectrum for 2-39b in $CDCl_3$ at 25 ^{o}C

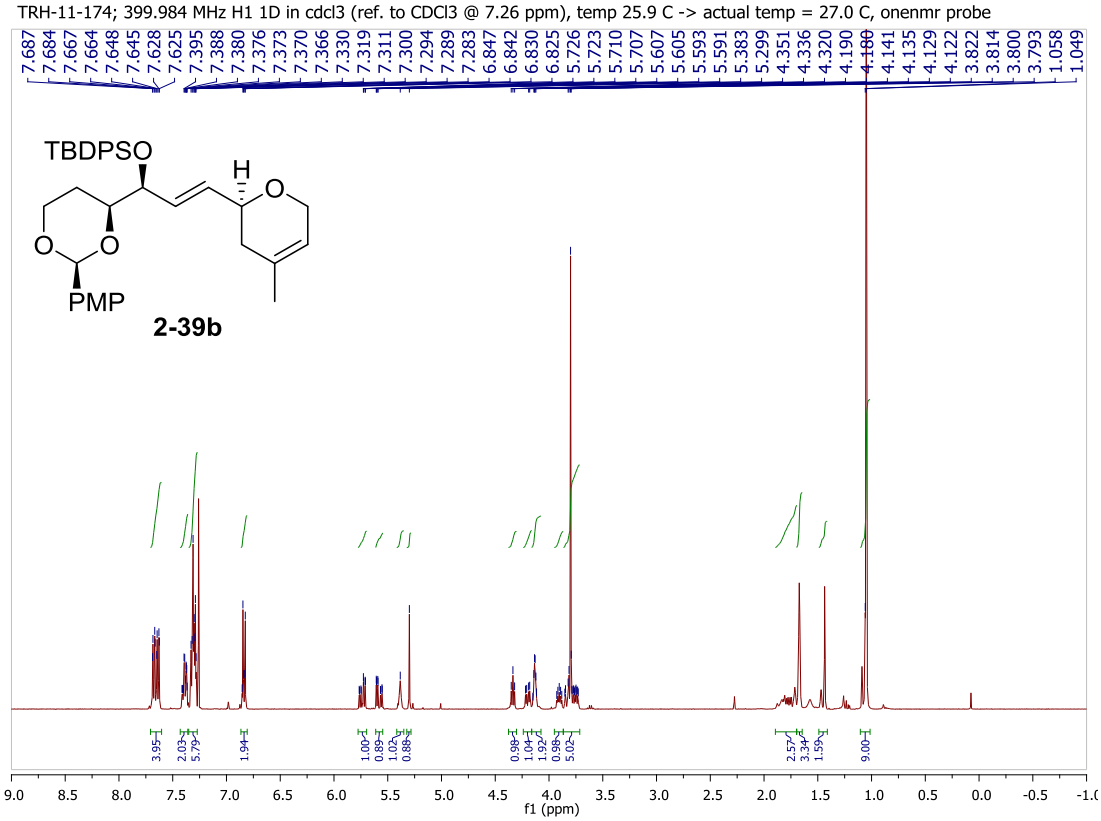

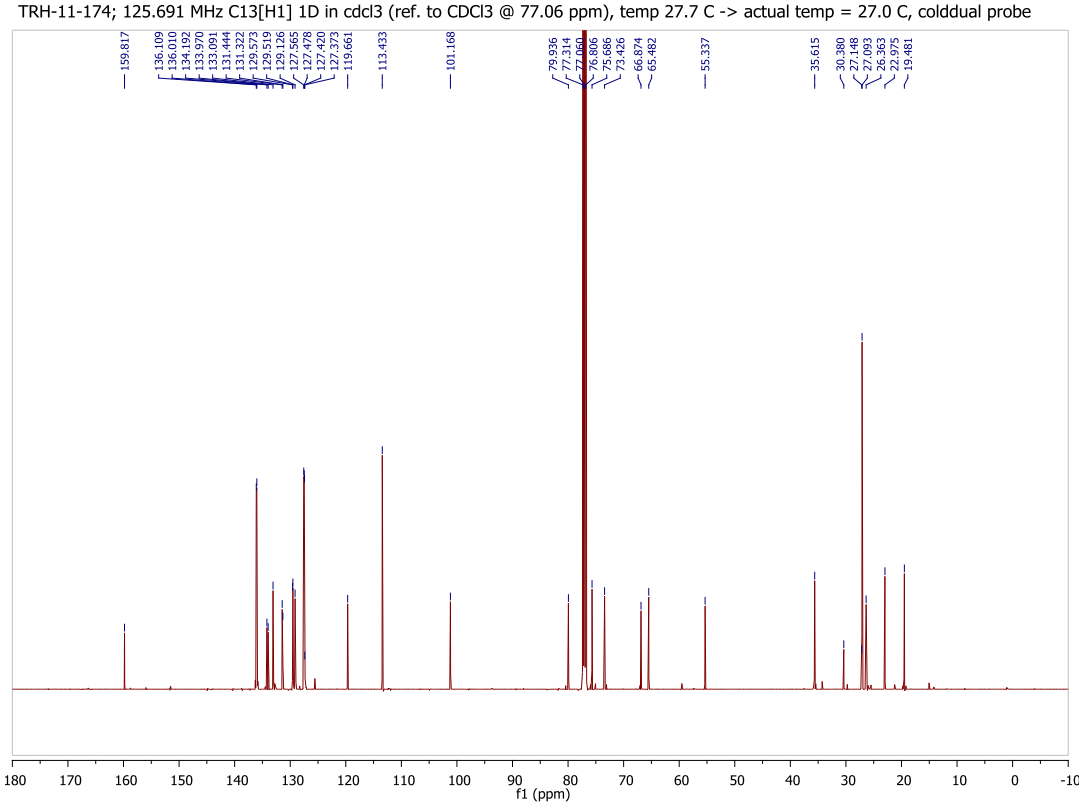

^{1}H and ^{13}C spectrum for 2-40a in C_6D_6 at 25 ^{o}C

TRH-7-65; 499.806 MHz H1 PRESAT in c6d6 (ref. to C6D6 @ 7.15 ppm), temp 27.7 C -> actual temp = 27.0 C, colddual probe

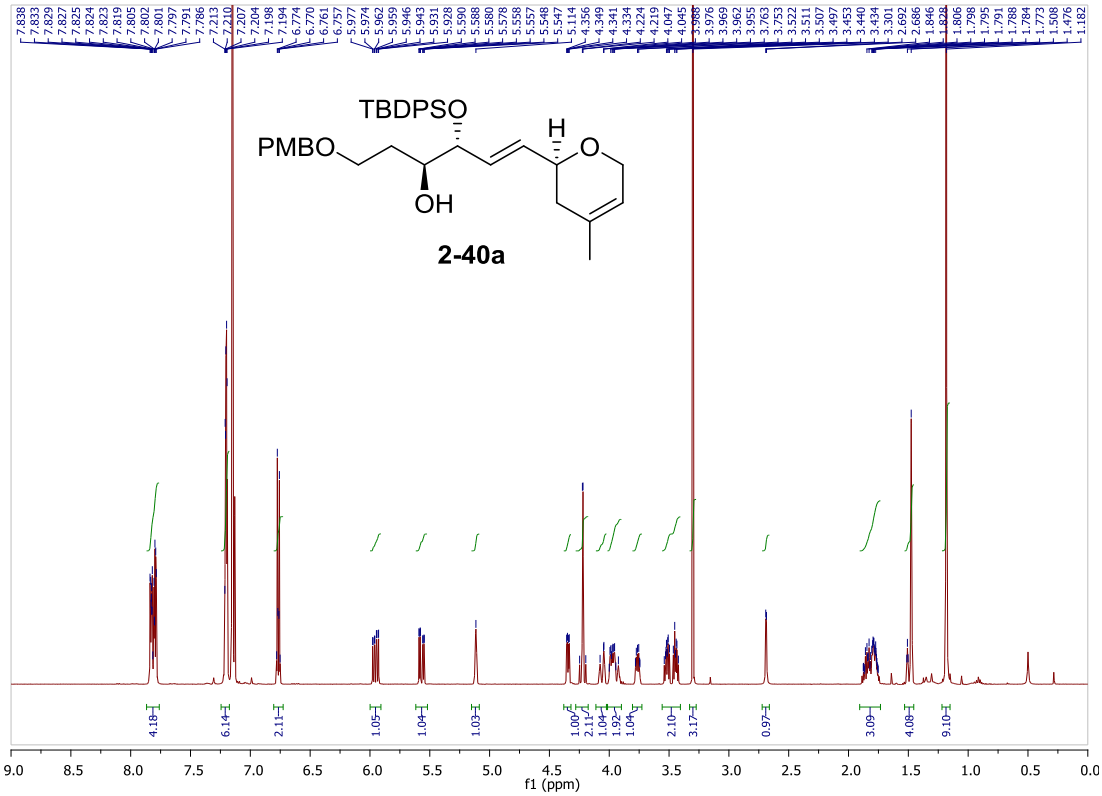

TRH-7-65; 125.691 MHz C13[H1] 1D in c6d6 (ref. to C6D6 @ 128.0 ppm), temp 27.7 C -> actual temp = 27.0 C, colddual probe

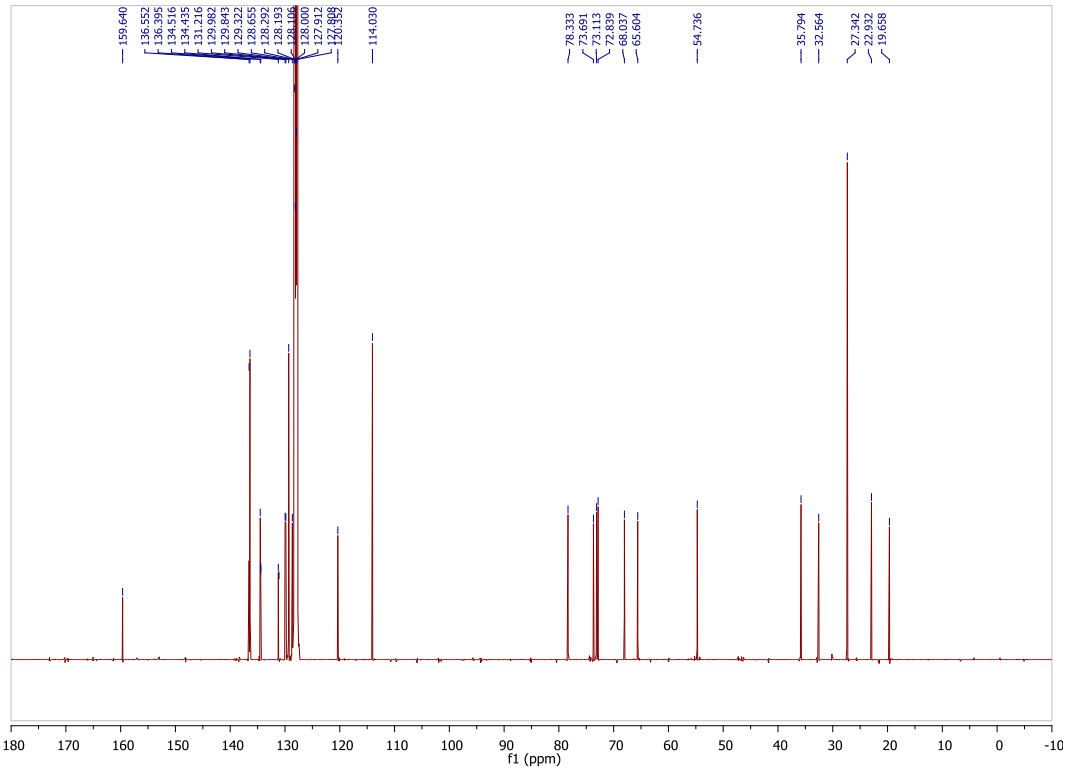

^{1}H (C_6D_6) and ^{13}C ($CDCl_3$) spectra for 2-40b at 25 ^{o}C

TRH-11-181; 400.389 MHz H1 PRESAT in c6d6 (ref. to C6D6 @ 7.15 ppm), temp 27.0 C -> actual temp = 27.0 C, m400gz probe

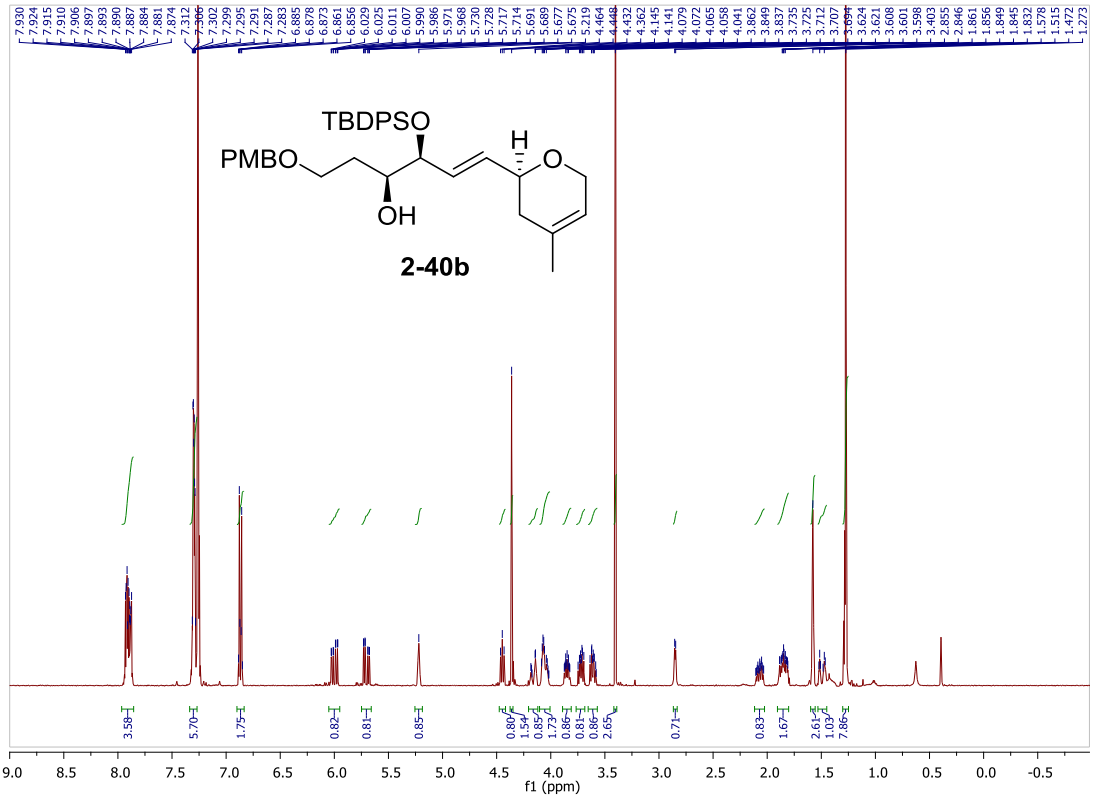

TRH-11-181; 125.691 MHz C13[H1] 1D in cdcl3 (ref. to CDCl3 @ 77.06 ppm), temp 27.7 C -> actual temp = 27.0 C, colddual probe

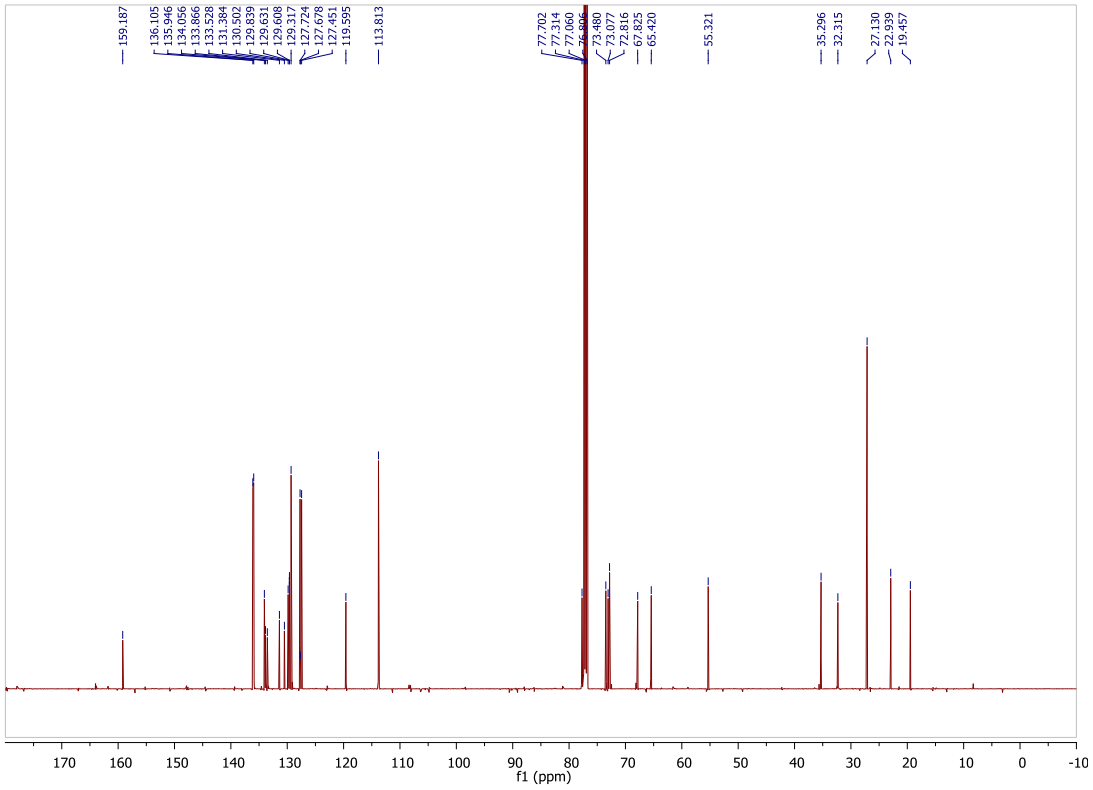

^{1}H and ^{13}C spectra for 2-40b in $CDCl_3$ at 25 ^{o}C

TRH-7-207; 499.806 MHz H1 PRESAT in cdcl3 (ref. to CDCl3 @ 7.26 ppm), temp 27.7 C -> actual temp = 27.0 C, colddual probe

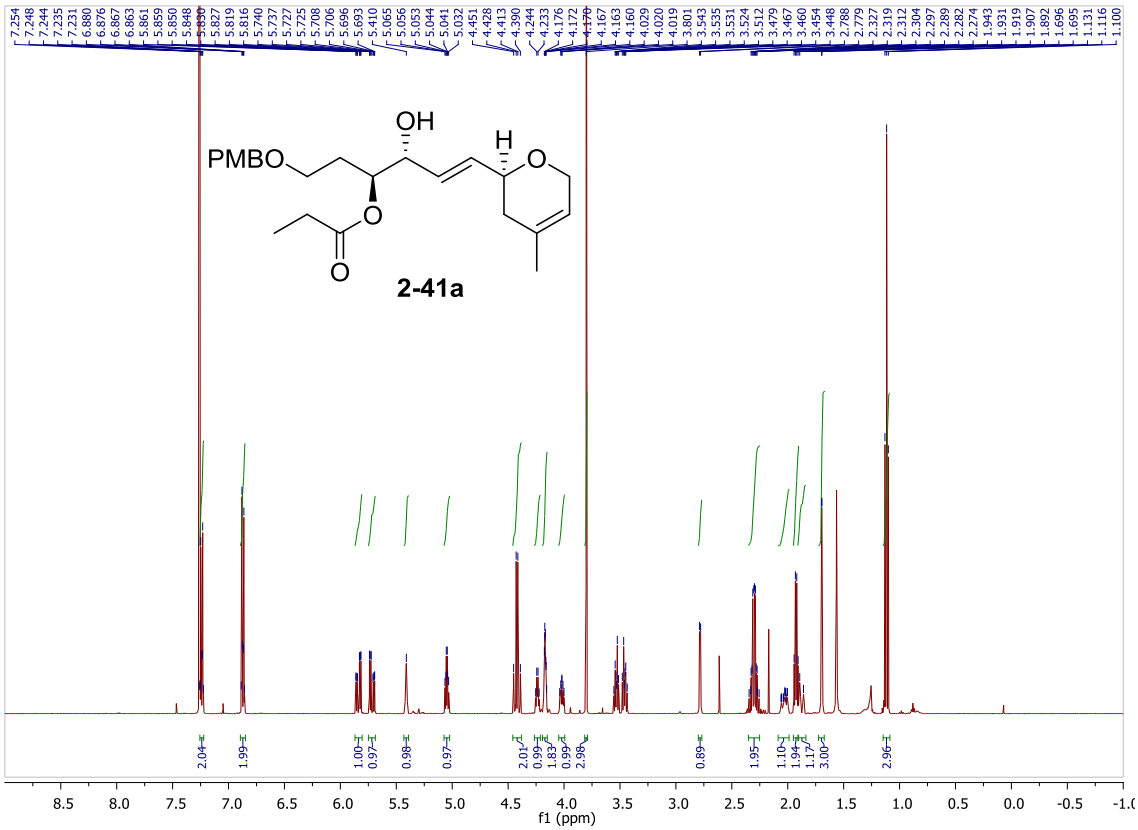

TRH-7-207; 125.691 MHz C13[H1] 1D in cdcl3 (ref. to CDCl3 @ 77.06 ppm), temp 27.7 C -> actual temp = 27.0 C, colddual probe

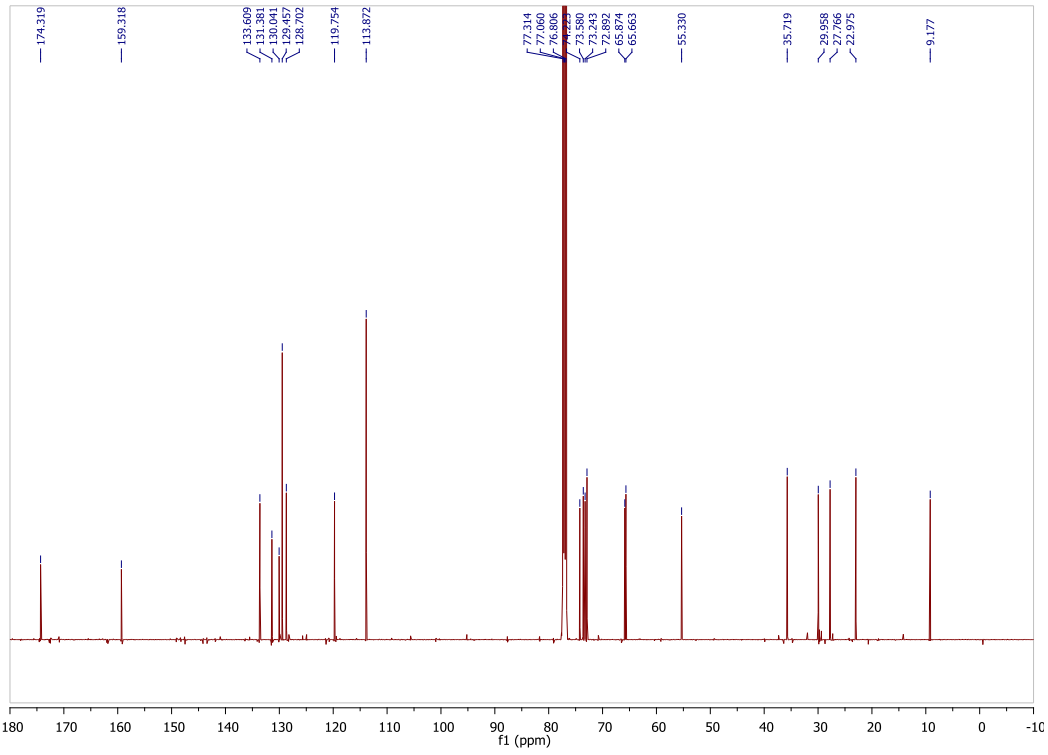

2D COSY of 2-41a in $CDCl_3$ (500 MHz)

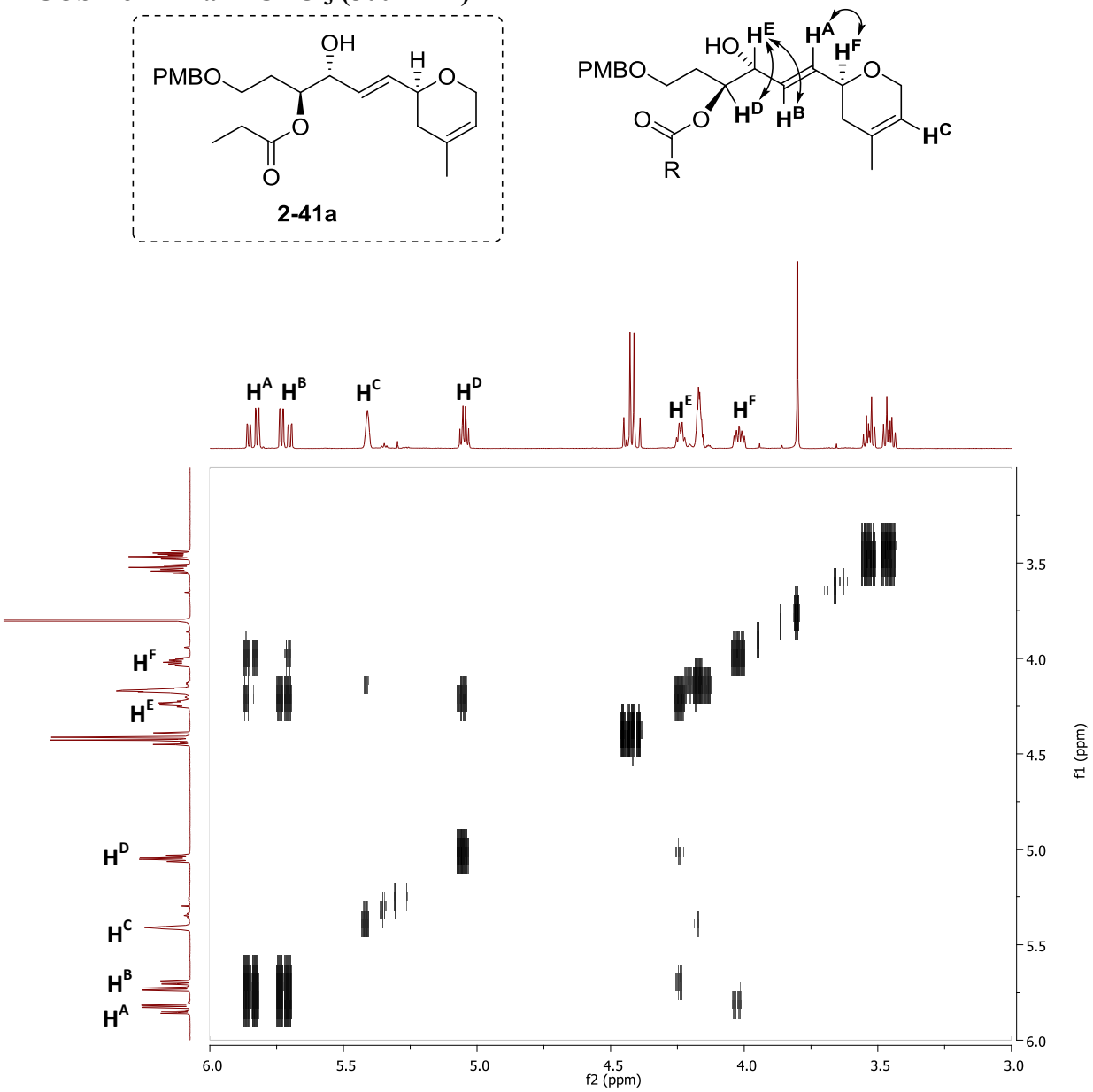

2D HSQC of 2-41a in $CDCl_3$ (500 MHz)

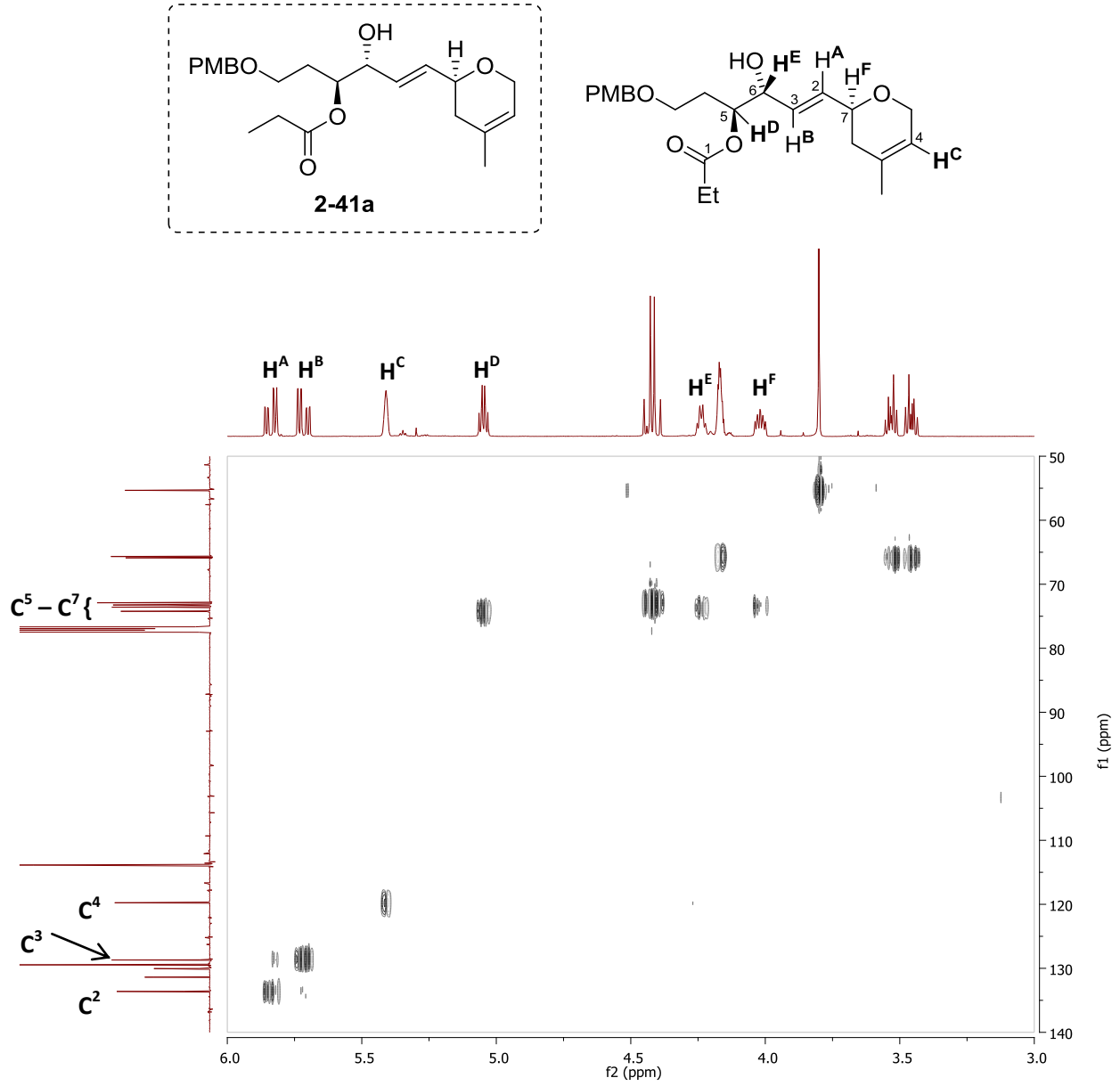

2D HMBC of 2-41a in $CDCl_3$ (500 MHz)

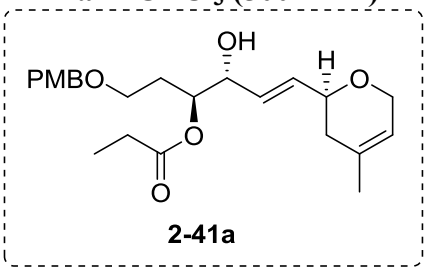

2-41a

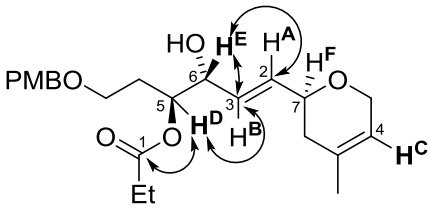

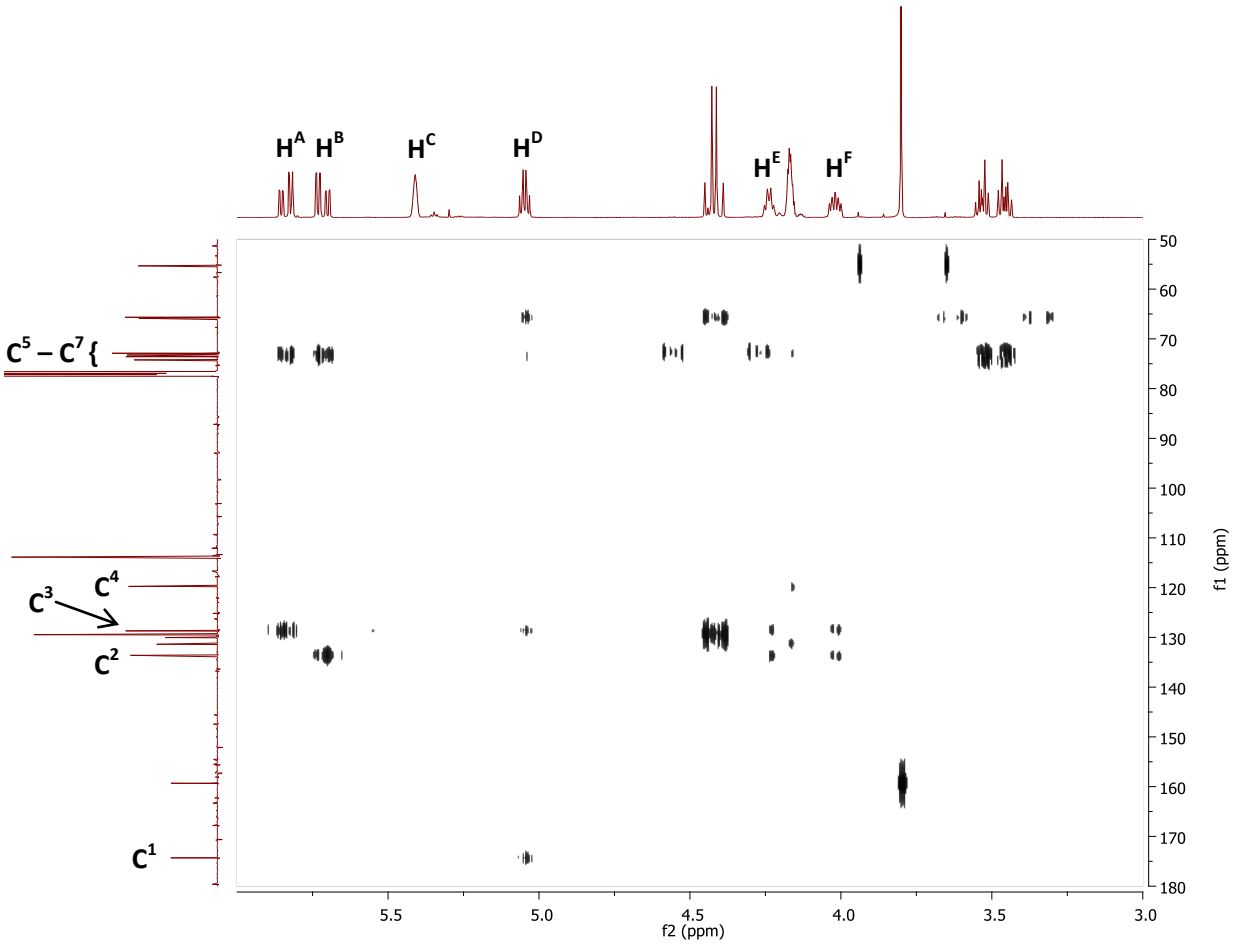

^{1}H and ^{13}C spectra for 2-41b in $CDCl_3$ at 25 ^{o}C

TRH-11-192B; 499.806 MHz H1 PRESAT in cdcl3 (ref. to CDCl3 @ 7.26 ppm), temp 27.7 C -> actual temp = 27.0 C, colddual probe

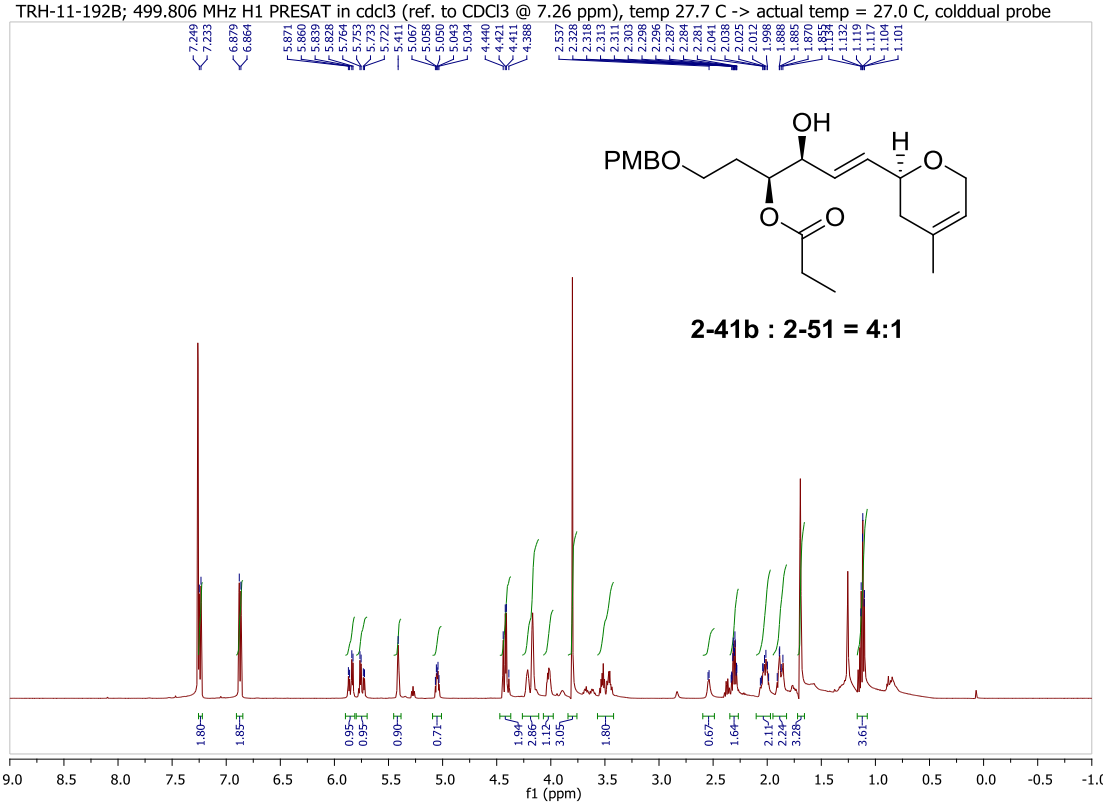

TRH-11-192B; 125.691 MHz C13[H1] 1D in cdcl3 (ref. to CDCl3 @ 77.06 ppm), temp 27.7 C -> actual temp = 27.0 C, colddual probe

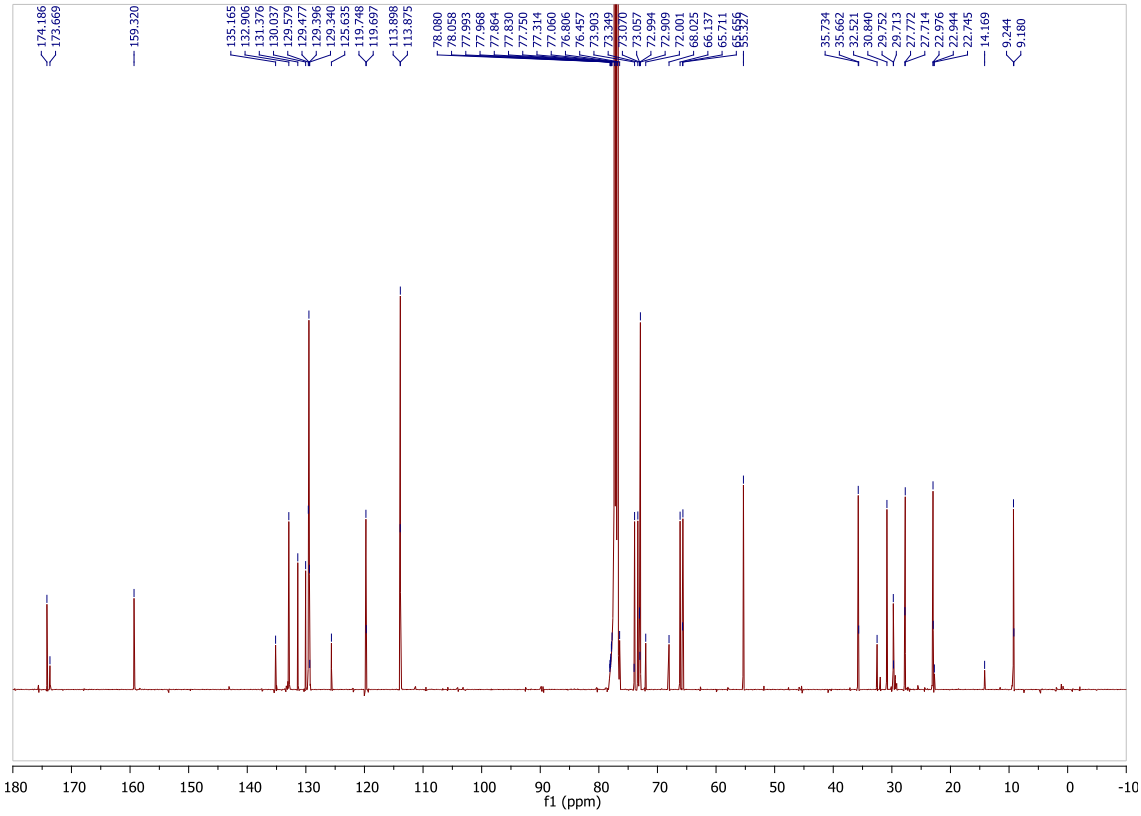

^{1}H and ^{13}C spectra for 2-51b in $CDCl_3$ at 25 ^{o}C

TRH-11-192A; 499.806 MHz H1 PRESAT in cdcl3 (ref. to CDCl3 @ 7.26 ppm), temp 27.7 C -> actual temp = 27.0 C, colddual probe

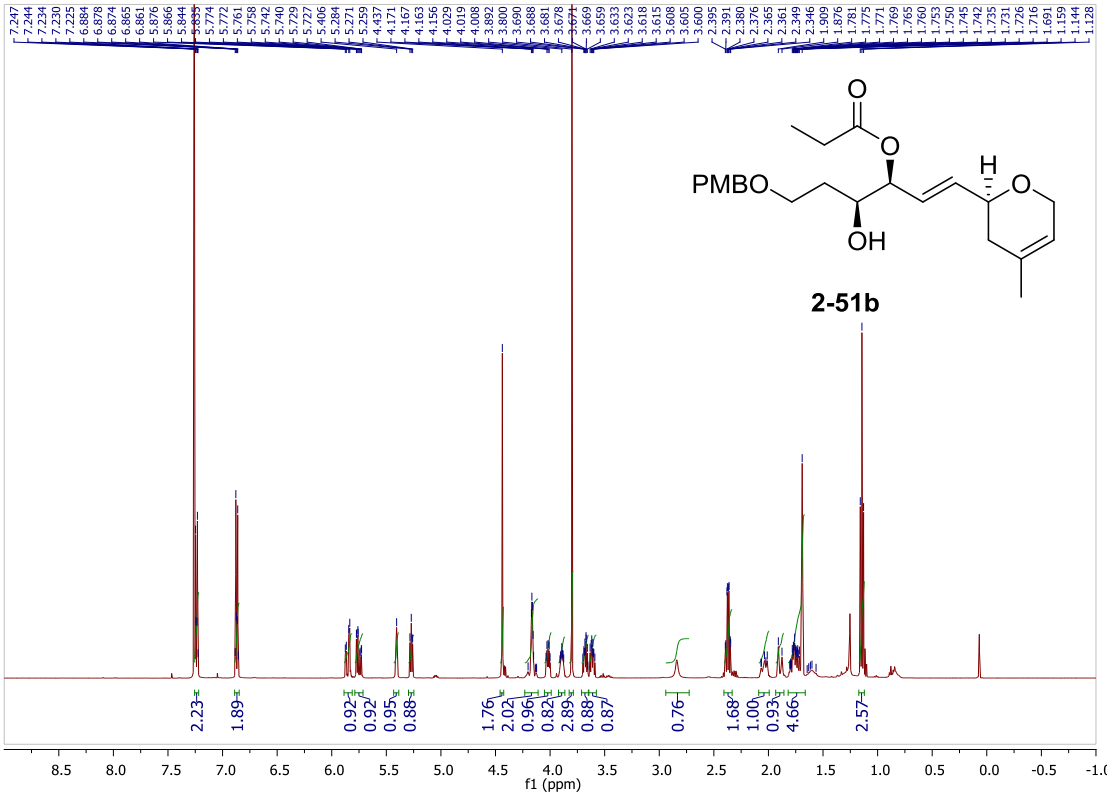

TRH-11-192A; 125.691 MHz C13[H1] 1D in cdcl3 (ref. to CDCl3 @ 77.06 ppm), temp 27.7 C -> actual temp = 27.0 C, colddual probe

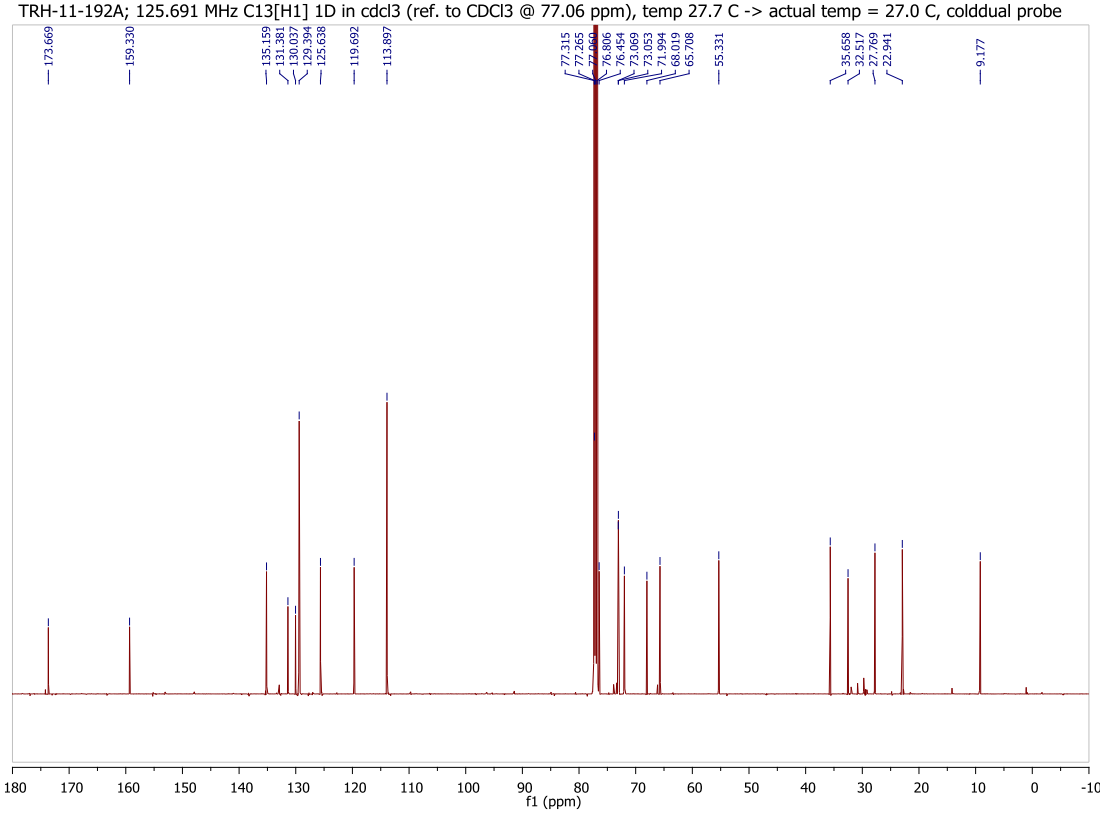

2D COSY of 2-51b in $CDCl_3$ (500 MHz)

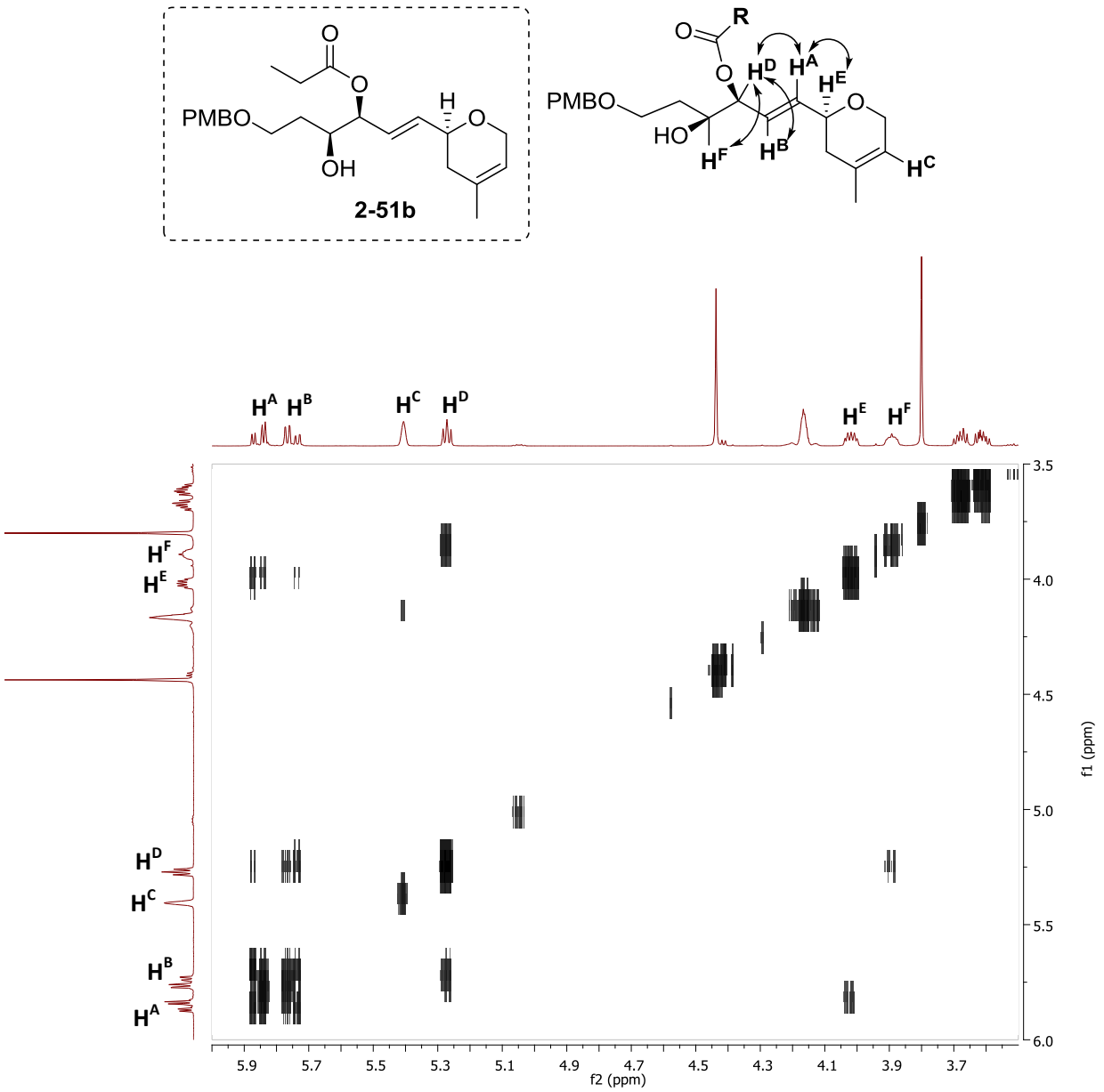

2D HMQC of 2-51b in $CDCl_3$ (500 MHz)

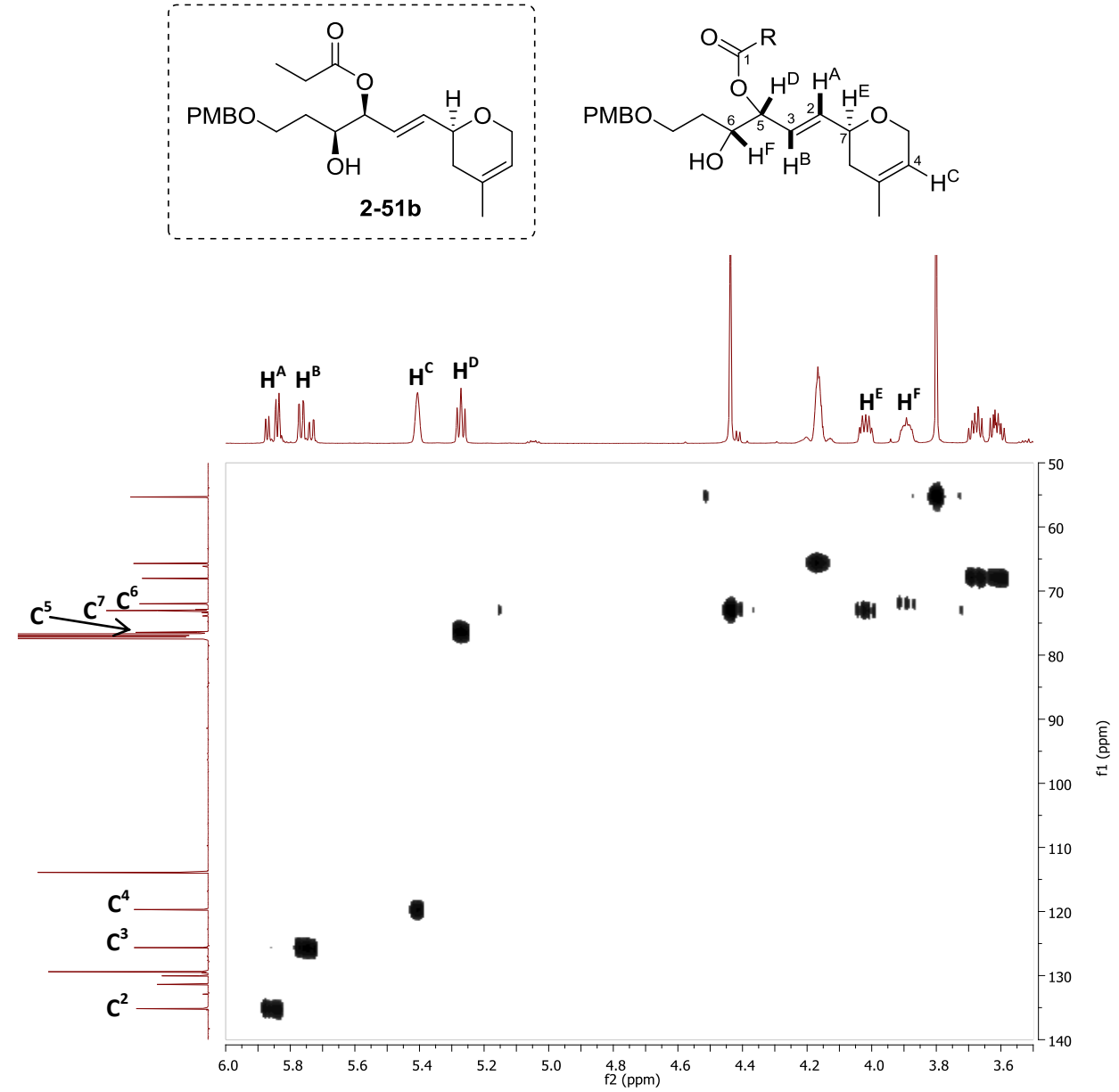

2D HMBC of 2-51b in $CDCl_3$ (500 MHz)

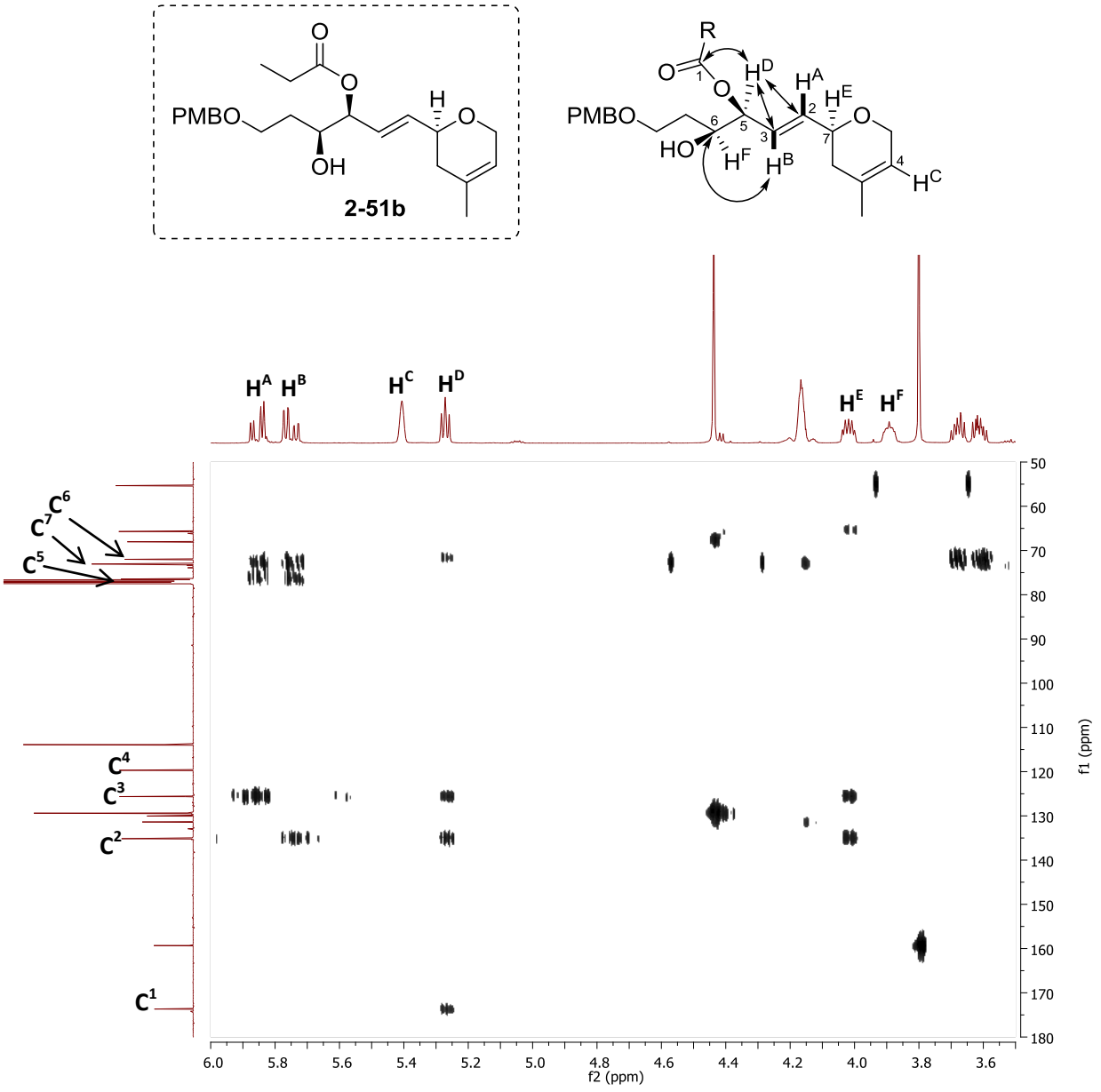

^{1}H and ^{13}C spectra for 2-42a in $CDCl_3$ at 25 ^{o}C

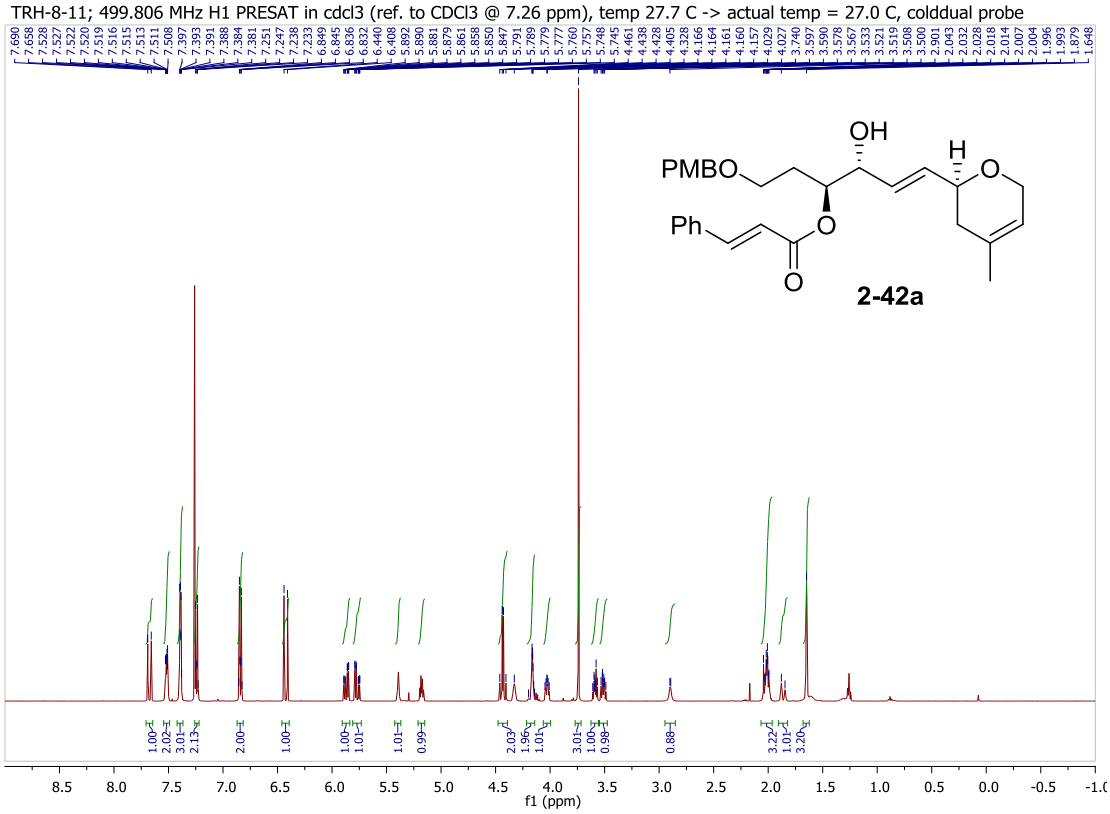

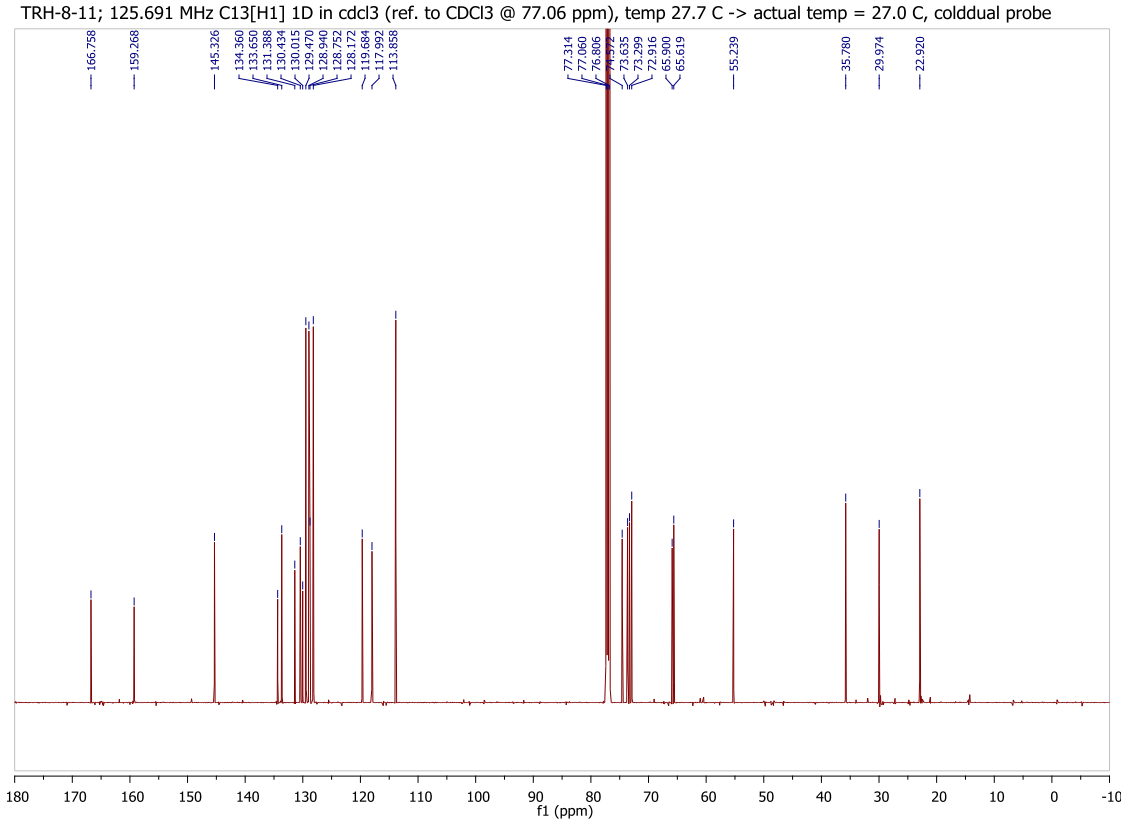

^{1}H and ^{13}C spectra for 2-43a in $CDCl_3$ at 25 ^{o}C

TRH-8-63; 499.806 MHz H1 PRESAT in cdcl3 (ref. to CDCl3 @ 7.26 ppm), temp 27.7 C -> actual temp = 27.0 C, colddual probe

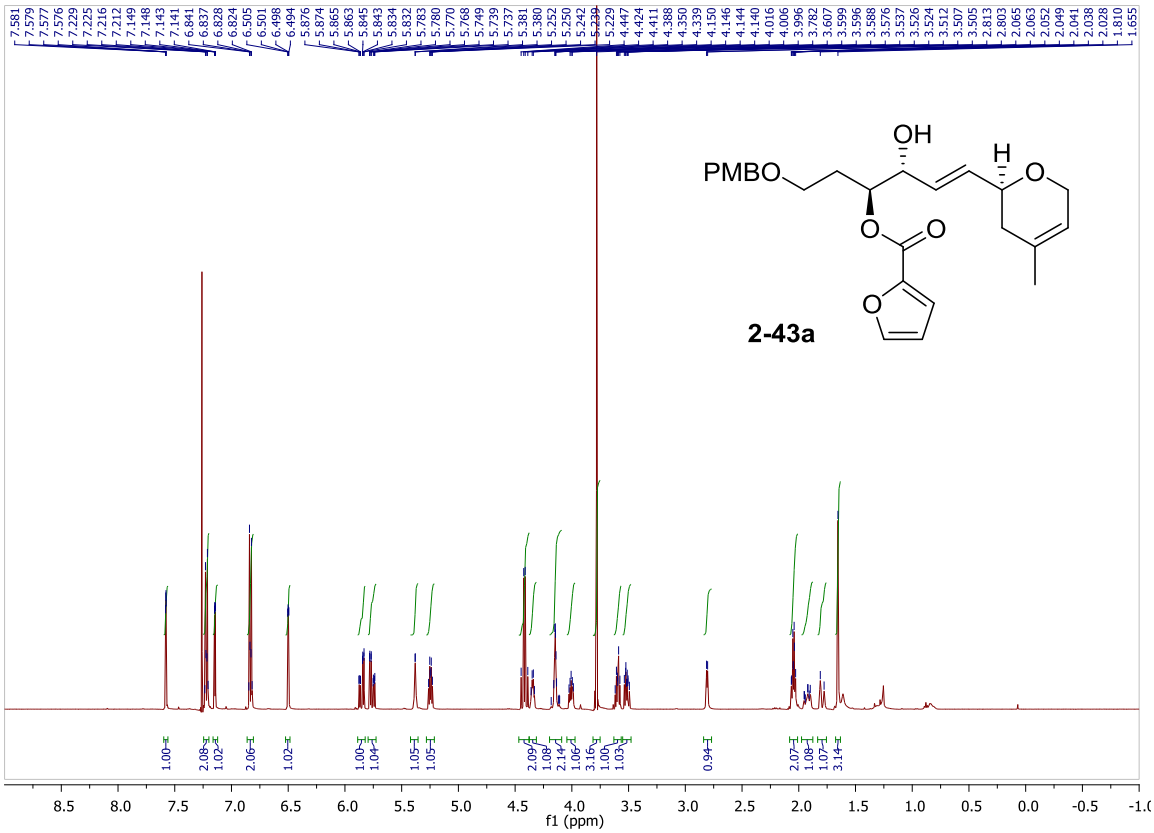

TRH-8-63; 125.691 MHz C13[H1] 1D in cdcl3 (ref. to CDCl3 @ 77.06 ppm), temp 27.7 C -> actual temp = 27.0 C, colddual probe

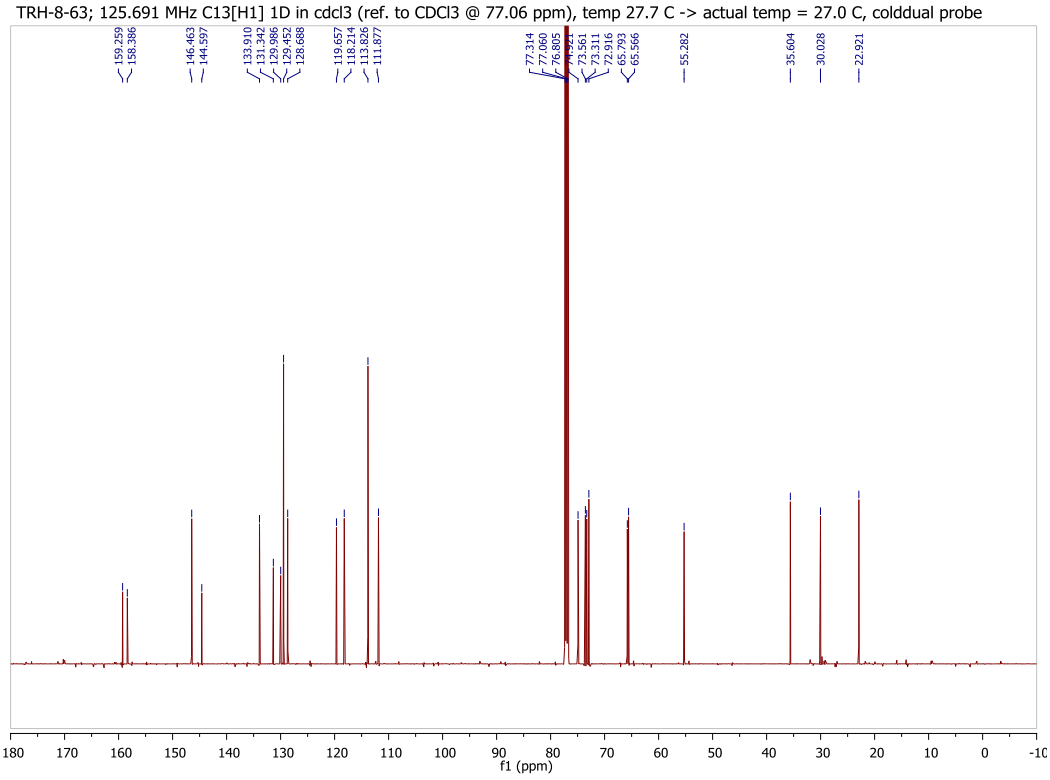

^{1}H and ^{13}C spectra for 2-43b in $CDCl_3$ at 25 ^{o}C

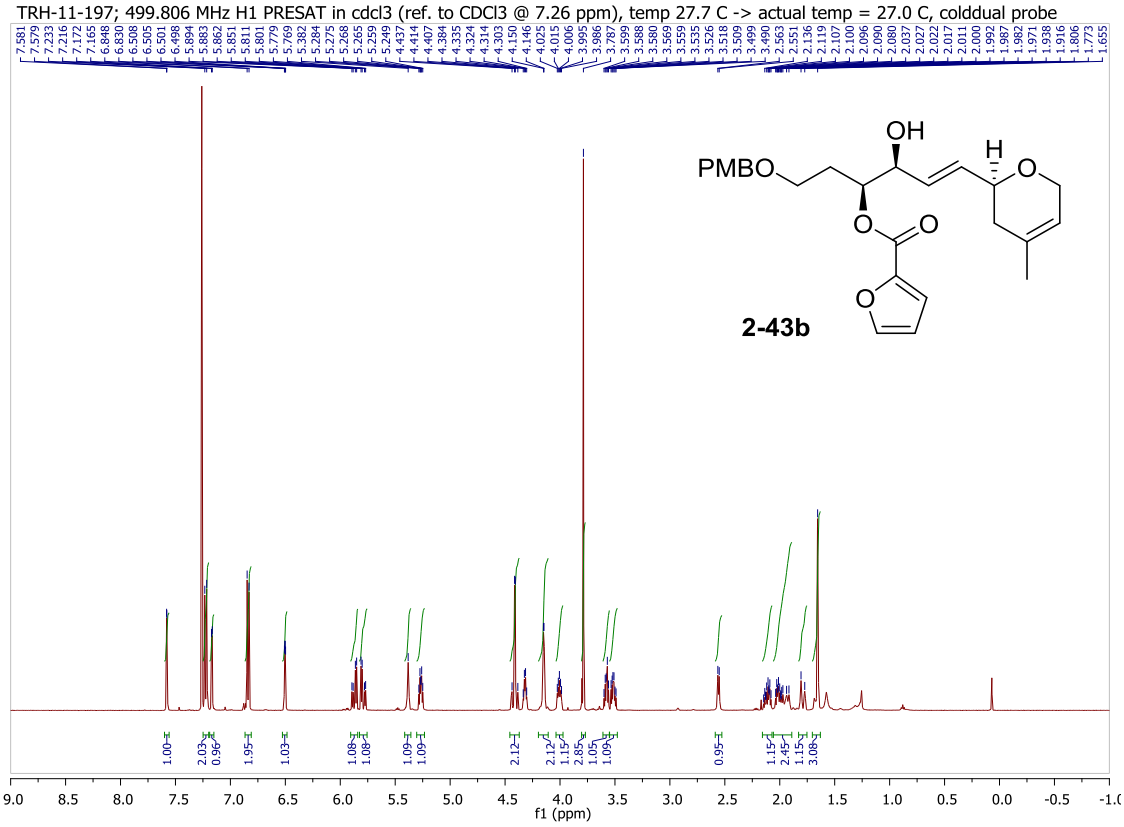

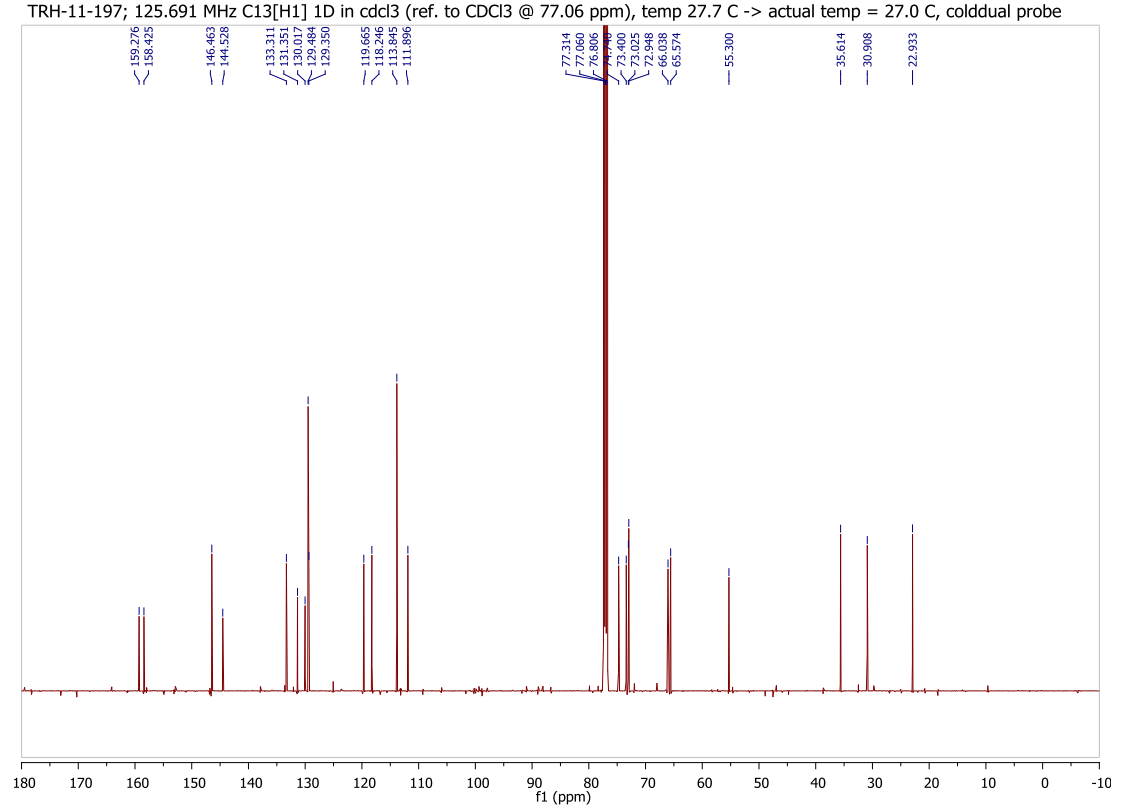

^{1}H and ^{13}C spectra for 2-44a in $CDCl_3$ at 25 ^{o}C

TRH-8-47; 499.806 MHz H1 PRESAT in cdcl3 (ref. to CDCl3 @ 7.26 ppm), temp 27.7 C -> actual temp = 27.0 C, colddual probe

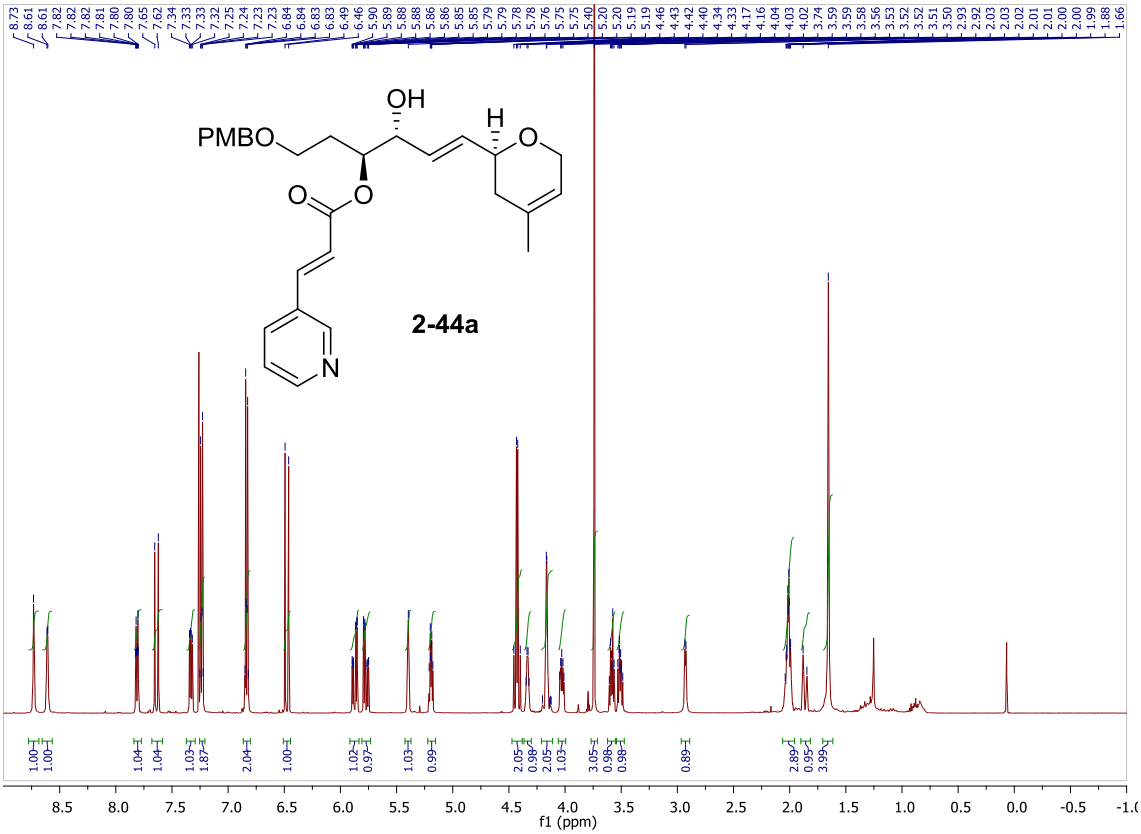

TRH-8-47; 125.691 MHz C13[H1] 1D in cdcl3 (ref. to CDCl3 @ 77.06 ppm), temp 27.7 C -> actual temp = 27.0 C, colddual probe

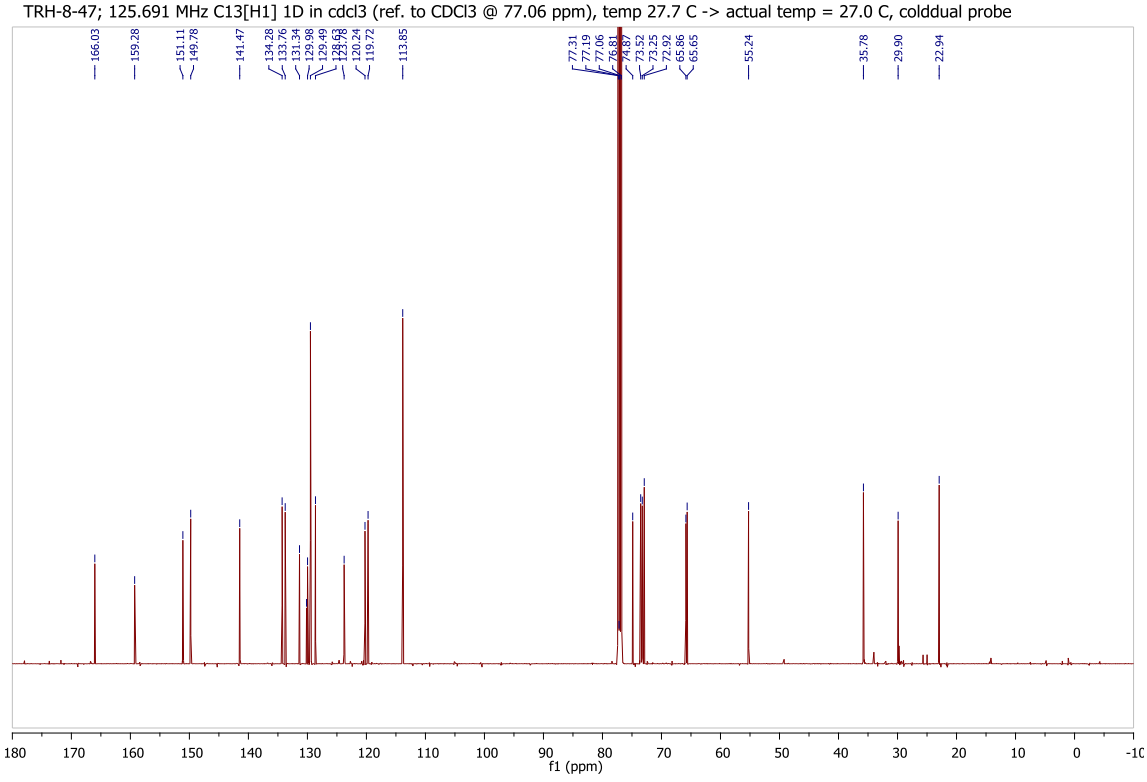

^{1}H and ^{13}C spectra for 2-45a in $CDCl_3$ at 25 ^{o}C

TRH-8-53; 499.806 MHz H1 PRESAT in cdcl3 (ref. to CDCl3 @ 7.26 ppm), temp 27.7 C -> actual temp = 27.0 C, colddual probe

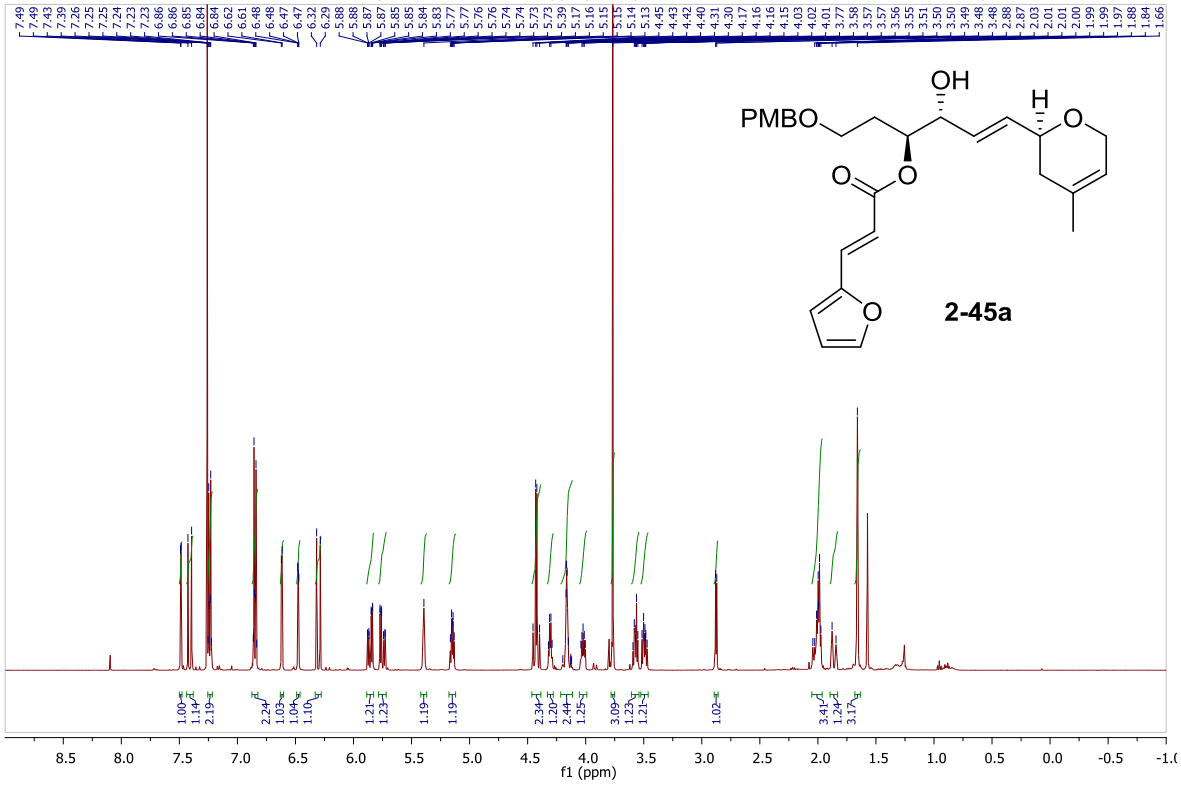

TRH-8-53; 125.691 MHz C13[H1] 1D in cdcl3 (ref. to CDCl3 @ 77.06 ppm), temp 27.7 C -> actual temp = 27.0 C, colddual probe

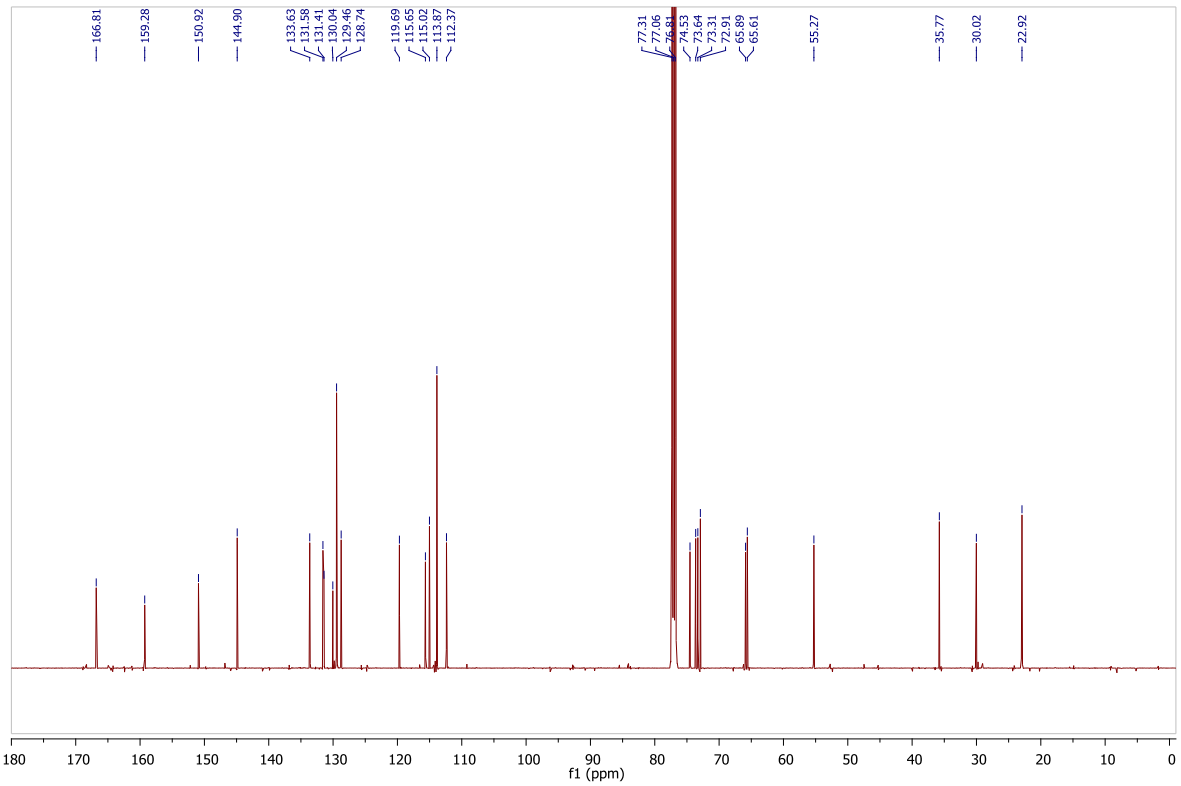

^{1}H and ^{13}C spectra for 2-46a in $CDCl_3$ at 25 ^{o}C

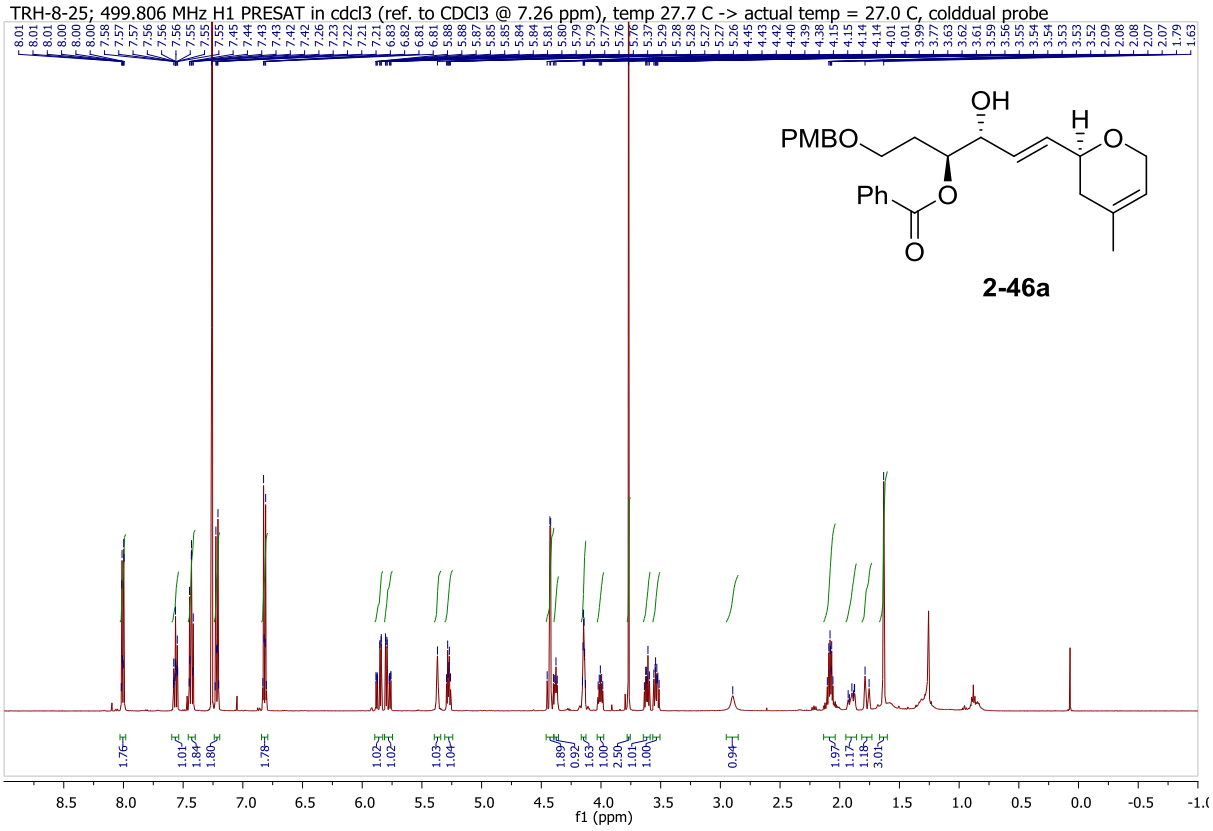

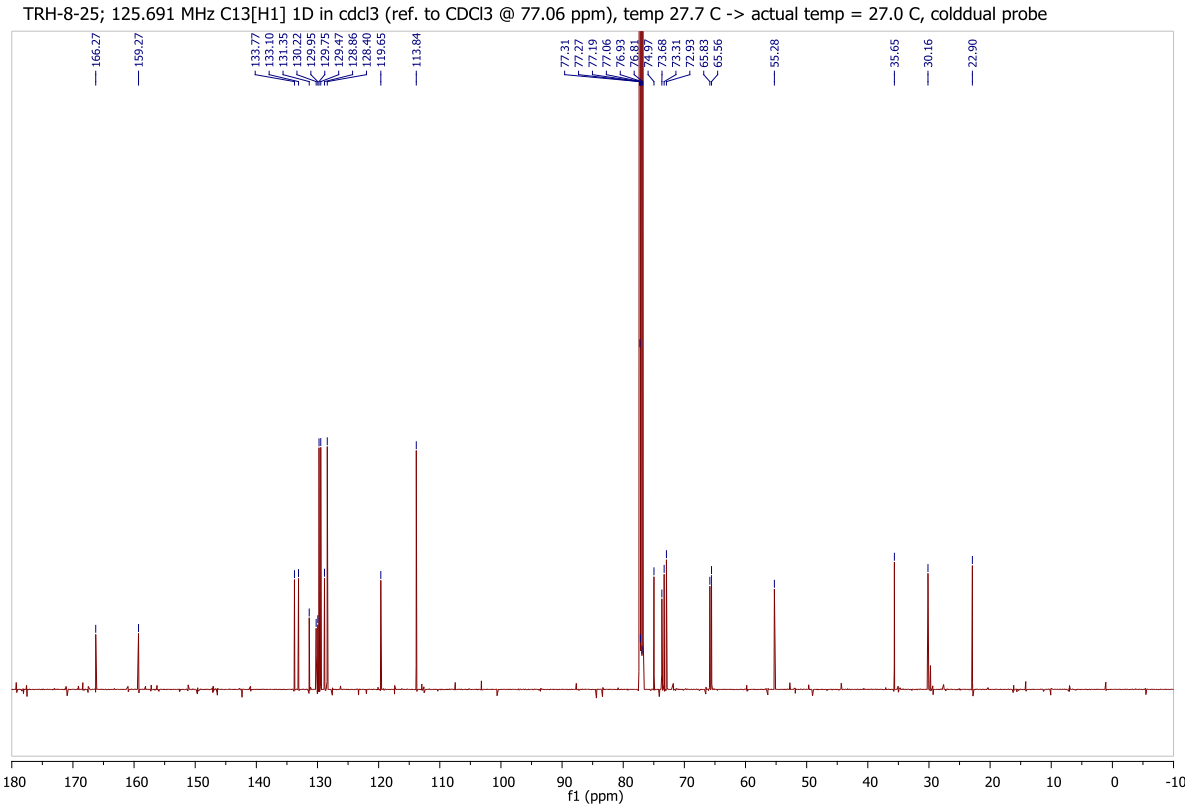

^{1}H and ^{13}C spectra for 2-47a in $CDCl_3$ at 25 ^{o}C

TRH-8-23; 499.806 MHz H1 PRESAT in cdcl3 (ref. to CDCl3 @ 7.26 ppm), temp 27.7 C -> actual temp = 27.0 C, colddual probe

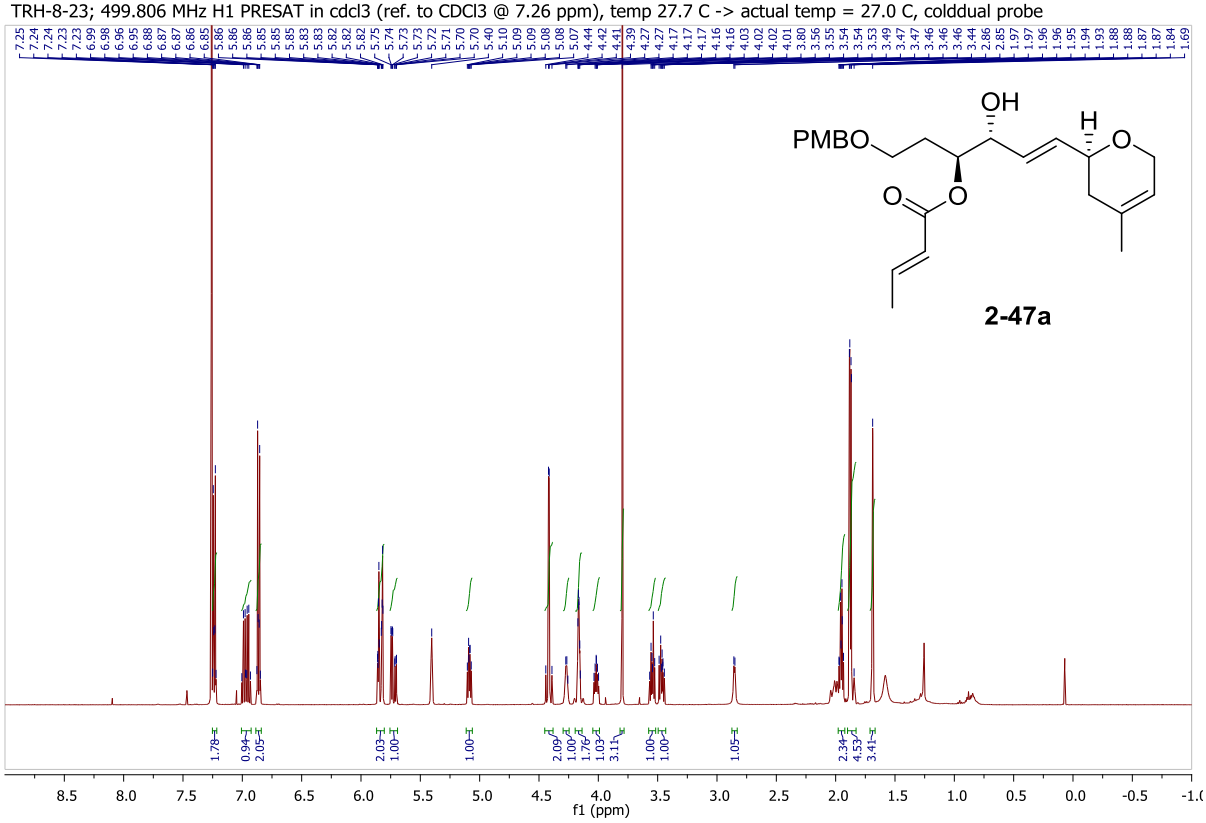

TRH-8-23; 125.691 MHz C13[H1] 1D in cdcl3 (ref. to CDCl3 @ 77.06 ppm), temp 27.7 C -> actual temp = 27.0 C, colddual probe

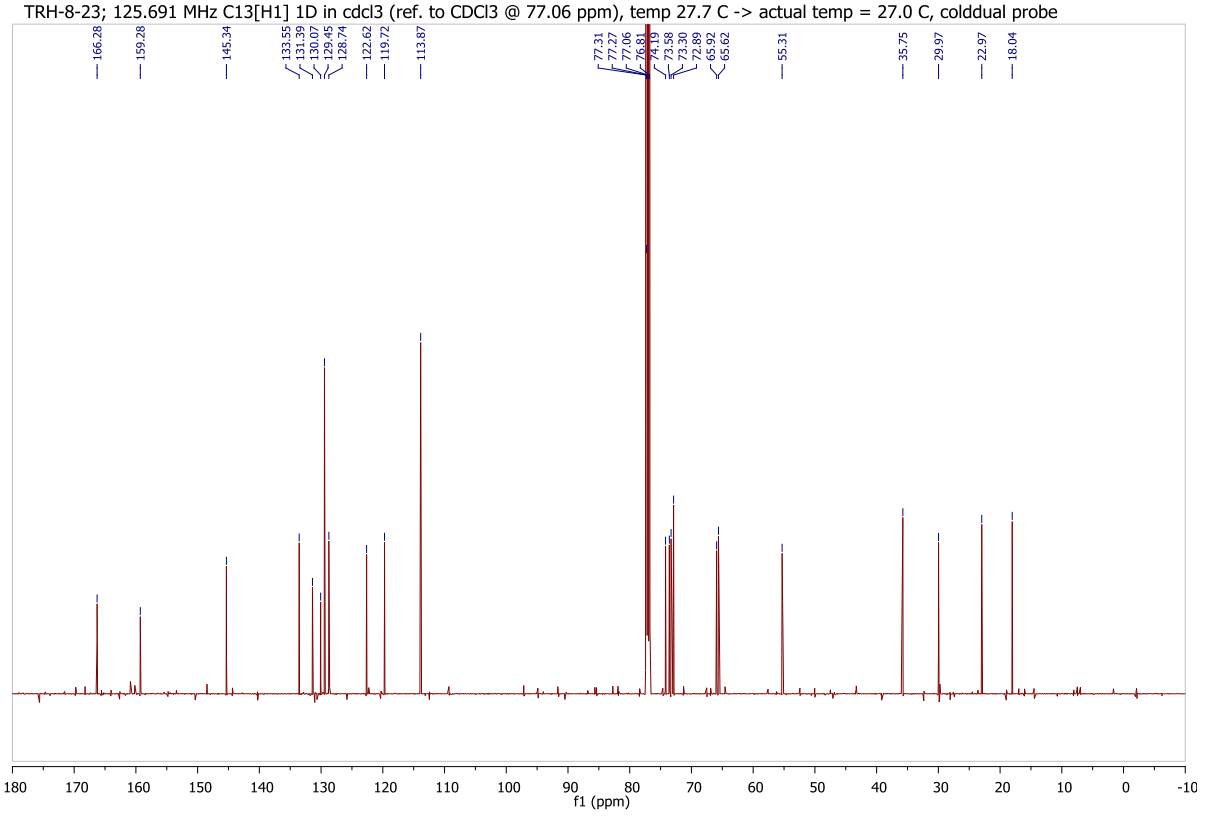

^{1}H and ^{13}C spectra for 2-48a in $CDCl_3$ at 25 ^{o}C

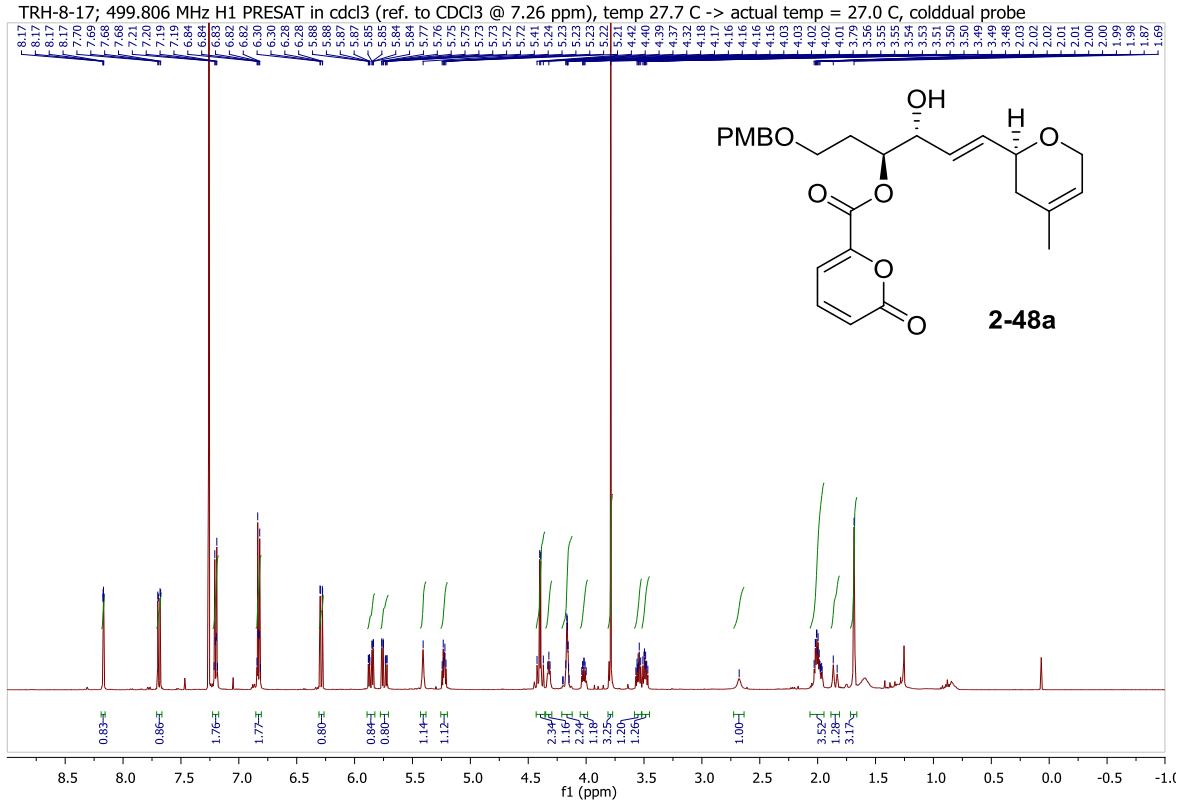

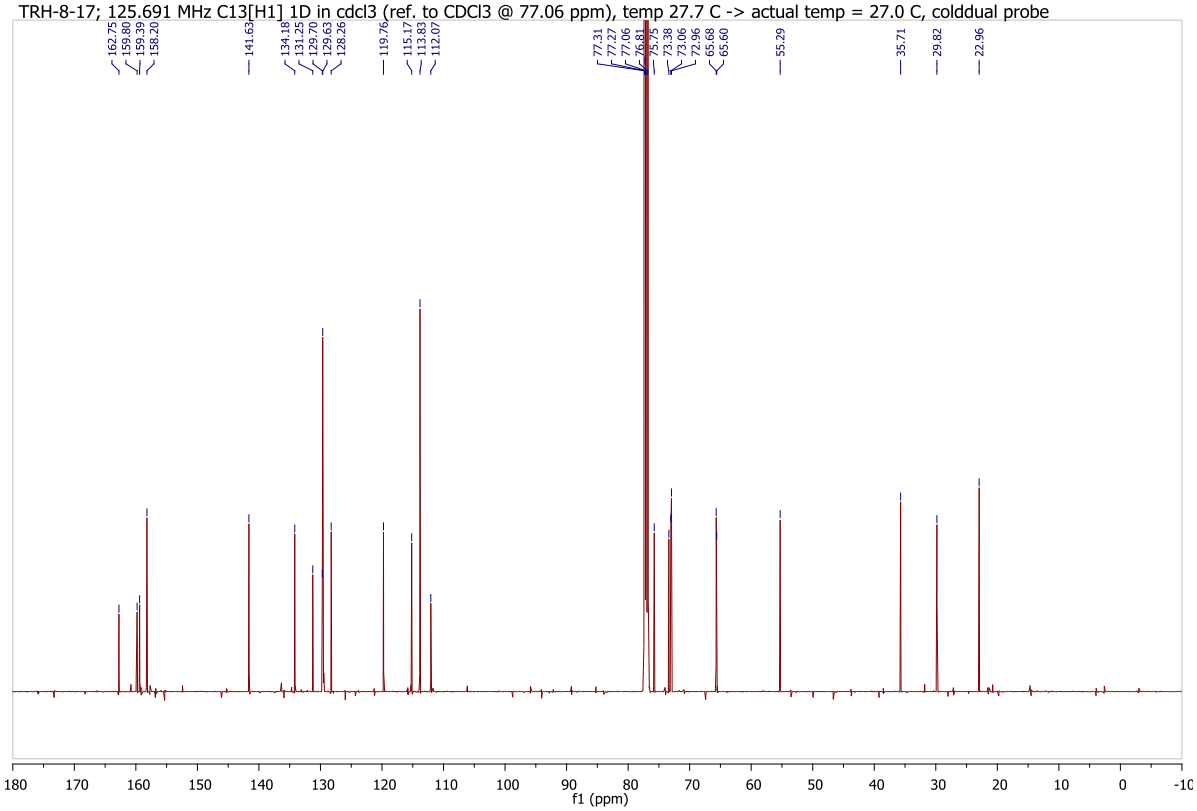

^{1}H and ^{13}C spectra for 2-49a in $CDCl_3$ at 25 ^{o}C

TRH-8-19; 499.806 MHz H1 PRESAT in cdcl3 (ref. to CDCl3 @ 7.26 ppm), temp 27.7 C -> actual temp = 27.0 C, colddual probe

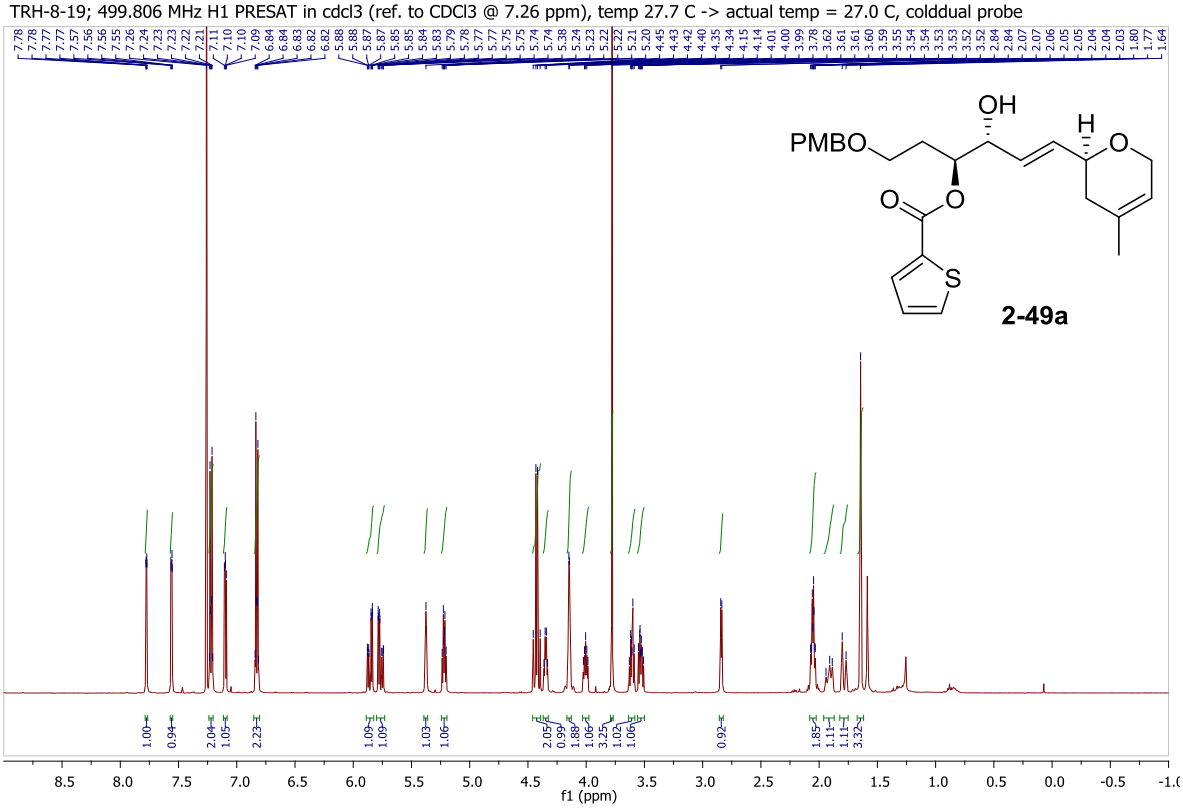

TRH-8-19; 125.691 MHz C13[H1] 1D in cdcl3 (ref. to CDCl3 @ 77.06 ppm), temp 27.7 C -> actual temp = 27.0 C, colddual probe

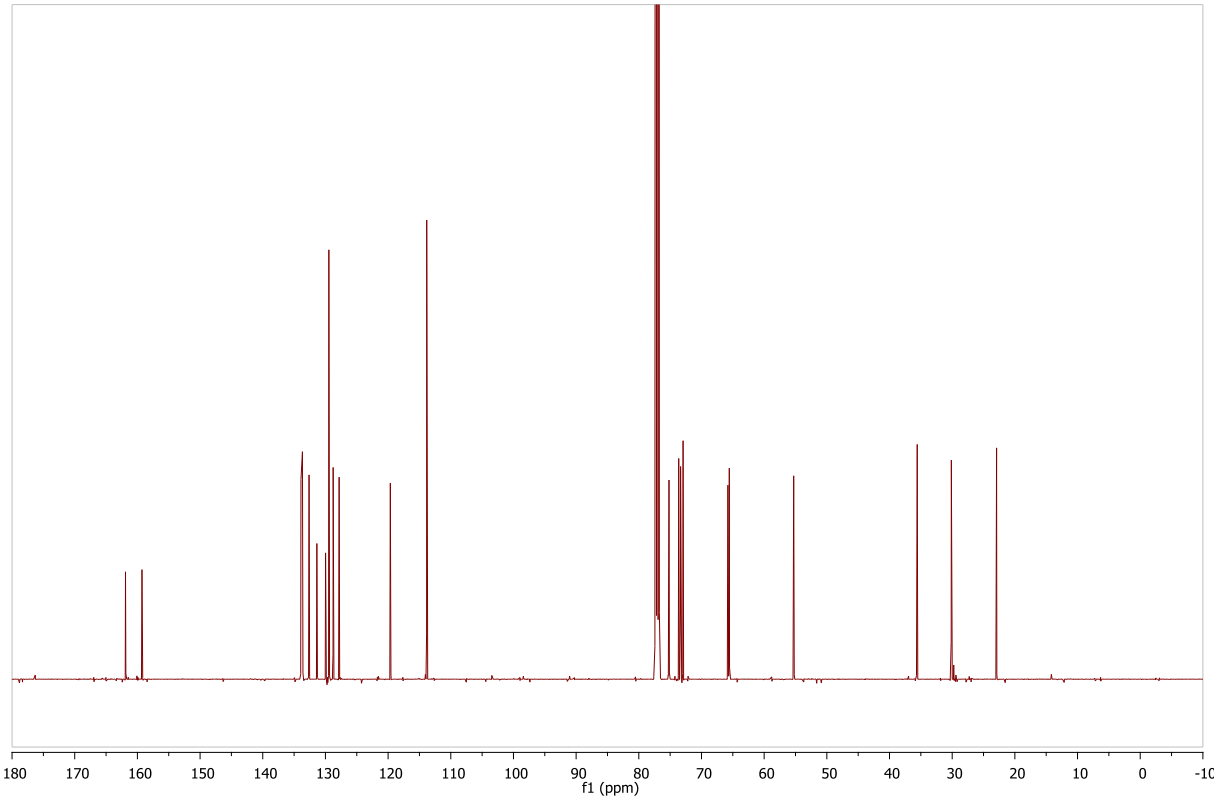

^{1}H and ^{13}C spectra for 2-50a in $CDCl_3$ at 25 ^{o}C

TRH-8-35; 499.806 MHz H1 PRESAT in cdcl3 (ref. to CDCl3 @ 7.26 ppm), temp 27.7 C -> actual temp = 27.0 C, colddual probe

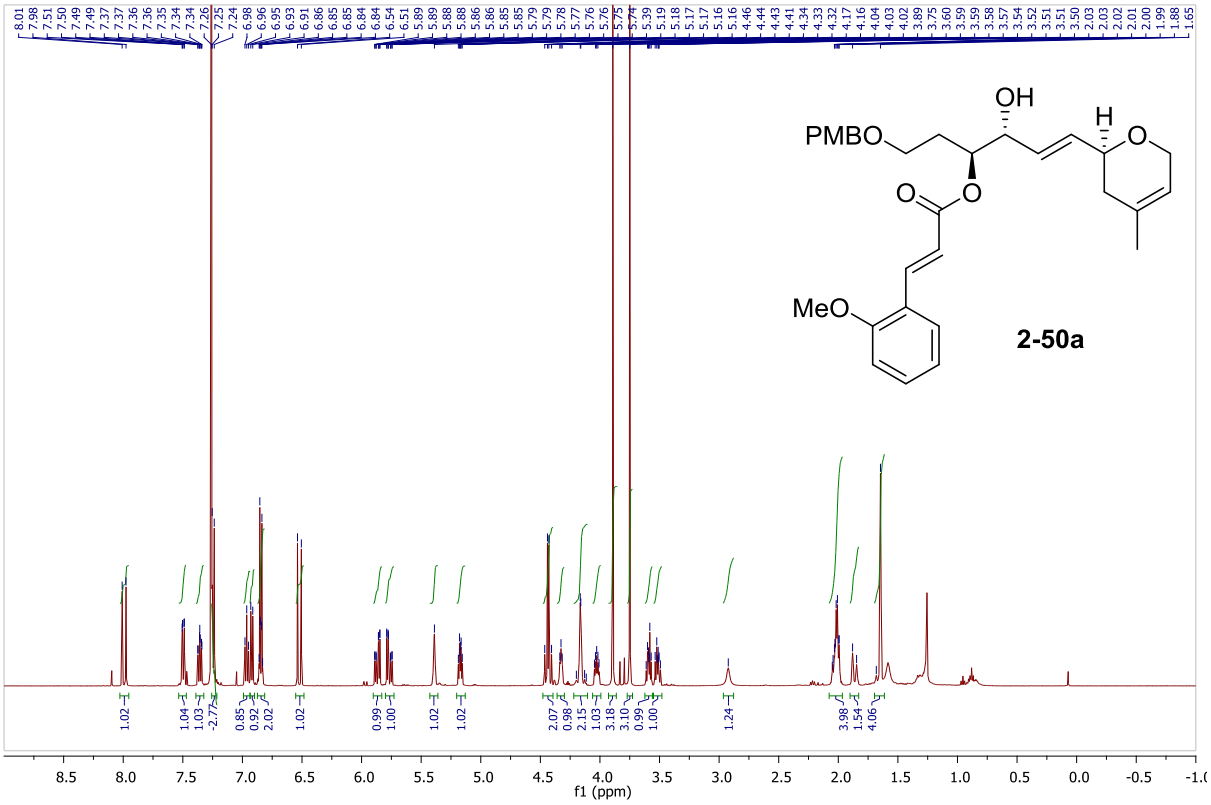

TRH-8-35; 125.691 MHz C13[H1] 1D in cdcl3 (ref. to CDCl3 @ 77.06 ppm), temp 27.7 C -> actual temp = 27.0 C, colddual probe

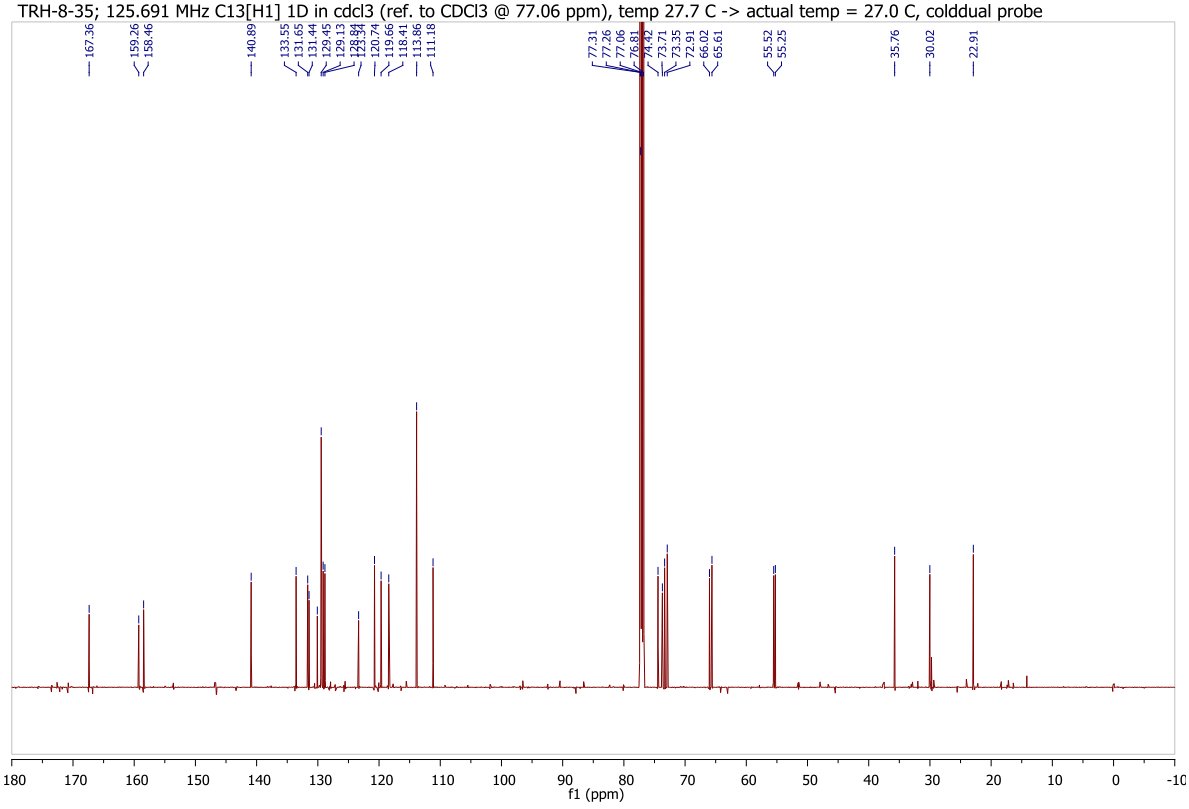

^{1}H and ^{13}C spectra for 3-52b in $CDCl_3$ at 25 ^{o}C

TRH-6-139; 499.806 MHz H1 PRESAT in cdcl3 (ref. to CDCl3 @ 7.26 ppm), temp 27.7 C -> actual temp = 27.0 C, colddual probe

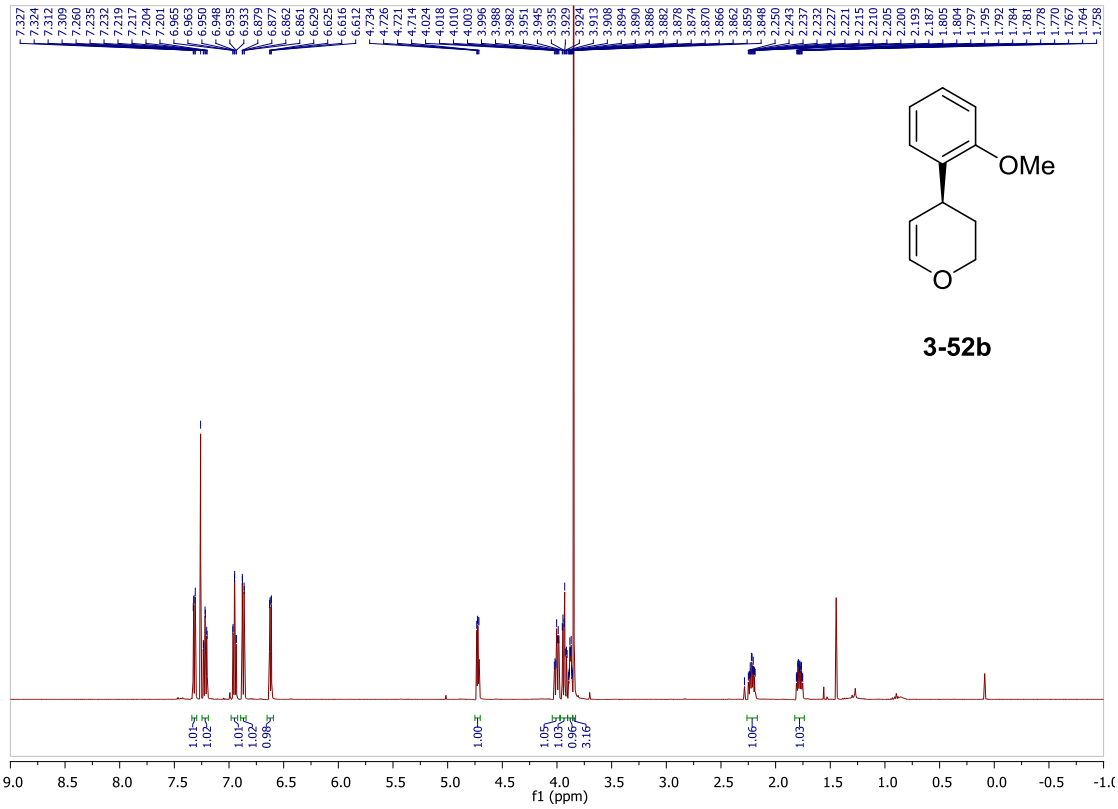

TRH-6-139; 125.691 MHz C13[H1] 1D in cdcl3 (ref. to CDCl3 @ 77.06 ppm), temp 27.7 C -> actual temp = 27.0 C, colddual probe

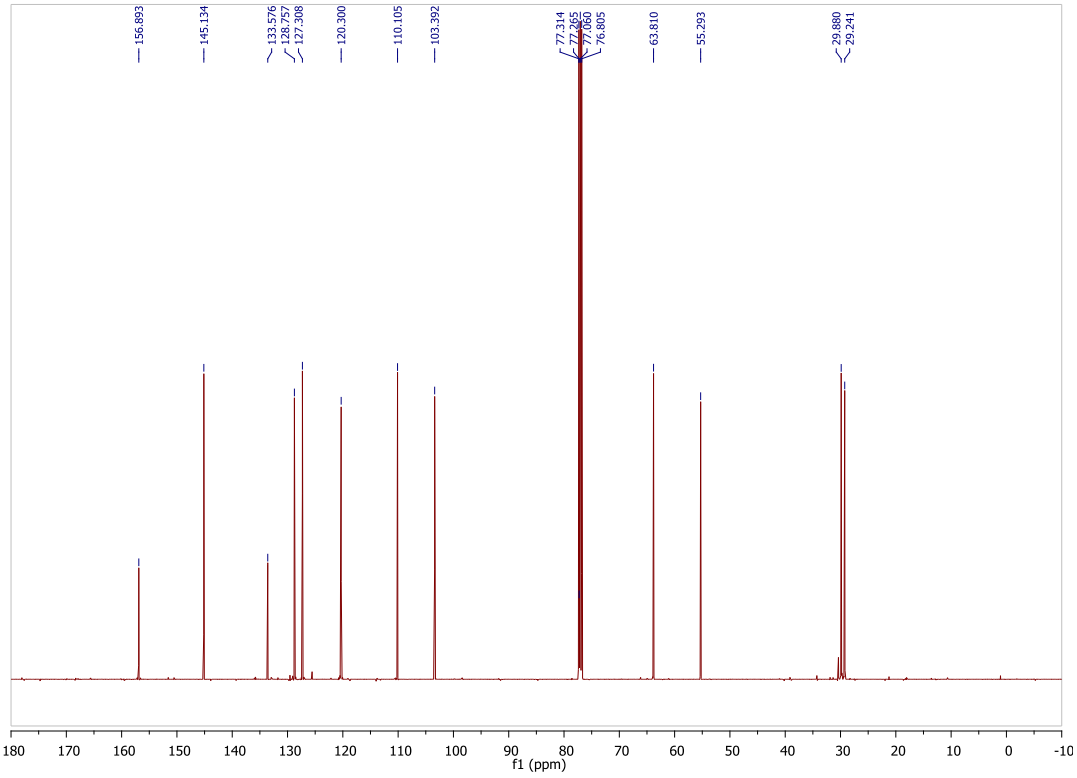

^{1}H and ^{13}C spectra for 3-52c in $CDCl_3$ at 25 ^{o}C

TRH-6-131; 499.806 MHz H1 PRESAT in cdcl3 (ref. to CDCl3 @ 7.26 ppm), temp 27.7 C -> actual temp = 27.0 C, colddual probe

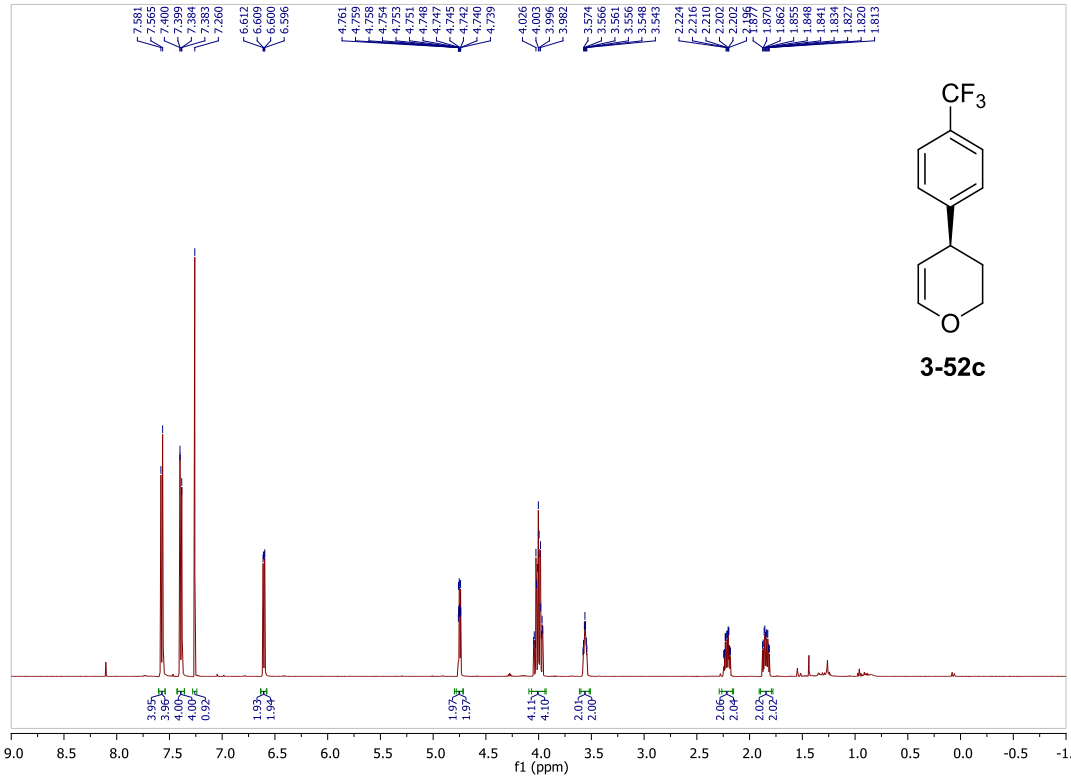

TRH-6-131, 125.691 MHz C13[H1] 1D in cdcl3 (ref. to CDCl3 @ 77.06 ppm), temp 27.7 C -> actual temp = 27.0 C, colddual probe

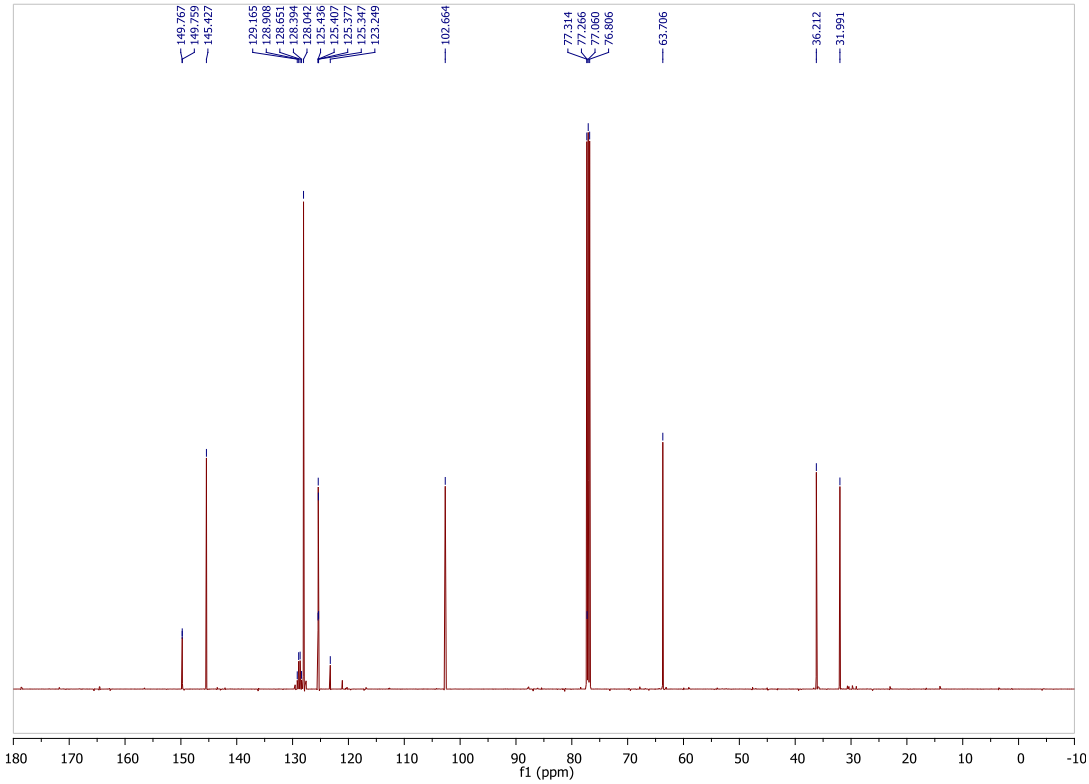

^{1}H and ^{13}C spectra for 3-52h in $CDCl_3$ at 25 ^{o}C

TRH-7-143; 498.118 MHz H1 1D in cdcl3 (ref. to CDCl3 @ 7.26 ppm), temp 26.4 C -> actual temp = 27.0 C, autoxdb probe

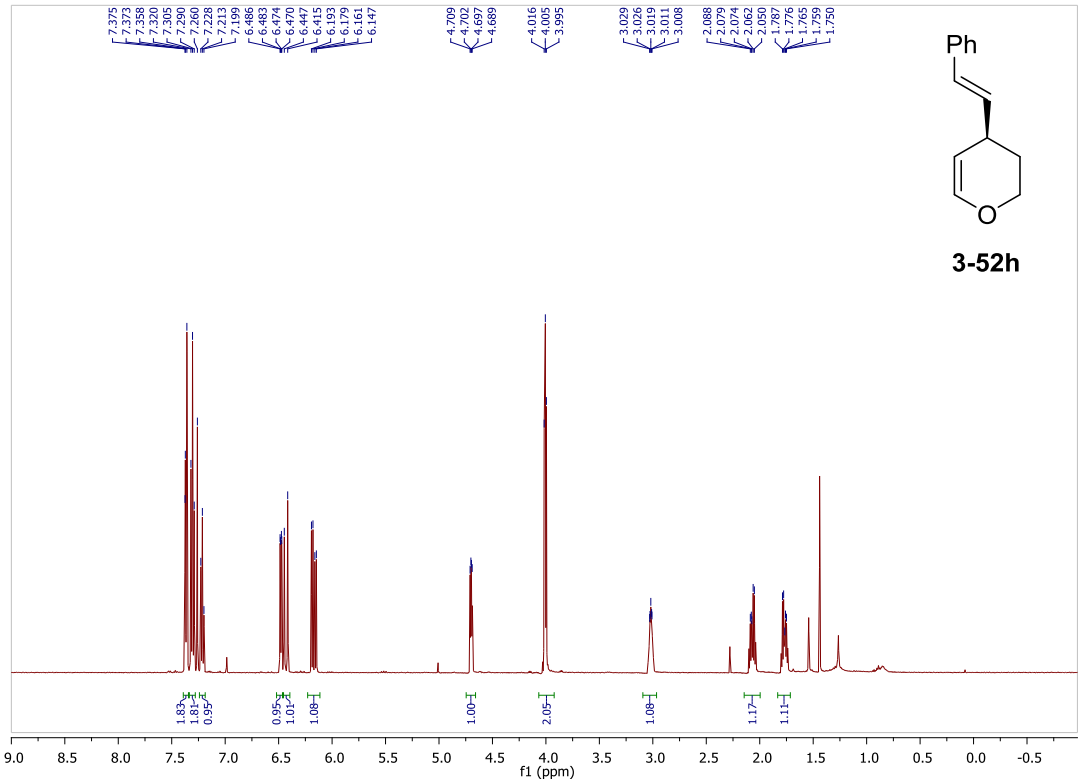

TRH-7-143; 125.266 MHz C13[H1] 1D in cdcl3 (ref. to CDCl3 @ 77.06 ppm), temp 26.4 C -> actual temp = 27.0 C, autoxdb probe

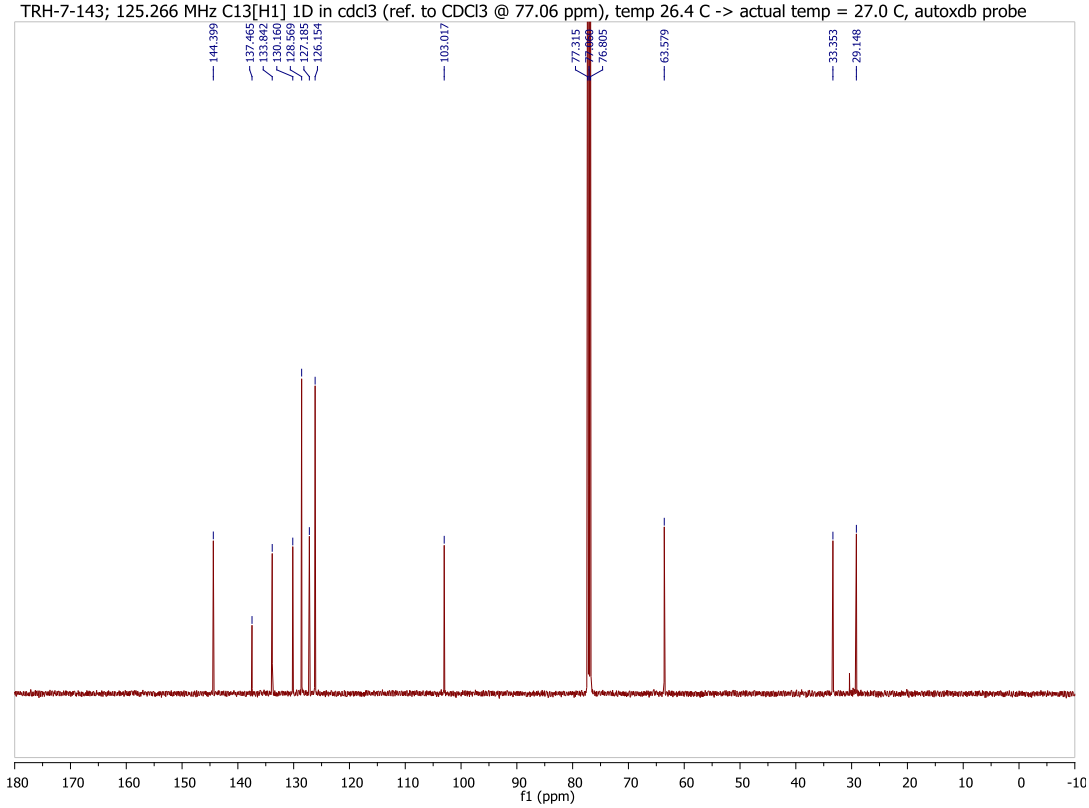

^{1}H and ^{13}C spectra for 3-52i in $CDCl_3$ at 25 ^{o}C

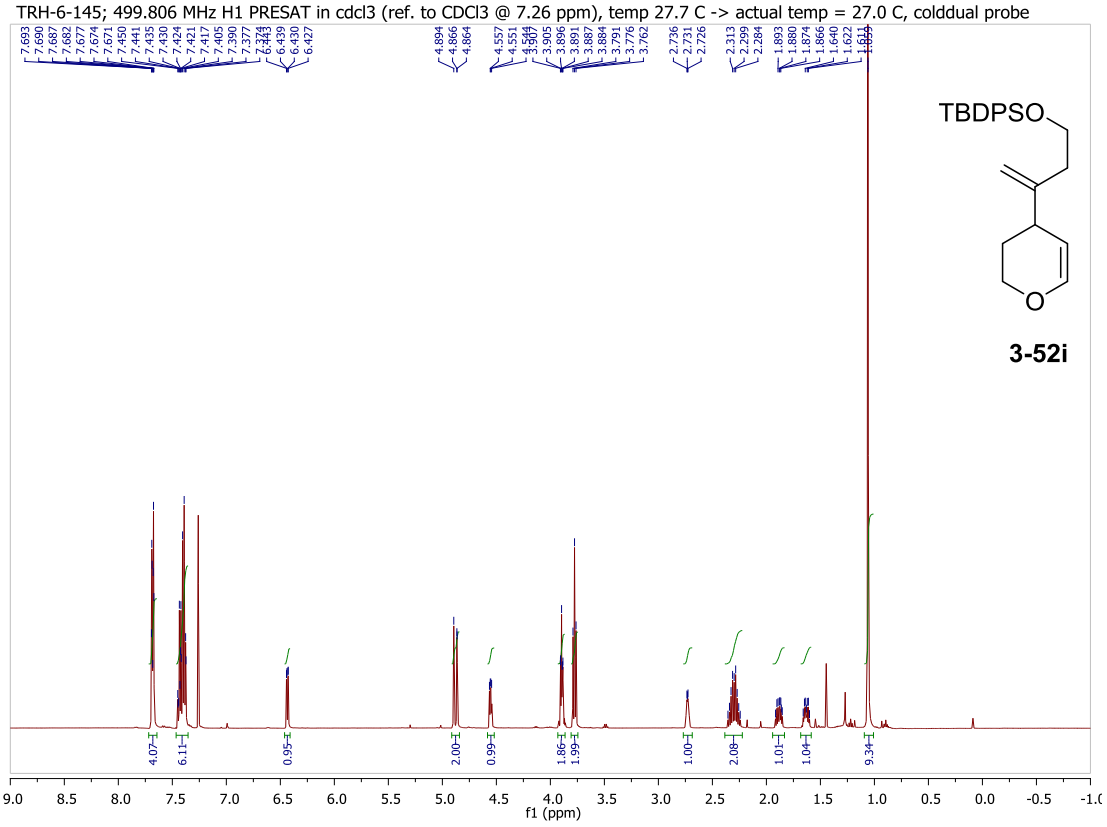

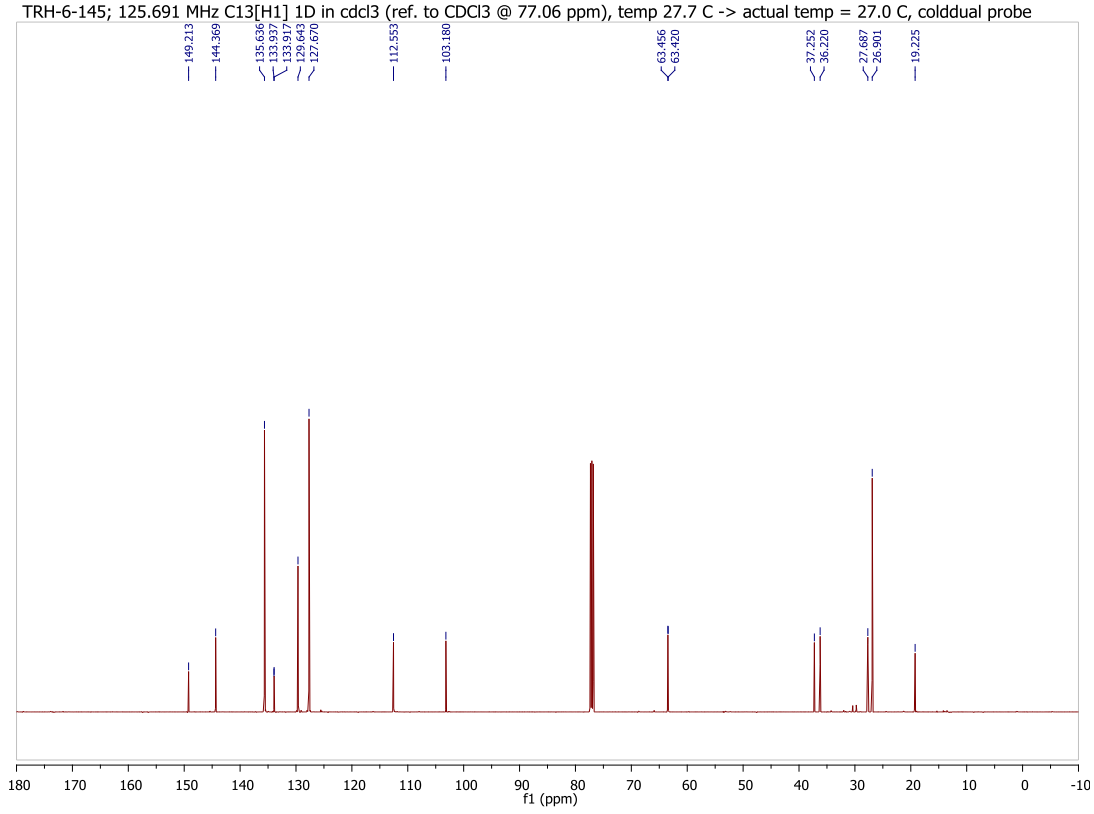

^{1}H and ^{13}C spectra for 3-52j in $CDCl_3$ at 25 ^{o}C

TRH-6-137; 498.118 MHz H1 1D in cdcl3 (ref. to CDCl3 @ 7.26 ppm), temp 26.4 C -> actual temp = 27.0 C, autoxdb probe

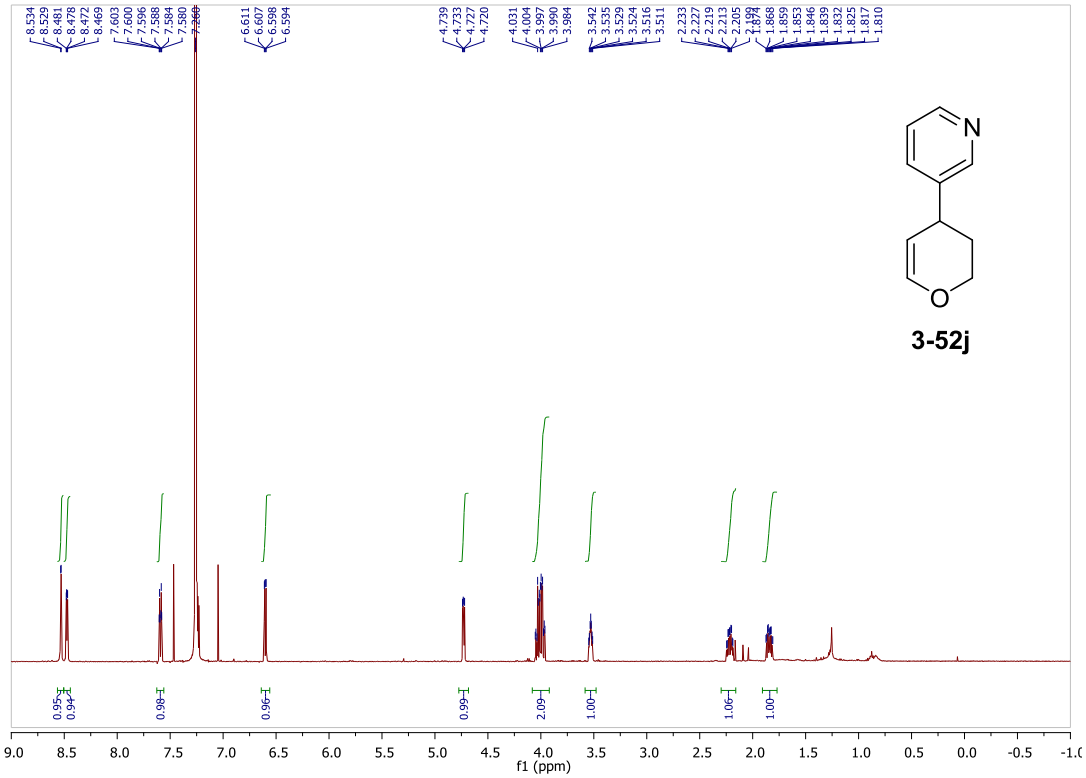

TRH-6-137; 125.266 MHz C13[H1] 1D in cdcl3 (ref. to CDCl3 @ 77.06 ppm), temp 26.4 C -> actual temp = 27.0 C, autoxdb probe

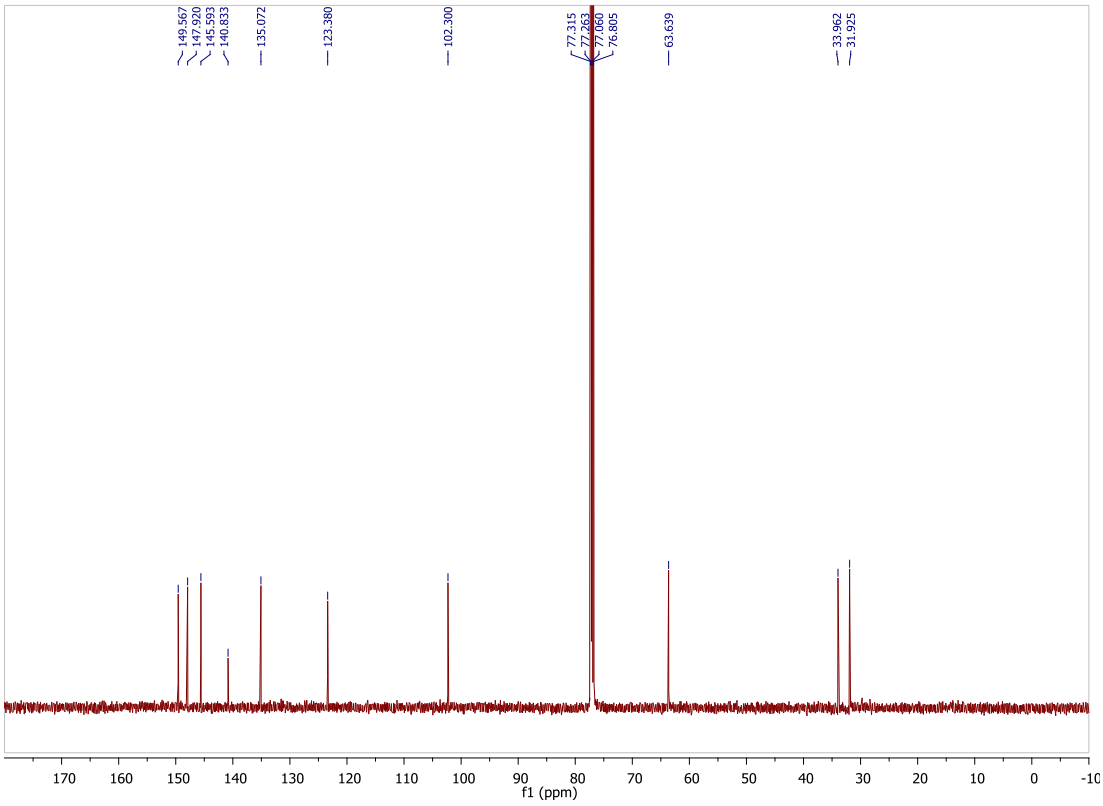

^{1}H and ^{13}C spectra for 3-52k in $CDCl_3$ at 25 ^{o}C

TRH-7-23; 400.392 MHz H1 PRESAT in cdcl3 (ref. to CDCl3 @ 7.26 ppm), temp 27.0 C -> actual temp = 27.0 C, m400gz probe

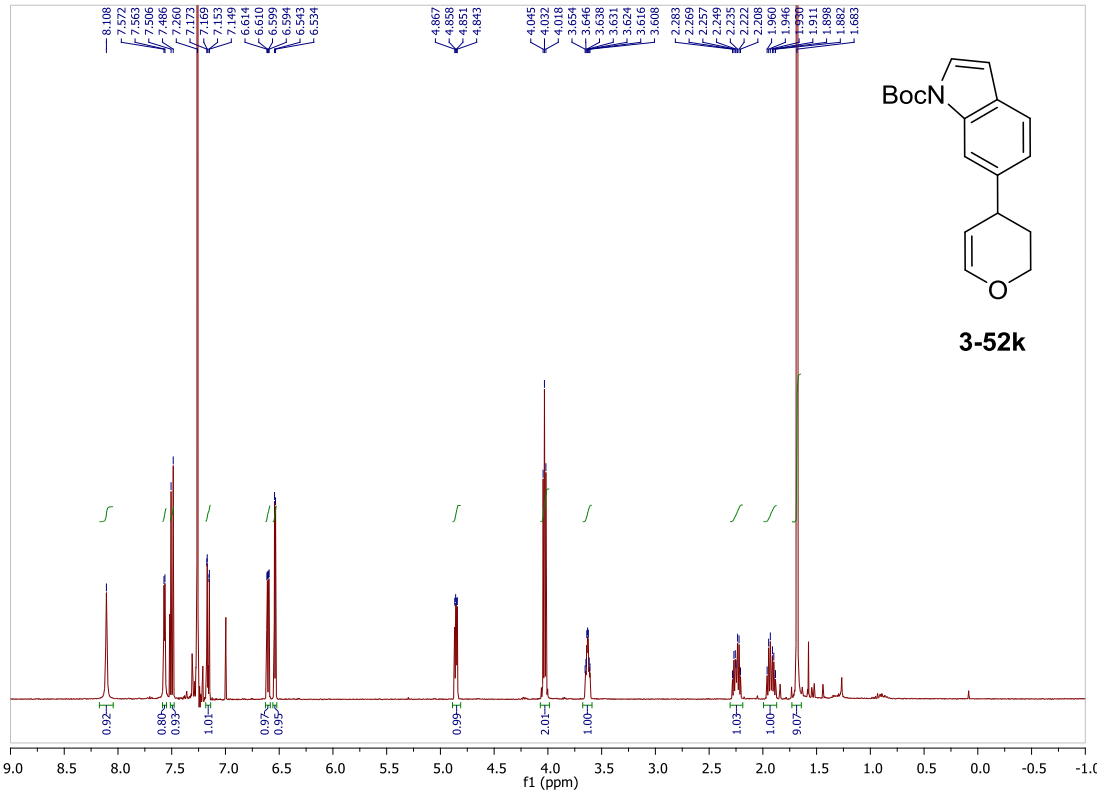

TRH-7-23; 125.690 MHz C13[H1] 1D in cdcl3 (ref. to CDCl3 @ 77.06 ppm), temp 27.7 C -> actual temp = 27.0 C, colddual probe

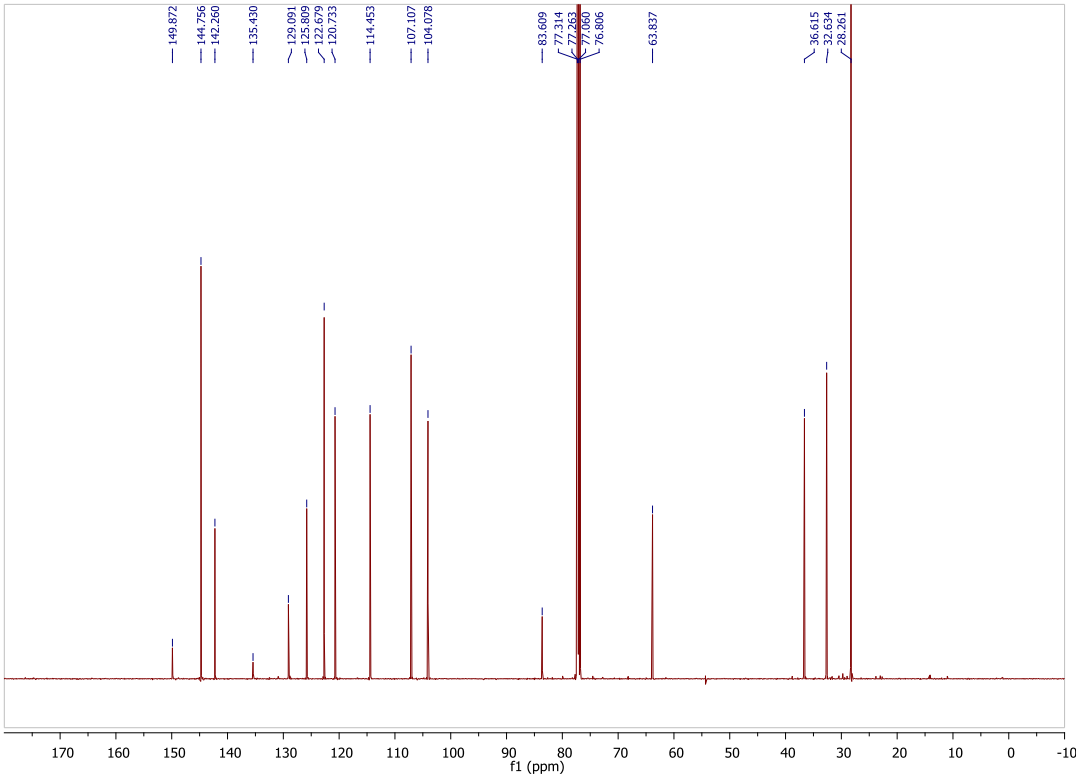

^{1}H and ^{13}C spectra for 3-53b in $CDCl_3$ at 25 ^{o}C

TRH-6-133; 499.806 MHz H1 PRESAT in cdcl3 (ref. to CDCl3 @ 7.26 ppm), temp 27.7 C -> actual temp = 27.0 C, colddual probe

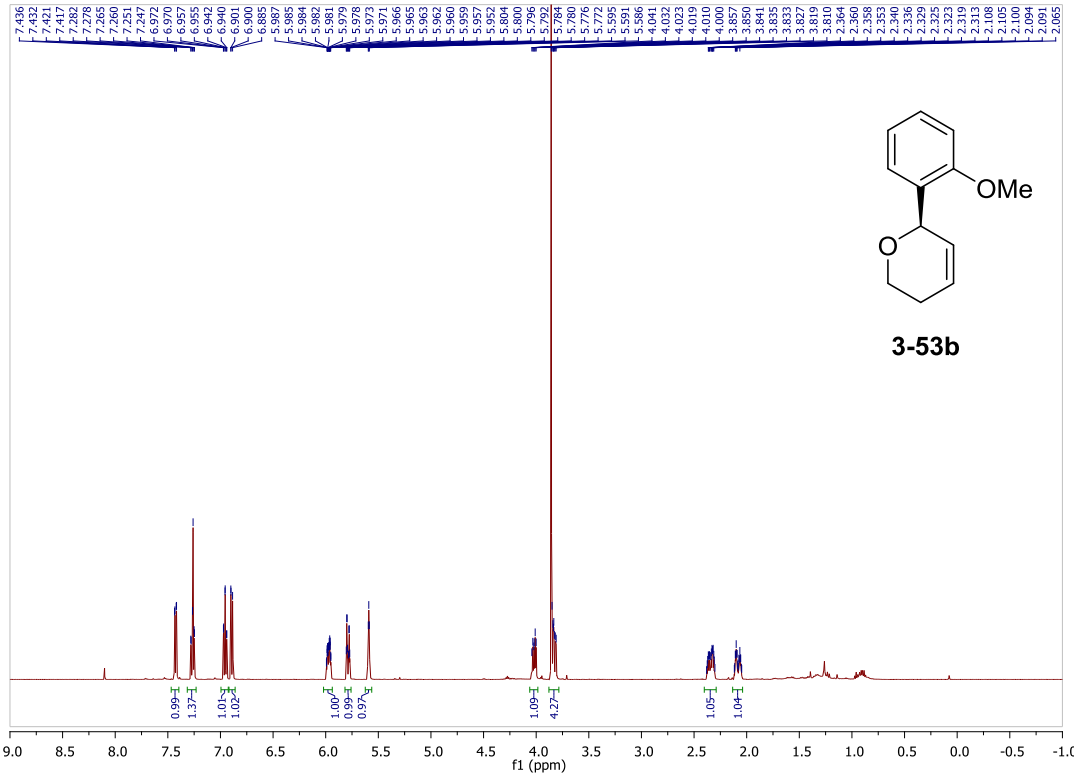

TRH-6-133; 125.691 MHz C13[H1] 1D in cdcl3 (ref. to CDCl3 @ 77.06 ppm), temp 27.7 C -> actual temp = 27.0 C, colddual probe

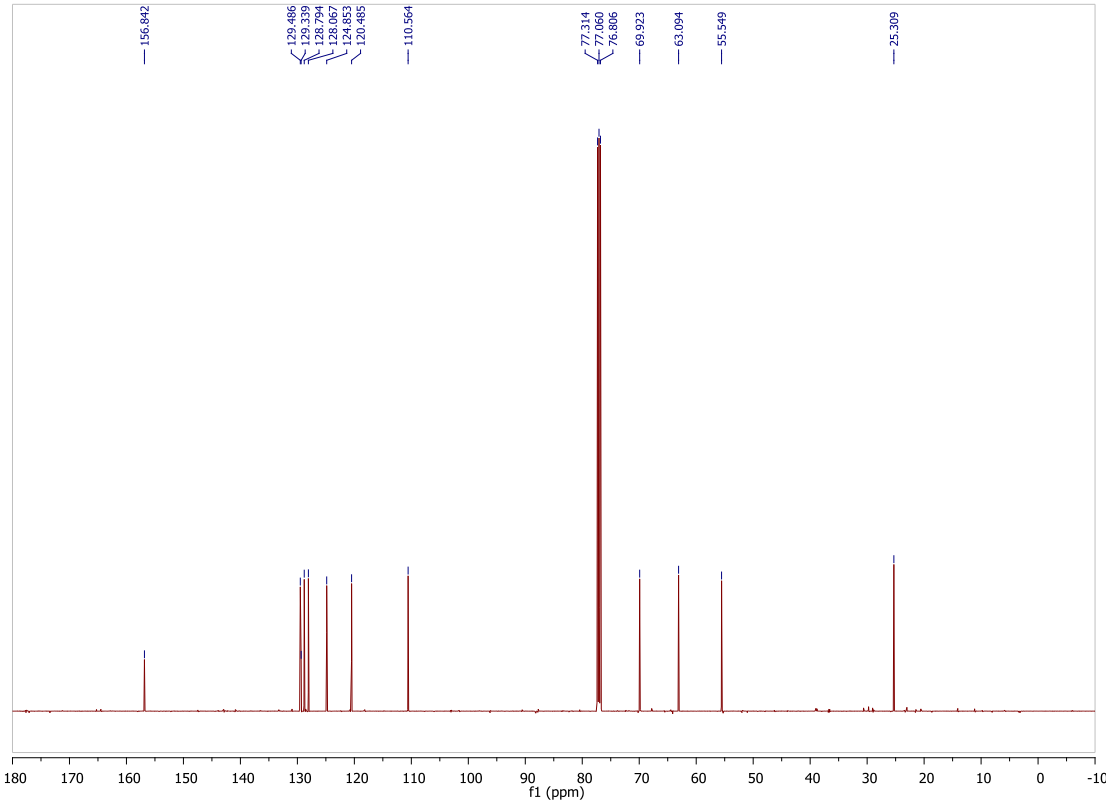

^{1}H and ^{13}C spectra for 3-53c in $CDCl_3$ at 25 ^{o}C

TRH-6-119; 499.806 MHz H1 PRESAT in cdcl3 (ref. to CDCl3 @ 7.26 ppm), temp 27.7 C -> actual temp = 27.0 C, colddual probe

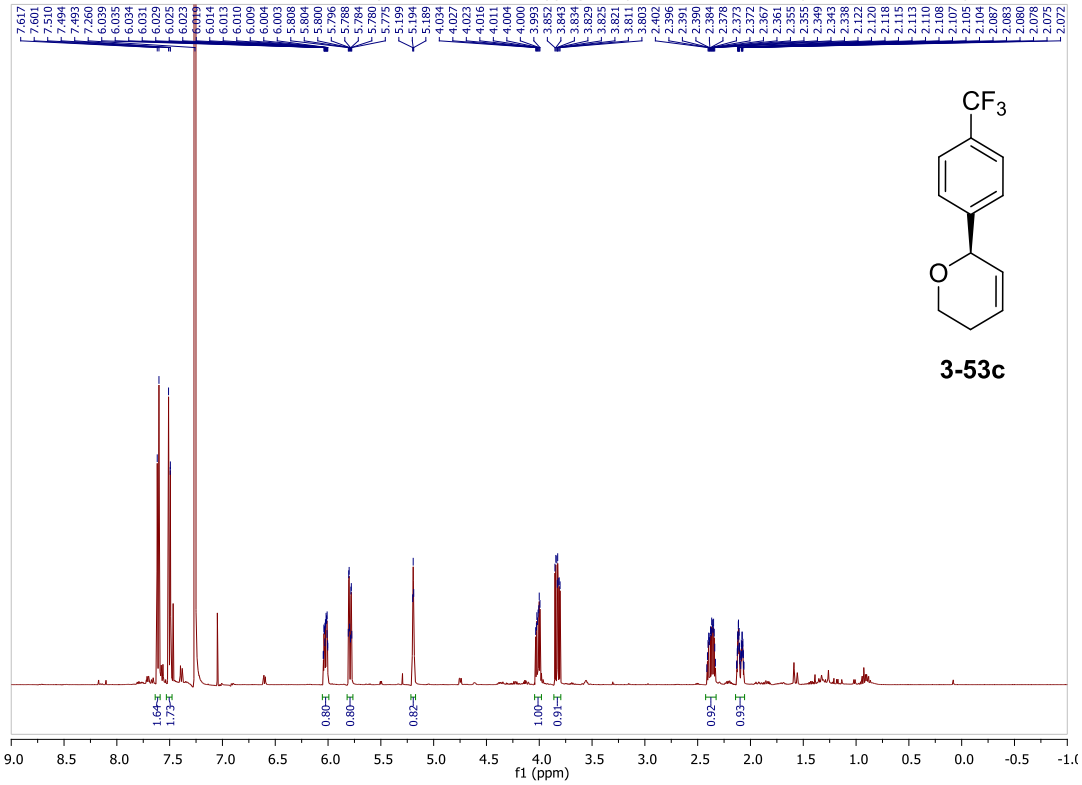

TRH-6-119; 125.691 MHz C13[H1] 1D in cdcl3 (ref. to CDCl3 @ 77.06 ppm), temp 27.7 C -> actual temp = 27.0 C, colddual probe

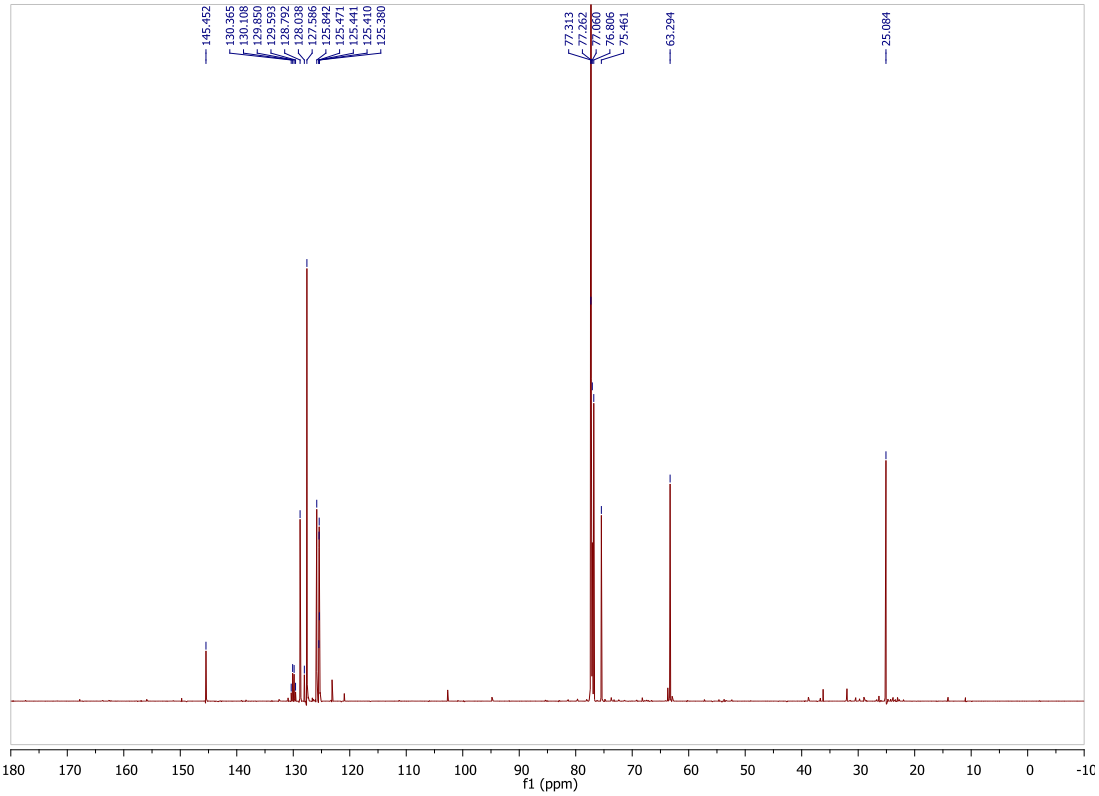

^{1}H and ^{13}C spectra for 3-53h in $CDCl_3$ at 25 ^{o}C

TRH-7-142; 499.806 MHz H1 PRESAT in cdcl3 (ref. to CDCl3 @ 7.26 ppm), temp 27.7 C -> actual temp = 27.0 C, colddual probe

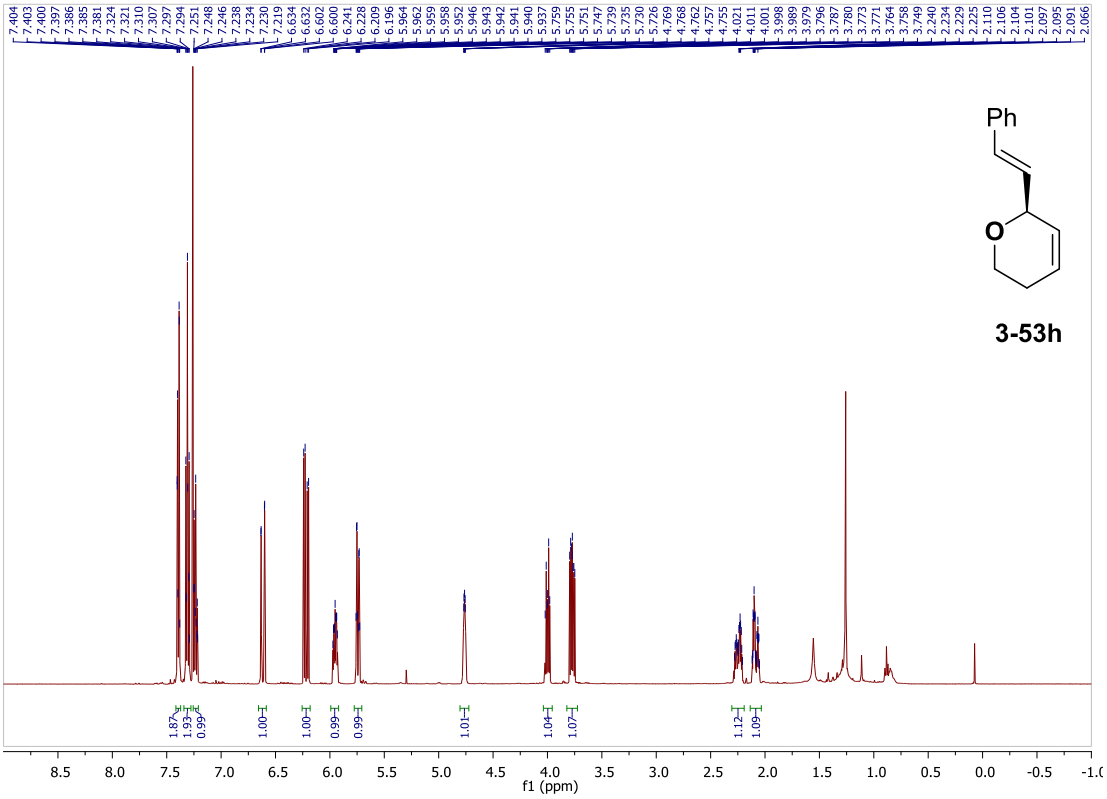

TRH-7-142; 125.691 MHz C13[H1] 1D in cdcl3 (ref. to CDCl3 @ 77.06 ppm), temp 27.7 C -> actual temp = 27.0 C, colddual probe

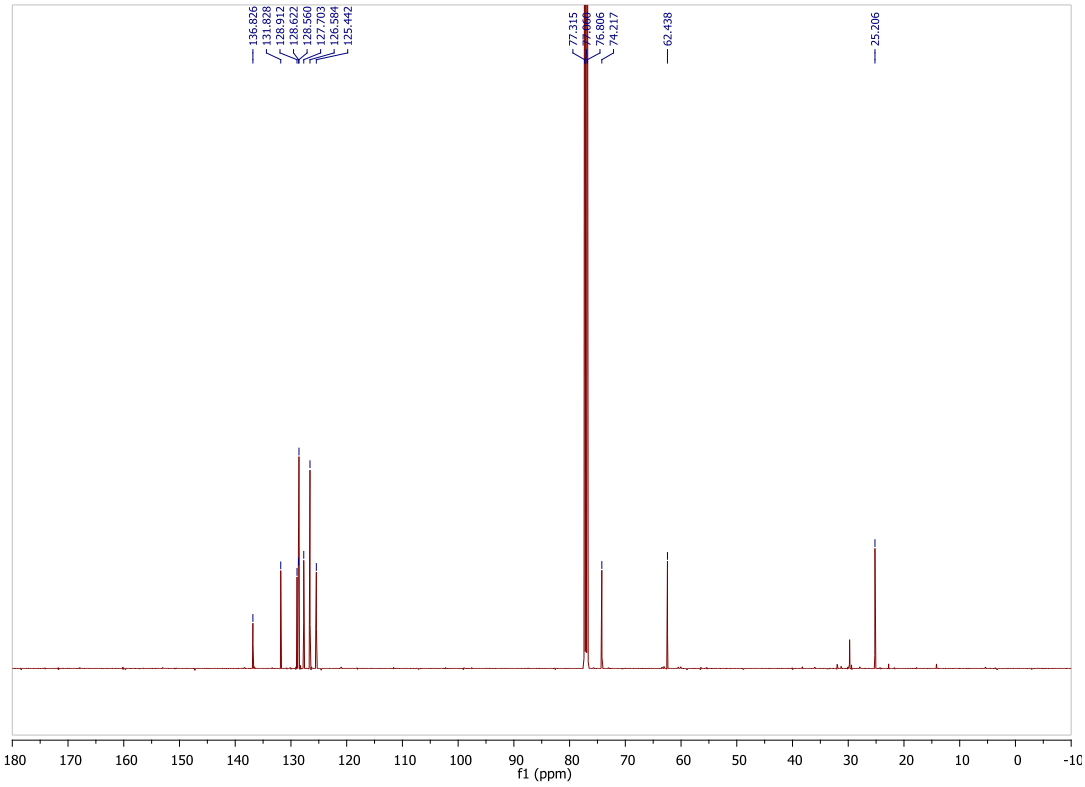

^{1}H and ^{13}C spectra for 3-53i in $CDCl_3$ at 25 ^{o}C

TRH-6-130; 499.806 MHz H1 PRESAT in cdcl3 (ref. to CDCl3 @ 7.26 ppm), temp 27.7 C -> actual temp = 27.0 C, colddual probe

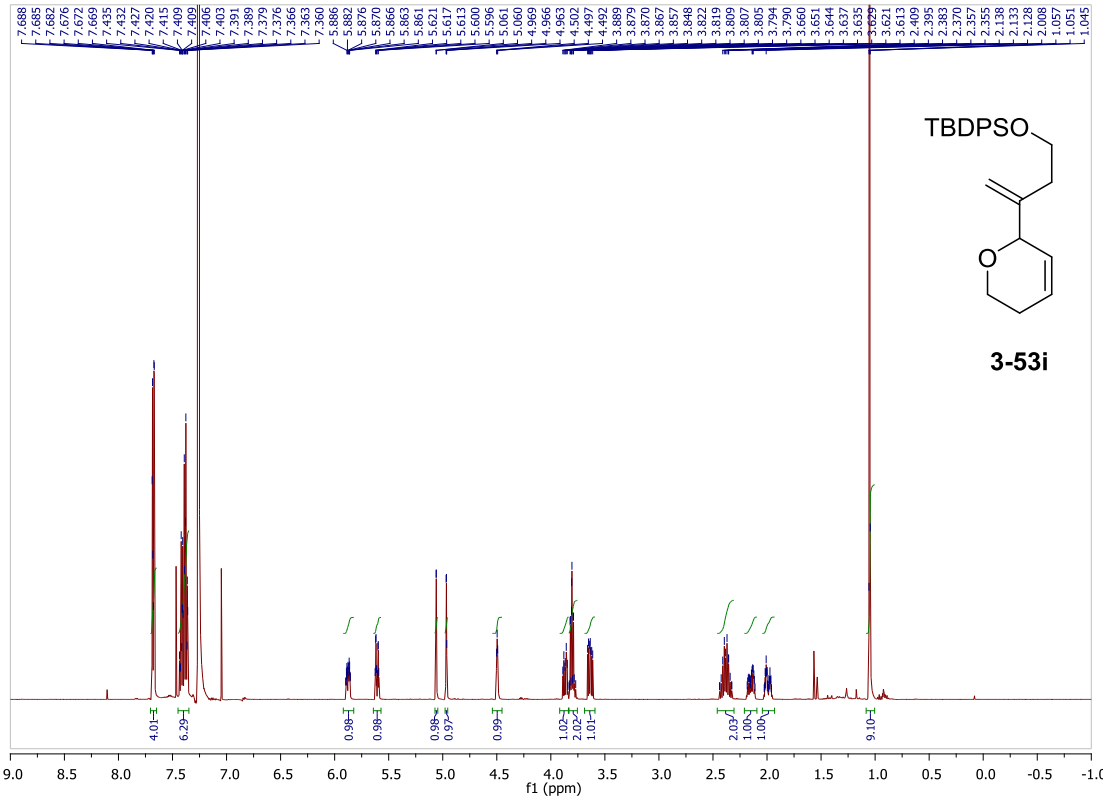

TRH-6-130; 125.691 MHz C13[H1] 1D in cdcl3 (ref. to CDCl3 @ 77.06 ppm), temp 27.7 C -> actual temp = 27.0 C, colddual probe

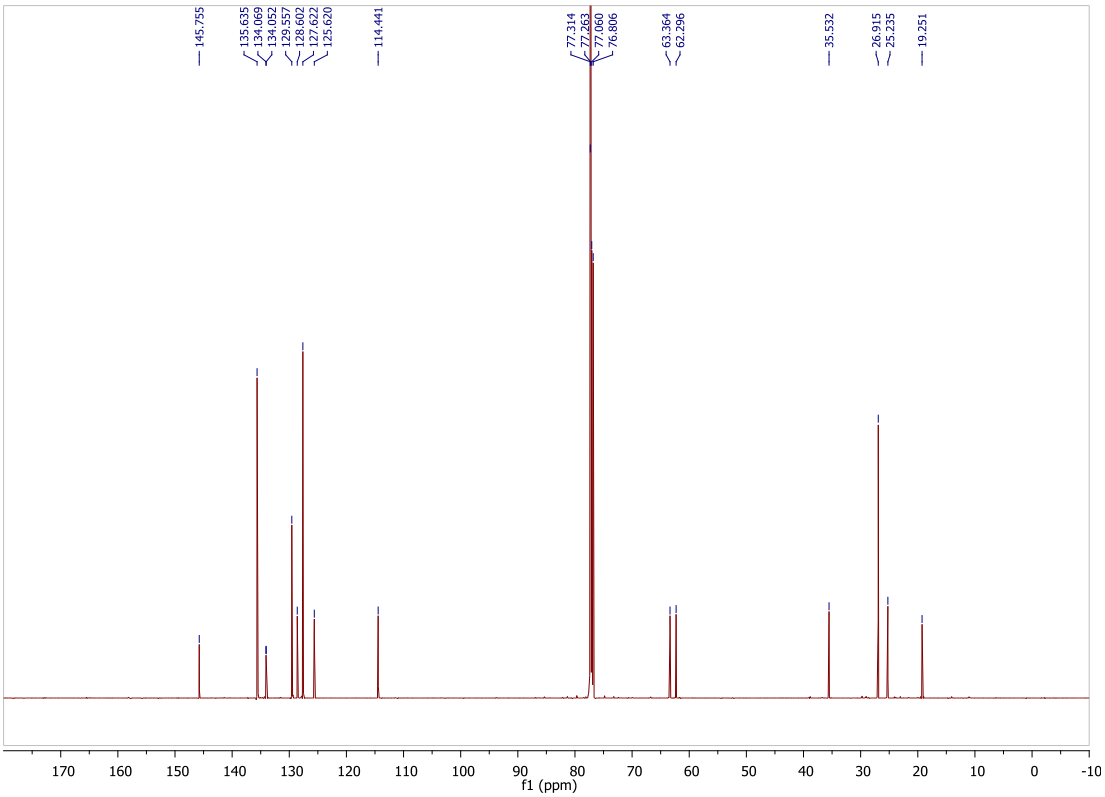

^{1}H and ^{13}C spectra for 3-53j in $CDCl_3$ at 25 ^{o}C

TRH-7-41; 498.118 MHz H1 1D in cdcl3 (ref. to CDCl3 @ 7.26 ppm), temp 26.4 C -> actual temp = 27.0 C, autoxdb probe

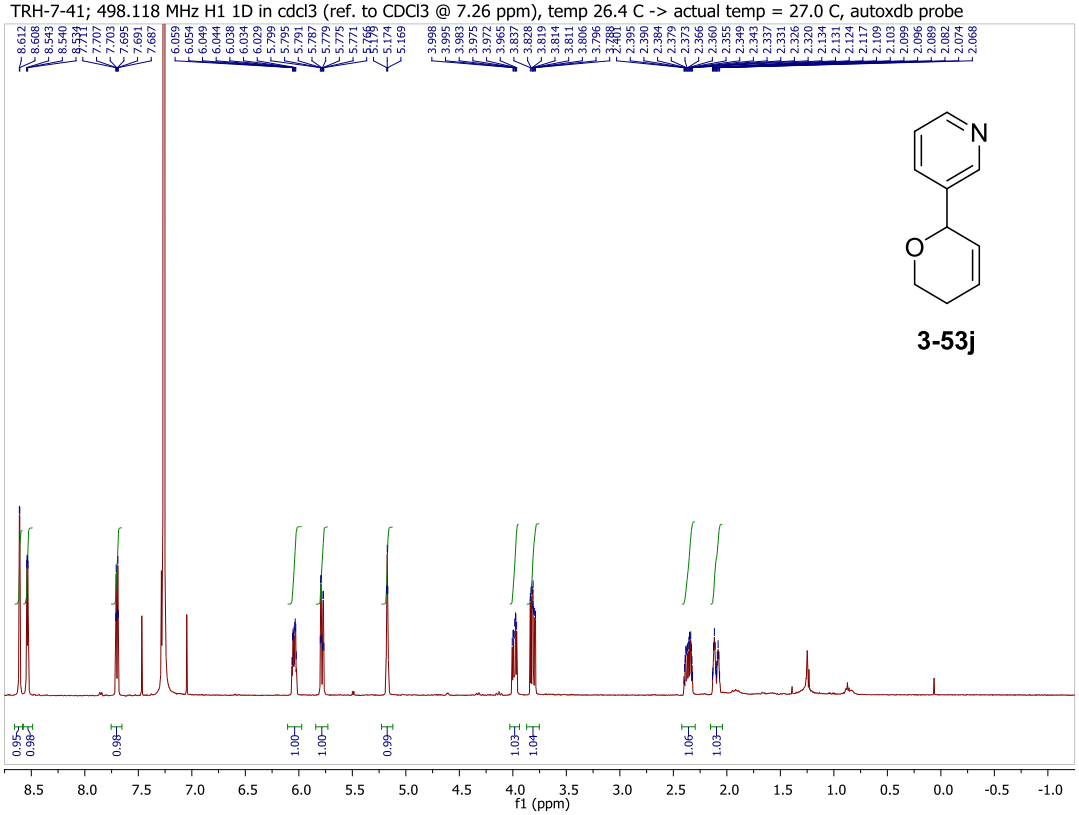

TRH-7-41; 125.690 MHz C13[H1] 1D in cdcl3 (ref. to CDCl3 @ 77.06 ppm), temp 27.7 C -> actual temp = 27.0 C, colddual probe

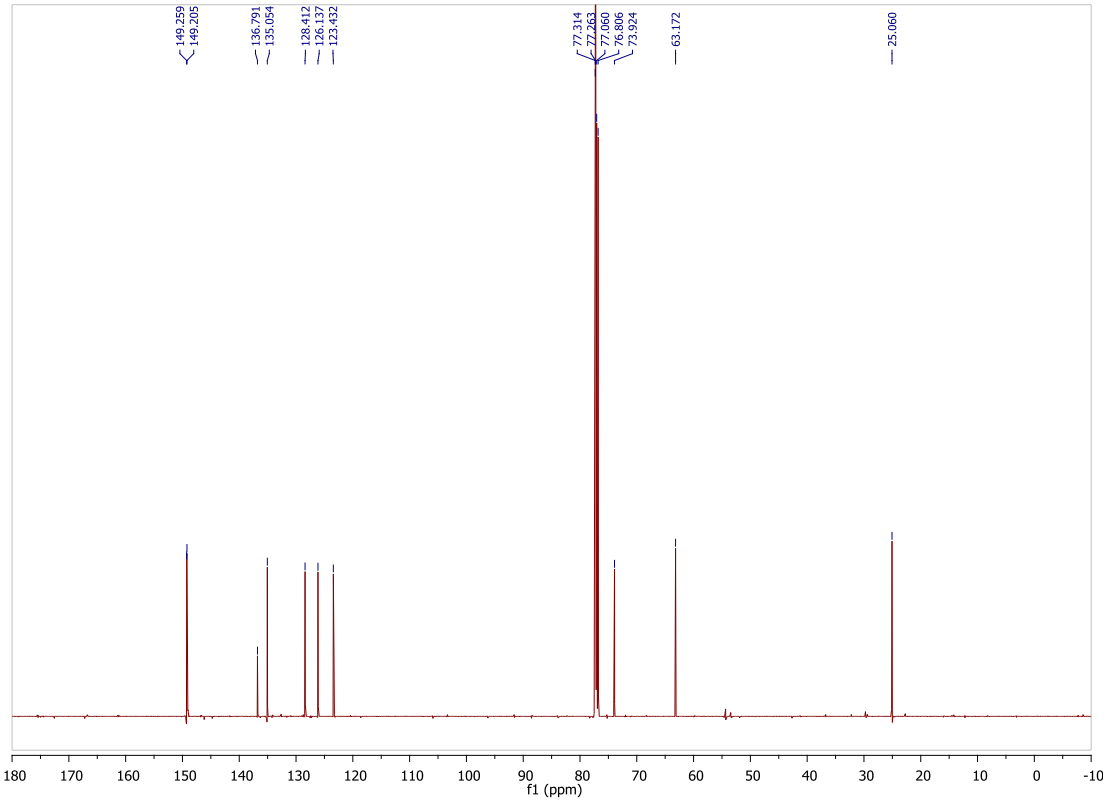

^{1}H and ^{13}C spectra for 3-53k in $CDCl_3$ at 25 ^{o}C

TRH-6-196; 498.118 MHz H1 1D in cdcl3 (ref. to CDCl3 @ 7.26 ppm), temp 26.4 C -> actual temp = 27.0 C, autoxdb probe

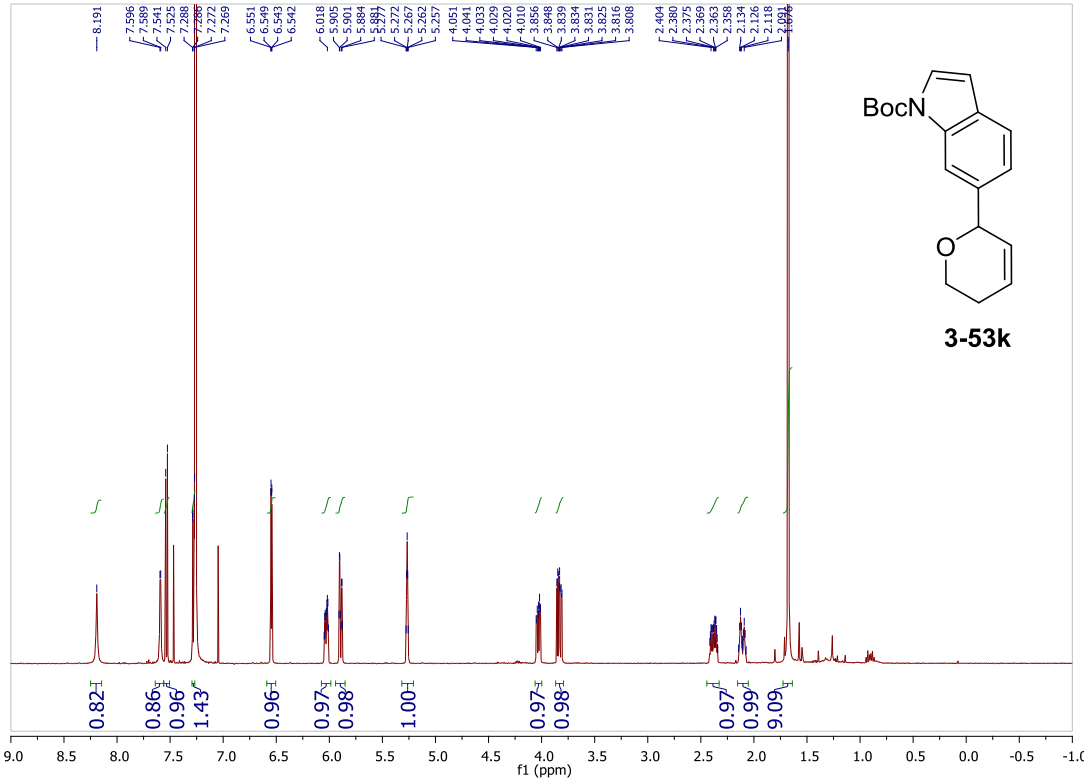

TRH-6-196; 100.689 MHz C13[H1] 1D in cdcl3 (ref. to CDCl3 @ 77.06 ppm), temp 27.0 C -> actual temp = 27.0 C, m400gz probe

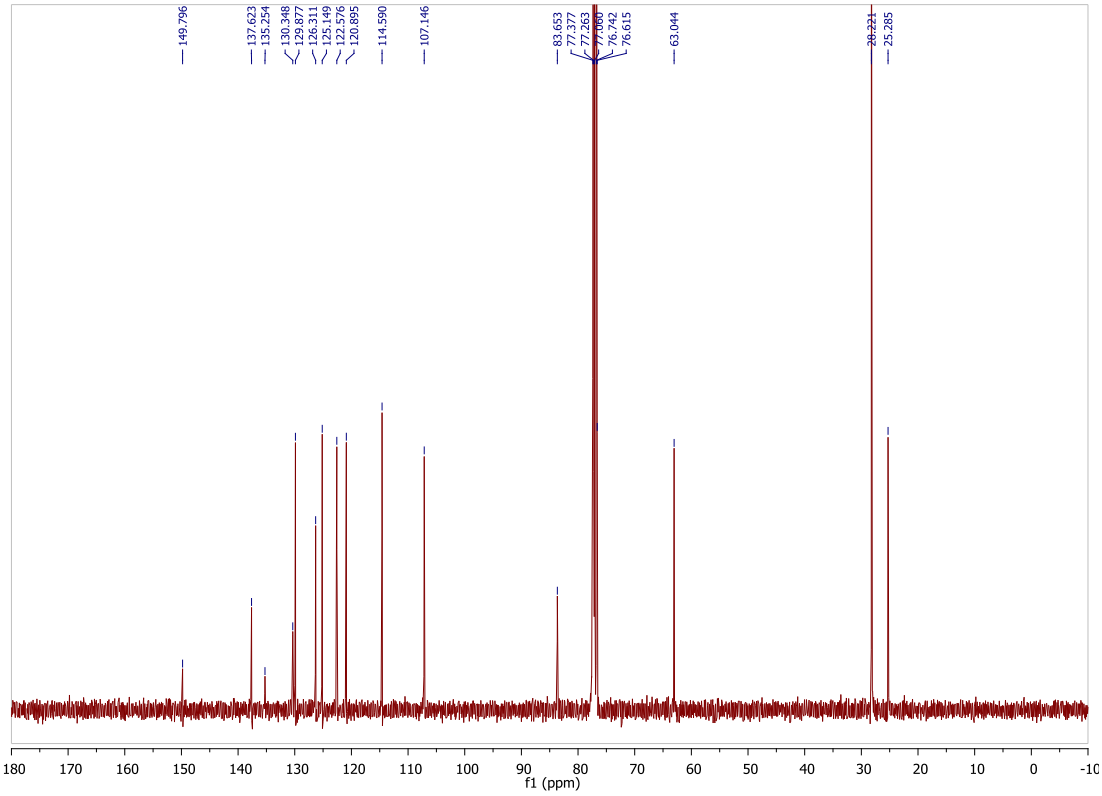

^{1}H and ^{13}C spectra for 3-57a/b in $CDCl_3$ at 25 ^{o}C

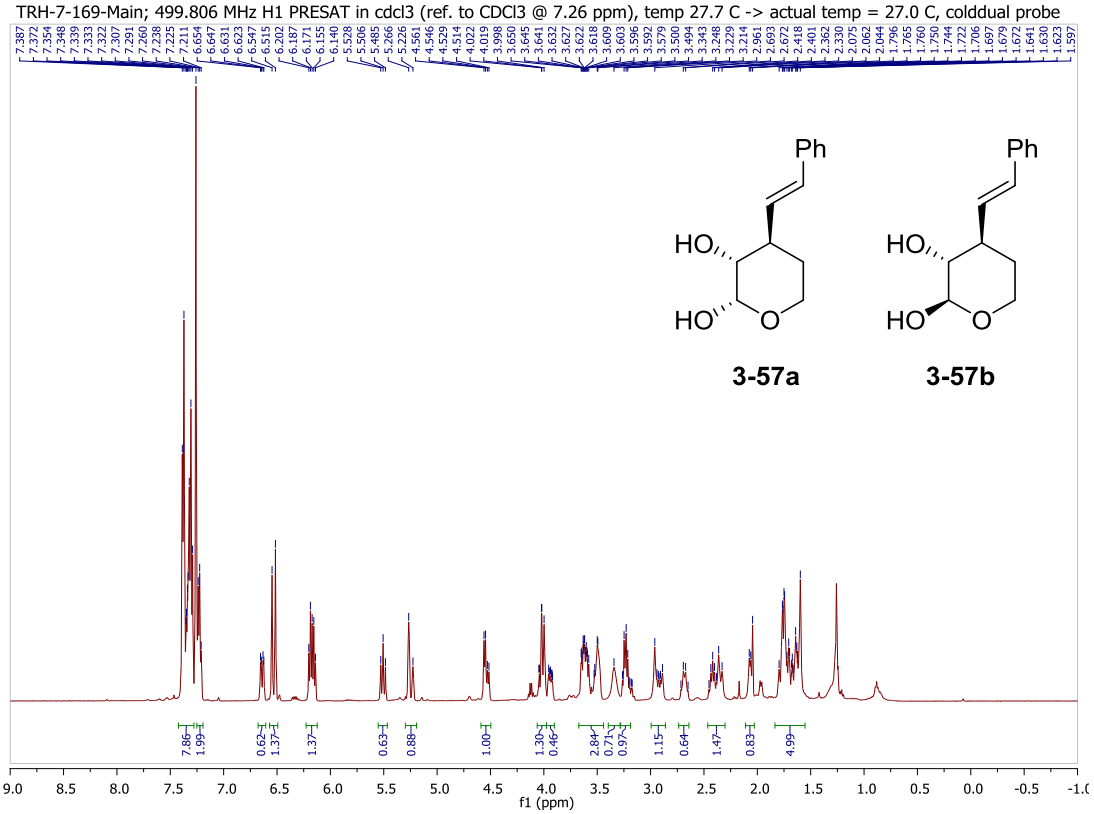

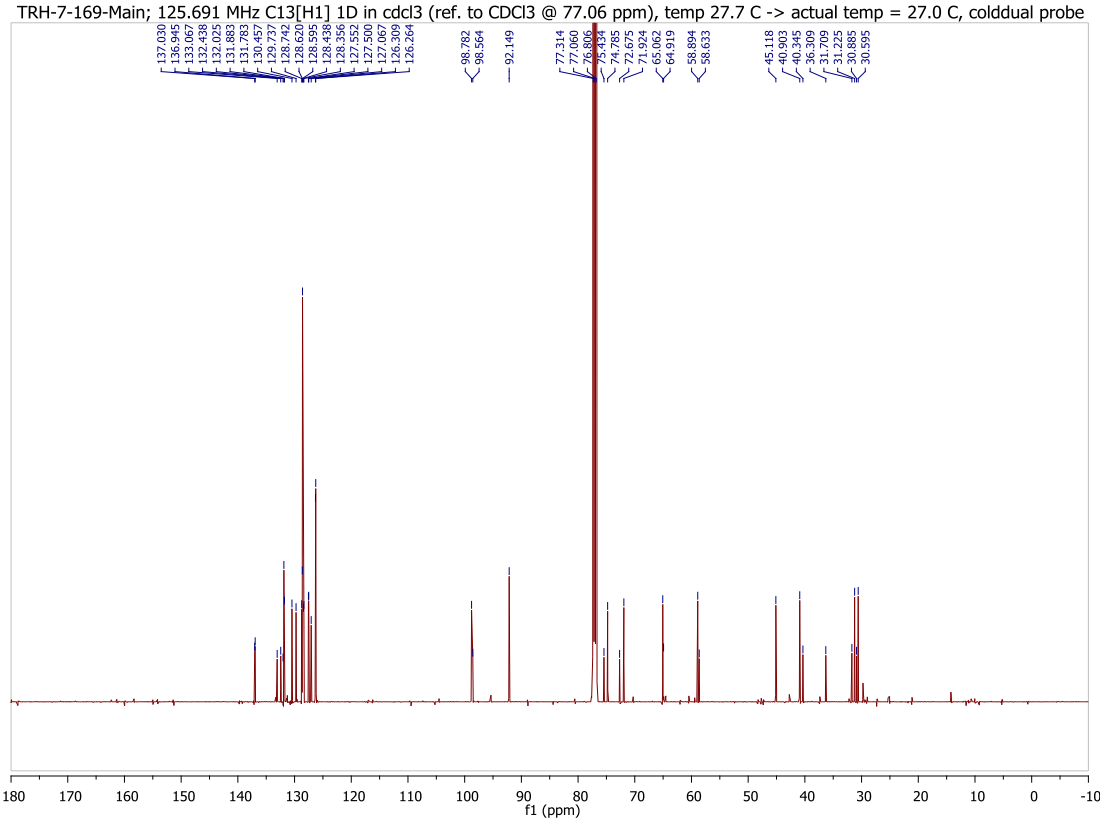

^{1}H and ^{13}C spectra for 3-72 in $CDCl_3$ at 25 ^{o}C

TRH-7-129; 499.806 MHz H1 PRESAT in cdcl3 (ref. to CDCl3 @ 7.26 ppm), temp 27.7 C -> actual temp = 27.0 C, colddual probe

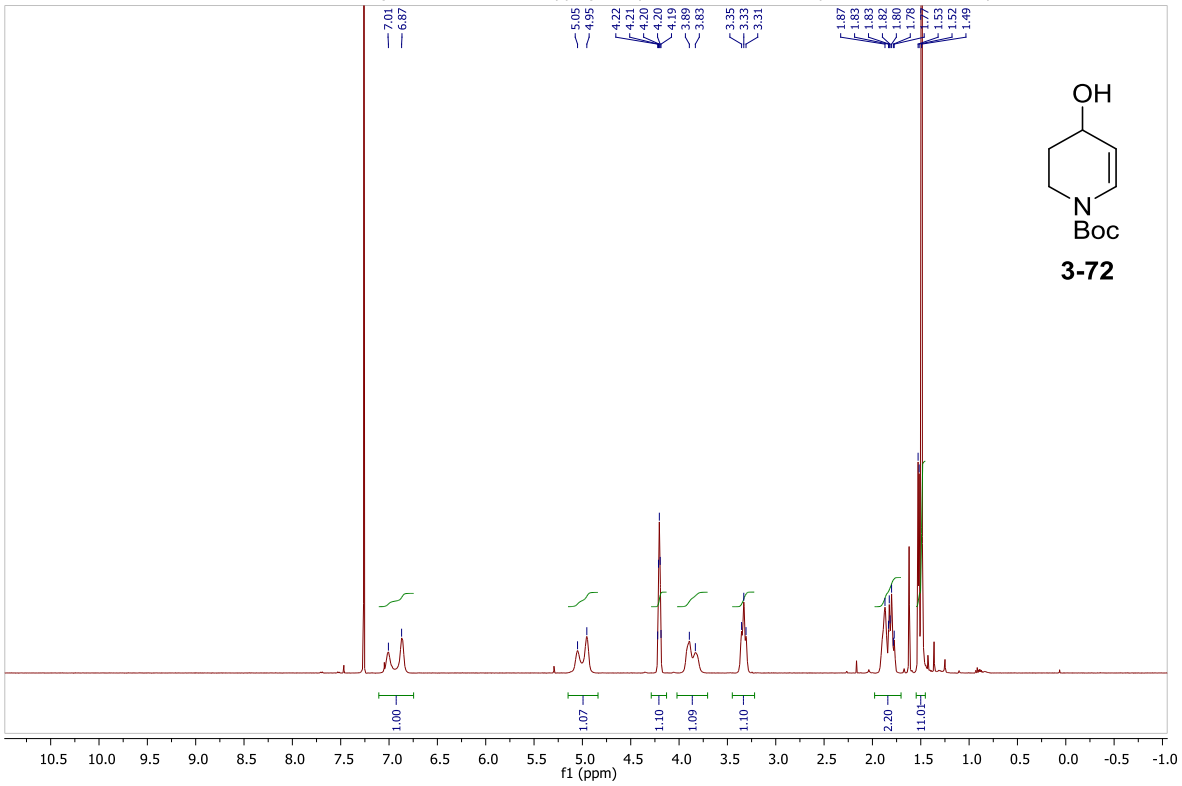

TRH-7-129; 125.691 MHz C13[H1] 1D in cdcl3 (ref. to CDCl3 @ 77.06 ppm), temp 27.7 C -> actual temp = 27.0 C, colddual probe

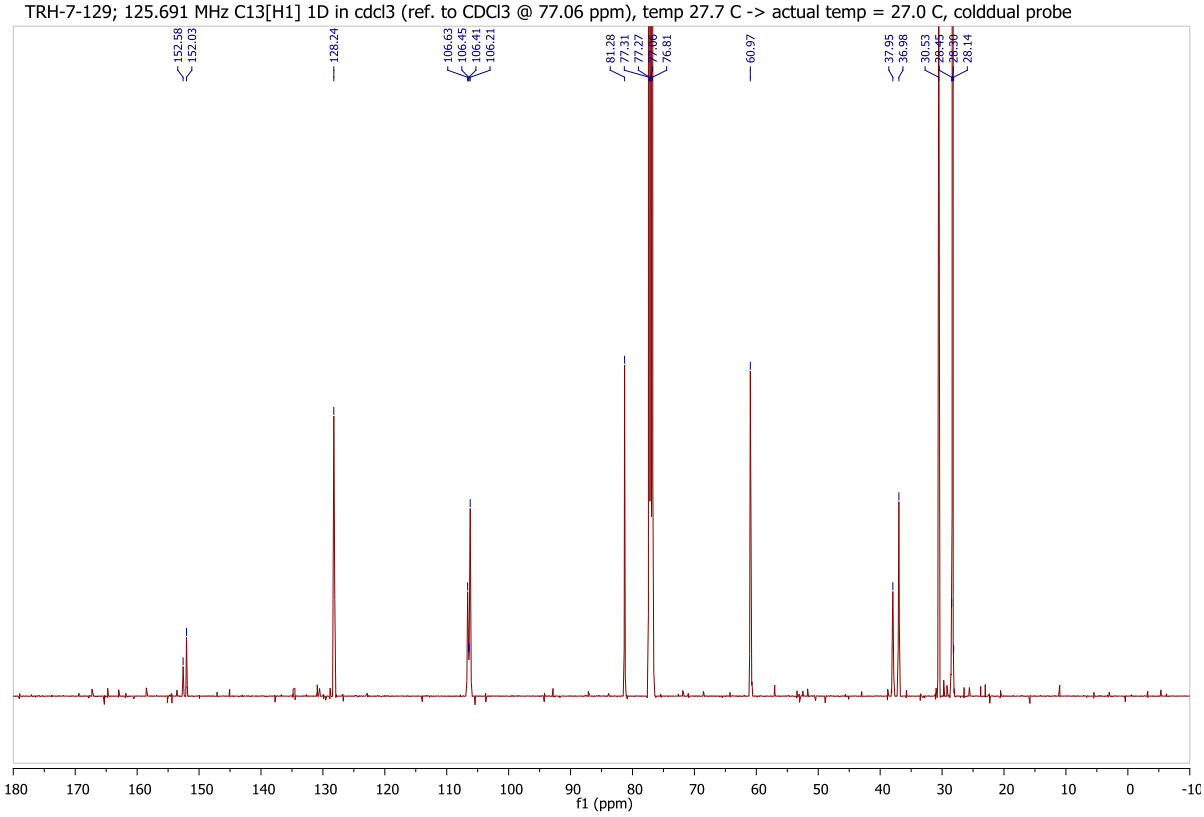

^{1}H and ^{13}C spectra for 4-6c in $CDCl_3$ at 25 ^{o}C

TRH-9-125; 499.806 MHz H1 PRESAT in cdcl3 (ref. to CDCl3 @ 7.26 ppm), temp 27.7 C -> actual temp = 27.0 C, colddual probe

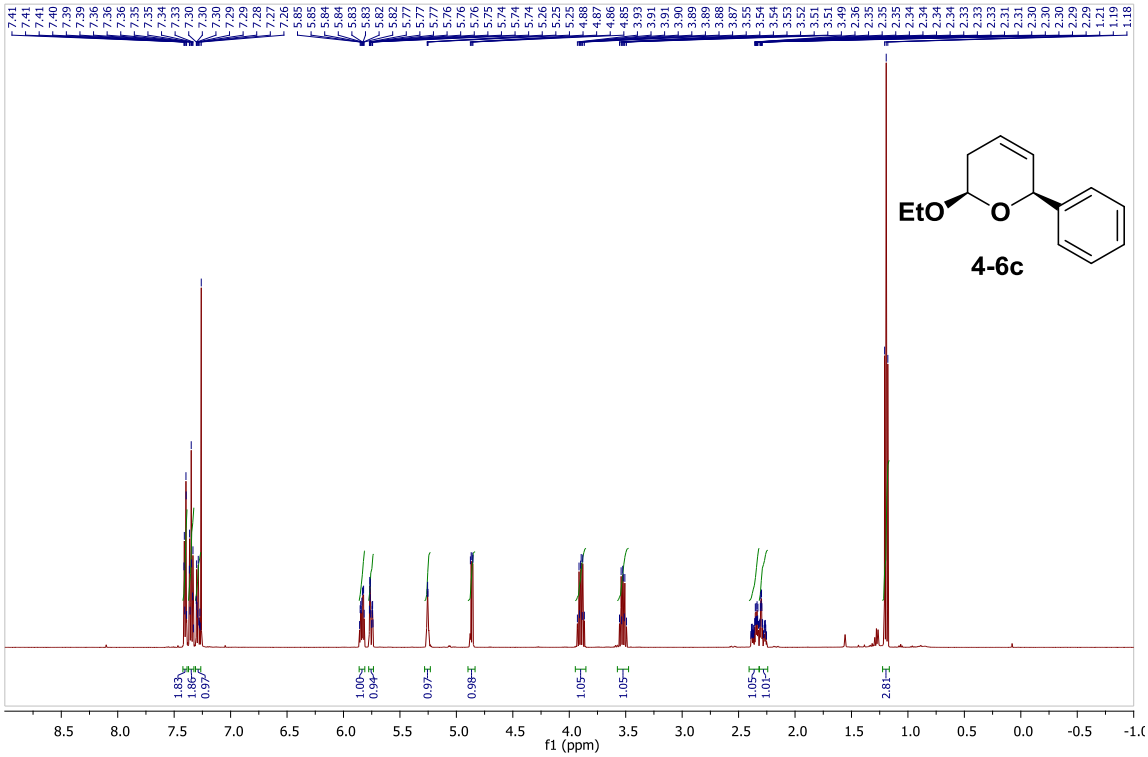

TRH-9-125; 125.691 MHz C13[H1] 1D in cdcl3 (ref. to CDCl3 @ 77.06 ppm), temp 27.7 C -> actual temp = 27.0 C, colddual probe

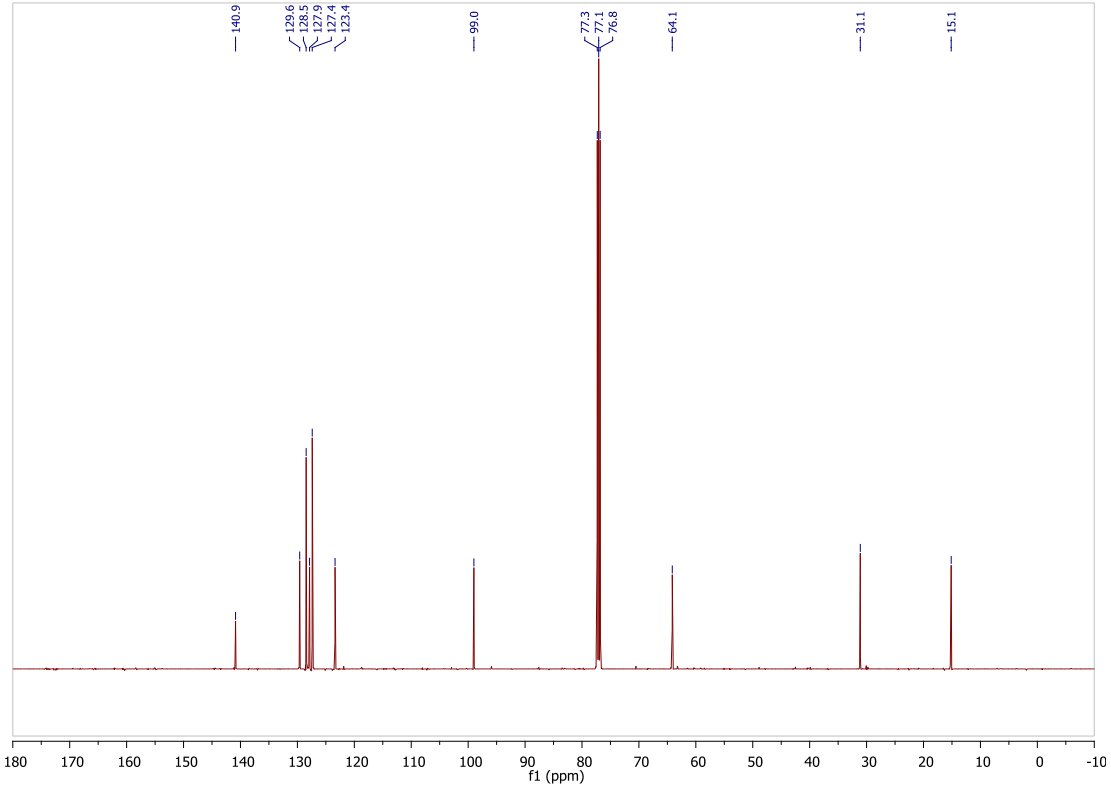

^{1}H and ^{13}C spectra for 4-7 in $CDCl_3$ at 25 ^{o}C

Taras, TRH-9-104; 499.806 MHz H1 PRESAT in cdcl3 (ref. to CDCl3 @ 7.26 ppm), temp 27.7 C -> actual temp = 27.0 C, colddual probe

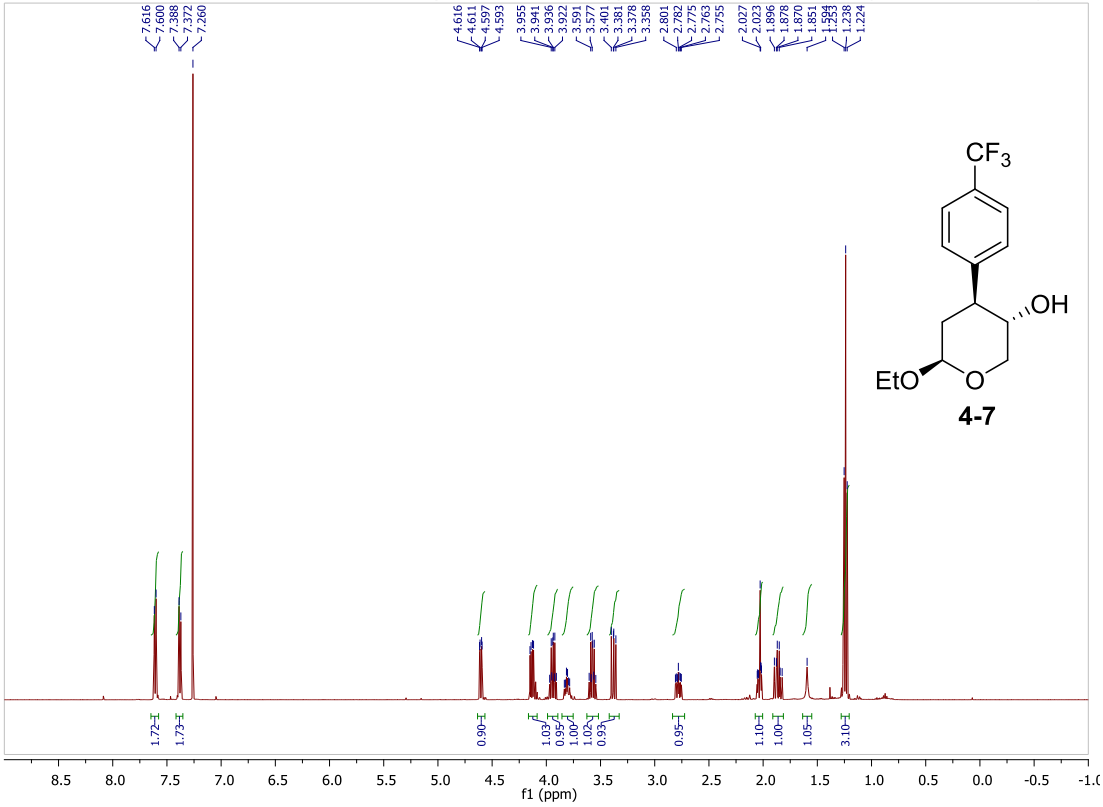

Taras, TRH-9-104; 125.691 MHz C13[H1] 1D in cdcl3 (ref. to CDCl3 @ 77.06 ppm), temp 27.7 C -> actual temp = 27.0 C, colddual probe

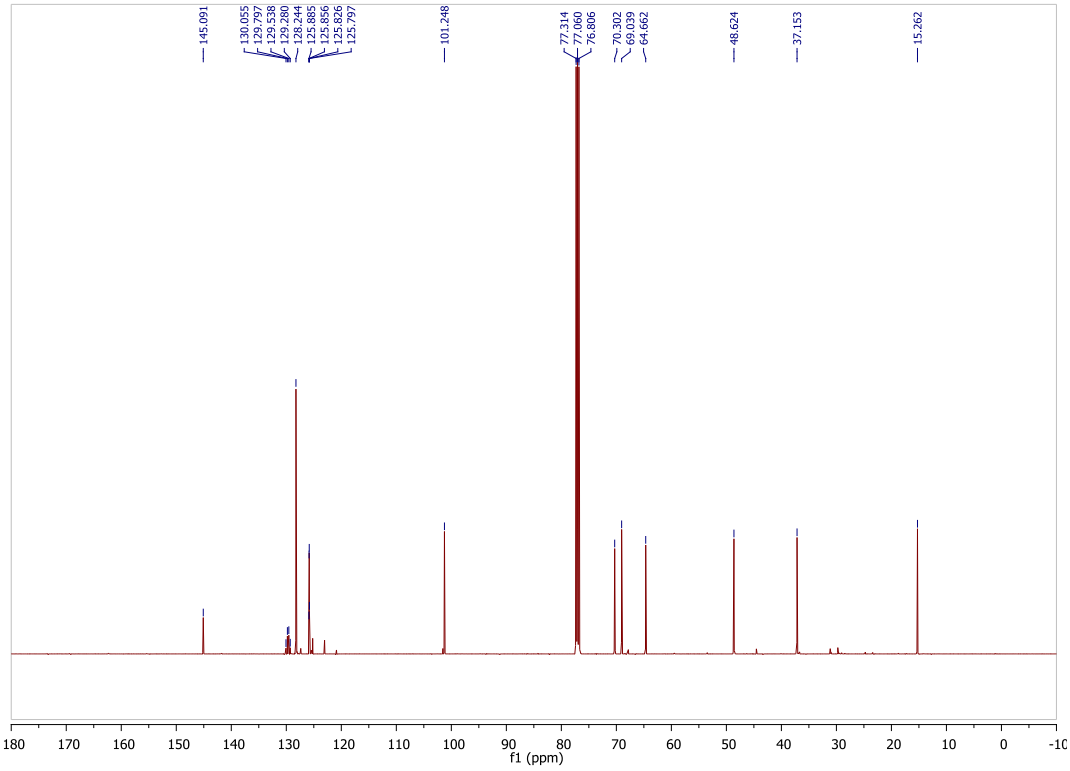

^{1}H and ^{13}C spectra for 4-9 in $CDCl_3$ at 25 ^{o}C

TRH-9-145; 400.389 MHz H1 PRESAT in cdcl3 (ref. to CDCl3 @ 7.26 ppm), temp 27.0 C -> actual temp = 27.0 C, m400gz probe

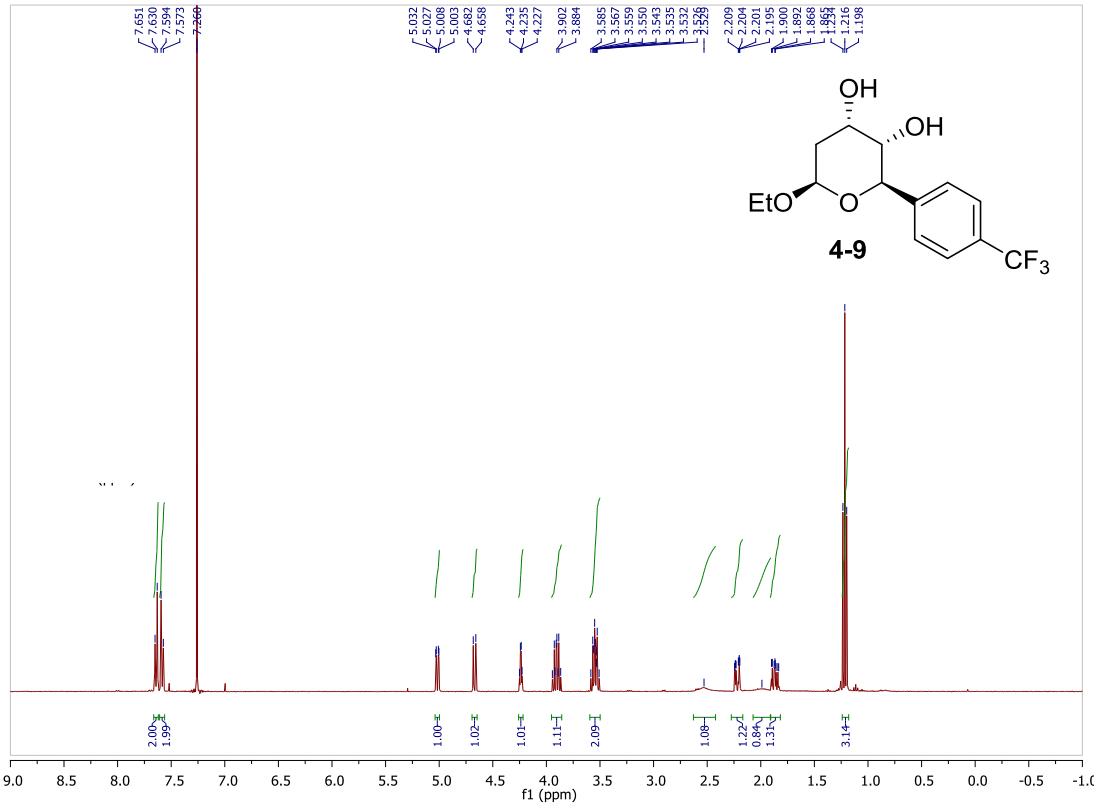

TRH-9-145; 100.688 MHz C13[H1] 1D in cdcl3 (ref. to CDCl3 @ 77.06 ppm), temp 27.0 C -> actual temp = 27.0 C, m400gz probe

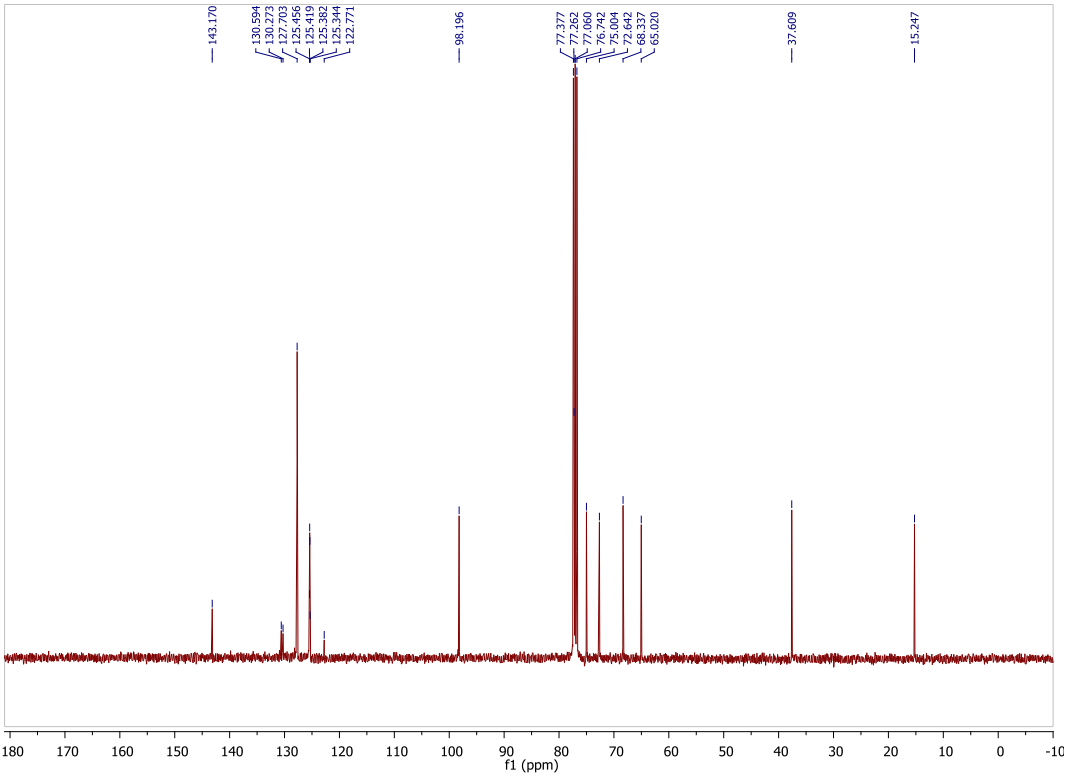

^{1}H and ^{13}C spectra for 4-10 in $CDCl_3$ at 25 ^{o}C

TRH-9-153; 499.806 MHz H1 PRESAT in cdcl3 (ref. to CDCl3 @ 7.26 ppm), temp 27.7 C -> actual temp = 27.0 C, colddual probe

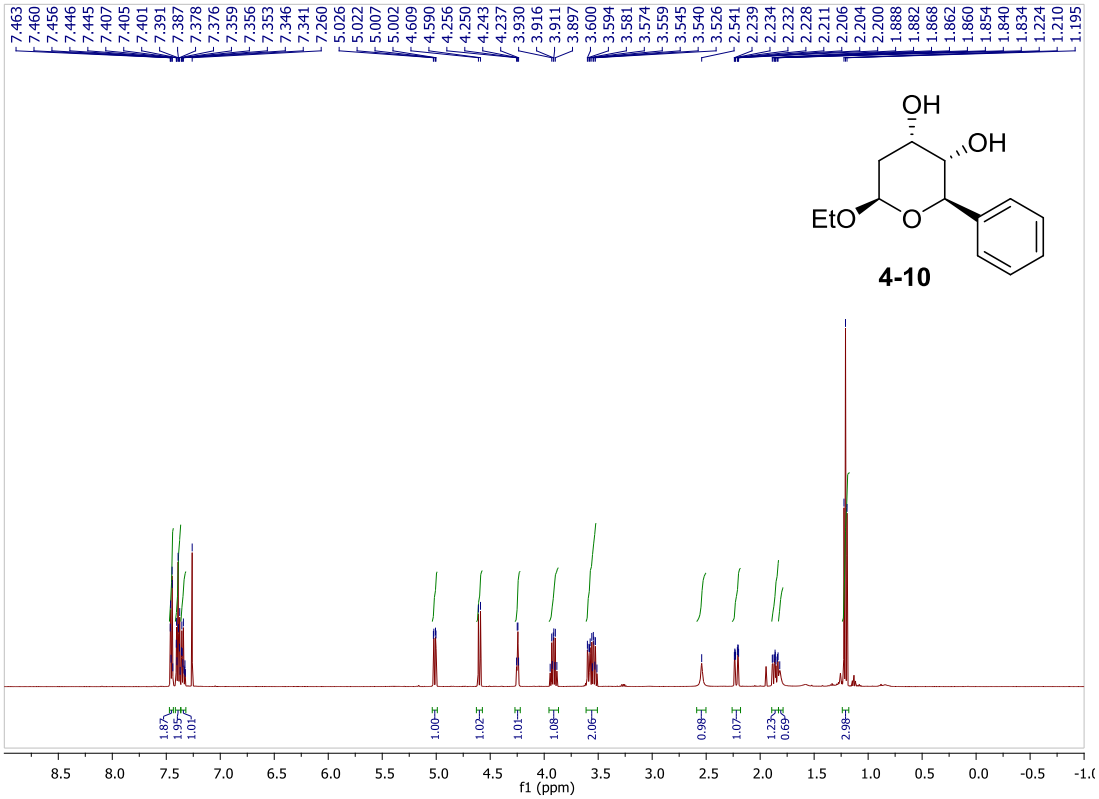

TRH-9-153; 125.691 MHz C13[H1] 1D in cdcl3 (ref. to CDCl3 @ 77.06 ppm), temp 27.7 C -> actual temp = 27.0 C, colddual probe

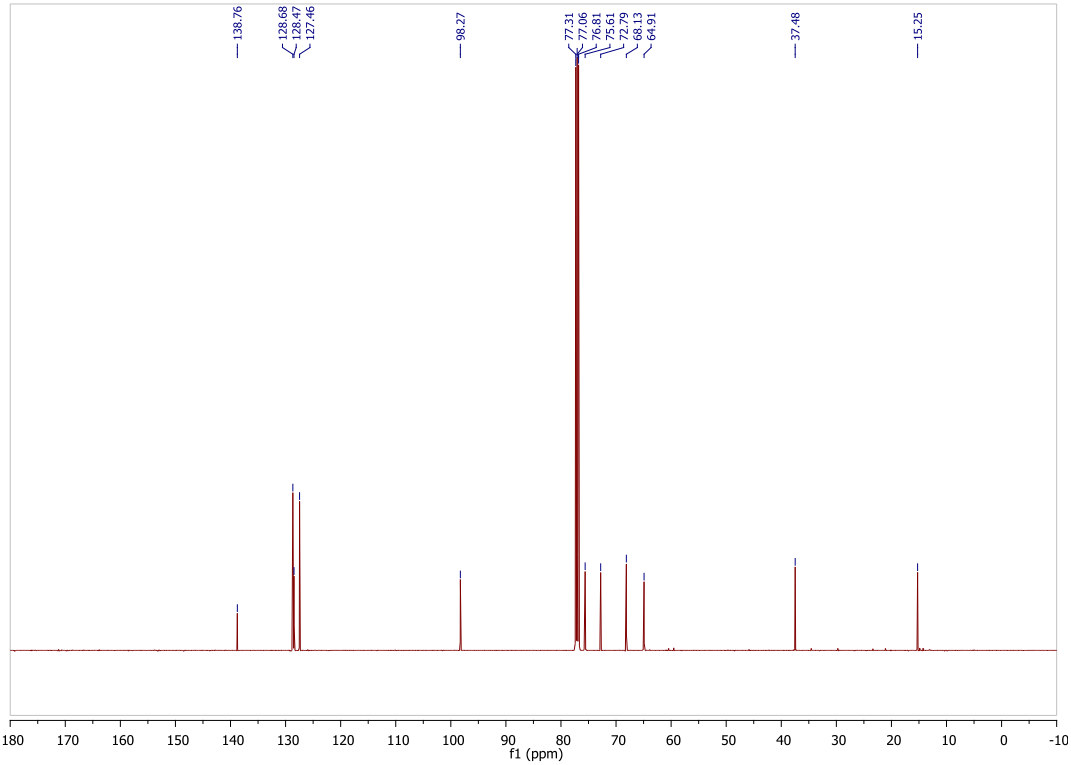

^{1}H and ^{13}C spectra for 4-10 in $CDCl_3$ at 25 ^{o}C

TRH-10-59; 499.806 MHz H1 PRESAT in cdcl3 (ref. to CDCl3 @ 7.26 ppm), temp 27.7 C -> actual temp = 27.0 C, colddual probe

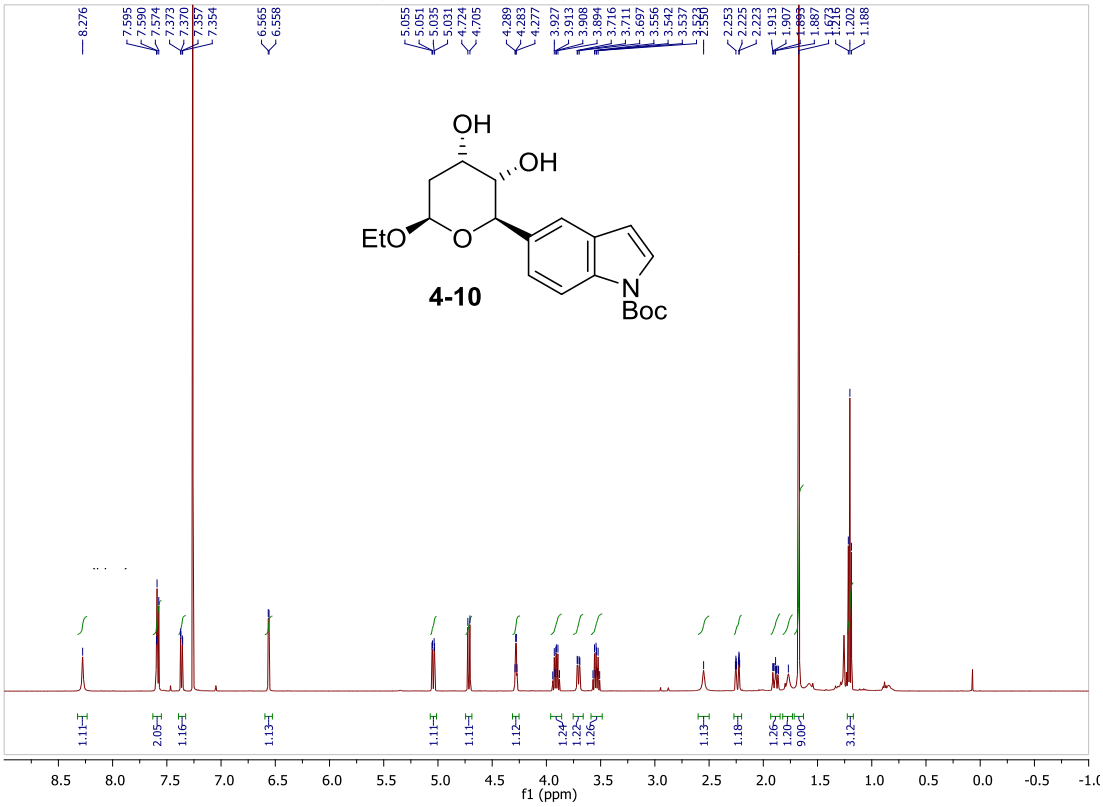

TRH-10-59; 125.691 MHz C13[H1] 1D in cdcl3 (ref. to CDCl3 @ 77.06 ppm), temp 27.7 C -> actual temp = 27.0 C, colddual probe

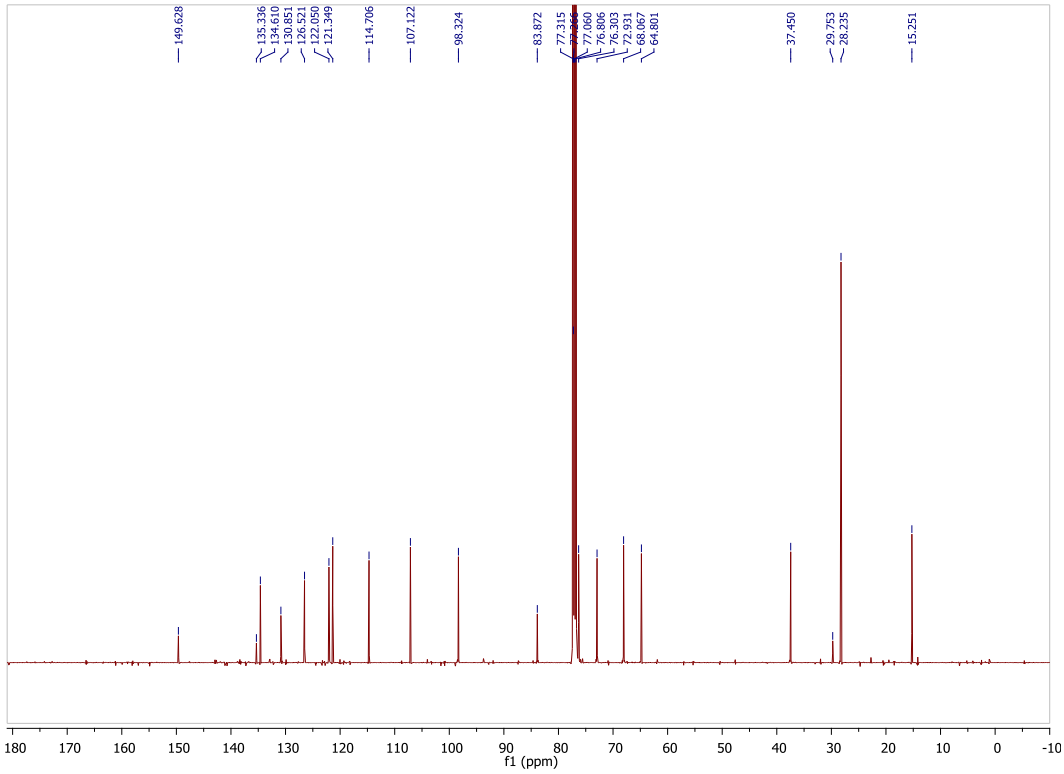

1D NOESY of 4-8 in $CDCl_3$ (500 MHz)

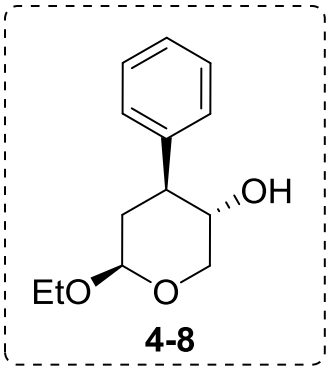

4-8

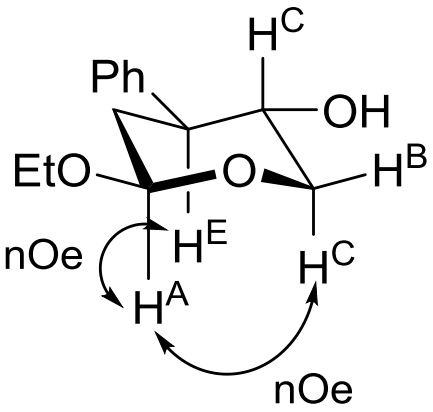

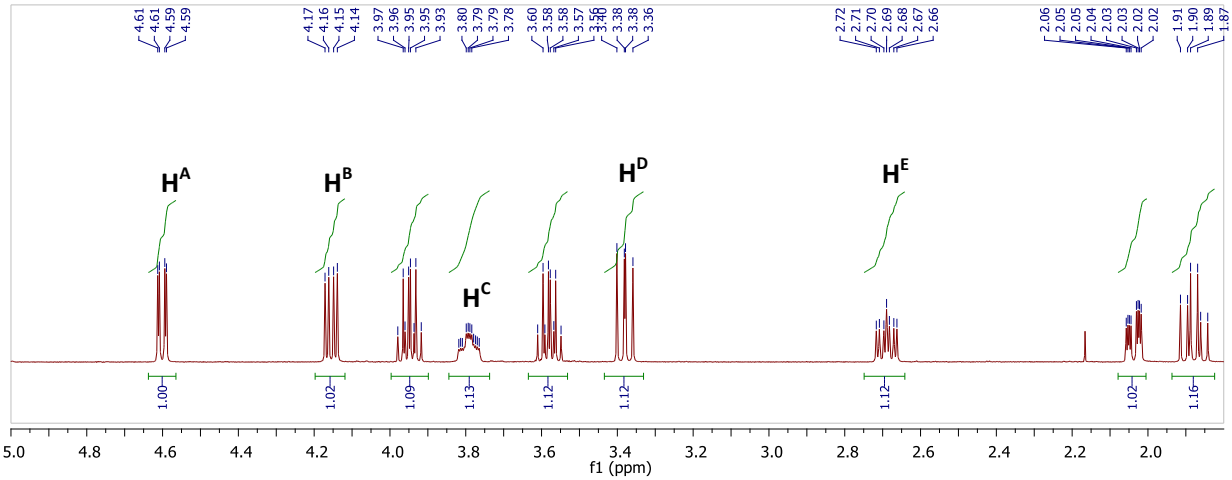

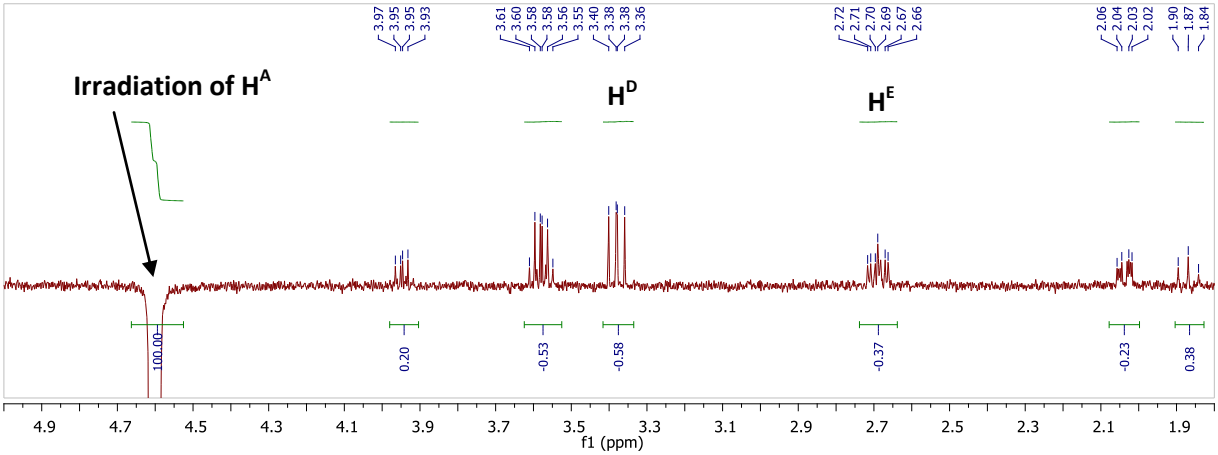

1D NOESY of 4-9 in $CDCl_3$ (500 MHz)

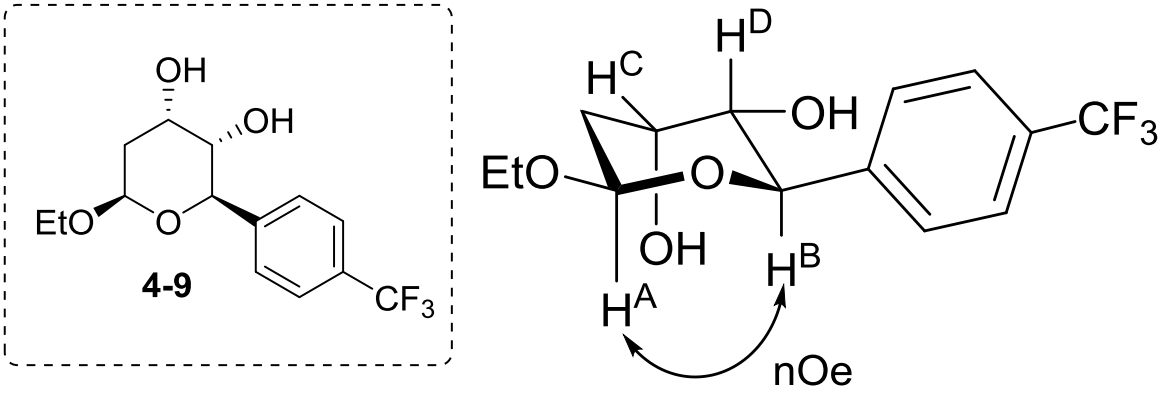

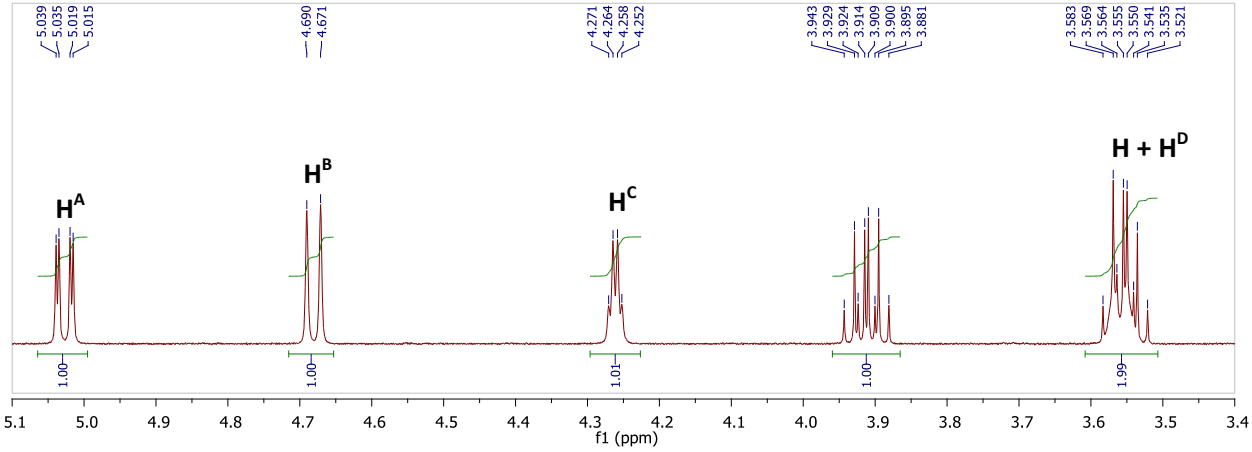

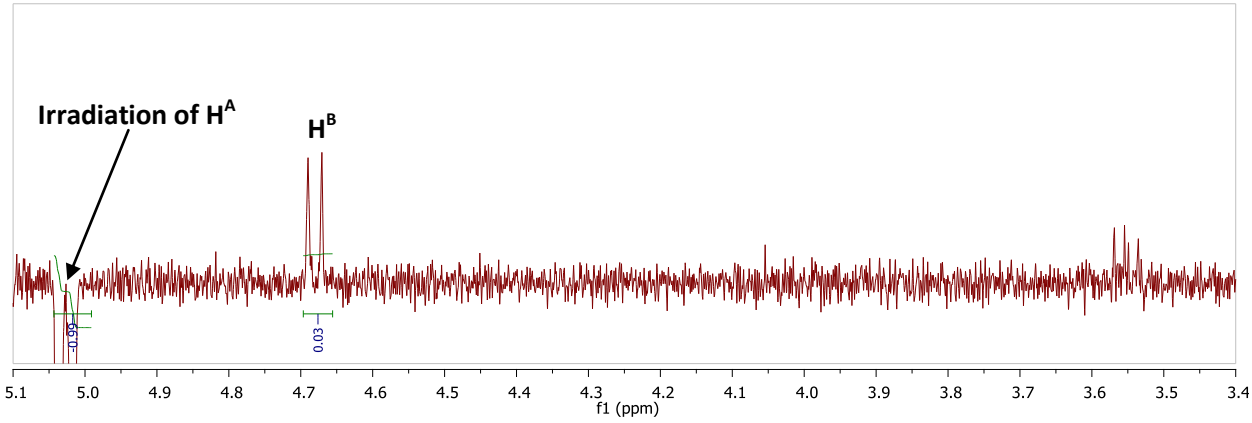

1D NOESY of 4-9 in $CDCl_3$ (500 MHz)

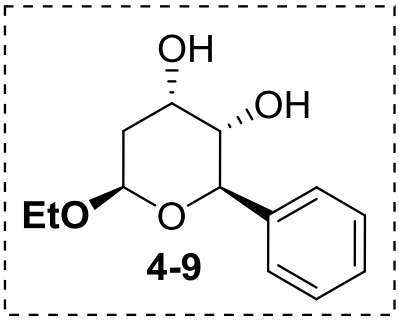

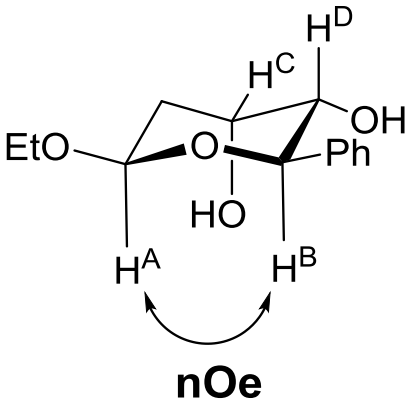

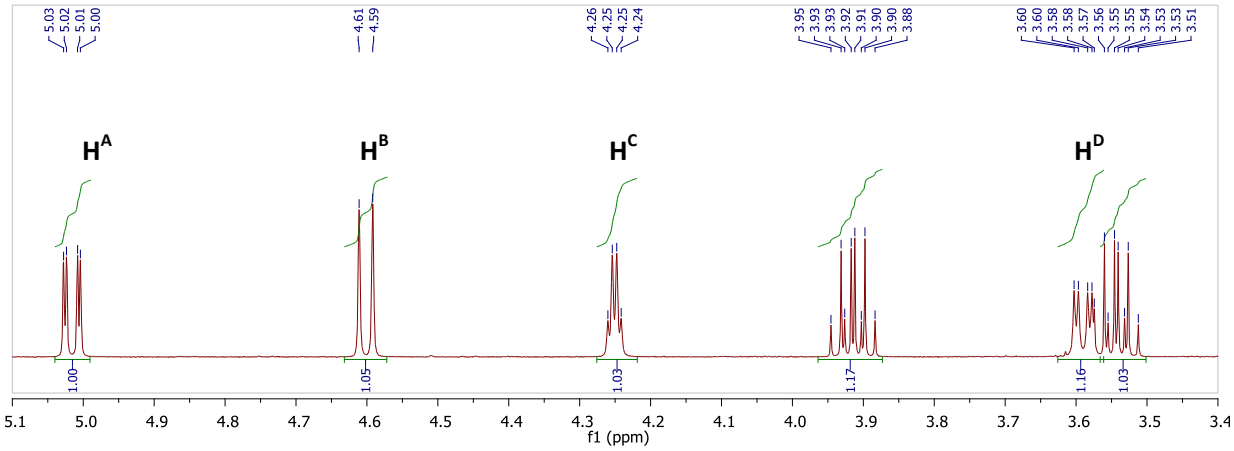

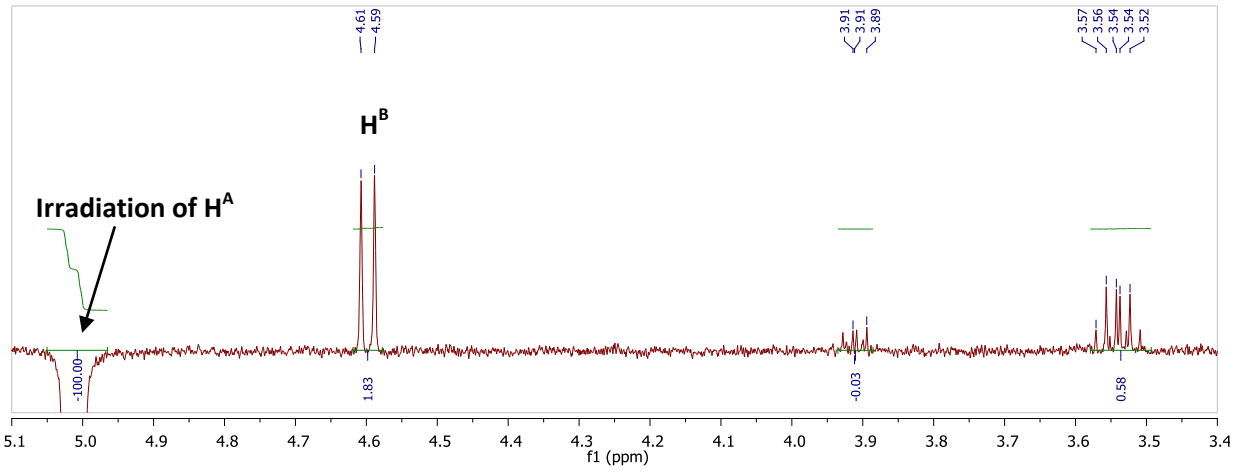

^{1}H and ^{13}C spectra for 4-25 in $CDCl_3$ at 25 ^{o}C

TRH-10-192; 499.806 MHz H1 PRESAT in cdcl3 (ref. to CDCl3 @ 7.26 ppm), temp 27.7 C -> actual temp = 27.0 C, colddual probe

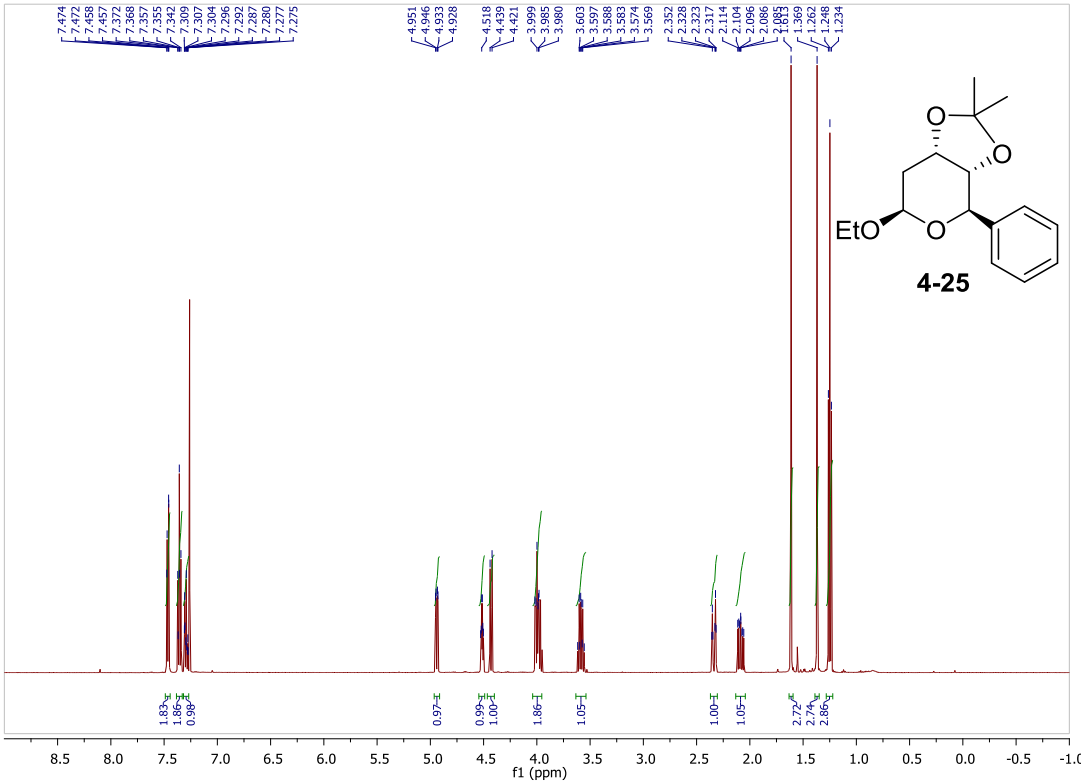

TRH-10-192; 125.691 MHz C13[H1] 1D in cdcl3 (ref. to CDCl3 @ 77.06 ppm), temp 27.7 C -> actual temp = 27.0 C, colddual probe

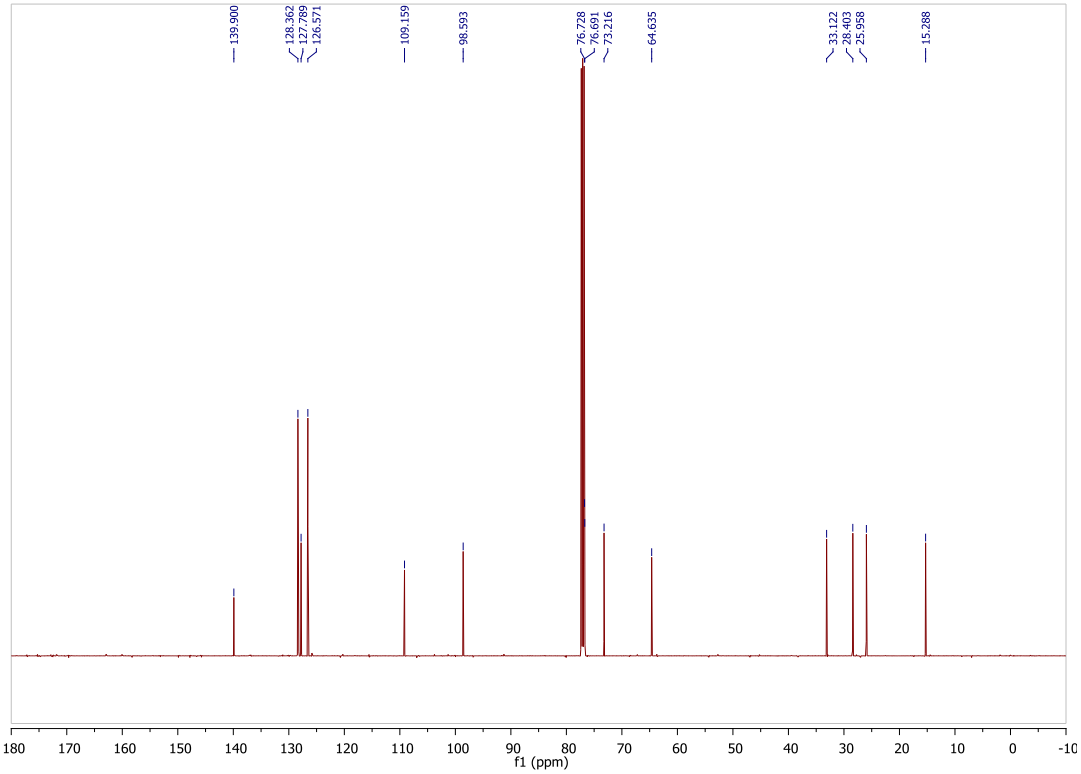

^{1}H and ^{13}C spectra for 4-26 in $CDCl_3$ at 25 ^{o}C

TRH-10-191, 699.769 MHz H1 PRESAT in cdcl3 (ref. to CDCl3 @ 7.26 ppm), temp 27.5 C -> actual temp = 27.0 C, coldid probe

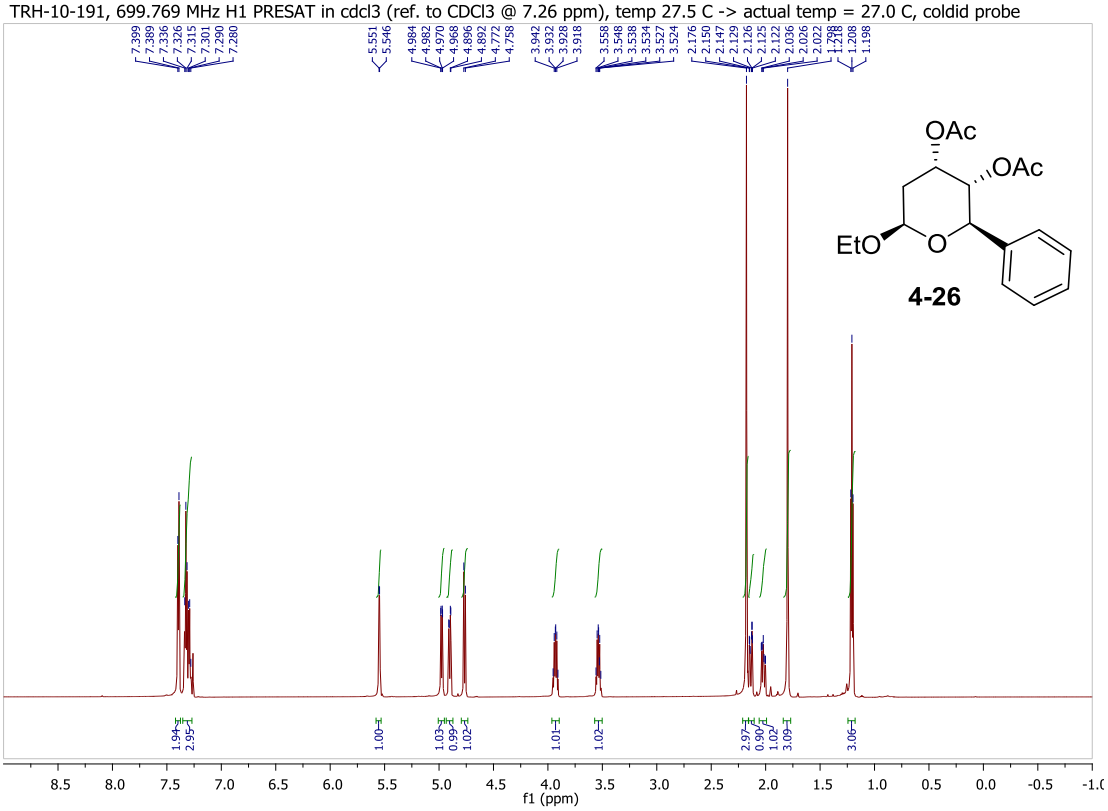

TRH-10-171; 175.976 MHz C13[H1] 1D in cdcl3 (ref. to CDCl3 @ 77.06 ppm), temp 27.5 C -> actual temp = 27.0 C, coldid probe

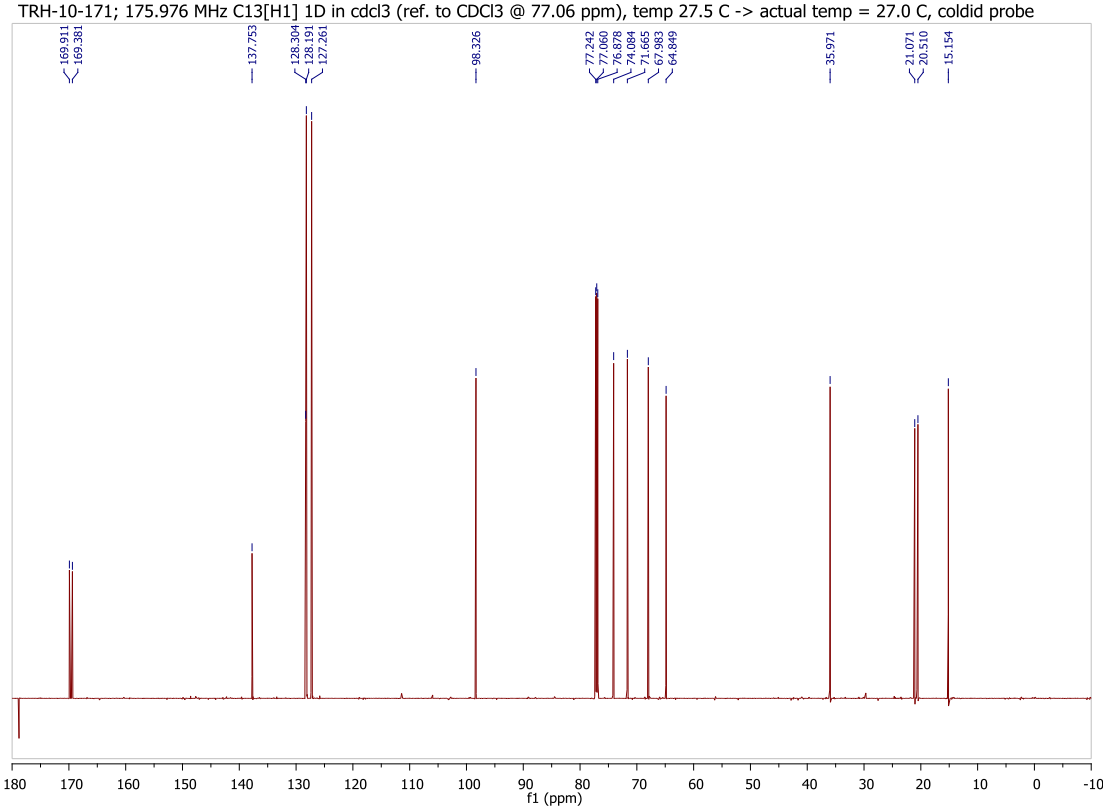

^{1}H and ^{13}C spectra for 4-27 in $CDCl_3$ at 25 ^{o}C

TRH-10-129; 699.769 MHz H1 PRESAT in cdcl3 (ref. to CDCl3 @ 7.26 ppm), temp 27.5 C -> actual temp = 27.0 C, coldid probe

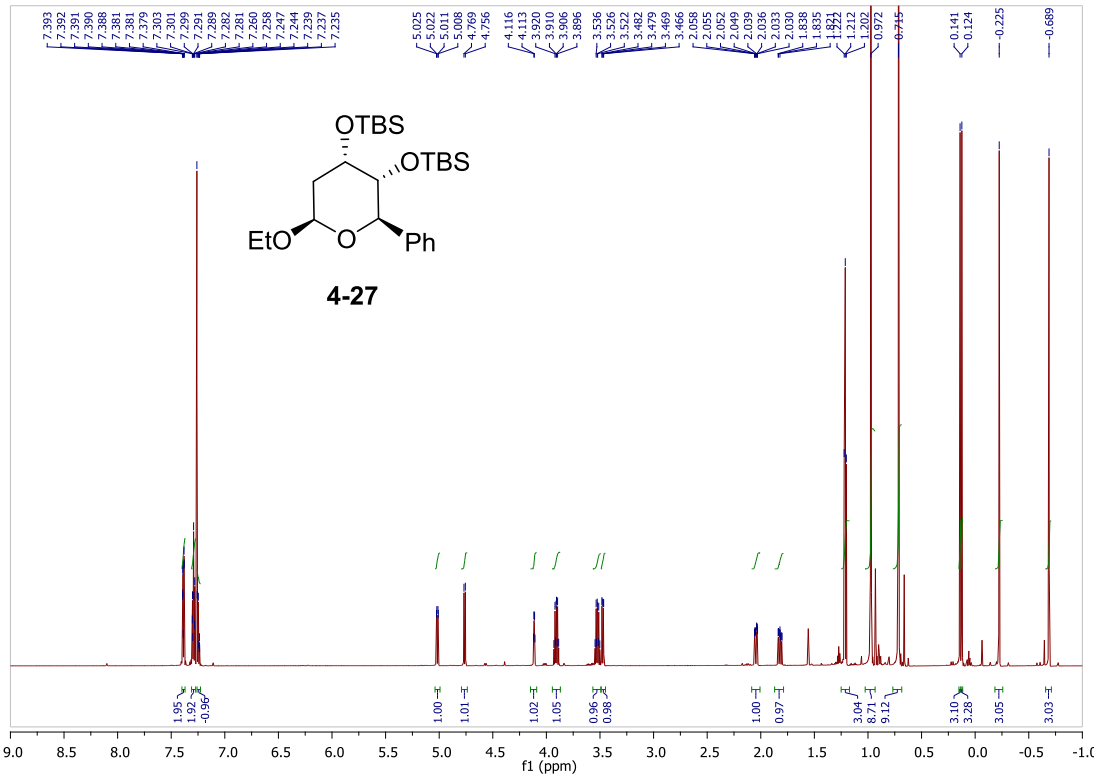

TRH-10-129; 699.769 MHz H1 PRESAT in cdcl3 (ref. to CDCl3 @ 7.26 ppm), temp 27.5 C -> actual temp = 27.0 C, coldid probe

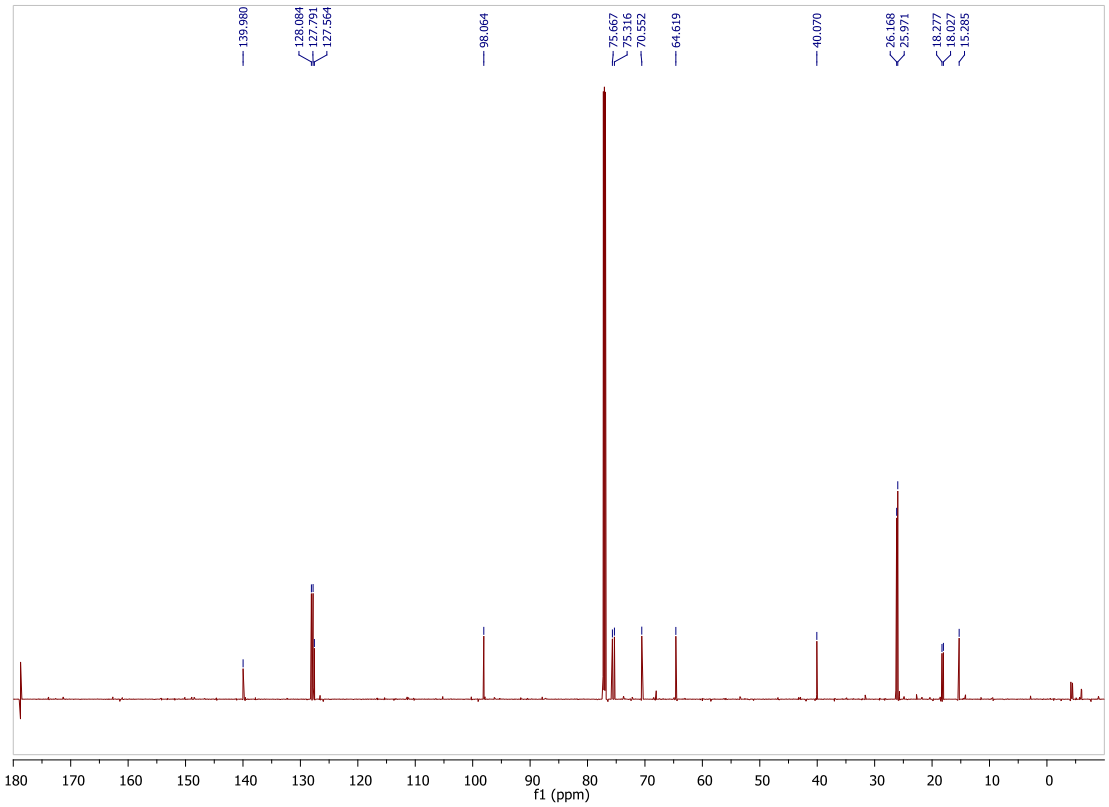

^{1}H and ^{13}C spectra for 4-28 in $CDCl_3$ at 25 ^{o}C

TRH-11-21; 699.769 MHz H1 PRESAT in cdcl3 (ref. to CDCl3 @ 7.26 ppm), temp 27.5 C -> actual temp = 27.0 C, coldid probe

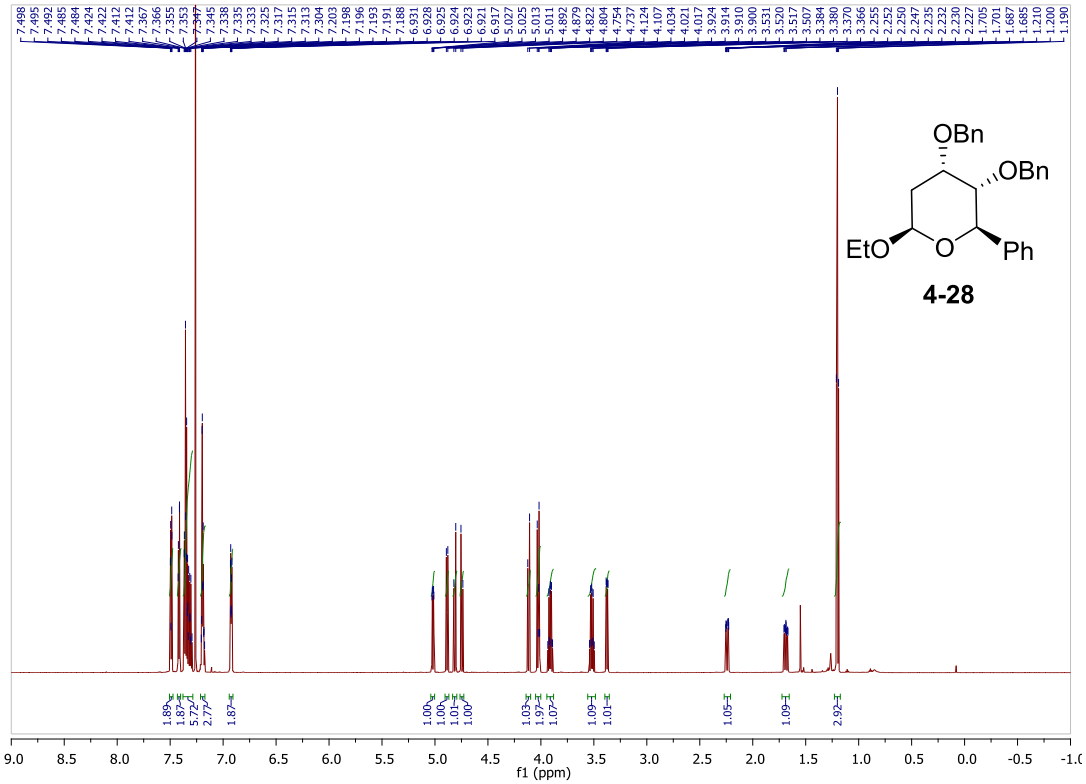

TRH-11-21; 175.976 MHz C13[H1] 1D in cdcl3 (ref. to CDCl3 @ 77.06 ppm), temp 27.5 C -> actual temp = 27.0 C, coldid probe

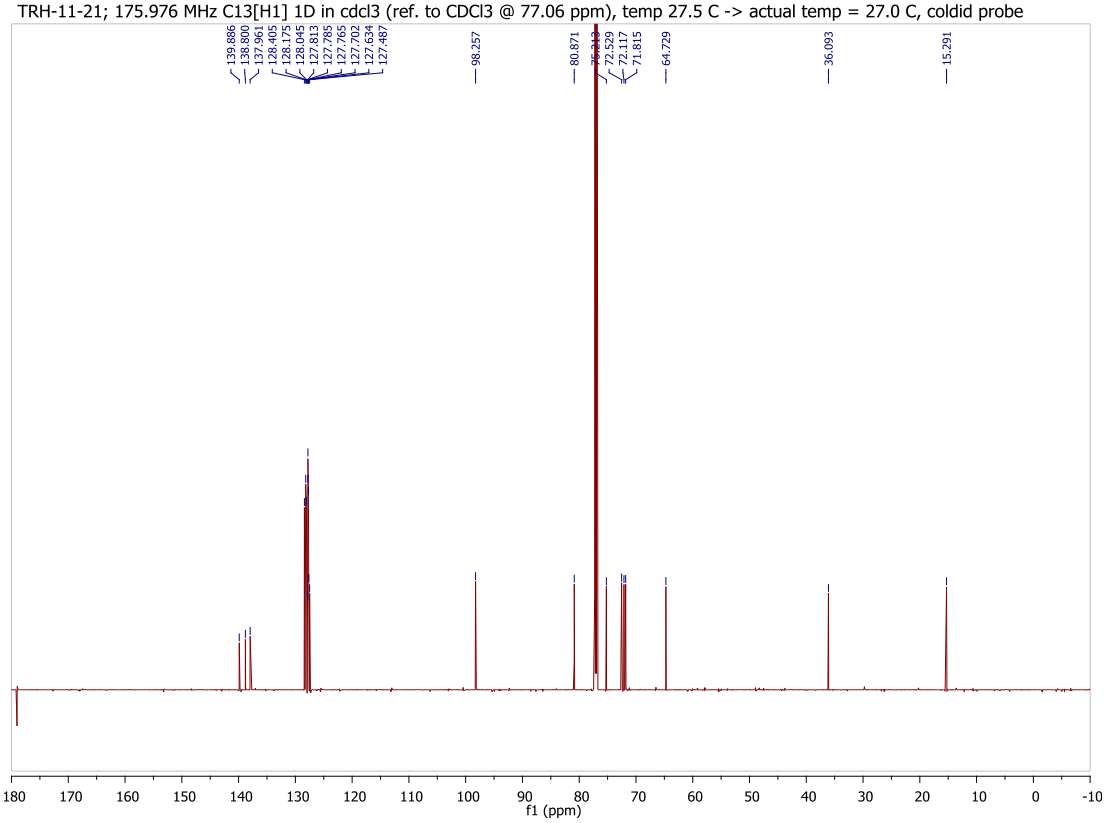

^{1}H and ^{13}C spectra for 4-35 in $CDCl_3$ at 25 ^{o}C

TRH-10-160; 699.769 MHz H1 PRESAT in cdcl3 (ref. to CDCl3 @ 7.26 ppm), temp 27.5 C -> actual temp = 27.0 C, coldid probe

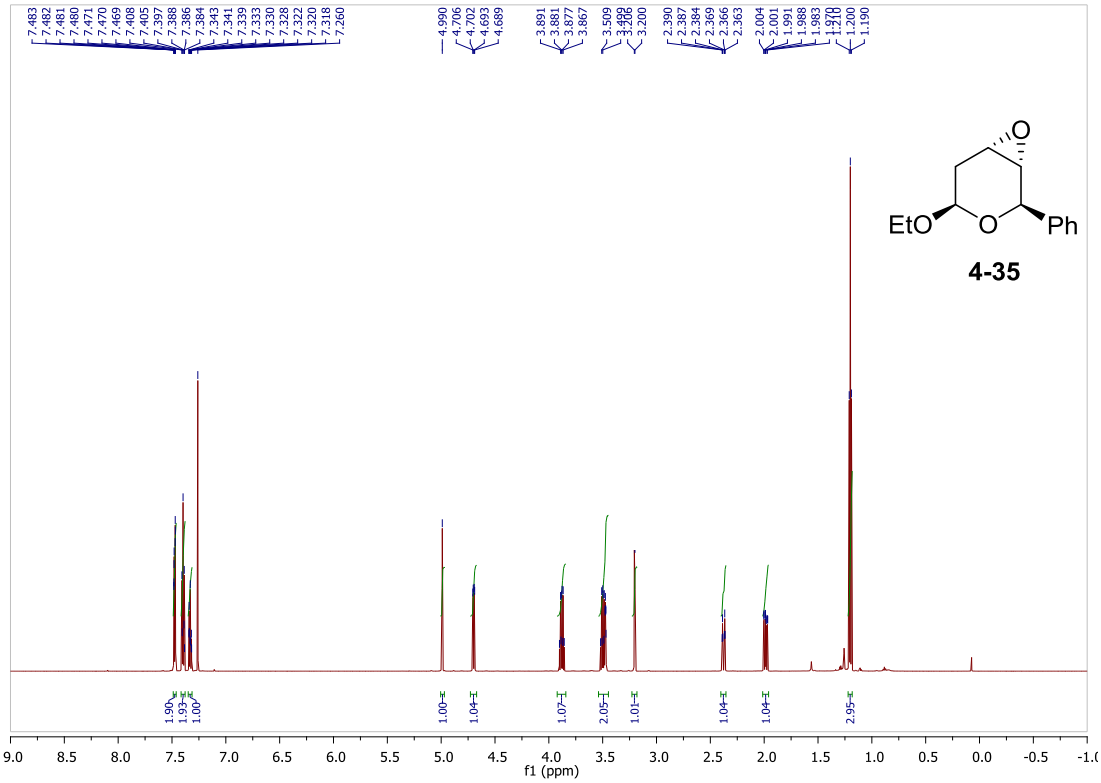

TRH-11-13; 125.691 MHz C13[H1] 1D in cdcl3 (ref. to CDCl3 @ 77.06 ppm), temp 27.7 C -> actual temp = 27.0 C, colddual probe

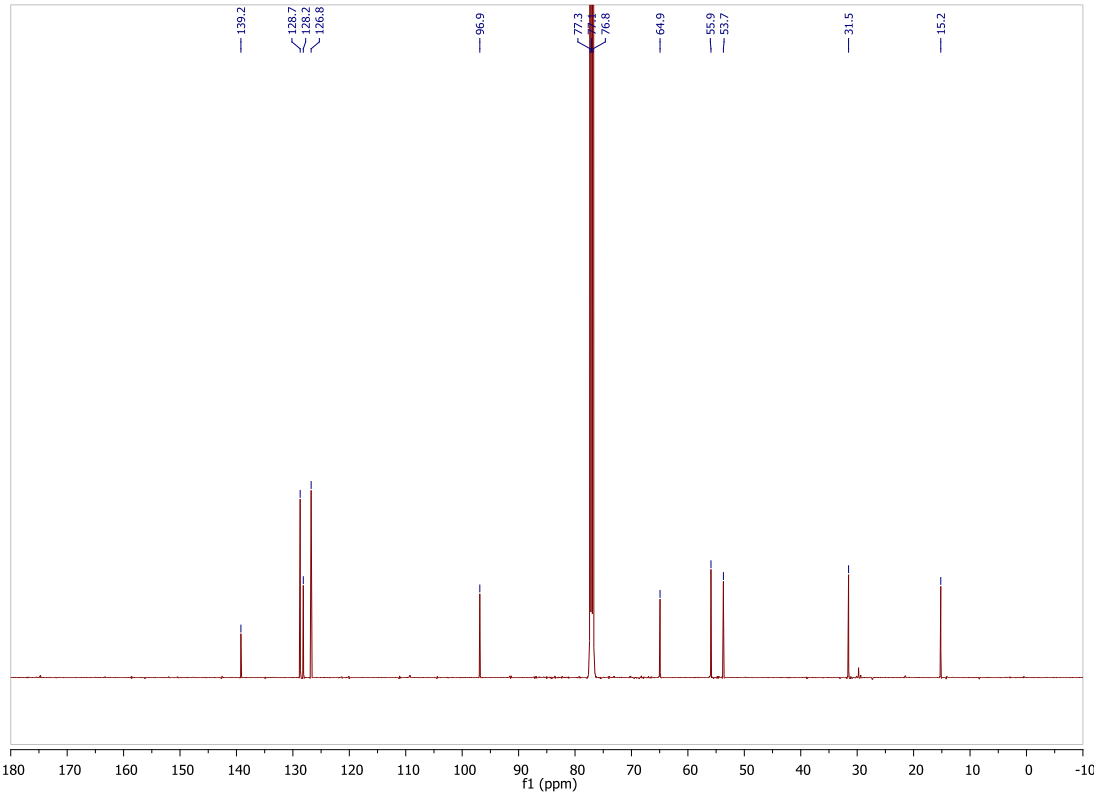

^{1}H and ^{13}C spectra for 4-34 in $CDCl_3$ at 25 ^{o}C

TRH-11-23; 699.769 MHz H1 PRESAT in cdcl3 (ref. to CDCl3 @ 7.26 ppm), temp 27.5 C -> actual temp = 27.0 C, coldid probe

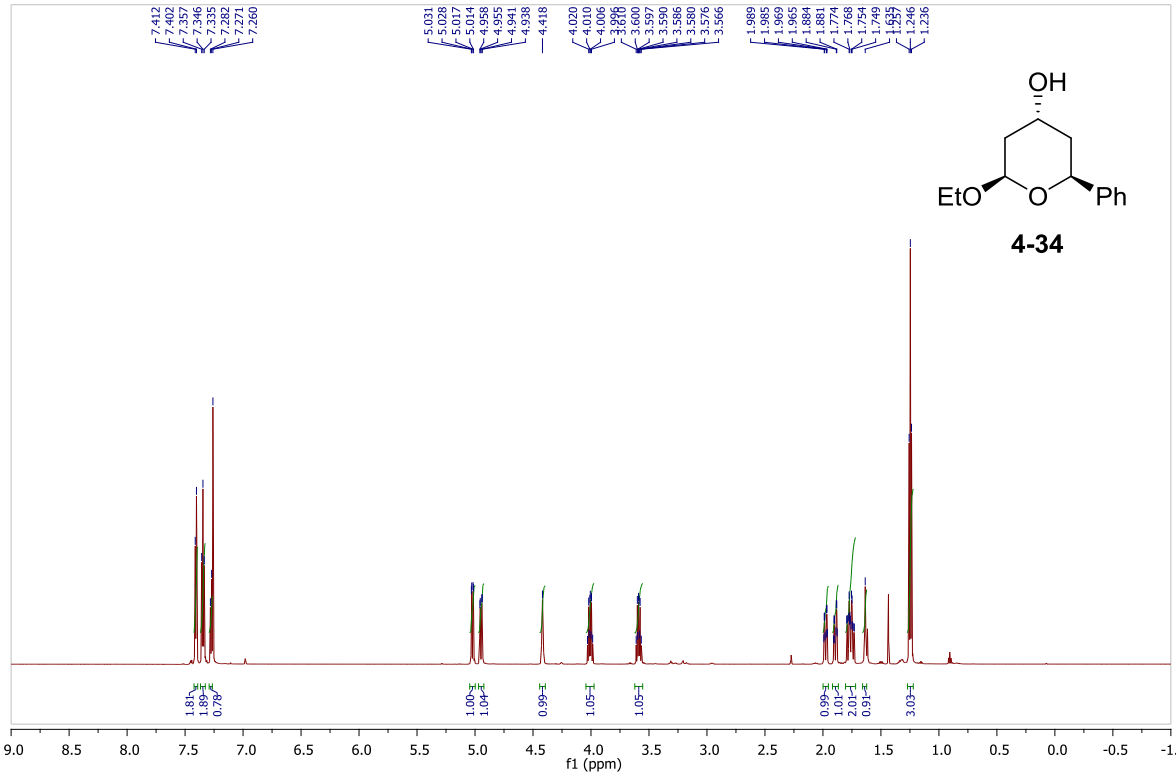

TRH-11-23; 175.976 MHz C13[H1] 1D in cdcl3 (ref. to CDCl3 @ 77.06 ppm), temp 27.5 C -> actual temp = 27.0 C, coldid probe

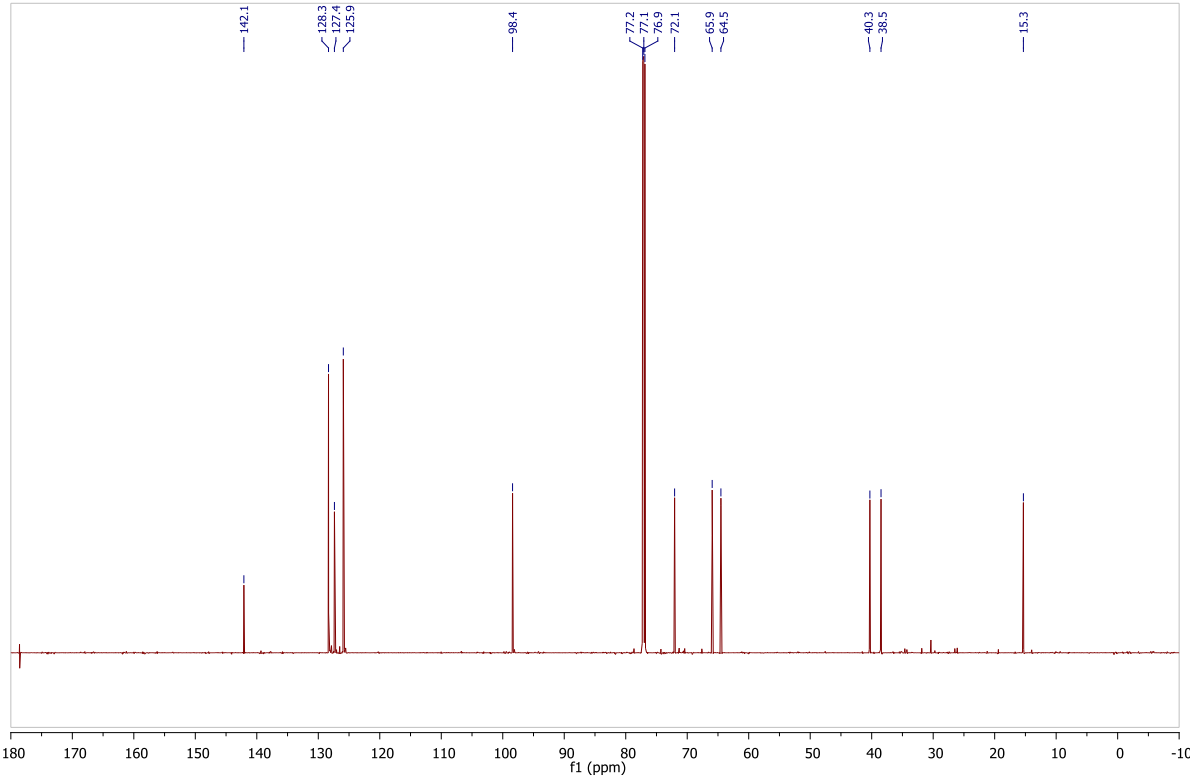

^{1}H and ^{13}C spectra for diospongin B in $CDCl_3$ at 25 ^{o}C

TRH-11-103; 400.389 MHz H1 PRESAT in cdcl3 (ref. to CDCl3 @ 7.26 ppm), temp 27.0 C -> actual temp = 27.0 C, m400gz probe

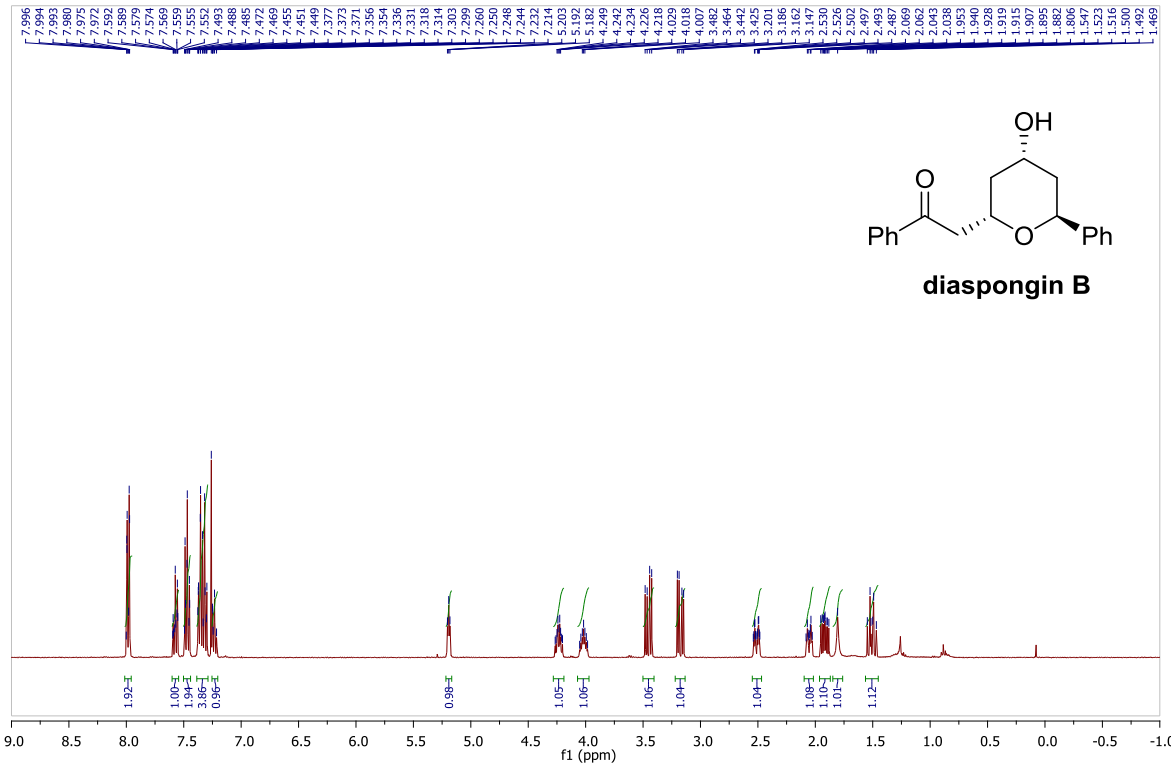

TRH-11-103; 100.688 MHz C13[H1] 1D in cdcl3 (ref. to CDCl3 @ 77.06 ppm), temp 27.0 C -> actual temp = 27.0 C, m400gz probe

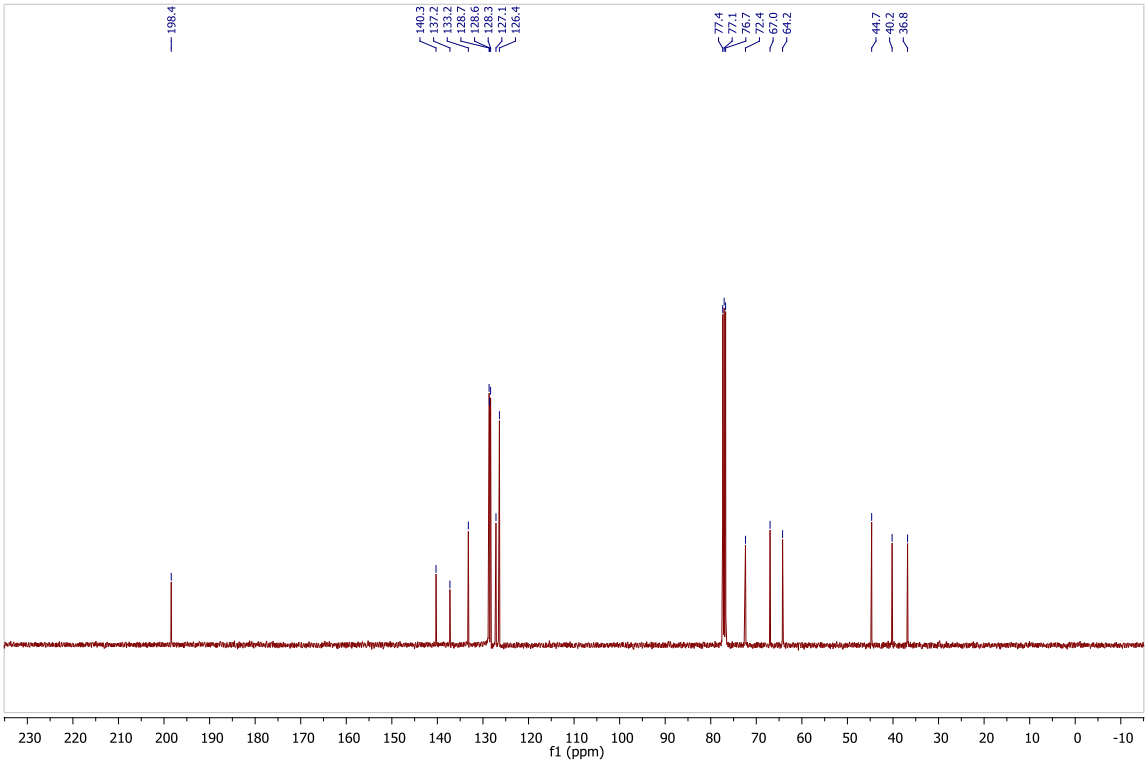

Appendix 2: Chromatograms for enantiomeric excess measurement (selected)

HPLC data for the racemic (top) and optically enriched (bottom) 3-52b

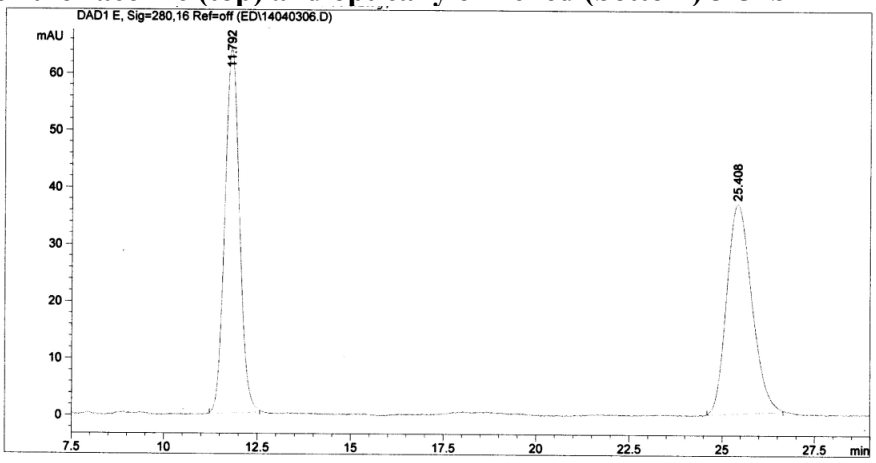


```
================================================================
                    Area Percent Report
================================================================

Sorted By             :      Signal
Multiplier            :      1.0000
Dilution              :      1.0000
Use Multiplier & Dilution Factor with ISTDs


Signal 1: DAD1 E, Sig=280,16 Ref=off

Peak RetTime Type  Width     Area      Height     Area
  #   [min]        [min]   [mAU*s]     [mAU]       %
----|-------|----|-------|----------|----------|--------|
   1  11.792 BB    0.4214 1739.64209   63.94012  49.9601
   2  25.408 BB    0.6496 1742.42163   36.71989  50.0399
```

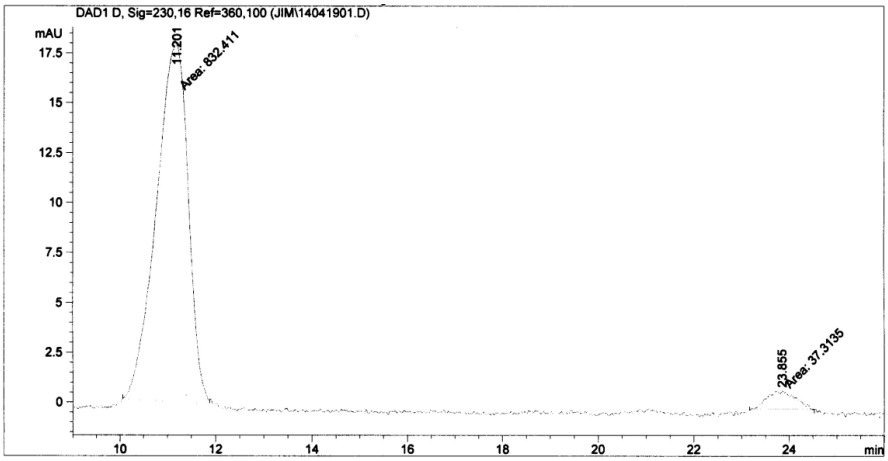


```
================================================================
                    Area Percent Report
================================================================

Sorted By             :      Signal
Multiplier            :      1.0000
Dilution              :      1.0000
Use Multiplier & Dilution Factor with ISTDs


Signal 1: DAD1 D, Sig=230,16 Ref=360,100

Peak RetTime Type  Width     Area      Height     Area
  #   [min]        [min]   [mAU*s]     [mAU]       %
----|-------|----|-------|----------|----------|--------|
   1  11.201 MM    0.7758  832.41101   17.88277  95.7097
   2  23.855 MM    0.6747   37.31351 9.21666e-1   4.2903
```

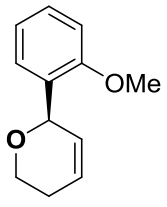

HPLC data for the racemic (top) and optically enriched (bottom) 3-52c

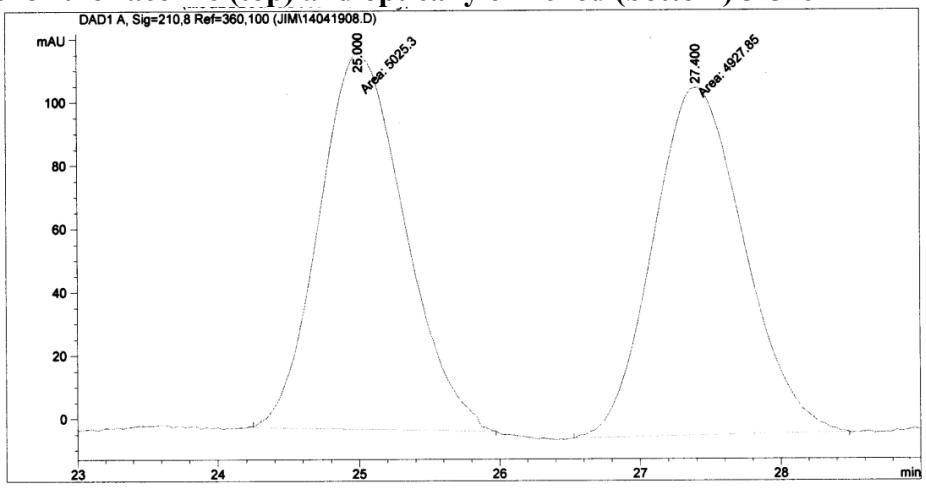


```
================================================================================
                            Area Percent Report
================================================================================

Sorted By             :      Signal
Multiplier            :      1.0000
Dilution              :      1.0000
Use Multiplier & Dilution Factor with ISTDs


Signal 1: DAD1 A, Sig=210,8 Ref=360,100

Peak RetTime Type  Width     Area      Height     Area
  #   [min]        [min]   [mAU*s]     [mAU]       %
----|-------|----|-------|----------|----------|--------|
   1  25.000 MM    0.7030 5025.30273  119.13275  50.4896
   2  27.400 MM    0.7486 4927.84863  109.71181  49.5104
```

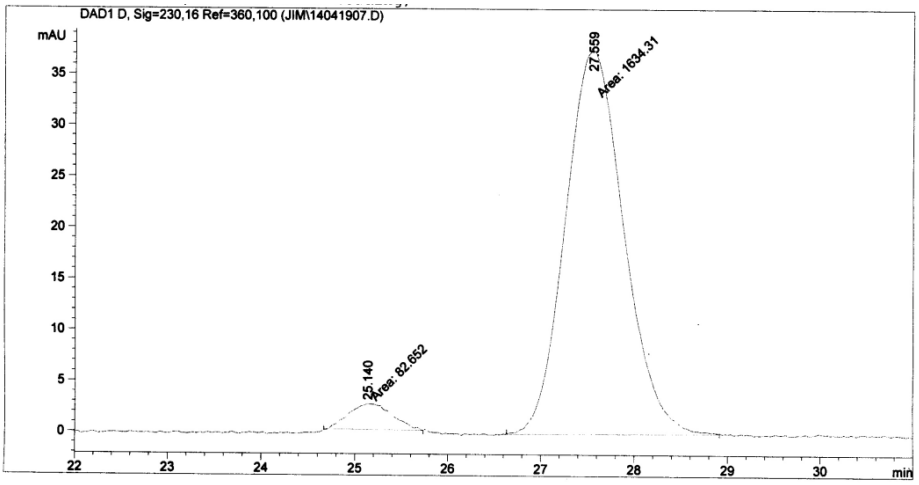


```
================================================================================
                            Area Percent Report
================================================================================

Sorted By             :      Signal
Multiplier            :      1.0000
Dilution              :      1.0000
Use Multiplier & Dilution Factor with ISTDs


Signal 1: DAD1 D, Sig=230,16 Ref=360,100

Peak RetTime Type  Width     Area      Height     Area
  #   [min]        [min]   [mAU*s]     [mAU]       %
----|-------|----|-------|----------|----------|--------|
   1  25.140 MM    0.5435   82.65195    2.53447   4.8138
   2  27.559 MM    0.7261 1634.31287   37.51581  95.1862
```

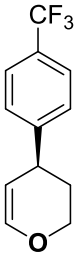

HPLC data for the racemic (top) and optically enriched (bottom) 3-57a

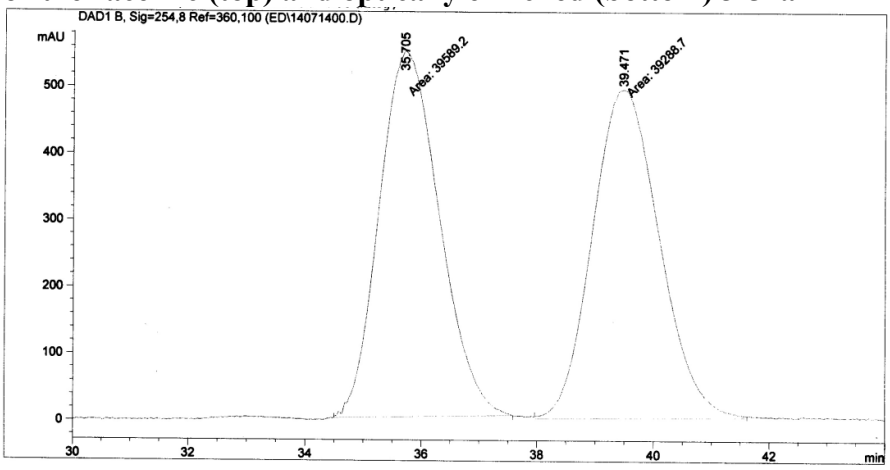


```
================================================================================
                              Area Percent Report
================================================================================

Sorted By             :      Signal
Multiplier            :      1.0000
Dilution              :      1.0000
Use Multiplier & Dilution Factor with ISTDs


Signal 1: DAD1 B, Sig=254,8 Ref=360,100

Peak RetTime Type  Width     Area      Height     Area
  #   [min]        [min]   [mAU*s]     [mAU]       %
----|-------|----|-------|----------|----------|--------|
   1  35.705 MM    1.2057 3.95892e4   547.26758  50.1905
   2  39.471 MM    1.3318 3.92887e4   491.66058  49.8095
```

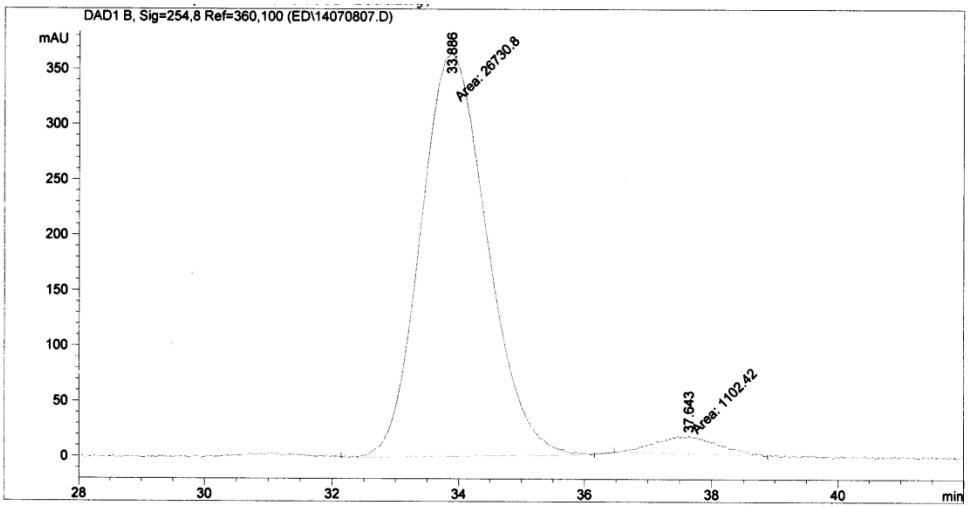


```
================================================================================
                              Area Percent Report
================================================================================

Sorted By             :      Signal
Multiplier            :      1.0000
Dilution              :      1.0000
Use Multiplier & Dilution Factor with ISTDs


Signal 1: DAD1 B, Sig=254,8 Ref=360,100

Peak RetTime Type  Width     Area      Height     Area
  #   [min]        [min]   [mAU*s]     [mAU]       %
----|-------|----|-------|----------|----------|--------|
   1  33.886 MM    1.2200 2.67308e4   365.17032  96.0392
   2  37.643 MM    1.1577 1102.42249   15.87115   3.9608
```

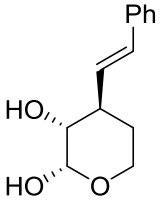

HPLC data for the racemic (top) and optically enriched (bottom) 3-53c

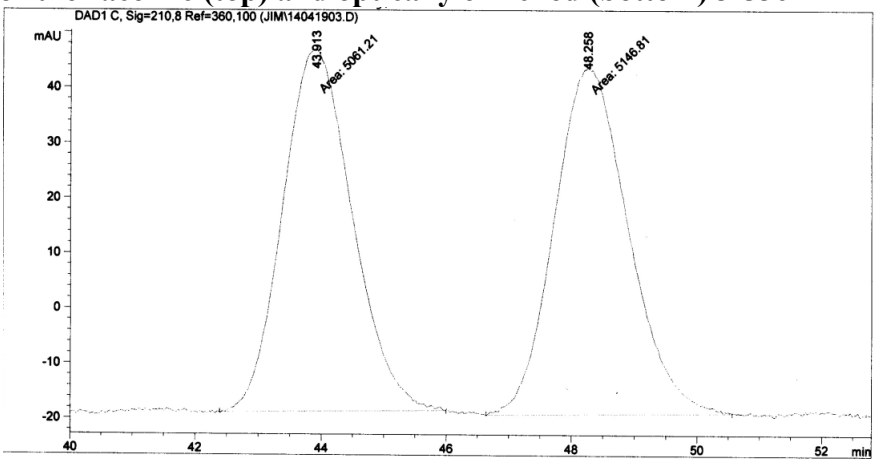


```
================================================================
                      Area Percent Report
================================================================

Sorted By             :      Signal
Multiplier            :      1.0000
Dilution              :      1.0000
Use Multiplier & Dilution Factor with ISTDs


Signal 1: DAD1 C, Sig=210,8 Ref=360,100

Peak RetTime Type  Width     Area      Height     Area
  #   [min]        [min]   [mAU*s]     [mAU]       %
----|-------|----|-------|----------|----------|--------|
   1  43.913 MM    1.2851 5061.21094   65.63991  49.5807
   2  48.258 MM    1.3654 5146.80615   62.82634  50.4193
```

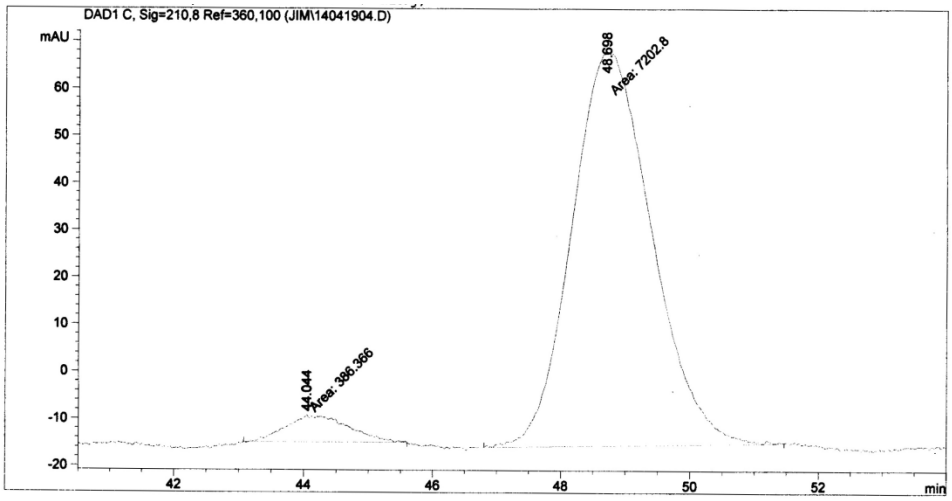


```
================================================================
                      Area Percent Report
================================================================

Sorted By             :      Signal
Multiplier            :      1.0000
Dilution              :      1.0000
Use Multiplier & Dilution Factor with ISTDs


Signal 1: DAD1 C, Sig=210,8 Ref=360,100

Peak RetTime Type  Width     Area      Height     Area
  #   [min]        [min]   [mAU*s]     [mAU]       %
----|-------|----|-------|----------|----------|--------|
   1  44.044 MM    1.1154  386.36633   5.77340   5.0910
   2  48.698 MM    1.4373 7202.79590  83.51940  94.9090
```

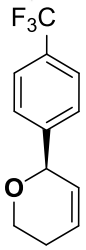

HPLC data for the racemic (top) and optically enriched (bottom) 3-53h

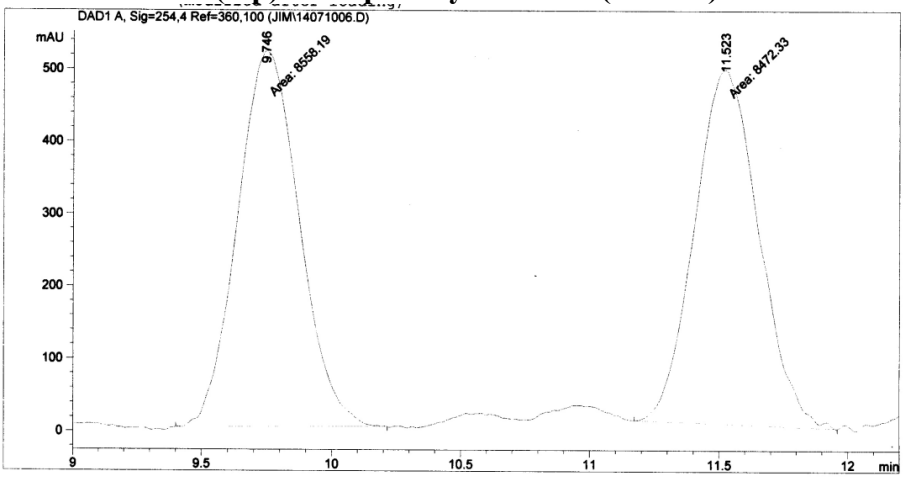


```
=====================================================================
                        Area Percent Report
=====================================================================

Sorted By             :      Signal
Multiplier            :      1.0000
Dilution              :      1.0000
Use Multiplier & Dilution Factor with ISTDs


Signal 1: DAD1 A, Sig=254,4 Ref=360,100

Peak RetTime Type  Width     Area      Height     Area
  #   [min]        [min]   [mAU*s]     [mAU]       %
----|-------|----|-------|----------|----------|--------|
   1   9.746 MM    0.2743 8558.18652  519.93268  50.2521
   2  11.523 MM    0.2888 8472.33496  488.99768  49.7479
```

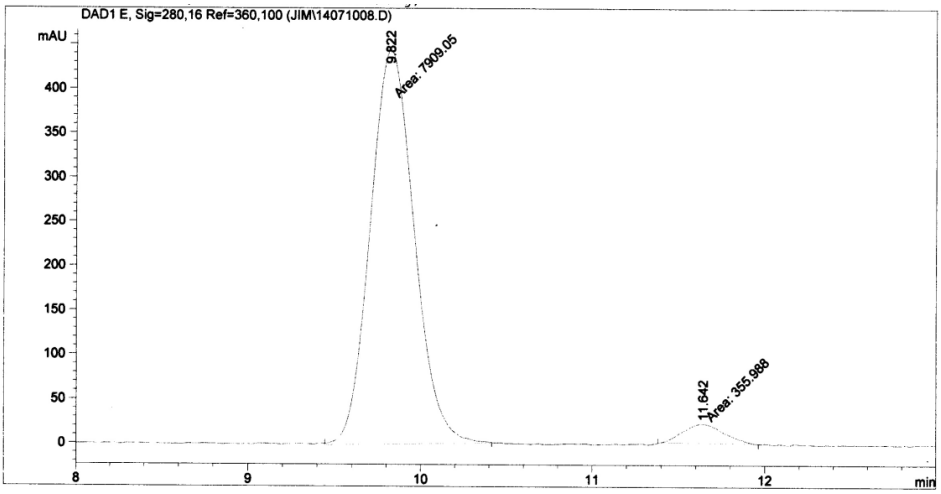


```
=====================================================================
                        Area Percent Report
=====================================================================

Sorted By             :      Signal
Multiplier            :      1.0000
Dilution              :      1.0000
Use Multiplier & Dilution Factor with ISTDs


Signal 1: DAD1 E, Sig=280,16 Ref=360,100

Peak RetTime Type  Width     Area      Height     Area
  #   [min]        [min]   [mAU*s]     [mAU]       %
----|-------|----|-------|----------|----------|--------|
   1   9.822 MM    0.2966 7909.05176  444.45425  95.6928
   2  11.642 MM    0.2762  355.98776   21.48442   4.3072
```

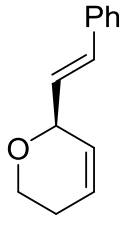

HPLC data for the racemic (top) and optically enriched (bottom) 4-8

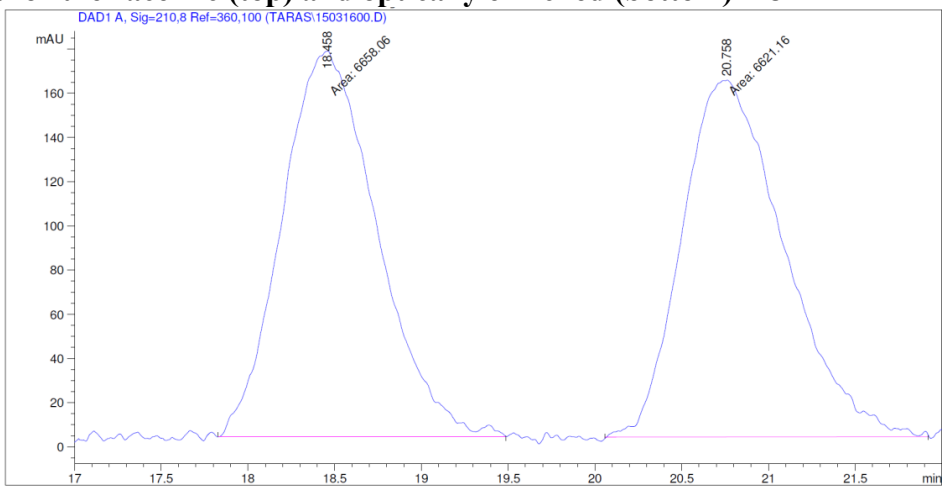


```
================================================================================
                            Area Percent Report
================================================================================

Sorted By             :      Signal
Multiplier            :      1.0000
Dilution              :      1.0000
Use Multiplier & Dilution Factor with ISTDs


Signal 1: DAD1 A, Sig=210,8 Ref=360,100

Peak RetTime Type  Width     Area      Height     Area
  #   [min]        [min]    [mAU*s]     [mAU]       %
----|-------|----|-------|----------|----------|--------|
   1  18.458 FM    0.6357 6658.05762  174.55846  50.1389
   2  20.758 MM    0.6835 6621.15771  161.46278  49.8611
```

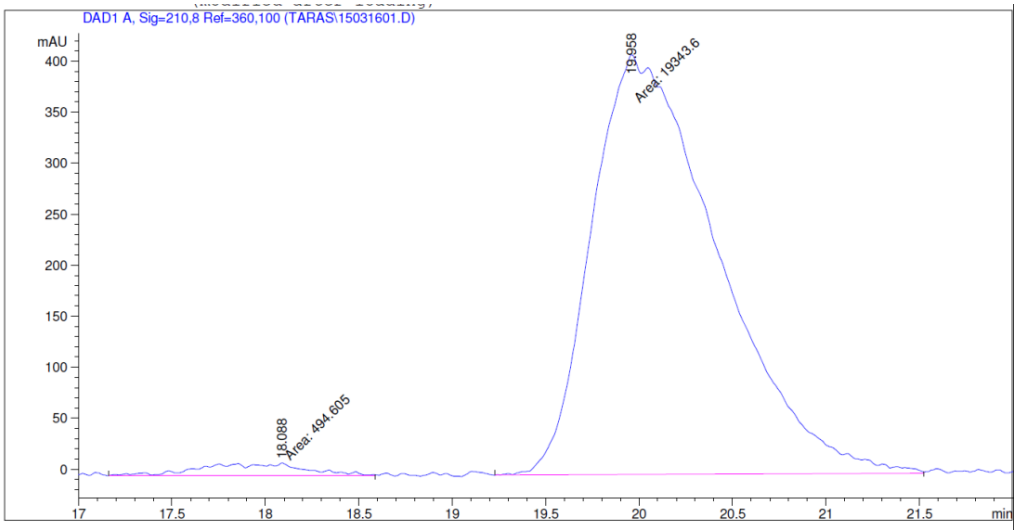


```
================================================================================
                            Area Percent Report
================================================================================

Sorted By             :      Signal
Multiplier            :      1.0000
Dilution              :      1.0000
Use Multiplier & Dilution Factor with ISTDs


Signal 1: DAD1 A, Sig=210,8 Ref=360,100

Peak RetTime Type  Width     Area      Height     Area
  #   [min]        [min]    [mAU*s]     [mAU]       %
----|-------|----|-------|----------|----------|--------|
   1  18.088 MF    0.6424  494.60522   12.83218   2.4932
   2  19.958 MF    0.7826 1.93436e4   411.93323  97.5068
```

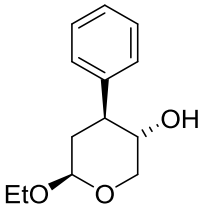

HPLC data for the racemic (top) and optically enriched (bottom) 4-5d

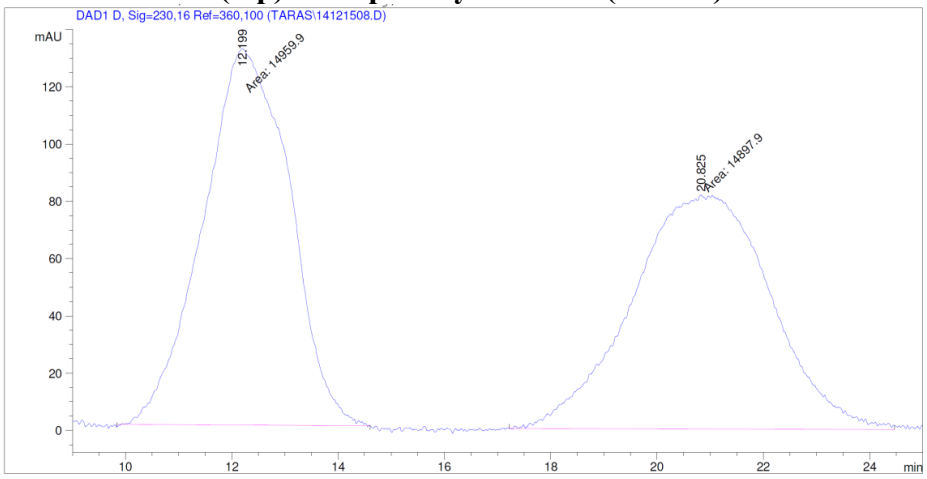


```
=====================================================================
                        Area Percent Report
=====================================================================

Sorted By             :      Signal
Multiplier            :      1.0000
Dilution              :      1.0000
Use Multiplier & Dilution Factor with ISTDs


Signal 1: DAD1 D, Sig=230,16 Ref=360,100

Peak RetTime Type  Width     Area      Height     Area
  #   [min]        [min]   [mAU*s]     [mAU]       %
----|-------|----|-------|----------|----------|--------|
   1  12.199 MM    1.8955 1.49599e4   131.53967  50.1037
   2  20.825 MF    3.0344 1.48979e4    81.82846  49.8963
```

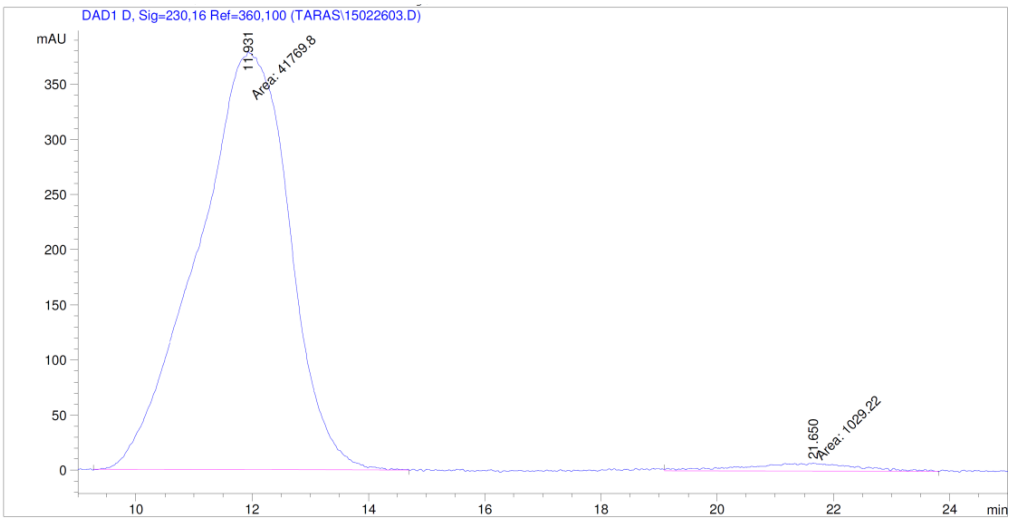


```
=====================================================================
                        Area Percent Report
=====================================================================

Sorted By             :      Signal
Multiplier            :      1.0000
Dilution              :      1.0000
Use Multiplier & Dilution Factor with ISTDs


Signal 1: DAD1 D, Sig=230,16 Ref=360,100

Peak RetTime Type  Width     Area      Height     Area
  #   [min]        [min]   [mAU*s]     [mAU]       %
----|-------|----|-------|----------|----------|--------|
   1  11.931 MM    1.8362 4.17698e4   379.13593  97.5952
   2  21.650 FM    2.2875 1029.22095    7.49903   2.4048
```

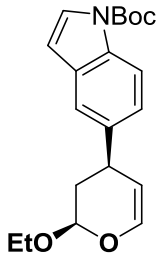

HPLC data for the racemic (top) and optically enriched (bottom) 4-5e

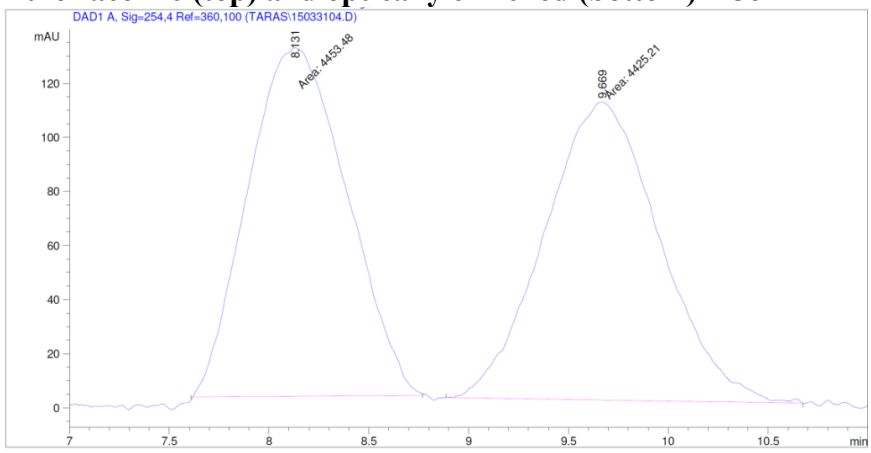


```
================================================================
                    Area Percent Report
================================================================

Sorted By             :      Signal
Multiplier            :      1.0000
Dilution              :      1.0000
Use Multiplier & Dilution Factor with ISTDs


Signal 1: DAD1 A, Sig=254,4 Ref=360,100

Peak RetTime Type  Width     Area      Height     Area
  #   [min]        [min]   [mAU*s]     [mAU]       %
----|-------|----|-------|----------|----------|--------|
   1   8.131 MF    0.5757 4453.48096  128.92000  50.1592
   2   9.669 MM    0.6689 4425.21436  110.26337  49.8408
```

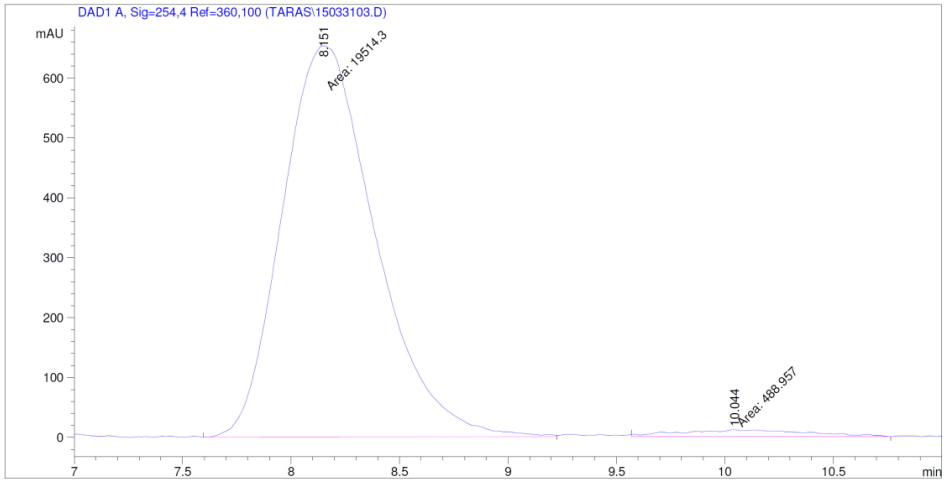


```
================================================================
                    Area Percent Report
================================================================

Sorted By             :      Signal
Multiplier            :      1.0000
Dilution              :      1.0000
Use Multiplier & Dilution Factor with ISTDs


Signal 1: DAD1 A, Sig=254,4 Ref=360,100

Peak RetTime Type  Width     Area      Height     Area
  #   [min]        [min]   [mAU*s]     [mAU]       %
----|-------|----|-------|----------|----------|--------|
   1   8.151 MF    0.4979 1.95143e4   653.22705  97.5556
   2  10.044 FM    0.7001  488.95691   11.64013   2.4444
```

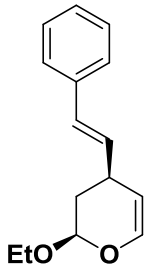

HPLC data for the racemic (top) and optically enriched (bottom) 4-10

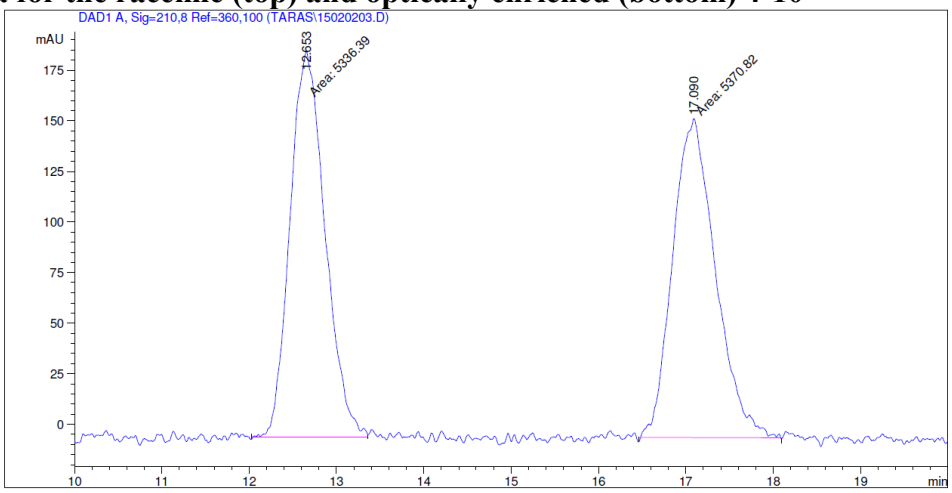


```
================================================================================
                            Area Percent Report
================================================================================

Sorted By             :      Signal
Multiplier            :      1.0000
Dilution              :      1.0000
Use Multiplier & Dilution Factor with ISTDs


Signal 1: DAD1 A, Sig=210,8 Ref=360,100

Peak RetTime Type  Width     Area      Height     Area
  #   [min]        [min]    [mAU*s]     [mAU]       %
----|-------|----|-------|----------|----------|--------|
   1  12.653 MF     0.4657 5336.38867  190.99638  49.8392
   2  17.090 FM     0.5665 5370.82324  158.01157  50.1608
```

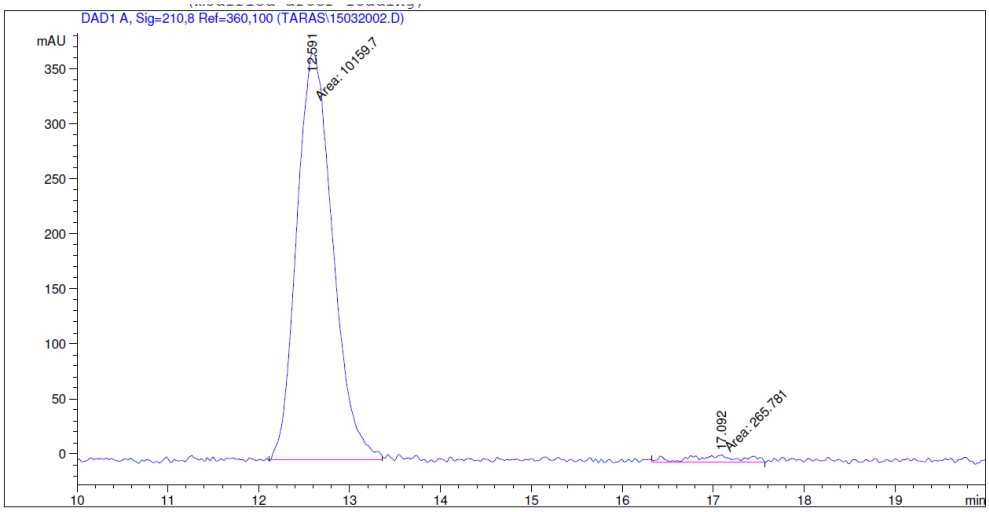


```
================================================================================
                            Area Percent Report
================================================================================

Sorted By             :      Signal
Multiplier            :      1.0000
Dilution              :      1.0000
Use Multiplier & Dilution Factor with ISTDs


Signal 1: DAD1 A, Sig=210,8 Ref=360,100

Peak RetTime Type  Width     Area      Height     Area
  #   [min]        [min]    [mAU*s]     [mAU]       %
----|-------|----|-------|----------|----------|--------|
   1  12.591 MF     0.4590 1.01597e4   368.88965  97.4507
   2  17.092 FM     0.6553  265.78055    6.75942   2.5493
```

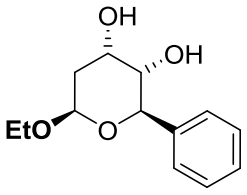

HPLC data for the racemic (top) and optically enriched (bottom) 4-11

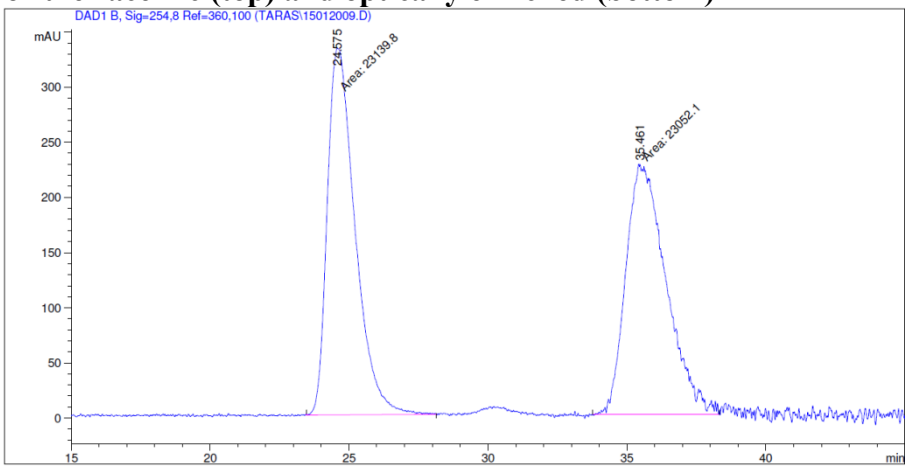


```
================================================================================
                            Area Percent Report
================================================================================

Sorted By             :      Signal
Multiplier            :      1.0000
Dilution              :      1.0000
Use Multiplier & Dilution Factor with ISTDs


Signal 1: DAD1 B, Sig=254,8 Ref=360,100

Peak RetTime Type  Width     Area      Height     Area
  #   [min]        [min]   [mAU*s]     [mAU]       %
----|-------|----|-------|----------|----------|--------|
   1  24.575 MM    1.1598 2.31397e4   332.51877  50.0949
   2  35.461 MM    1.6897 2.30521e4   227.37604  49.9051
```

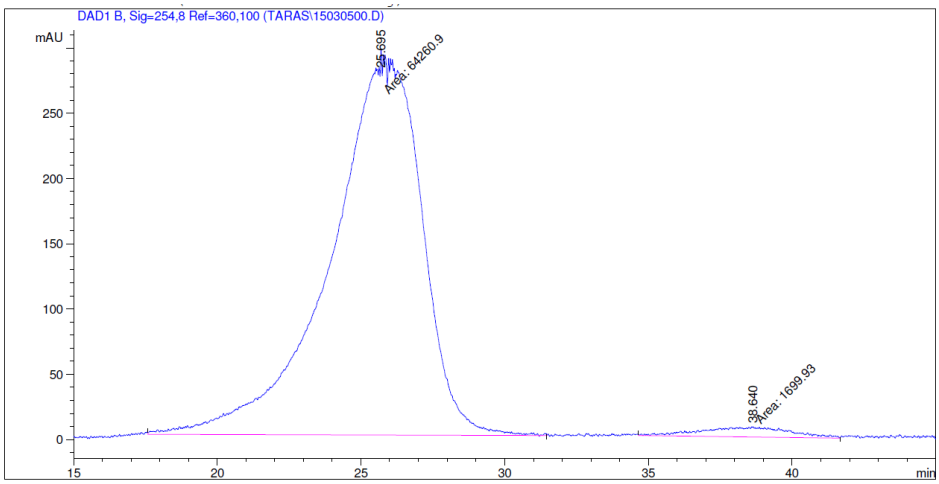


```
================================================================================
                            Area Percent Report
================================================================================

Sorted By             :      Signal
Multiplier            :      1.0000
Dilution              :      1.0000
Use Multiplier & Dilution Factor with ISTDs


Signal 1: DAD1 B, Sig=254,8 Ref=360,100

Peak RetTime Type  Width     Area      Height     Area
  #   [min]        [min]   [mAU*s]     [mAU]       %
----|-------|----|-------|----------|----------|--------|
   1  25.695 MM    3.6248 6.42609e4   295.47260  97.4228
   2  38.640 MM    3.5041 1699.92957    8.08547   2.5772
```

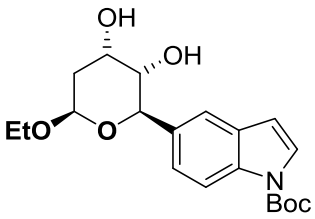

HPLC data for the racemic (top) and optically enriched (bottom) 4-6e

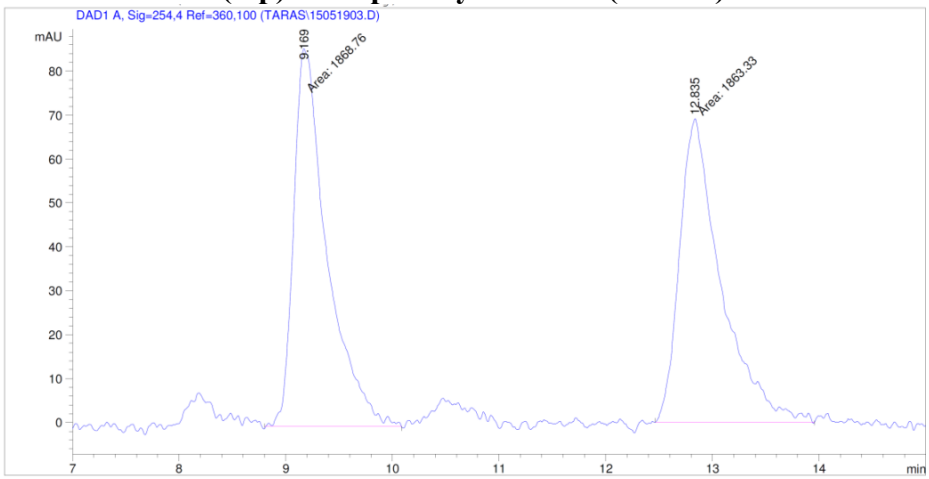


```
=====================================================================
                      Area Percent Report
=====================================================================

Sorted By             :      Signal
Multiplier            :      1.0000
Dilution              :      1.0000
Use Multiplier & Dilution Factor with ISTDs


Signal 1: DAD1 A, Sig=254,4 Ref=360,100

Peak RetTime Type  Width     Area      Height     Area
  #   [min]       [min]   [mAU*s]     [mAU]       %
----|-------|----|-------|----------|----------|--------|
   1   9.169 MF    0.3618 1868.75989   86.08758  50.0727
   2  12.835 MM    0.4488 1863.33301   69.19574  49.9273
```

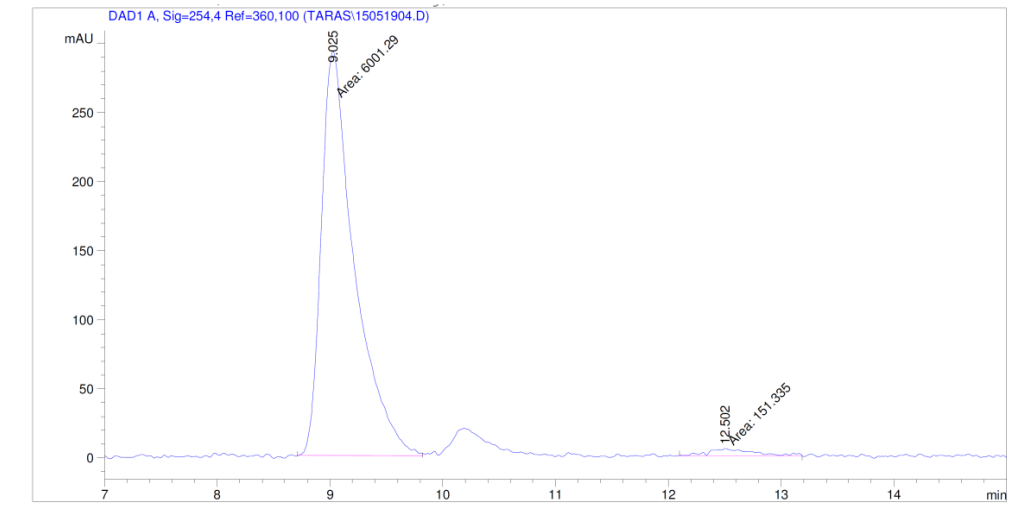


```
=====================================================================
                      Area Percent Report
=====================================================================

Sorted By             :      Signal
Multiplier            :      1.0000
Dilution              :      1.0000
Use Multiplier & Dilution Factor with ISTDs


Signal 1: DAD1 A, Sig=254,4 Ref=360,100

Peak RetTime Type  Width     Area      Height     Area
  #   [min]       [min]   [mAU*s]     [mAU]       %
----|-------|----|-------|----------|----------|--------|
   1   9.025 MF    0.3412 6001.29297  293.18839  97.5403
   2  12.502 MF    0.4635  151.33517    5.44123   2.4597
```

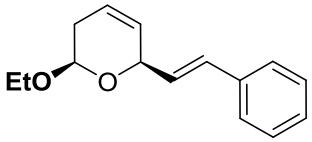

Appendix 3: Crystal Structure Report

X-ray Crystallographic data for 4-8

XCL Code: DGH1502 **Date:** 15 May 2015

Compound: Ethyl 2,3-dideoxy-3-phenylpentopyranoside

Formula: $C_{13}H_{18}O_3$

Supervisor: D. G. Hall **Crystallographer:** R. McDonald

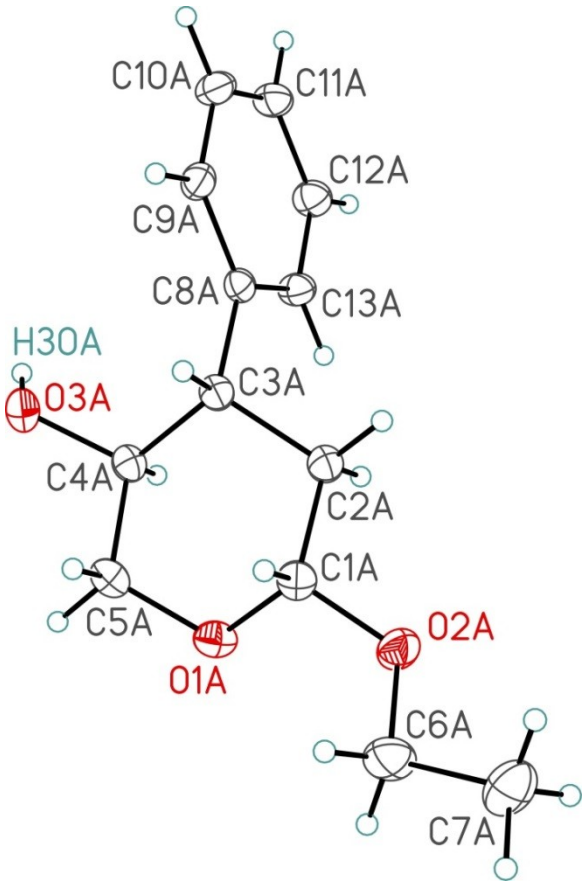

For further information regarding this X-ray, please contact the X-ray crystallography laboratory at the University of Alberta:
Dr. Robert McDonald E-Mail: Bob.McDonald@ualberta.ca
Dr. Michael J. Ferguson E-Mail: Michael.Ferguson@ualberta.ca **Lab:** E3-09; **Office:** E3-13 Gunning/Lemieux Chemistry Centre
Phone: +1 780 492 2485; **Fax:** +1 780 492 8231

X-Ray Crystallography Laboratory, Department of Chemistry, University of Alberta, Edmonton, Alberta, T6G 2G2, Canada

X-ray Crystallographic data for 4-9

XCL Code: DGH1504 **Date:** 8 June 2015

Compound: Ethyl 2-deoxy-5-{4-(trifluoromethyl)phenyl}pentopyranoside

Formula: $C_{14}H_{17}F_3O_4$

Supervisor: D. G. Hall **Crystallographer:** R. McDonald

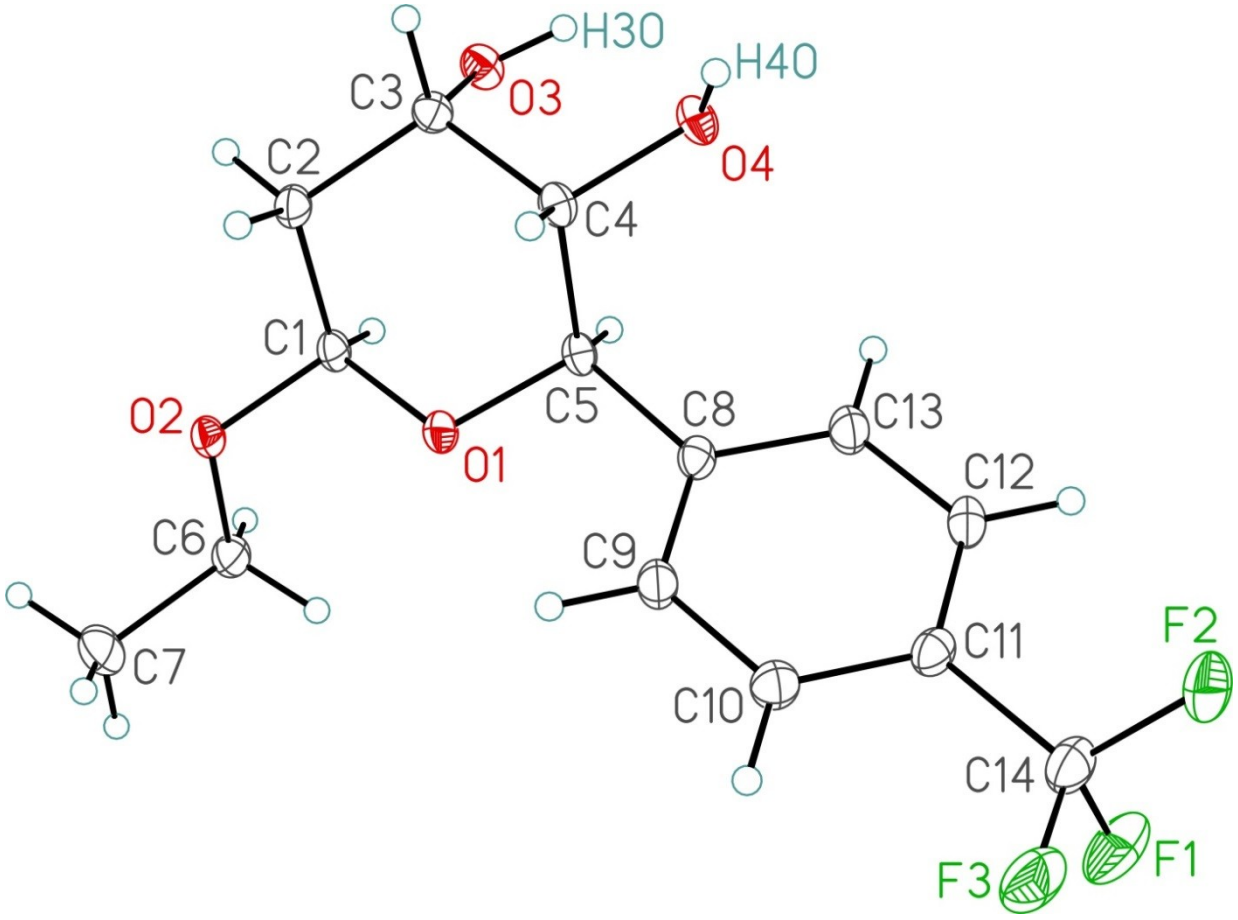

For further information regarding this X-ray, please contact the X-ray crystallography laboratory at the University of Alberta:
Dr. Robert McDonald E-Mail: Bob.McDonald@ualberta.ca
Dr. Michael J. Ferguson E-Mail: Michael.Ferguson@ualberta.ca **Lab:** E3-09; **Office:** E3-13 Gunning/Lemieux Chemistry Centre
Phone: +1 780 492 2485; **Fax:** +1 780 492 8231

X-Ray Crystallography Laboratory, Department of Chemistry, University of Alberta, Edmonton, Alberta, T6G 2G2, Canada

X-ray Crystallographic data for 4-10

XCL Code: DGH1501 **Date:** 15 April 2015

Compound: Ethyl 2-deoxy-5-phenylpentopyranoside

Formula: $C_{13}H_{18}O_4$

Supervisor: D. G. Hall **Crystallographer:** R. McDonald

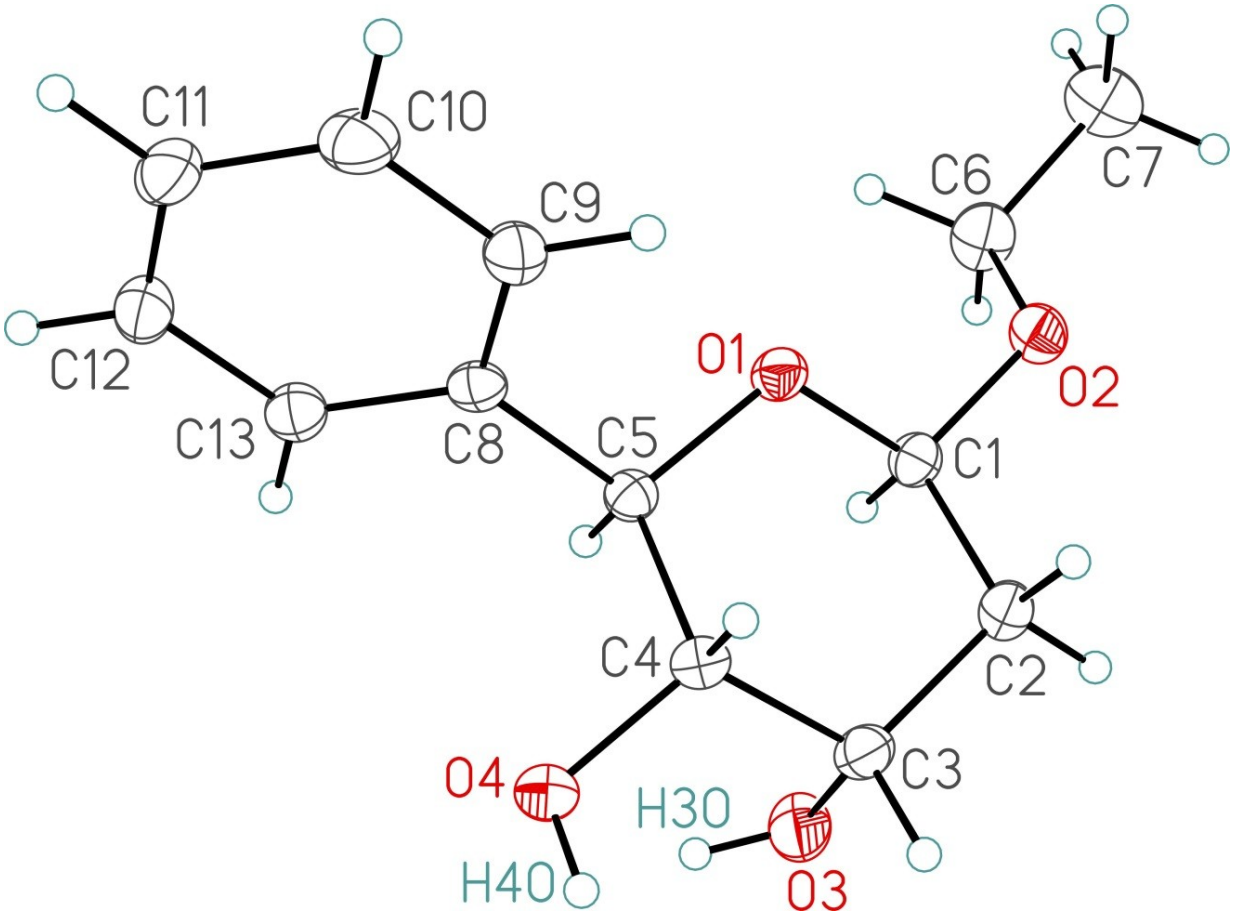

For further information regarding this X-ray, please contact the X-ray crystallography laboratory at the University of Alberta:
Dr. Robert McDonald E-Mail: Bob.McDonald@ualberta.ca
Dr. Michael J. Ferguson E-Mail: Michael.Ferguson@ualberta.ca **Lab:** E3-09; **Office:** E3-13 Gunning/Lemieux Chemistry Centre
Phone: +1 780 492 2485; **Fax:** +1 780 492 8231

X-Ray Crystallography Laboratory, Department of Chemistry, University of Alberta, Edmonton, Alberta, T6G 2G2, Canada

X-ray Crystallographic data for 4-35

XCL Code: DGH1503 **Date:** 25 May 2015

Compound: Ethyl 3,4-anhydro-2-deoxy-5-phenylpentopyranoside

Formula: $C_{13}H_{16}O_3$

Supervisor: D. G. Hall **Crystallographer:** R. McDonald

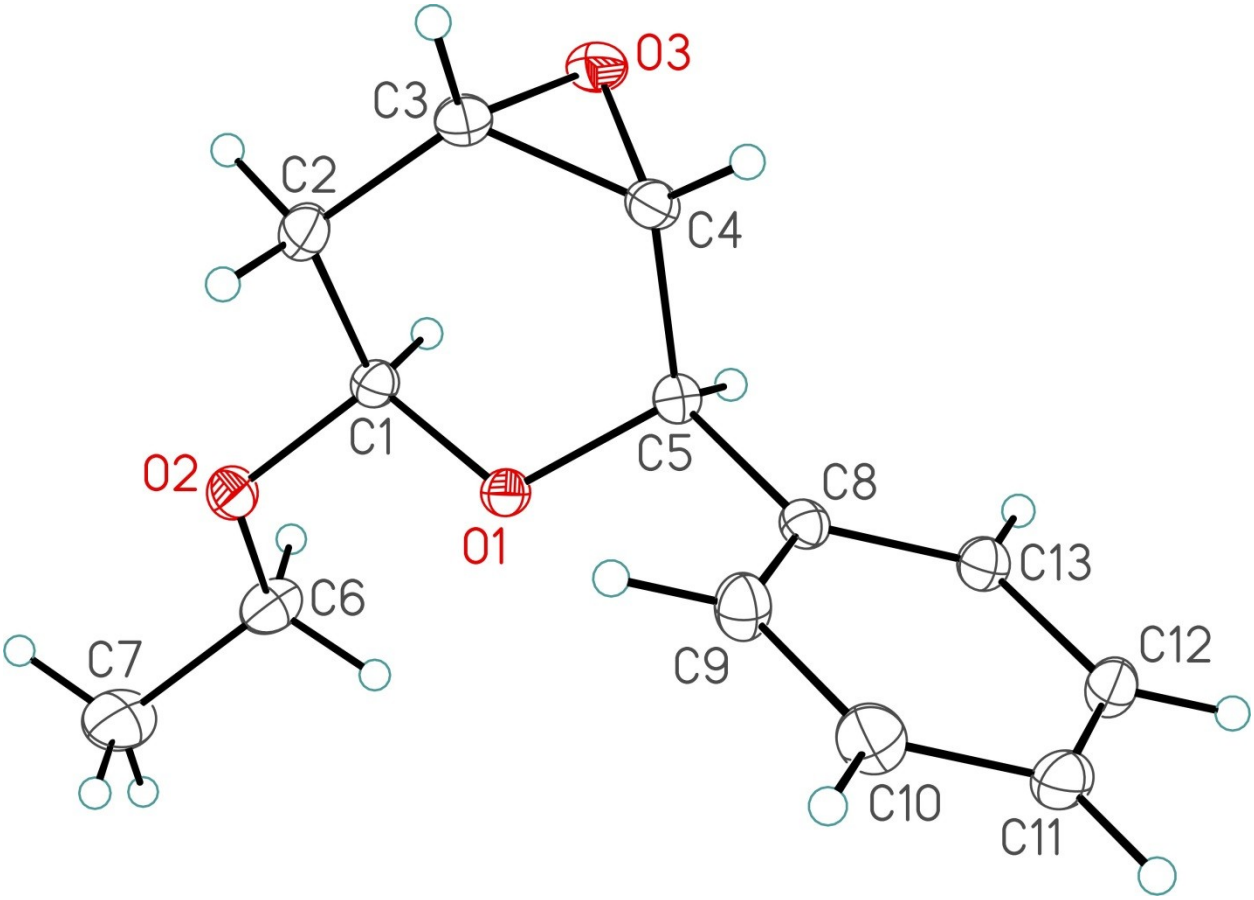

For further information regarding this X-ray, please contact the X-ray crystallography laboratory at the University of Alberta:
Dr. Robert McDonald E-Mail: Bob.McDonald@ualberta.ca
Dr. Michael J. Ferguson E-Mail: Michael.Ferguson@ualberta.ca **Lab:** E3-09; **Office:** E3-13 Gunning/Lemieux Chemistry Centre
Phone: +1 780 492 2485; **Fax:** +1 780 492 8231

X-Ray Crystallography Laboratory, Department of Chemistry, University of Alberta, Edmonton, Alberta, T6G 2G2, Canada